Title: Cosmology with Gravitational Lensing

Date: Jan 23, 2009 04:00 PM

URL: http://pirsa.org/09010041

Abstract:

Cosmology with gravitational lensing

Priya Natarajan
Radcliffe Institute for Advanced Study
and
Yale University

Collaborators:

- Andrew Davis (Yale)
- Latchezar Benatov (Yale)
- Julie Comerford (Berkeley)
- Kenneth Rines (W Washington)
- Jean-Paul Kneib (Marseille)
- Sean Moran (JHU)
- Tommaso Treu (UCSB)
- Gabriella De Lucia (MPA)
- Volker Springel (MPA)
- Ian Smail (Durham)
- Marceau Limousin (Toulouse)
- Daisuke Nagai (Yale)
- Andrey Kravtsov (Chicago)
- Richard Ellis (Caltech)
- Eric Jullo (JPL)
- Stephane Bardeau (IAP)
- Graham Smith (Birmingham)
- Good fair-trade coffee
- Fine wine, dark chocolate

Talk Outline

Lensing tests of the Cold Dark Matter paradigm

- Lensing basics
- Application to clusters of galaxies

Dark matter properties

(i) Mass profiles of clusters: modeling accuracy

(ii) Substructure: mass function of DM halos; spatial distribution of DM halos

(iii) Density profiles of DM halos: slopes; existence of cores

(iv) Tidal stripping: galaxy orbits and dynamics; implications for the nature of DM

(v) Concentration-Mass relation

(vi) Lensing cross sections and arc statistics: superlenses; structure along the line of sight

Lensing constraints on dark energy

(i) cluster arcs

(ii) Feasibility of this geometric technique

Future prospects

(i) clusters as gravitational telescopes

(ii) X-ray-SZ

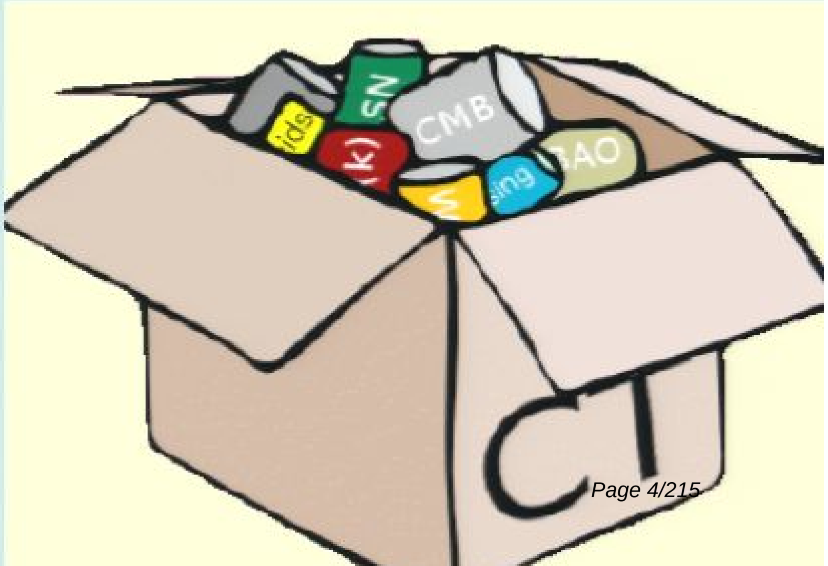

Composition of the Cosmos

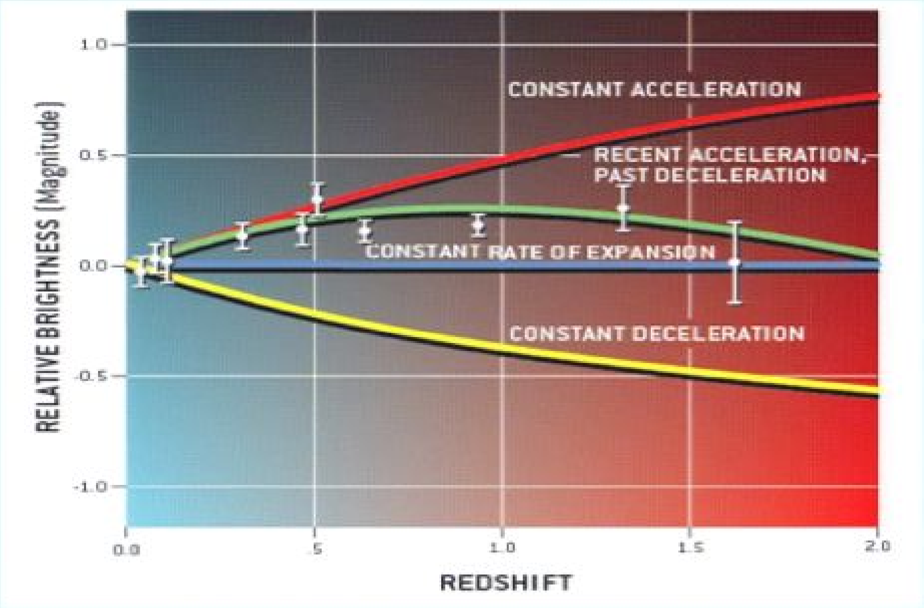

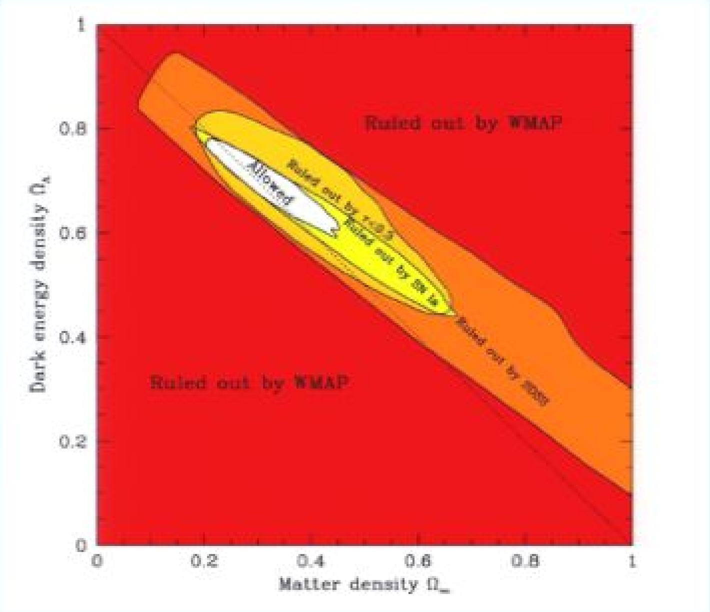

Compelling cosmological evidence for non-baryonic DM

$\Omega_d h^2($ 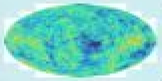 $)= 0.113$

WIMPS: Weakly Interacting Massive Particles - the lightest neutralino, motivated by SUSY, mean scattering time-scale longer than Hubble time

Riess+ 98 Perlmutter +99;
Tegmark+ 03; Spergel+ 03; 06;
WMAP SDSS 2dF

Measuring lensing signals

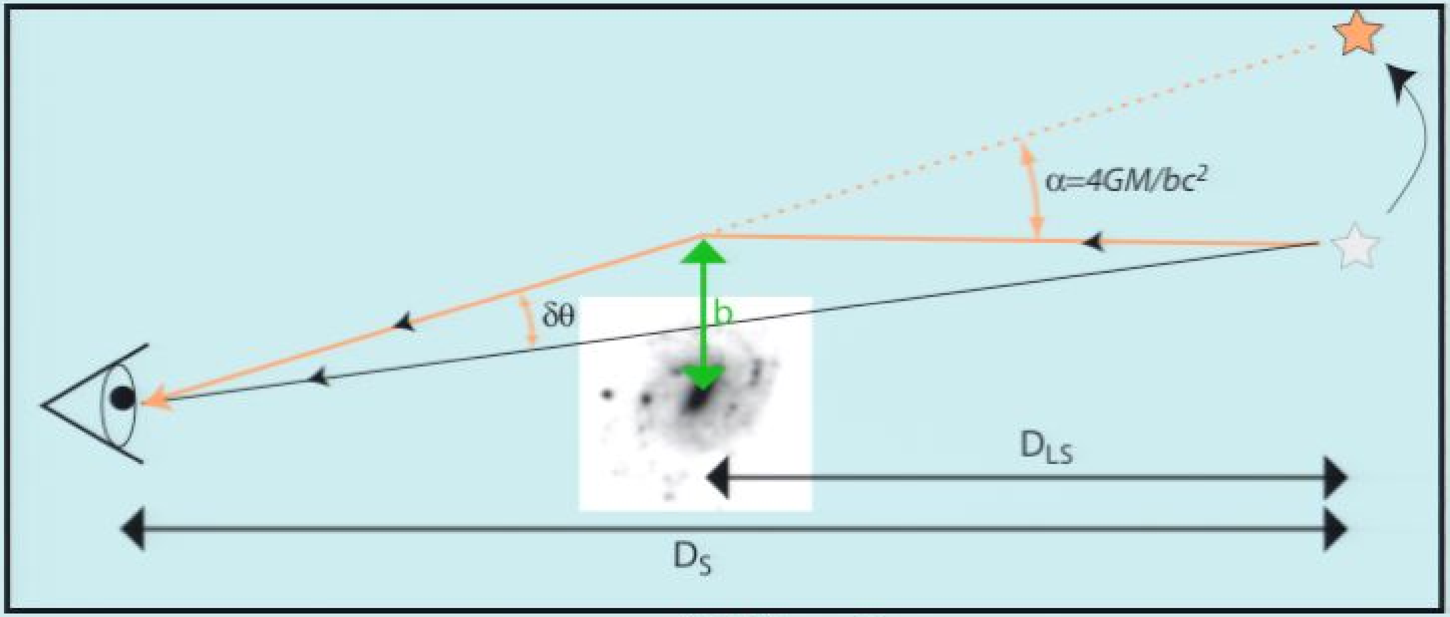

$$\delta\theta = \frac{4GM}{bc^2} \frac{D_{LS}}{D_S}$$

We observe this deflection angle (more precisely, gradients of the deflection angle).

Cosmology changes growth rate of mass structures in the Universe.

Cosmology changes the geometric distance factors.

The deflection is proportional to the mass

Blandford & Narayan 92; Schneider Ehlers & Falco 92; Bartelmann & Narayan 97;

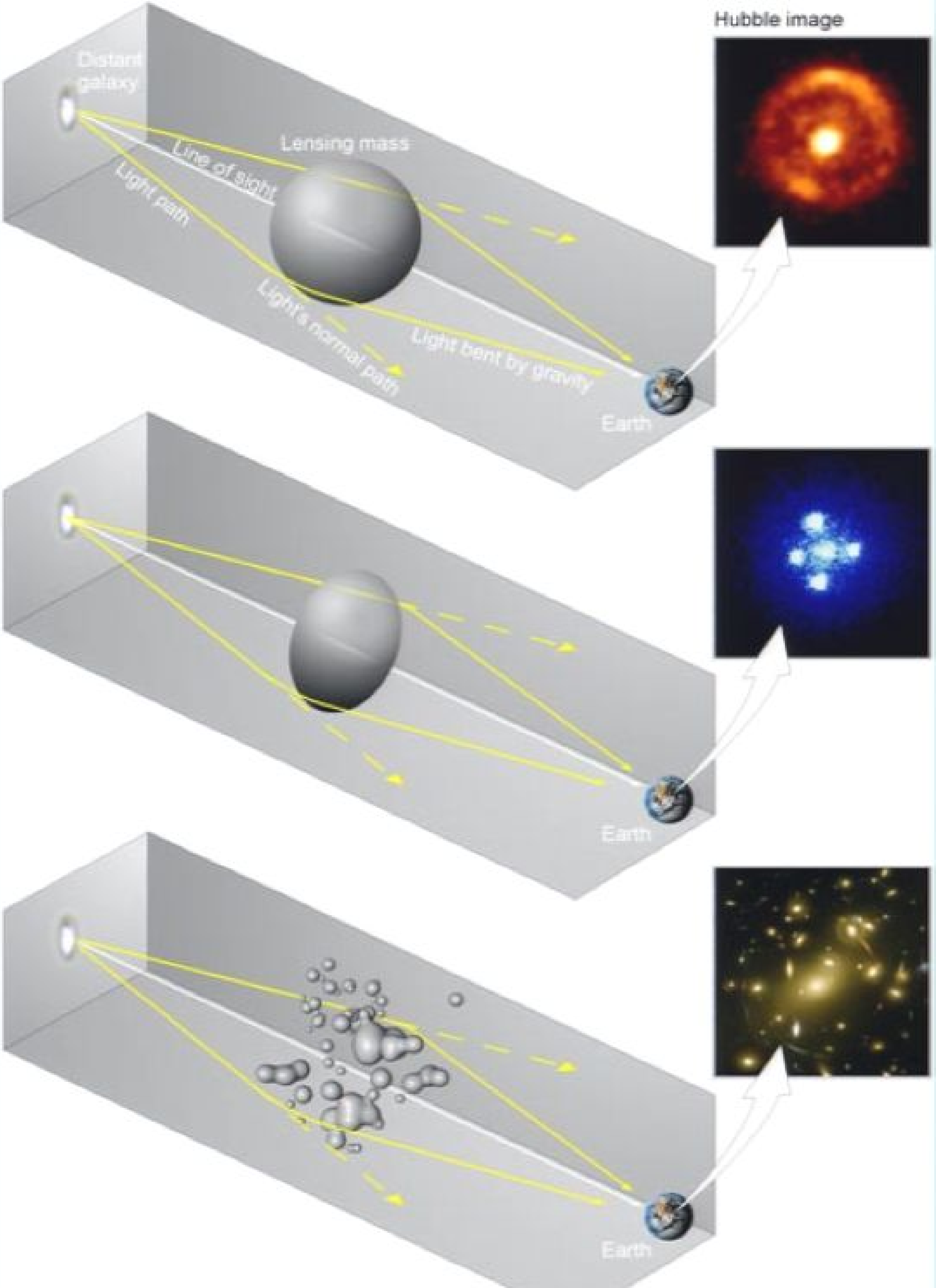
Hubble image
Distant galaxy
Lensing mass
Line of sight
Light path
Light's normal path
Light bent by gravity
Earth
Earth
Earth

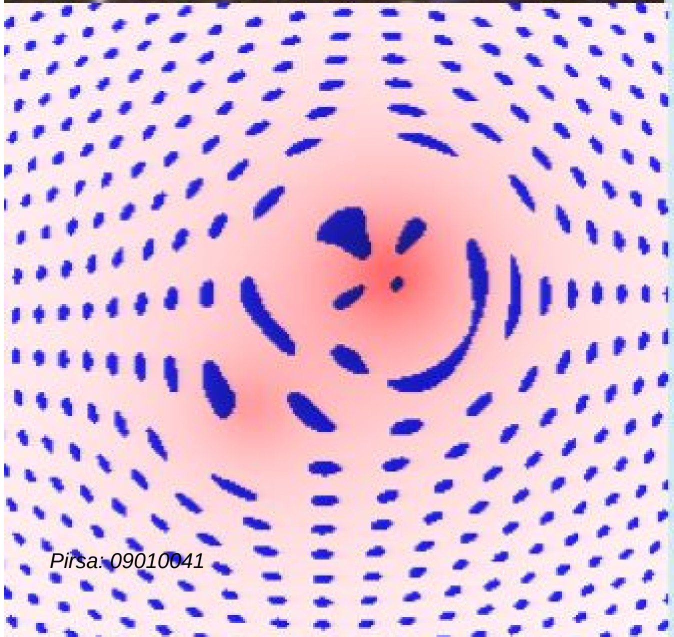

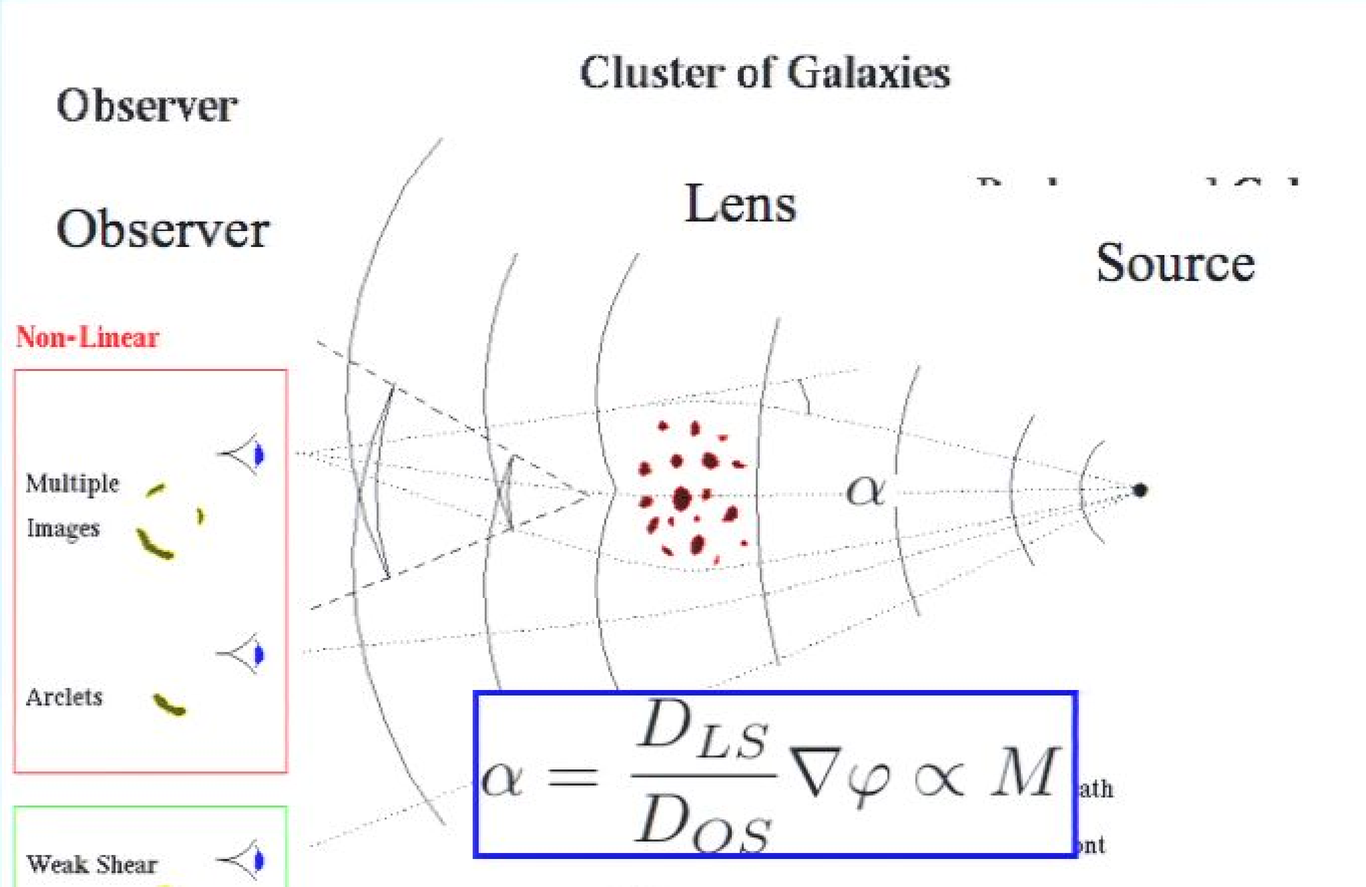

$$\alpha = \frac{D_{LS}}{D_{OS}} \nabla \varphi \propto M$$

- - - - Multiple Images Area

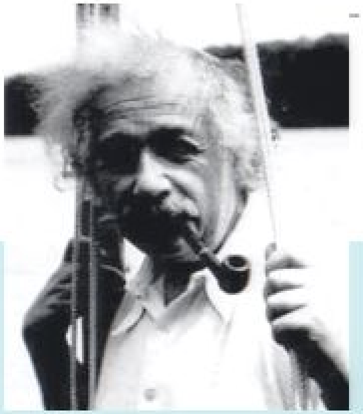

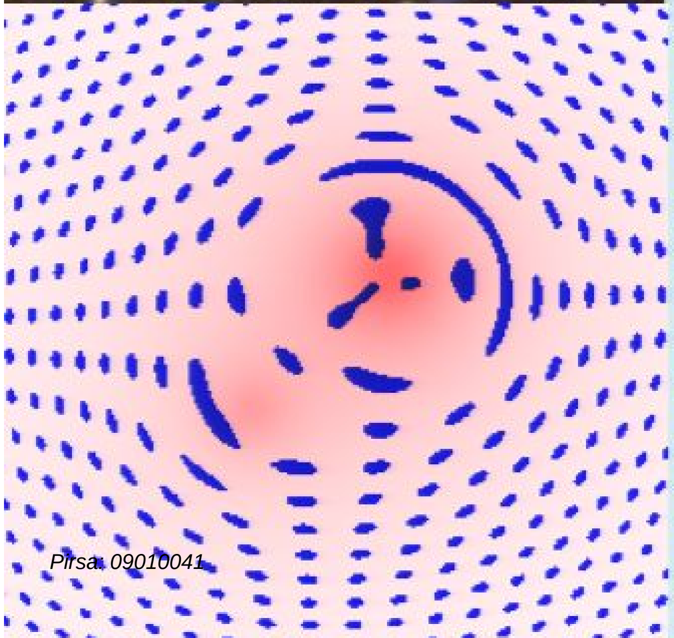

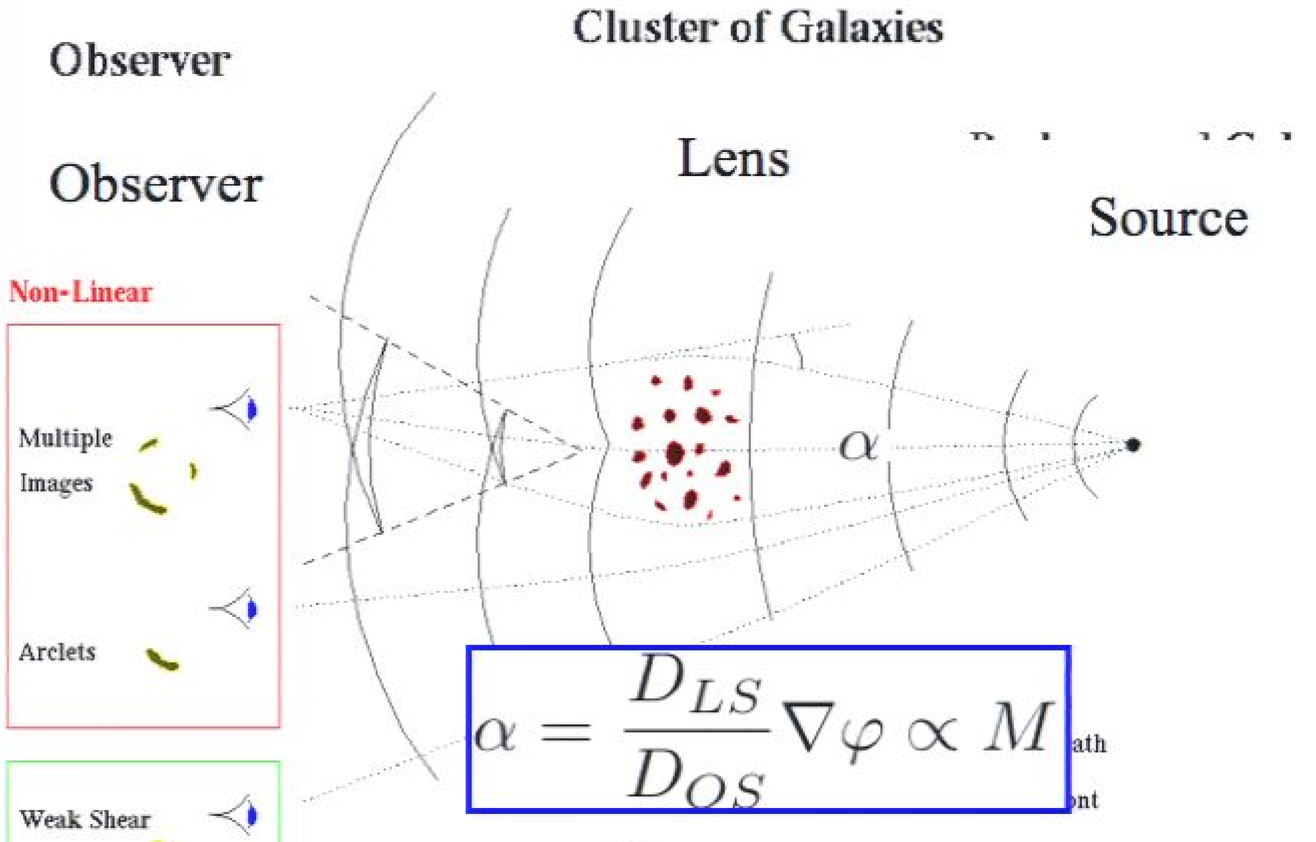

$$\boxed{\alpha = \frac{D_{LS}}{D_{OS}}\nabla\varphi \propto M}$$

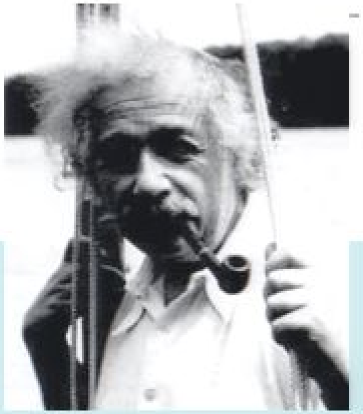

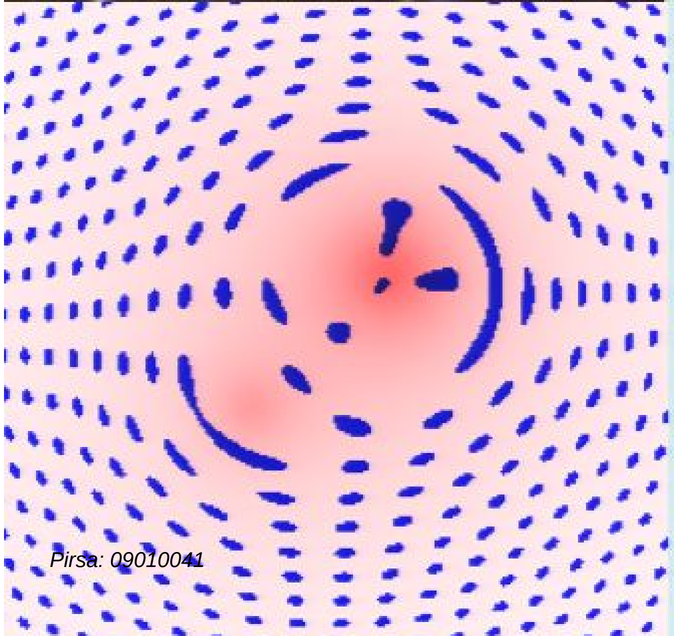

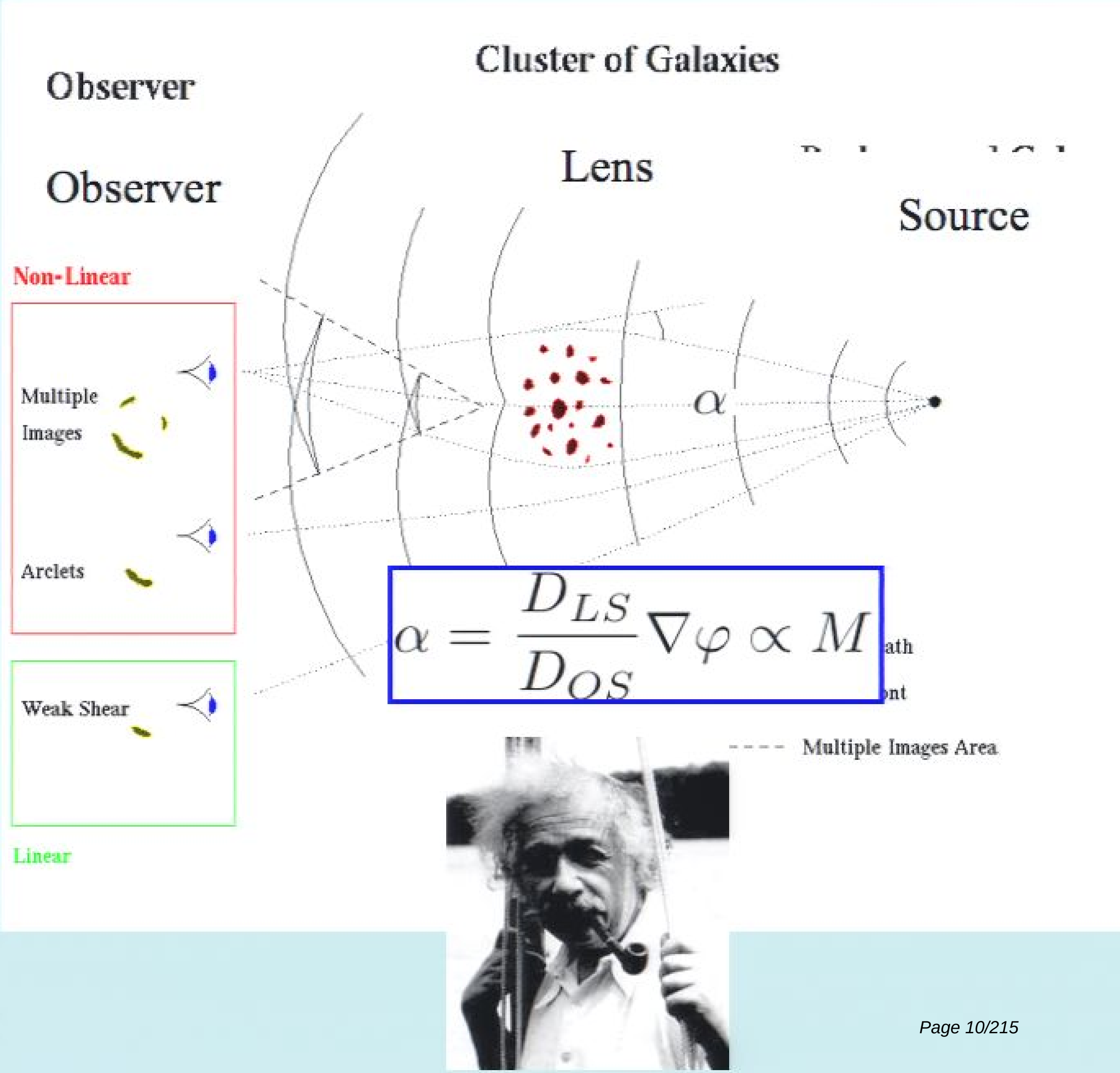

$$\alpha = \frac{D_{LS}}{D_{OS}} \nabla \varphi \propto M$$

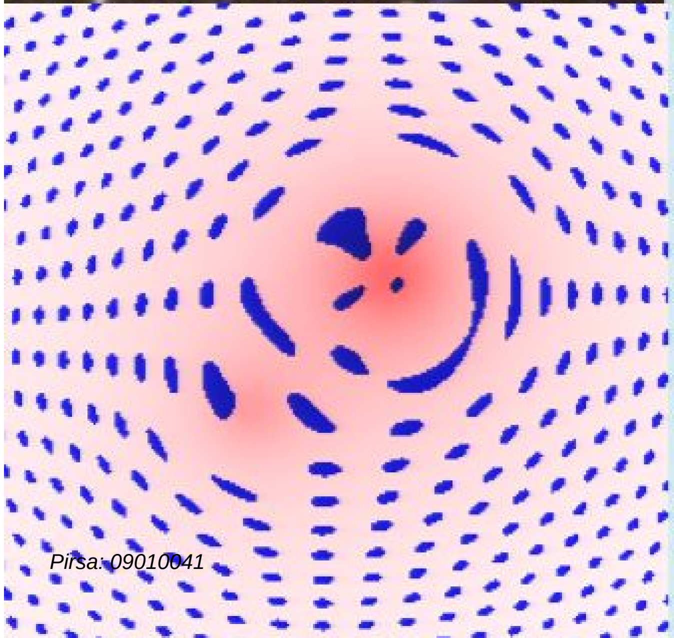

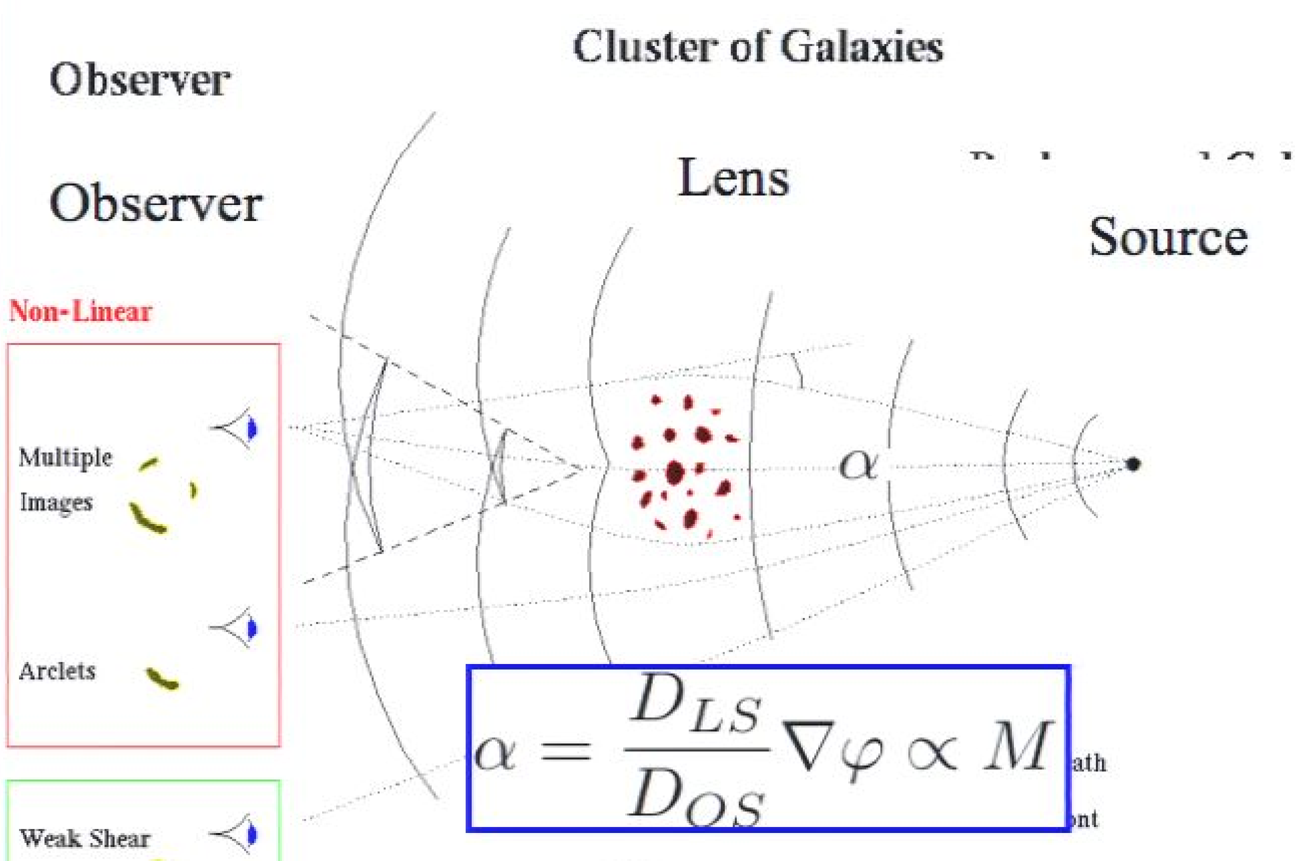

$$\alpha = \frac{D_{LS}}{D_{OS}} \nabla \varphi \propto M$$

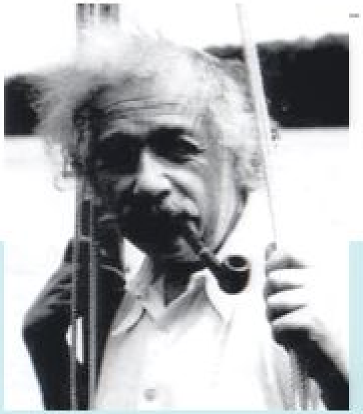

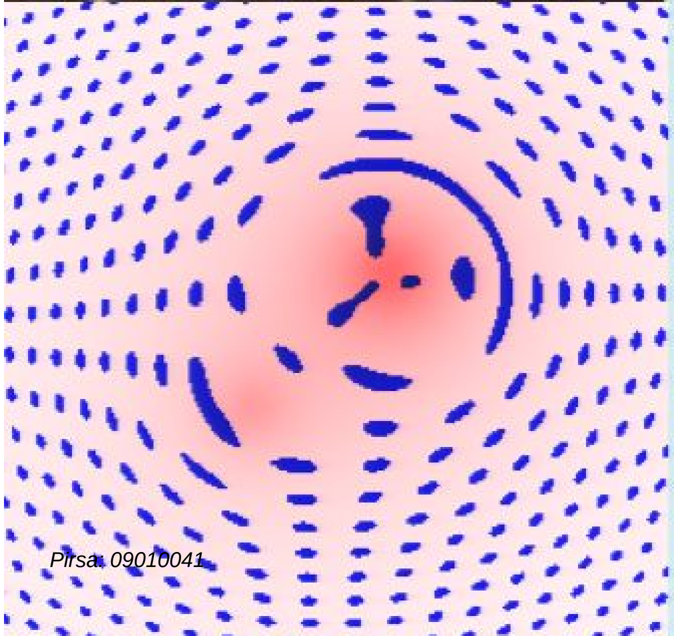

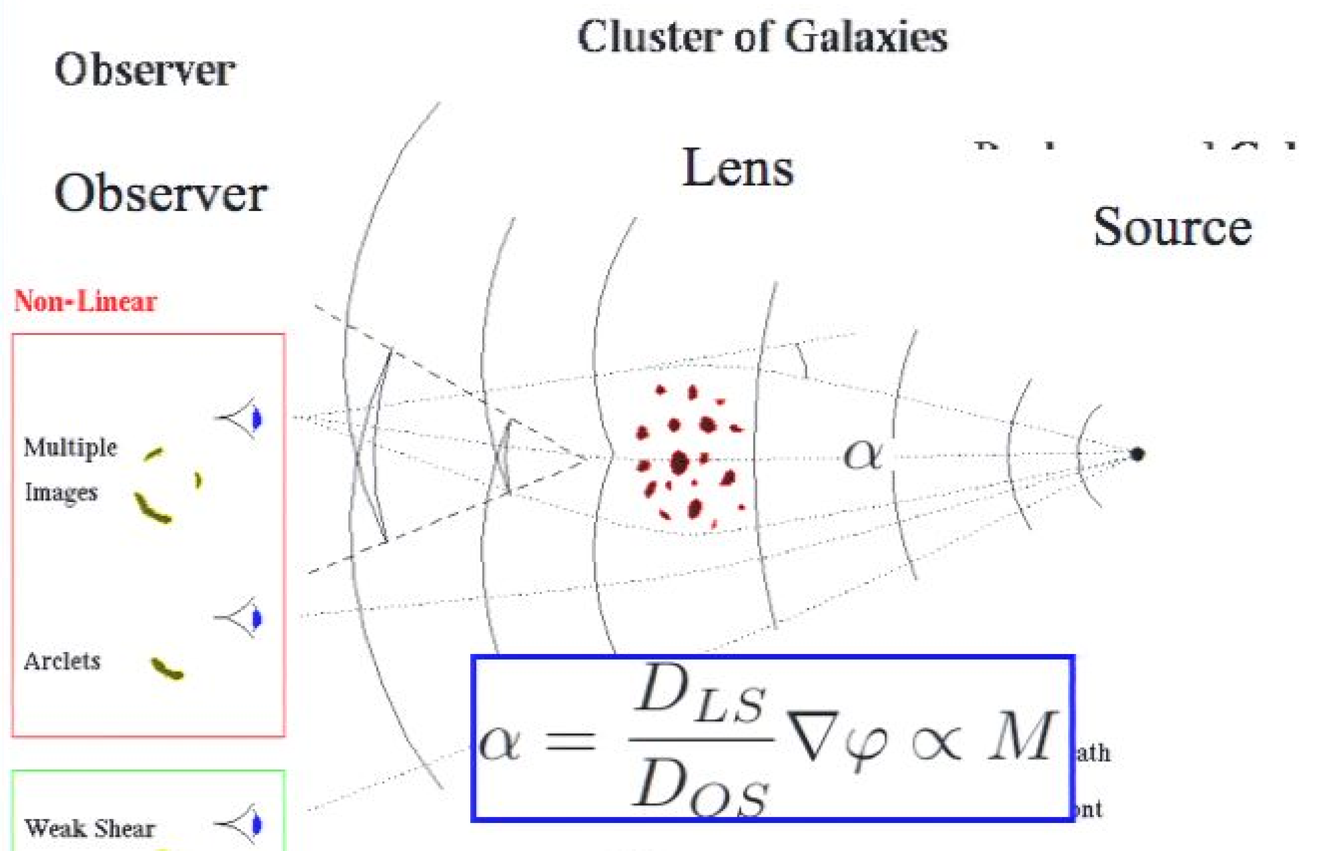

$$\boxed{\alpha = \frac{D_{LS}}{D_{OS}} \nabla \varphi \propto M}$$

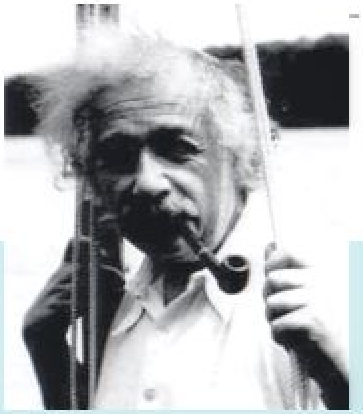

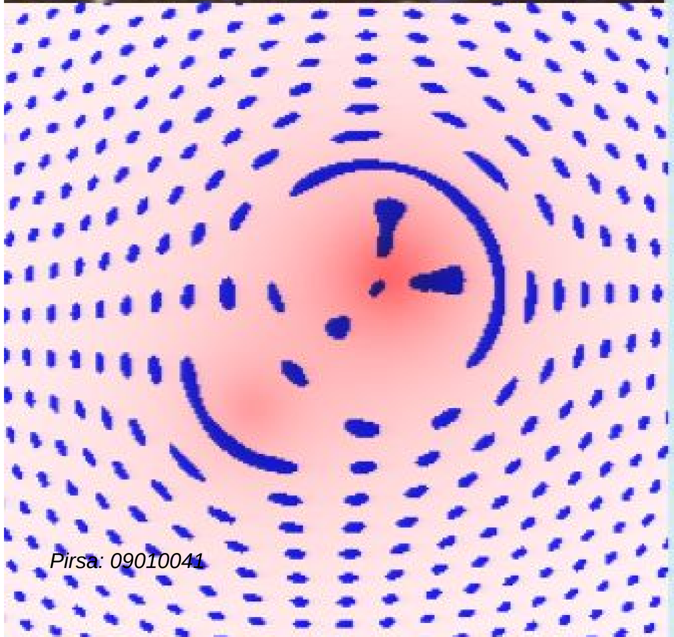

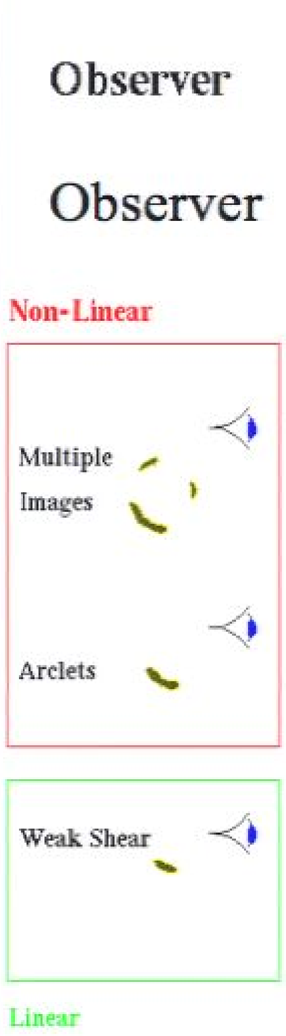

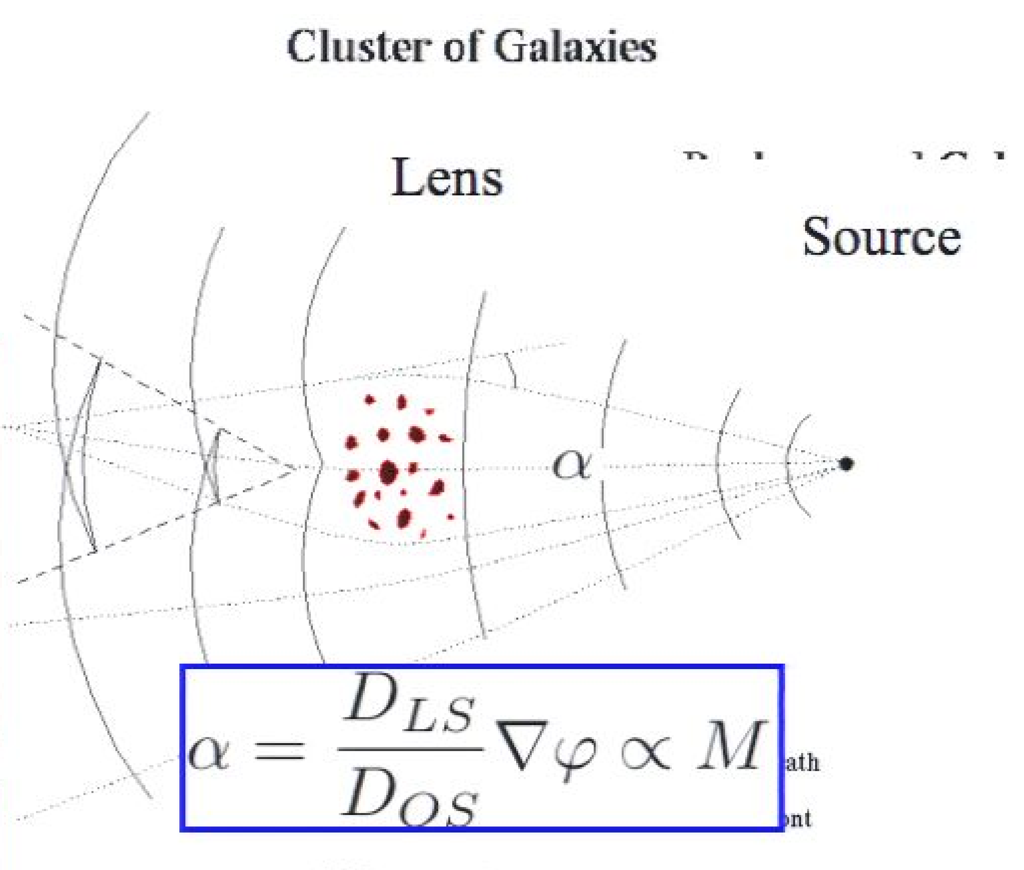

$$\boxed{\alpha = \frac{D_{LS}}{D_{OS}} \nabla\varphi \propto M}$$

Multiple Images Area

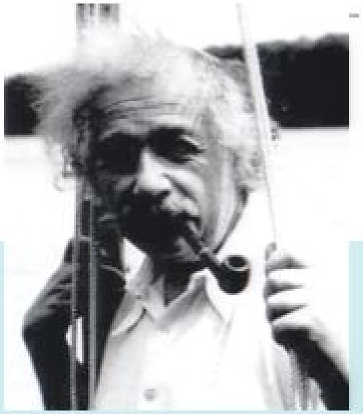

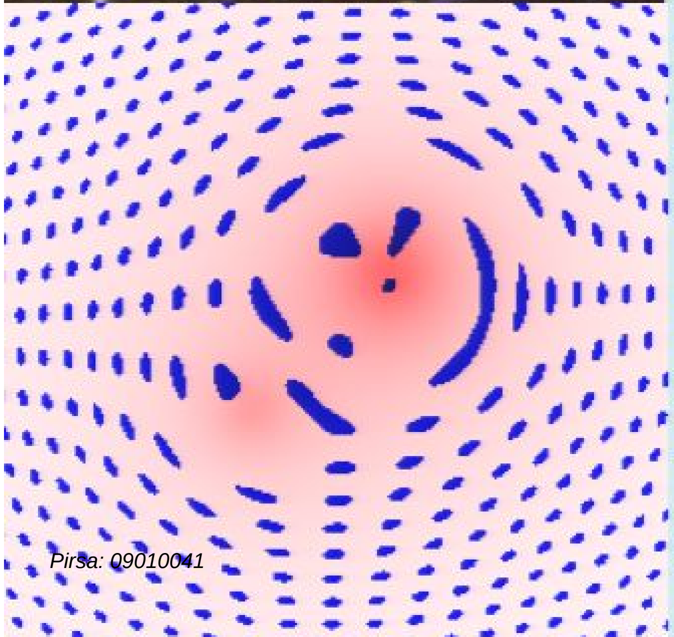

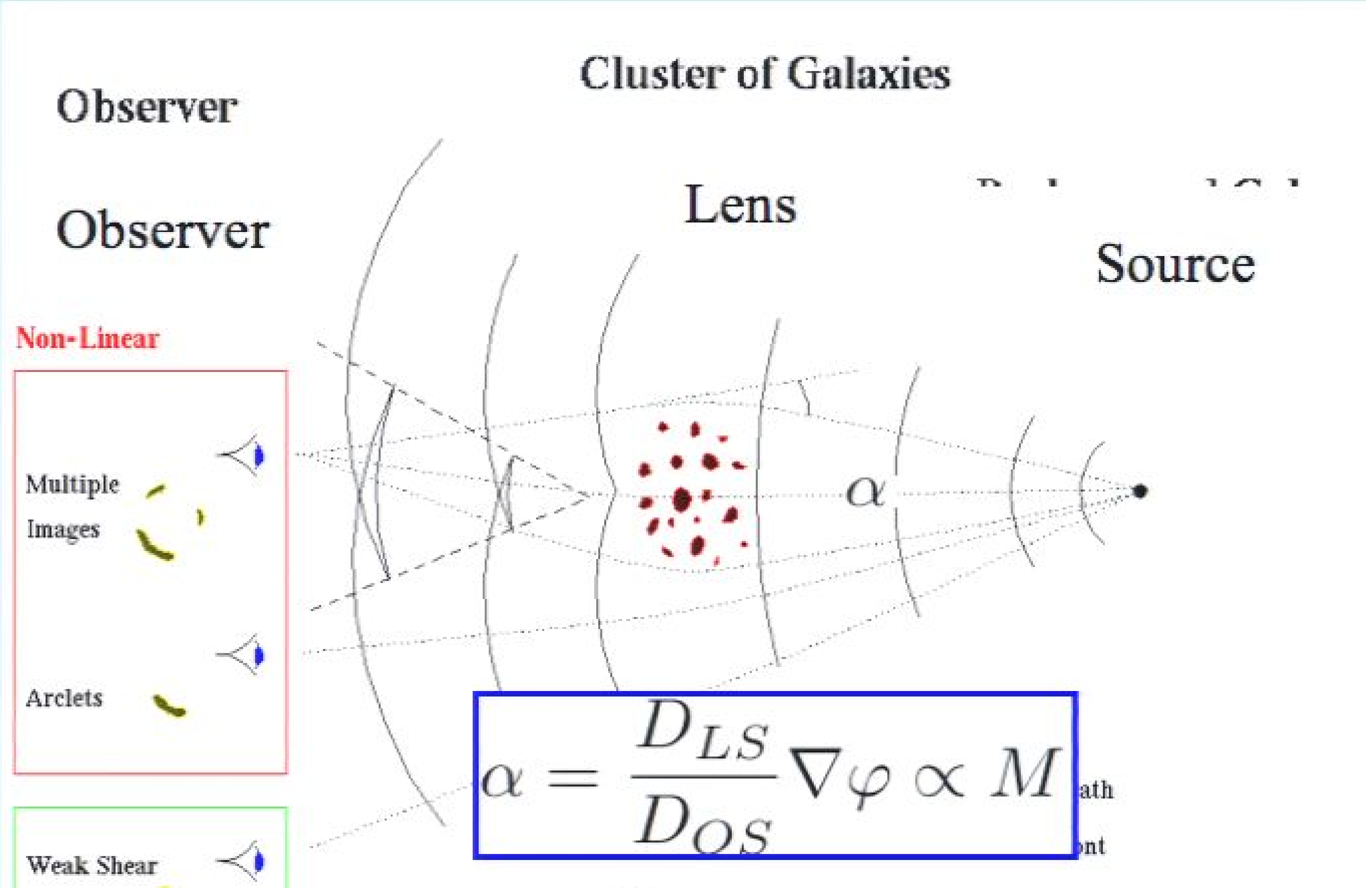

$$\boxed{\alpha = \frac{D_{LS}}{D_{OS}} \nabla\varphi \propto M}$$

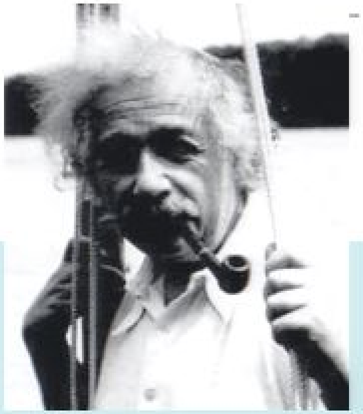

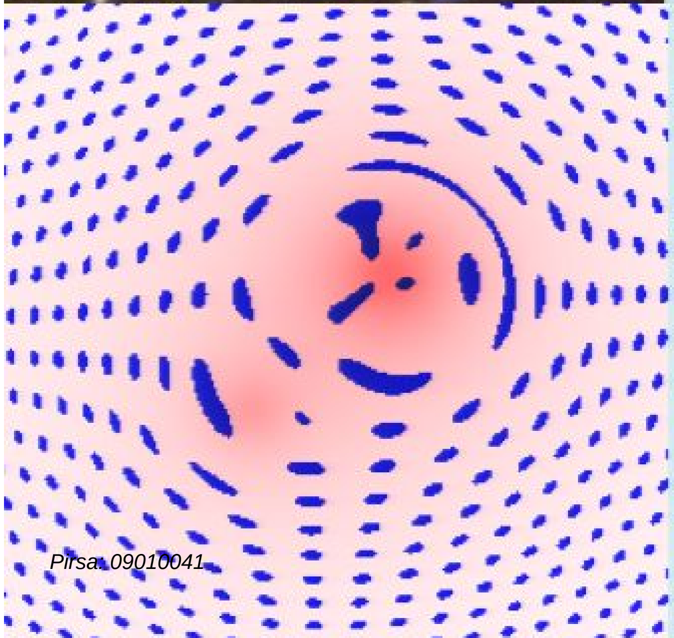

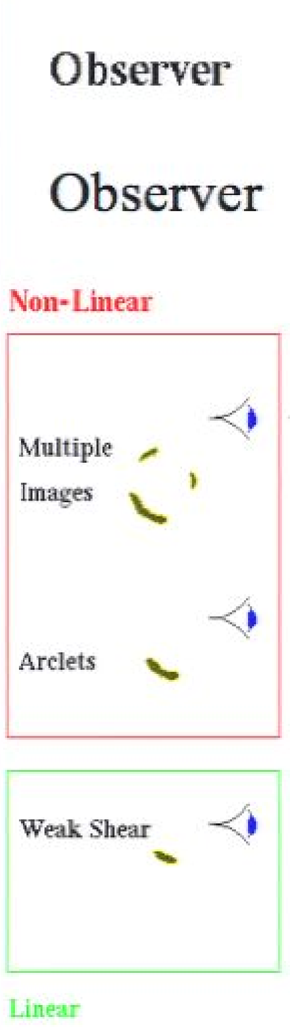

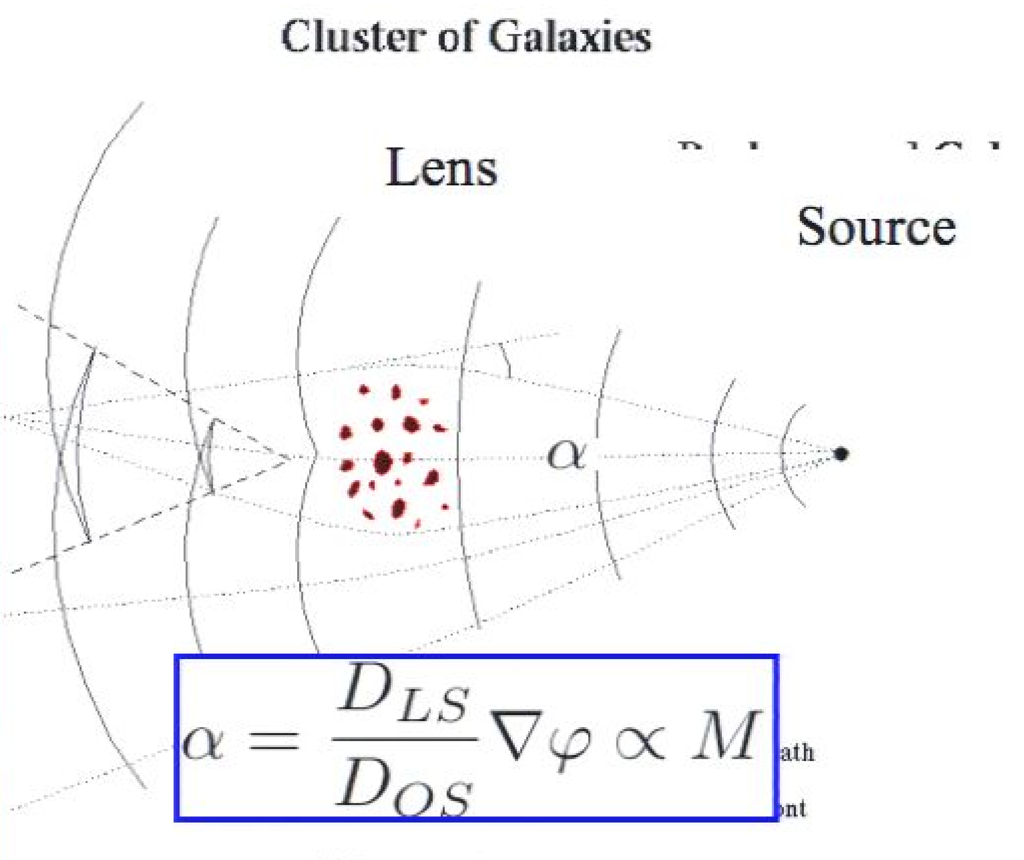

$$\alpha = \frac{D_{LS}}{D_{OS}} \nabla \varphi \propto M$$

Multiple Images Area

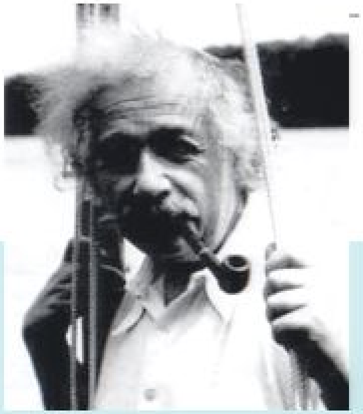

CFHT 1990

Z_cluster=0.375

Z_arc=0.725 (Soucail et al 1988)

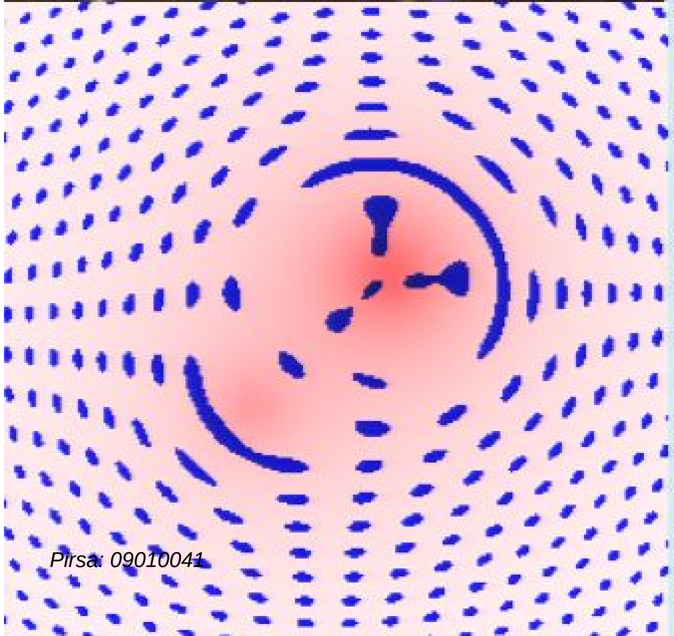

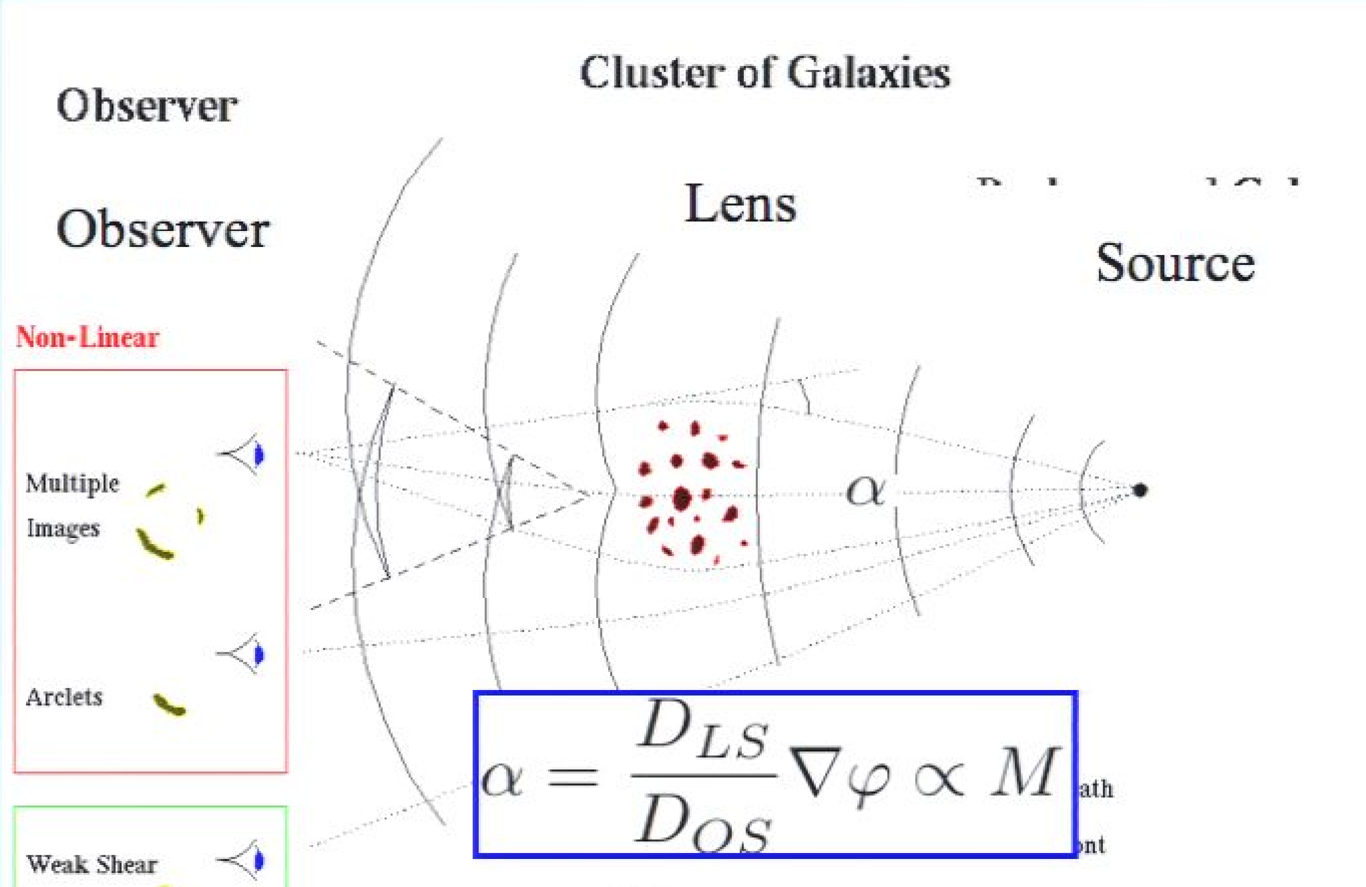

$$\alpha = \frac{D_{LS}}{D_{OS}} \nabla \varphi \propto M$$

Linear

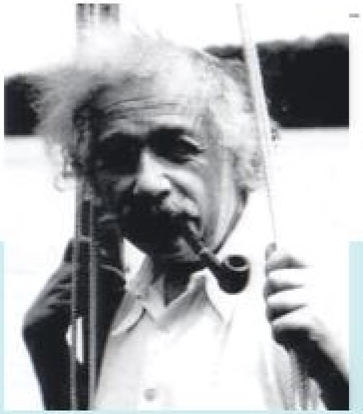

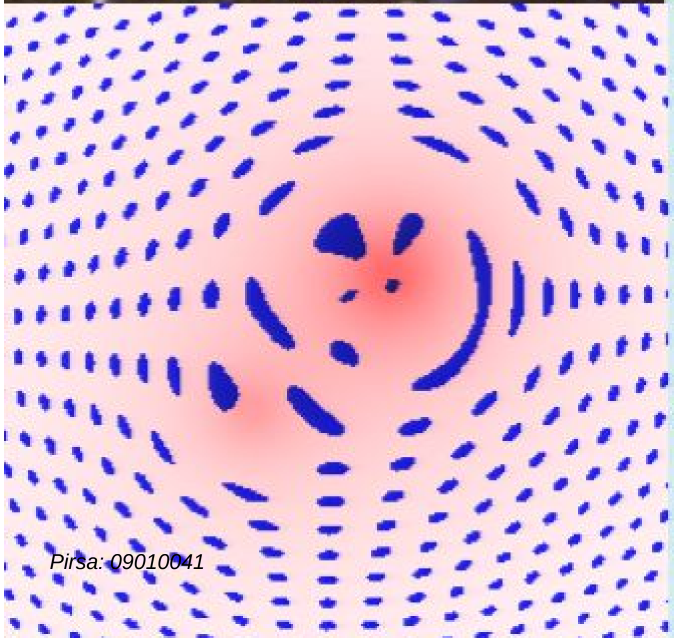

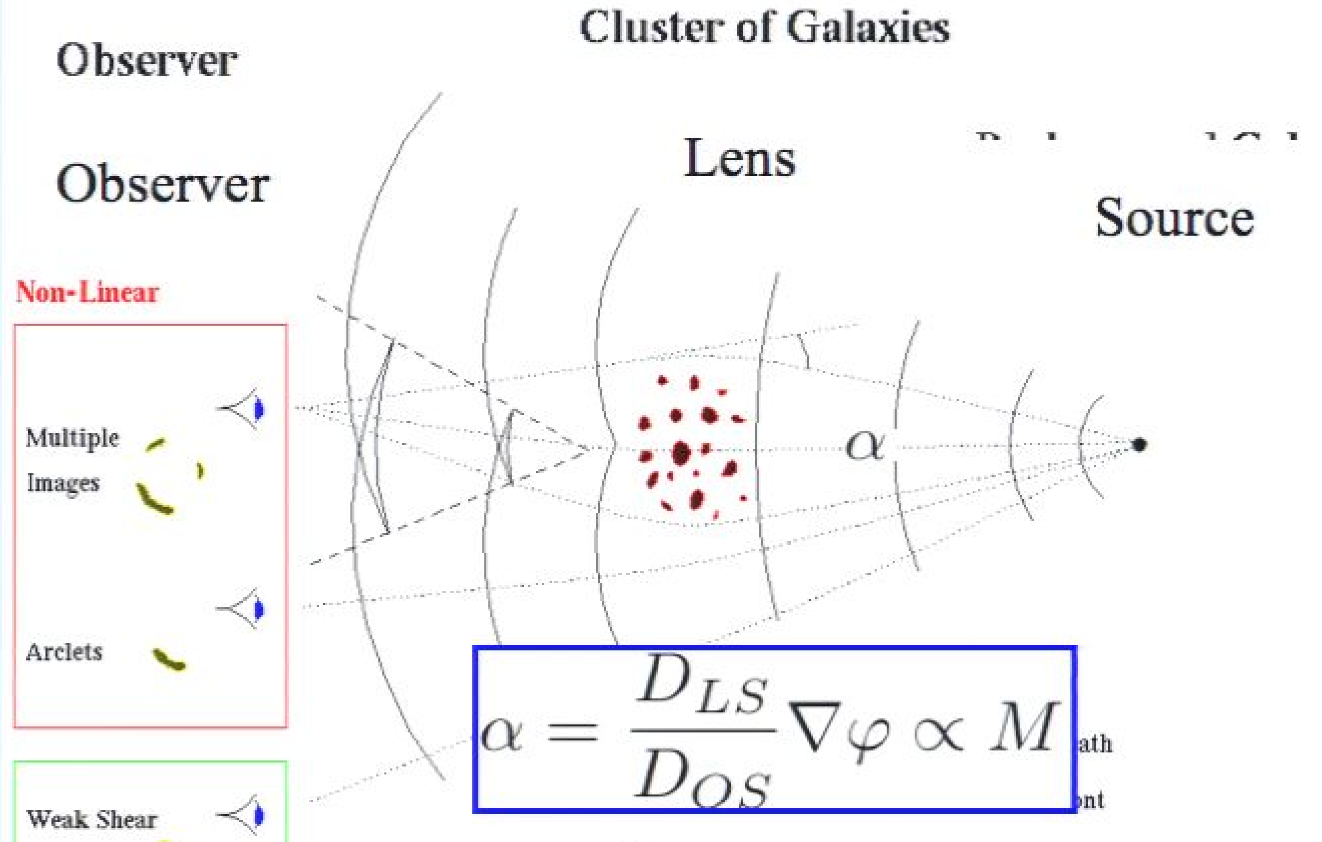

$$\alpha = \frac{D_{LS}}{D_{OS}} \nabla \varphi \propto M$$

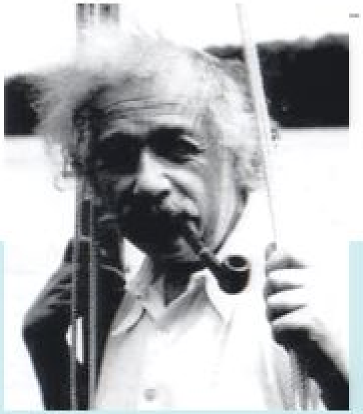

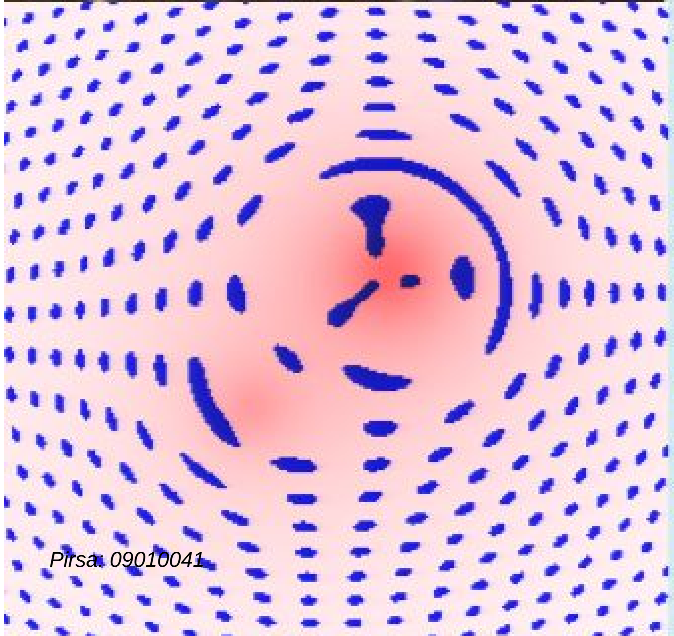

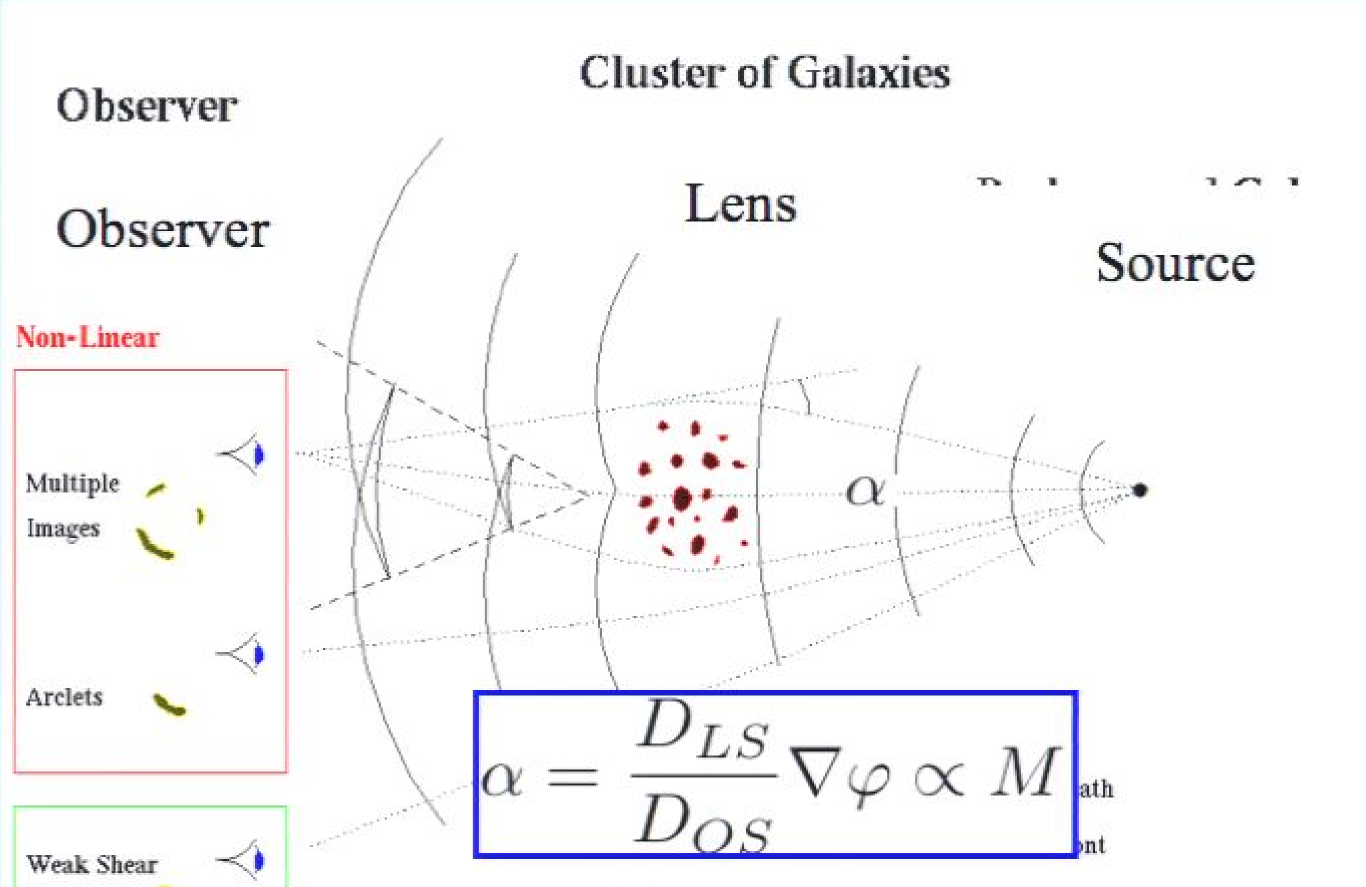

$$\boxed{\alpha = \frac{D_{LS}}{D_{OS}} \nabla\varphi \propto M}$$

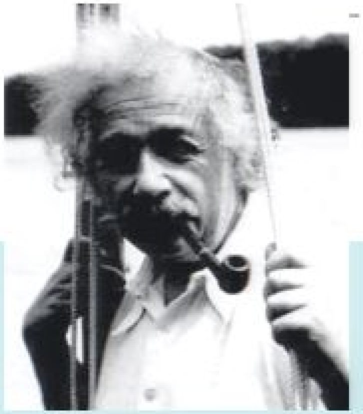

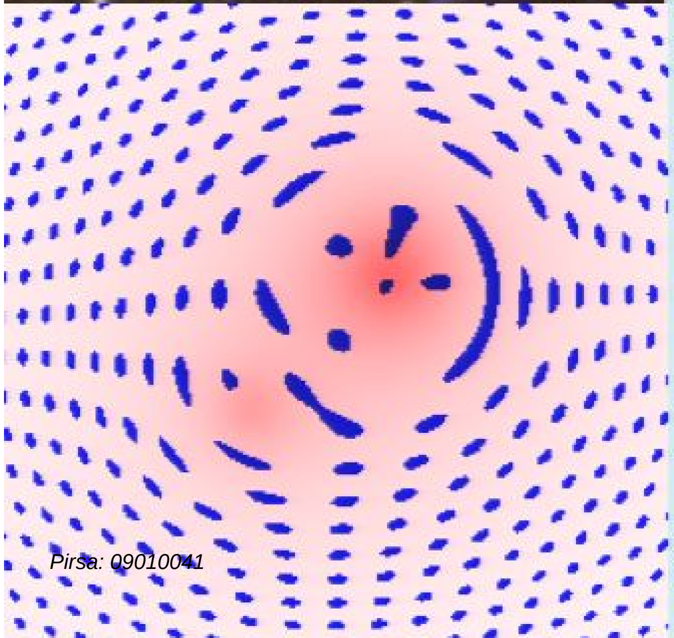

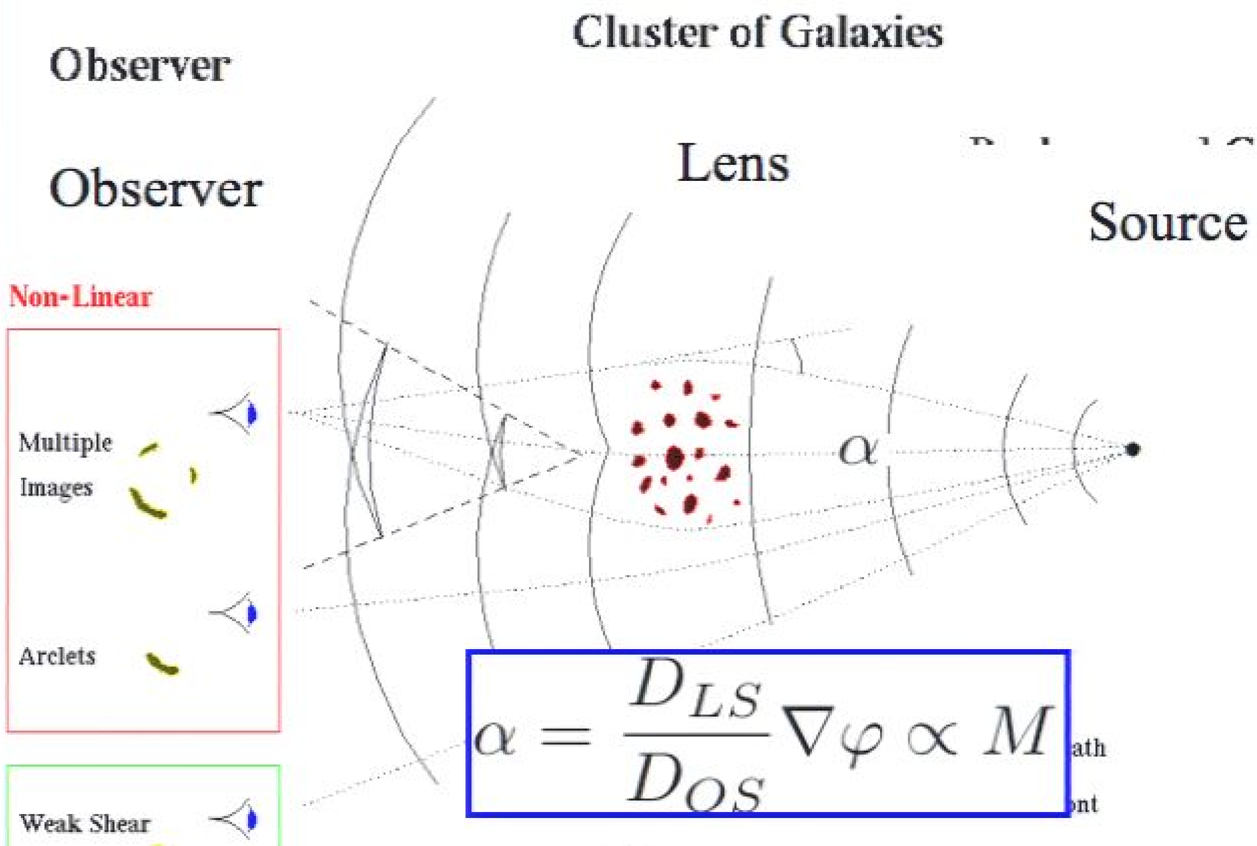

$$\alpha = \frac{D_{LS}}{D_{OS}} \nabla\varphi \propto M$$

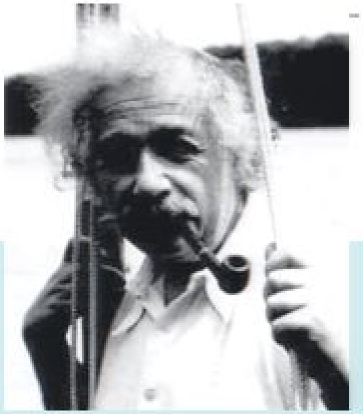

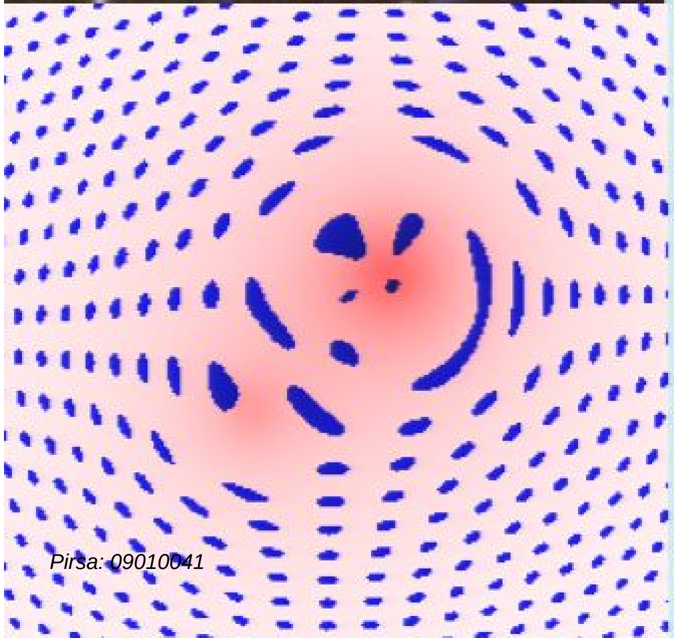

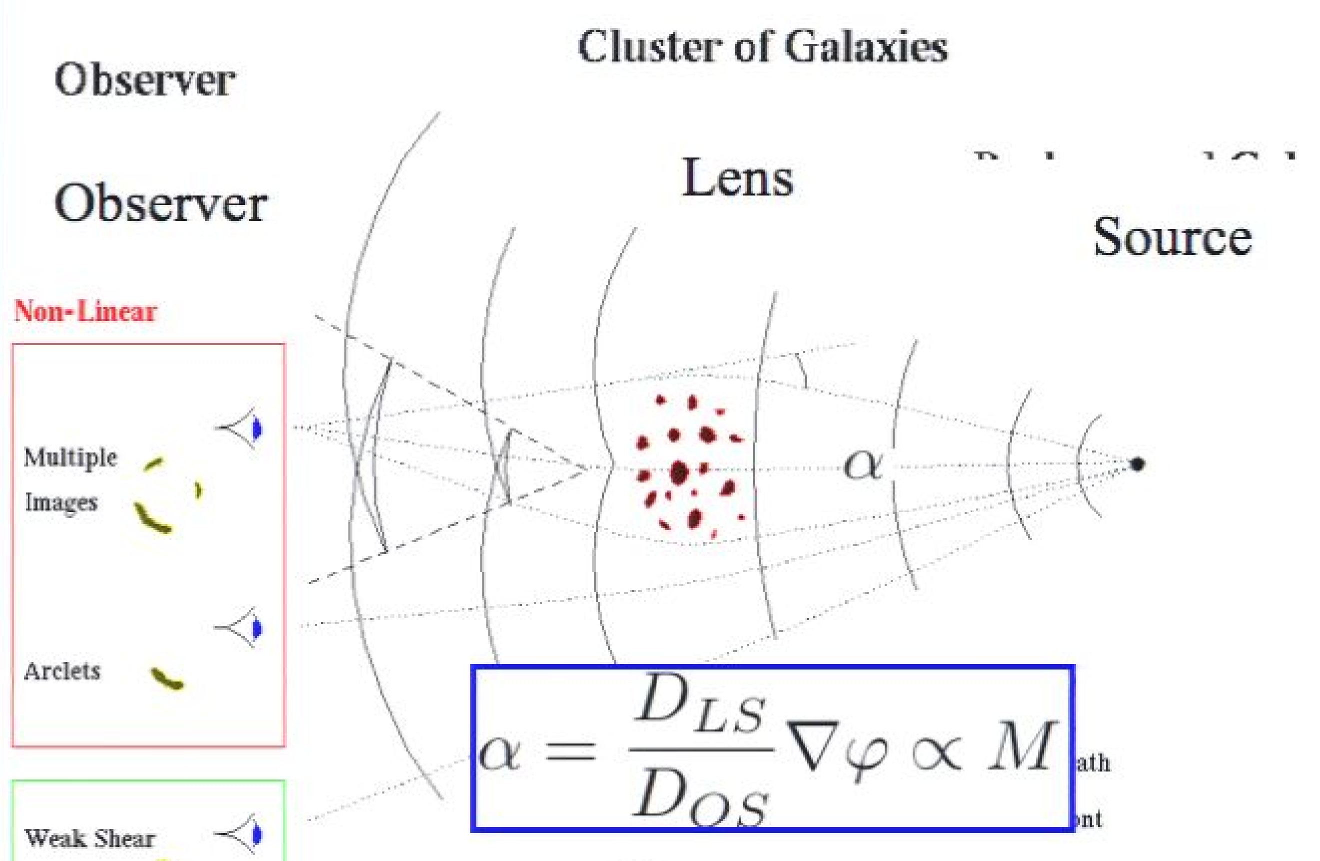

$$\alpha = \frac{D_{LS}}{D_{OS}} \nabla \varphi \propto M$$

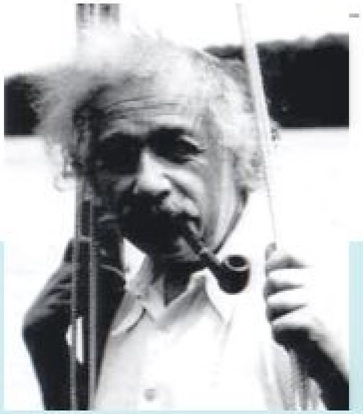

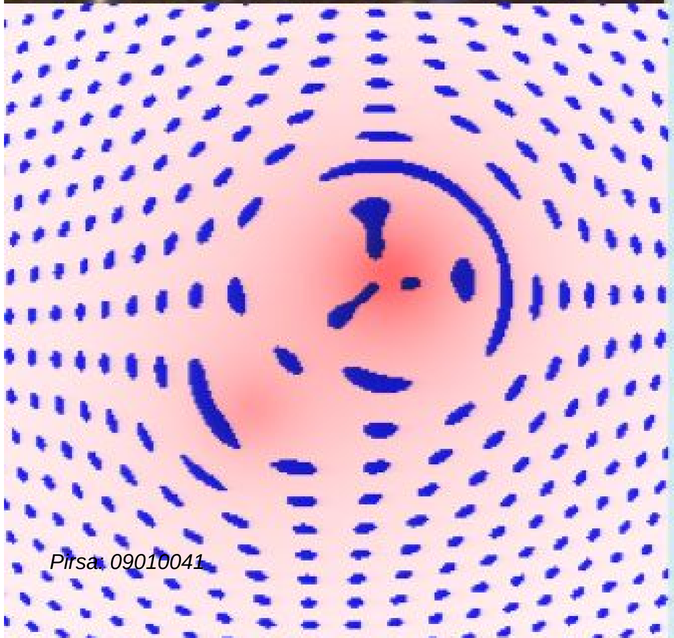

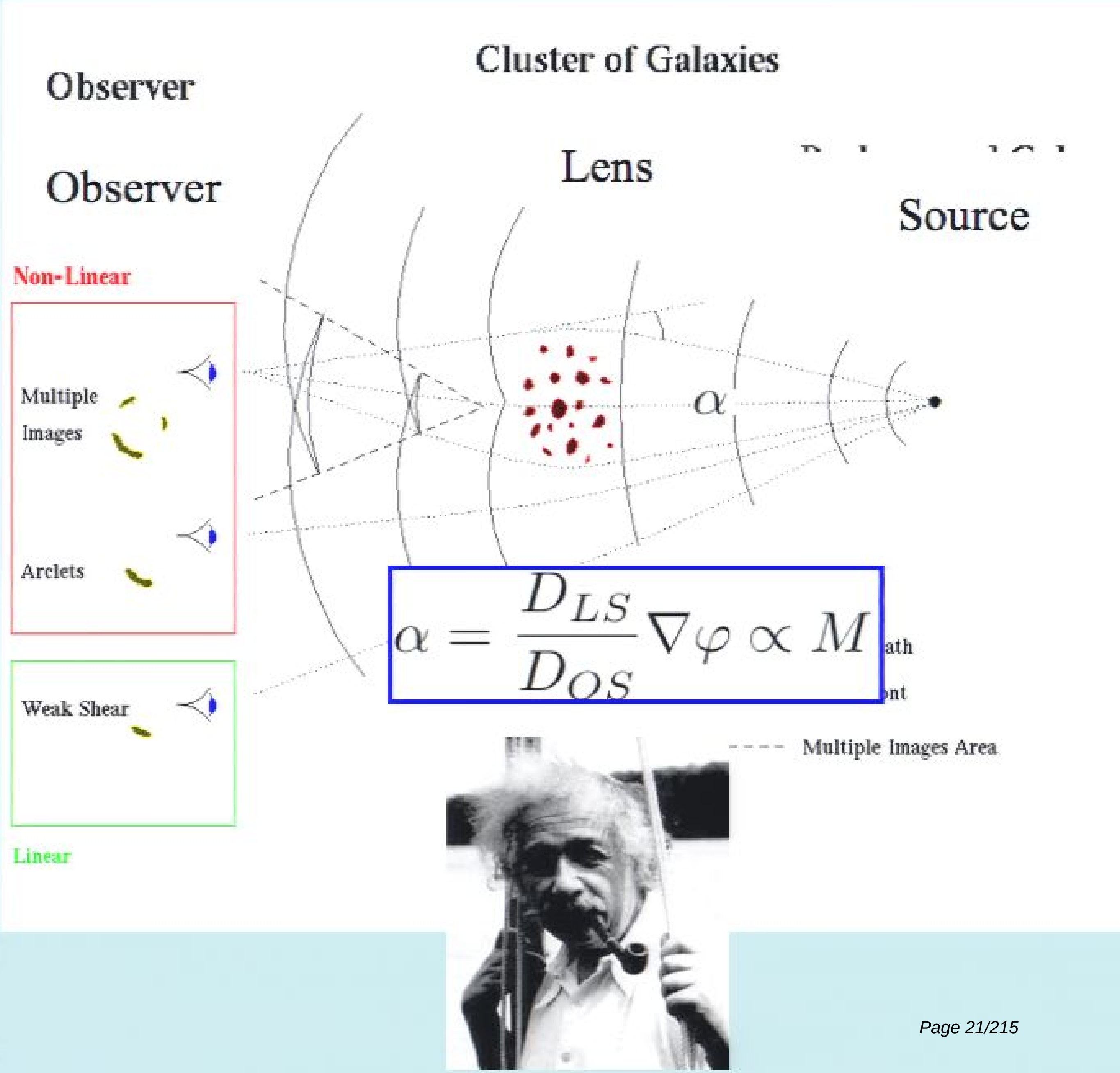

$$\alpha = \frac{D_{LS}}{D_{OS}} \nabla \varphi \propto M$$

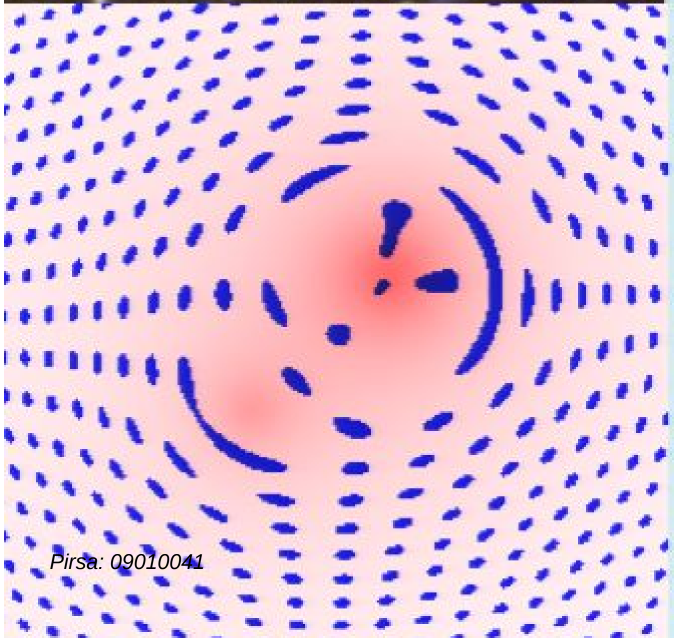

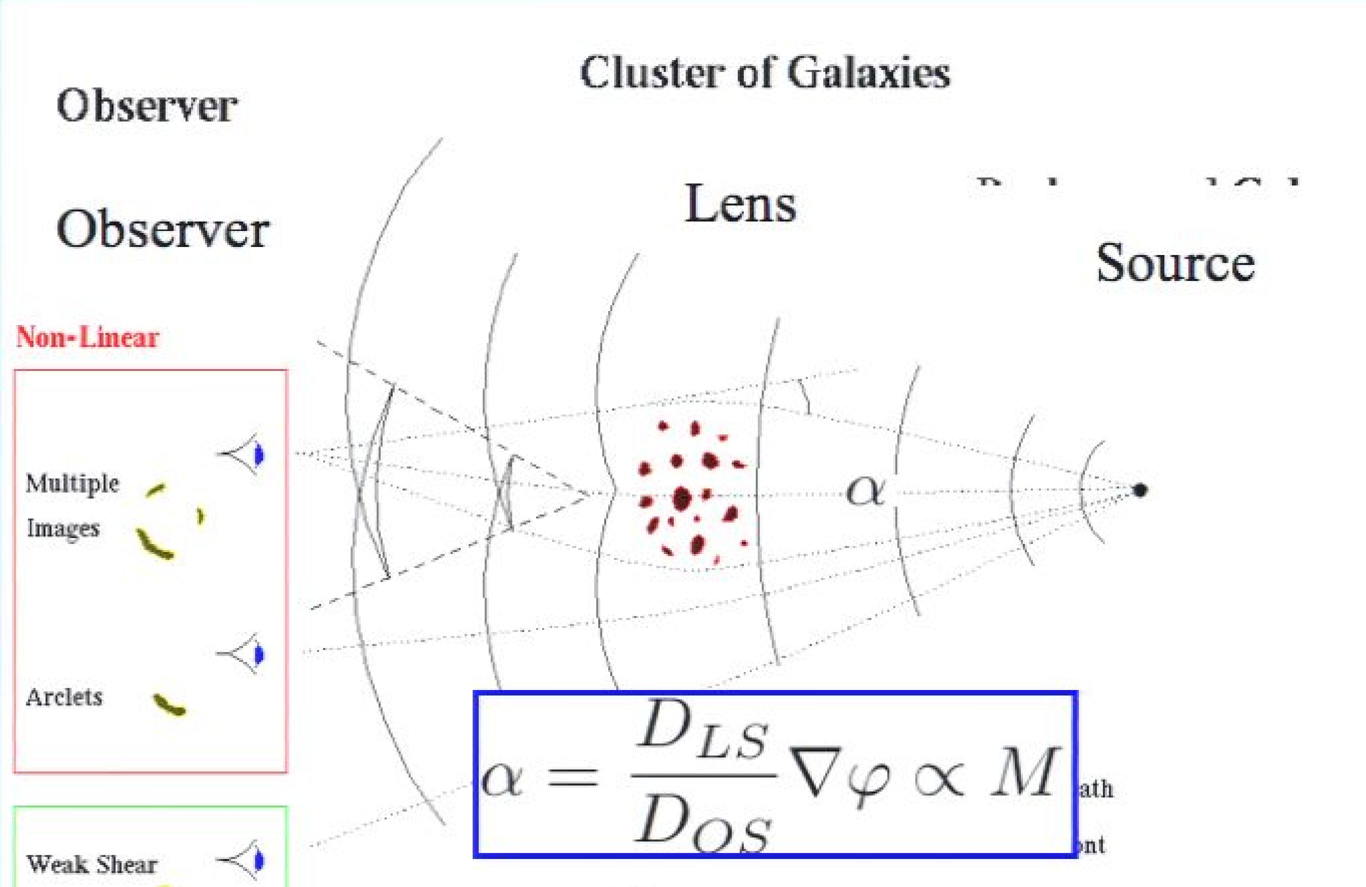

$$\alpha = \frac{D_{LS}}{D_{OS}} \nabla \varphi \propto M$$

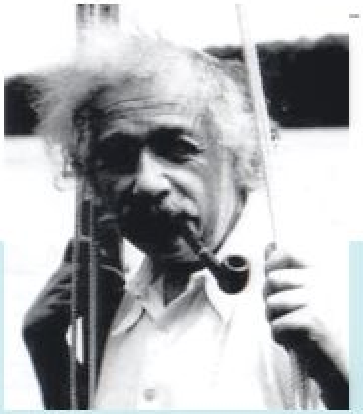

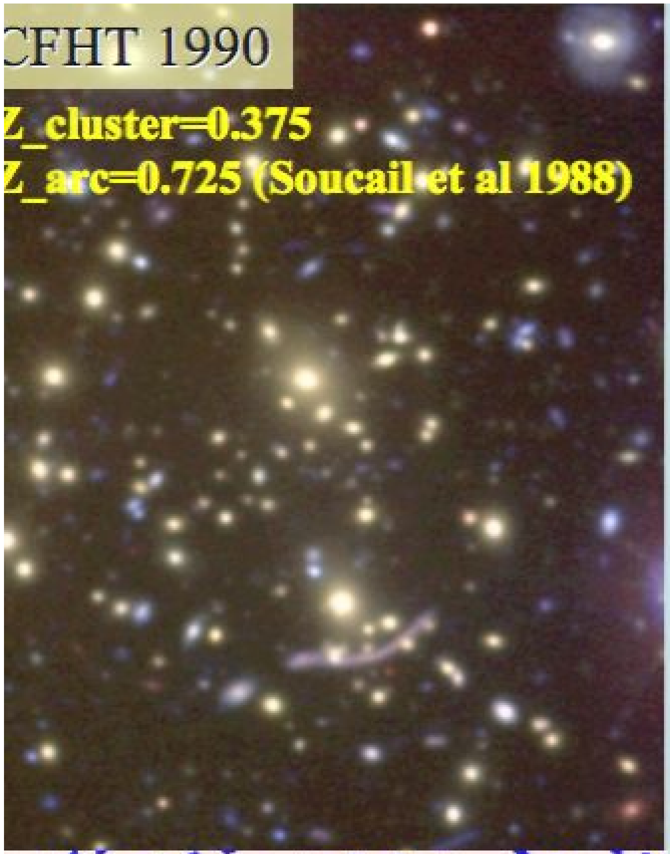

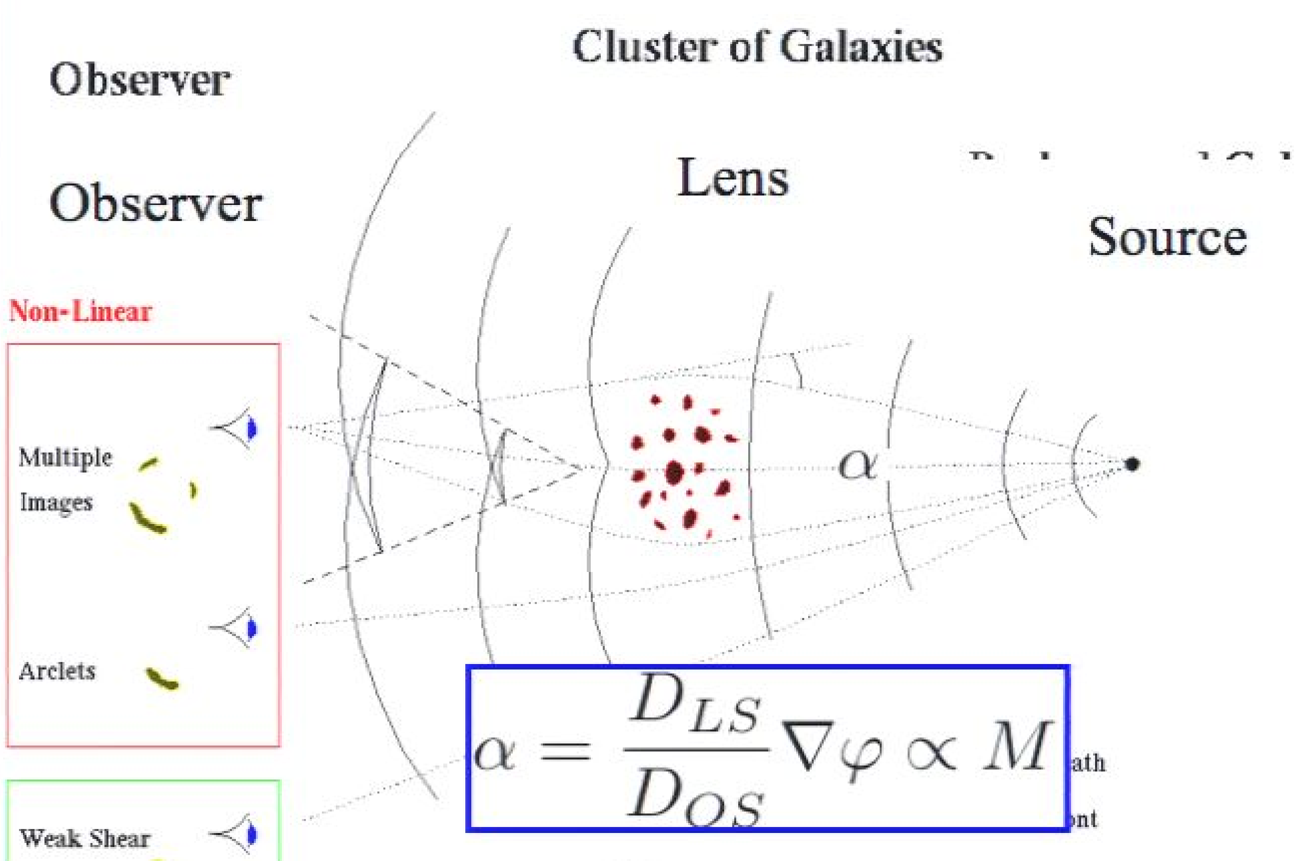

$$\alpha = \frac{D_{LS}}{D_{OS}} \nabla \varphi \propto M$$

- - - - Multiple Images Area

Linear

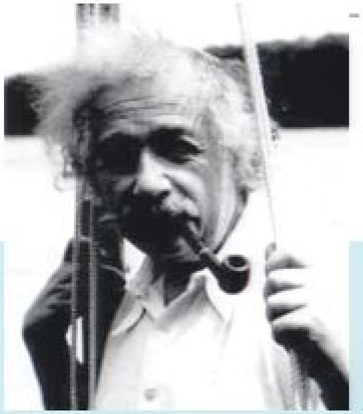

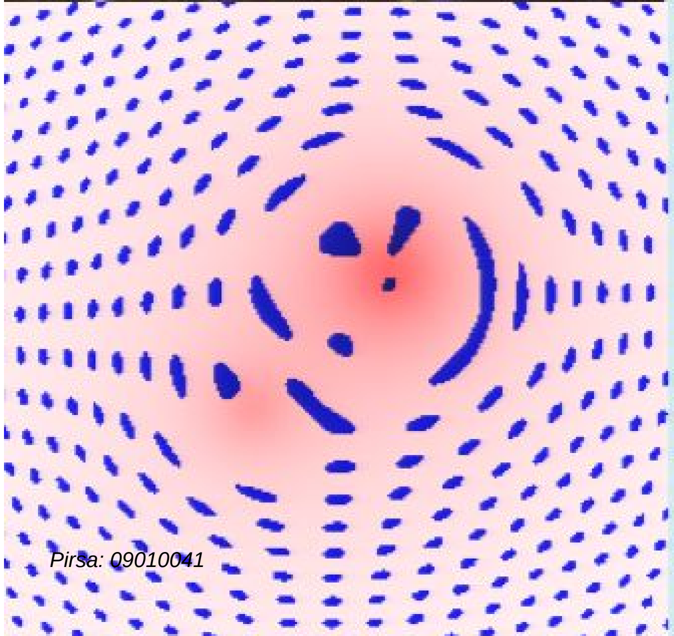


CFHT 1990

Z_cluster=0.375

Z_arc=0.725 (Soucail et al 1988)

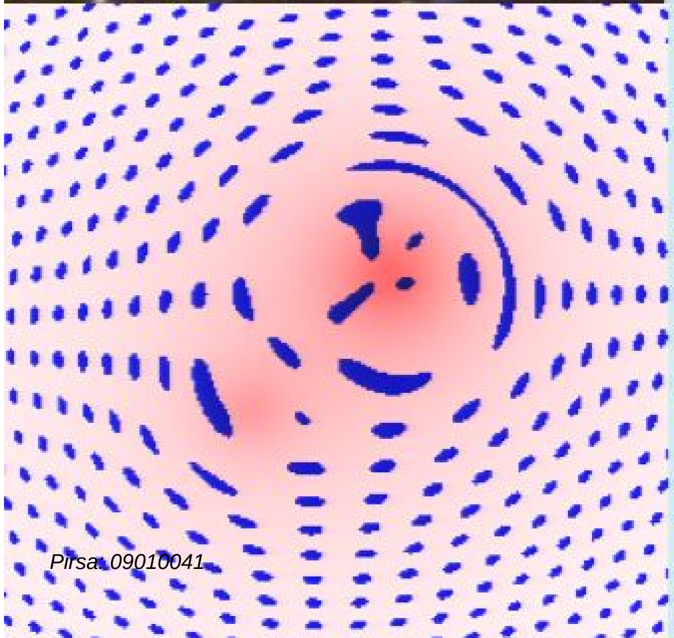

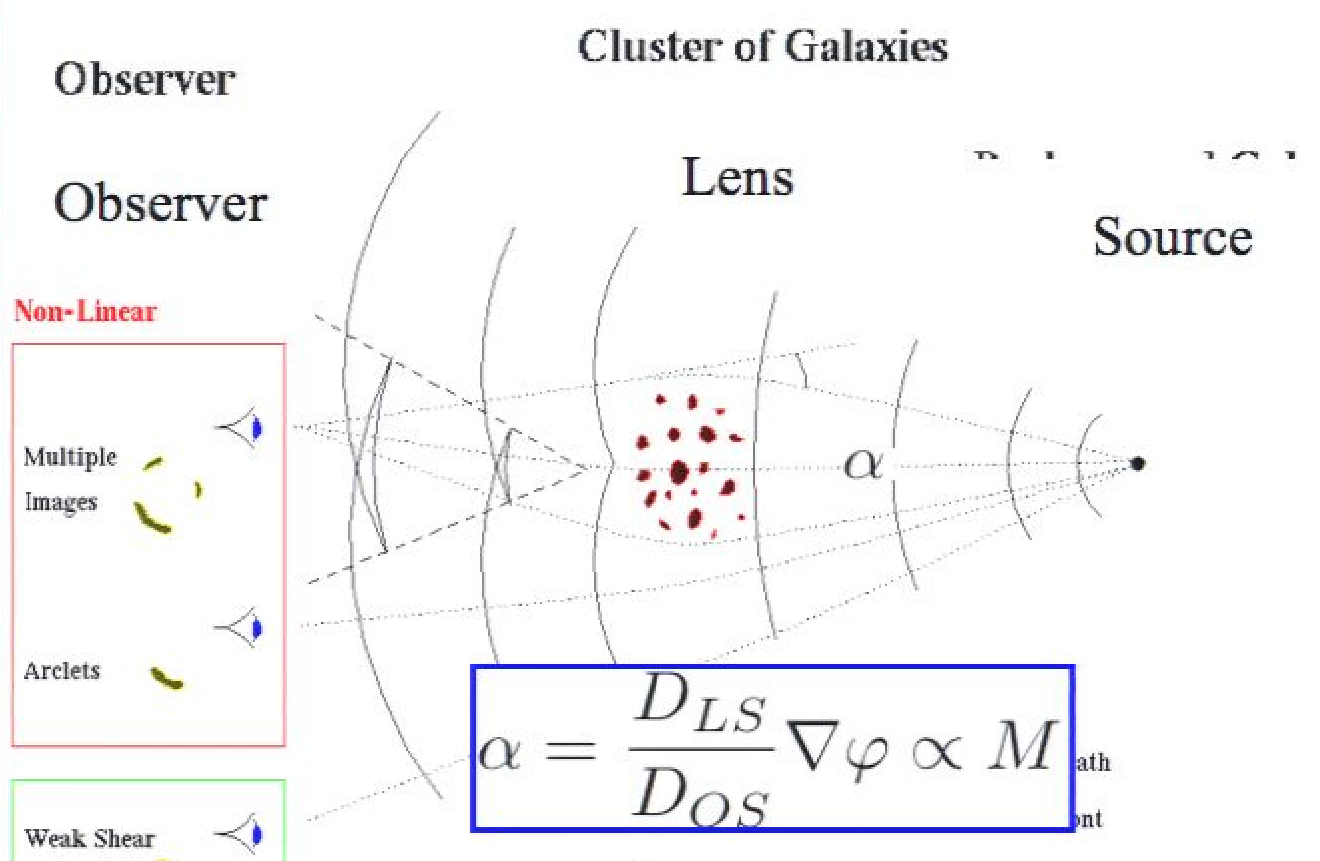

$$\alpha = \frac{D_{LS}}{D_{OS}} \nabla\varphi \propto M$$

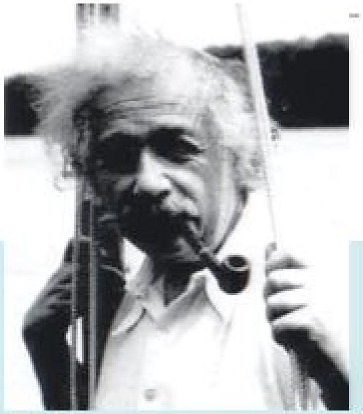

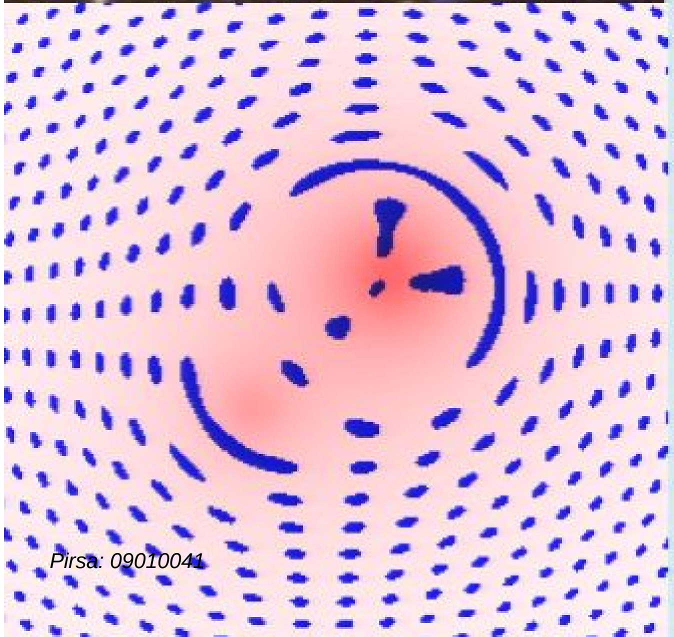

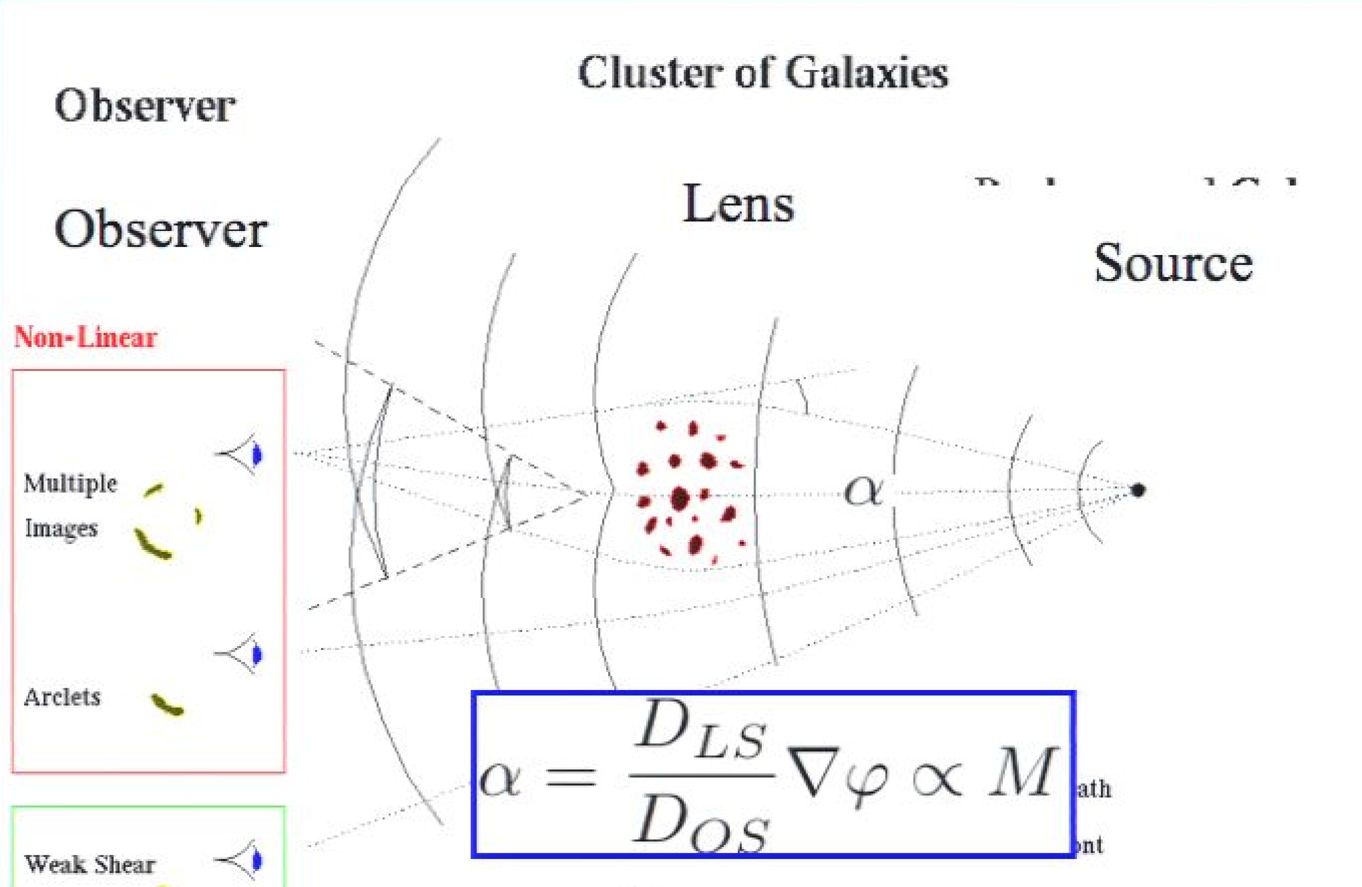

$$\alpha = \frac{D_{LS}}{D_{OS}} \nabla \varphi \propto M$$

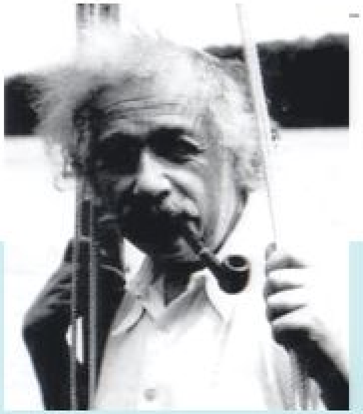


CFHT 1990

Z_cluster=0.375

Z_arc=0.725 (Soucail et al 1988)

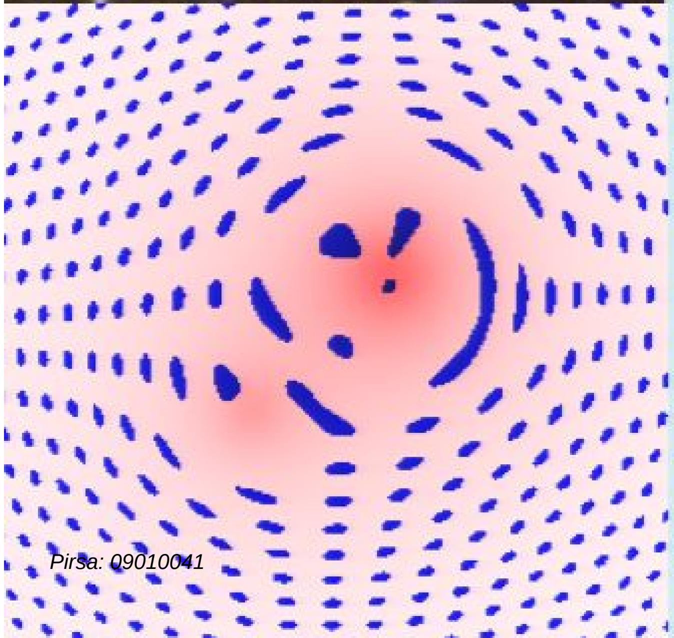

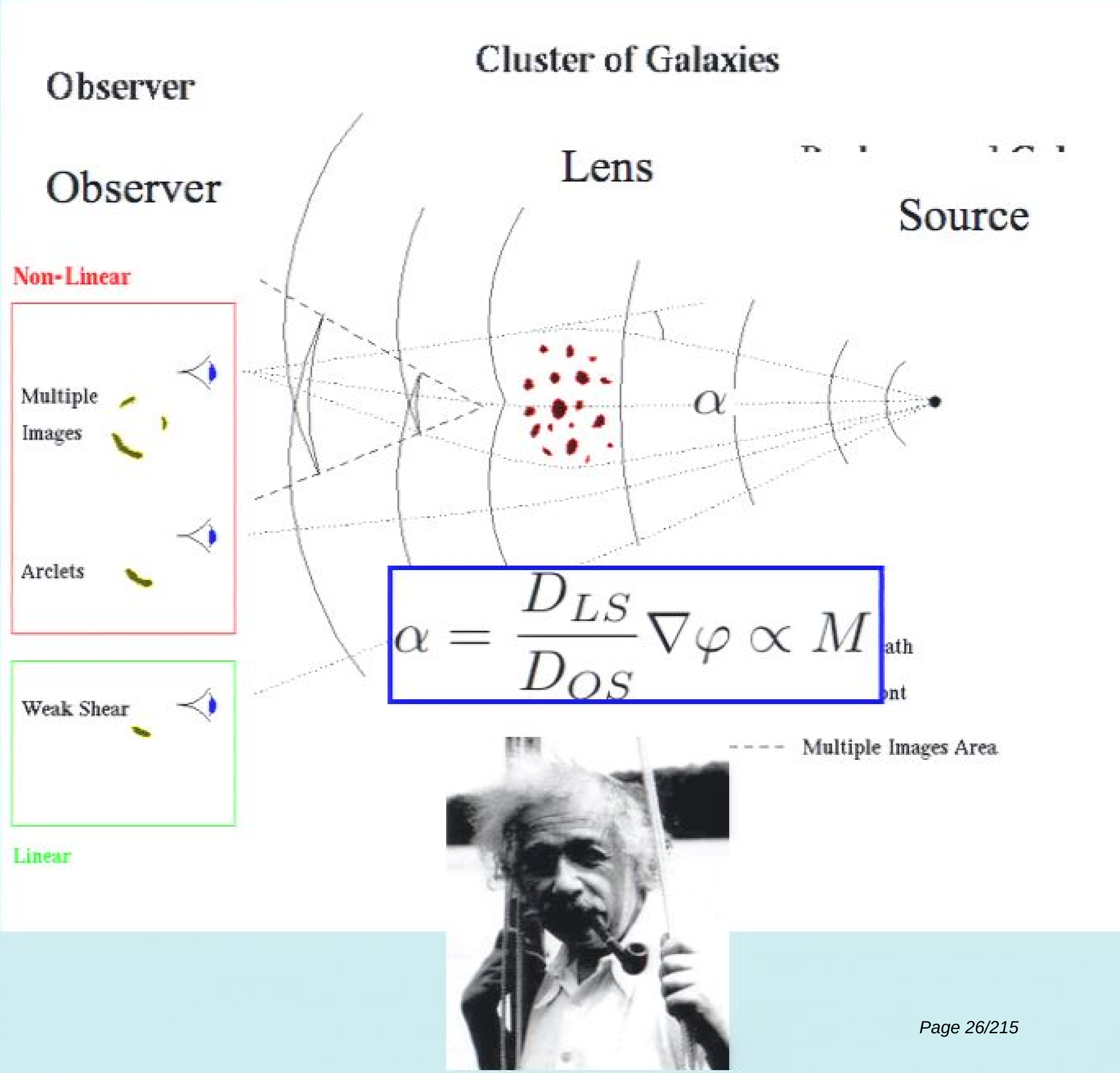

$$\boxed{\alpha = \frac{D_{LS}}{D_{OS}} \nabla \varphi \propto M}$$

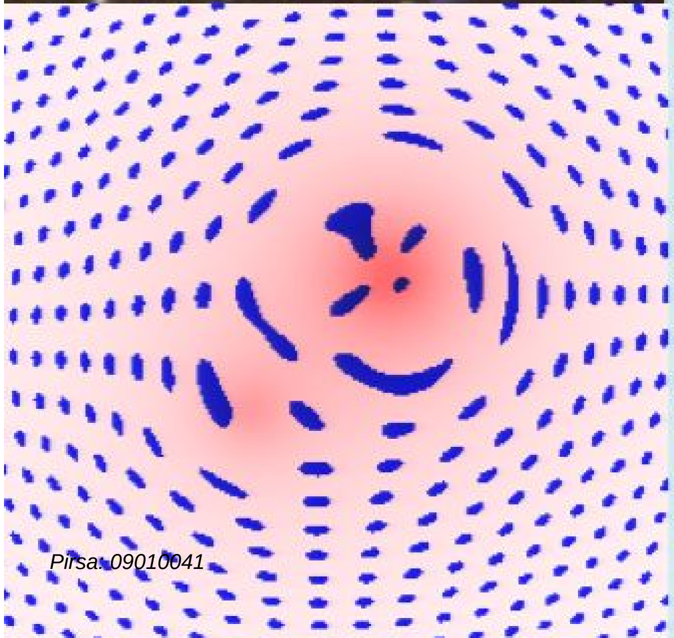

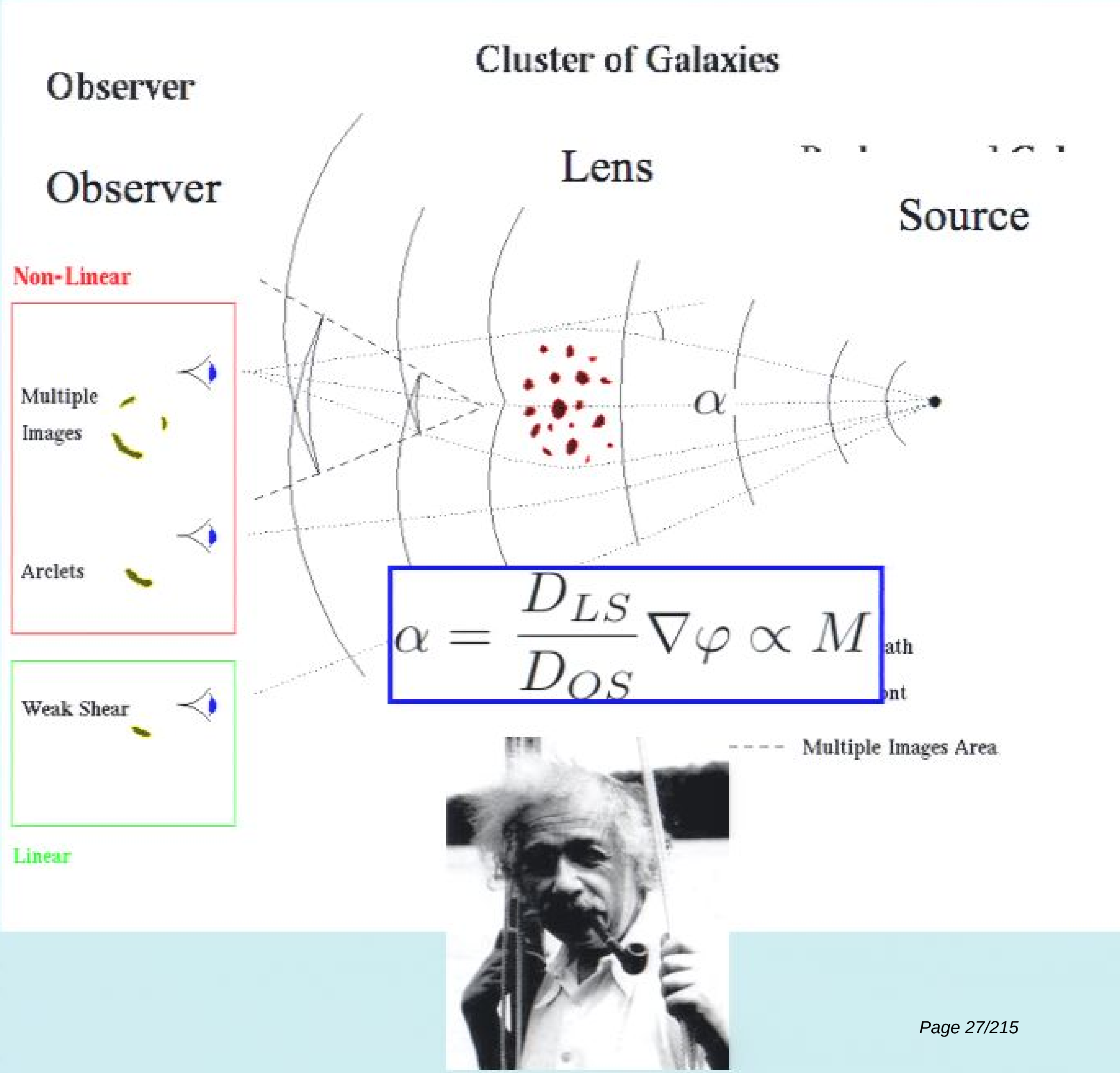

$$\alpha = \frac{D_{LS}}{D_{OS}} \nabla \varphi \propto M$$


CFHT 1990

Z_cluster=0.375

Z_arc=0.725 (Soucail et al 1988)

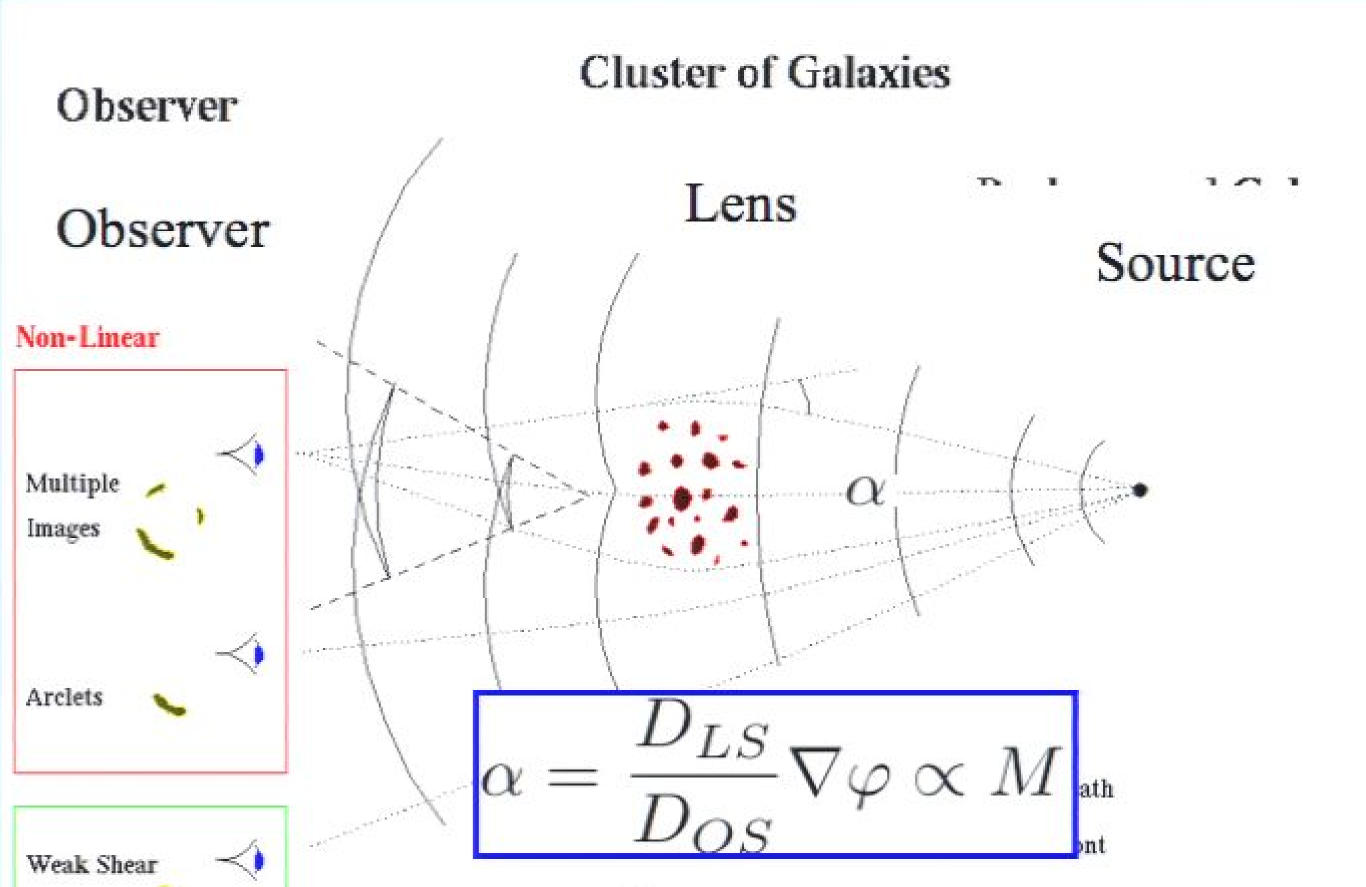

$$\alpha = \frac{D_{LS}}{D_{OS}} \nabla \varphi \propto M$$

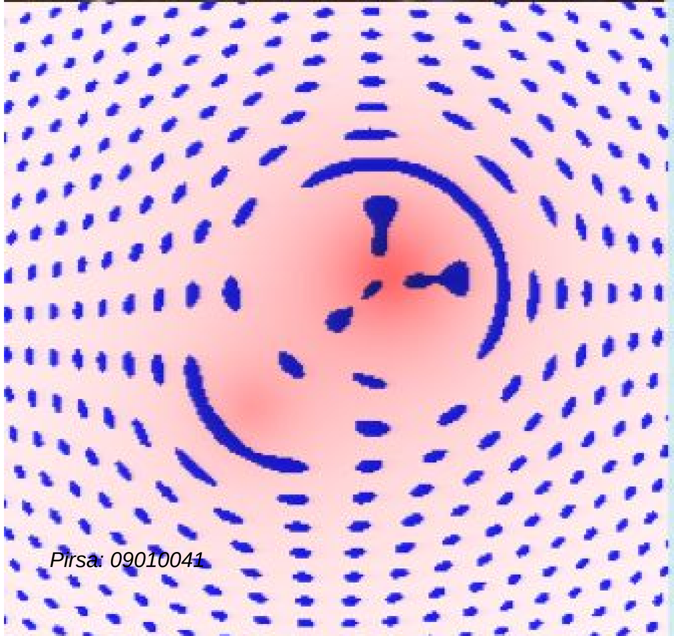

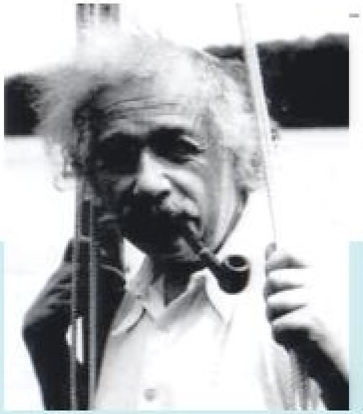

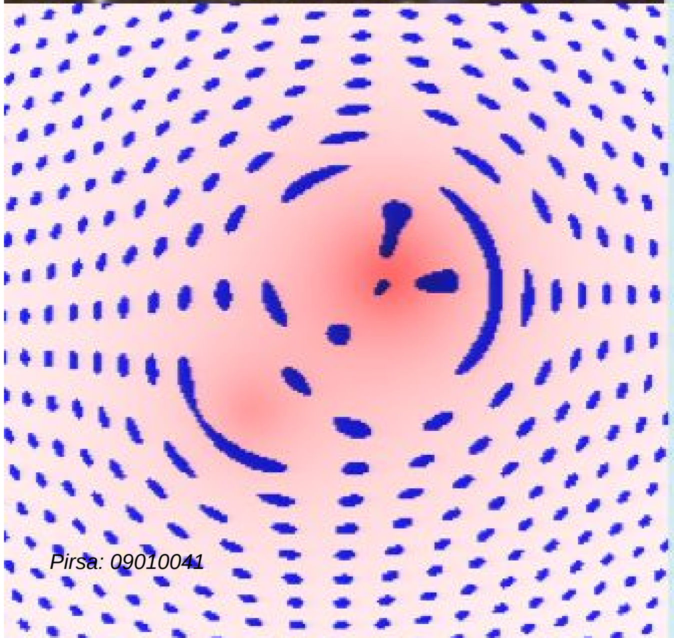

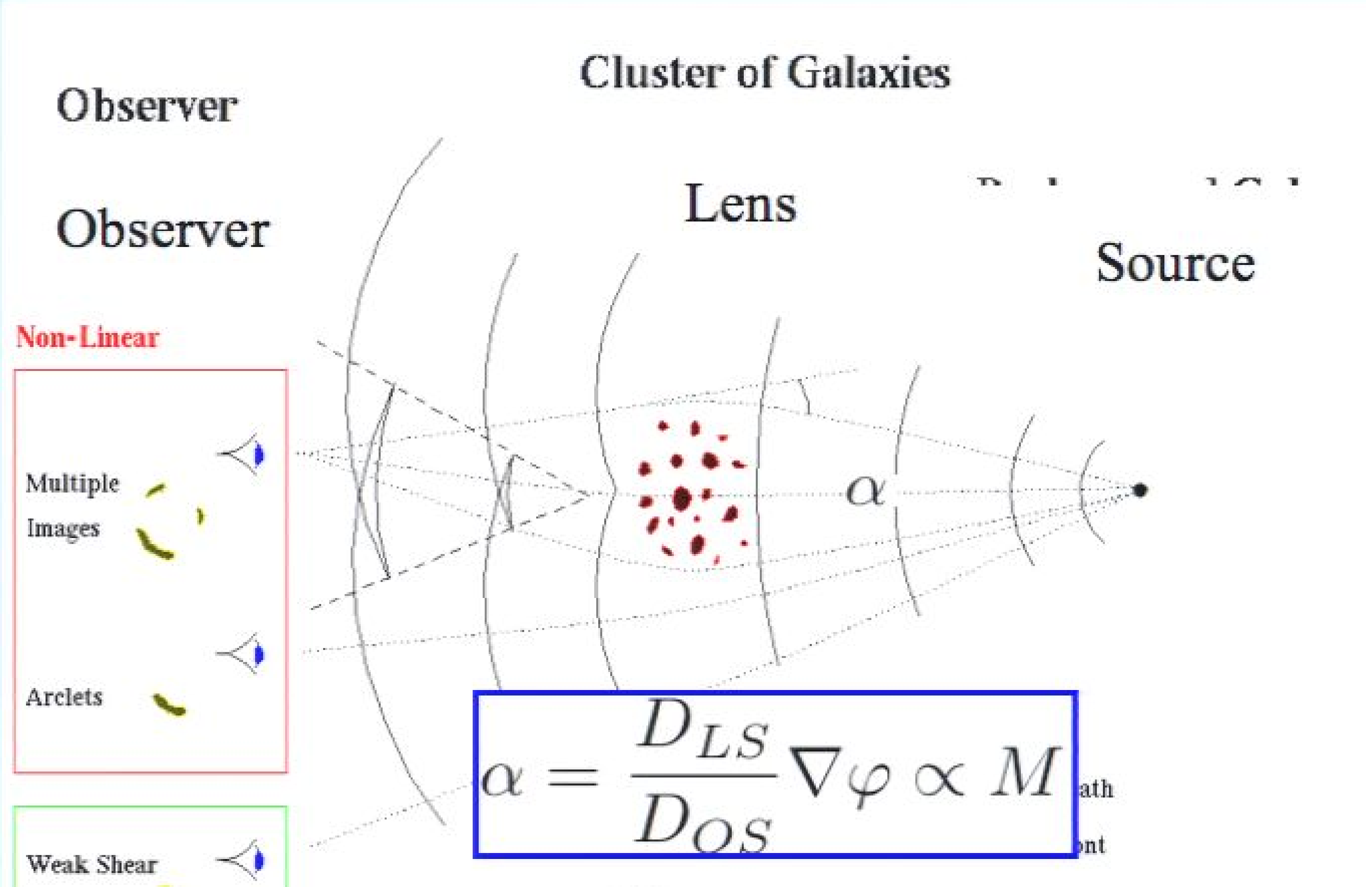

$$\alpha = \frac{D_{LS}}{D_{OS}} \nabla \varphi \propto M$$

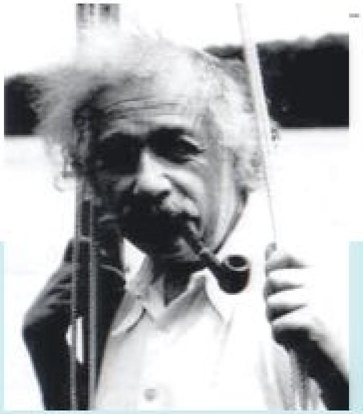

CFHT 1990

Z_cluster=0.375

Z_arc=0.725 (Soucail et al 1988)

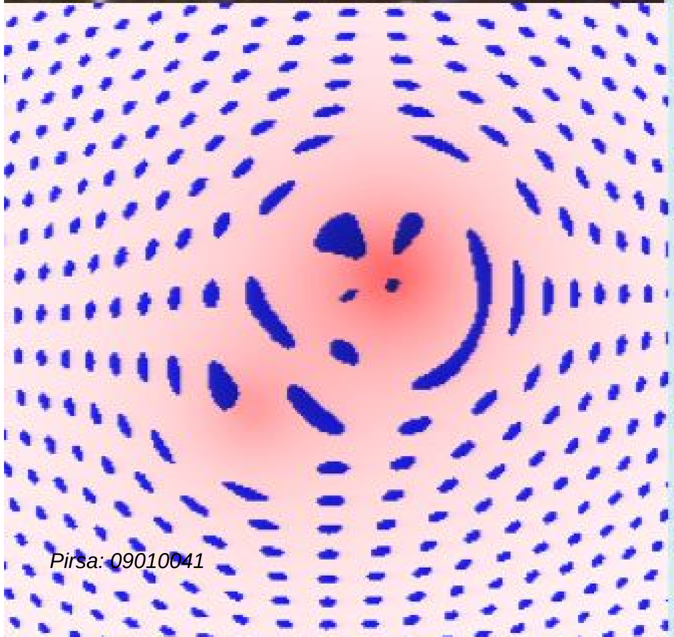

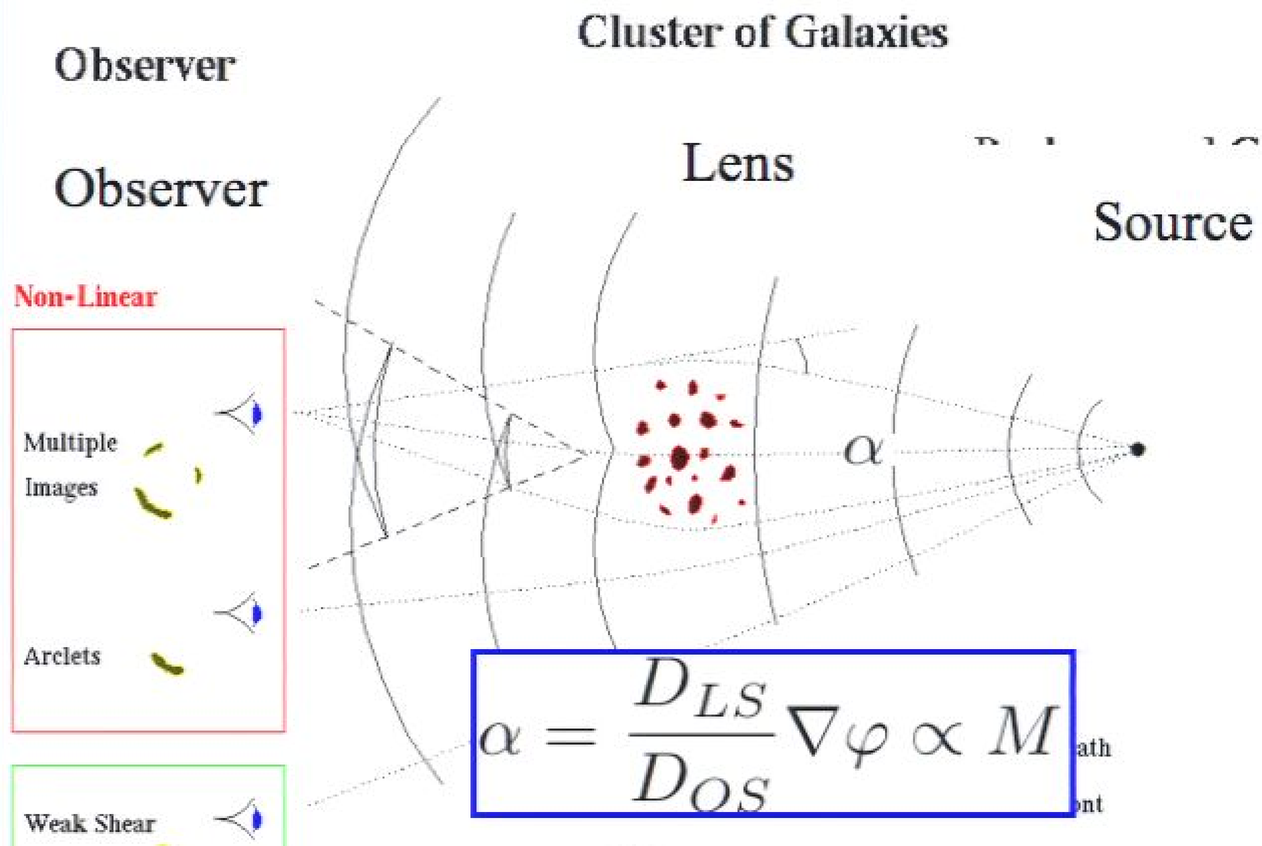

$$\boxed{\alpha = \frac{D_{LS}}{D_{OS}} \nabla \varphi \propto M}$$

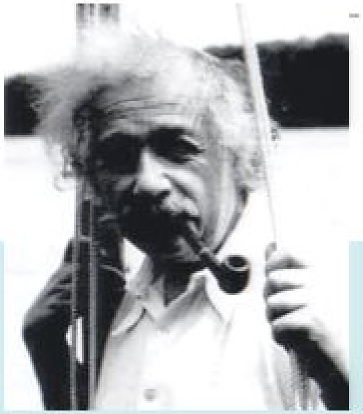

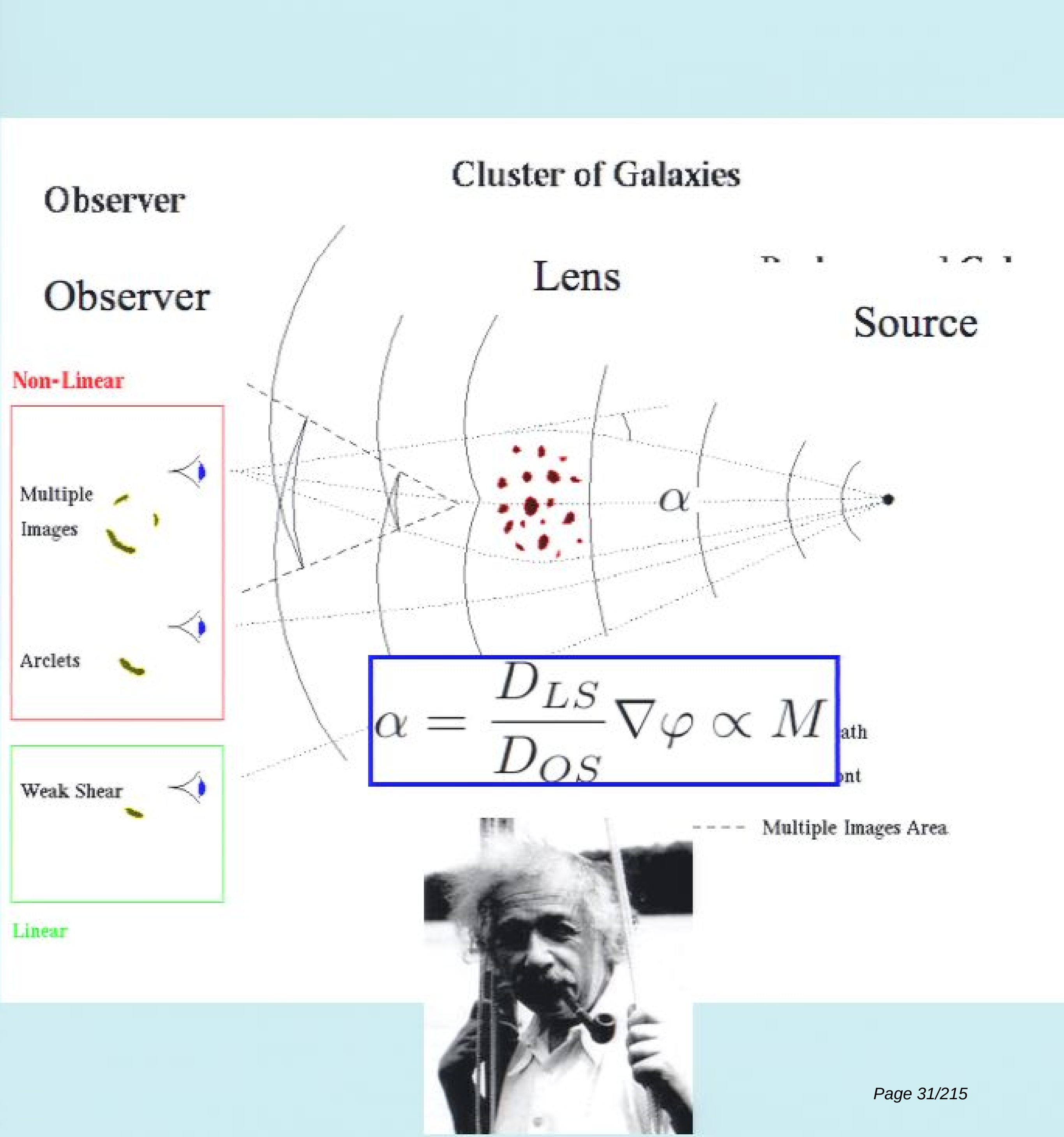

$$\alpha = \frac{D_{LS}}{D_{OS}} \nabla \varphi \propto M$$

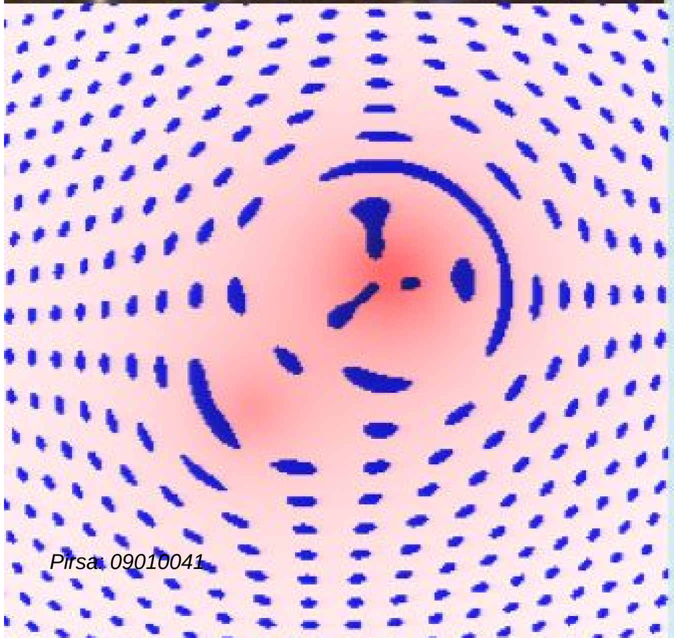

CFHT 1990

Z_cluster=0.375

Z_arc=0.725 (Soucail et al 1988)

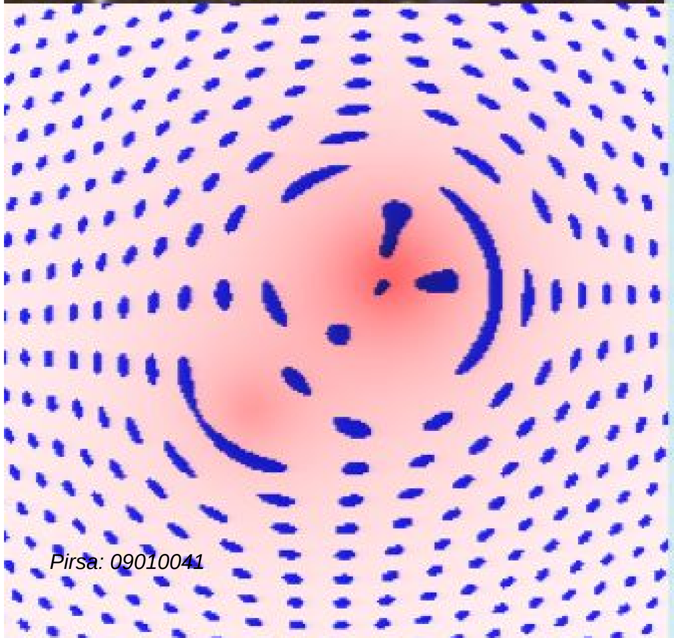

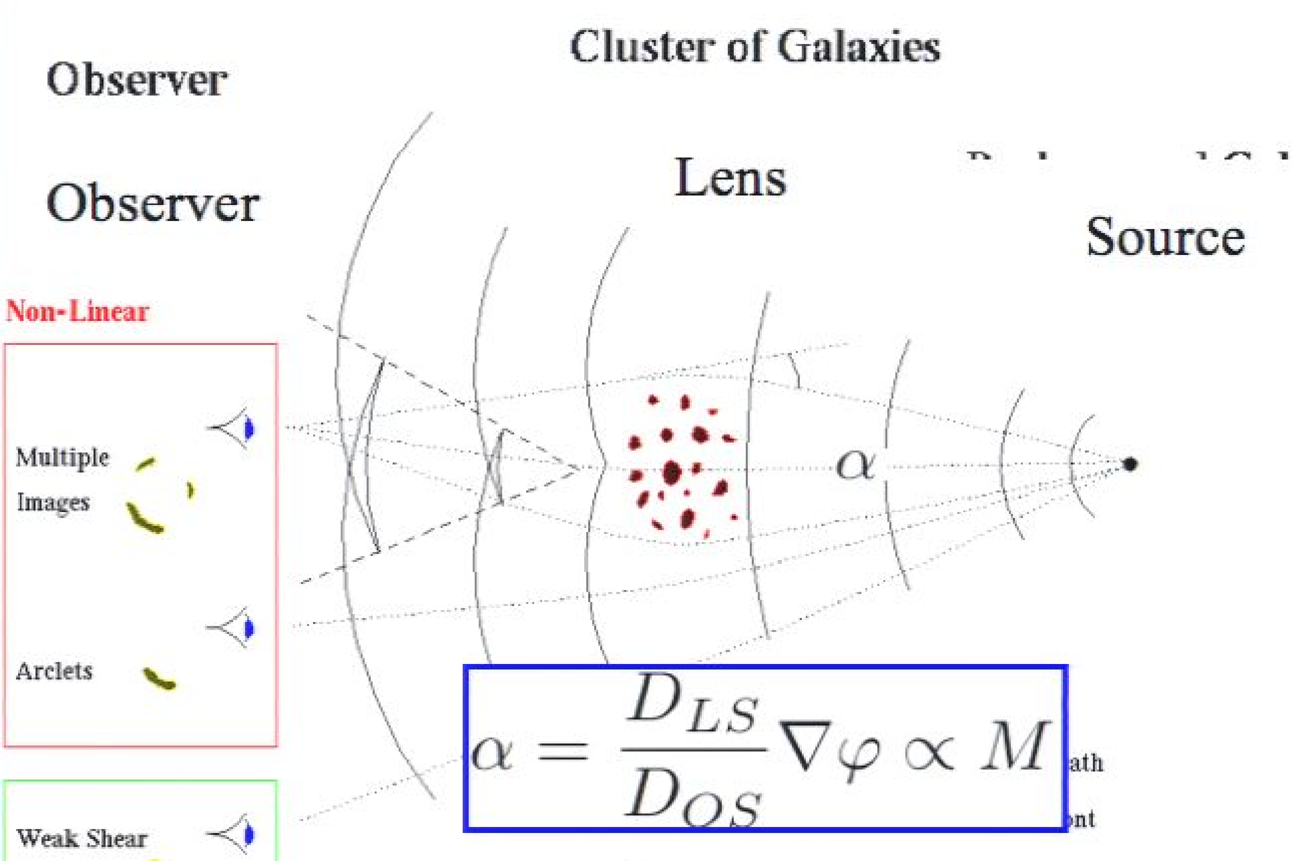

$$\alpha = \frac{D_{LS}}{D_{OS}} \nabla \varphi \propto M$$

- - - - Multiple Images Area

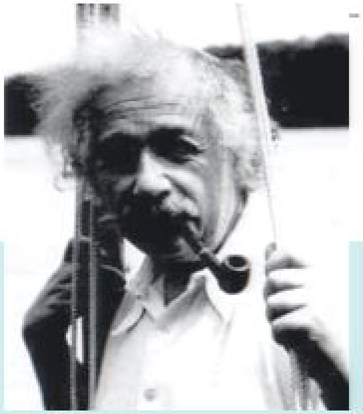

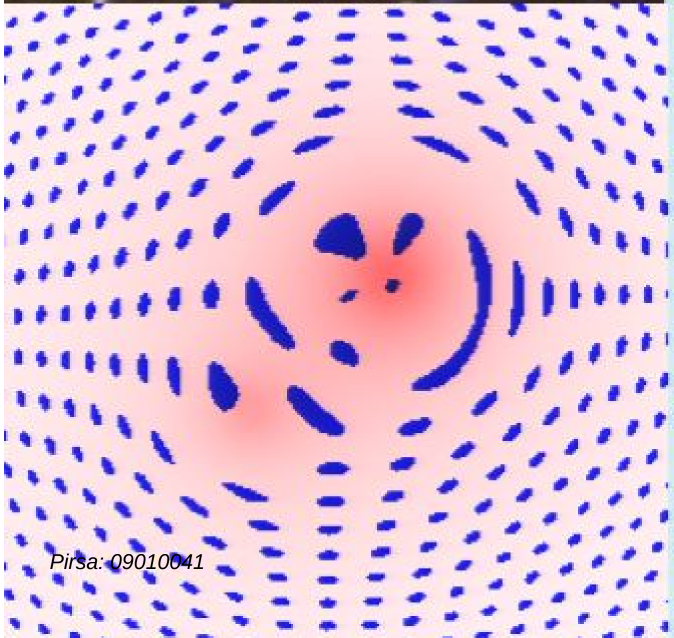

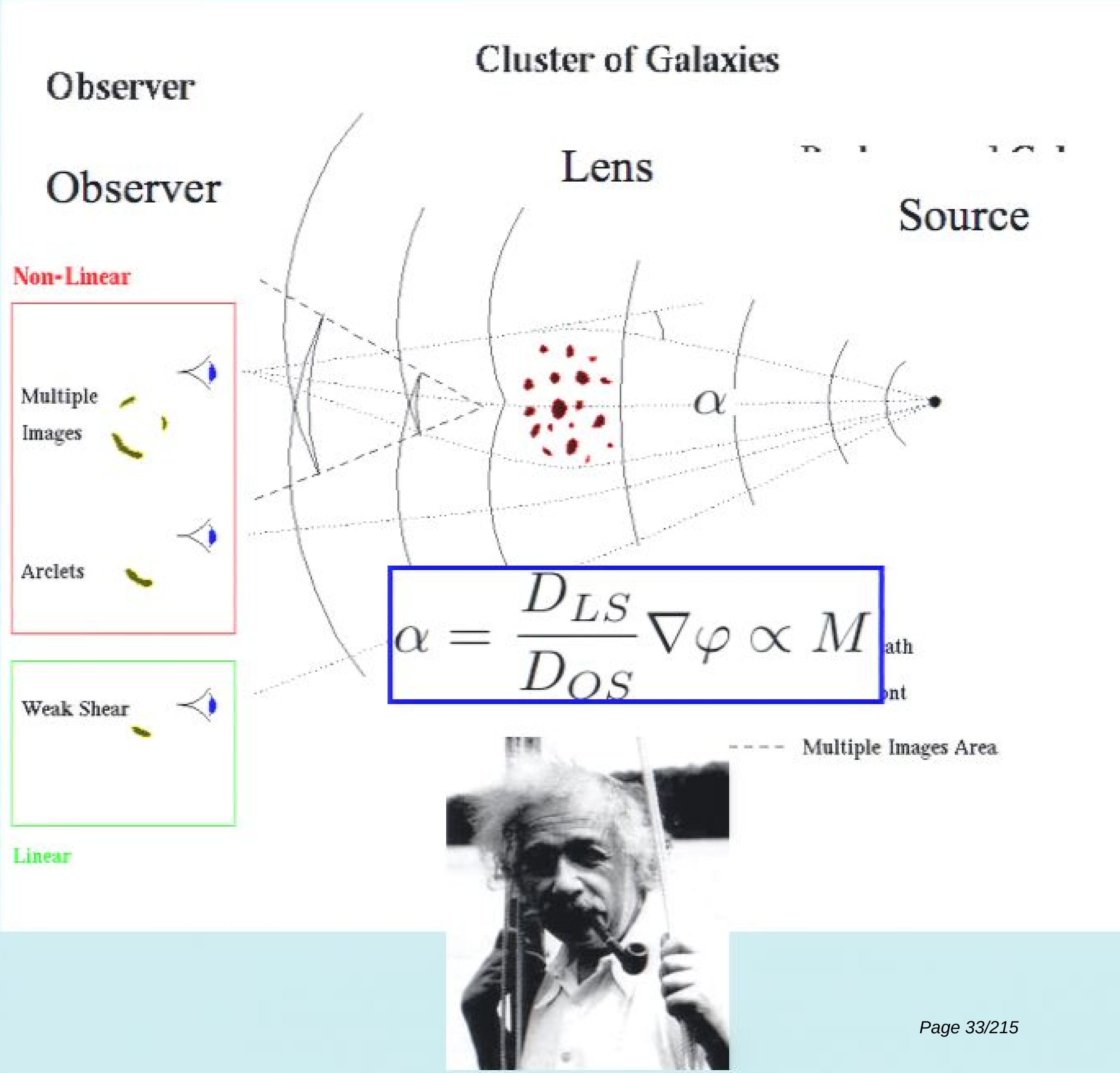

$$\alpha = \frac{D_{LS}}{D_{OS}} \nabla\varphi \propto M$$

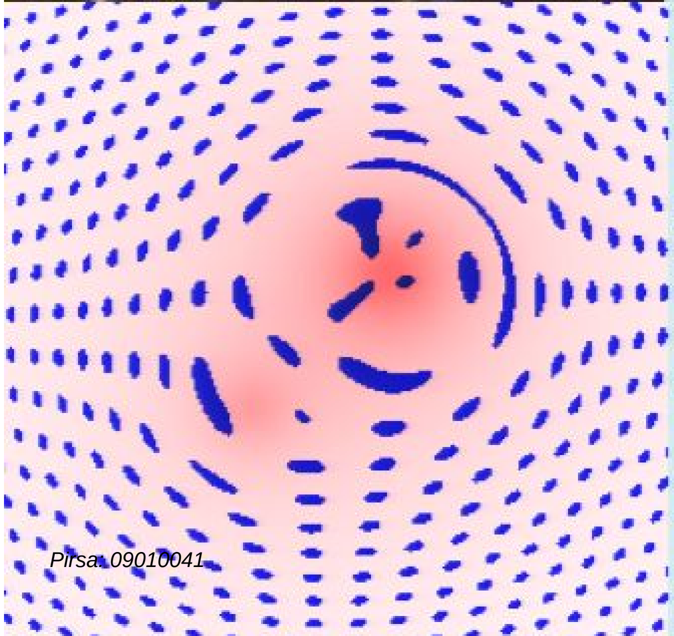

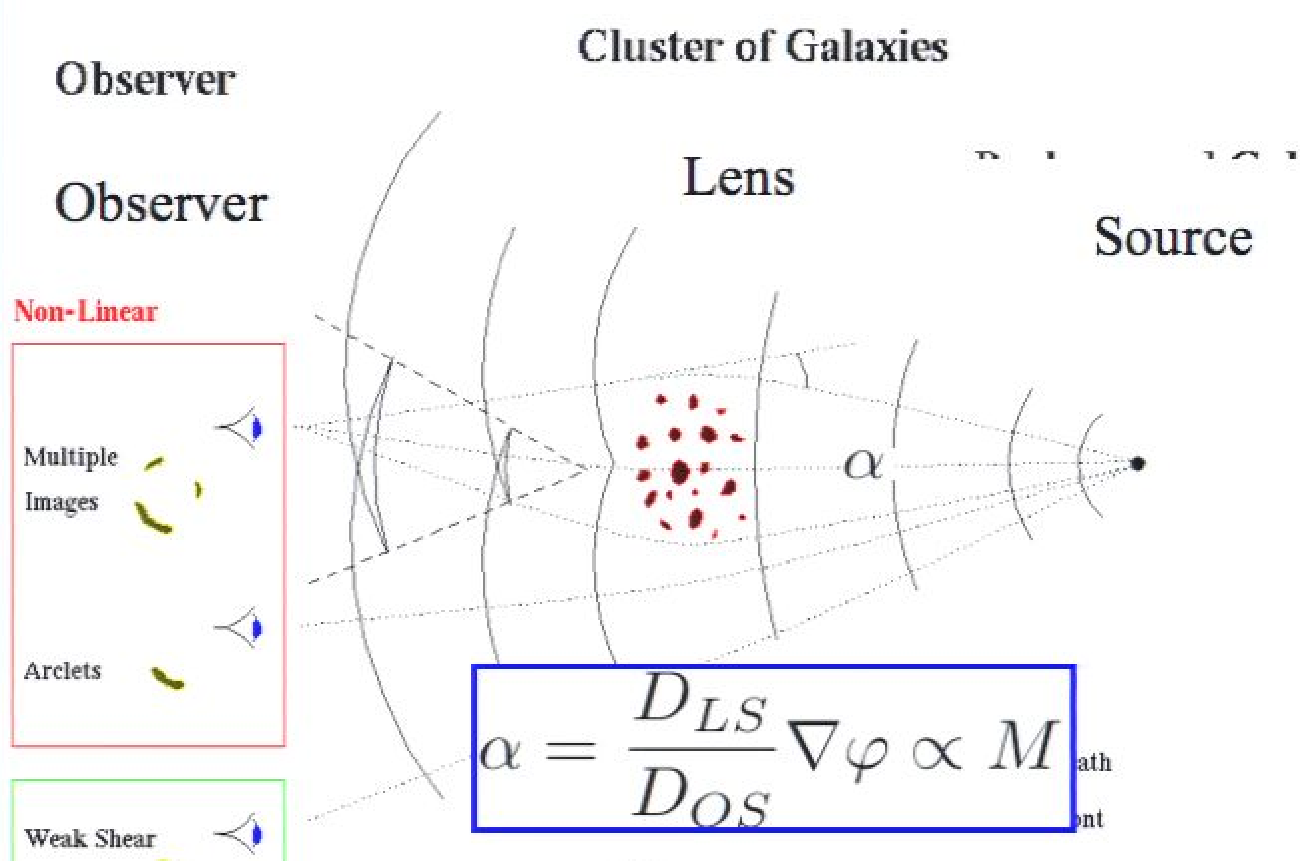

$$\boxed{\alpha = \frac{D_{LS}}{D_{OS}} \nabla \varphi \propto M}$$

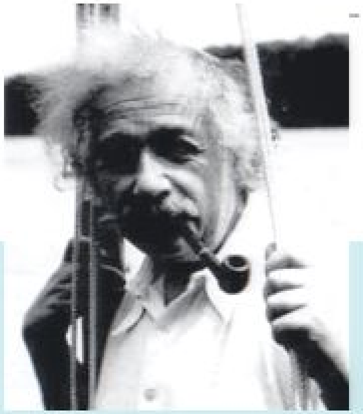

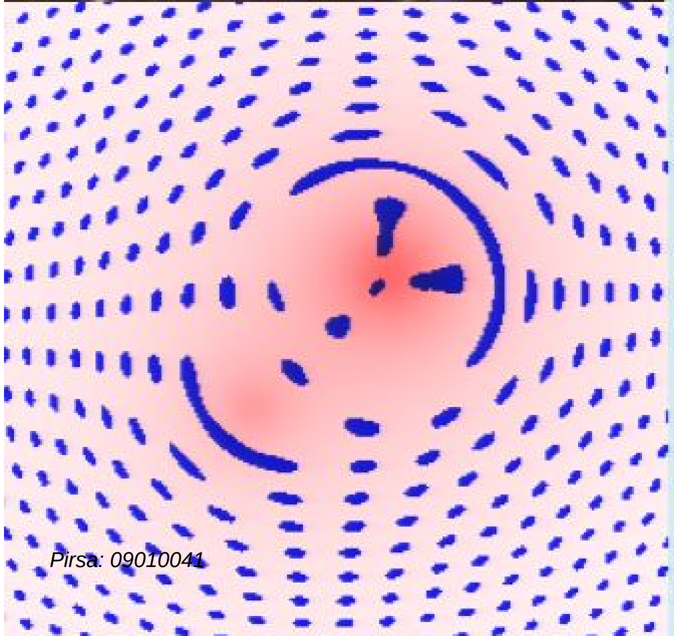

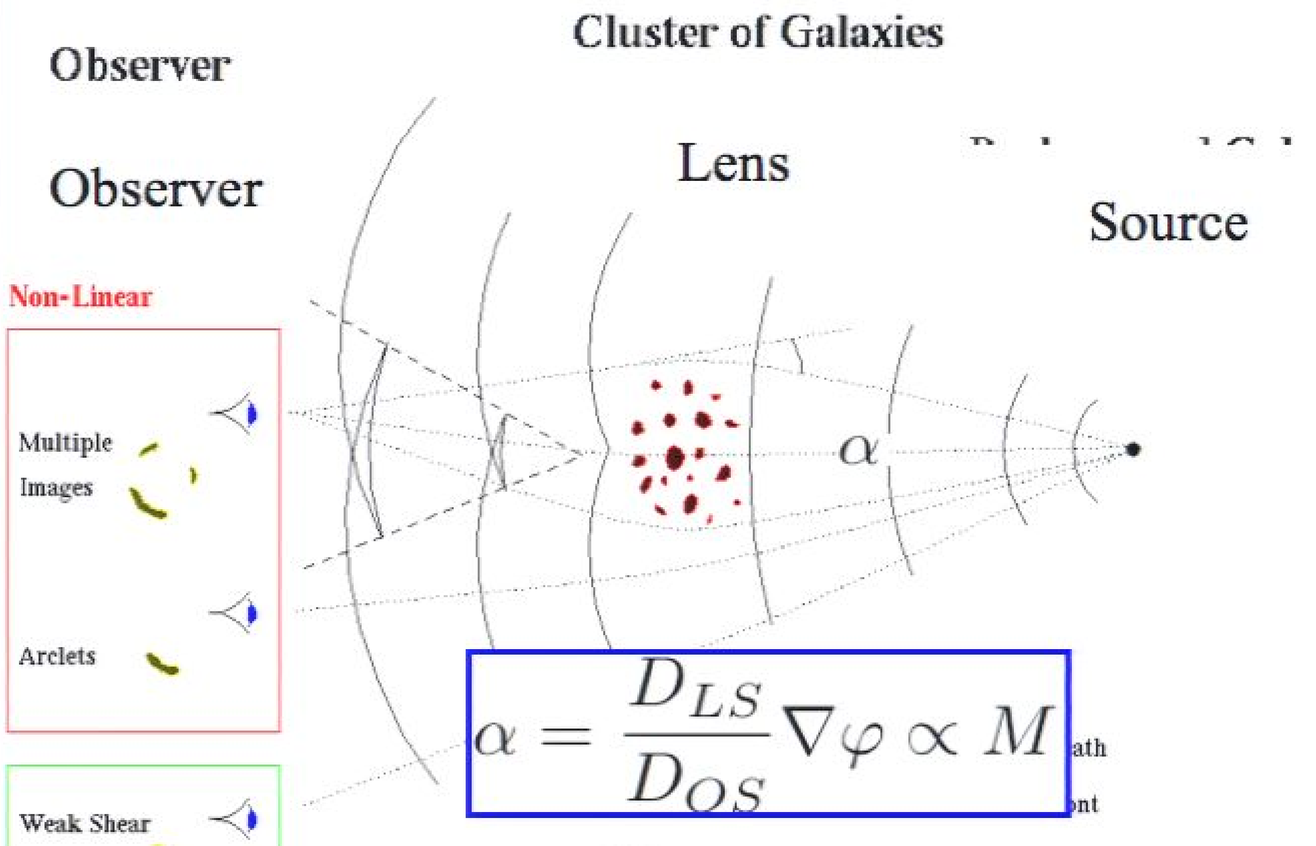

$$\alpha = \frac{D_{LS}}{D_{OS}} \nabla \varphi \propto M$$

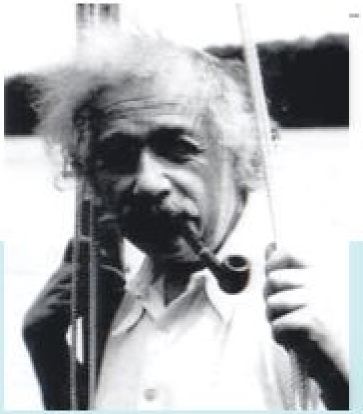

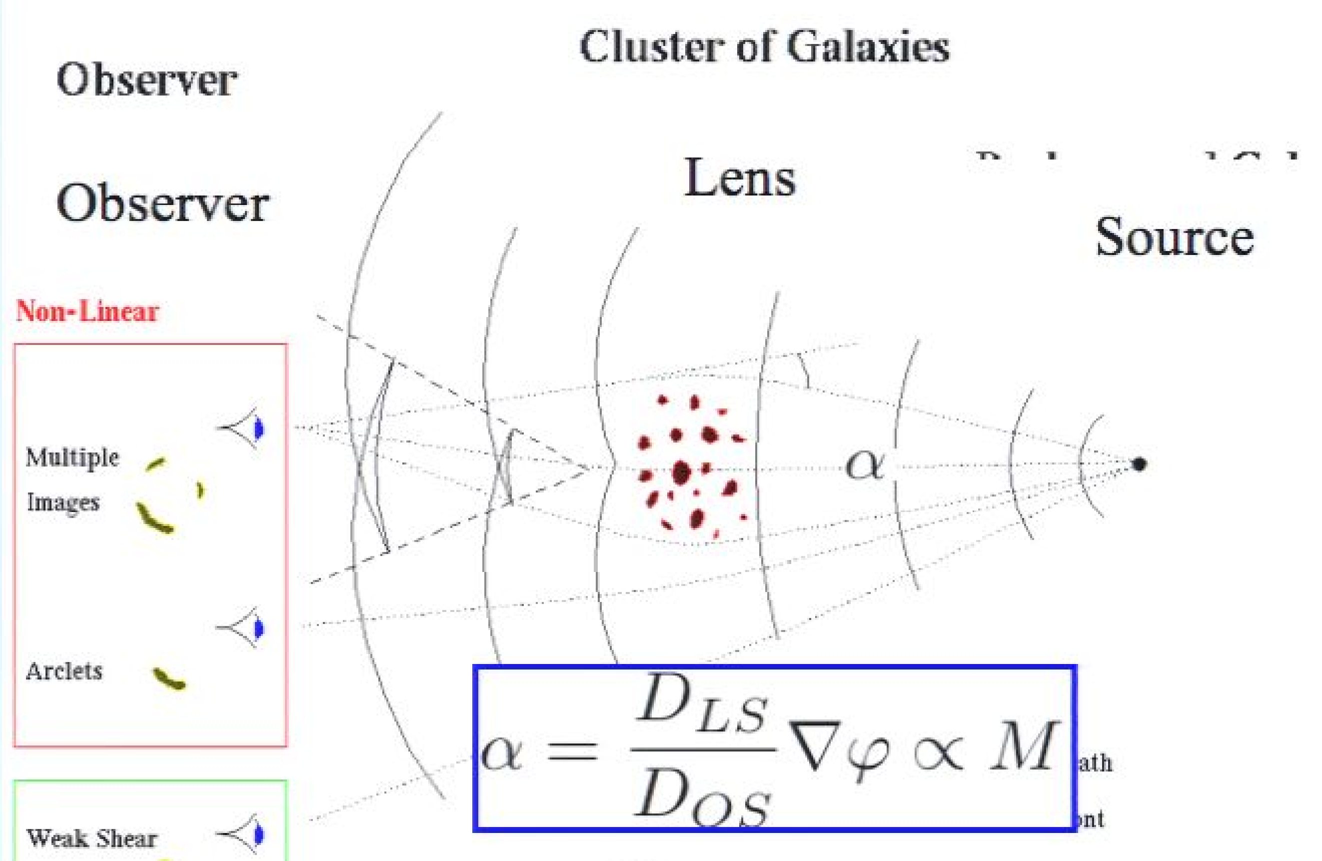

$$\alpha = \frac{D_{LS}}{D_{OS}} \nabla \varphi \propto M$$

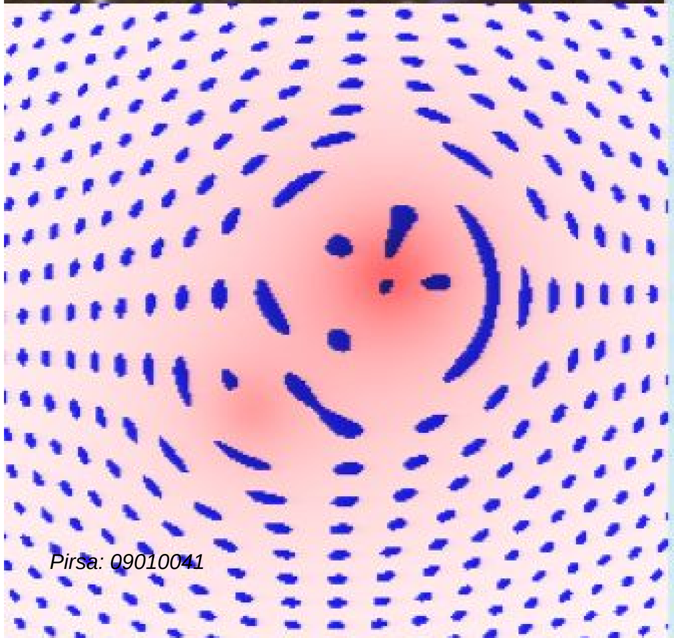

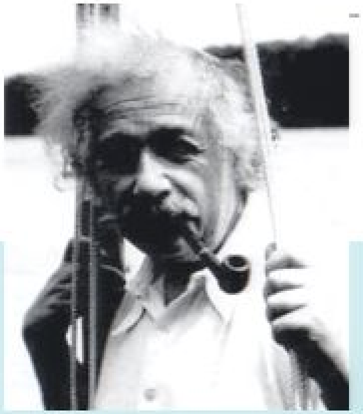

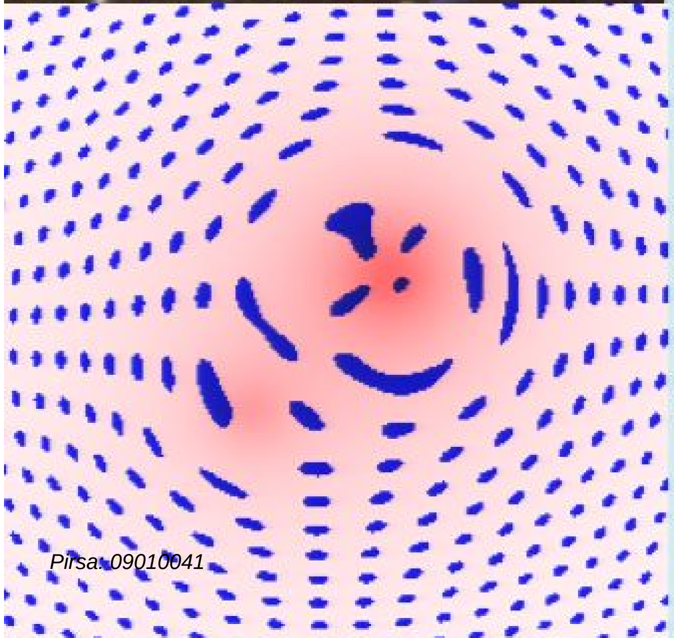

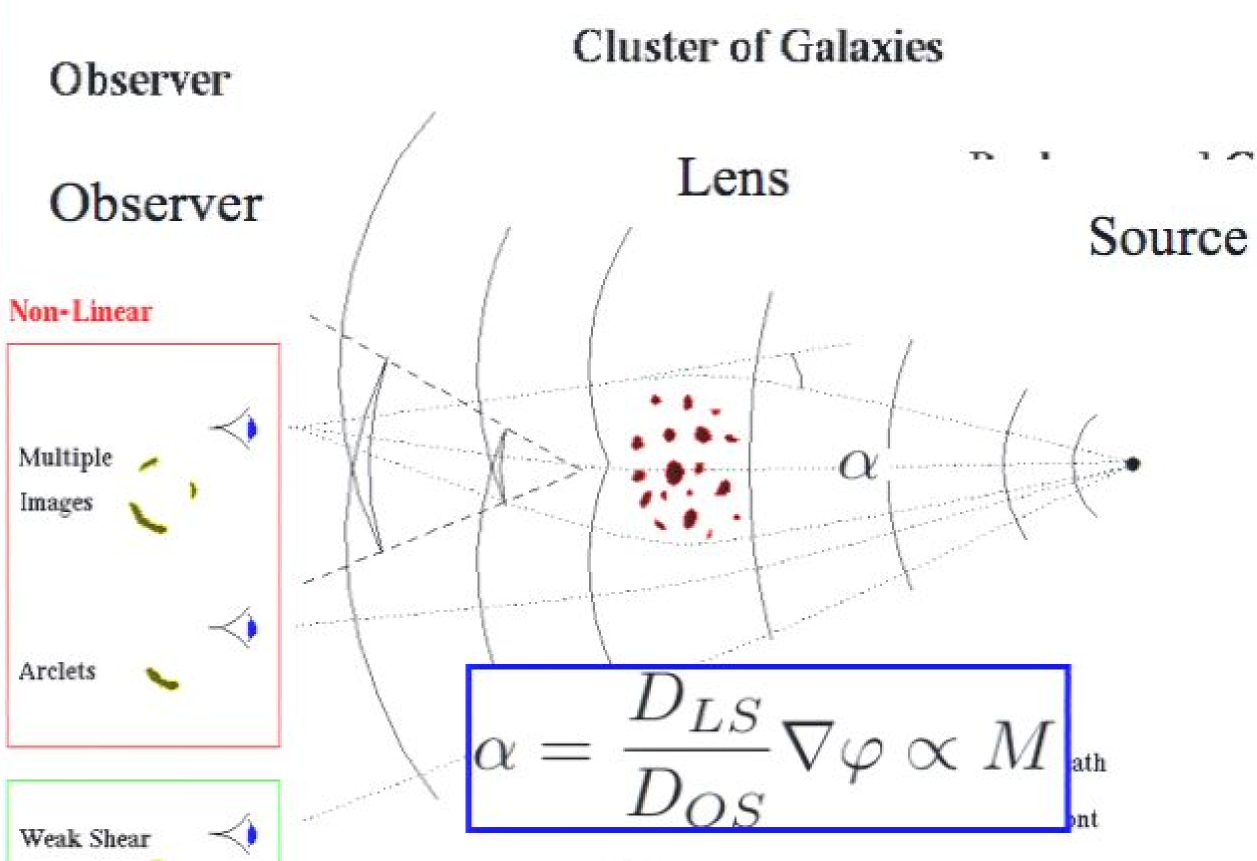

$$\boxed{\alpha = \frac{D_{LS}}{D_{OS}} \nabla \varphi \propto M}$$

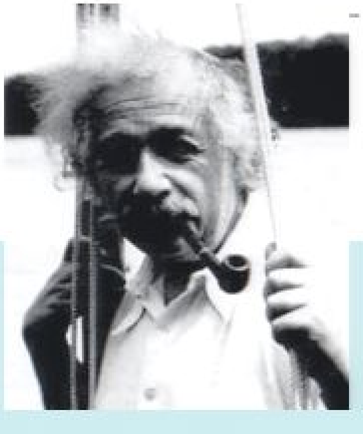

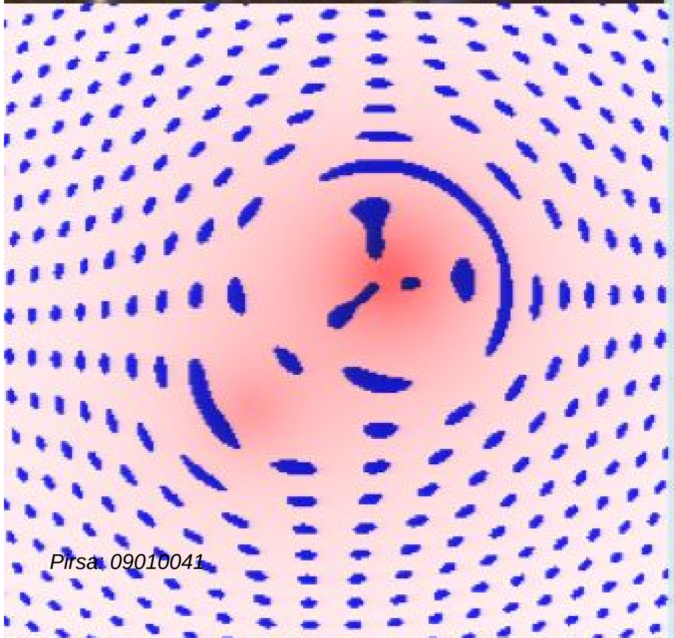

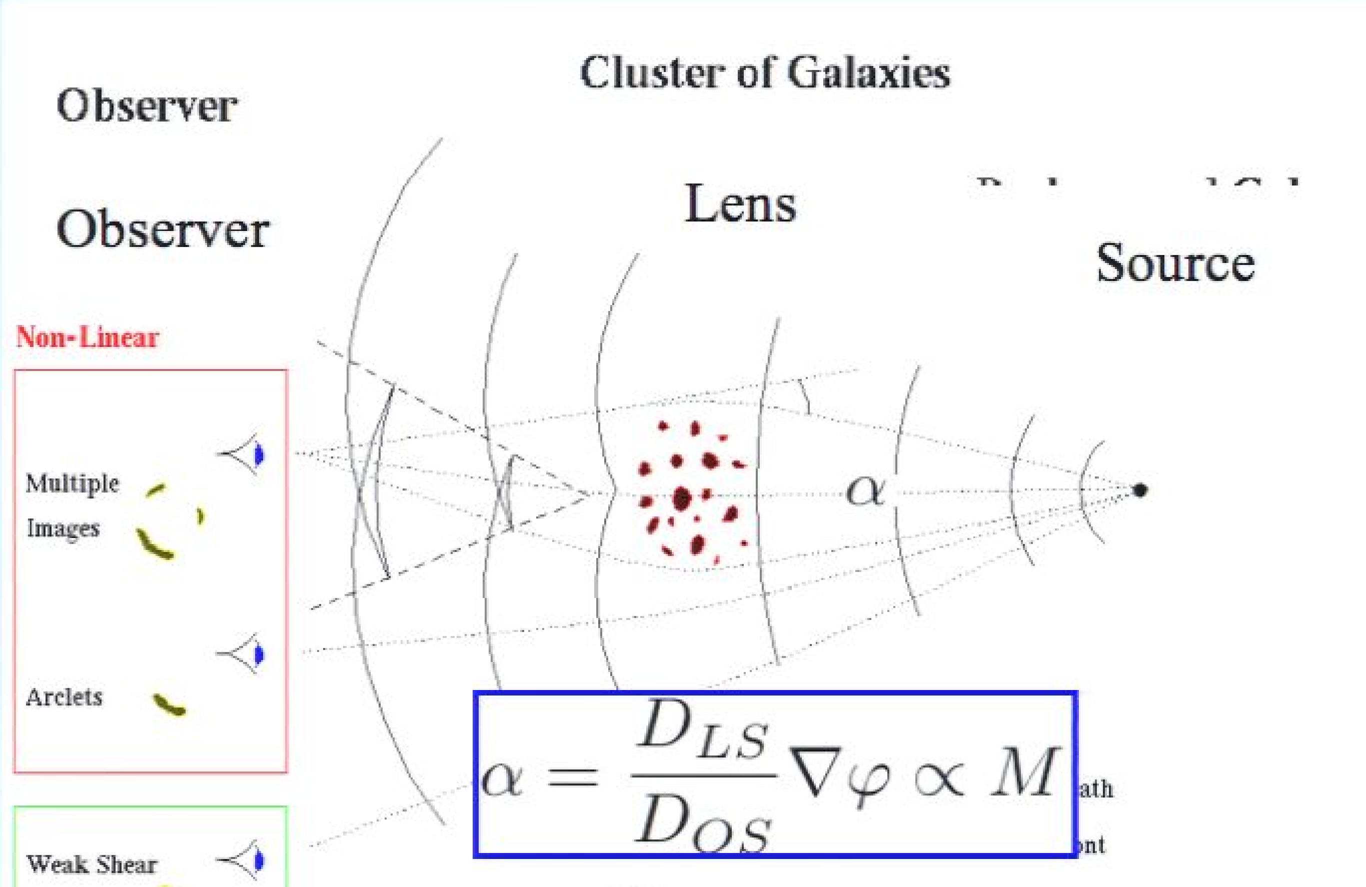

$$\alpha = \frac{D_{LS}}{D_{OS}} \nabla \varphi \propto M$$

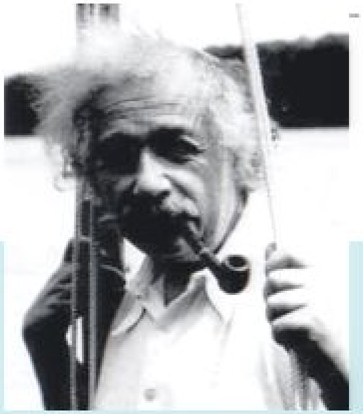

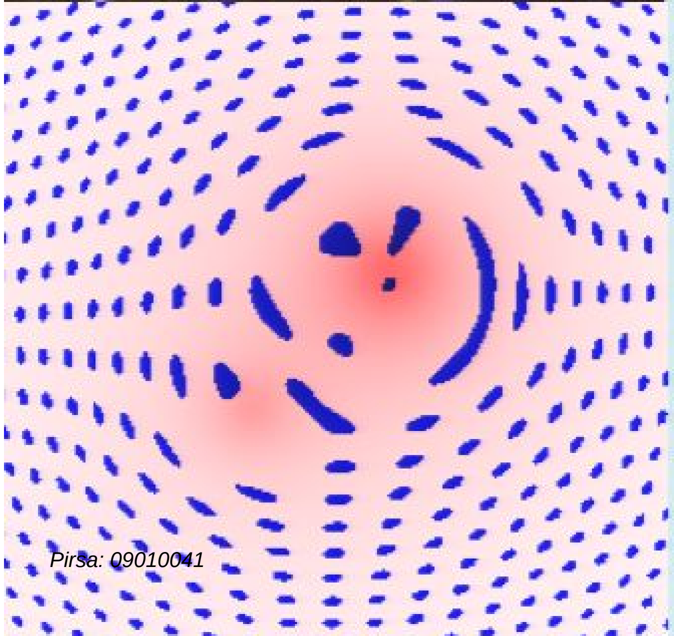

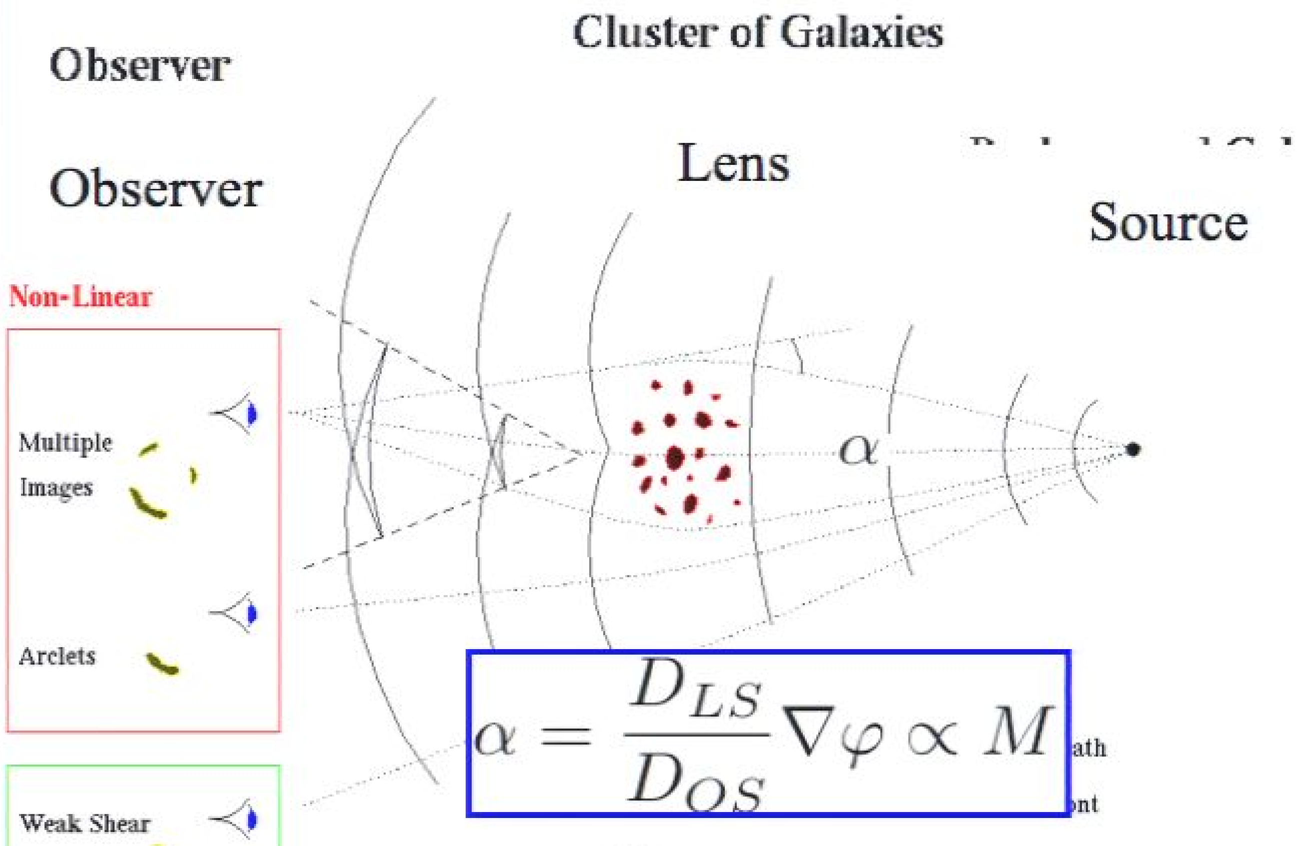

$$\alpha = \frac{D_{LS}}{D_{OS}} \nabla \varphi \propto M$$

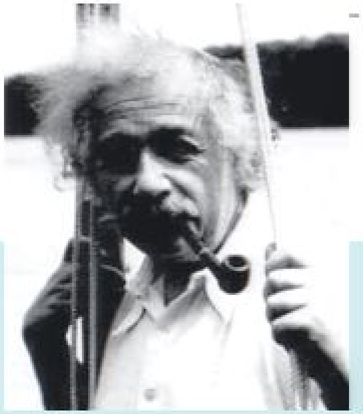

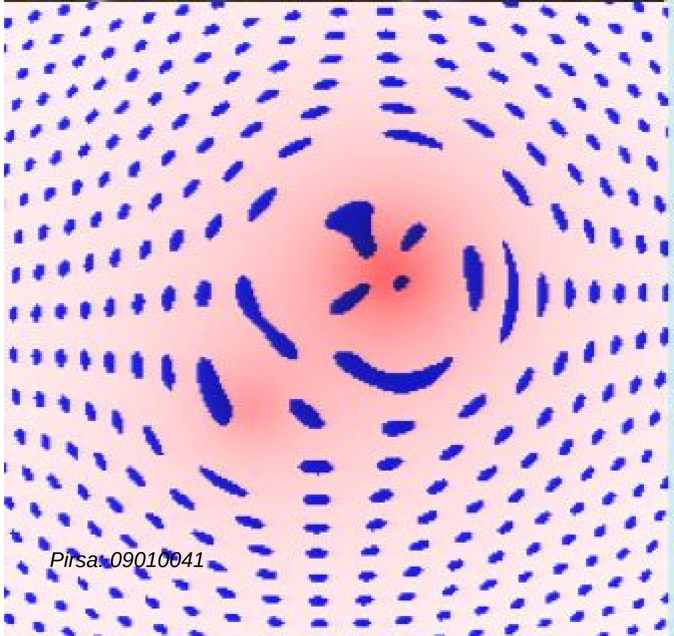

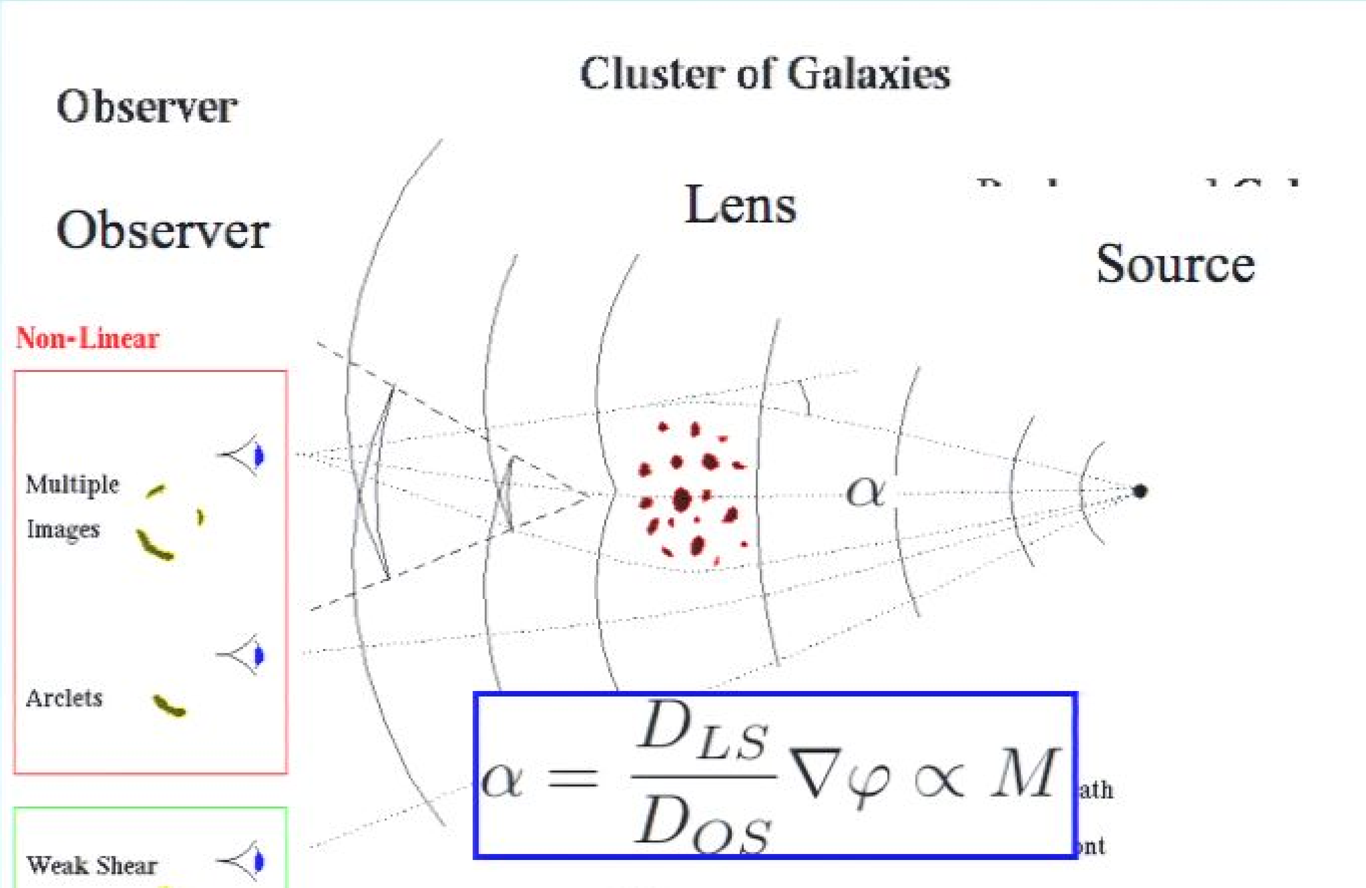

$$\alpha = \frac{D_{LS}}{D_{OS}} \nabla \varphi \propto M$$

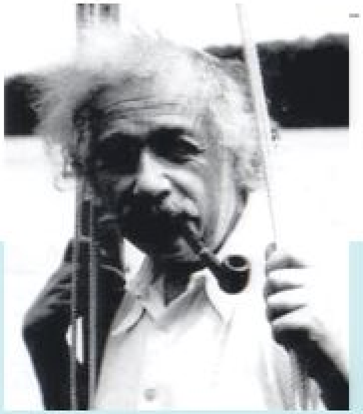

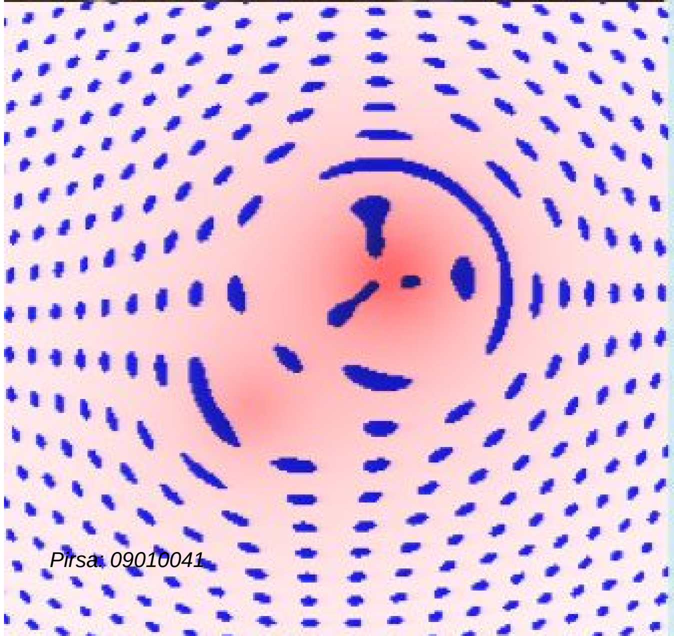

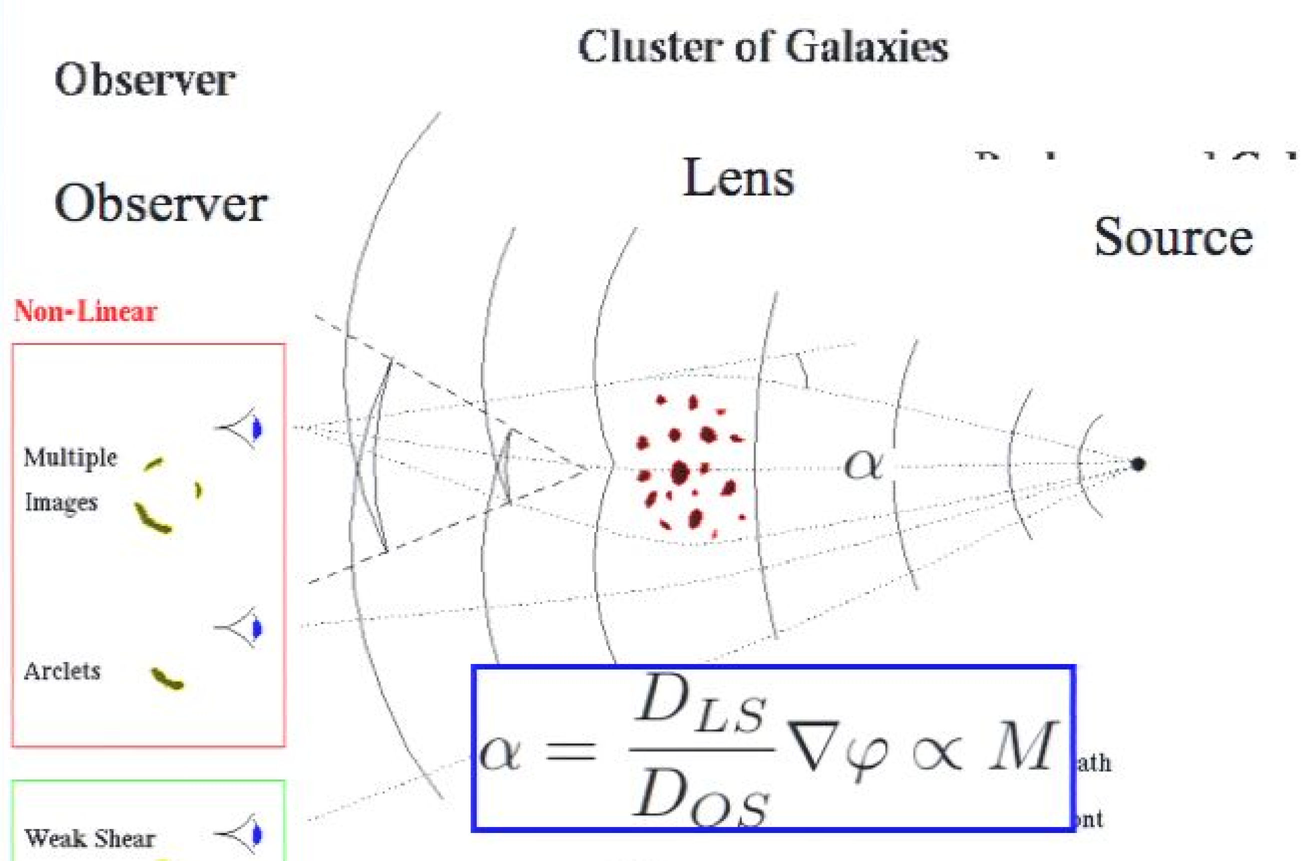

$$\alpha = \frac{D_{LS}}{D_{OS}} \nabla \varphi \propto M$$

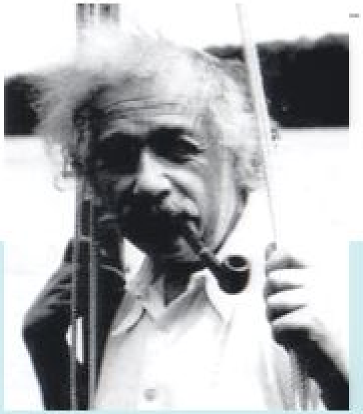

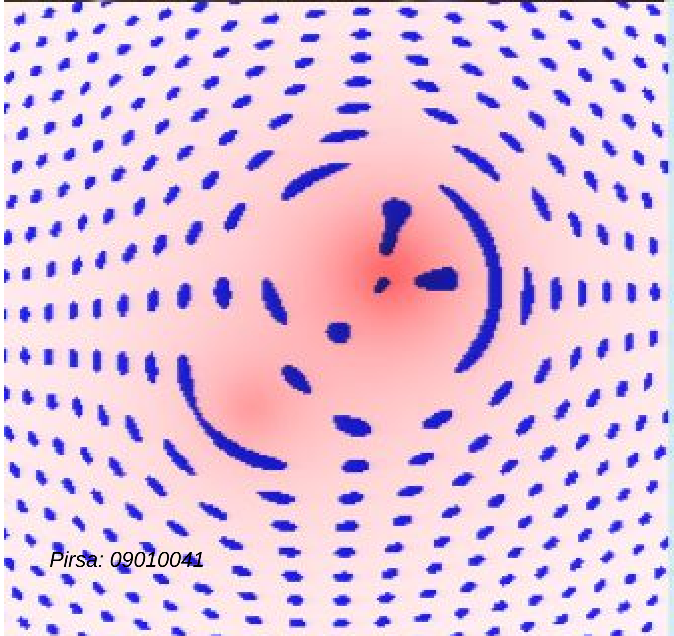

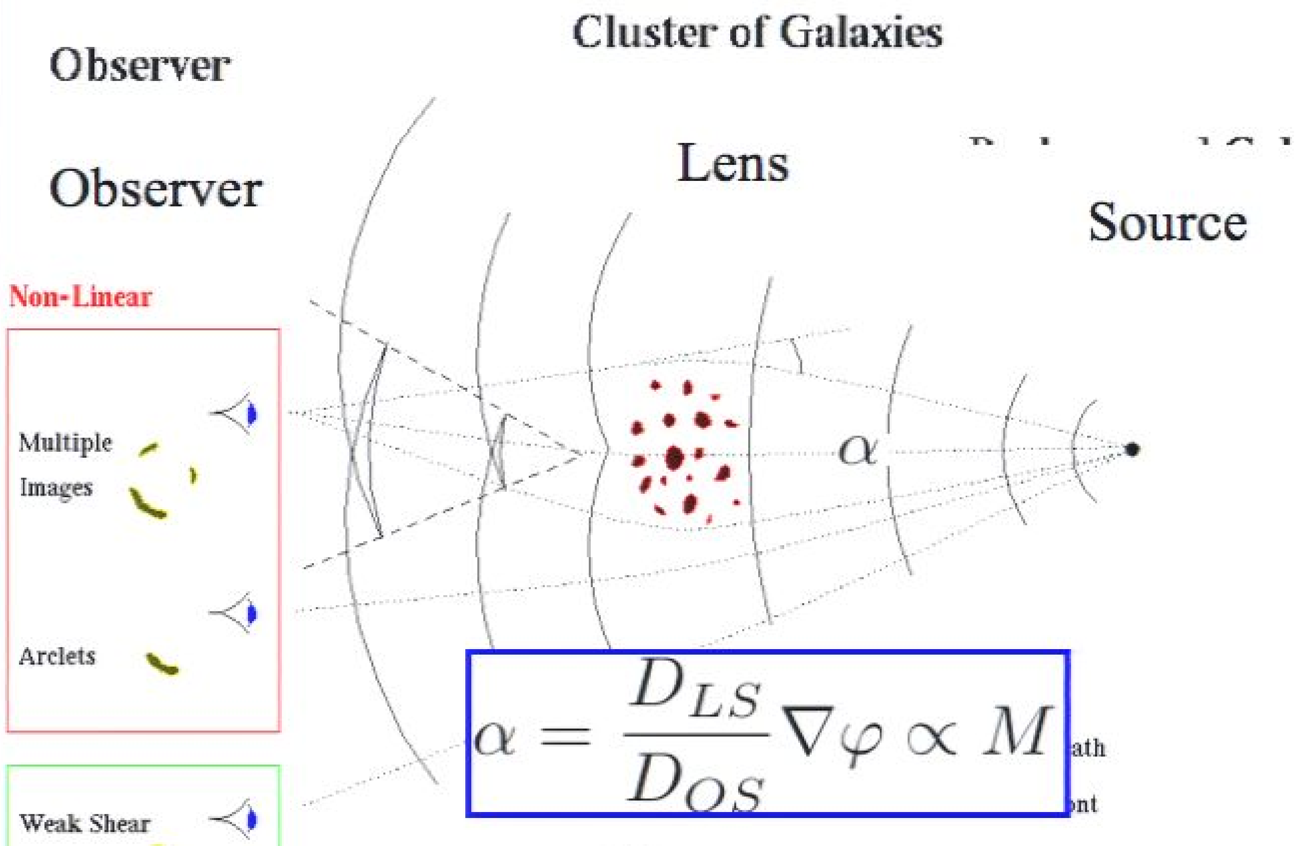

$$\alpha = \frac{D_{LS}}{D_{OS}} \nabla \varphi \propto M$$

- - - - Multiple Images Area

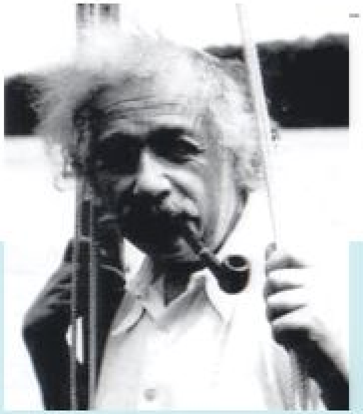

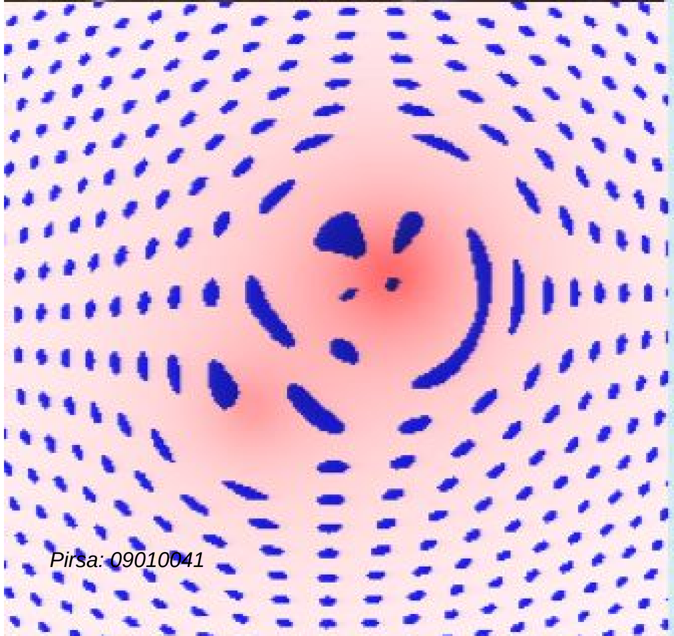

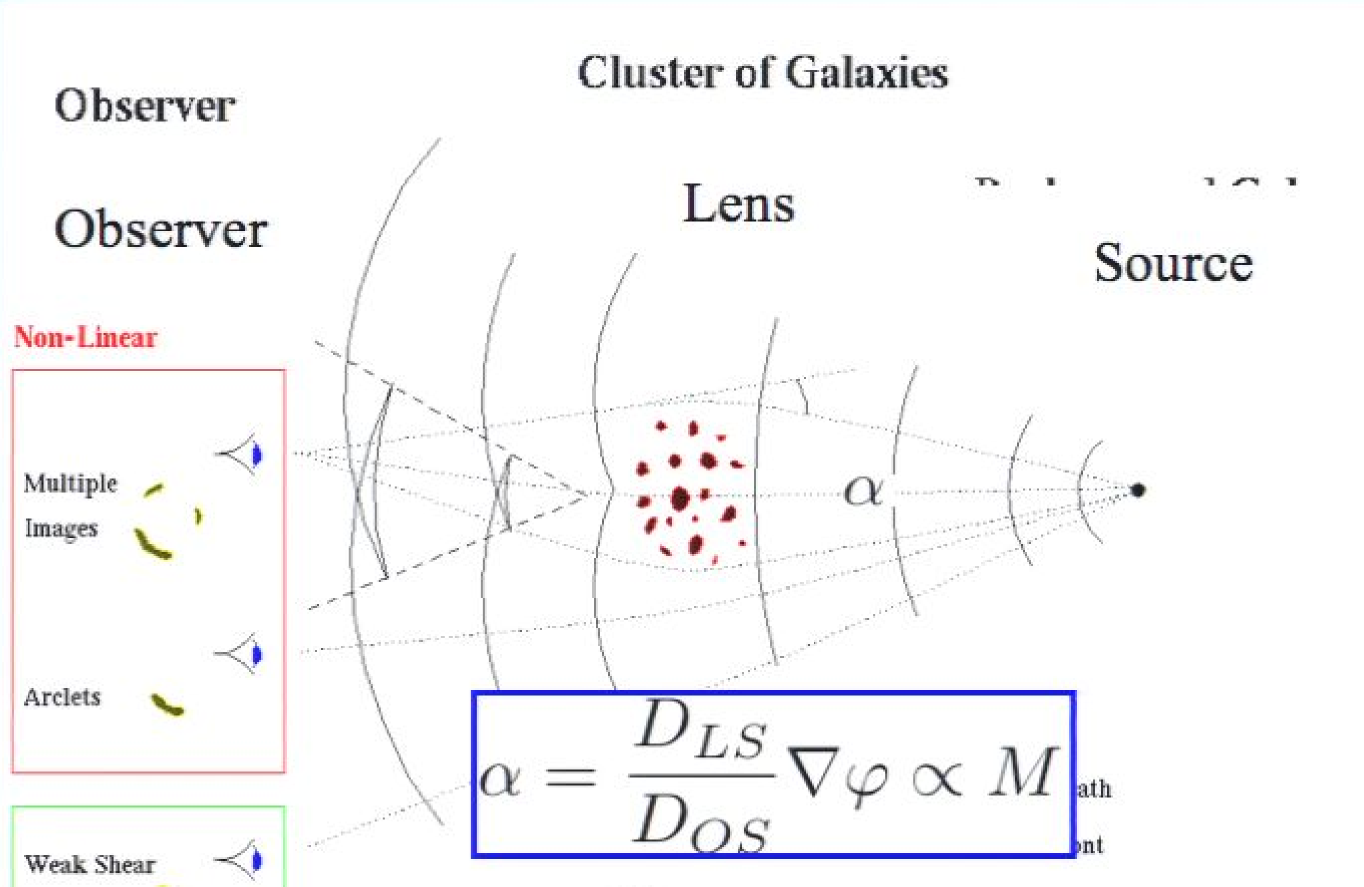

$$\alpha = \frac{D_{LS}}{D_{OS}} \nabla \varphi \propto M$$

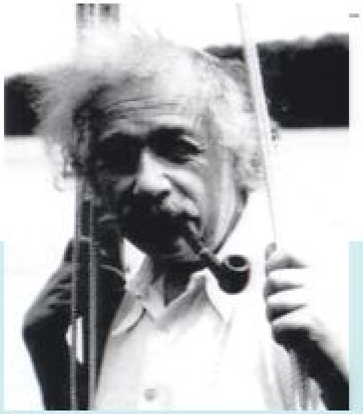

CFHT 1990

Z_cluster=0.375

Z_arc=0.725 (Soucail et al 1988)

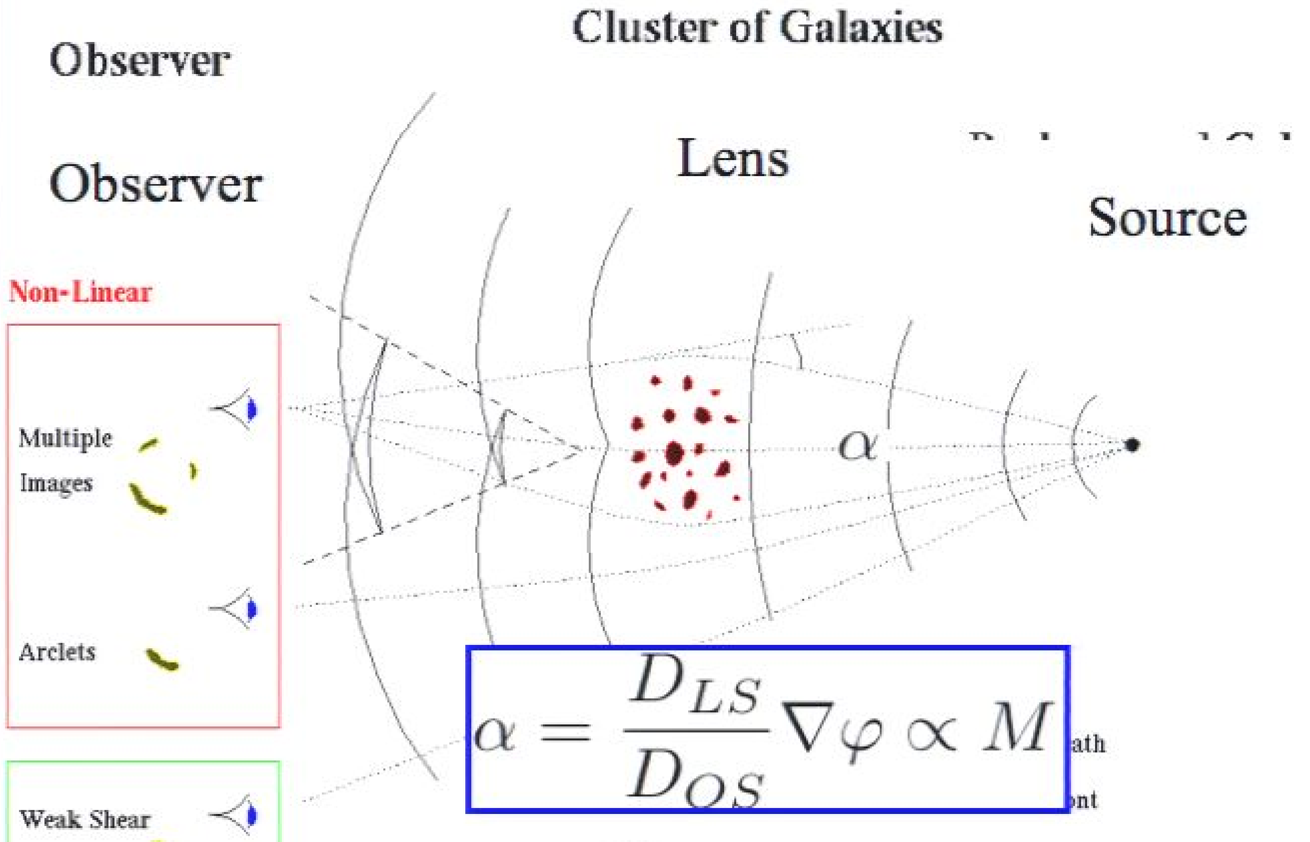

$$\alpha = \frac{D_{LS}}{D_{OS}} \nabla \varphi \propto M$$

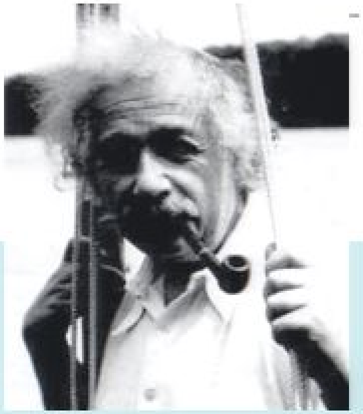

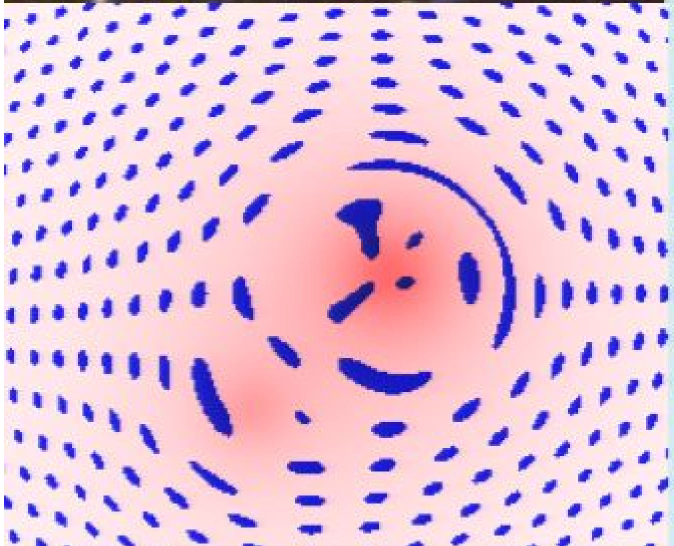

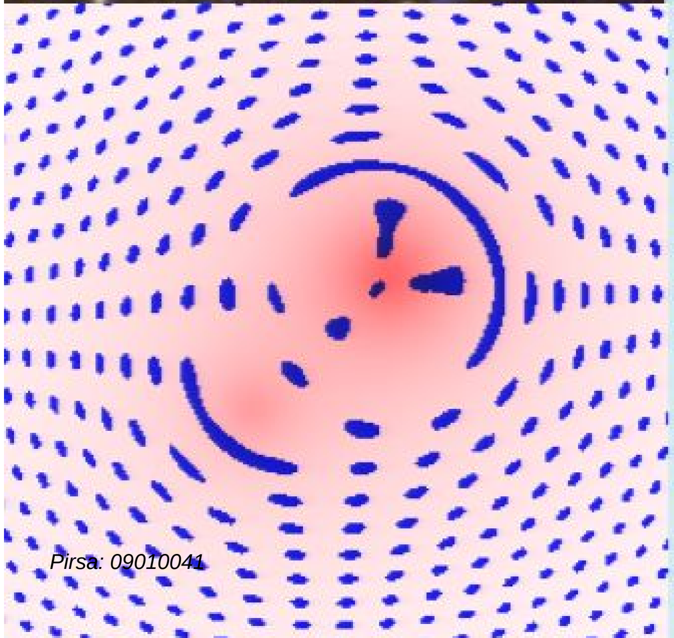

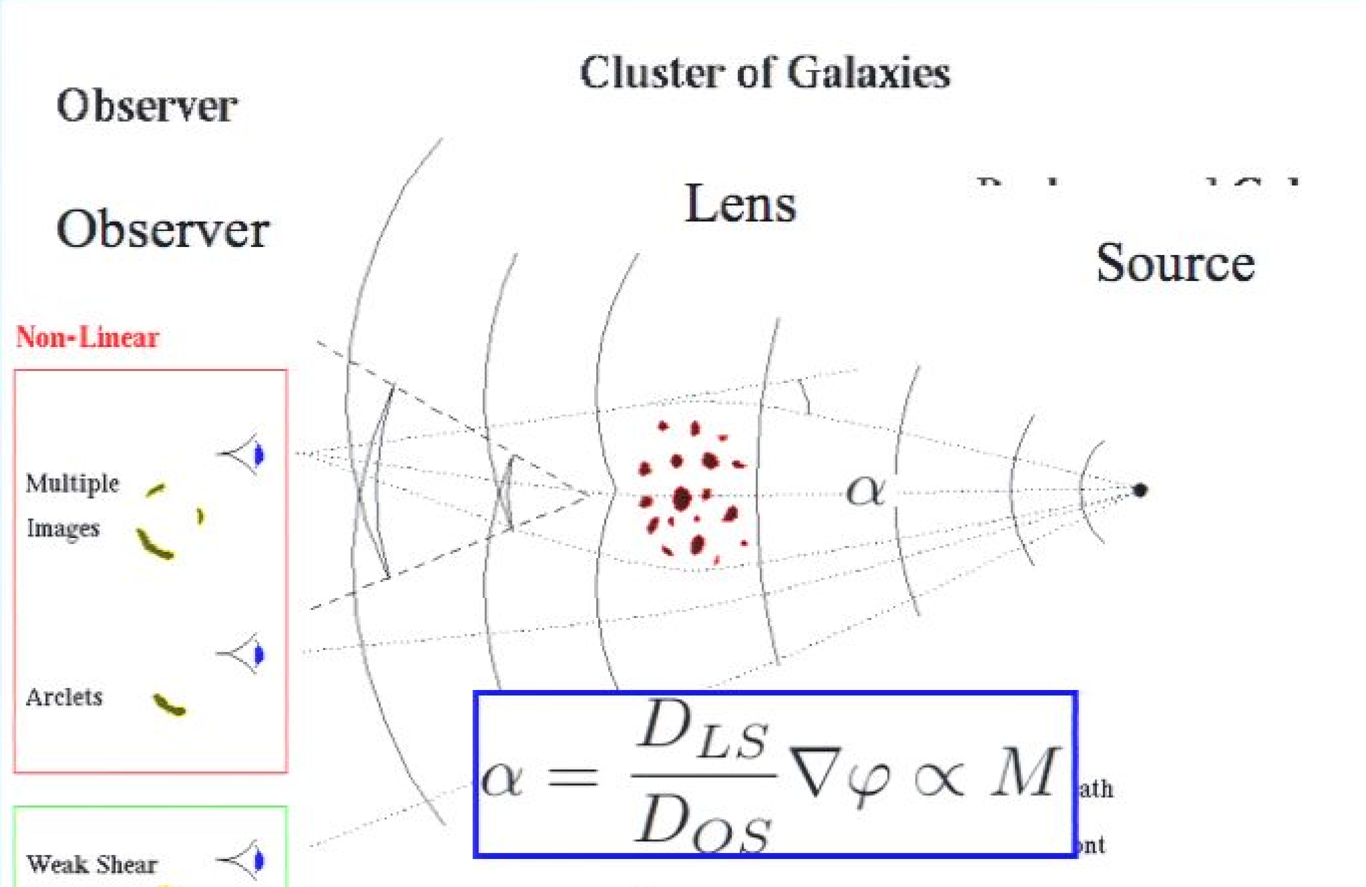

$$\boxed{\alpha = \frac{D_{LS}}{D_{OS}} \nabla \varphi \propto M}$$

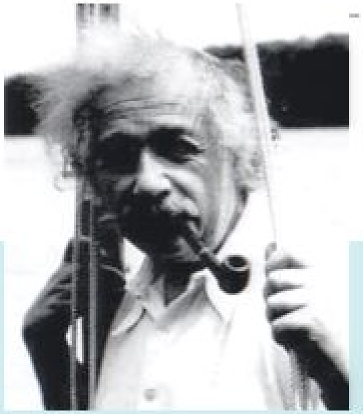

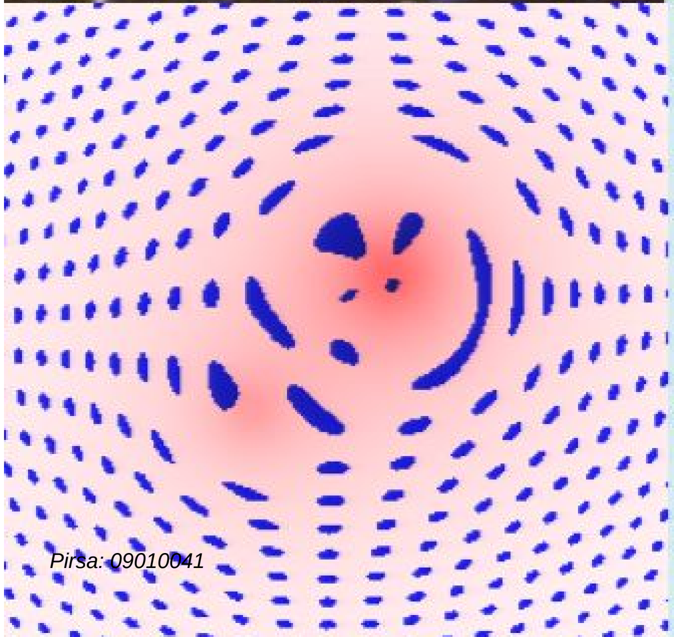

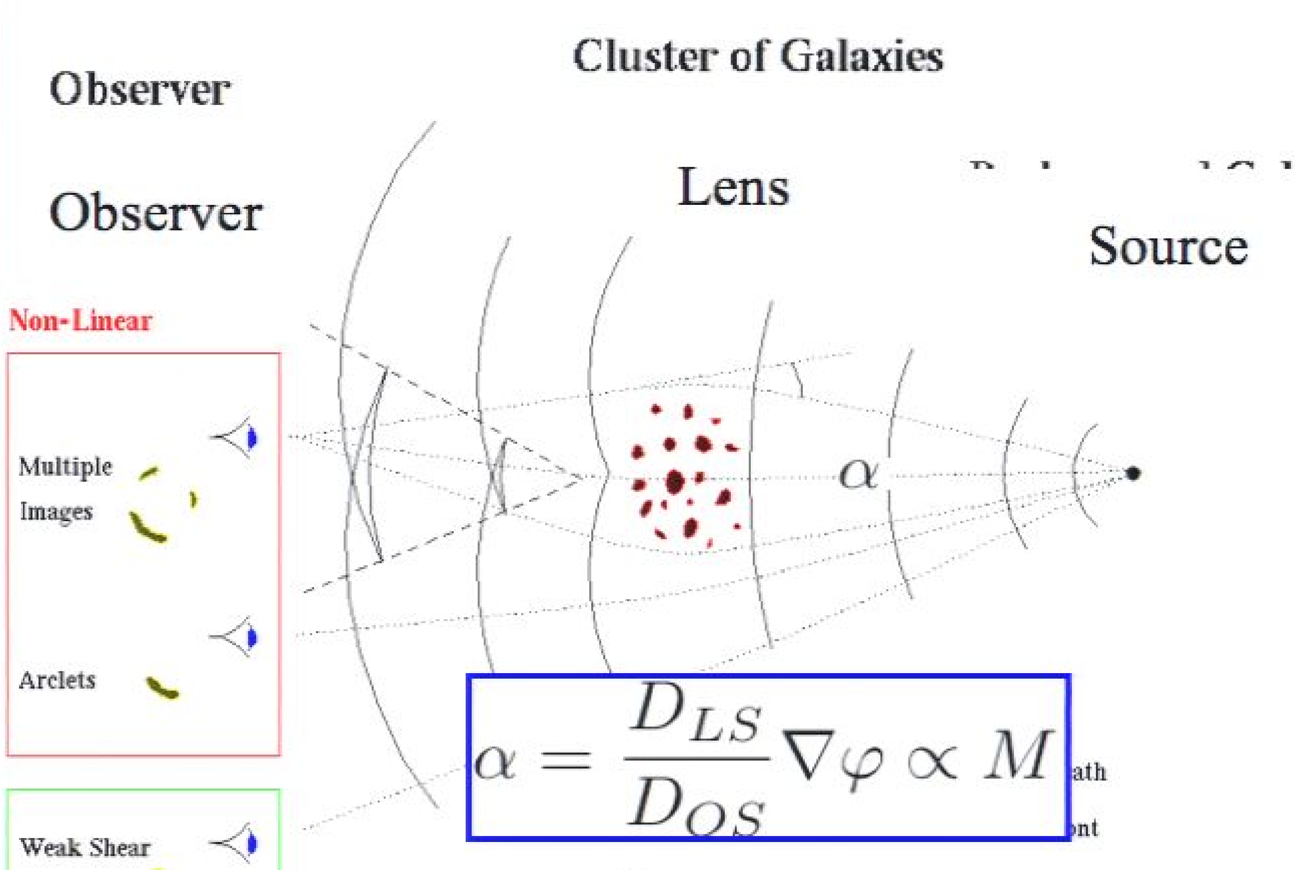

$$\boxed{\alpha = \frac{D_{LS}}{D_{OS}} \nabla \varphi \propto M}$$

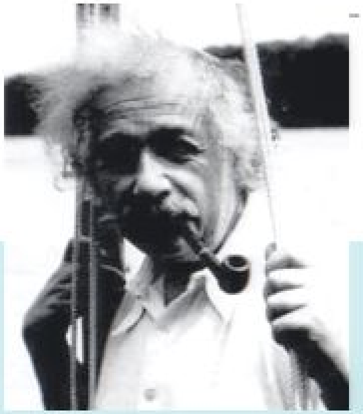

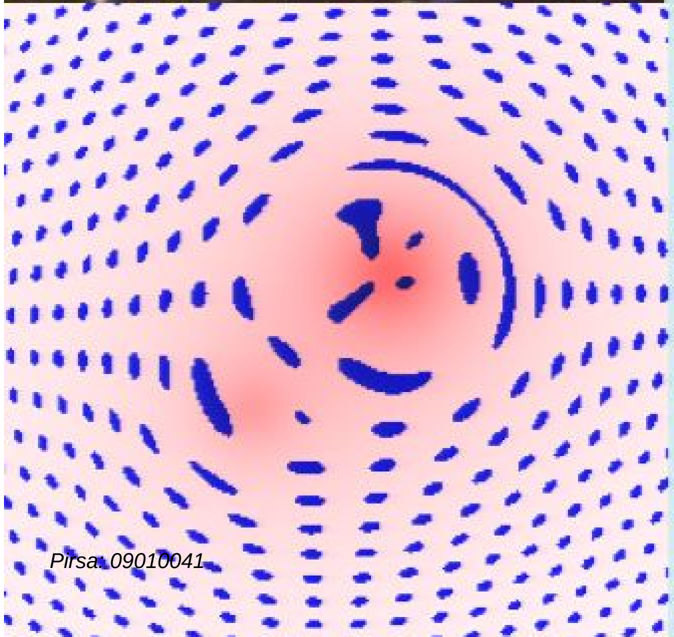

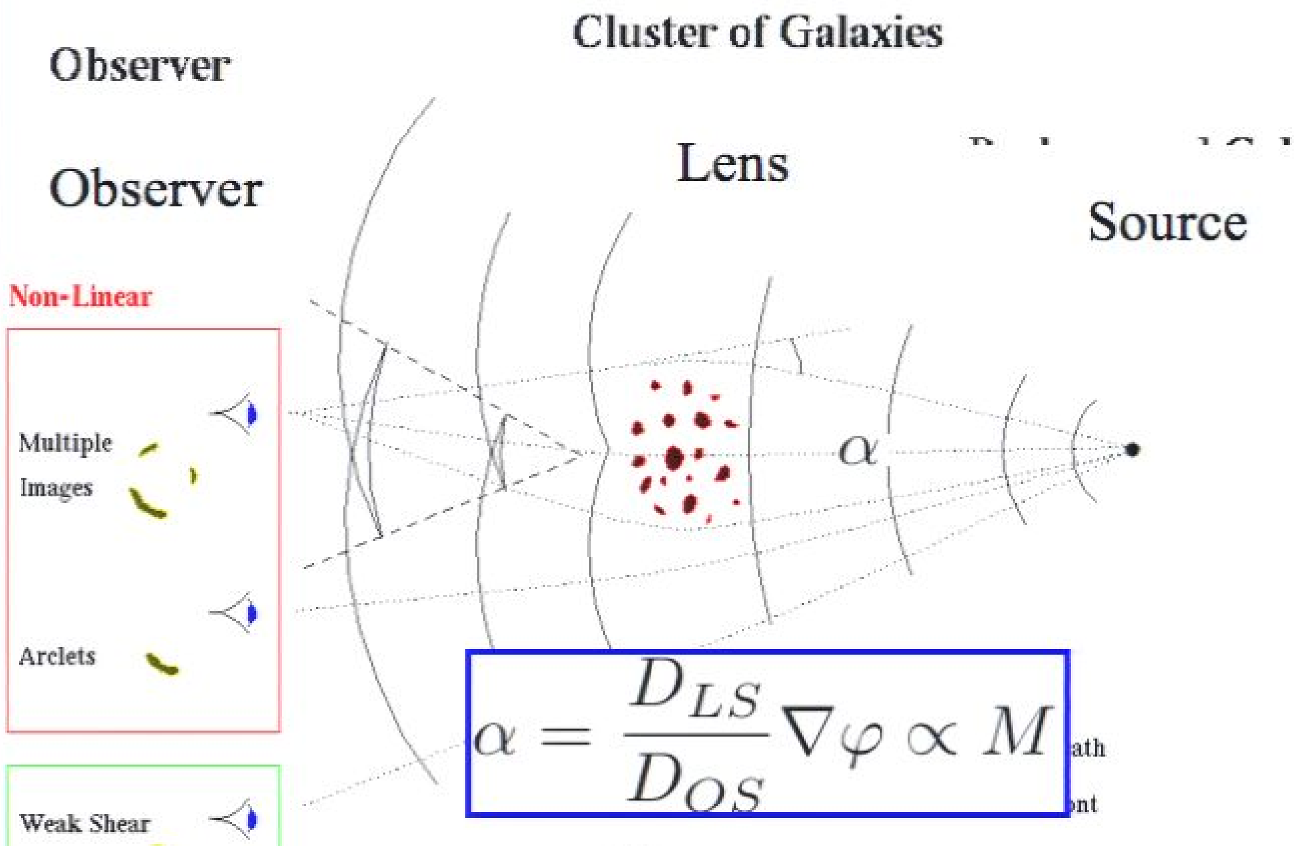

$$\alpha = \frac{D_{LS}}{D_{OS}} \nabla \varphi \propto M$$

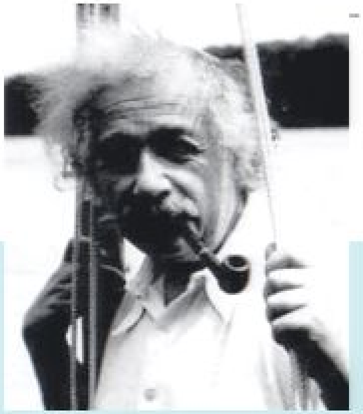


CFHT 1990

Z_cluster=0.375

Z_arc=0.725 (Soucail et al 1988)

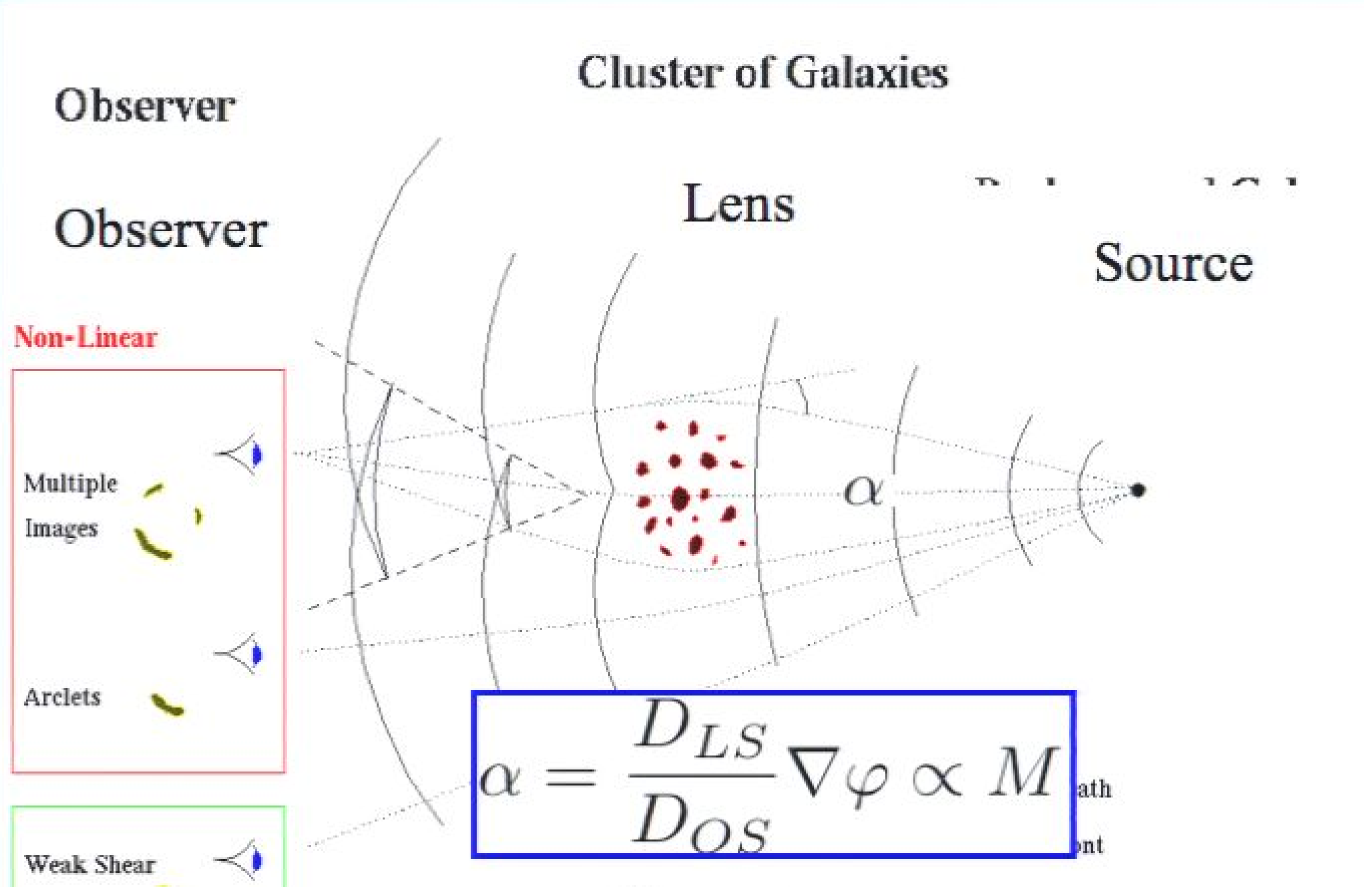

$$\alpha = \frac{D_{LS}}{D_{OS}} \nabla \varphi \propto M$$

Linear

Multiple Images Area

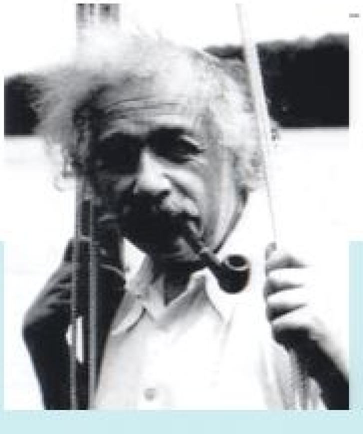

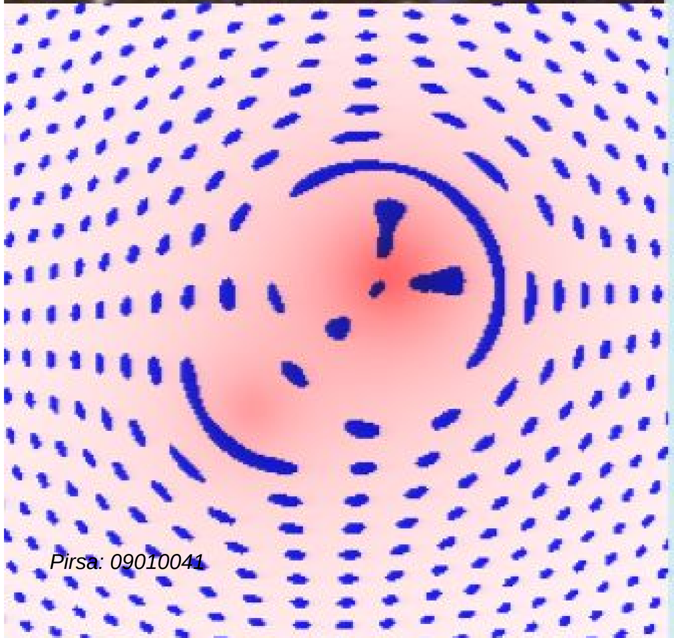

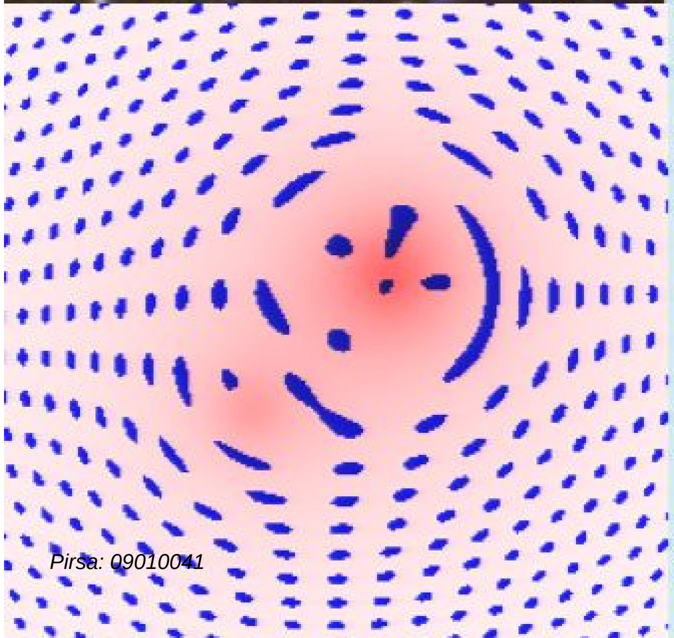

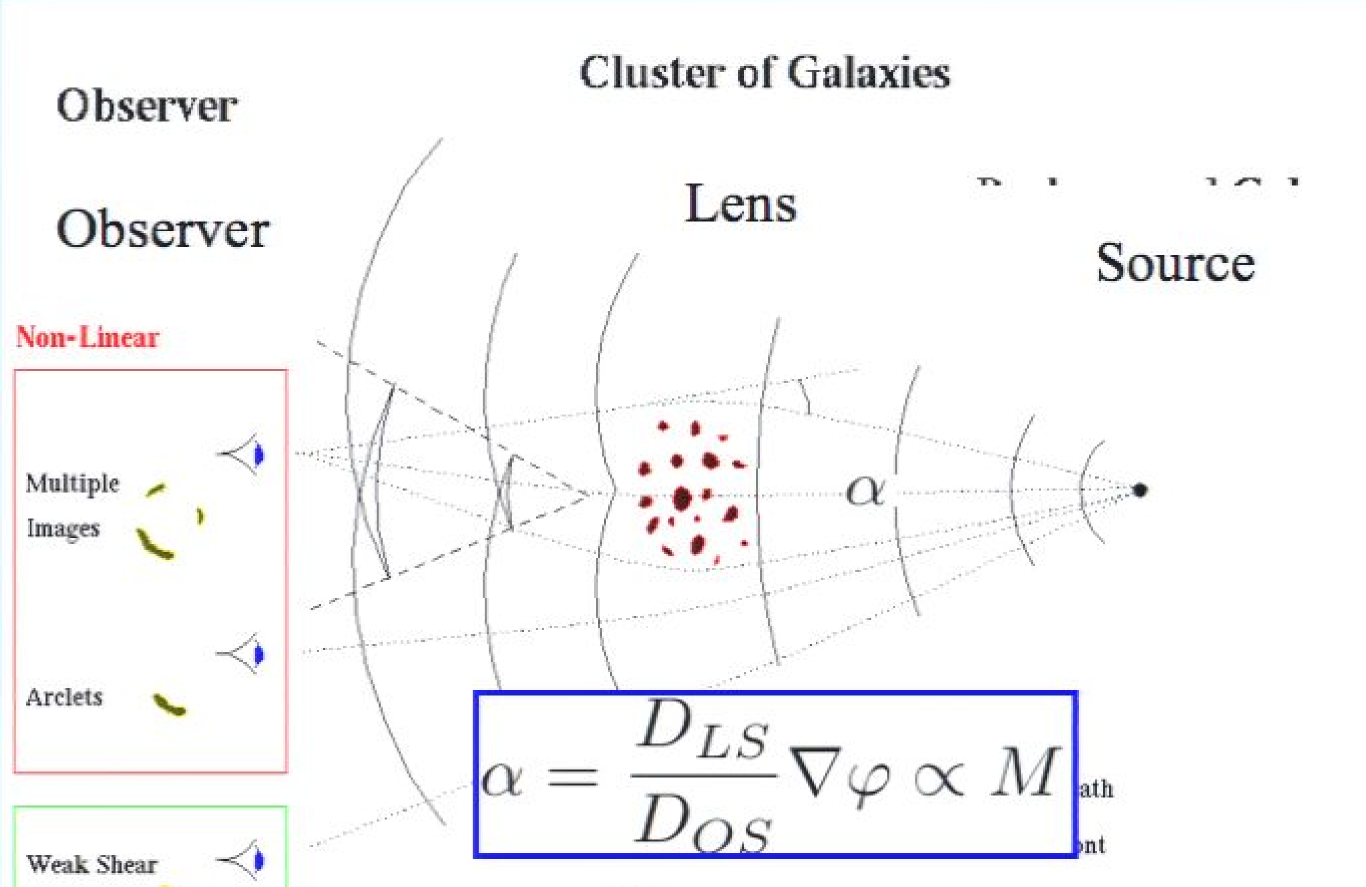

$$\alpha = \frac{D_{LS}}{D_{OS}} \nabla \varphi \propto M$$

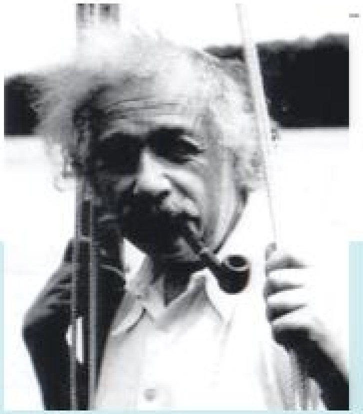

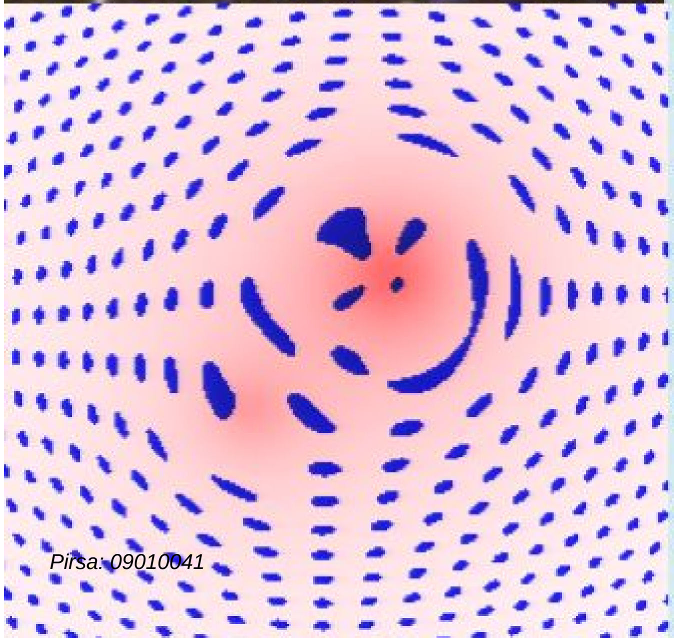

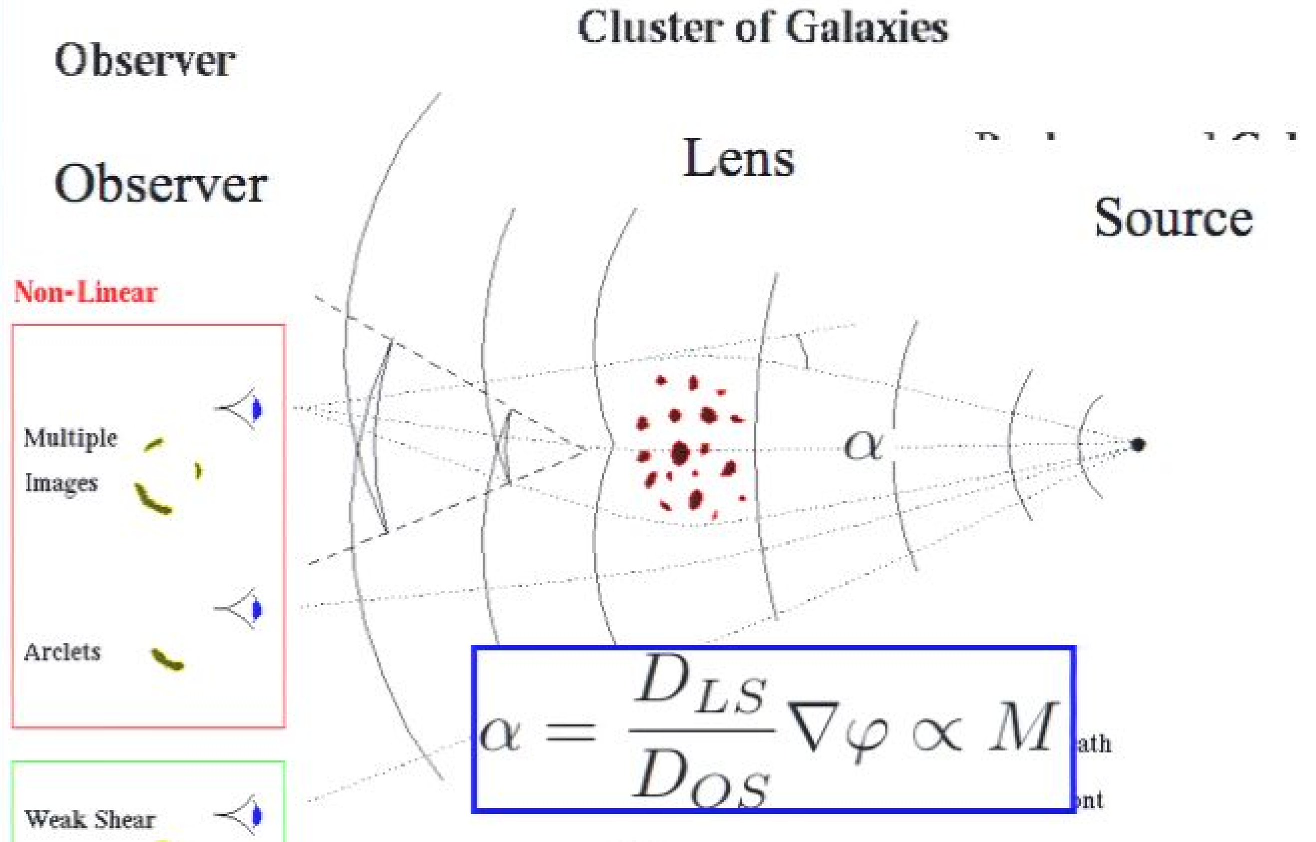

$$\alpha = \frac{D_{LS}}{D_{OS}} \nabla \varphi \propto M$$

- - - - Multiple Images Area

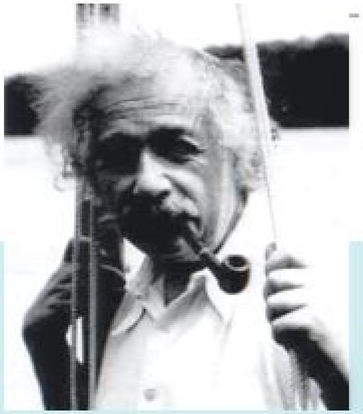

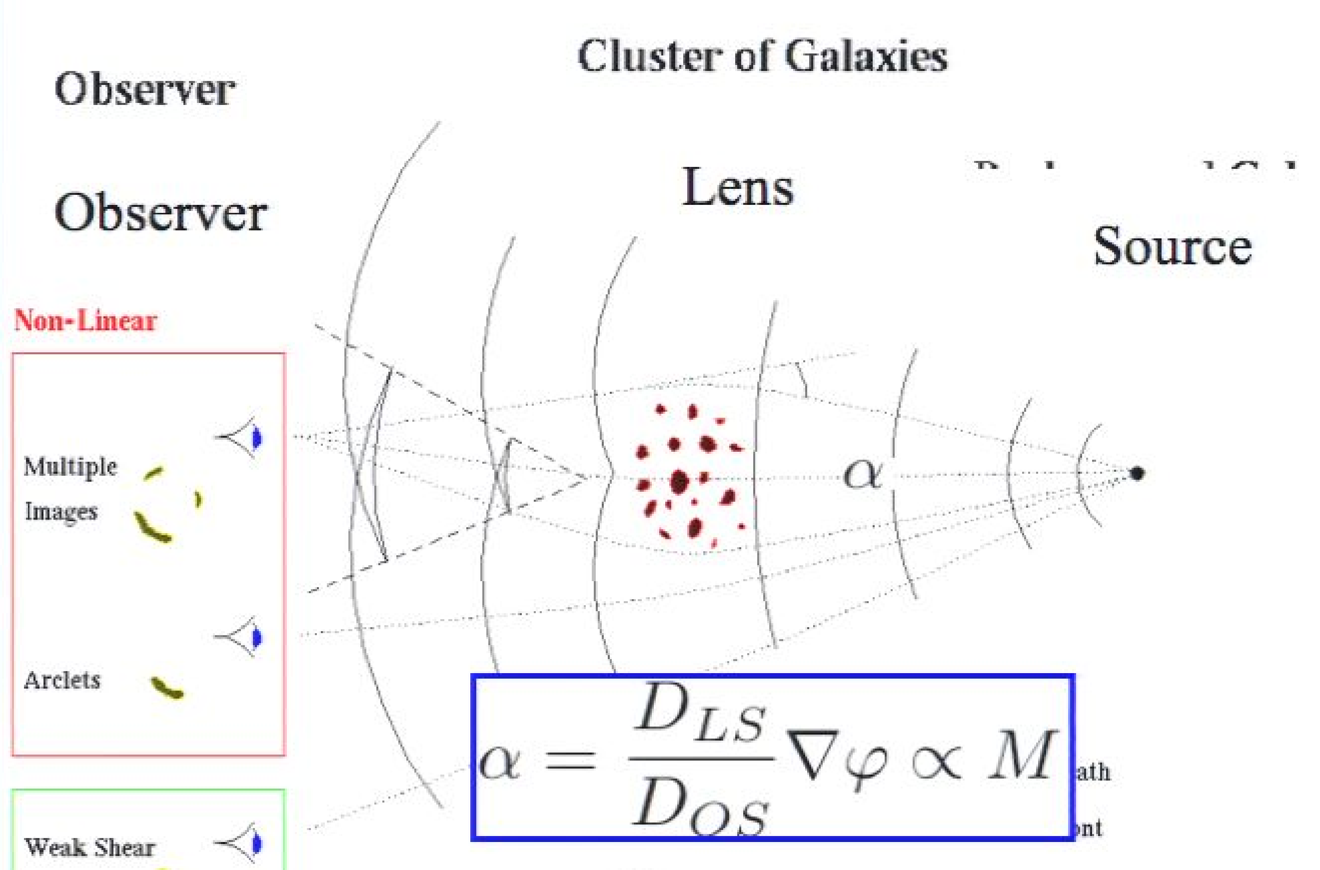

$$\alpha = \frac{D_{LS}}{D_{OS}} \nabla\varphi \propto M$$

Multiple Images Area

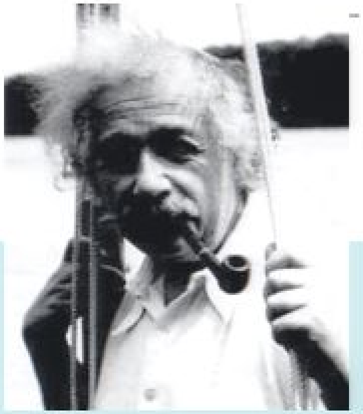

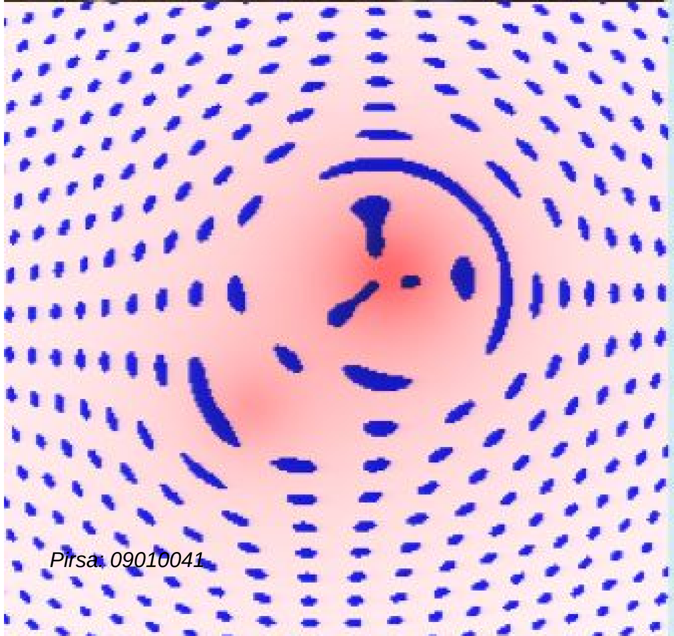

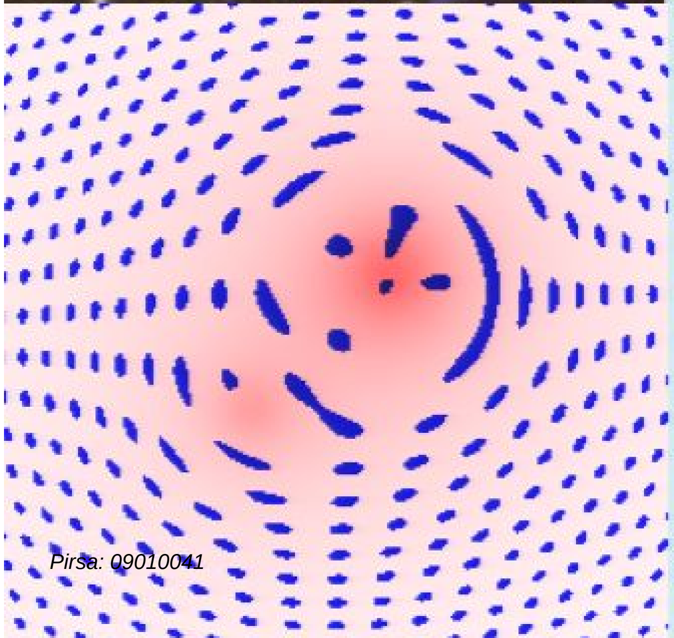

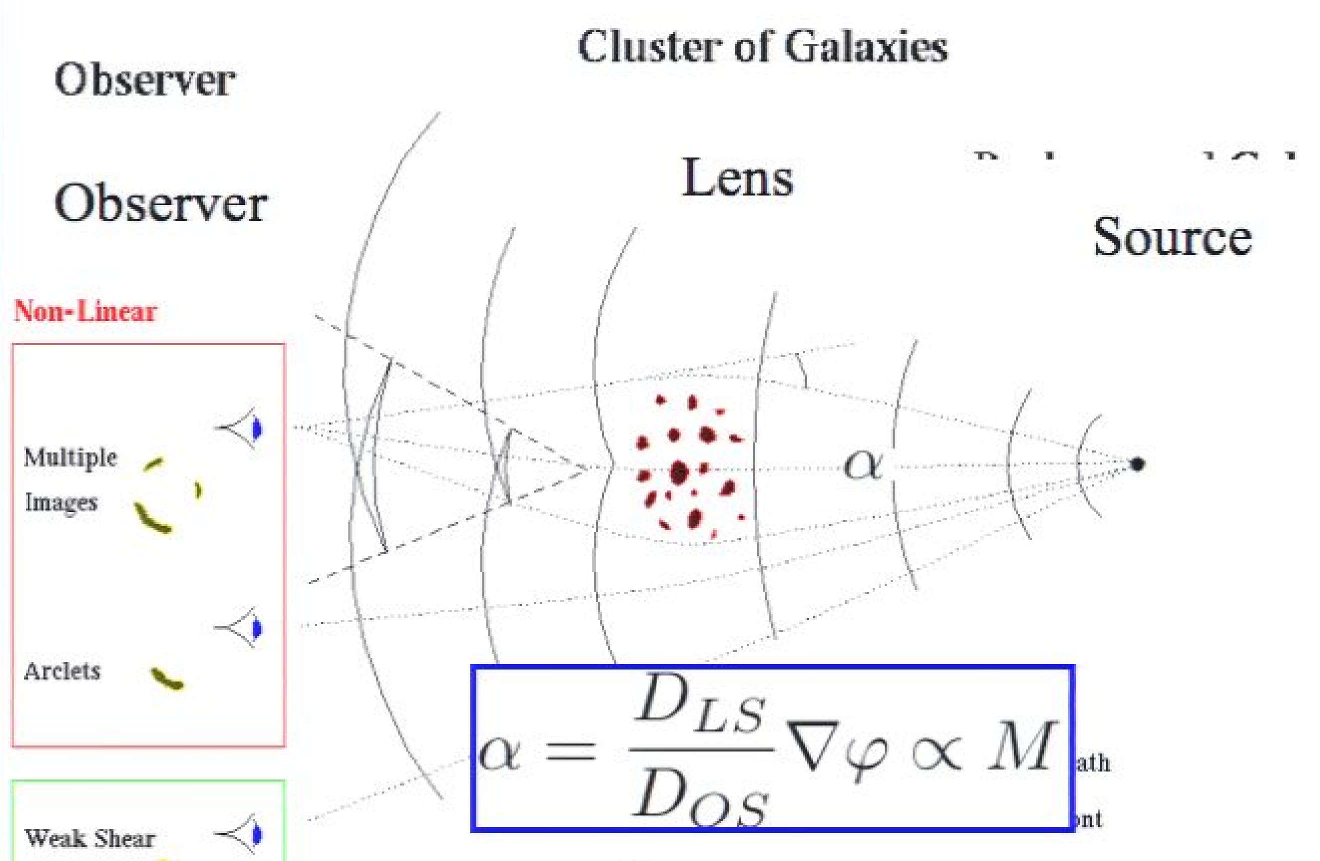

$$\alpha = \frac{D_{LS}}{D_{OS}} \nabla \varphi \propto M$$

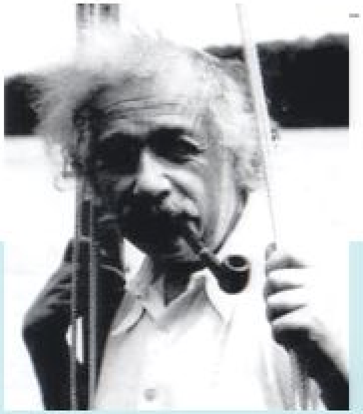


CFHT 1990

Z_cluster=0.375

Z_arc=0.725 (Soucail et al 1988)

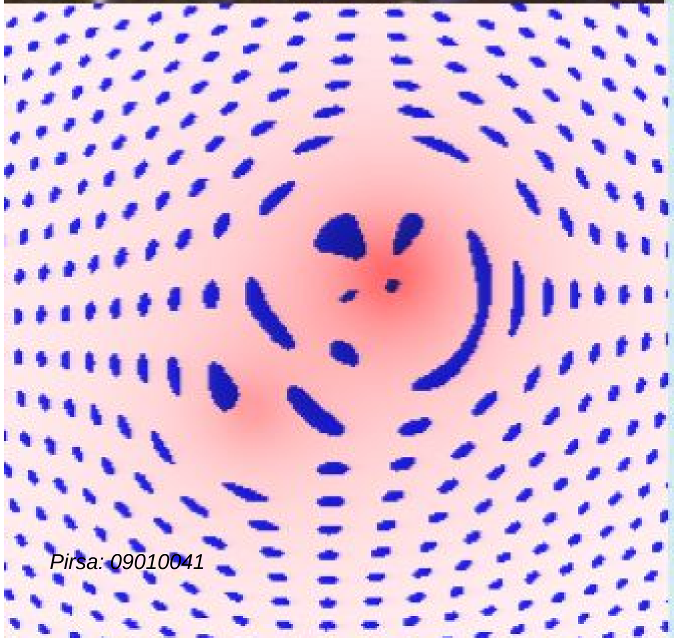

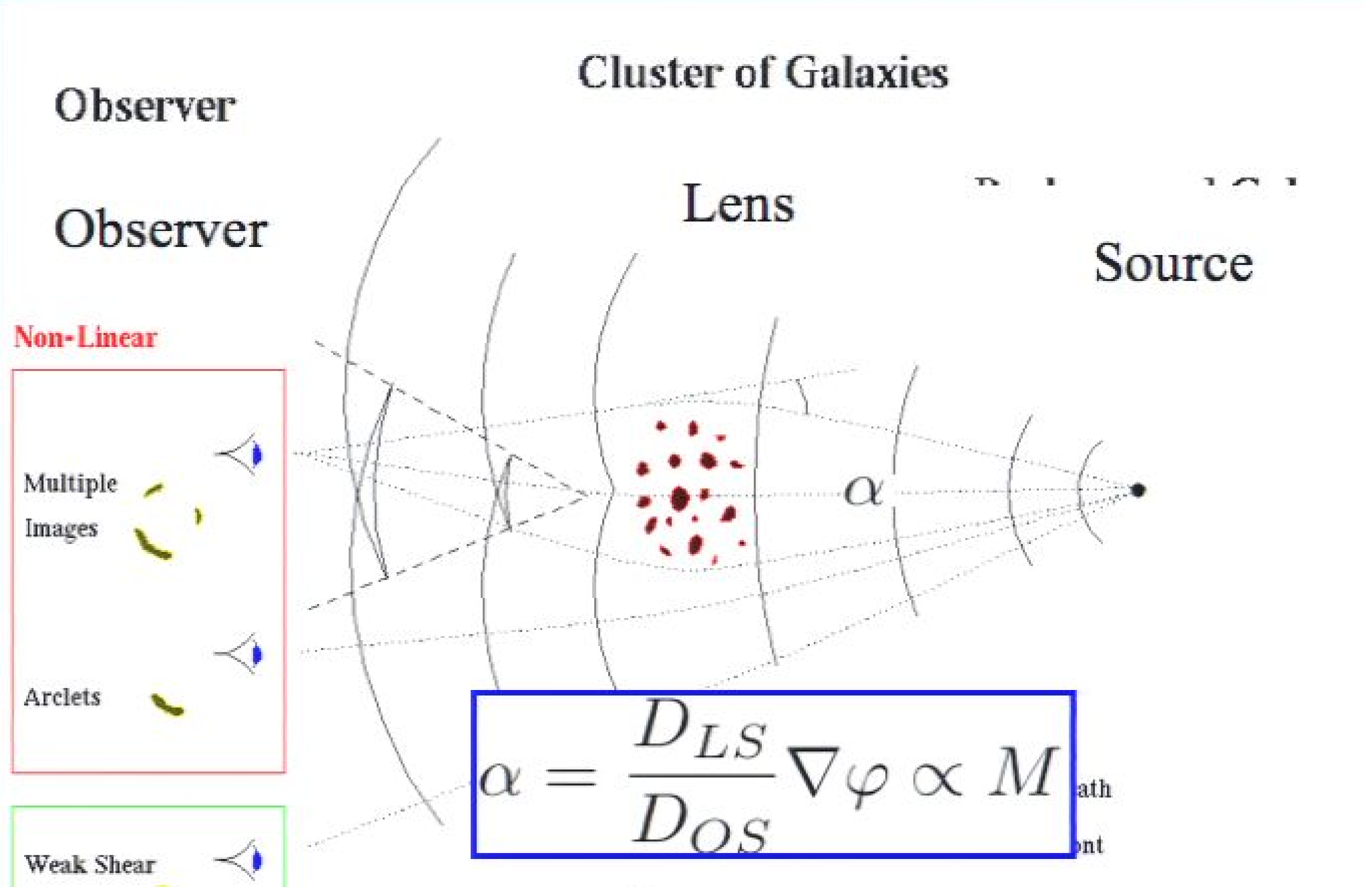

$$\alpha = \frac{D_{LS}}{D_{OS}} \nabla \varphi \propto M$$

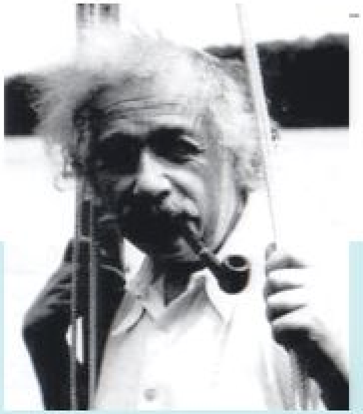

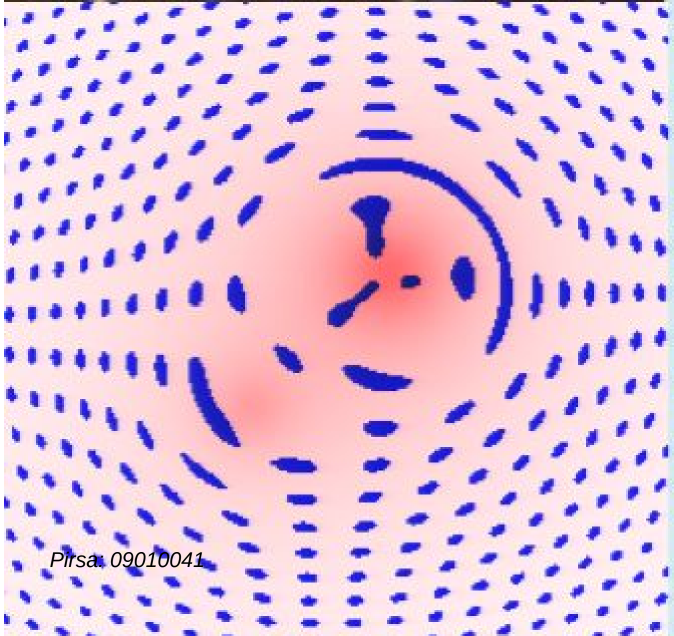

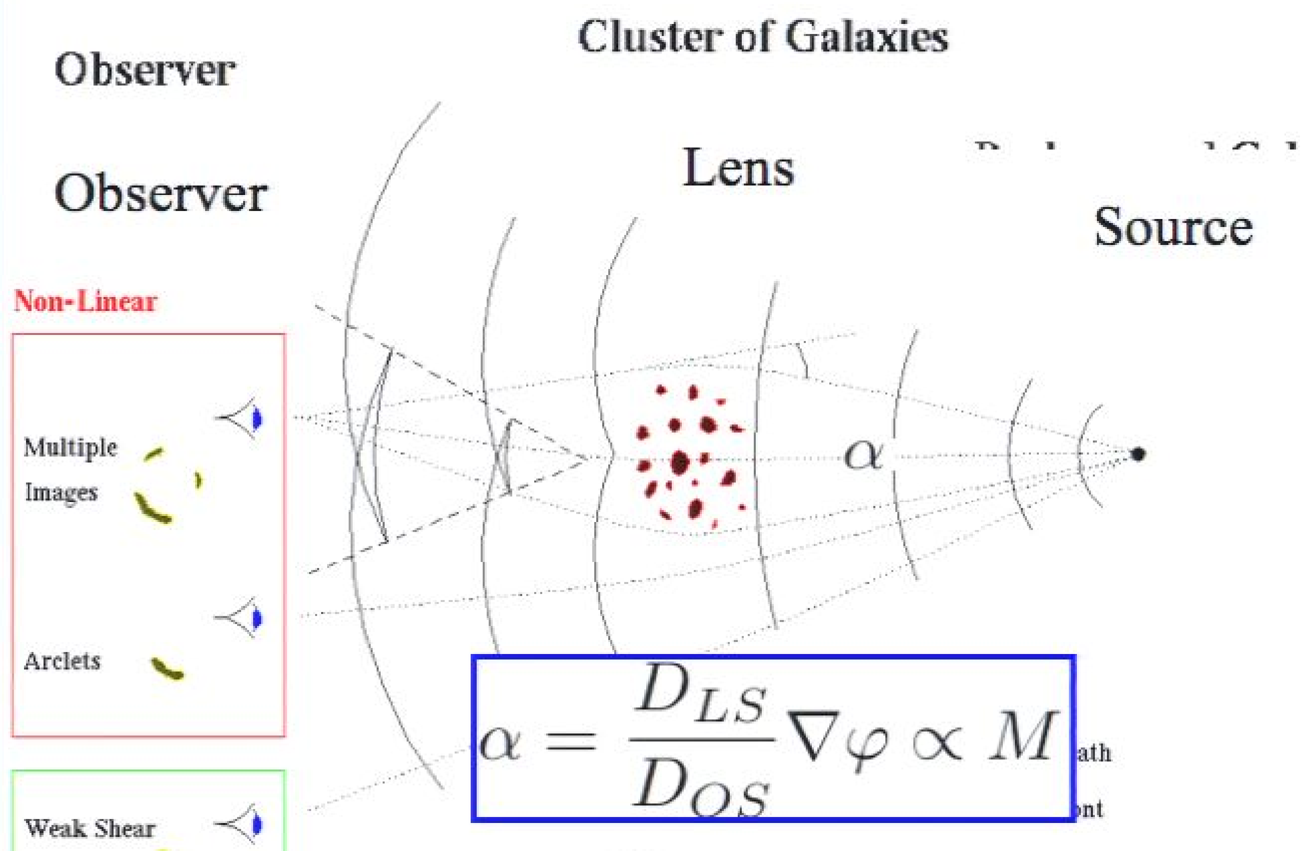

$$\alpha = \frac{D_{LS}}{D_{OS}} \nabla \varphi \propto M$$

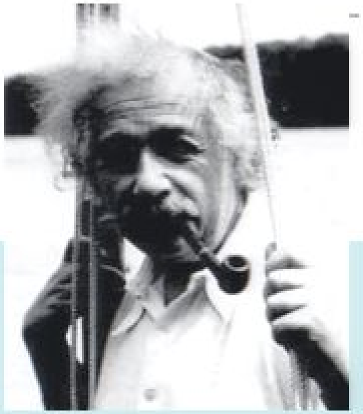

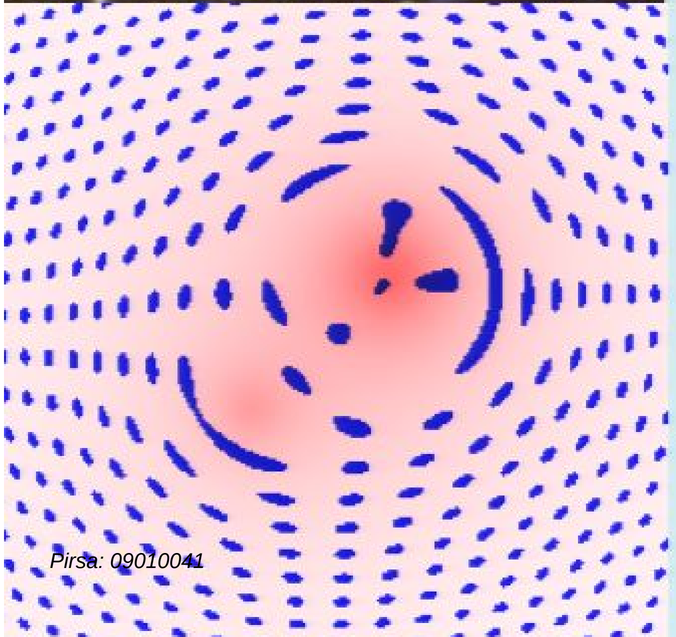

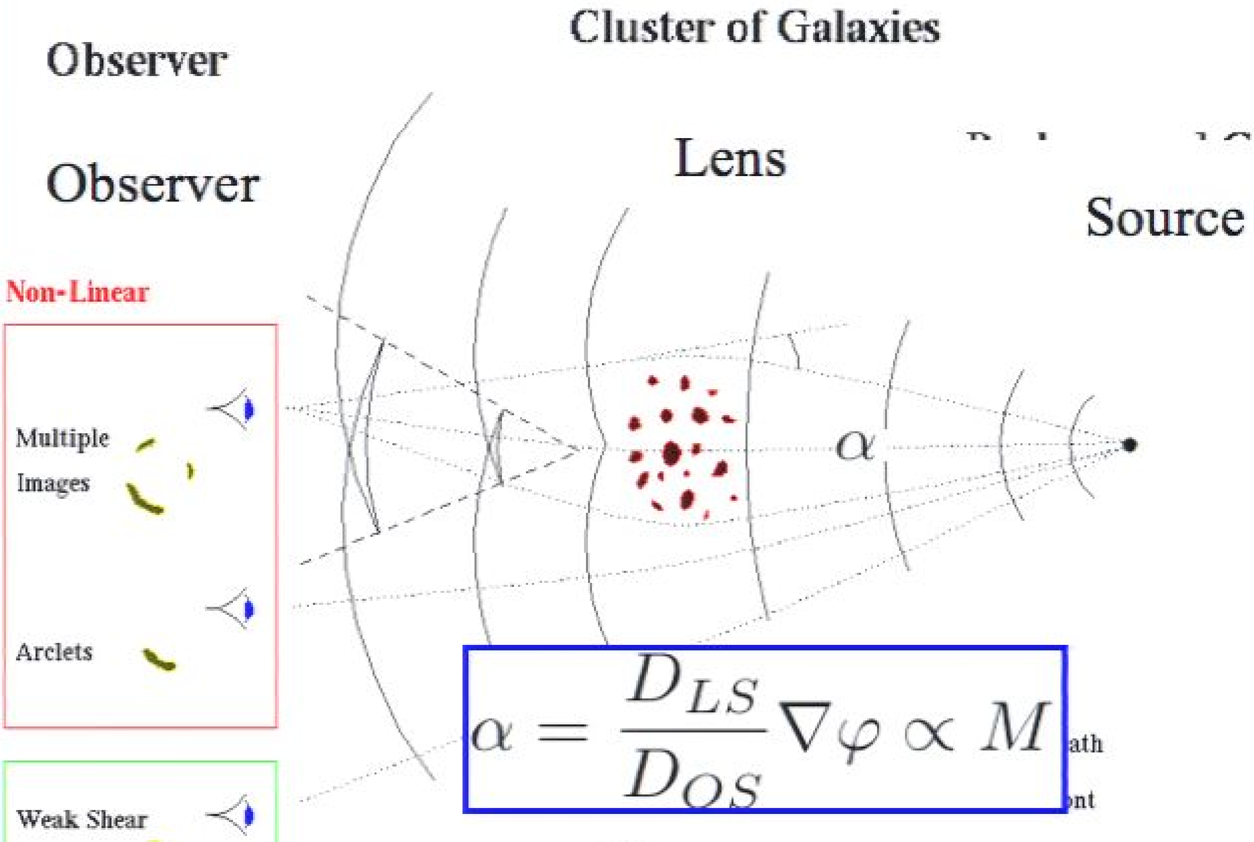

$$\boxed{\alpha = \frac{D_{LS}}{D_{OS}} \nabla\varphi \propto M}$$

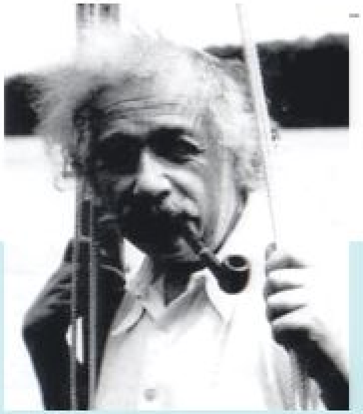

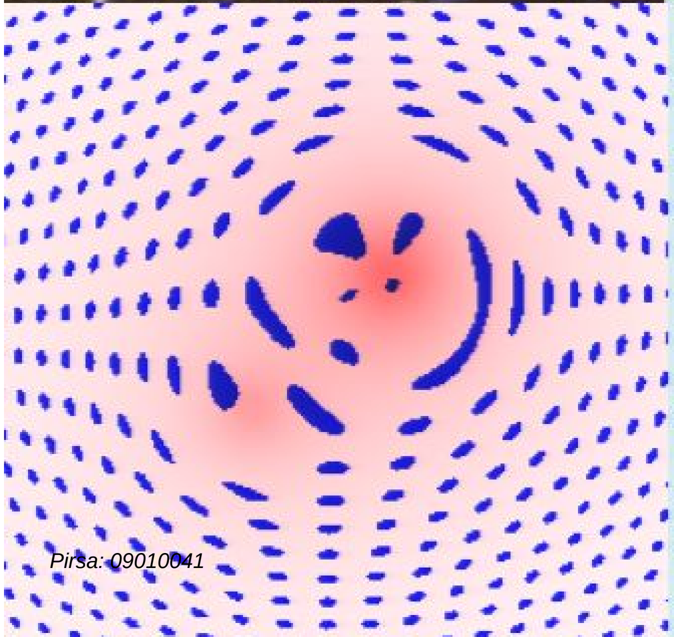

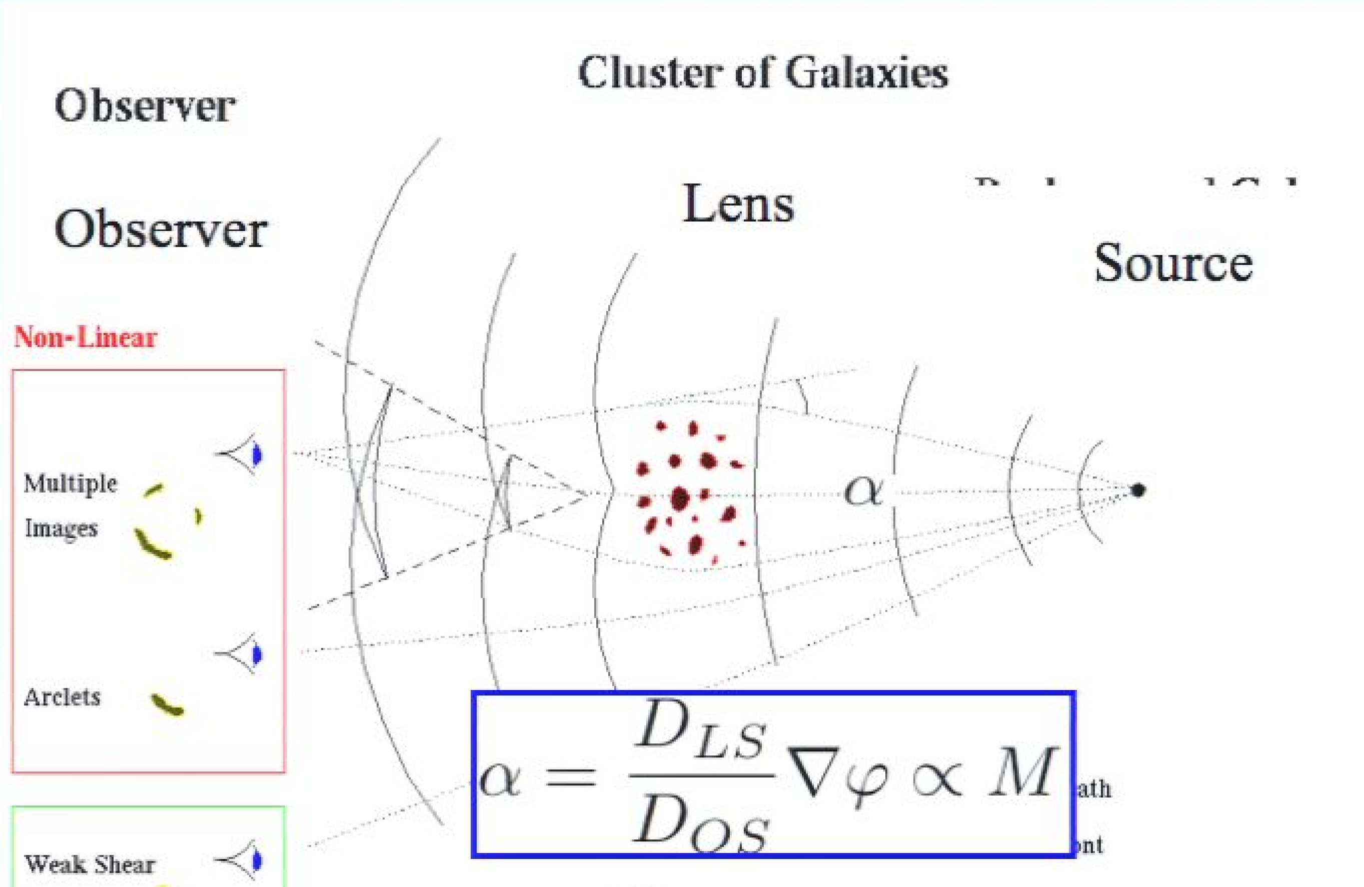

$$\alpha = \frac{D_{LS}}{D_{OS}} \nabla \varphi \propto M$$

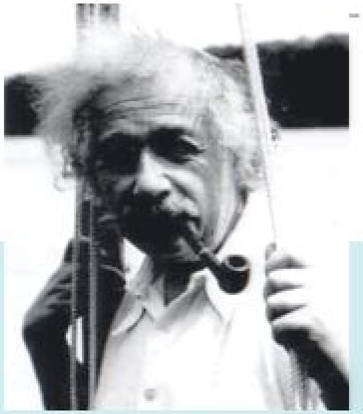

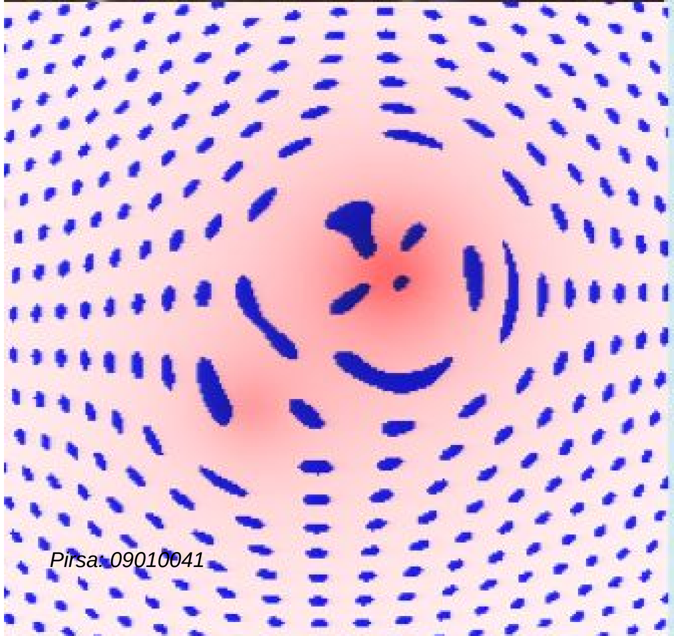

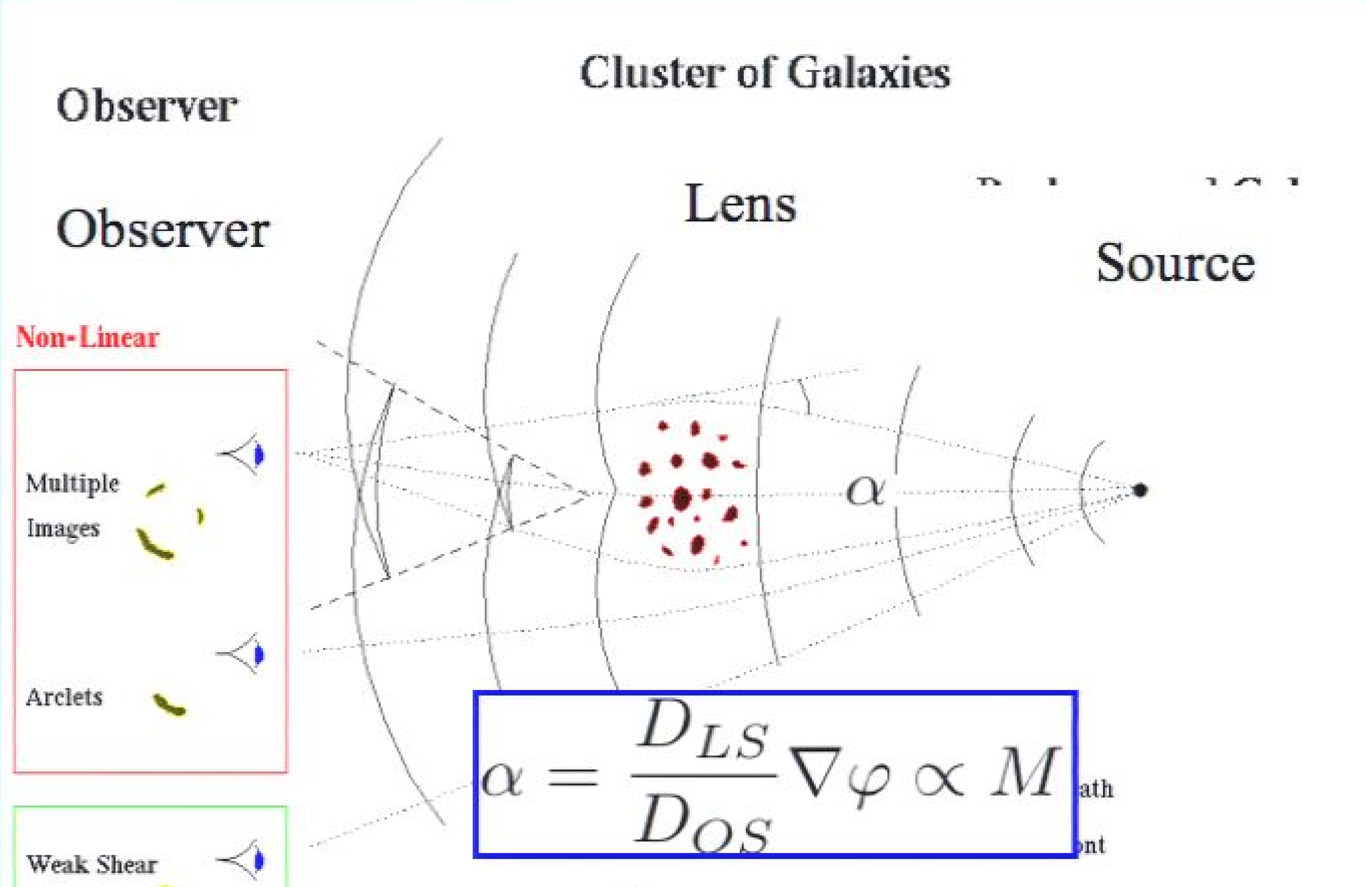

$$\alpha = \frac{D_{LS}}{D_{OS}} \nabla \varphi \propto M$$

Multiple Images Area

Linear

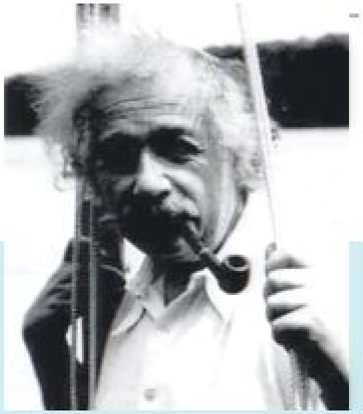

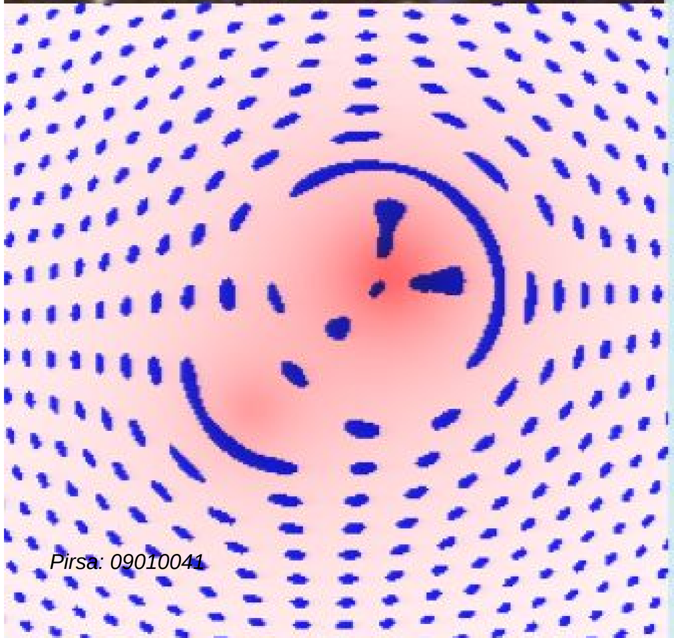

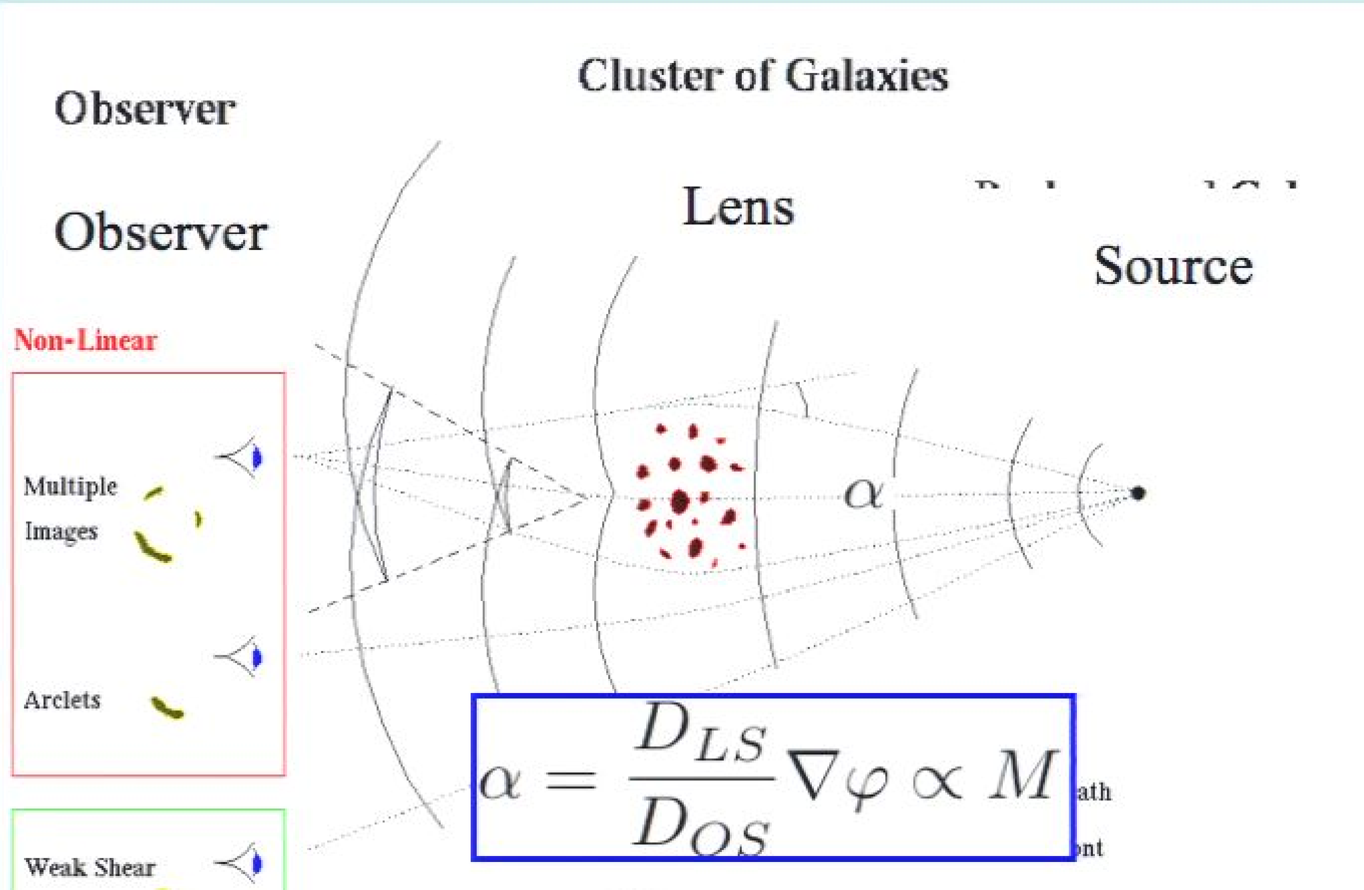

$$\boxed{\alpha = \frac{D_{LS}}{D_{OS}} \nabla \varphi \propto M}$$

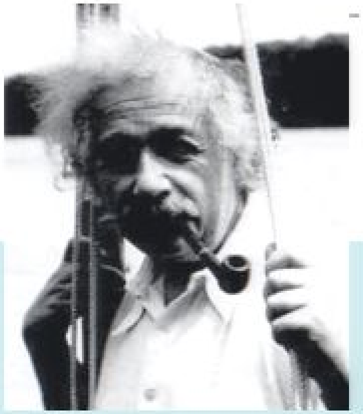

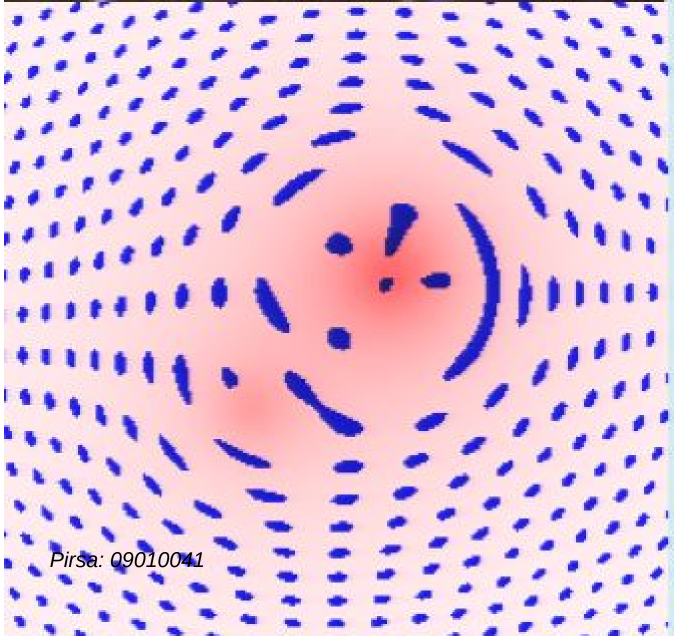

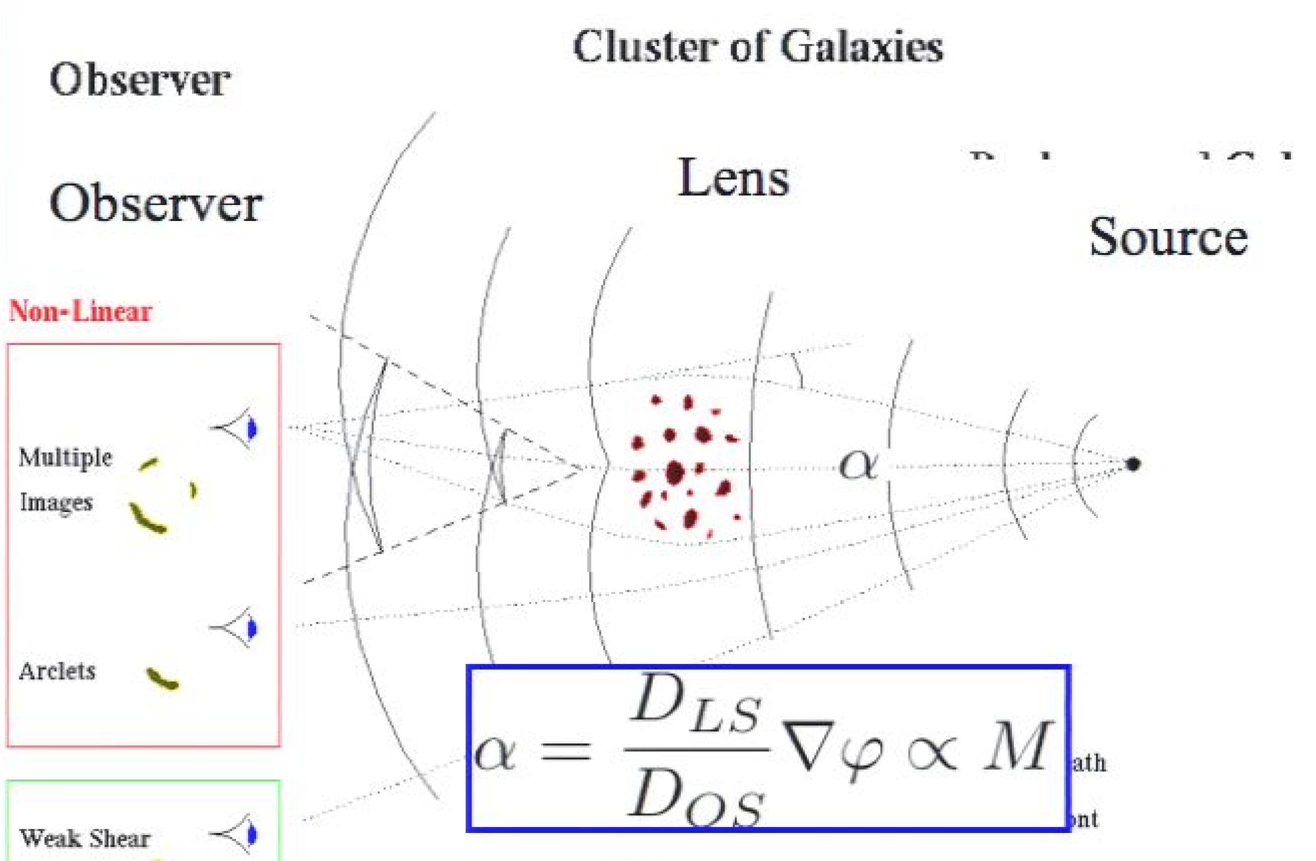

$$\boxed{\alpha = \frac{D_{LS}}{D_{OS}} \nabla \varphi \propto M}$$

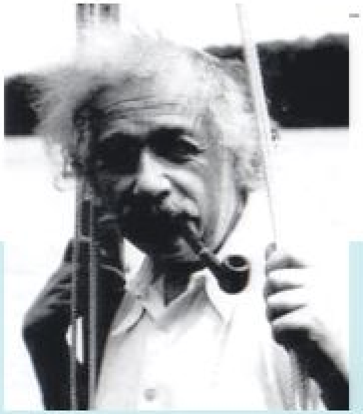

CFHT 1990

Z_cluster=0.375

Z_arc=0.725 (Soucail et al 1988)

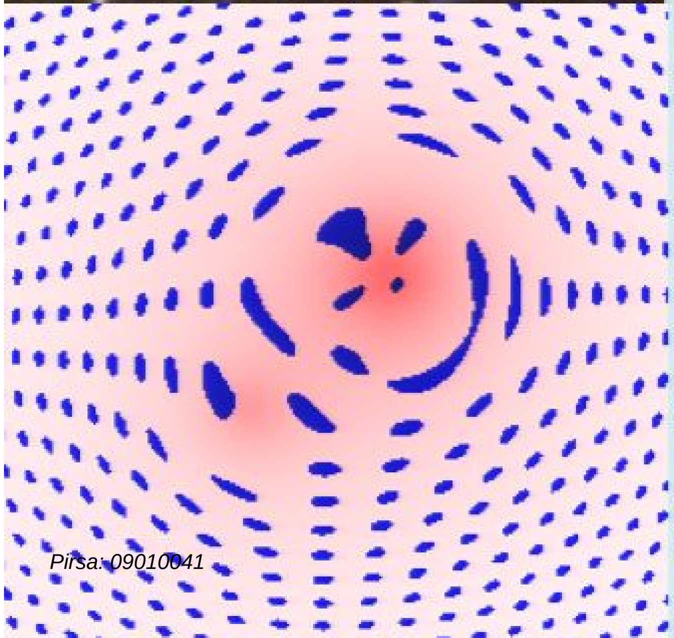

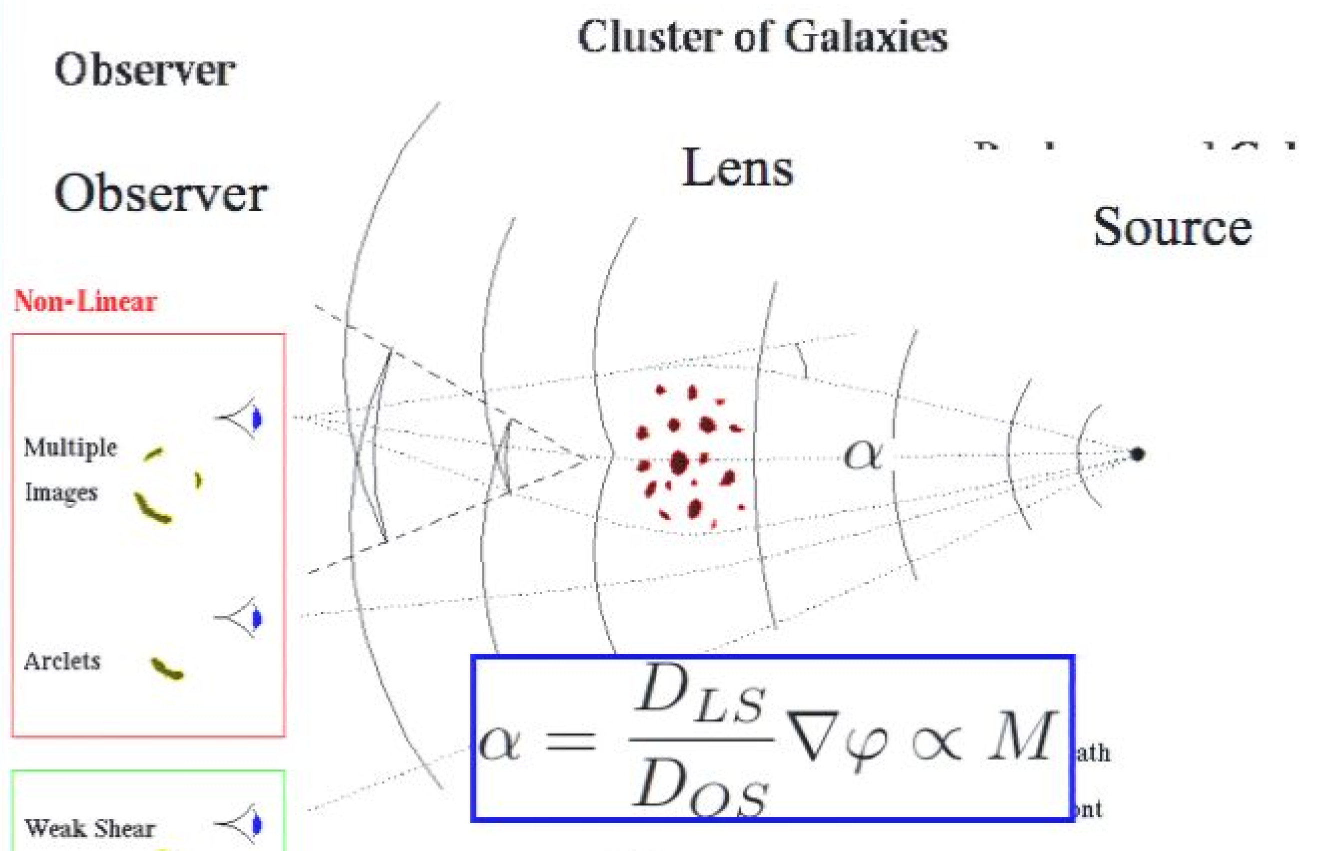

$$\alpha = \frac{D_{LS}}{D_{OS}} \nabla\varphi \propto M$$

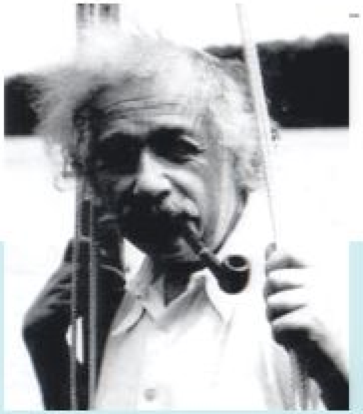

CFHT 1990

Z_cluster=0.375

Z_arc=0.725 (Soucail et al 1988)

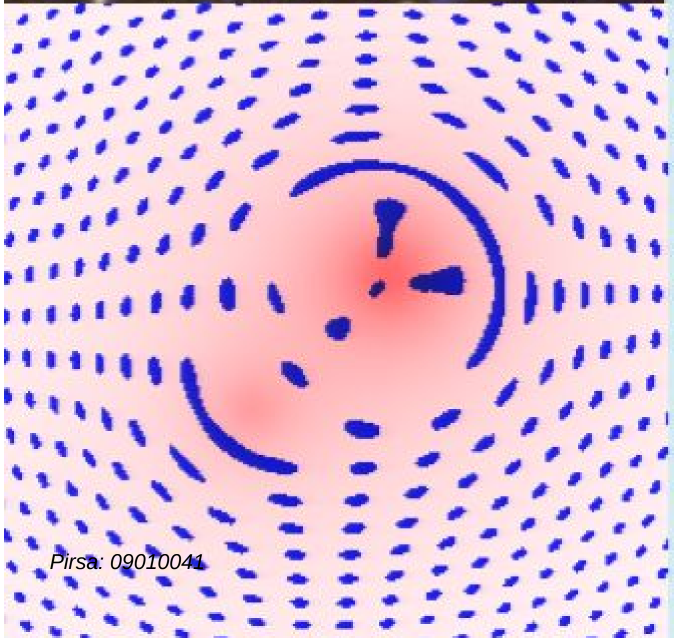

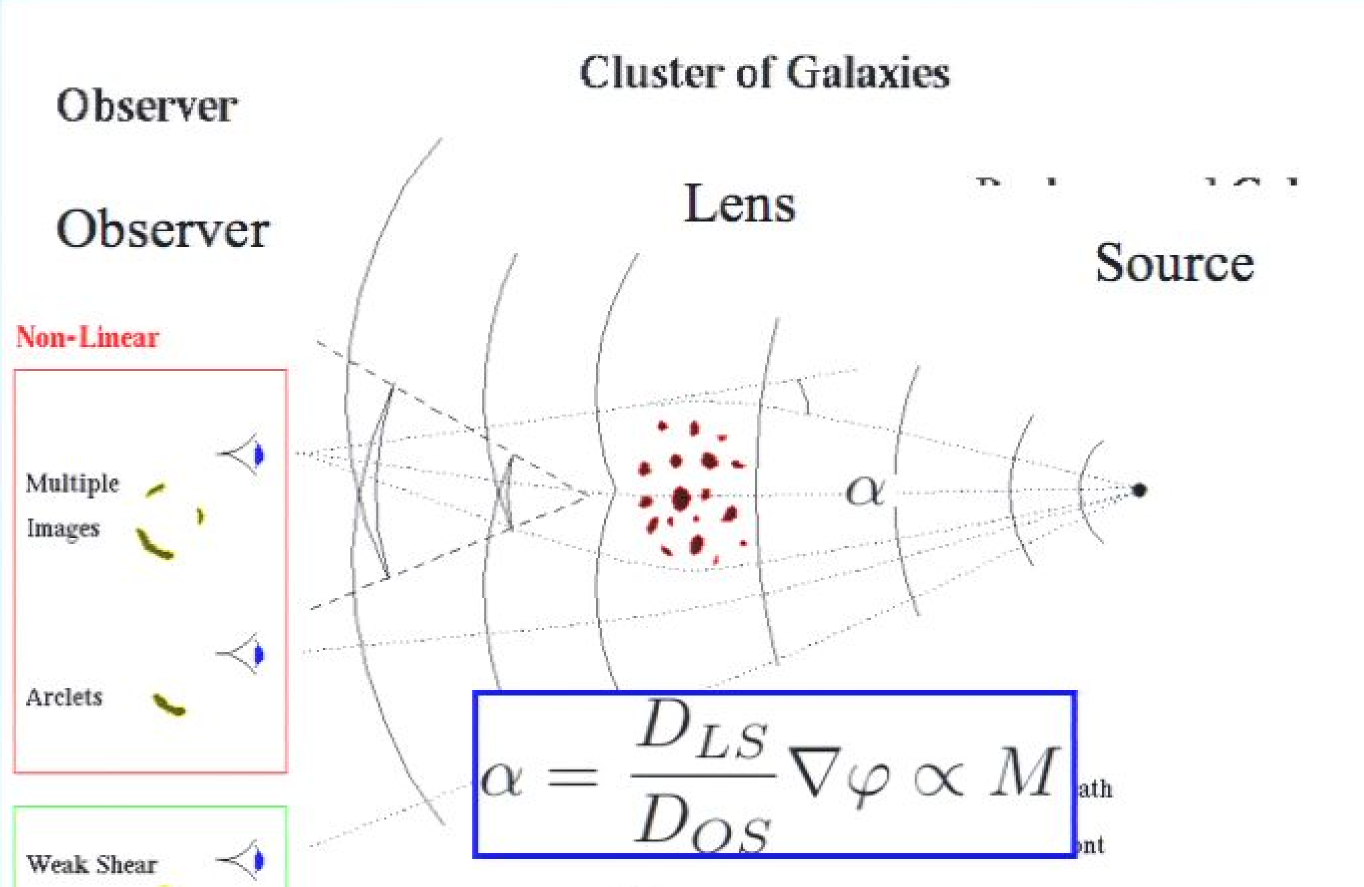

$$\alpha = \frac{D_{LS}}{D_{OS}} \nabla \varphi \propto M$$

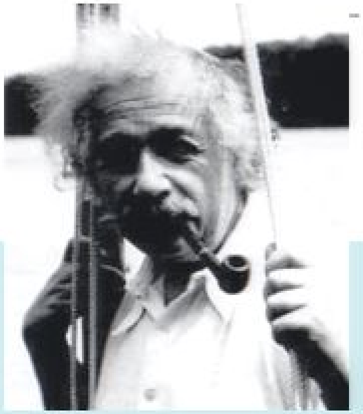

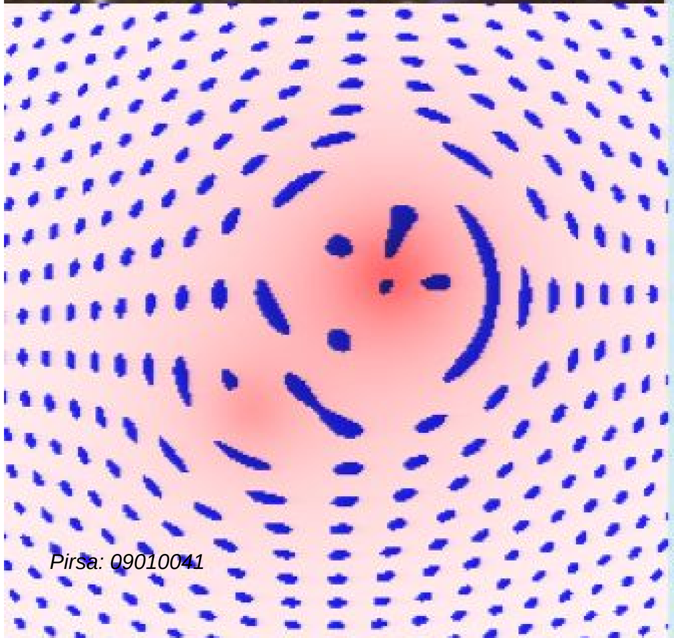

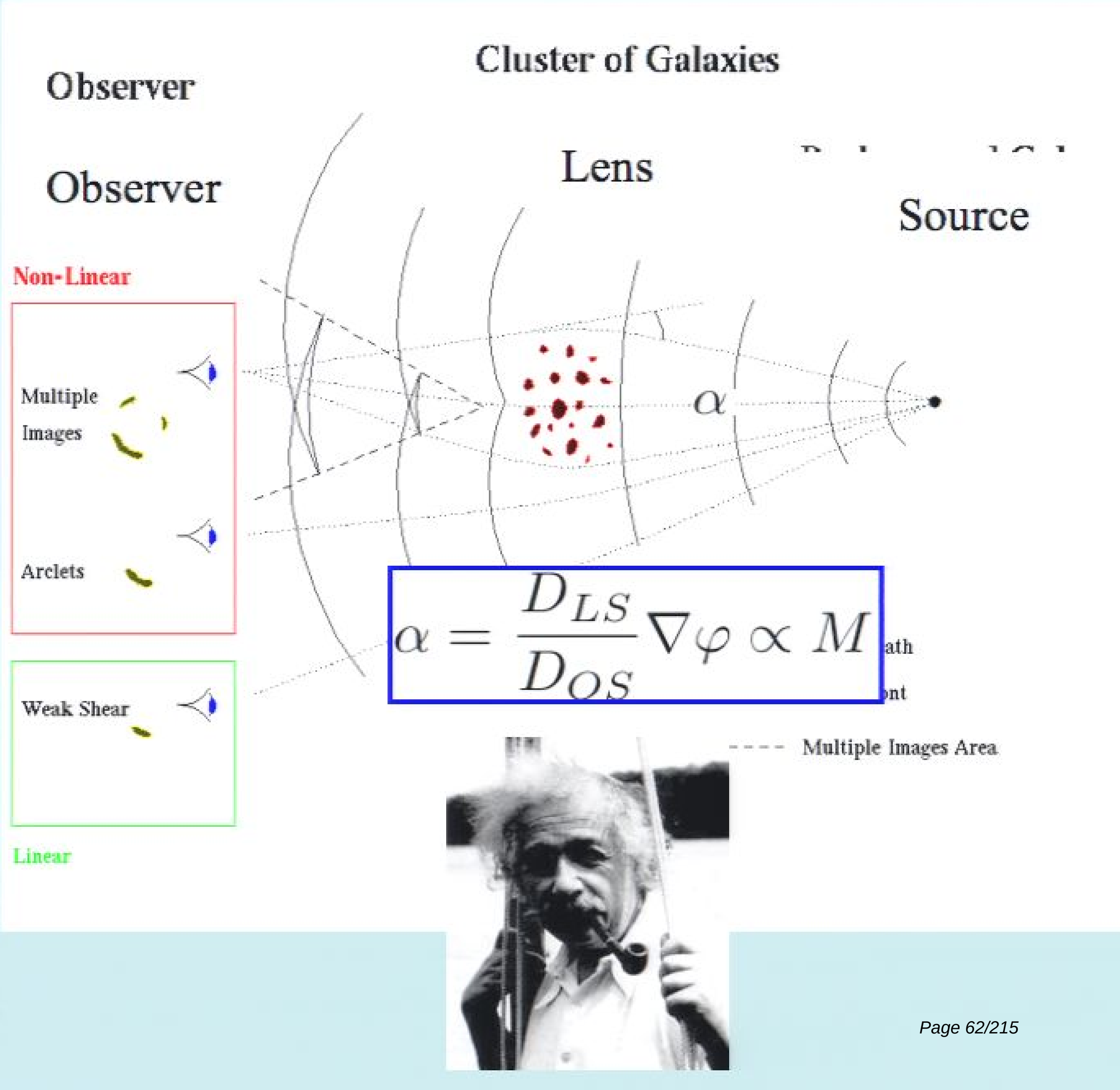

$$\alpha = \frac{D_{LS}}{D_{OS}} \nabla \varphi \propto M$$

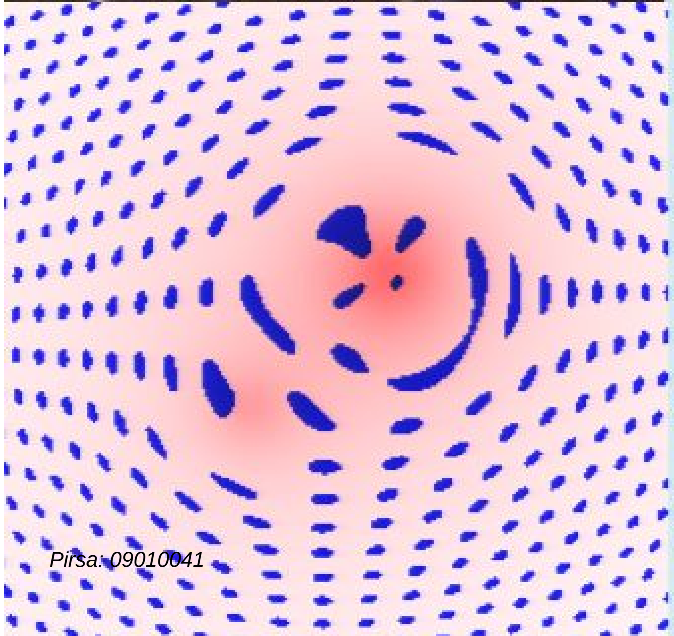

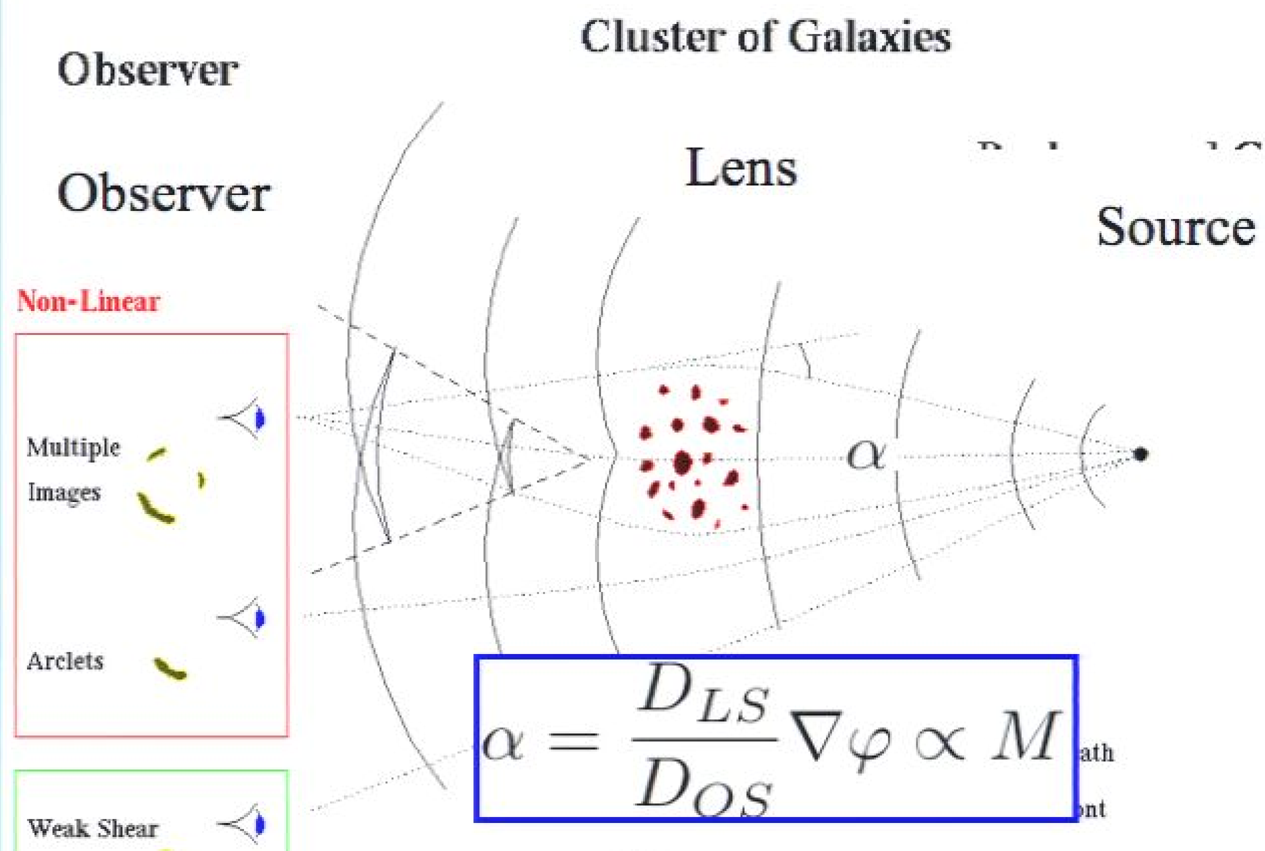

$$\alpha = \frac{D_{LS}}{D_{OS}} \nabla \varphi \propto M$$

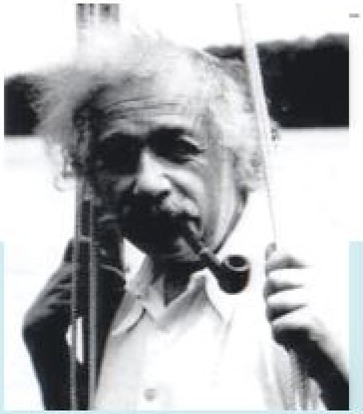

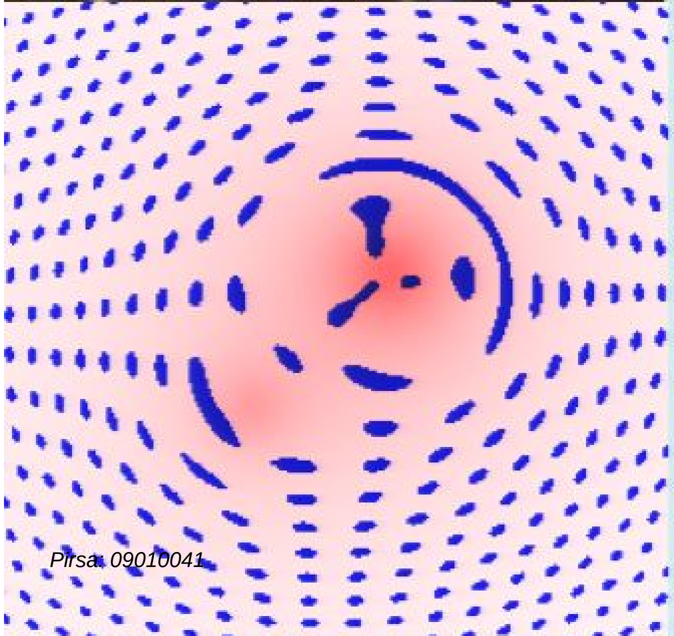

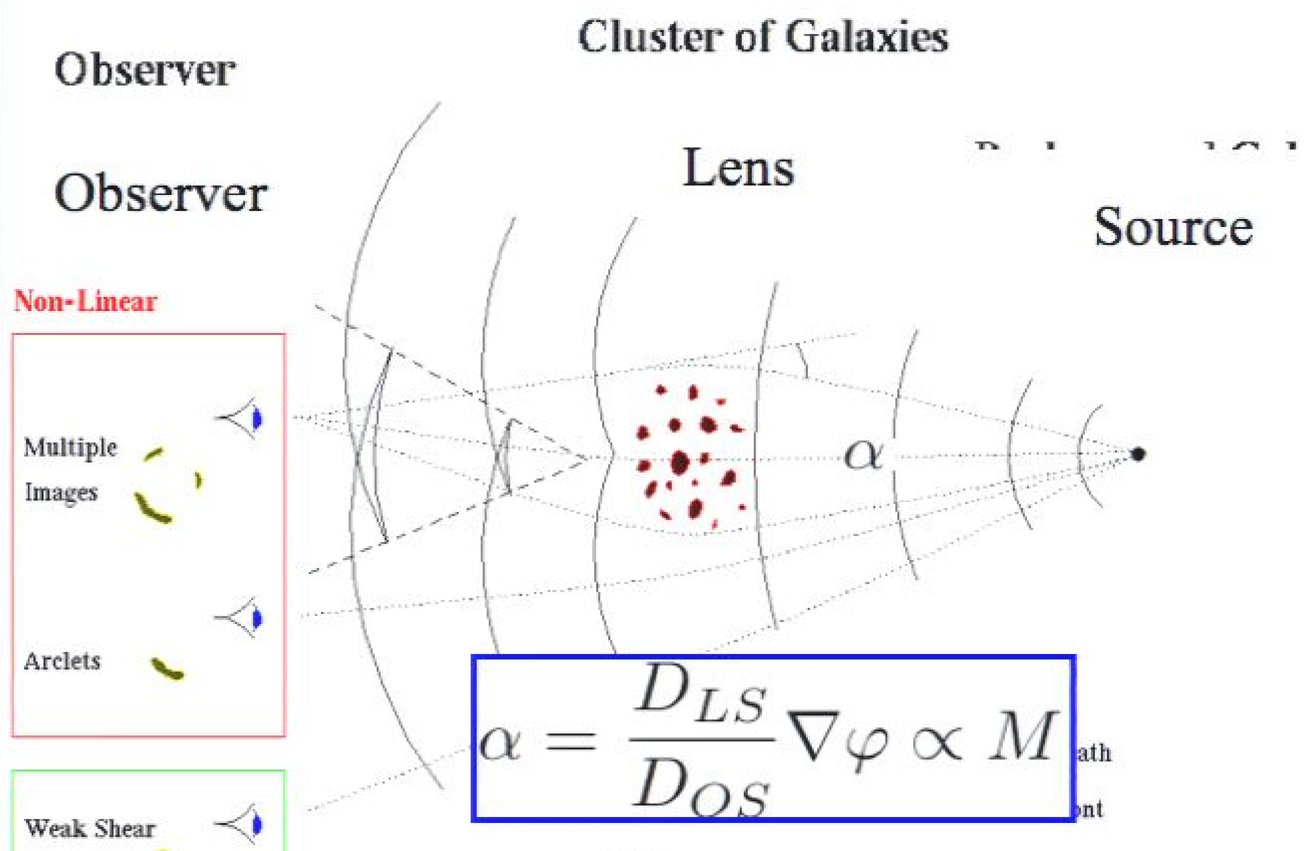

$$\boxed{\alpha = \frac{D_{LS}}{D_{OS}} \nabla \varphi \propto M}$$

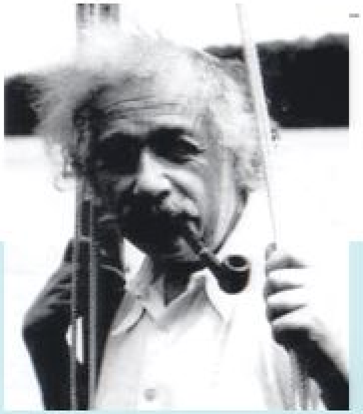

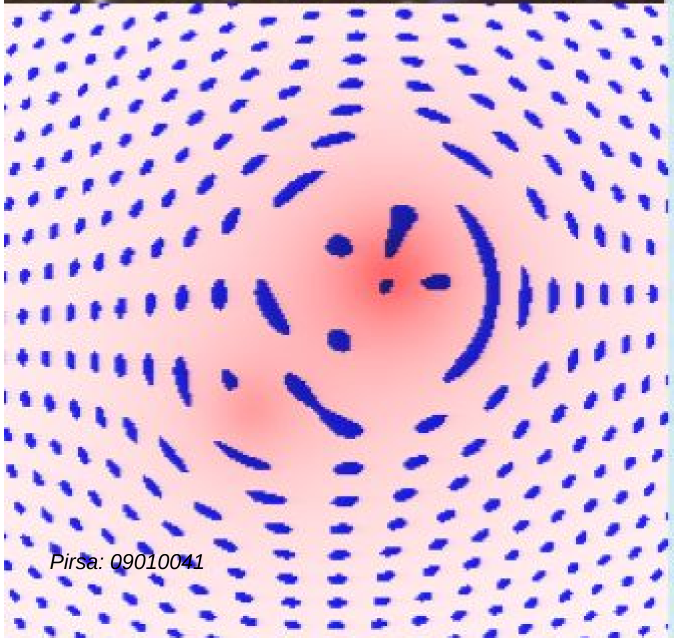

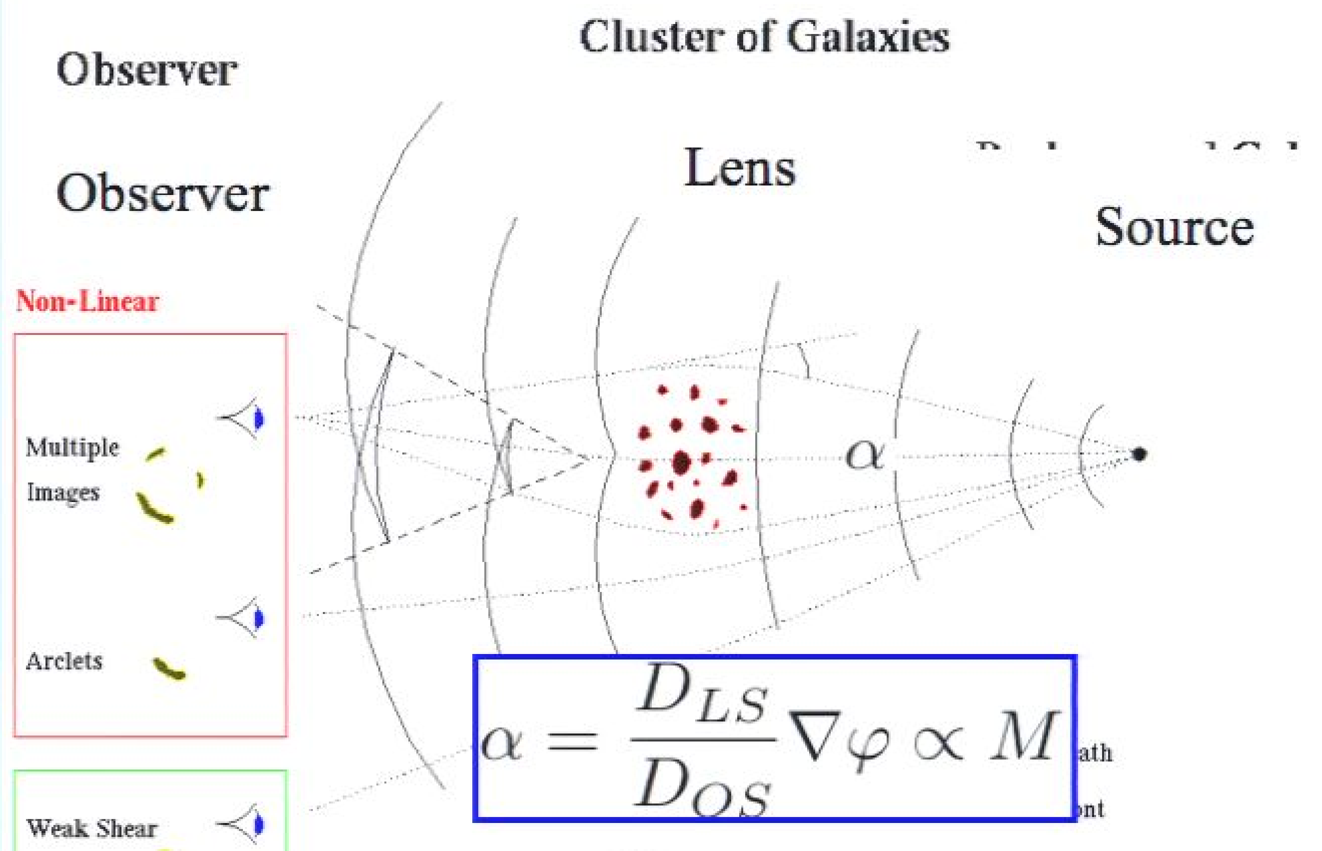

$$\alpha = \frac{D_{LS}}{D_{OS}} \nabla \varphi \propto M$$

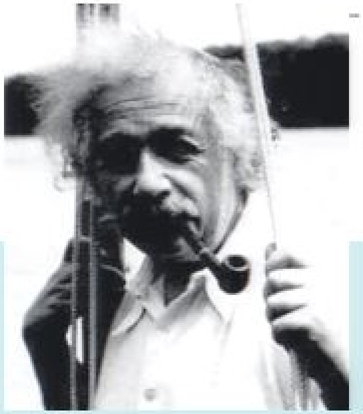

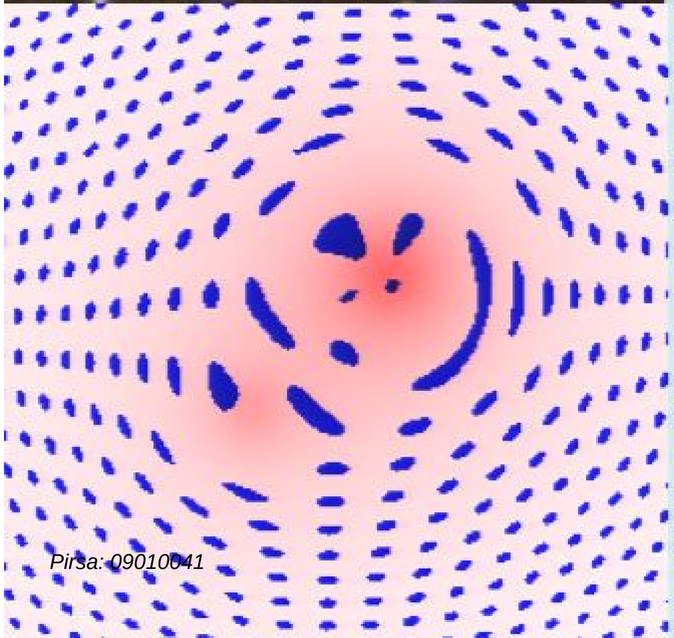

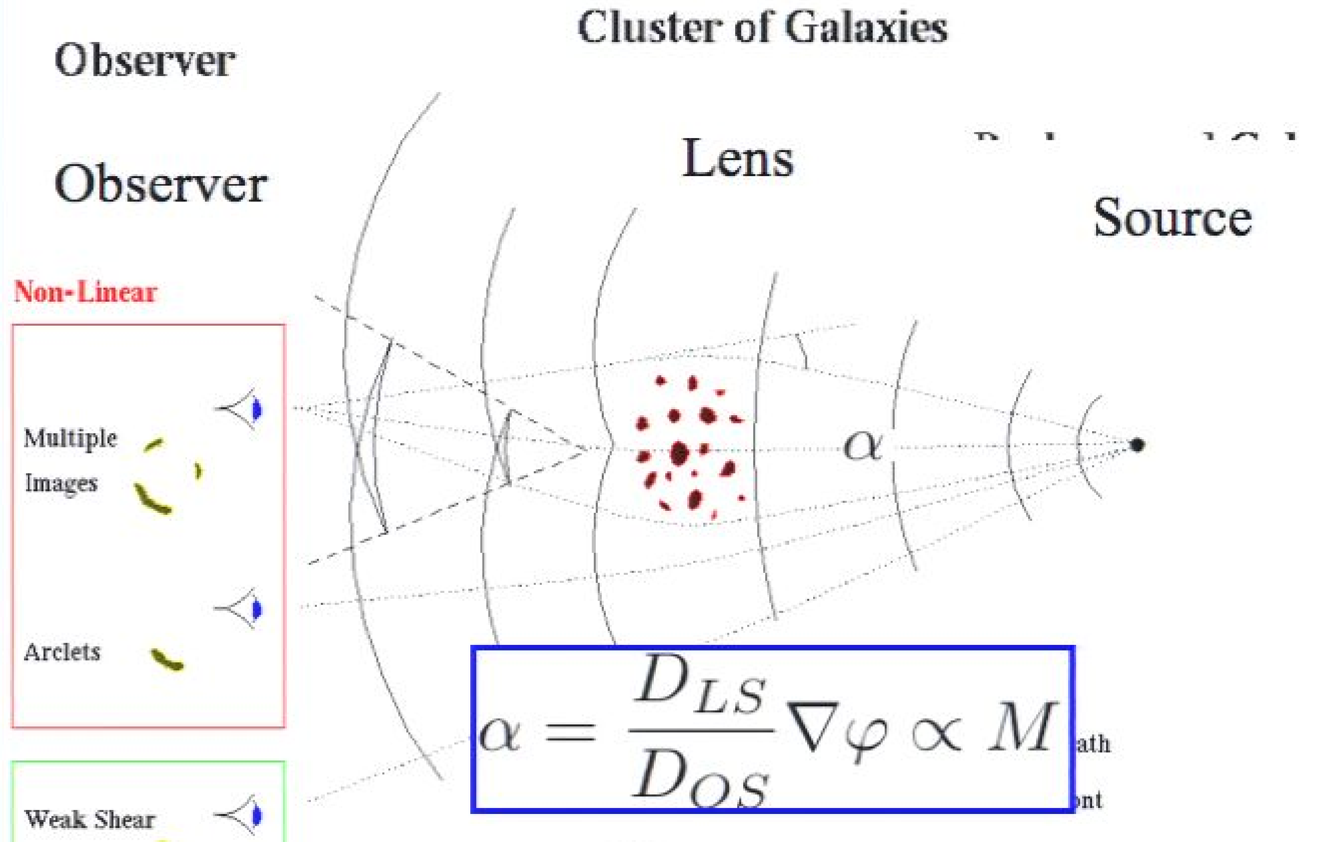

$$\alpha = \frac{D_{LS}}{D_{OS}} \nabla \varphi \propto M$$

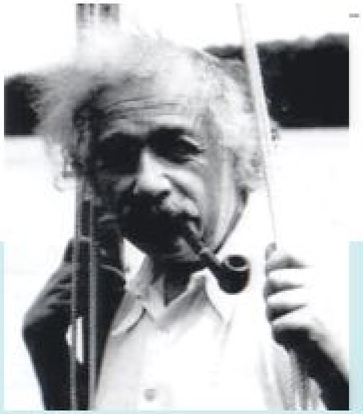

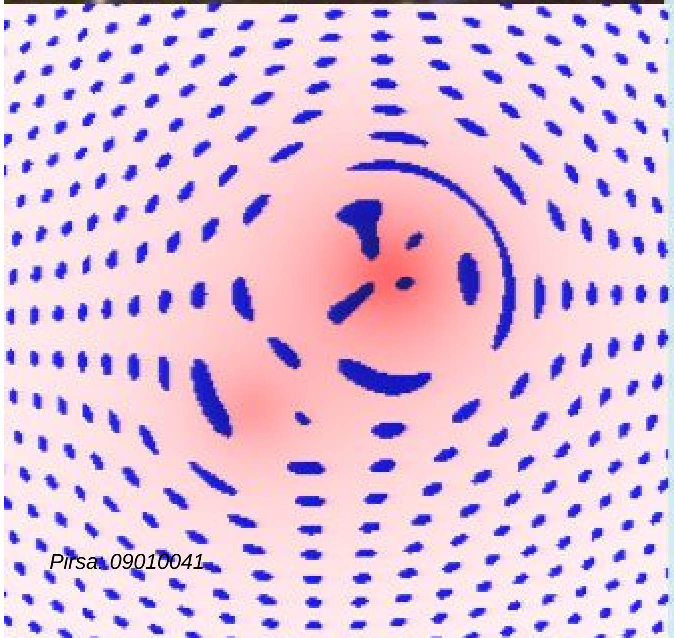

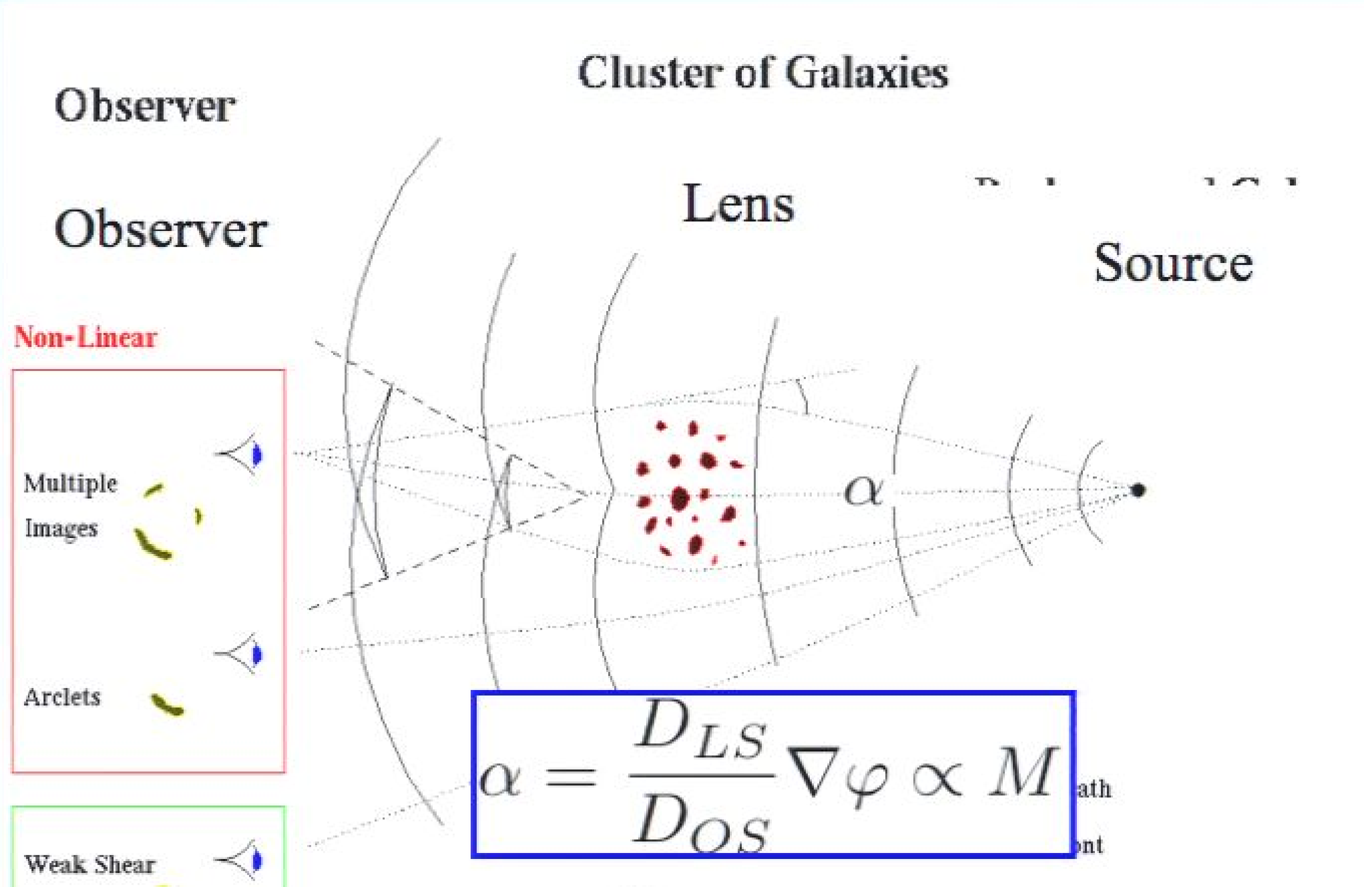

$$\alpha = \frac{D_{LS}}{D_{OS}} \nabla \varphi \propto M$$

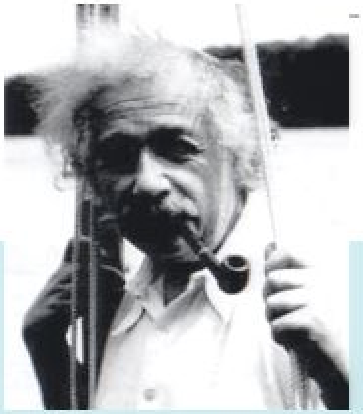


CFHT 1990
Z_cluster=0.375
Z_arc=0.725 (Soucail et al 1988)

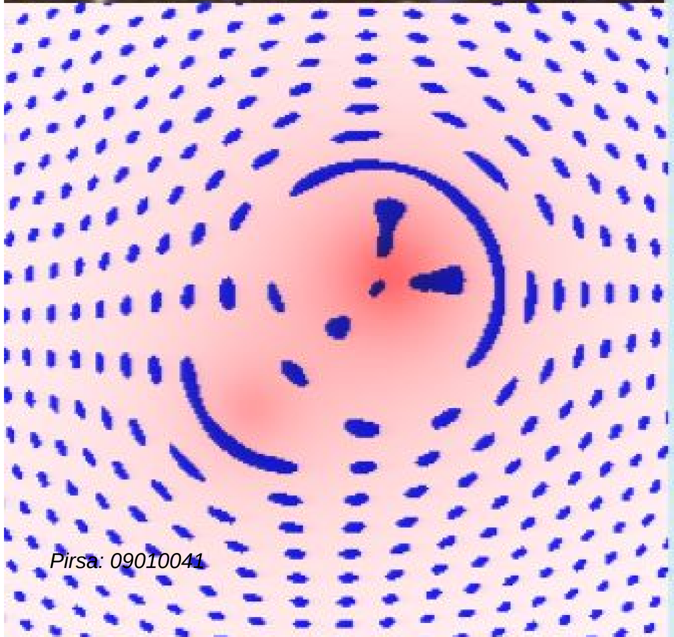

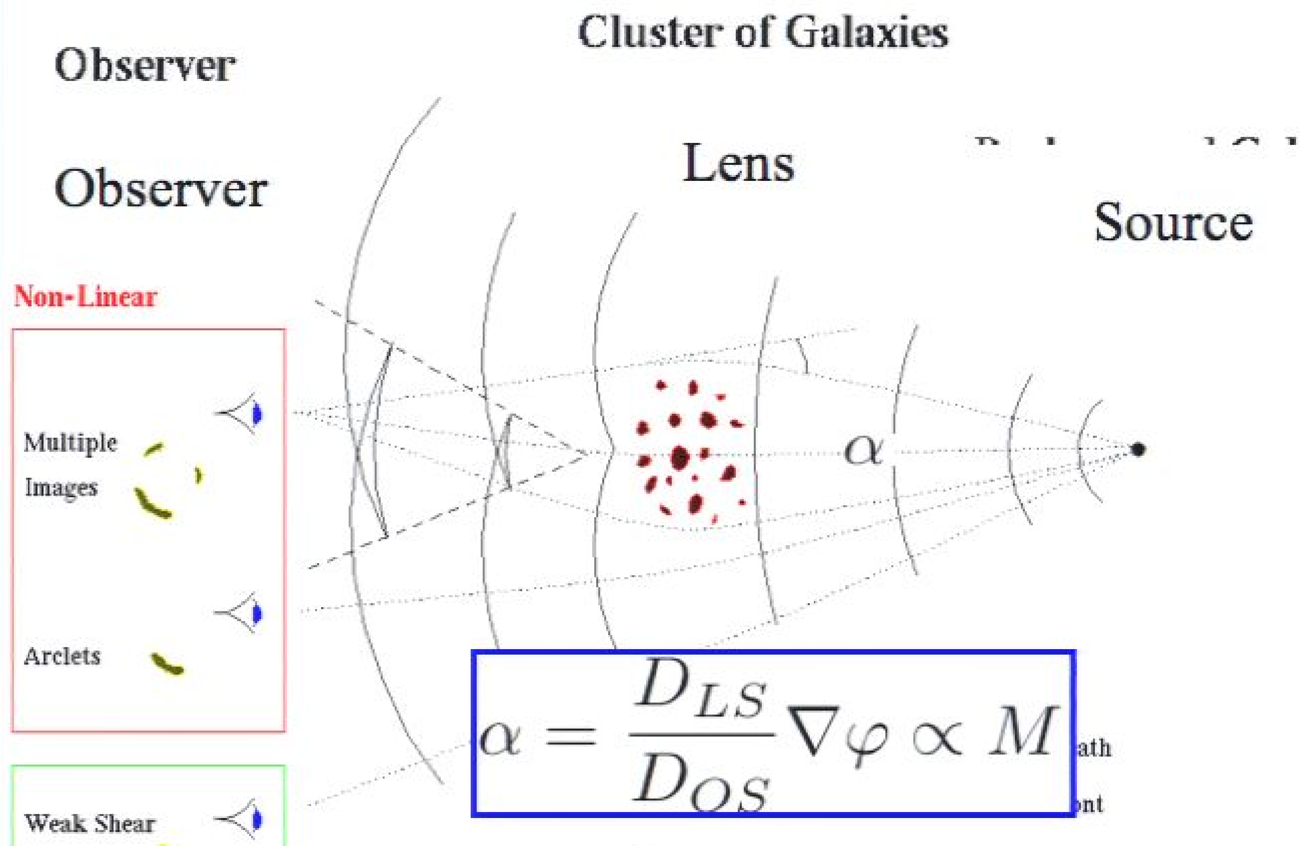

$$\alpha = \frac{D_{LS}}{D_{OS}} \nabla \varphi \propto M$$

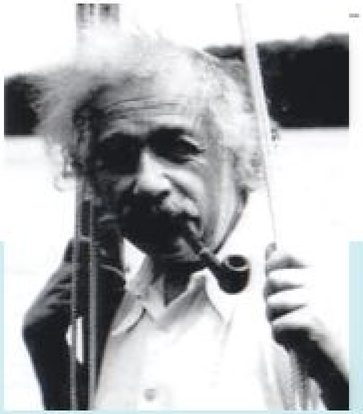

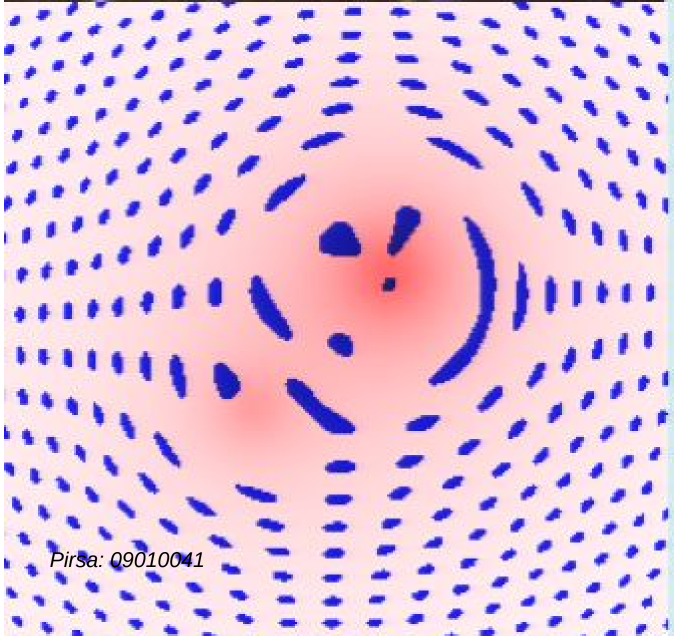

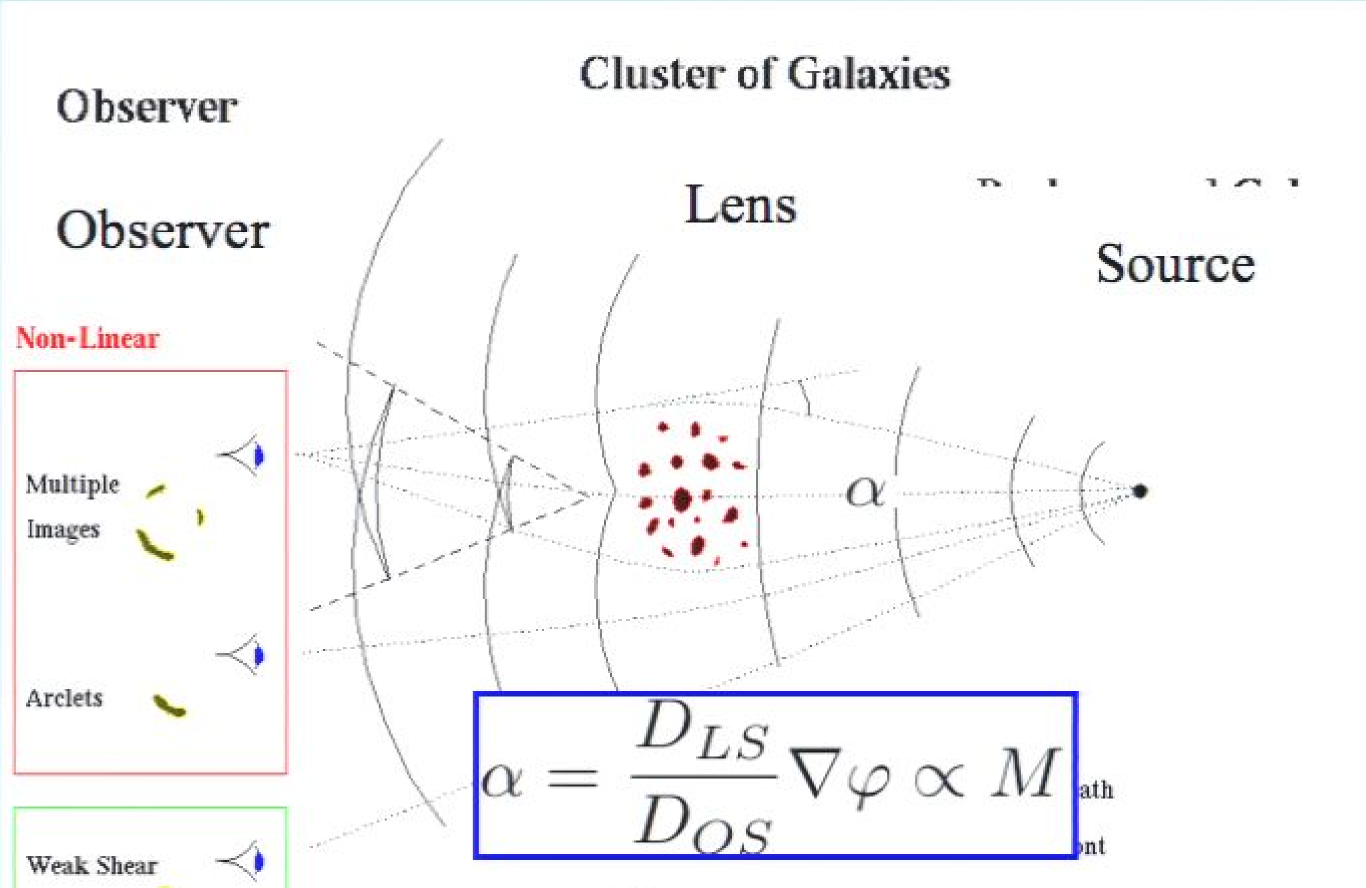

$$\alpha = \frac{D_{LS}}{D_{OS}} \nabla \varphi \propto M$$

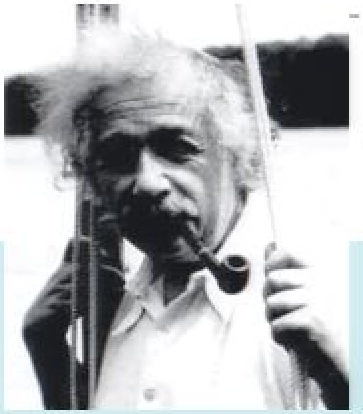

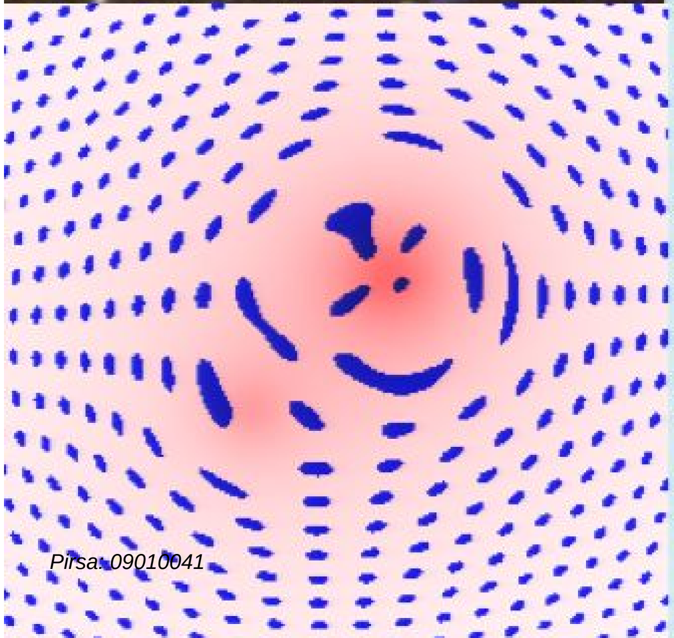

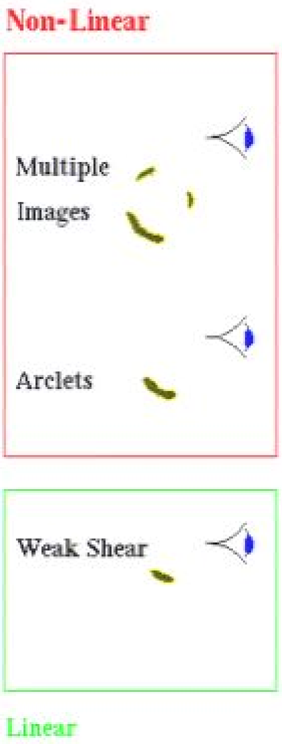

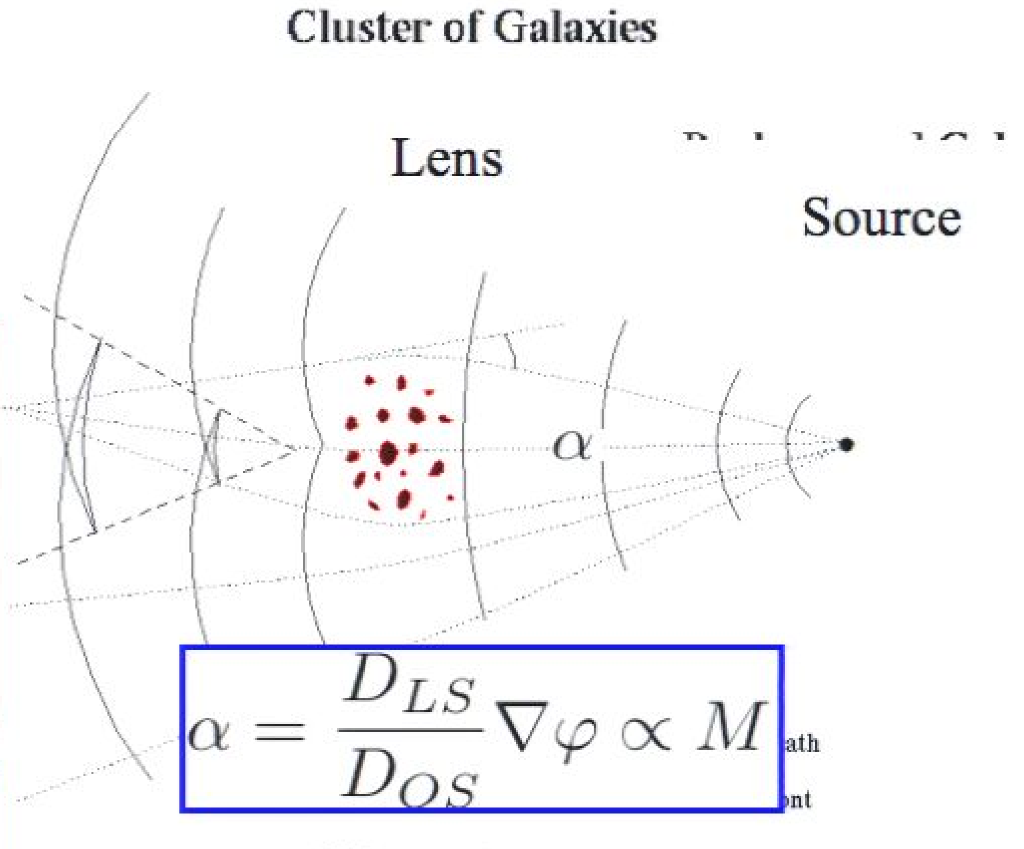

$$\alpha = \frac{D_{LS}}{D_{OS}} \nabla \varphi \propto M$$

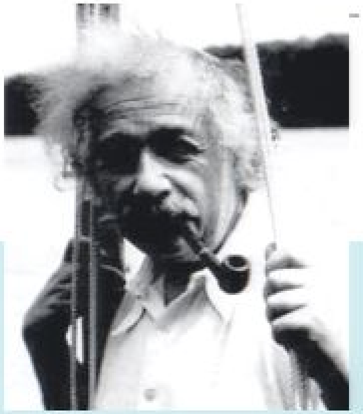

CFHT 1990

Z_cluster=0.375

Z_arc=0.725 (Soucail et al 1988)

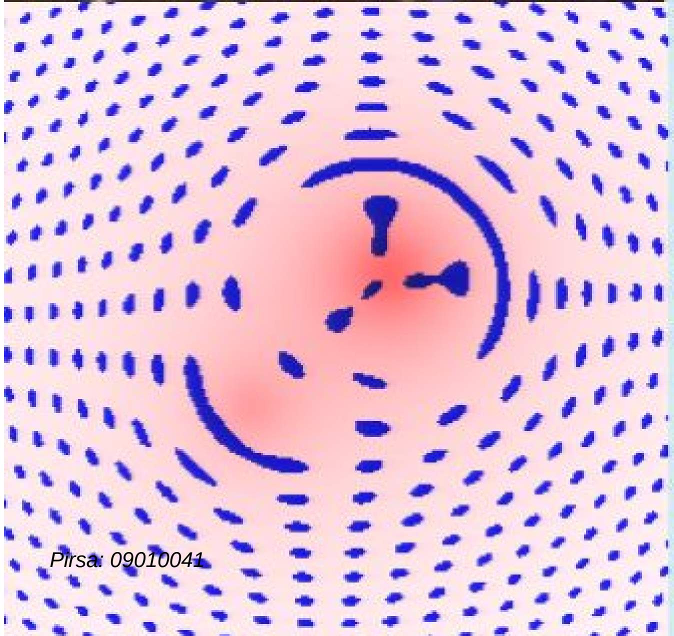

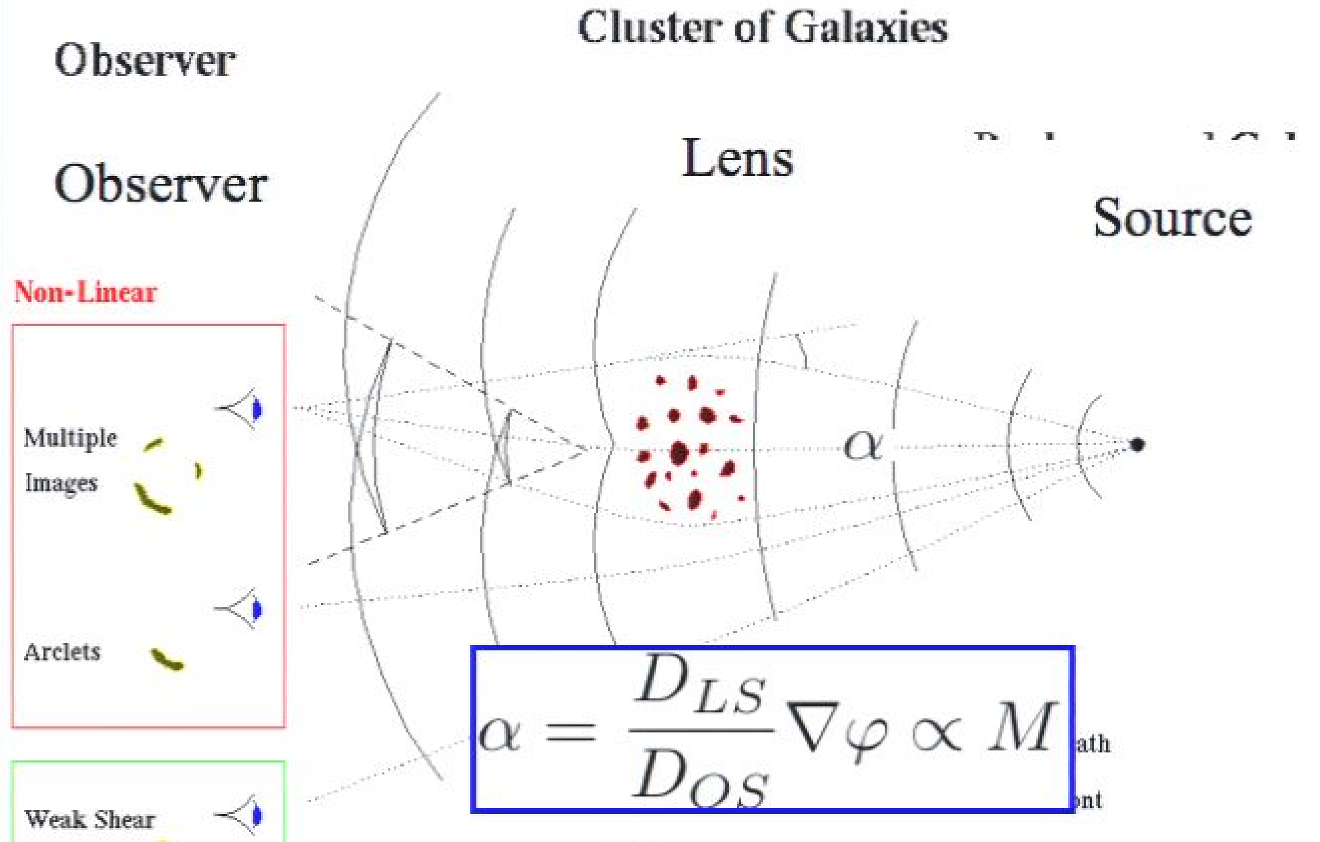

$$\alpha = \frac{D_{LS}}{D_{OS}} \nabla \varphi \propto M$$

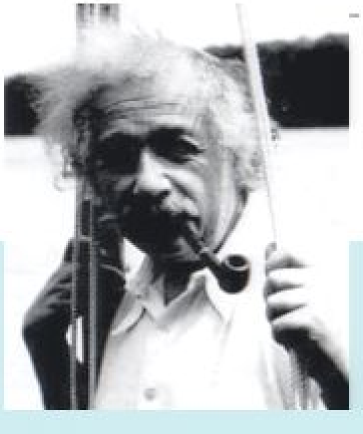

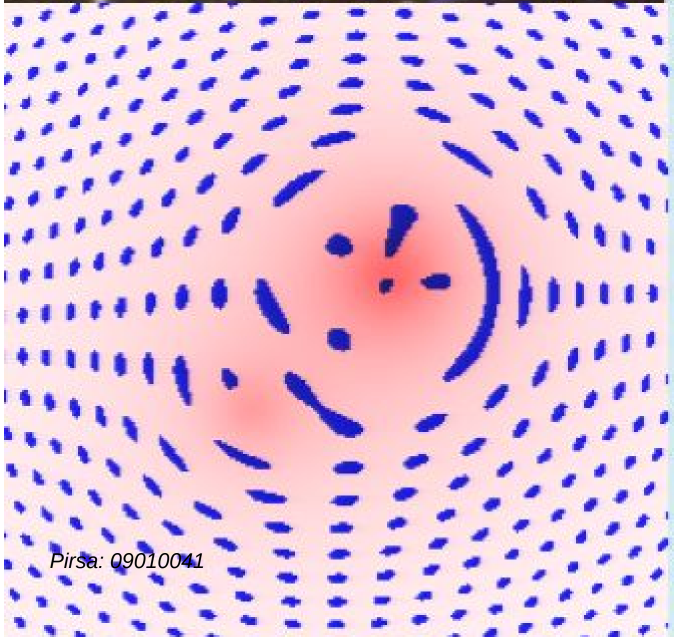

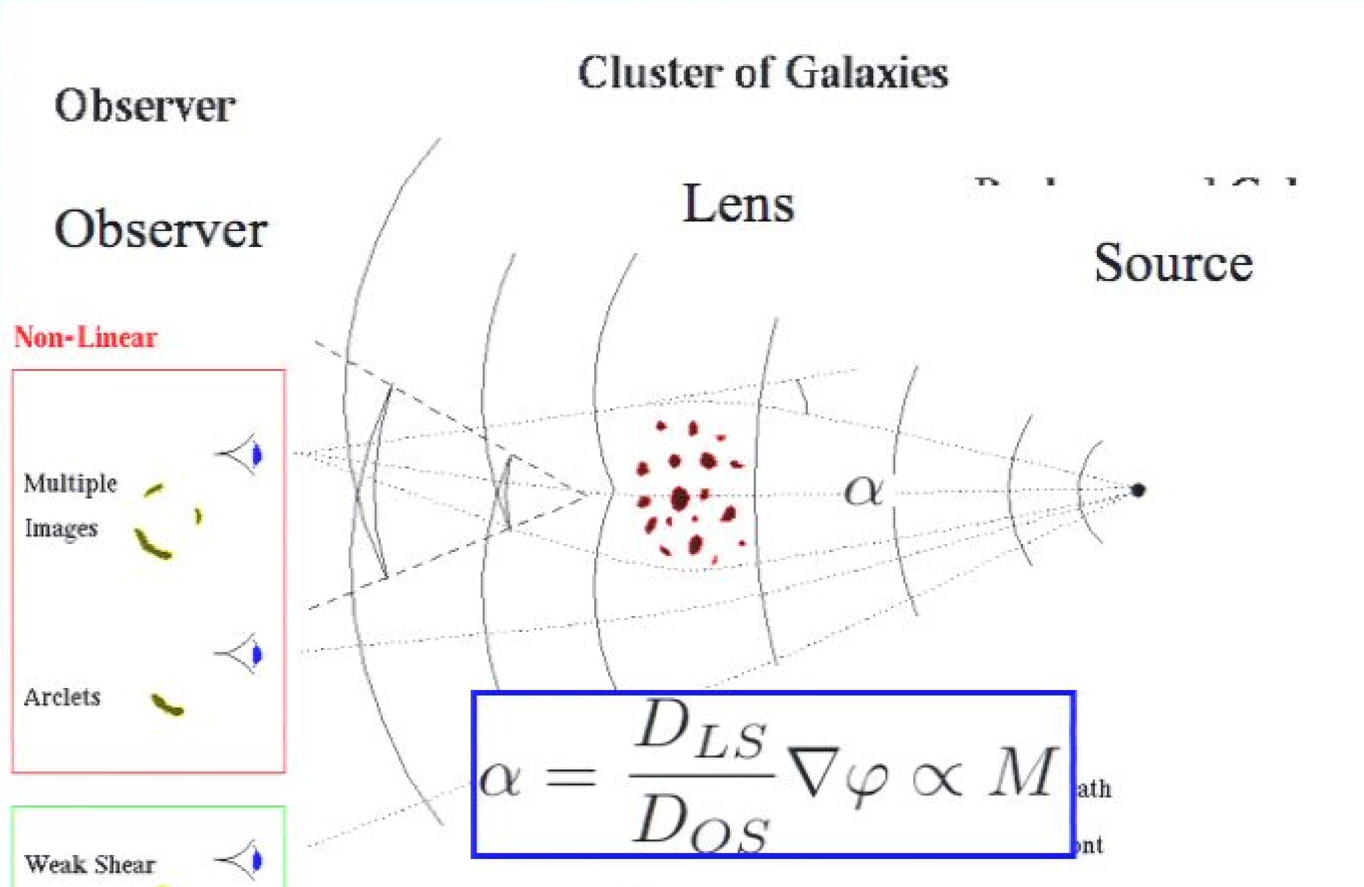

$$\alpha = \frac{D_{LS}}{D_{OS}} \nabla \varphi \propto M$$

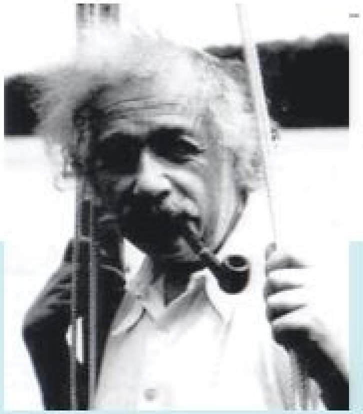

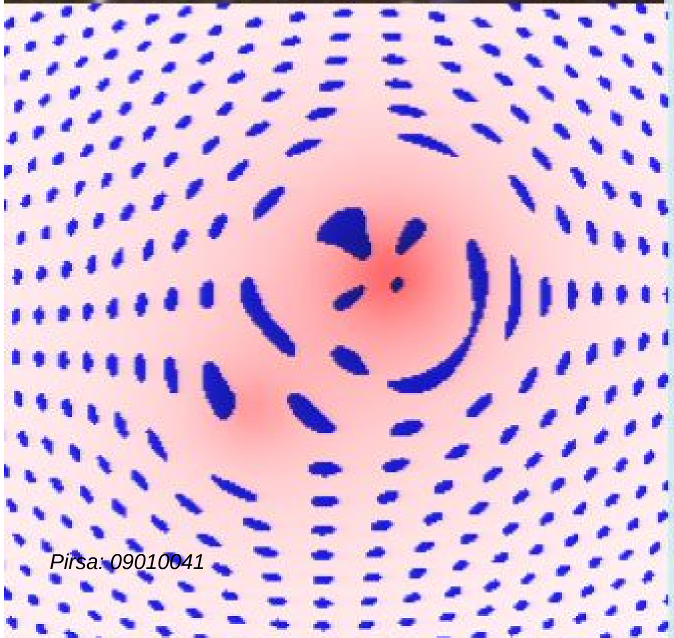

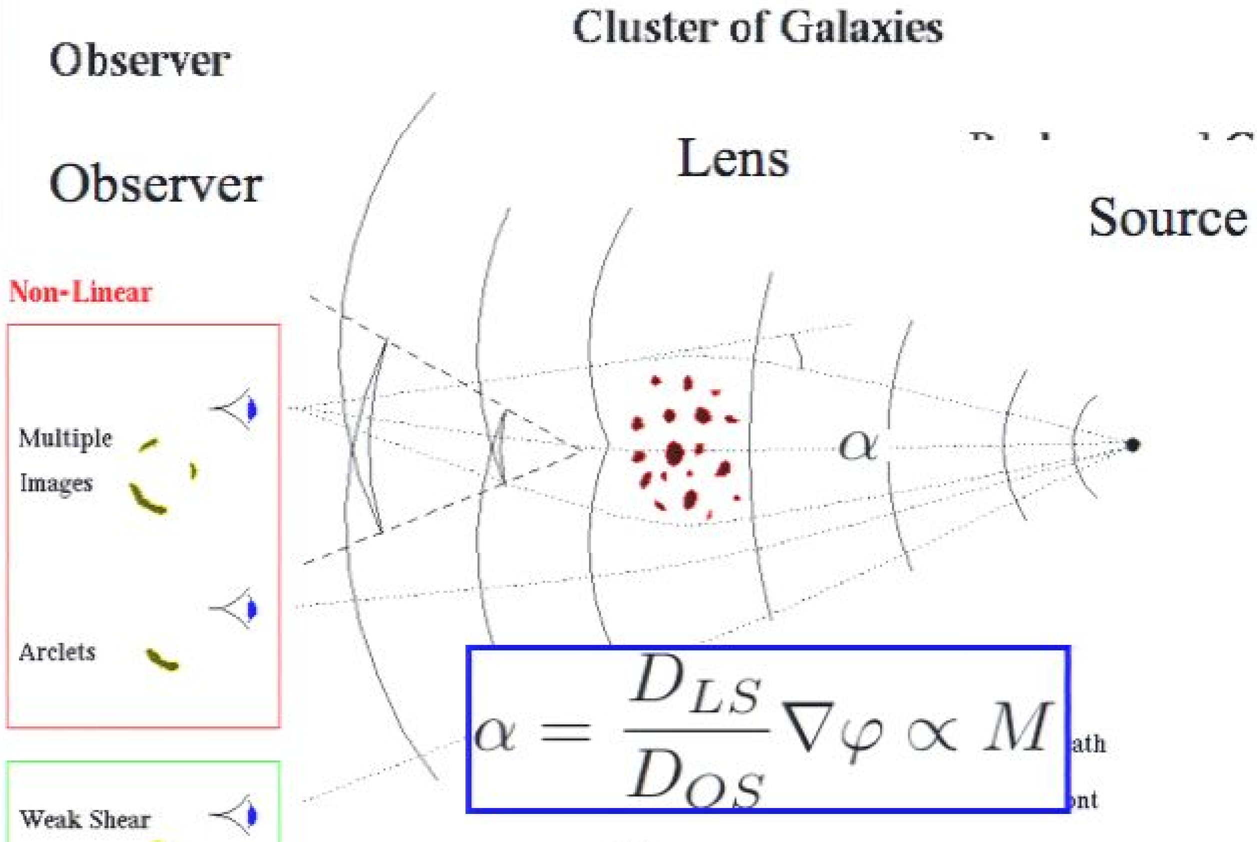

$$\boxed{\alpha = \frac{D_{LS}}{D_{OS}} \nabla \varphi \propto M}$$

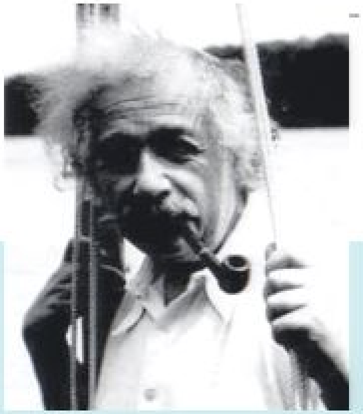

CFHT 1990

Z_cluster=0.375

Z_arc=0.725 (Soucail et al 1988)

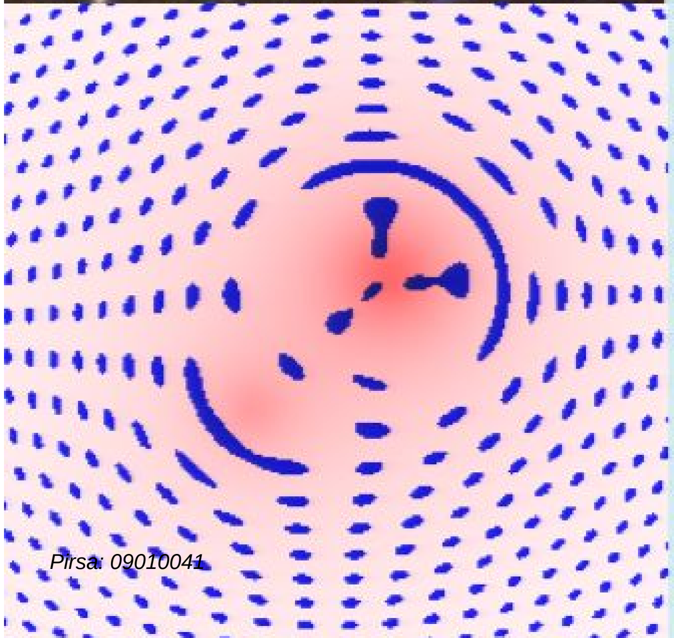

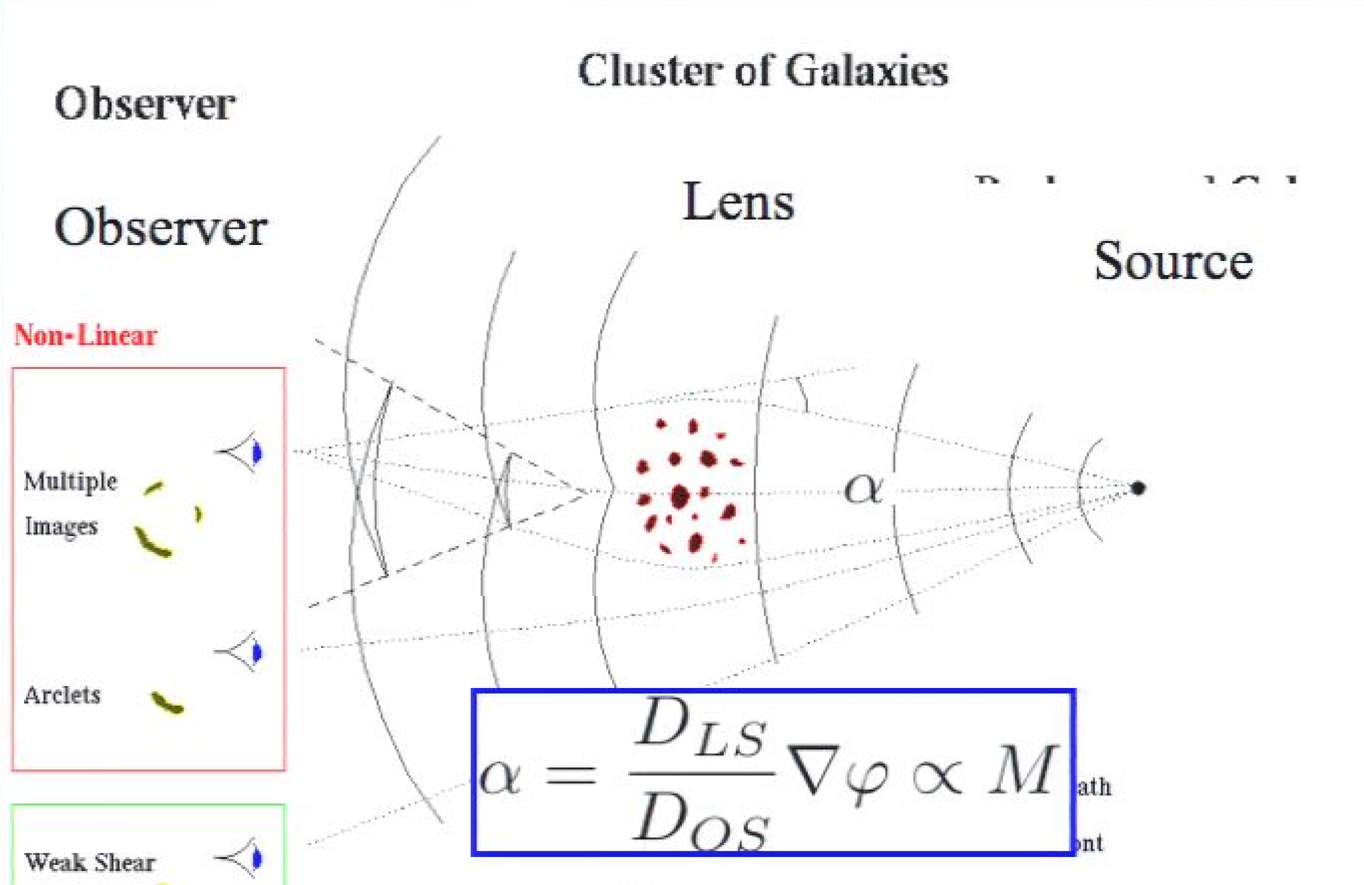

$$\alpha = \frac{D_{LS}}{D_{OS}} \nabla \varphi \propto M$$

- - - - Multiple Images Area

Linear

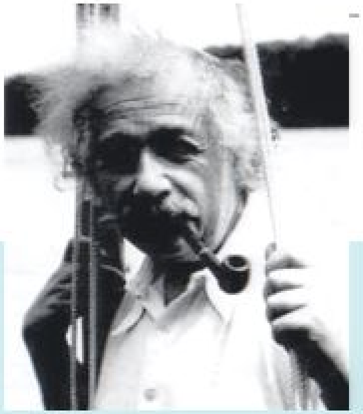

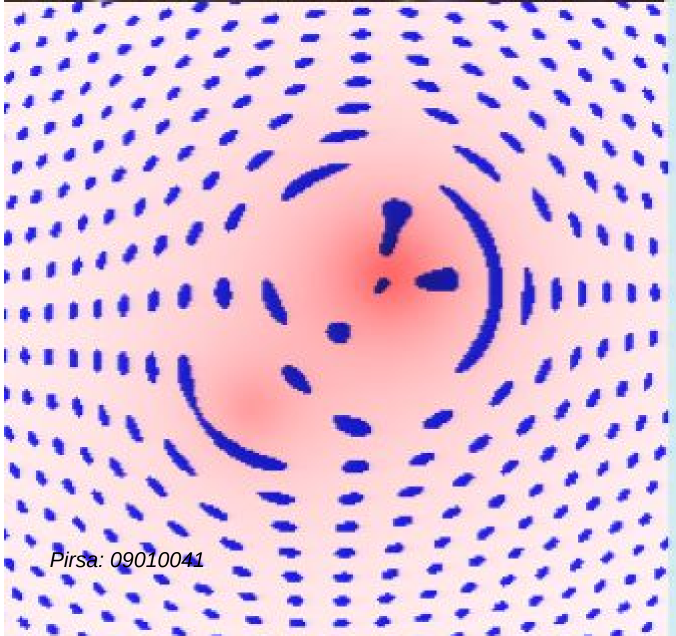

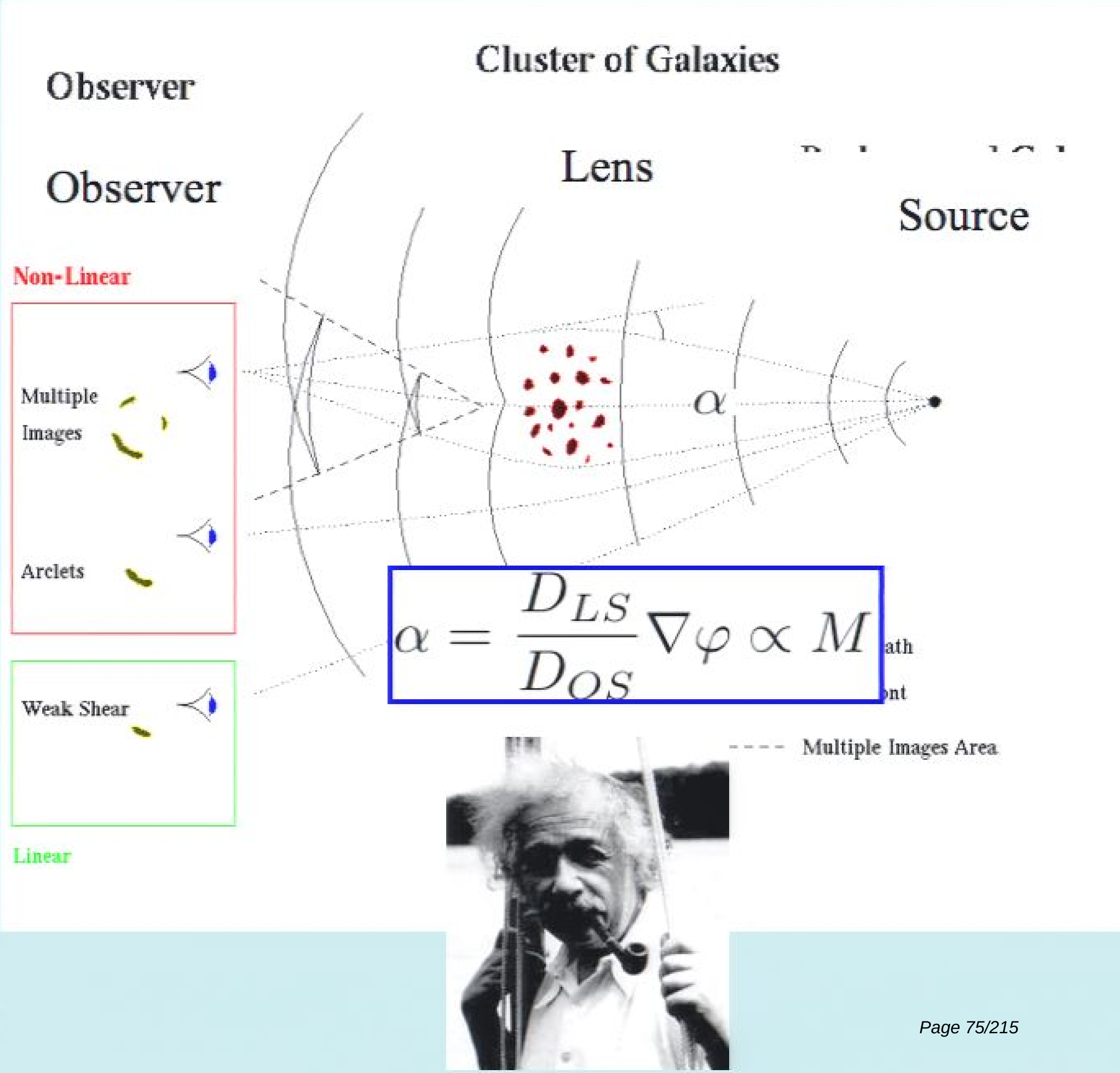

$$\alpha = \frac{D_{LS}}{D_{OS}} \nabla \varphi \propto M$$

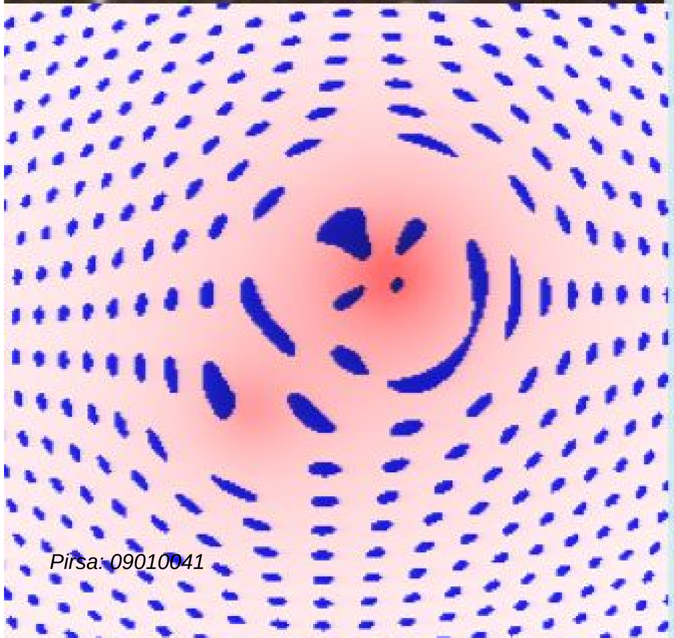

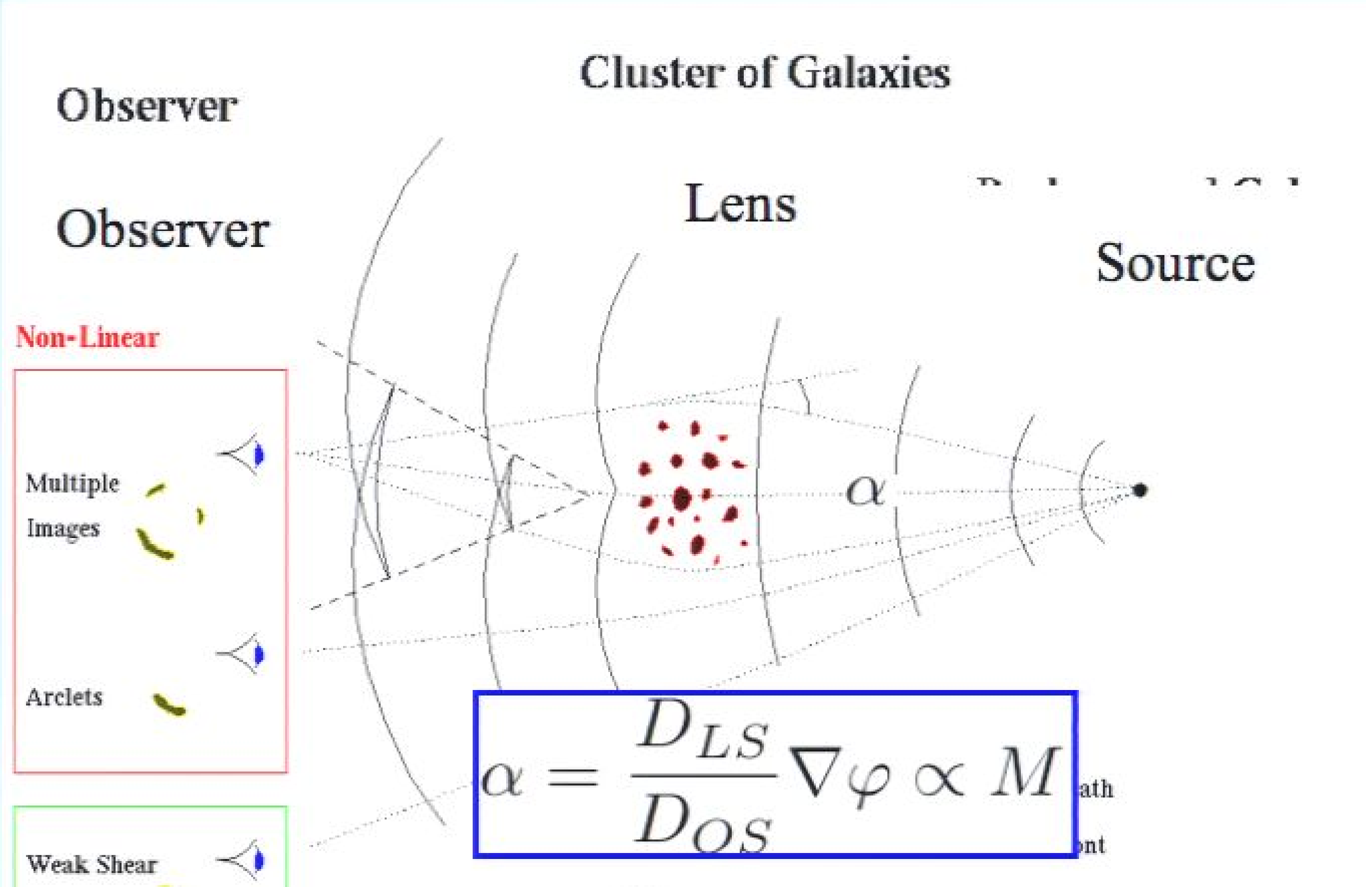

$$\alpha = \frac{D_{LS}}{D_{OS}}\nabla\varphi \propto M$$

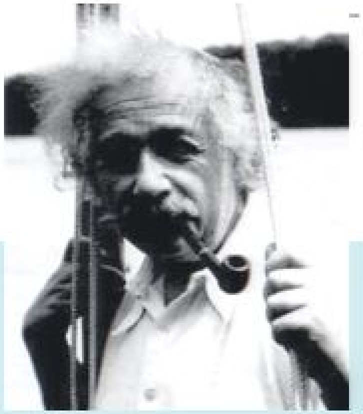

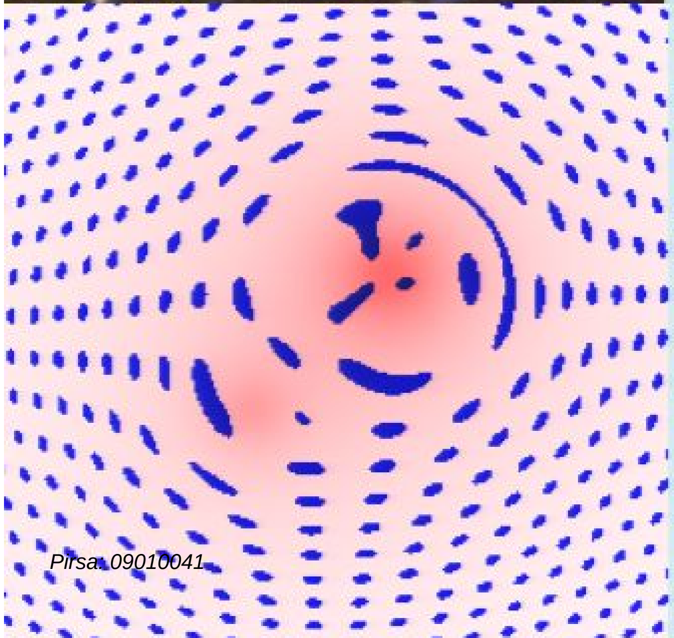

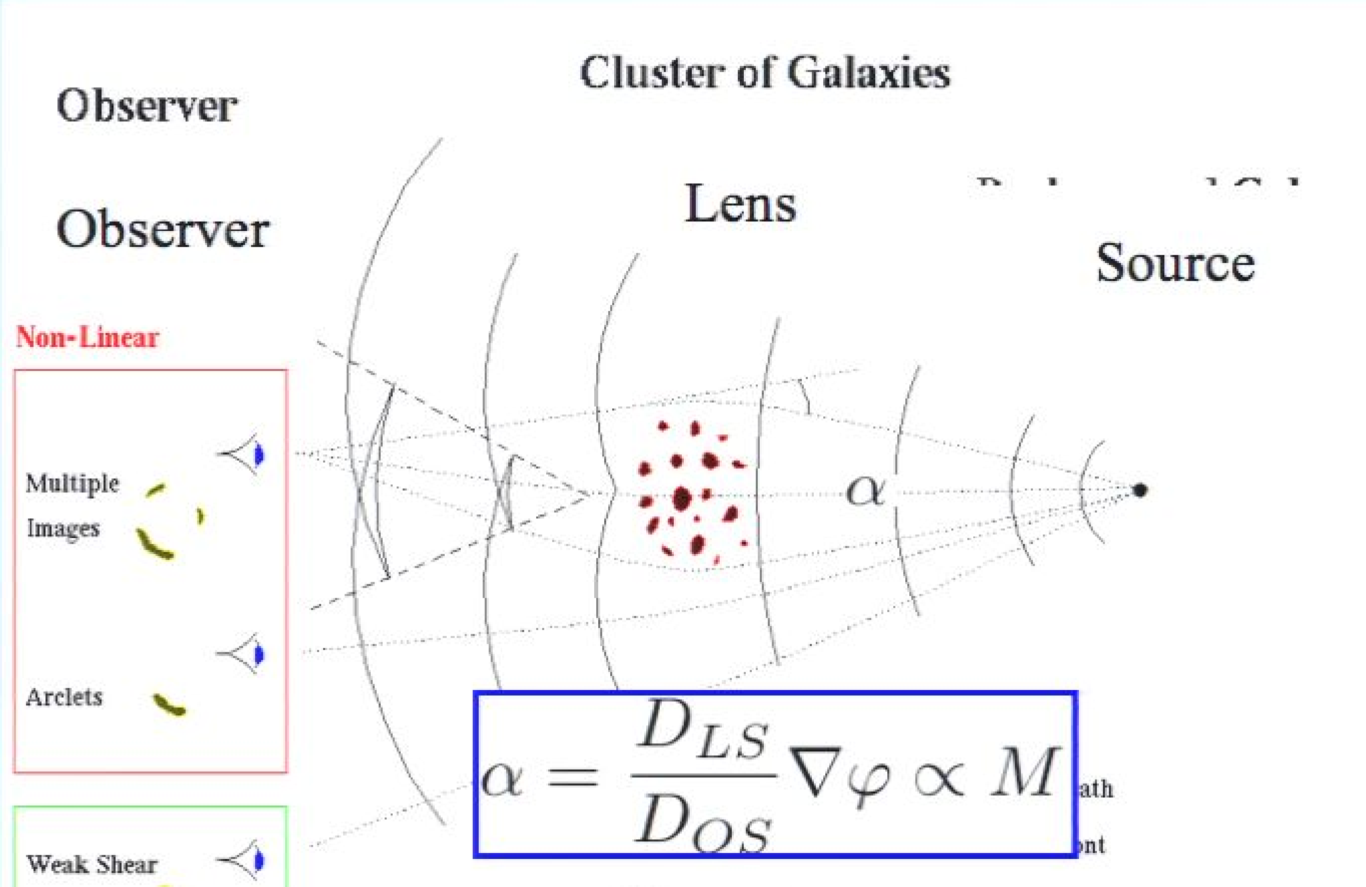

$$\alpha = \frac{D_{LS}}{D_{OS}}\nabla\varphi \propto M$$

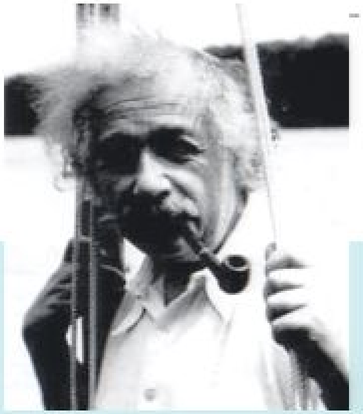

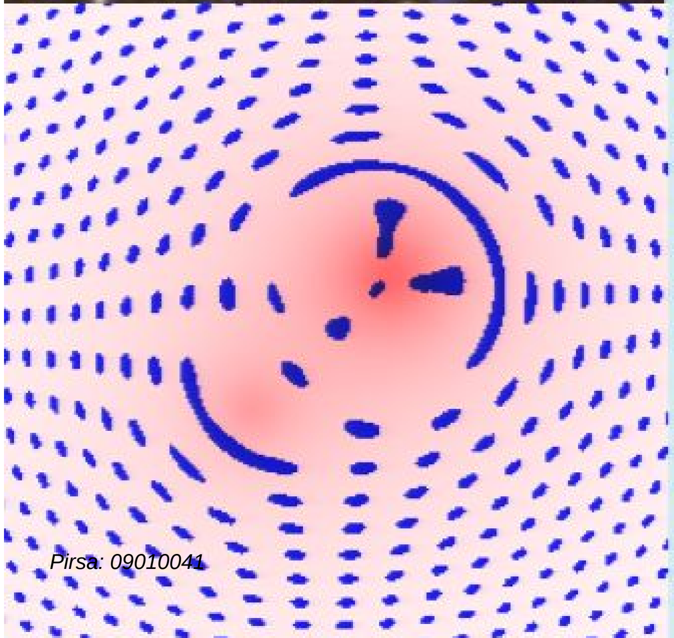

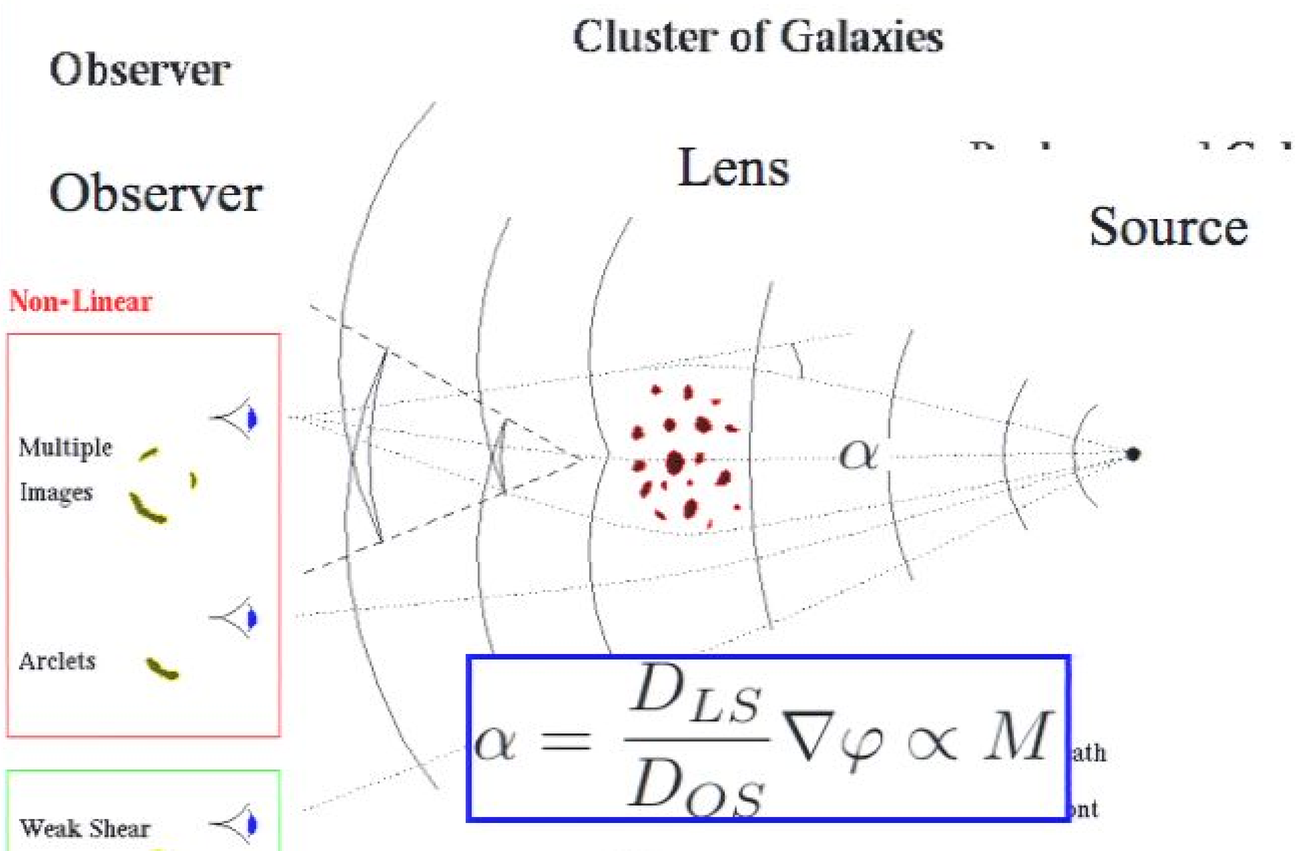

$$\alpha = \frac{D_{LS}}{D_{OS}} \nabla \varphi \propto M$$

- - - - Multiple Images Area

Linear

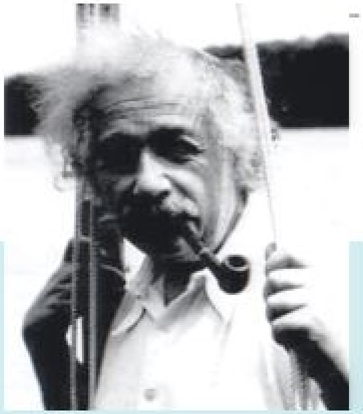

CFHT 1990

Z_cluster=0.375

Z_arc=0.725 (Soucail et al 1988)

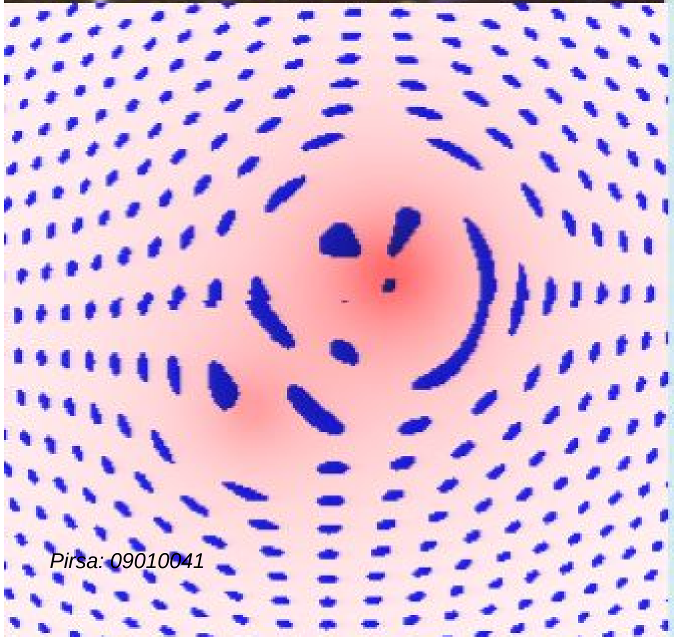

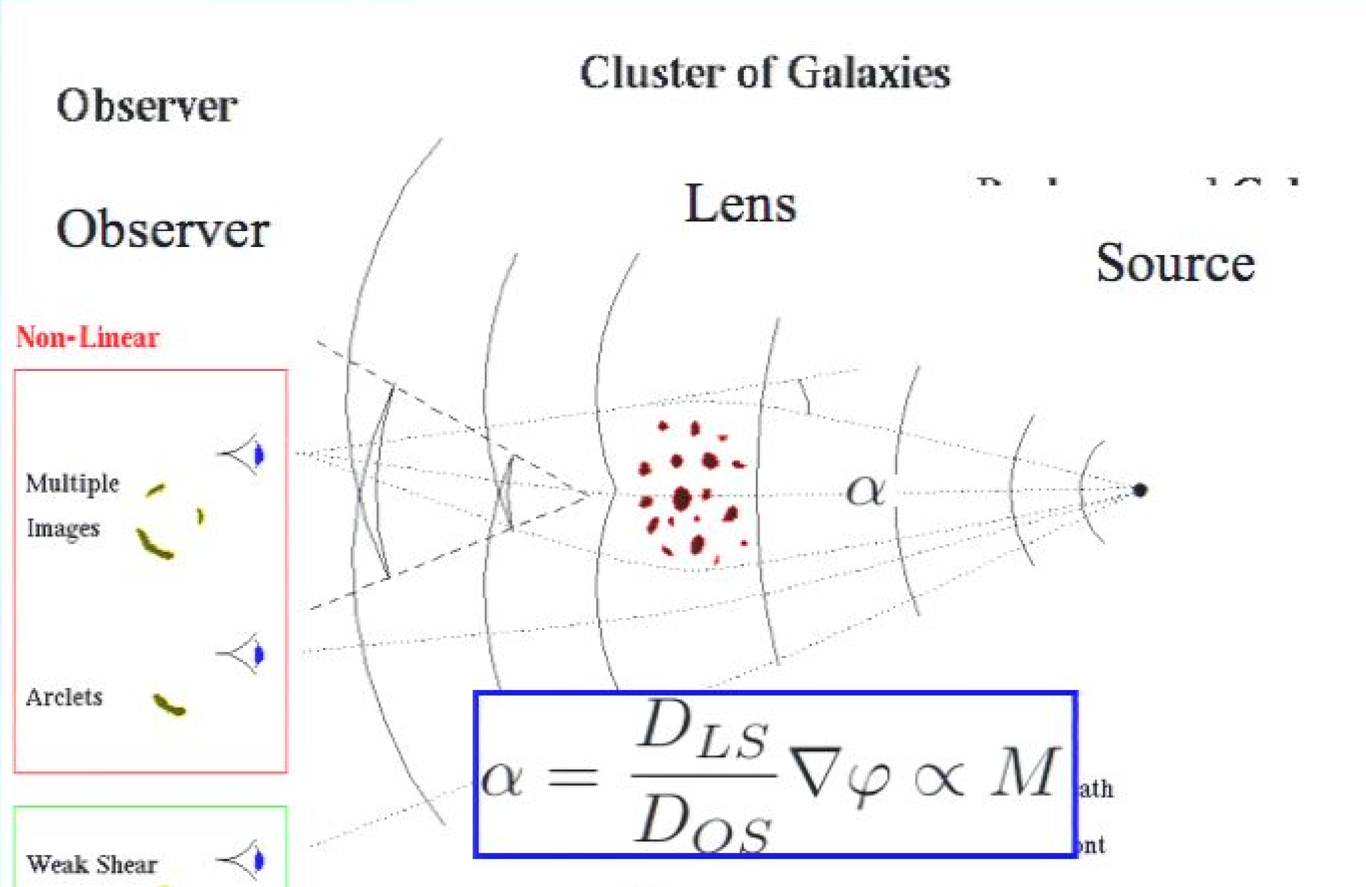

$$\alpha = \frac{D_{LS}}{D_{OS}} \nabla \varphi \propto M$$

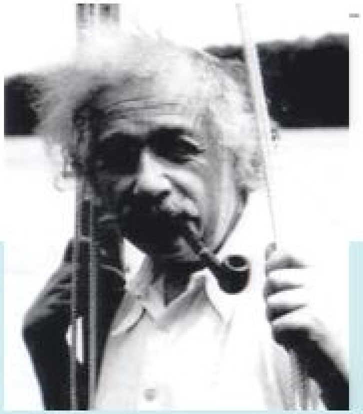

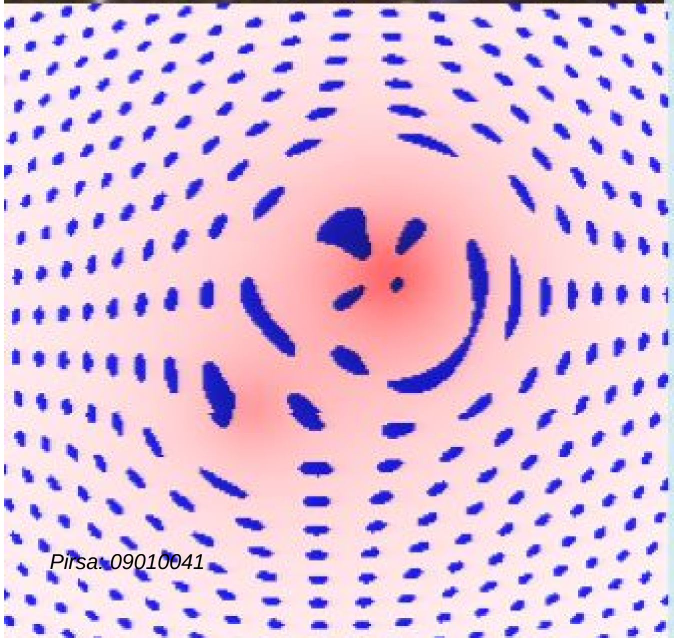

Observer

Observer

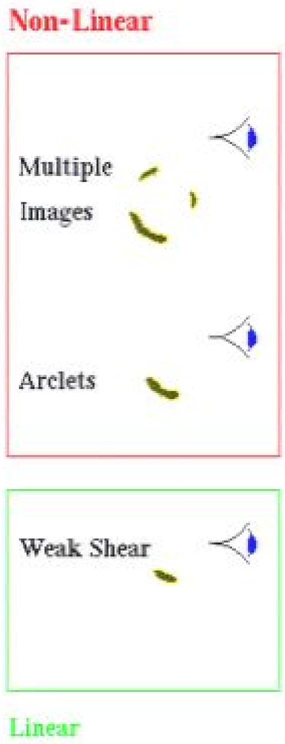

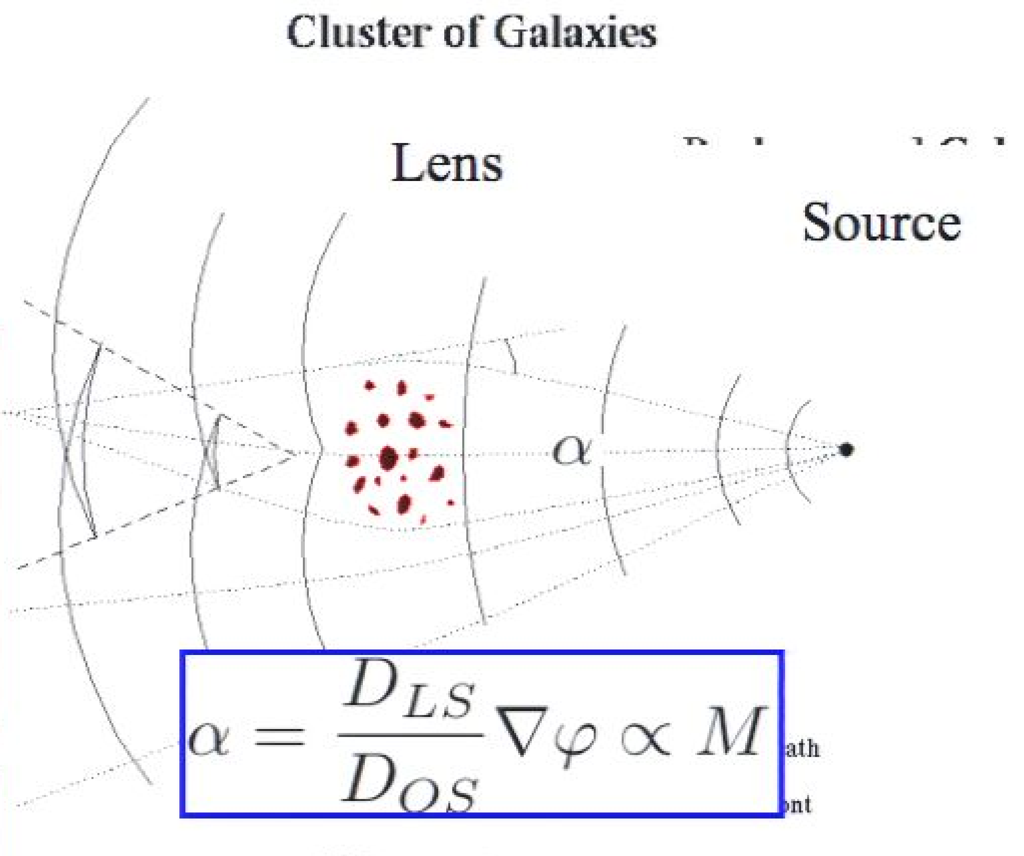

$$\alpha = \frac{D_{LS}}{D_{OS}} \nabla \varphi \propto M$$

- - - Multiple Images Area

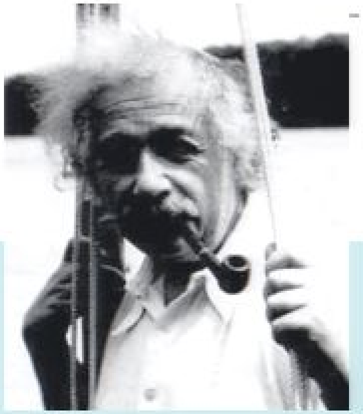

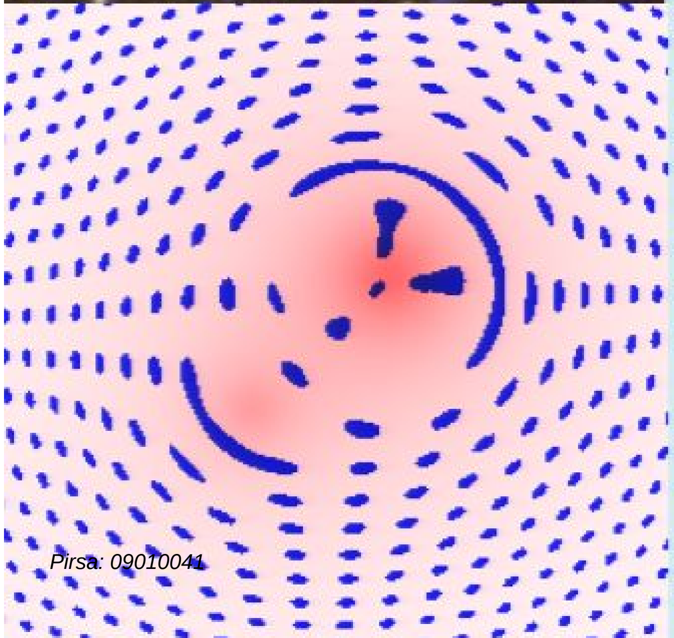

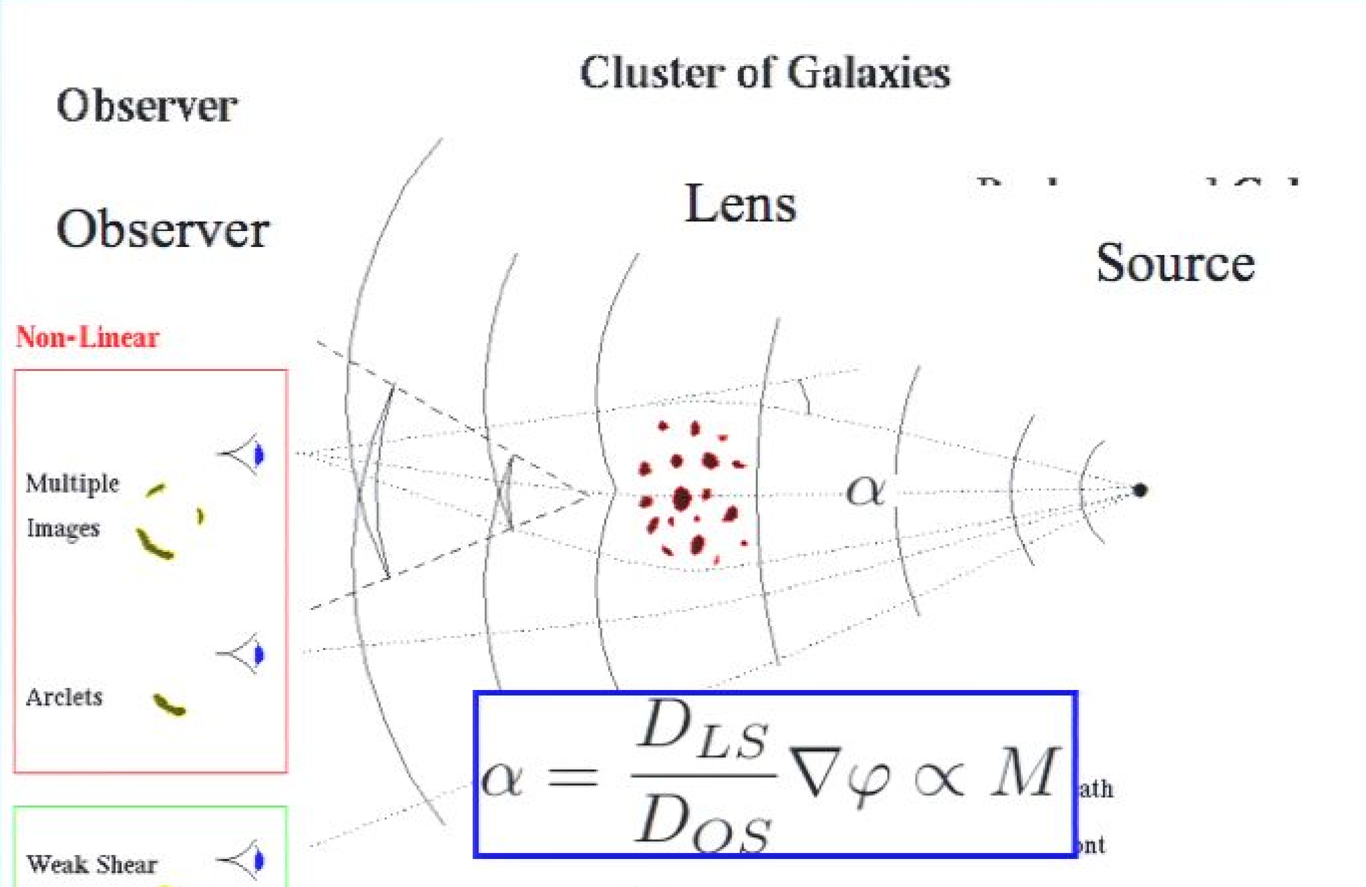

$$\alpha = \frac{D_{LS}}{D_{OS}} \nabla \varphi \propto M$$

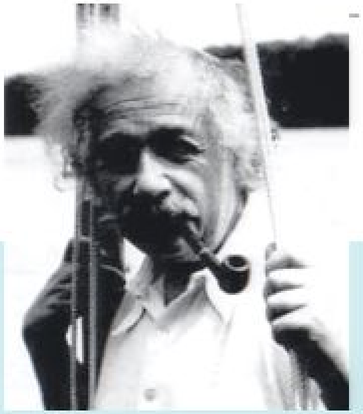

CFHT 1990

Z_cluster=0.375

Z_arc=0.725 (Soucail et al 1988)

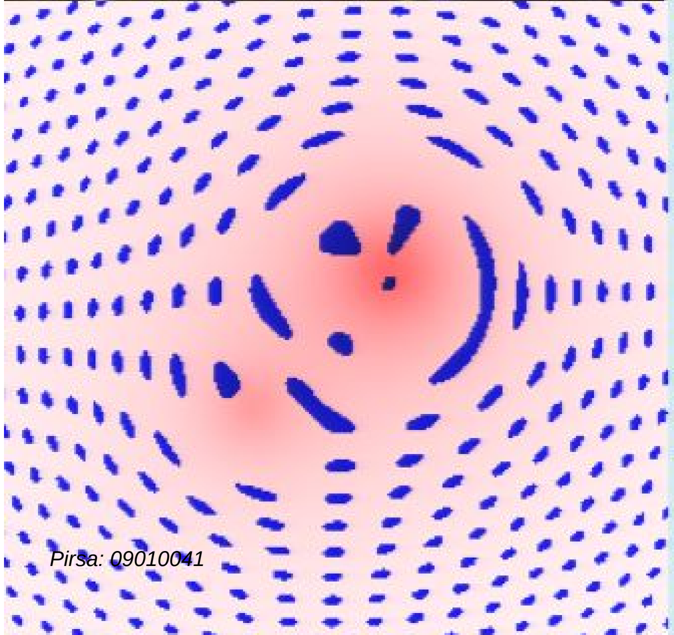

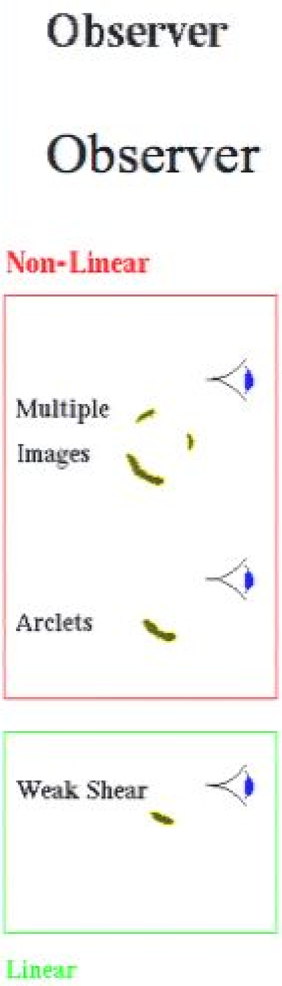

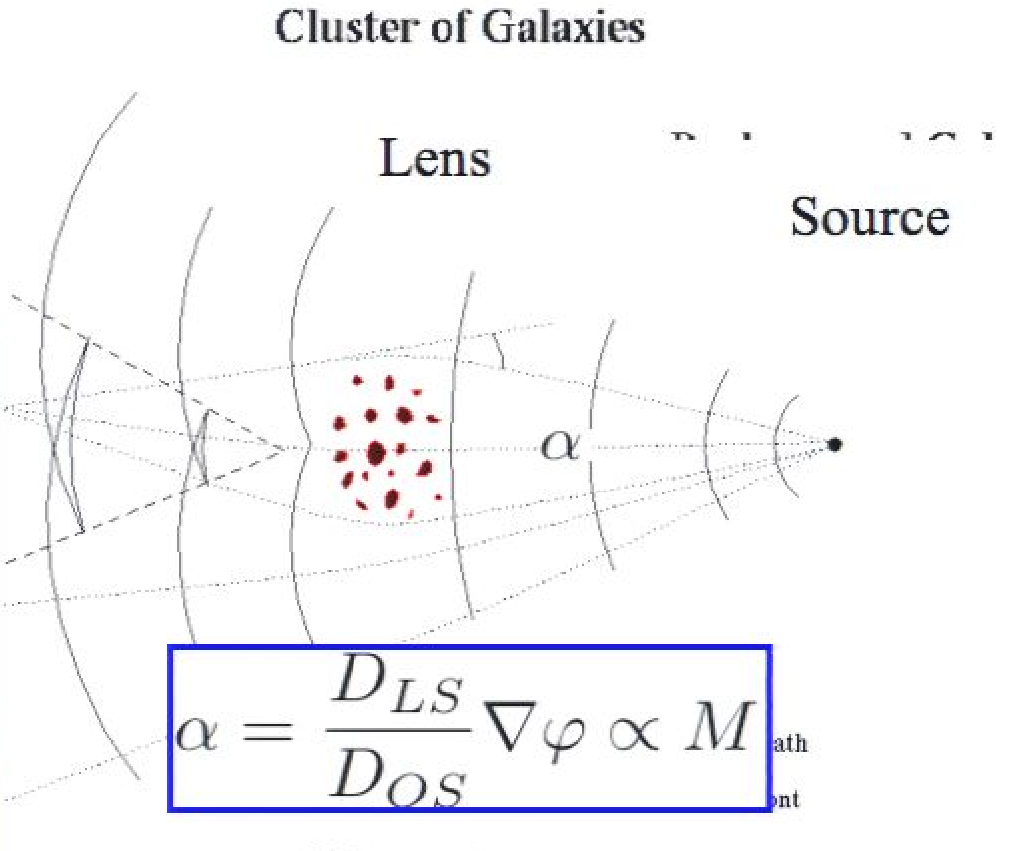

$$\boxed{\alpha = \frac{D_{LS}}{D_{OS}} \nabla \varphi \propto M}$$

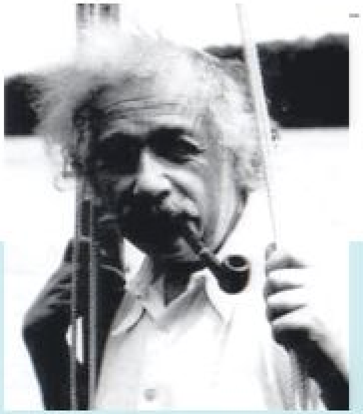


CFHT 1990

Z_cluster=0.375

Z_arc=0.725 (Soucail et al 1988)

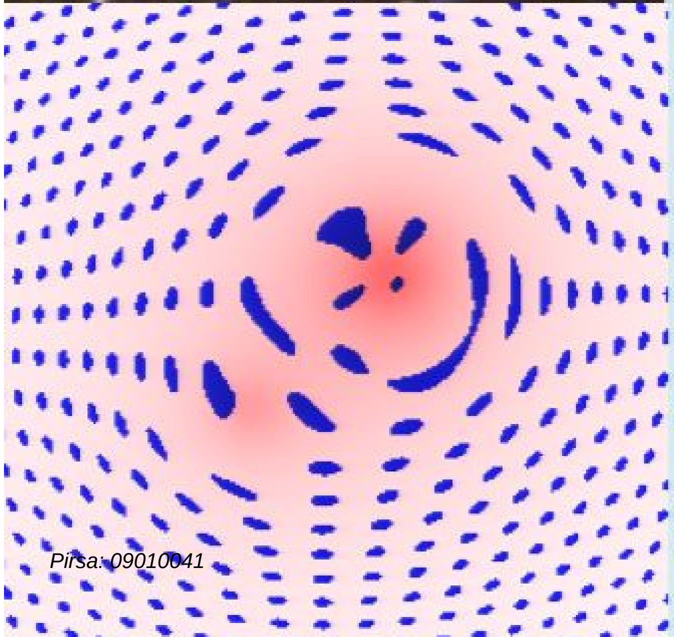

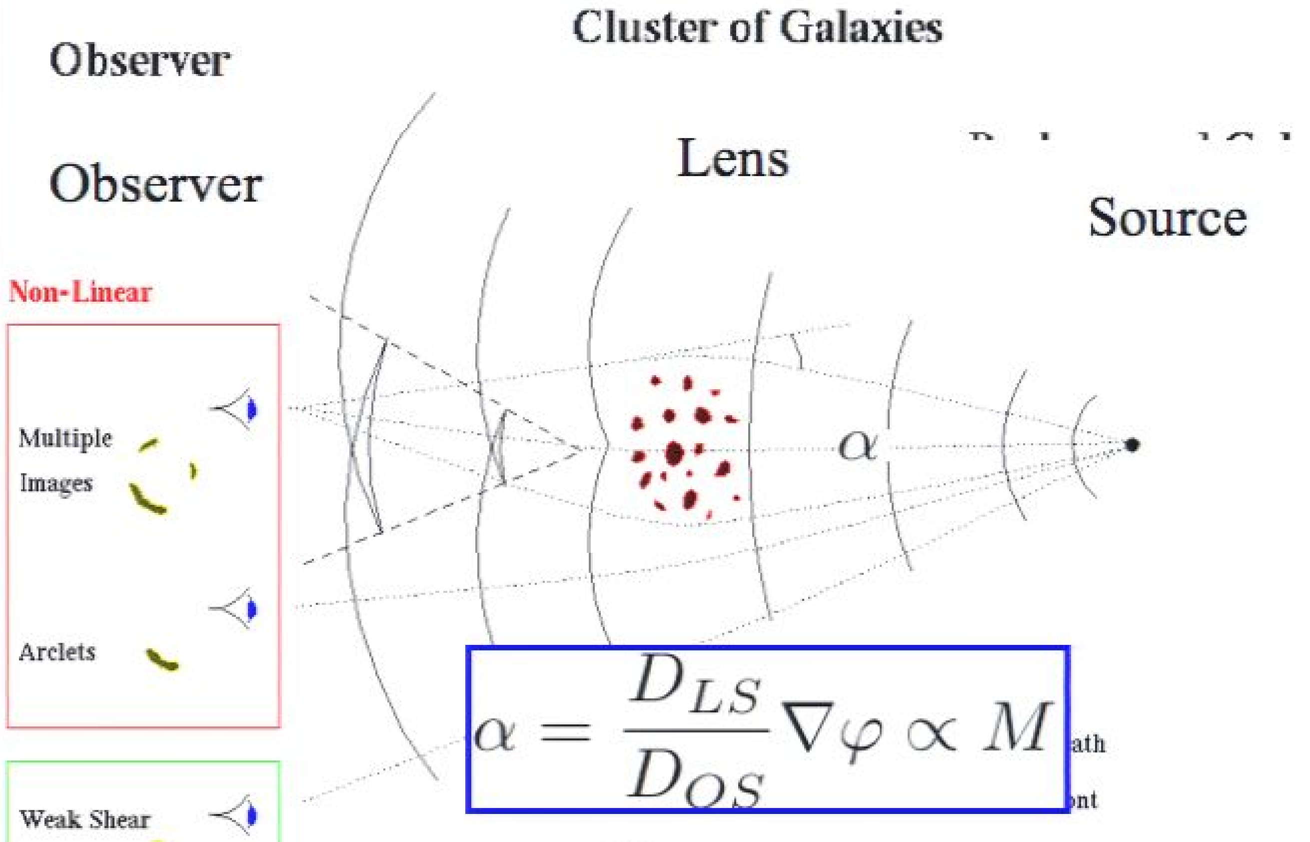

$$\alpha = \frac{D_{LS}}{D_{OS}} \nabla \varphi \propto M$$

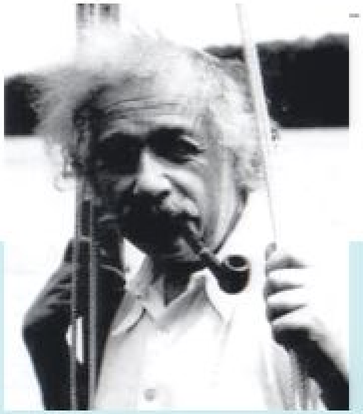


CFHT 1990

Z_cluster=0.375

Z_arc=0.725 (Soucail et al 1988)

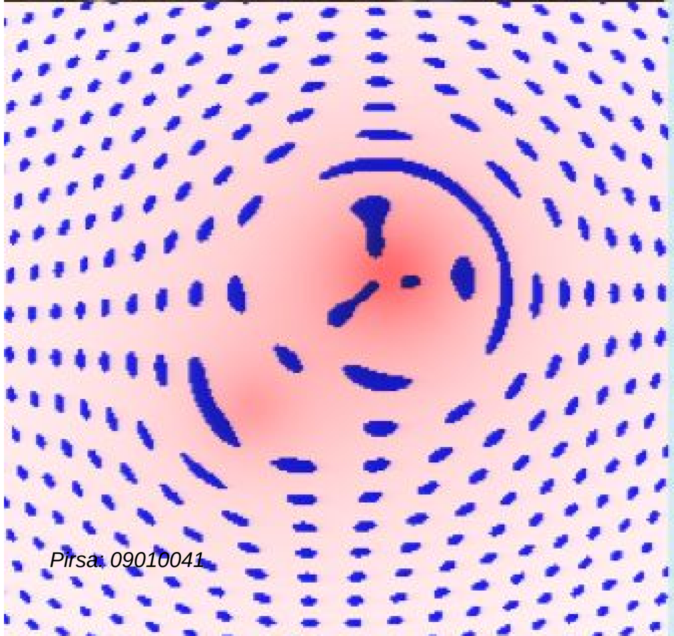

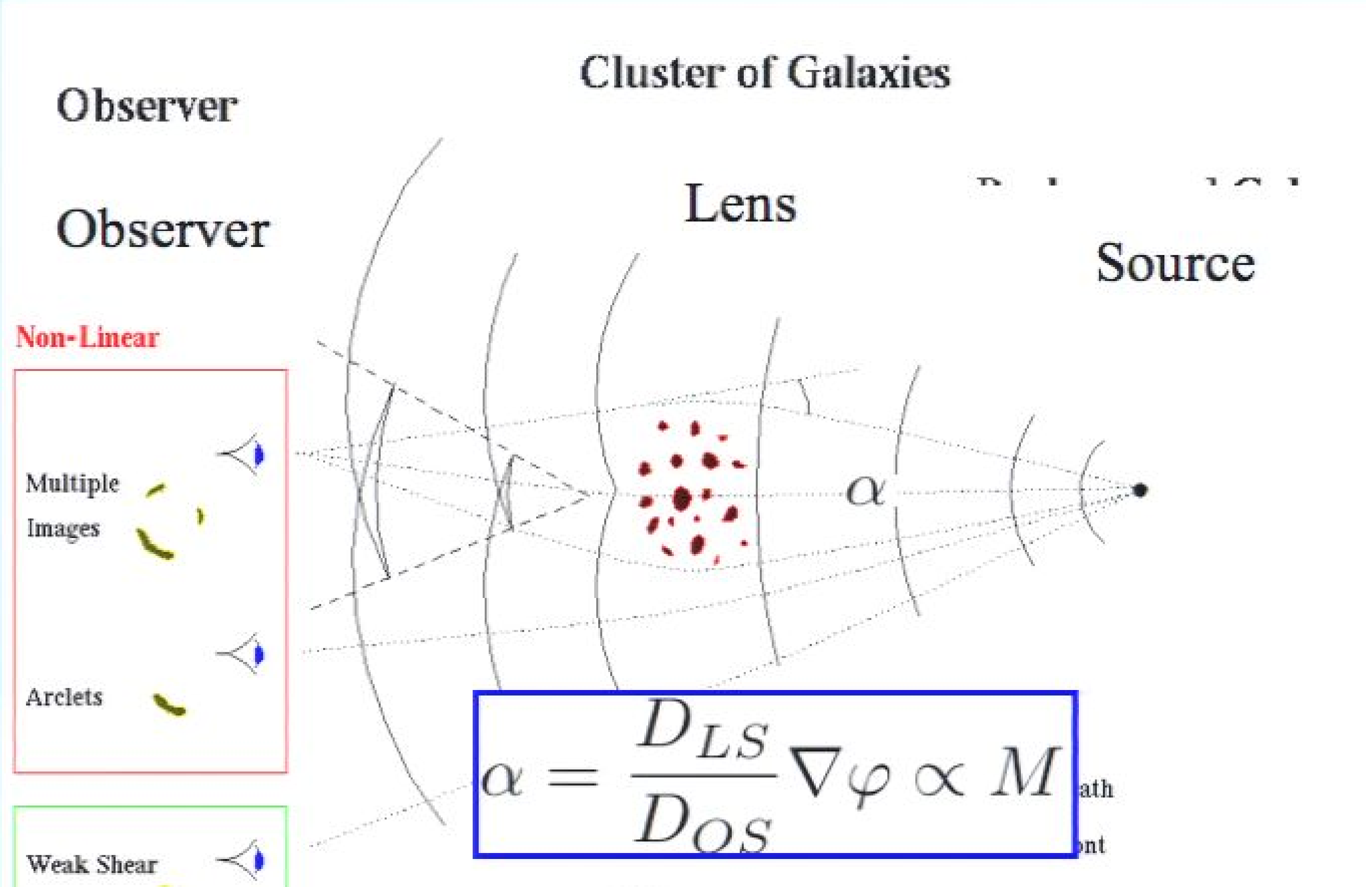

$$\alpha = \frac{D_{LS}}{D_{OS}} \nabla \varphi \propto M$$

Multiple Images Area

Linear

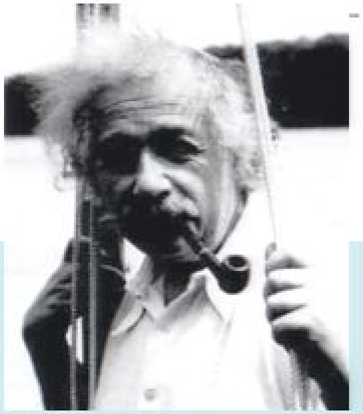

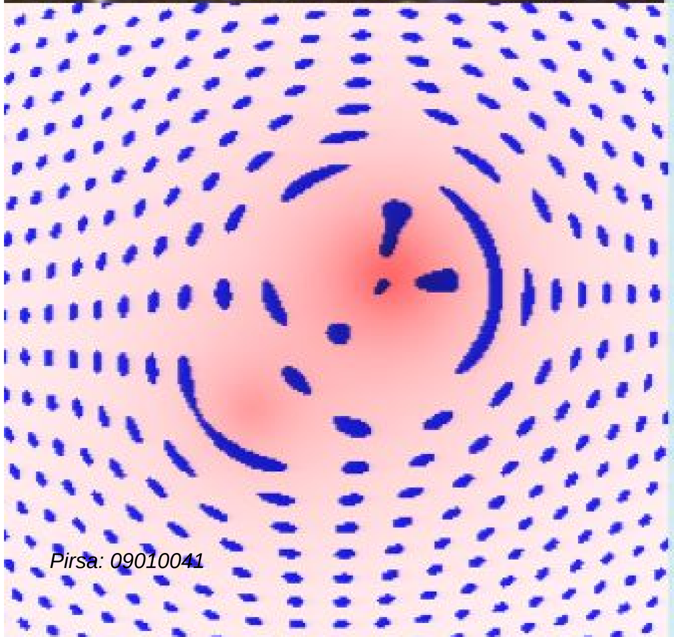

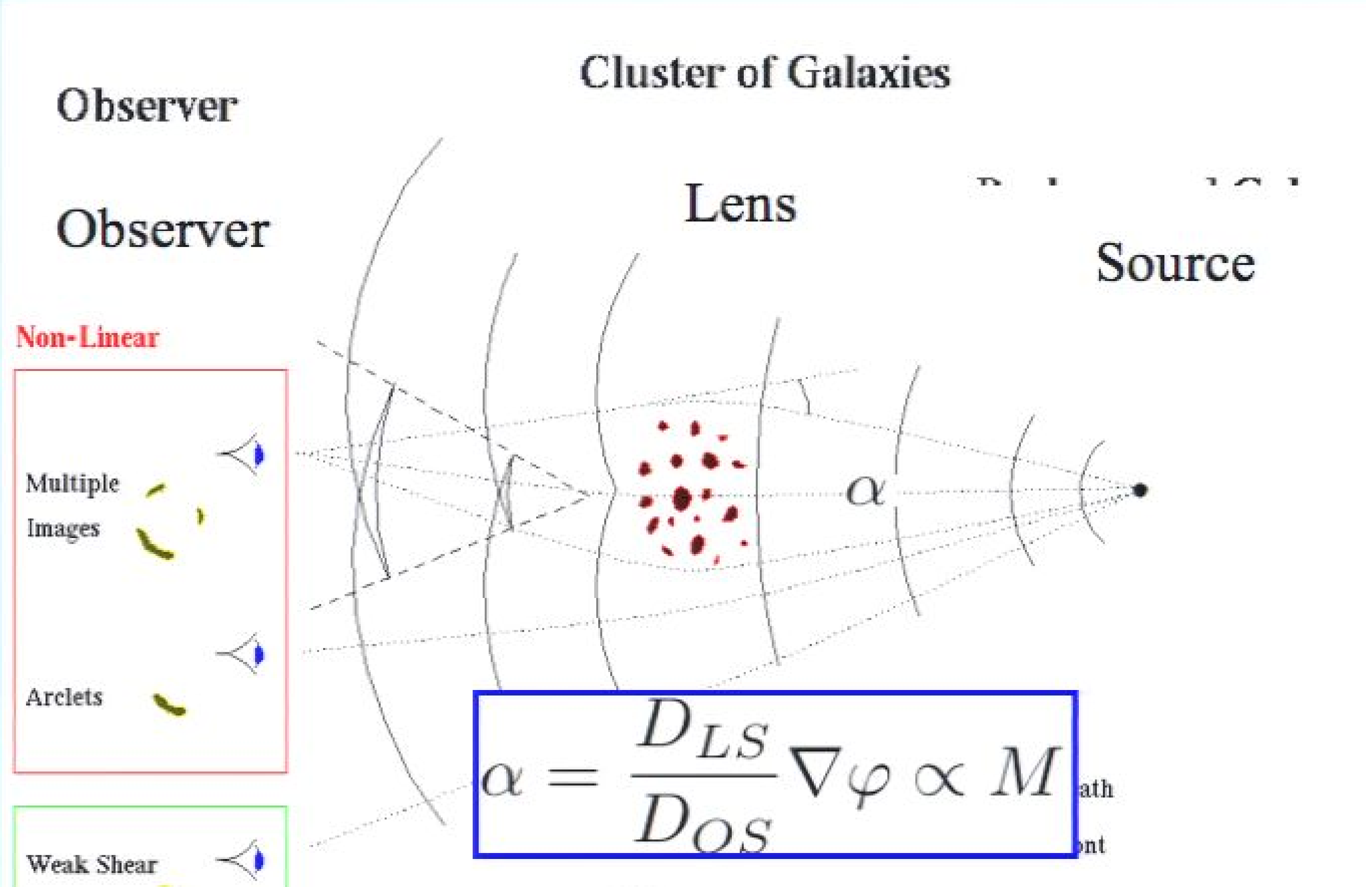

$$\alpha = \frac{D_{LS}}{D_{OS}} \nabla \varphi \propto M$$

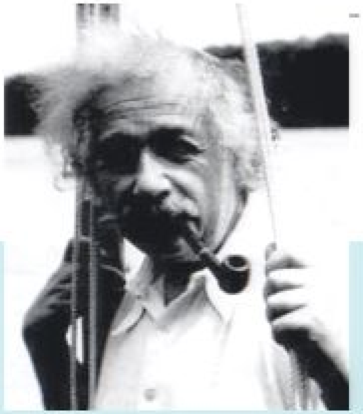

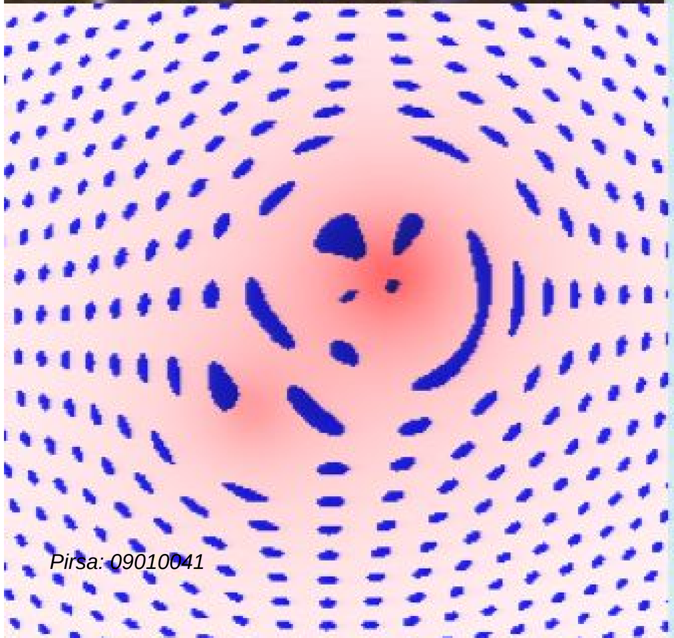

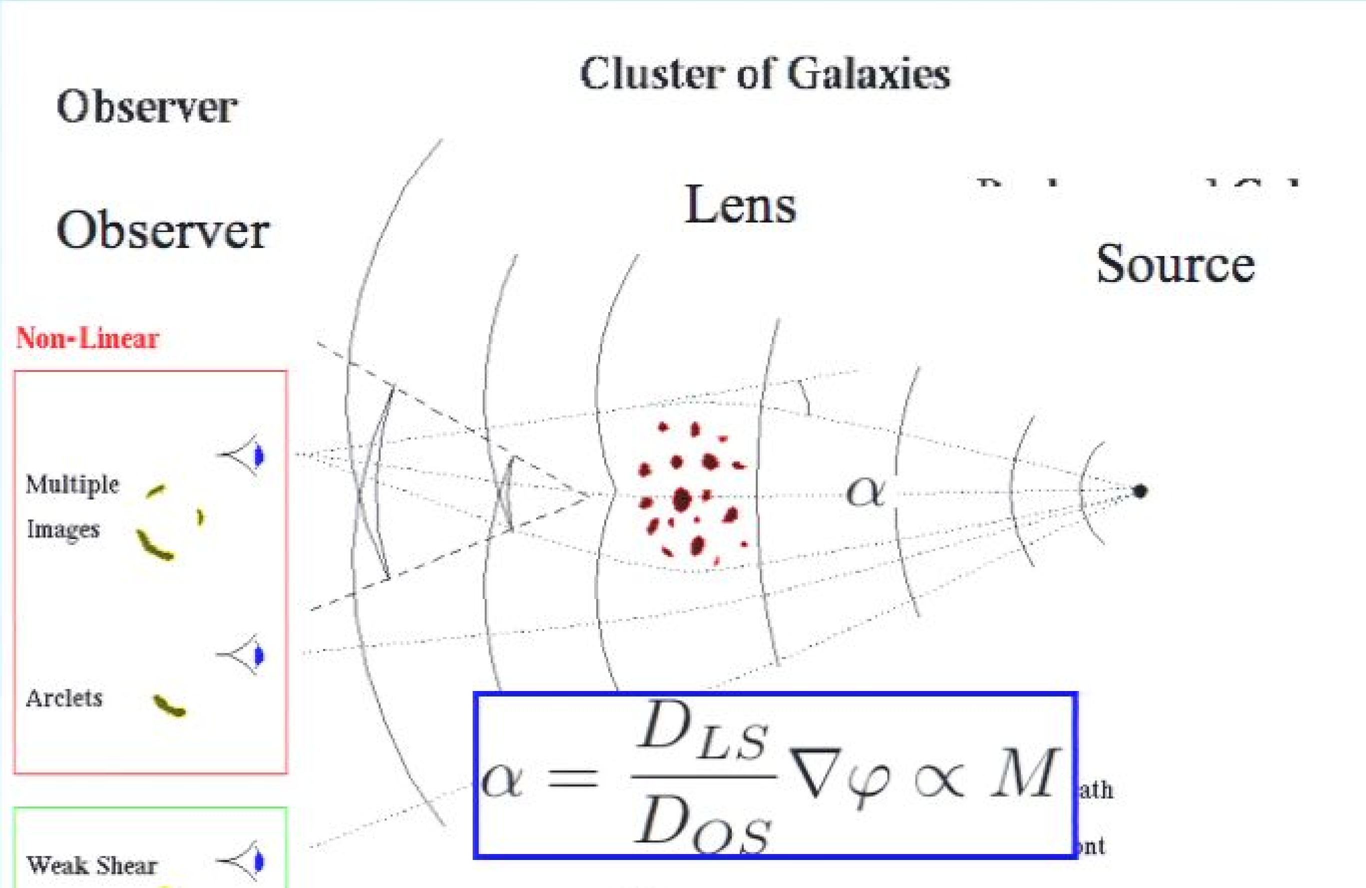

$$\alpha = \frac{D_{LS}}{D_{OS}} \nabla \varphi \propto M$$

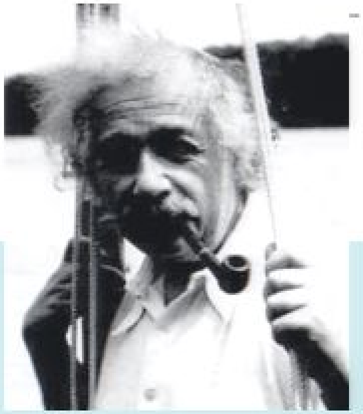

CFHT 1990

Z_cluster=0.375

Z_arc=0.725 (Soucail et al 1988)

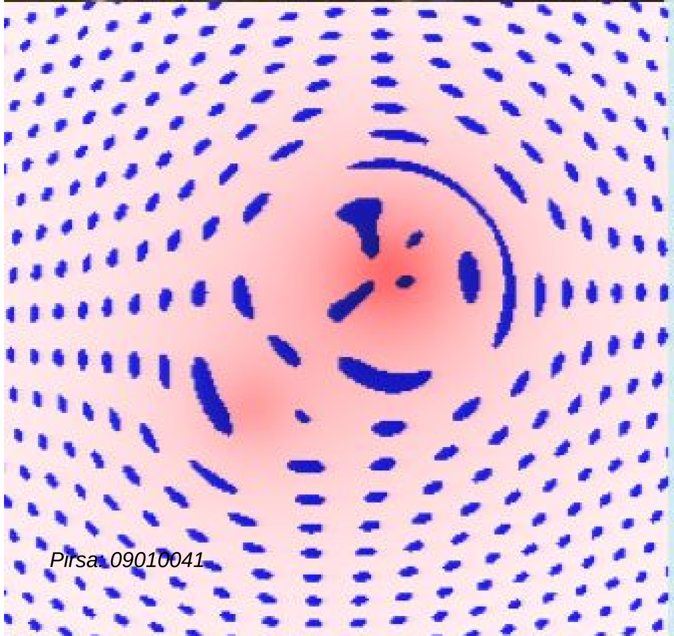

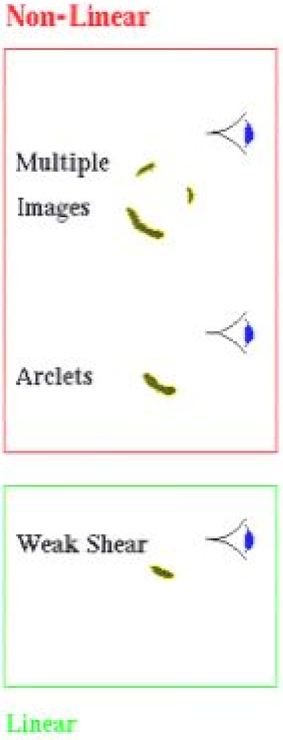

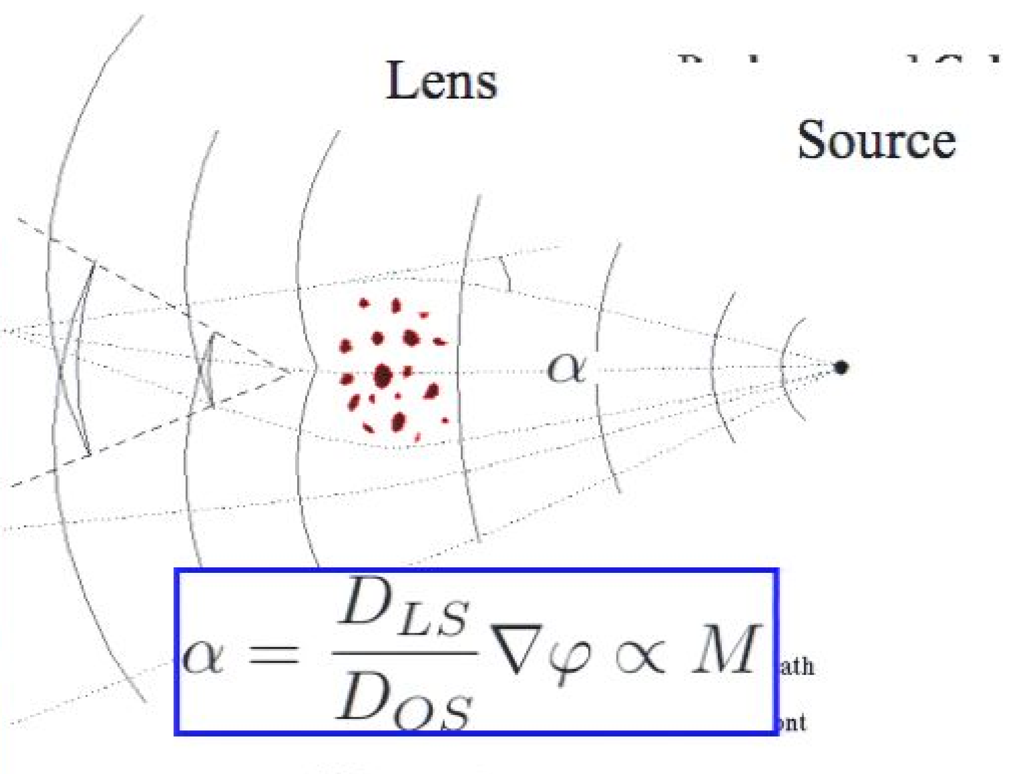

$$\alpha = \frac{D_{LS}}{D_{OS}} \nabla \varphi \propto M$$

- - - - Multiple Images Area

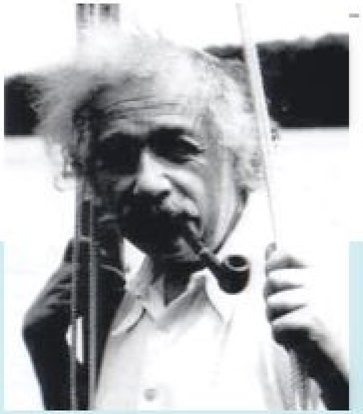

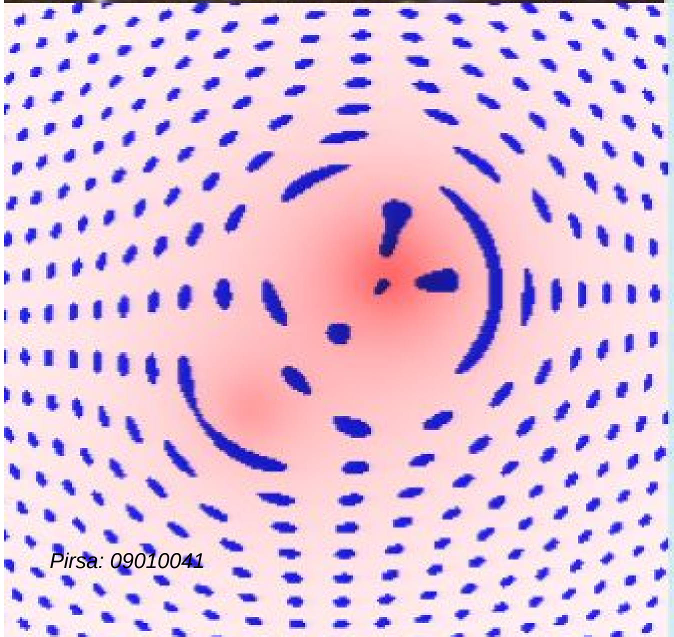

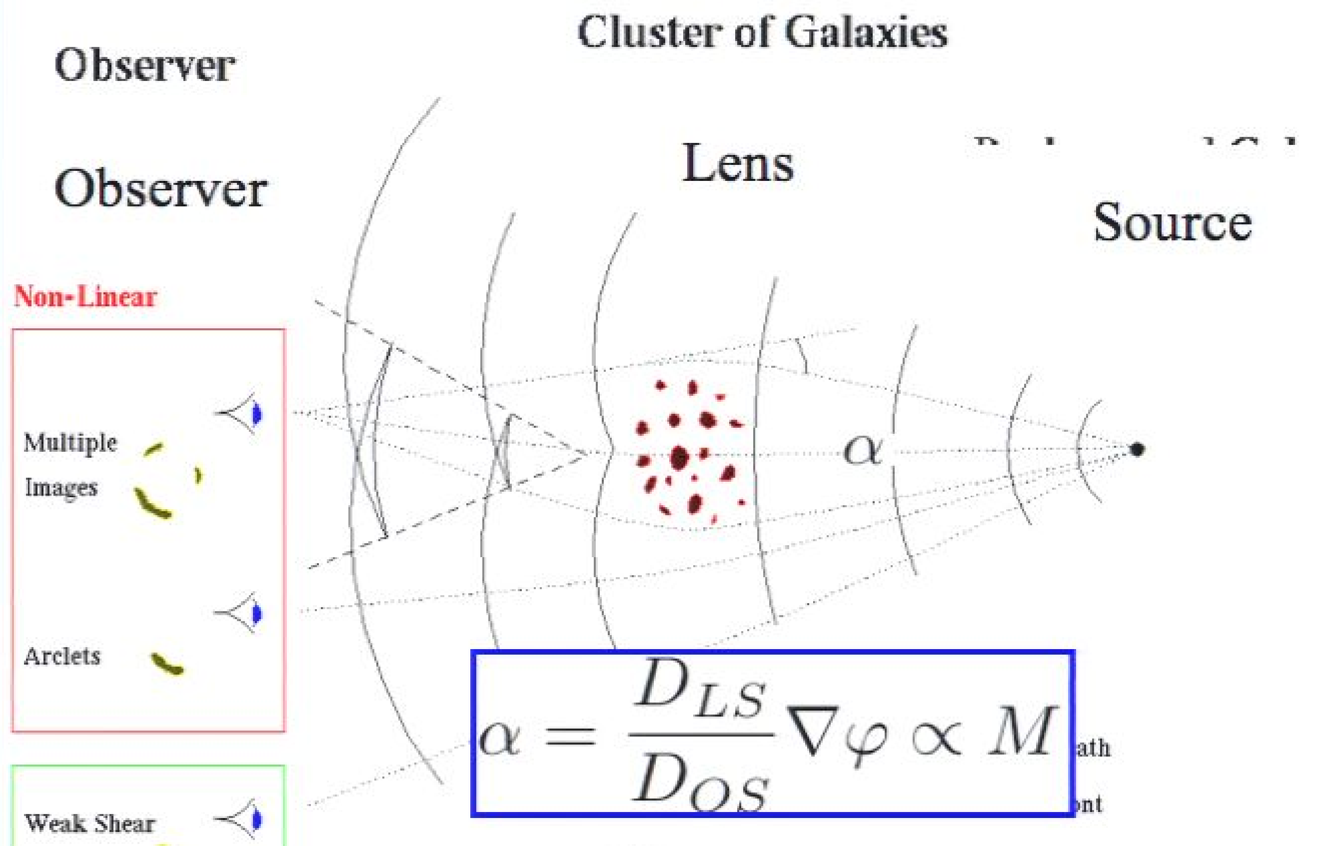

$$\alpha = \frac{D_{LS}}{D_{OS}} \nabla \varphi \propto M$$

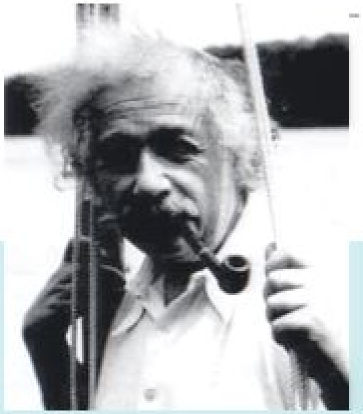

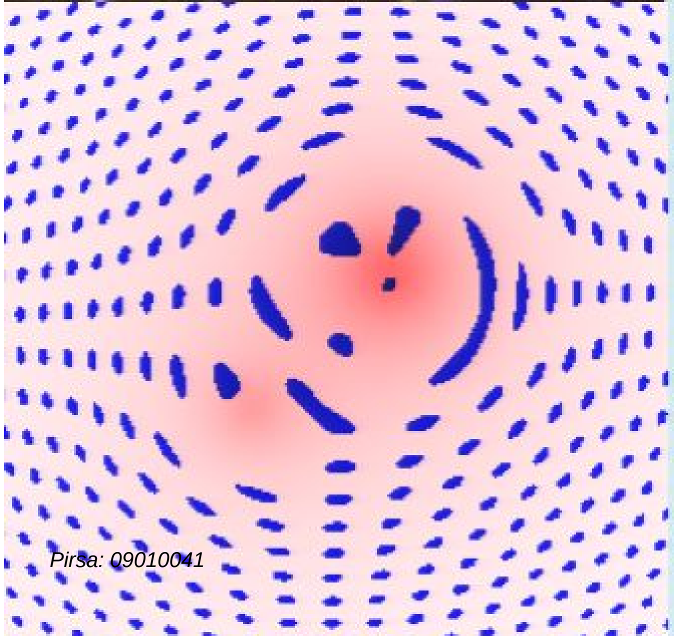

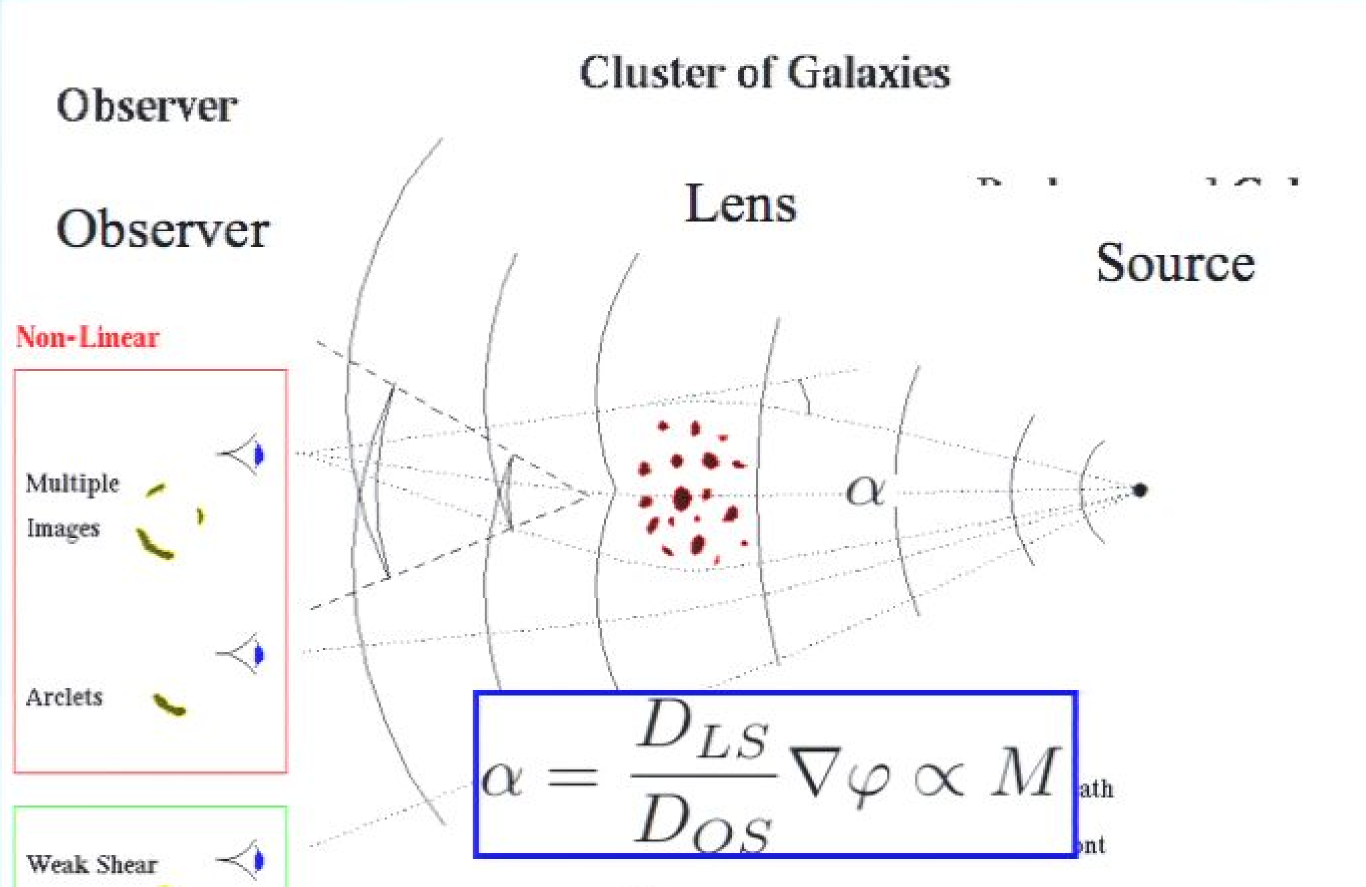

$$\alpha = \frac{D_{LS}}{D_{OS}} \nabla \varphi \propto M$$

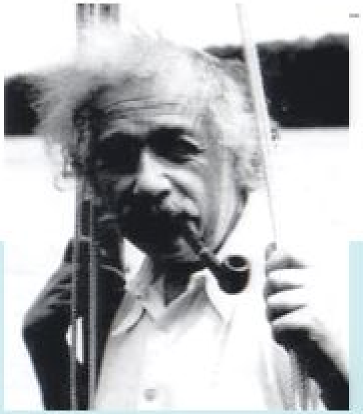

ath

nt

Multiple Images Area

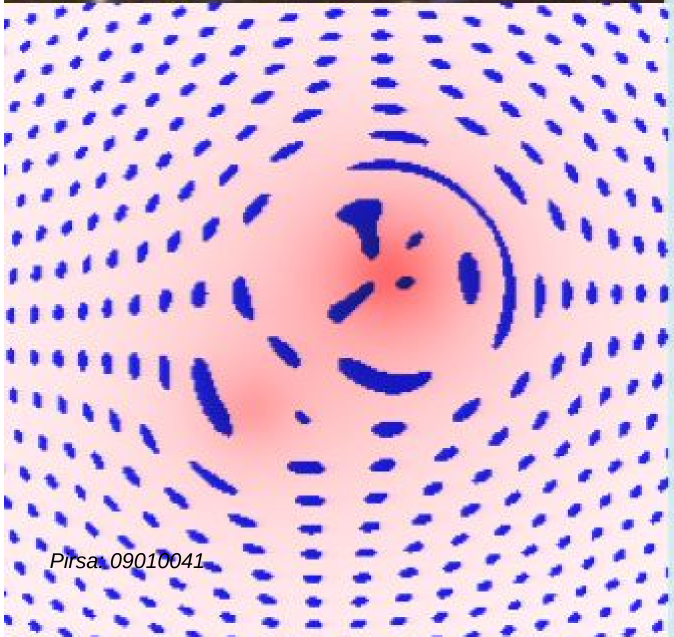

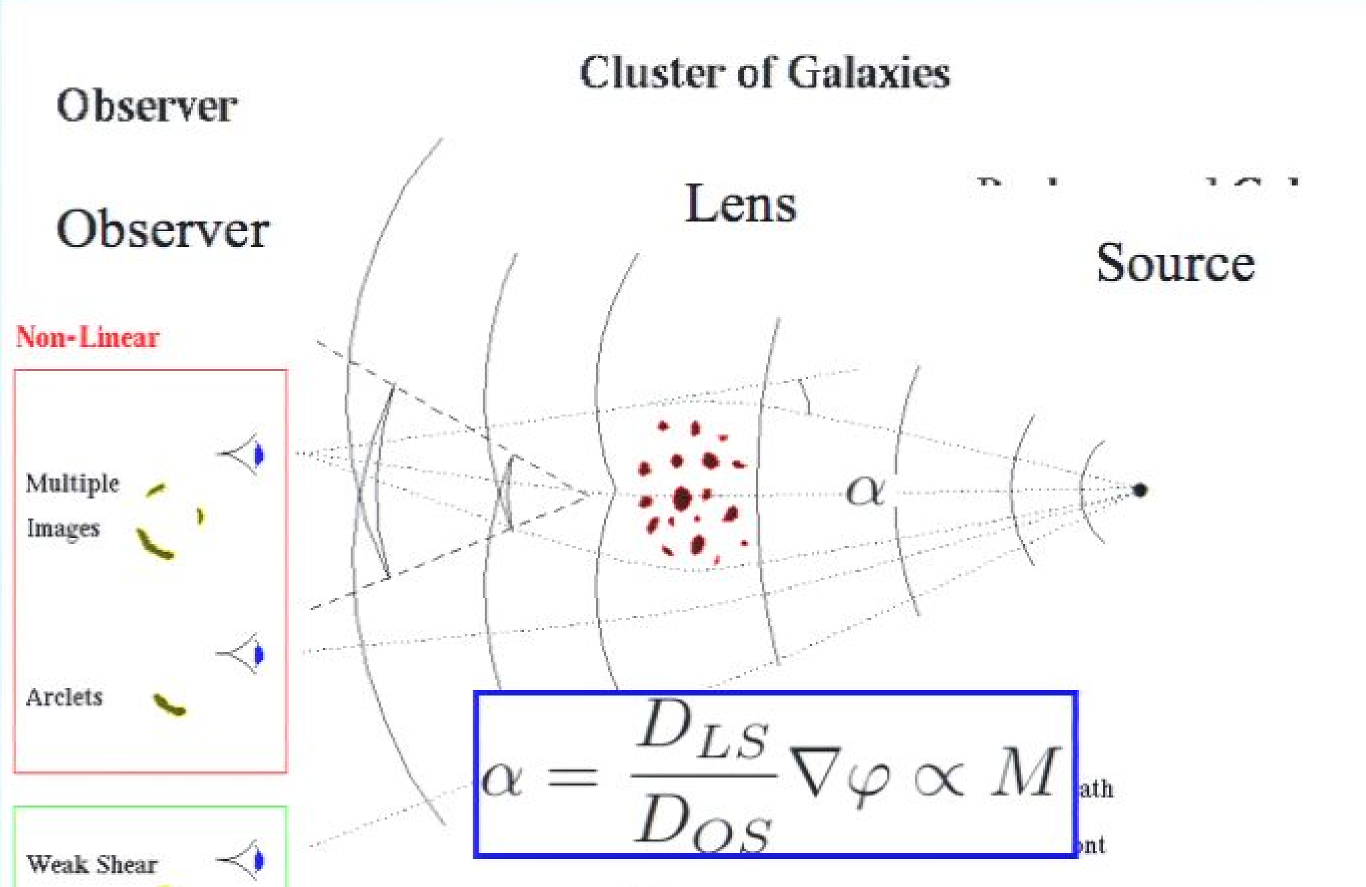

$$\alpha = \frac{D_{LS}}{D_{OS}} \nabla \varphi \propto M$$

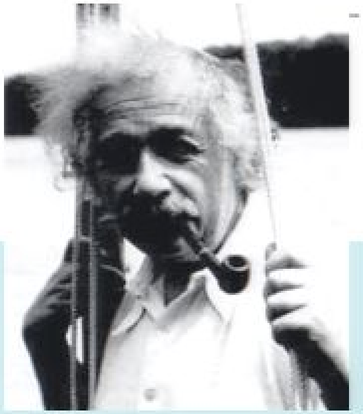

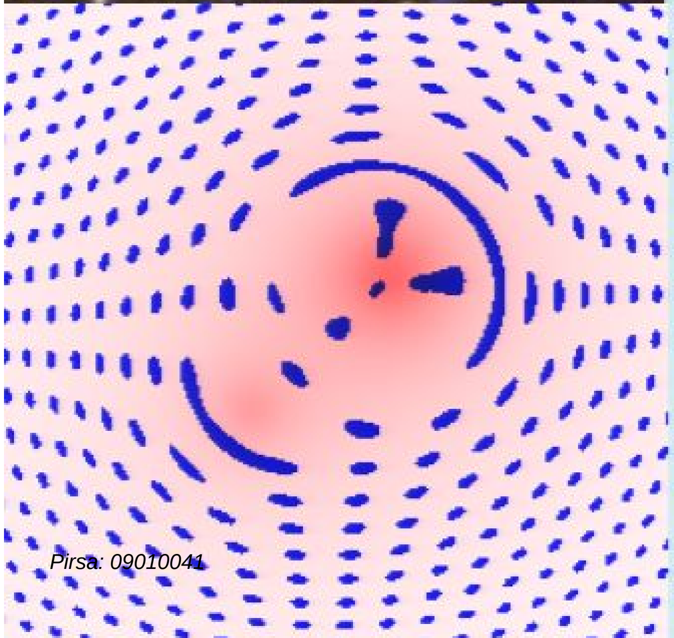

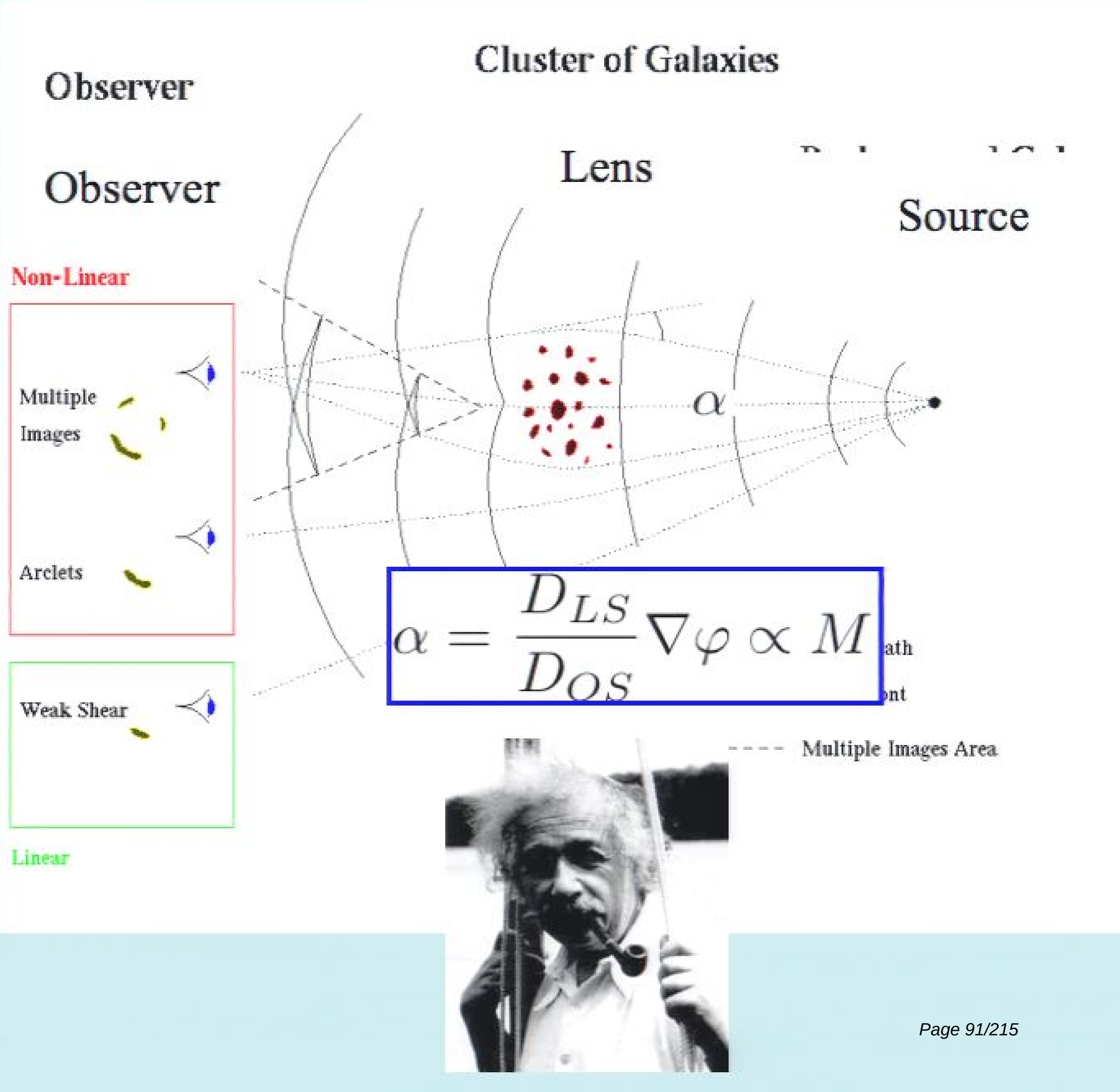

$$\alpha = \frac{D_{LS}}{D_{OS}} \nabla \varphi \propto M$$

CFHT 1990

Z_cluster=0.375

Z_arc=0.725 (Soucail et al 1988)

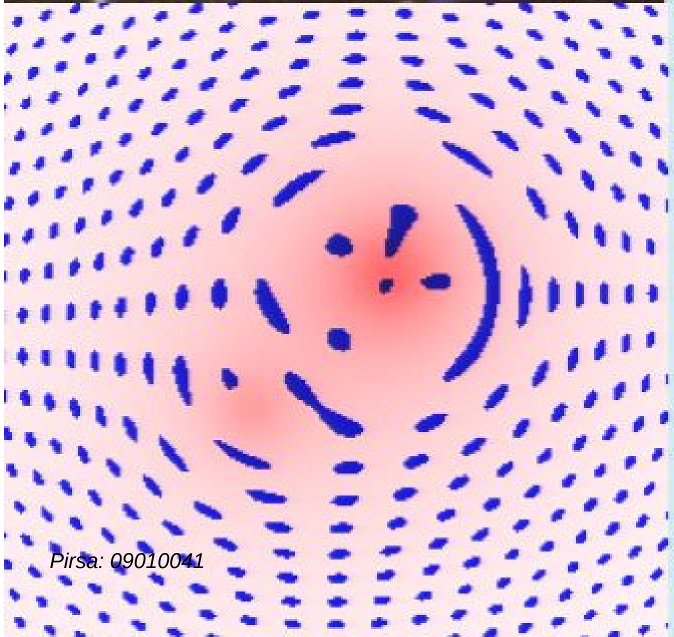

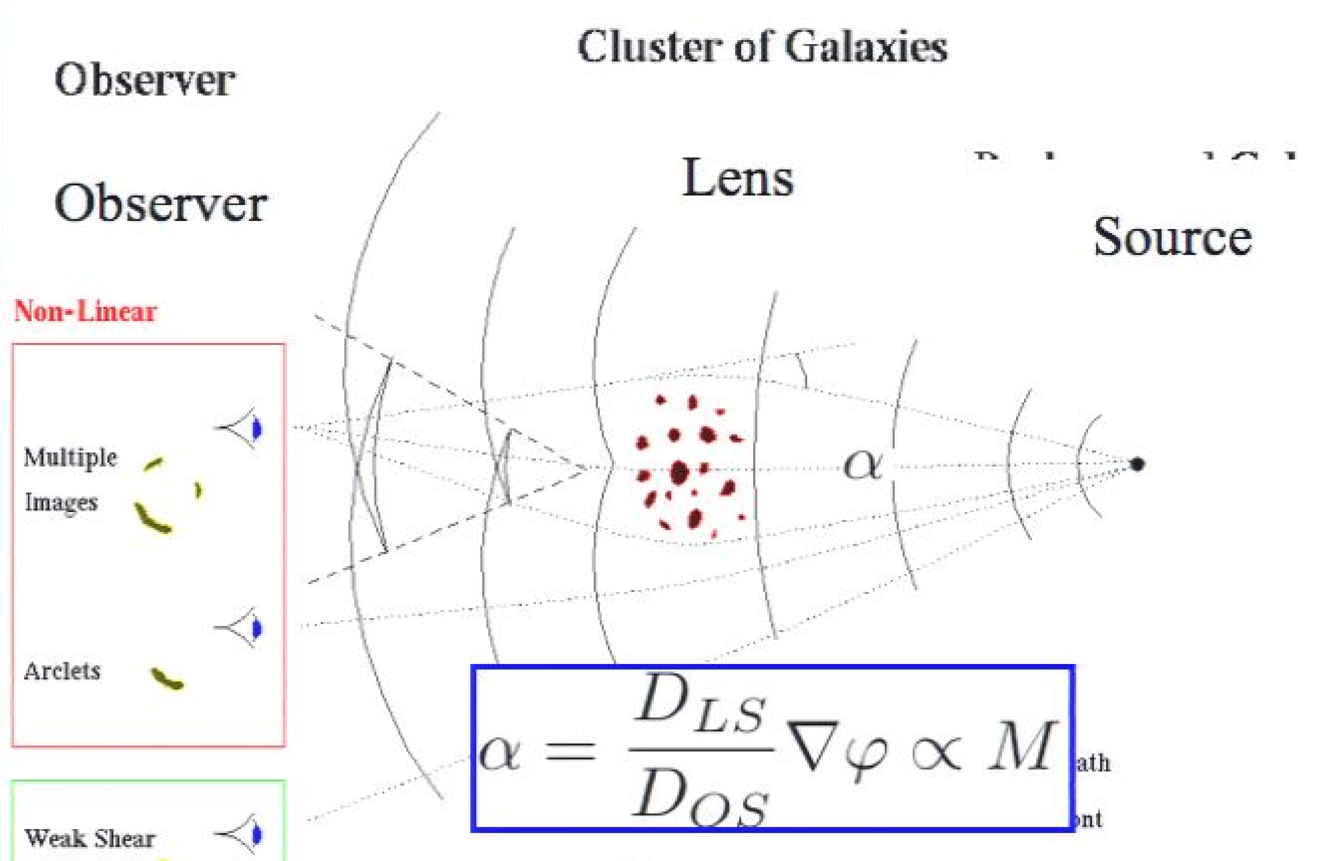

$$\alpha = \frac{D_{LS}}{D_{OS}} \nabla \varphi \propto M$$

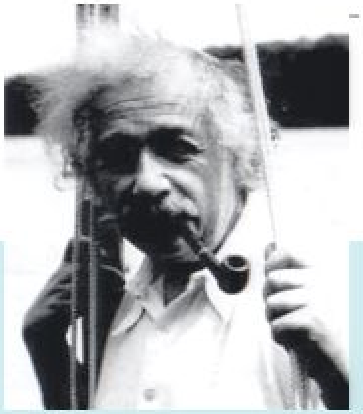


CFHT 1990

Z_cluster=0.375

Z_arc=0.725 (Soucail et al 1988)

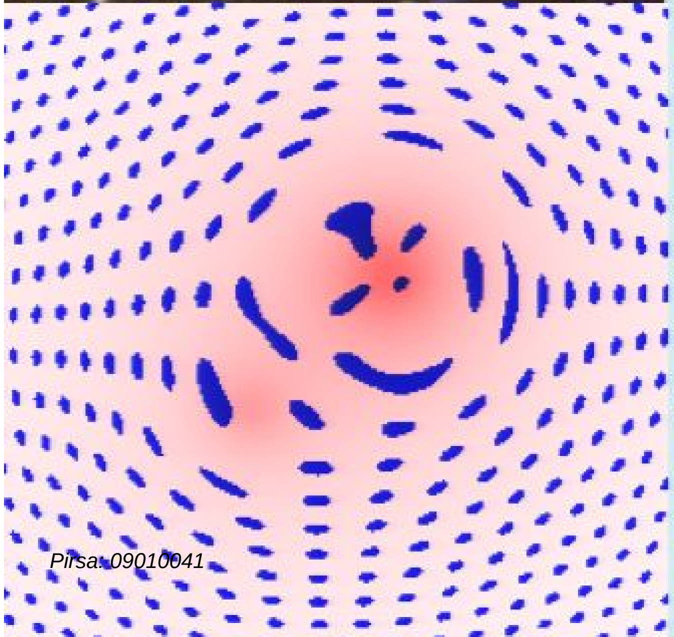

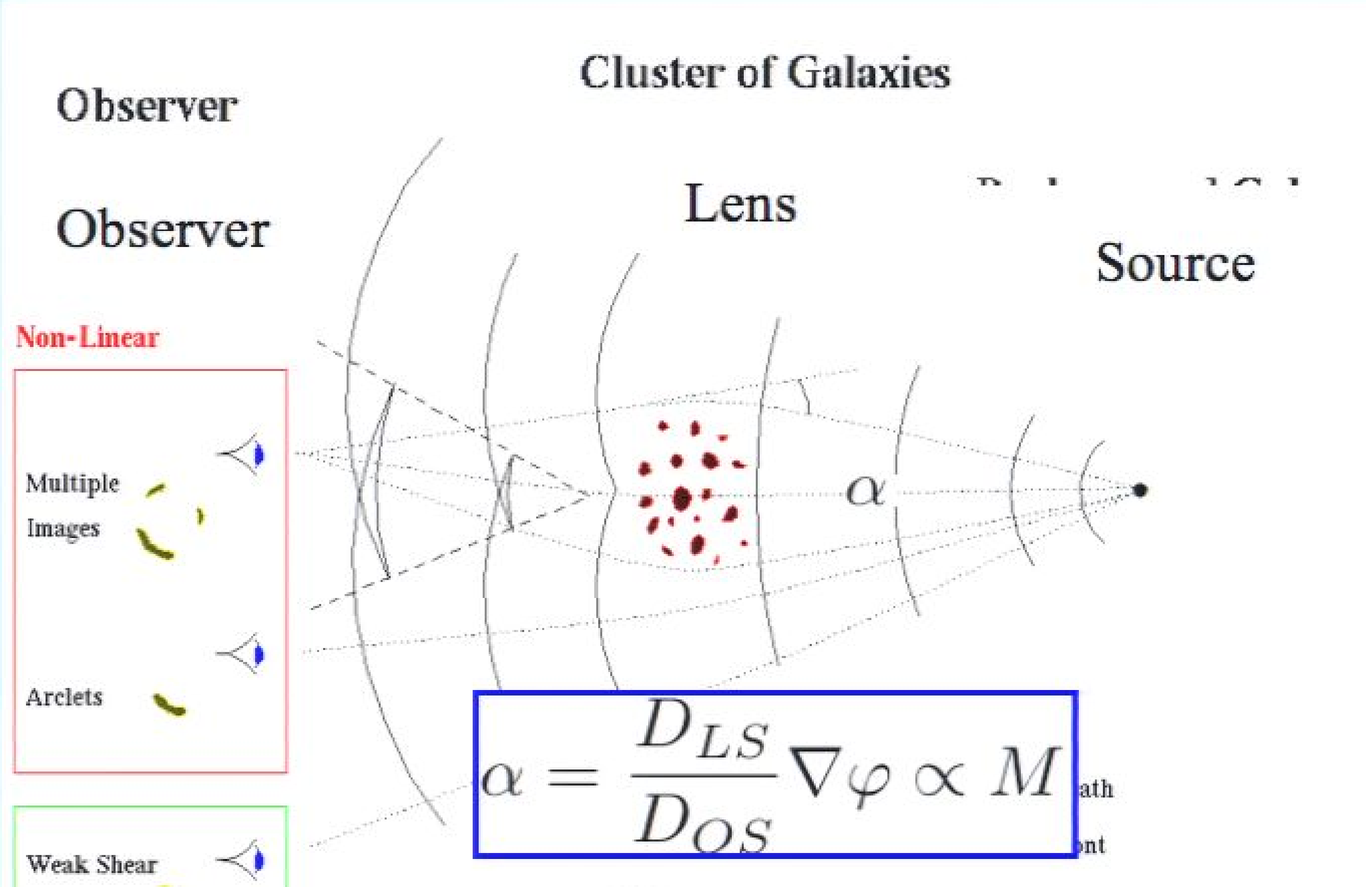

$$\alpha = \frac{D_{LS}}{D_{OS}} \nabla \varphi \propto M$$

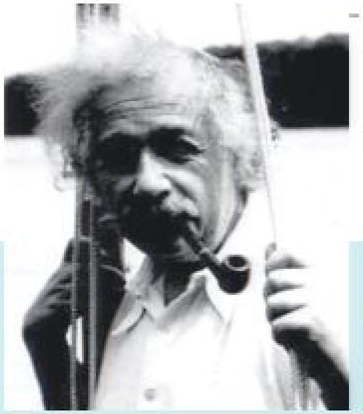

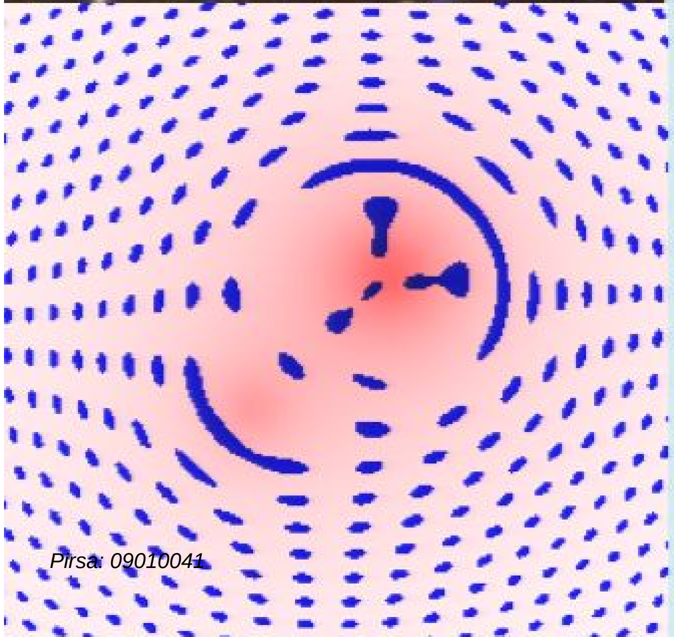

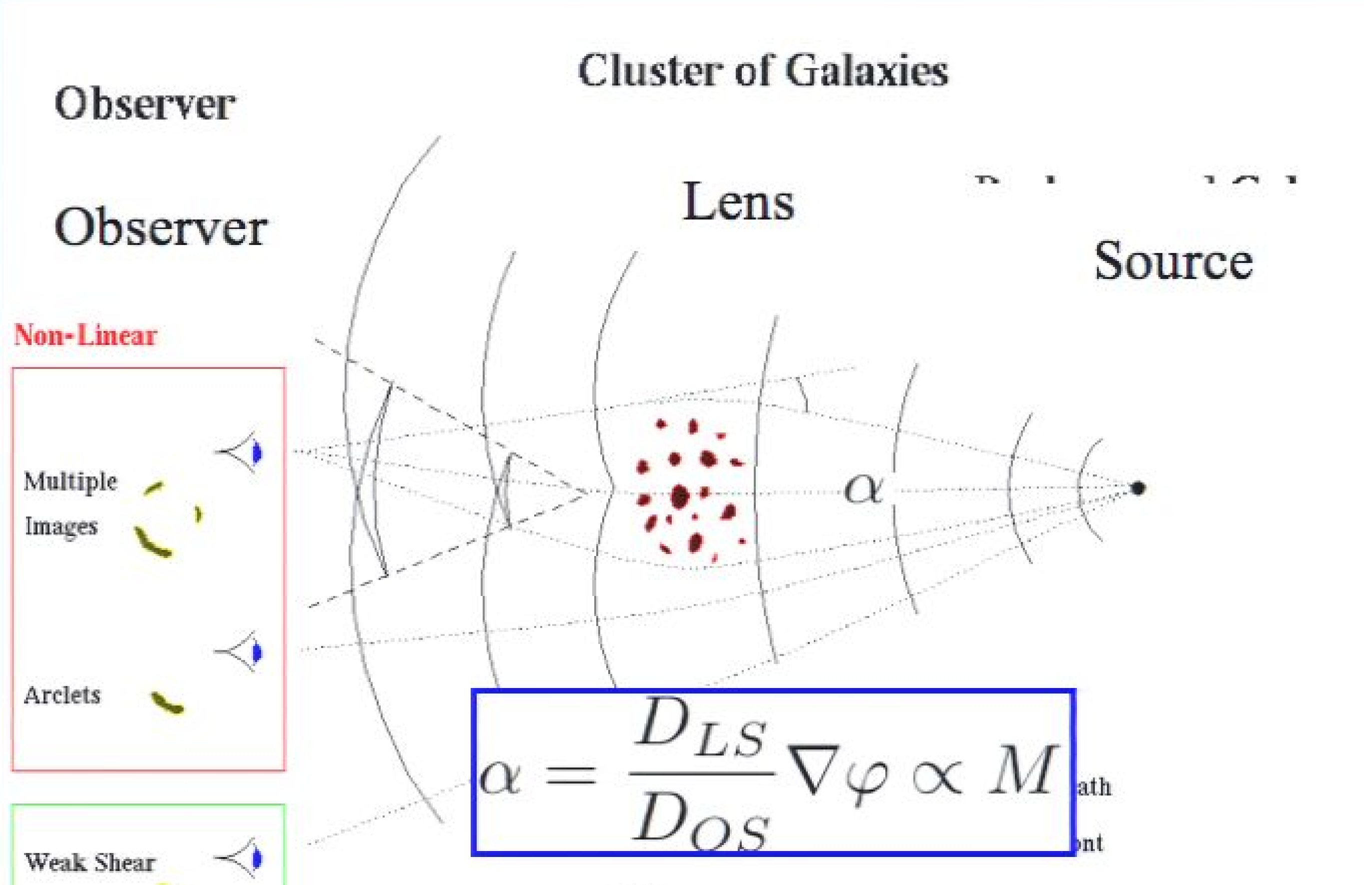

$$\alpha = \frac{D_{LS}}{D_{OS}} \nabla \varphi \propto M$$

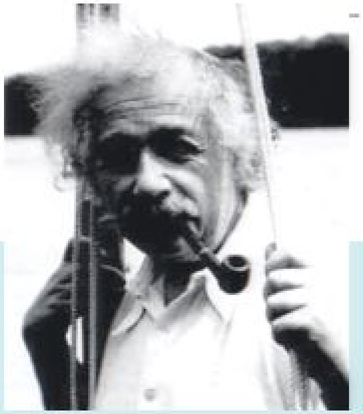

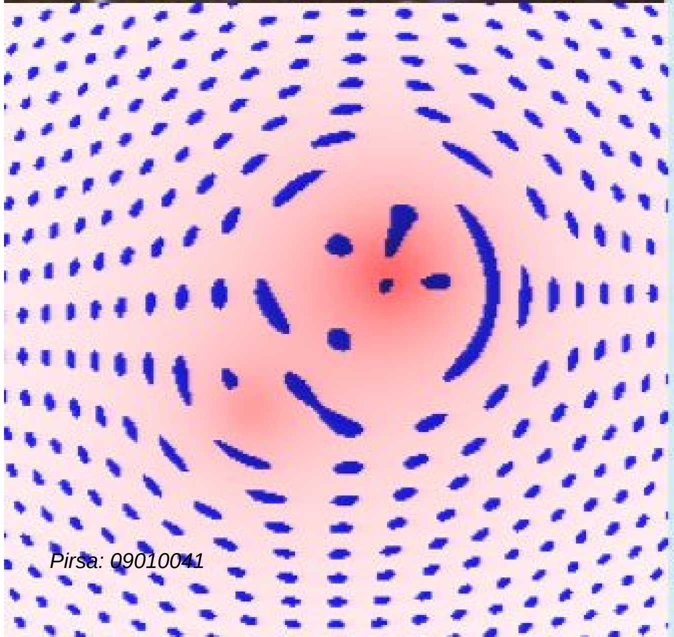

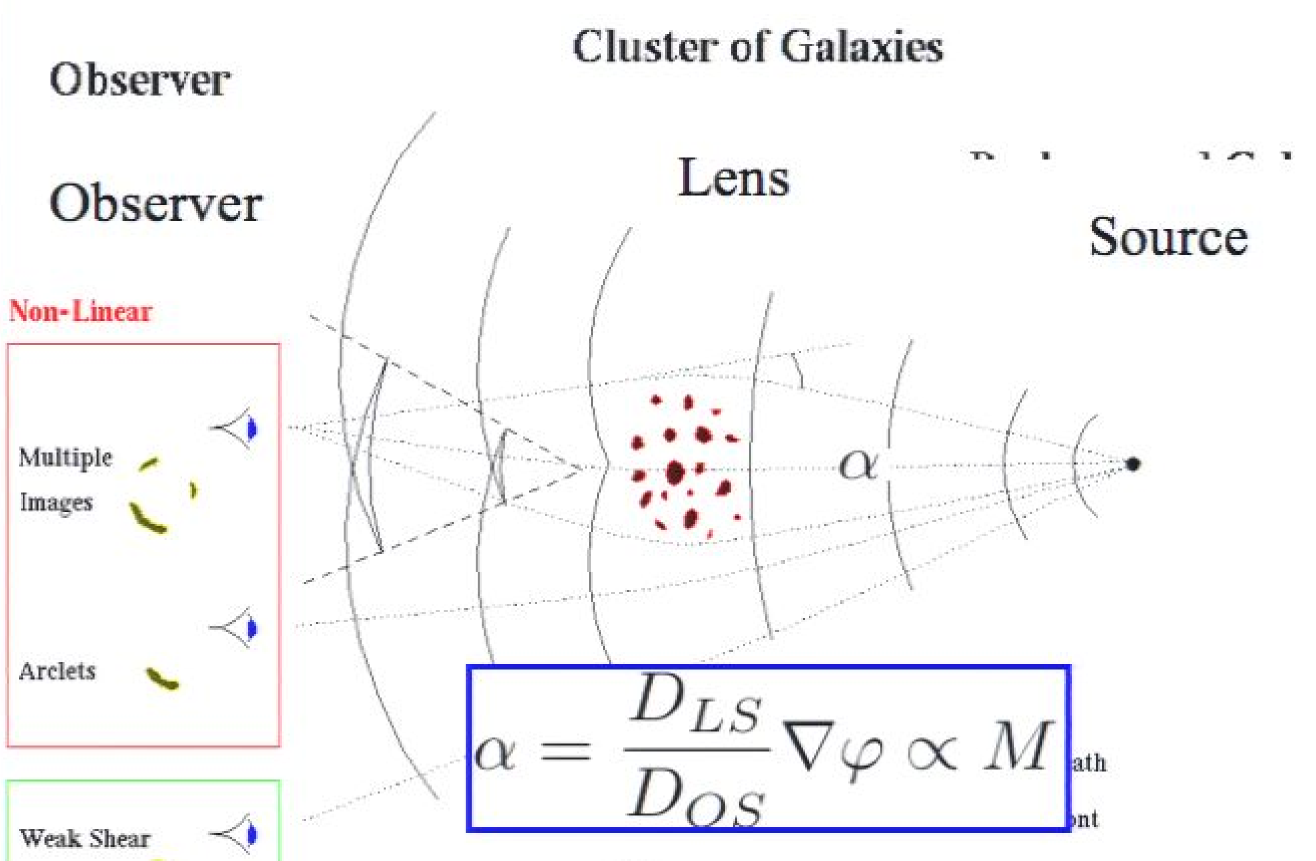

$$\alpha = \frac{D_{LS}}{D_{OS}} \nabla \varphi \propto M$$

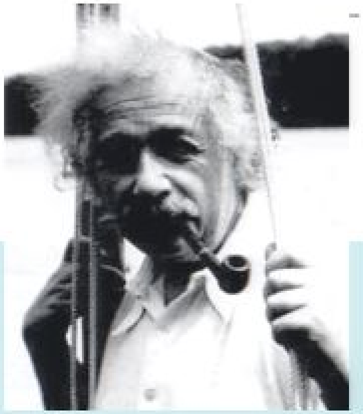

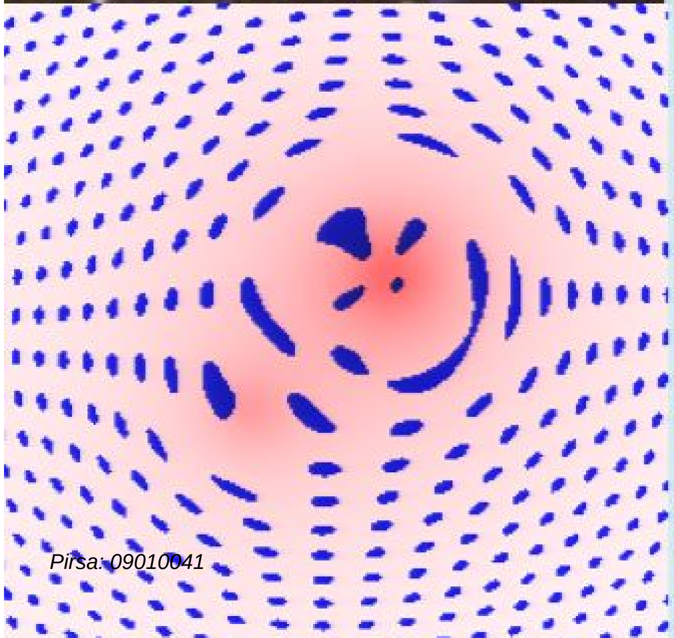

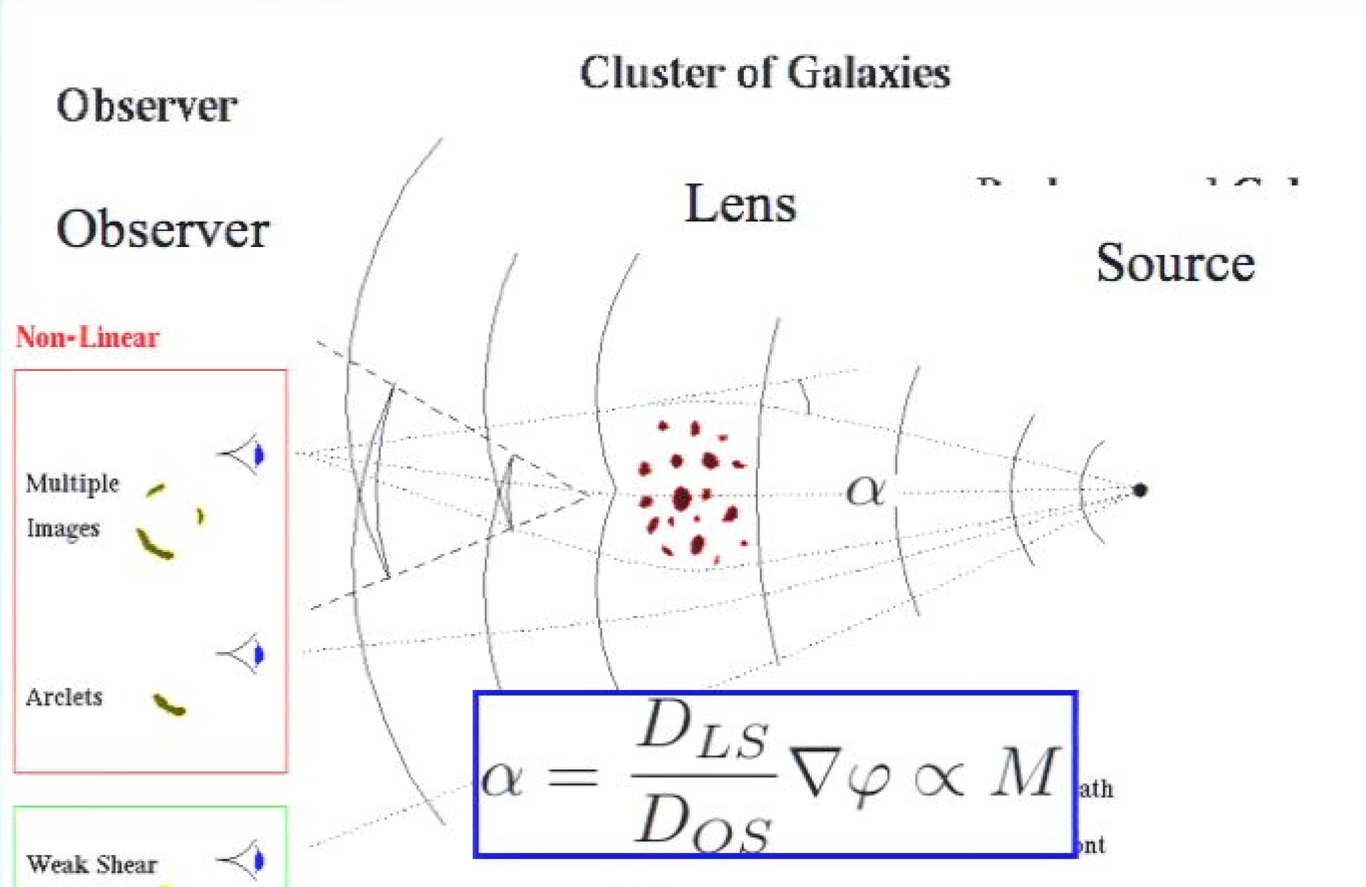

$$\boxed{\alpha = \frac{D_{LS}}{D_{OS}} \nabla \varphi \propto M}$$

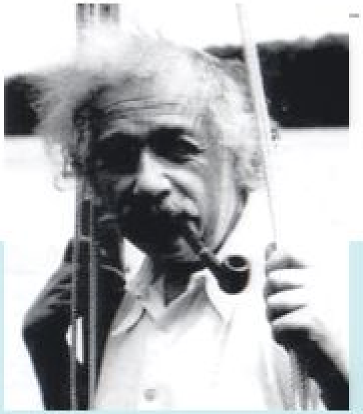

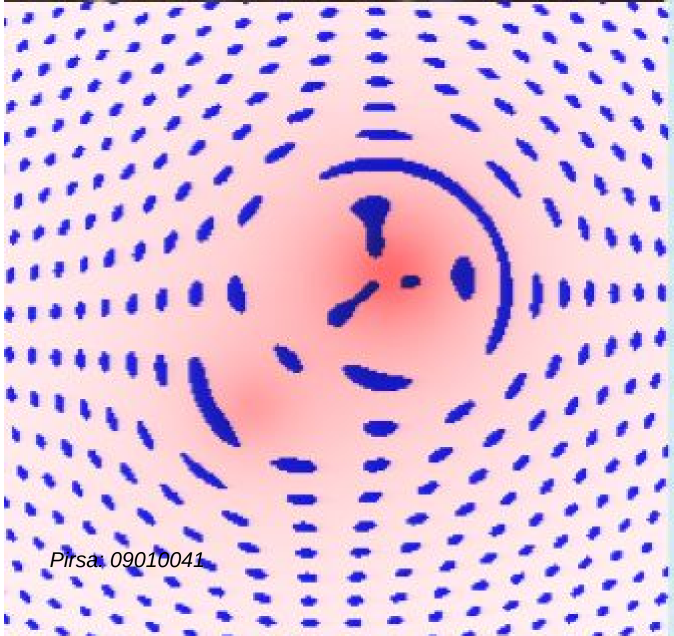

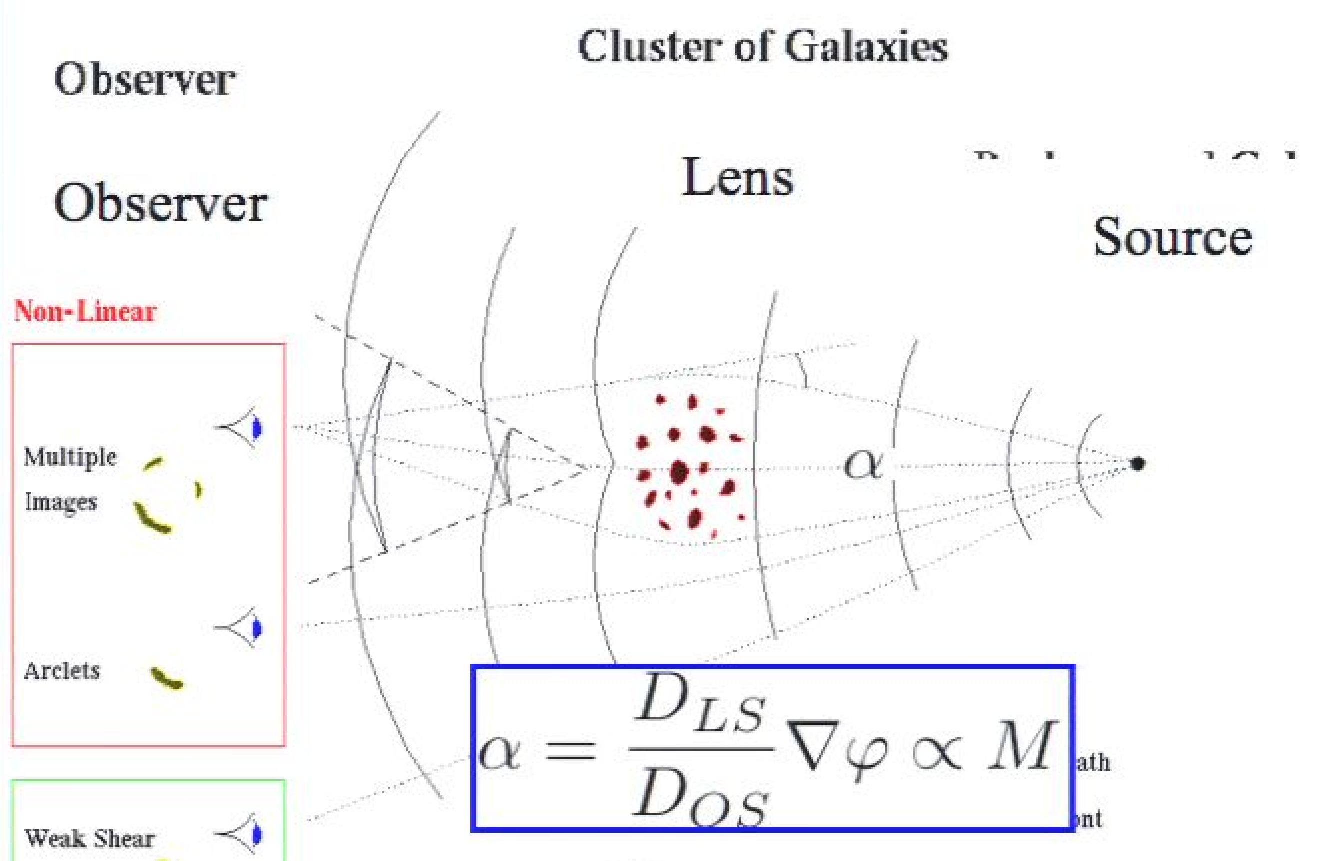

$$\alpha = \frac{D_{LS}}{D_{OS}} \nabla \varphi \propto M$$

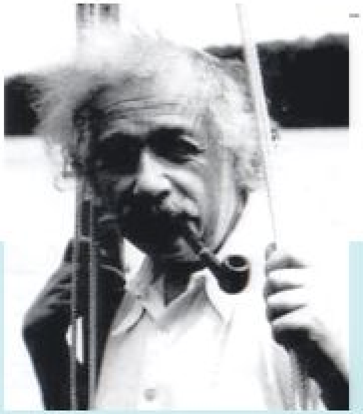

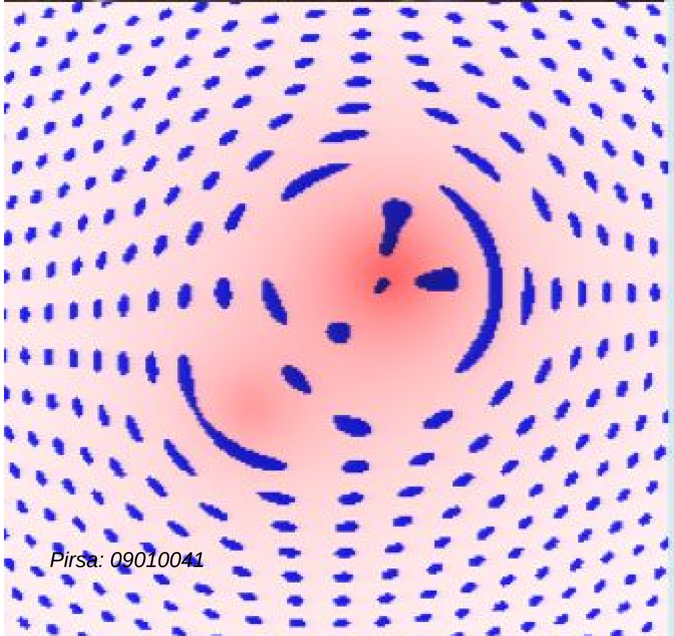

Observer

Observer

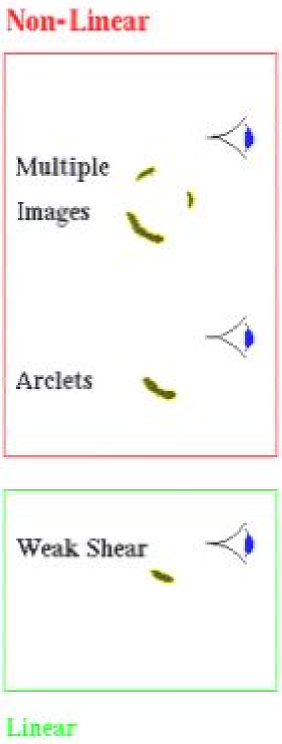

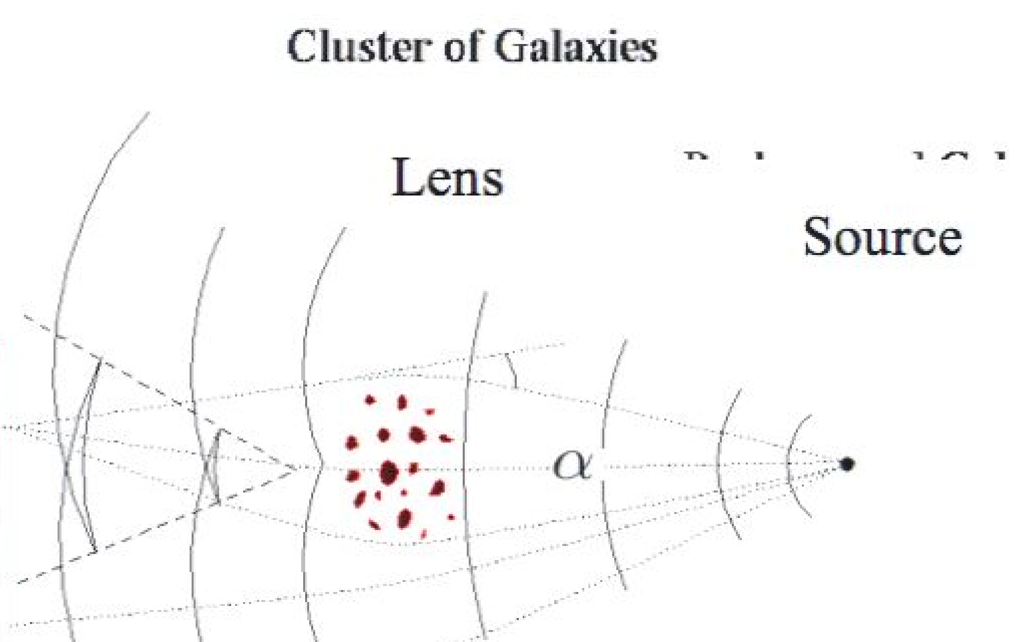

$$\boxed{\alpha = \frac{D_{LS}}{D_{OS}} \nabla \varphi \propto M}$$

- - - - Multiple Images Area

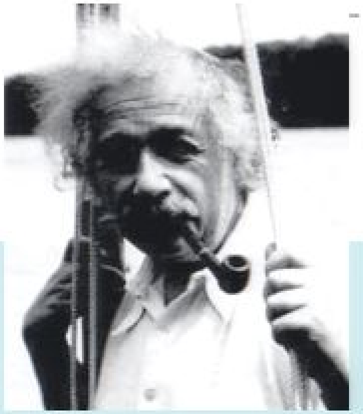

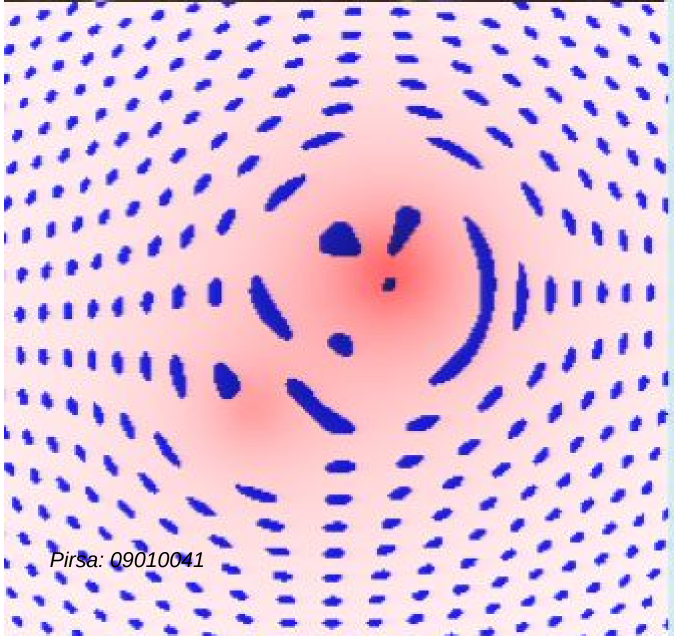

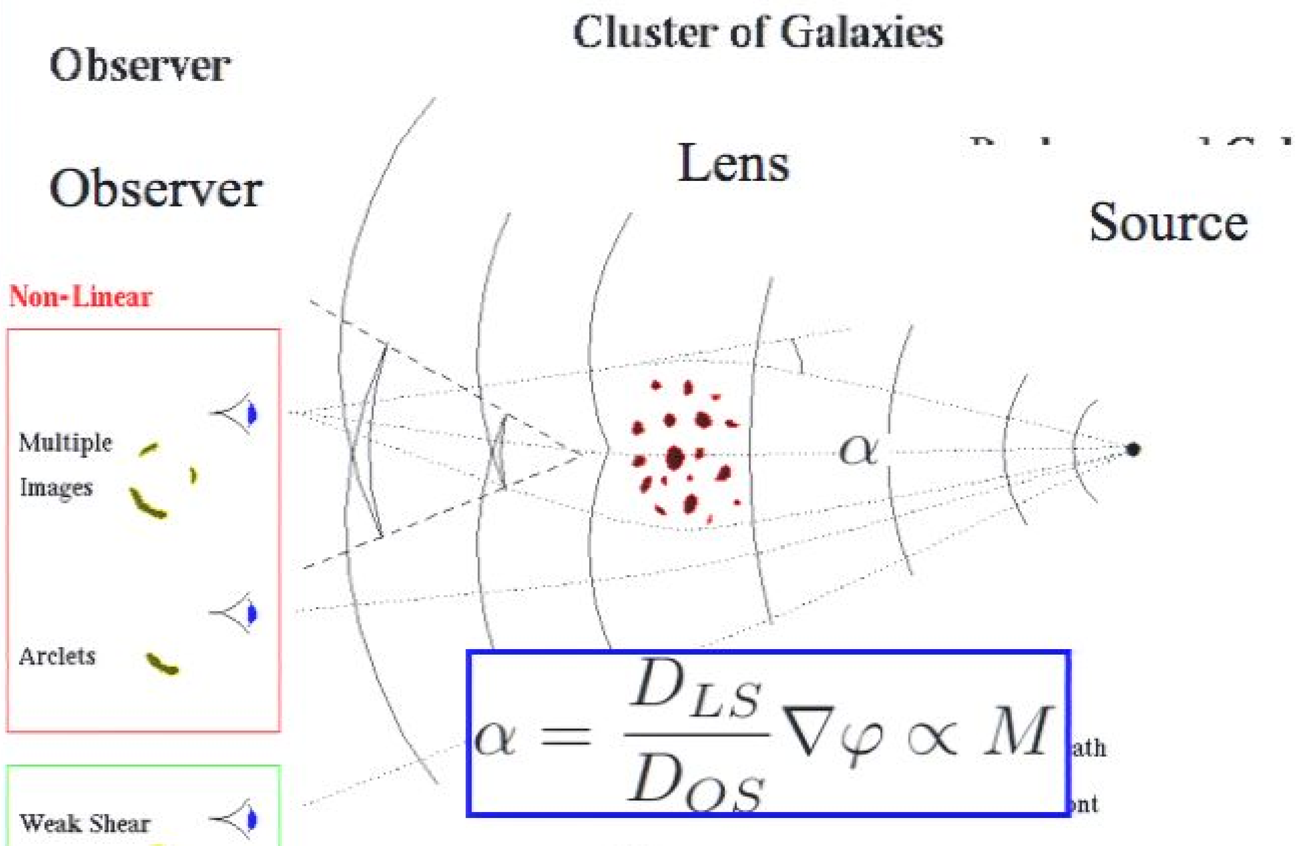

$$\alpha = \frac{D_{LS}}{D_{OS}} \nabla \varphi \propto M$$

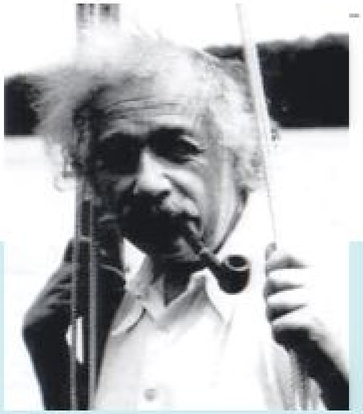

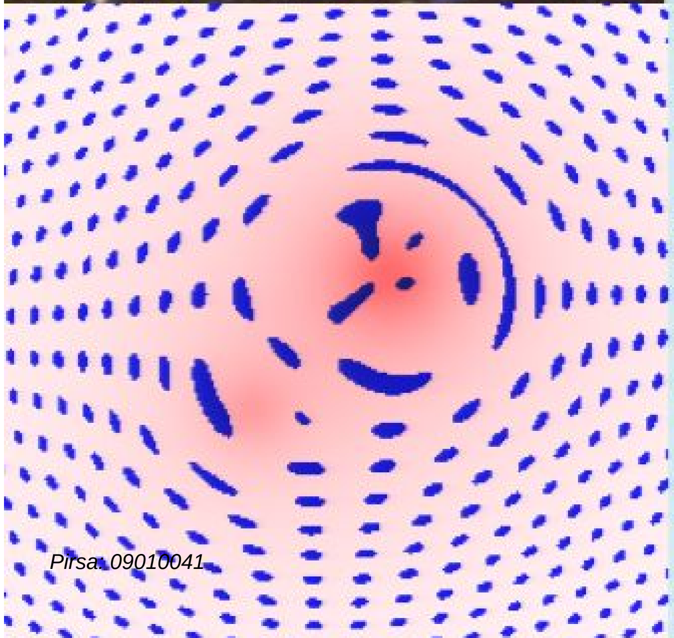

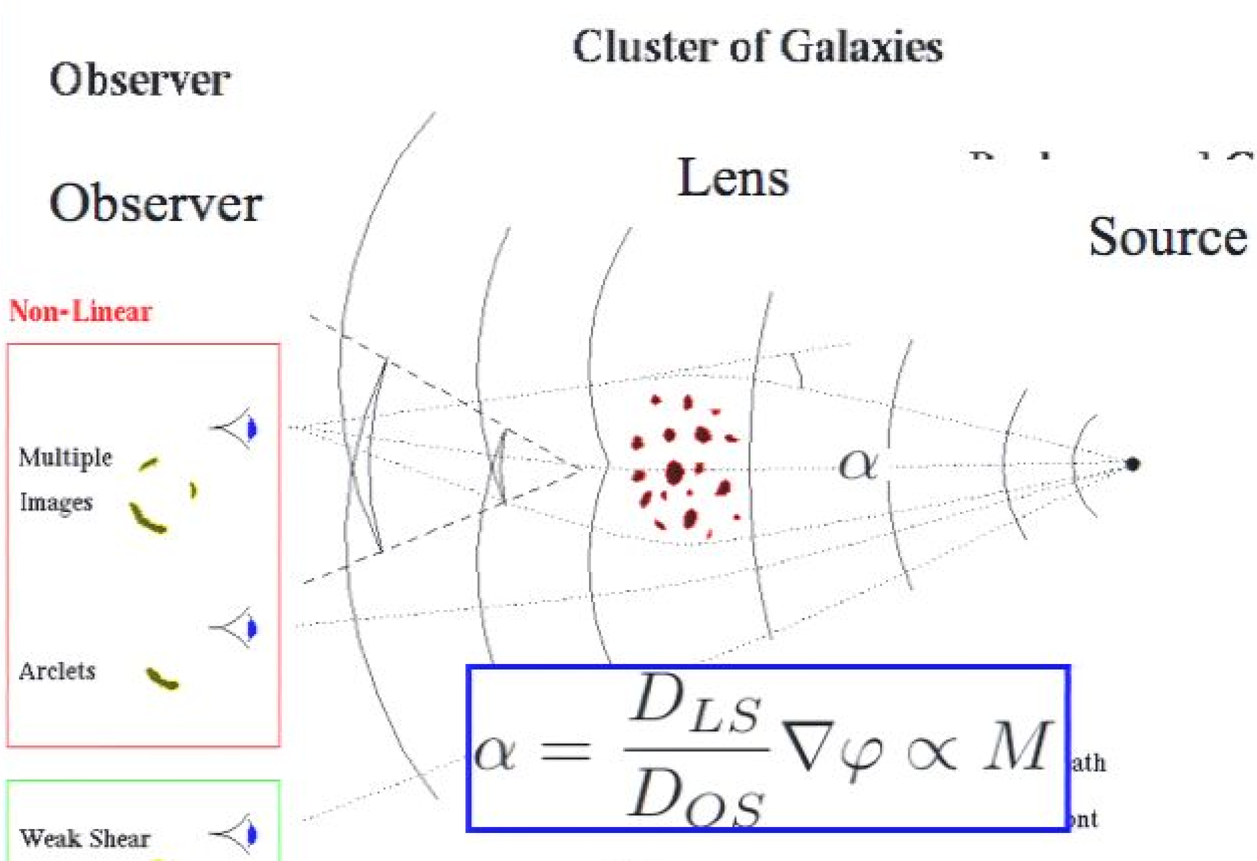

$$\alpha = \frac{D_{LS}}{D_{OS}} \nabla\varphi \propto M$$

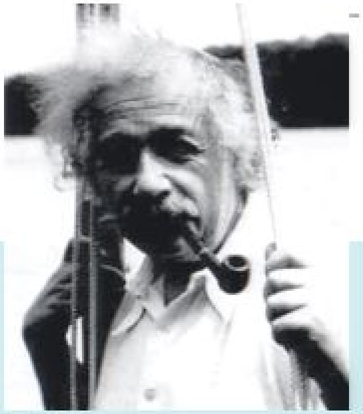

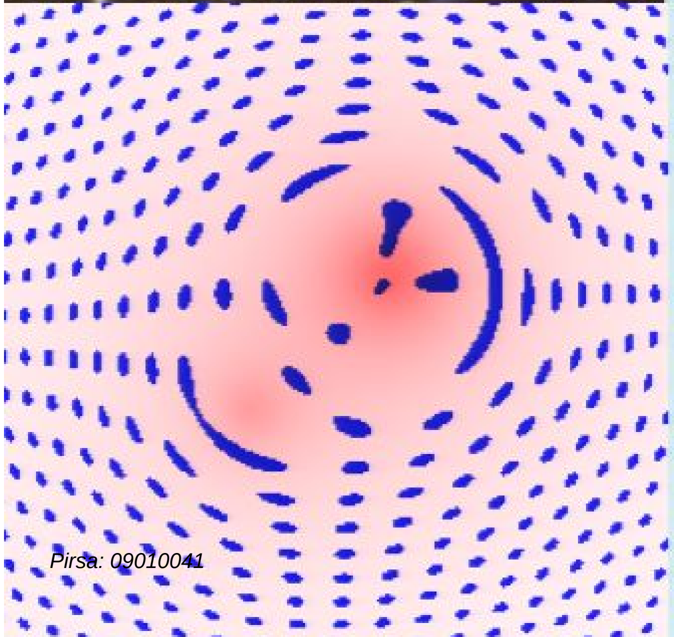

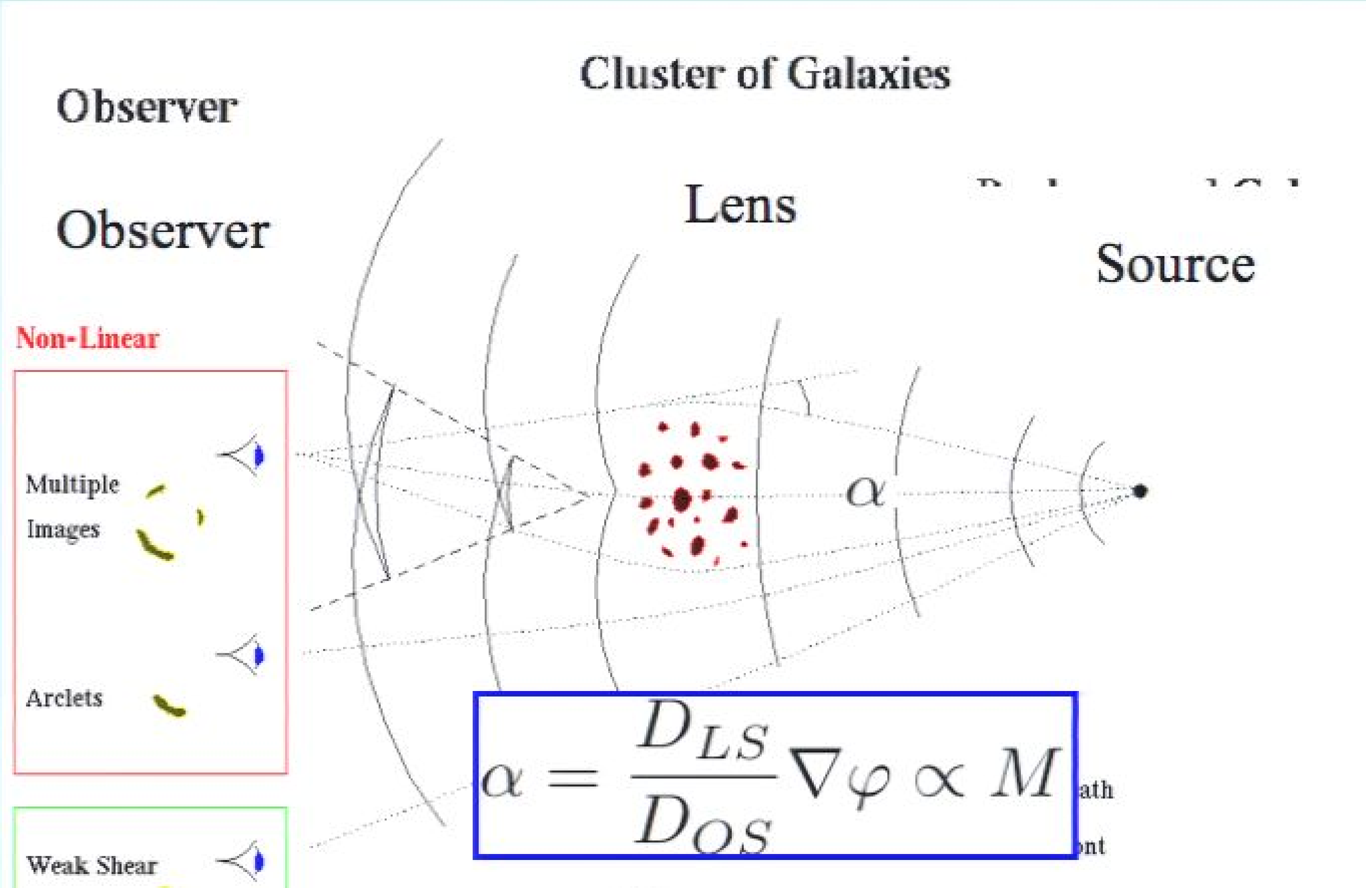

$$\alpha = \frac{D_{LS}}{D_{OS}} \nabla \varphi \propto M$$

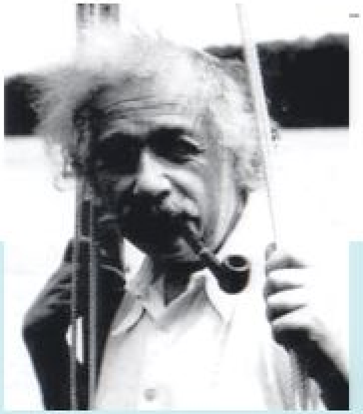

CFHT 1990

Z_cluster=0.375

Z_arc=0.725 (Soucail et al 1988)

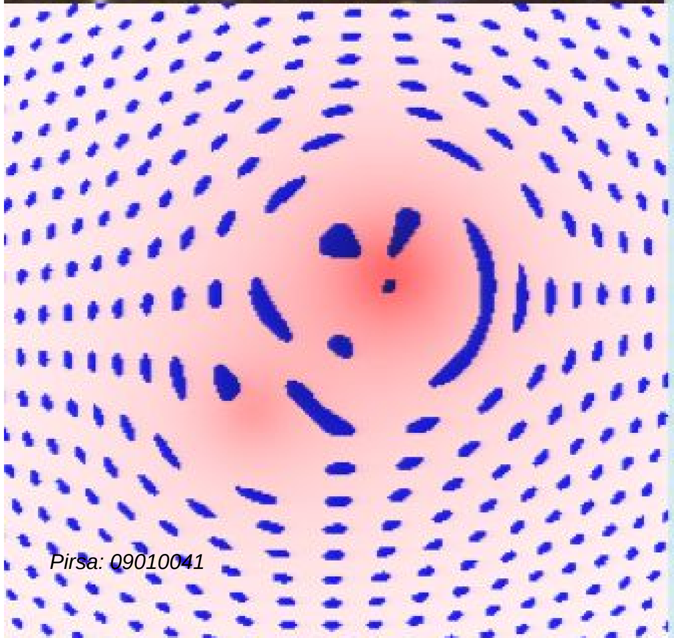

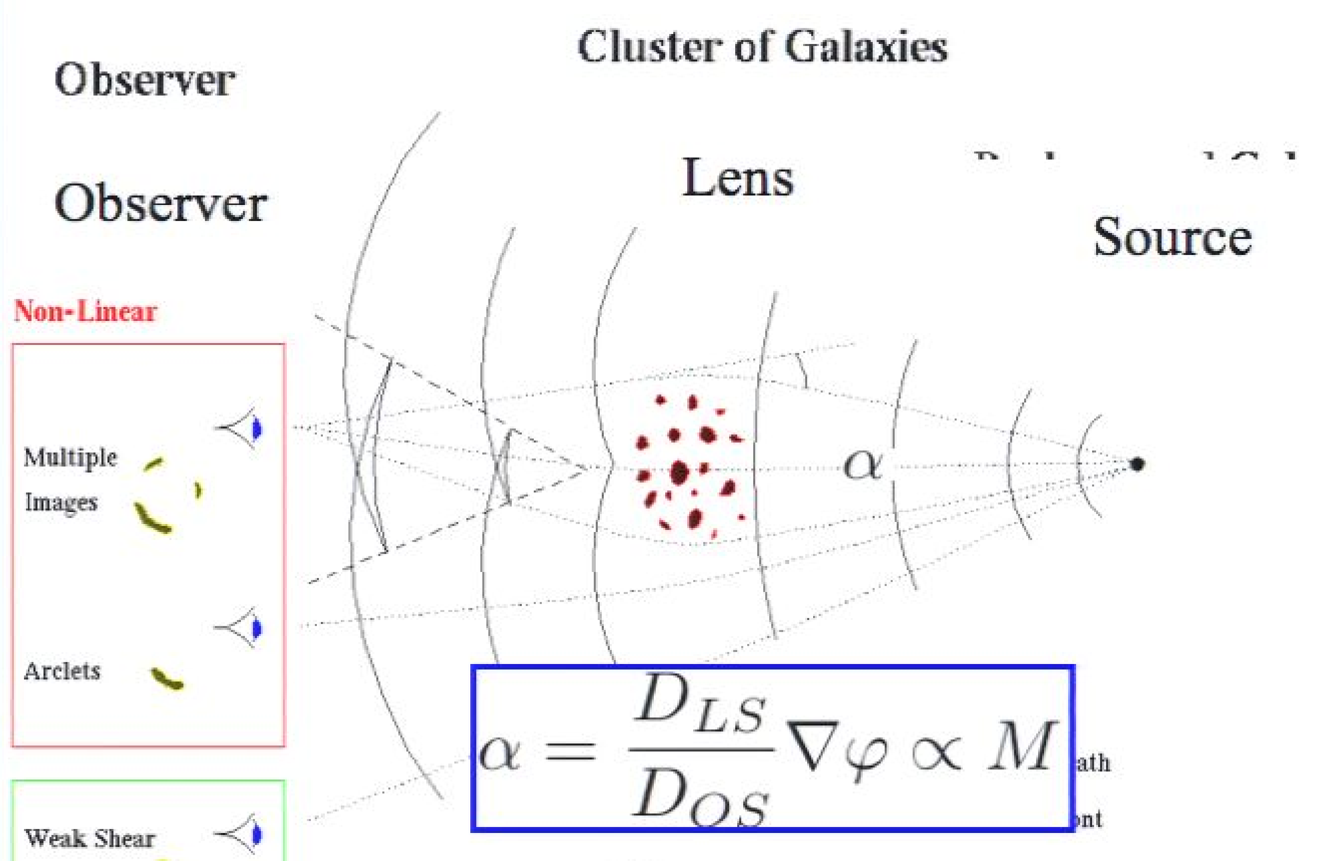

$$\alpha = \frac{D_{LS}}{D_{OS}}\nabla\varphi \propto M$$

Multiple Images Area

Linear

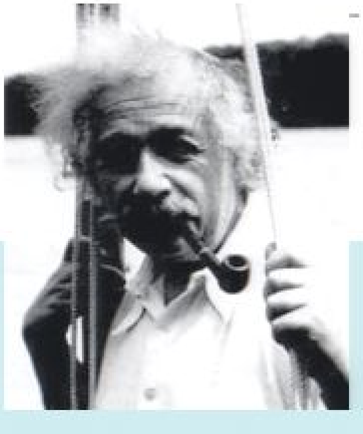

CFHT 1990

Z_cluster=0.375

Z_arc=0.725 (Soucail et al 1988)

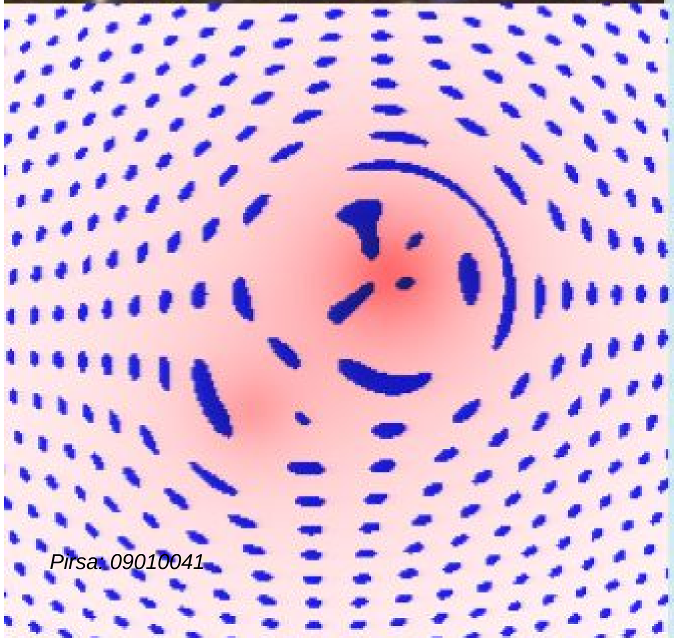

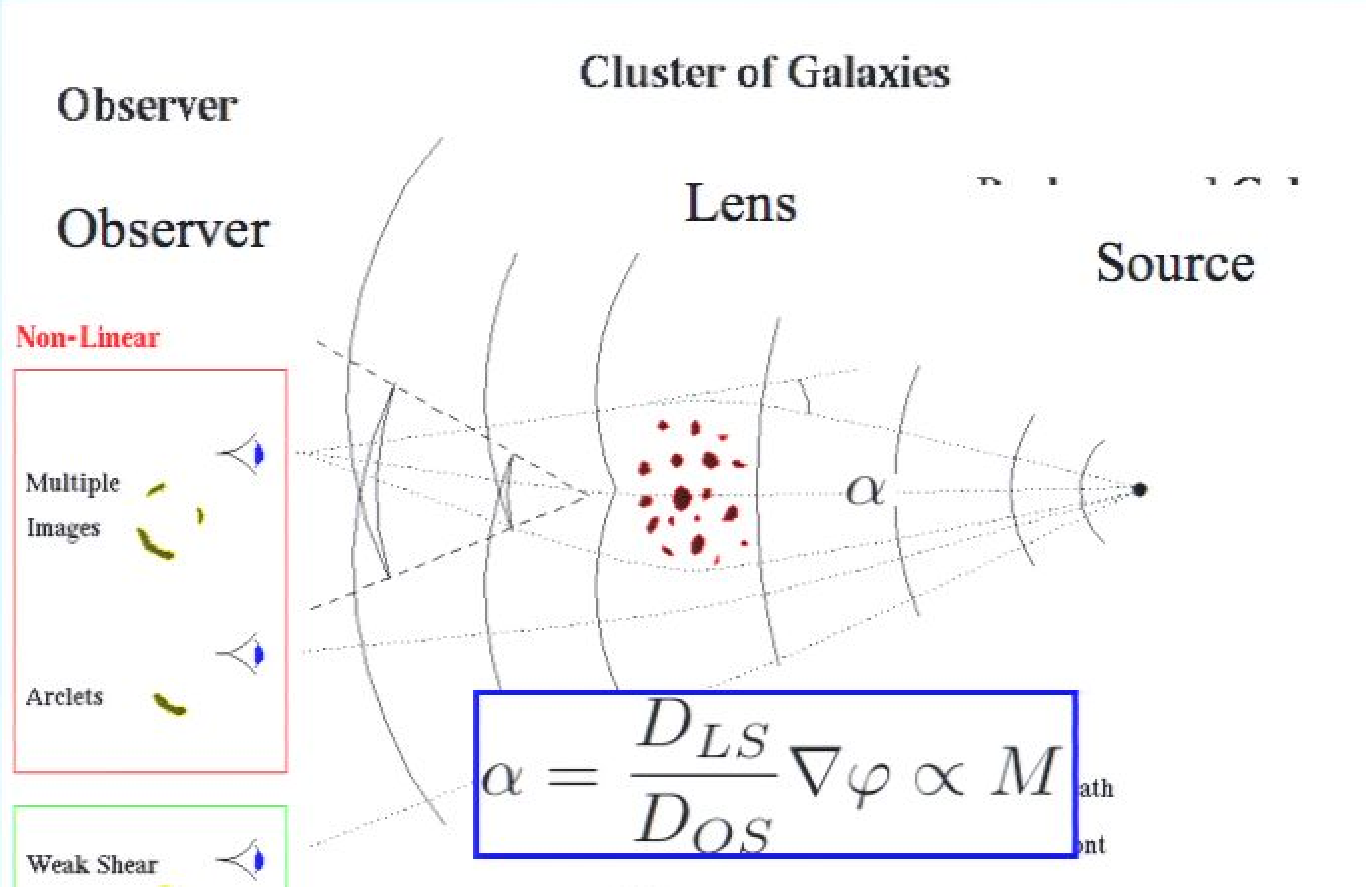

$$\alpha = \frac{D_{LS}}{D_{OS}} \nabla \varphi \propto M$$

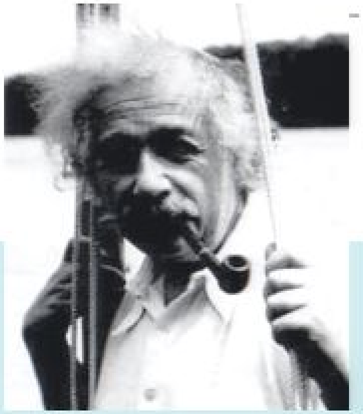

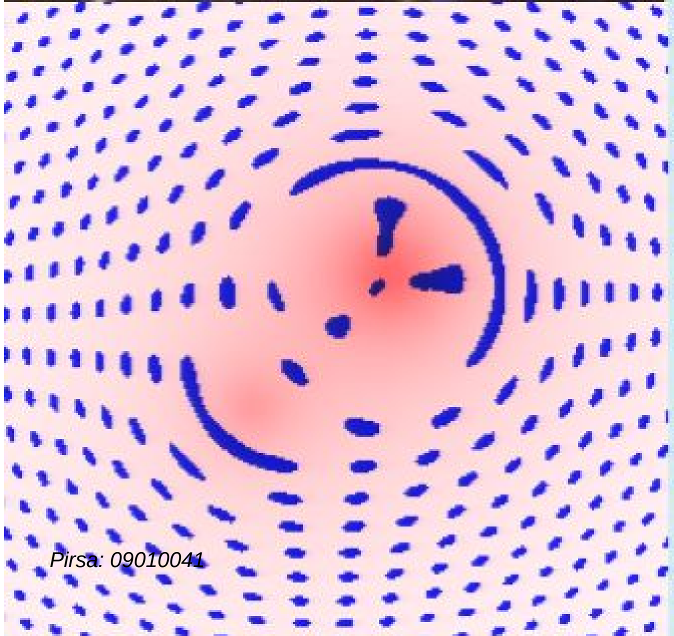

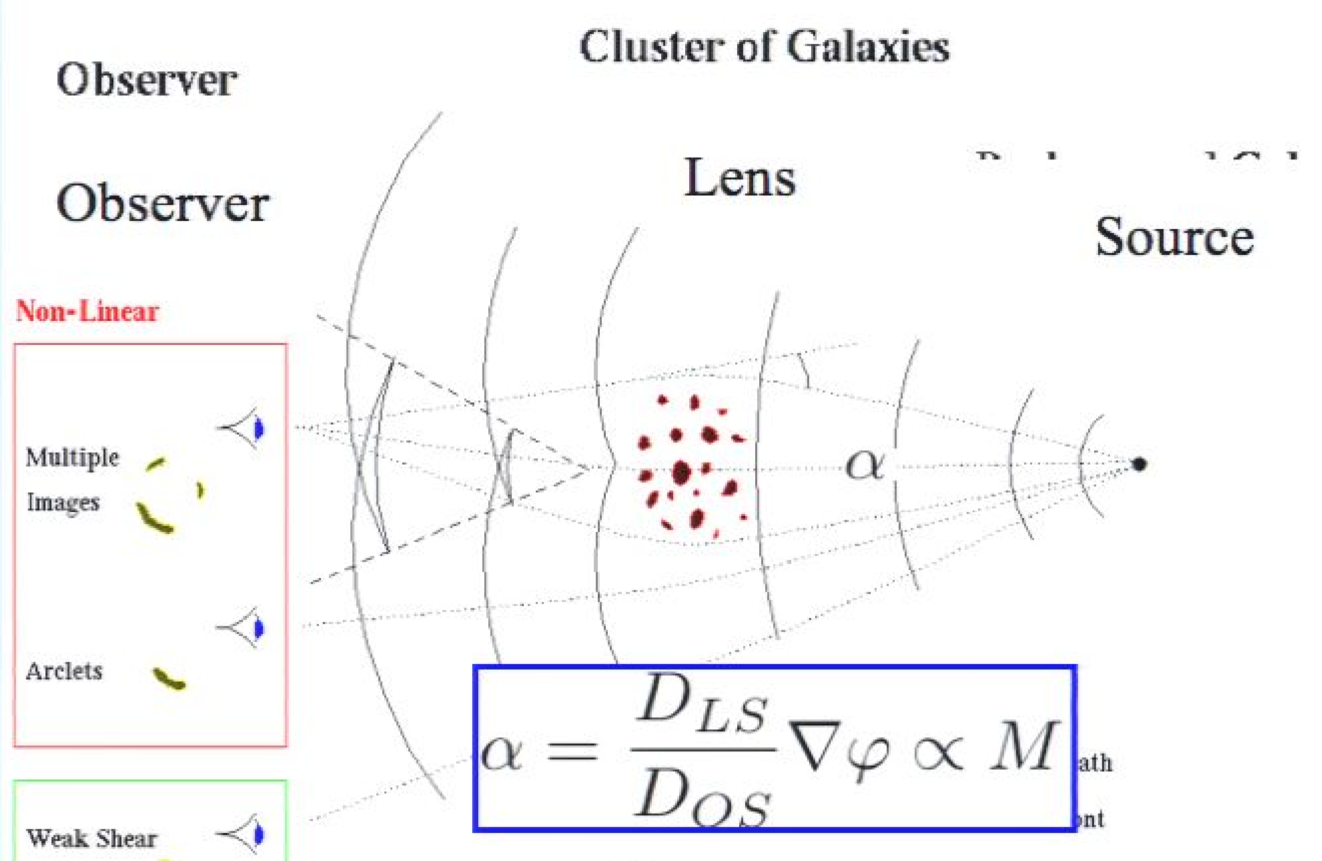

$$\alpha = \frac{D_{LS}}{D_{OS}} \nabla \varphi \propto M$$

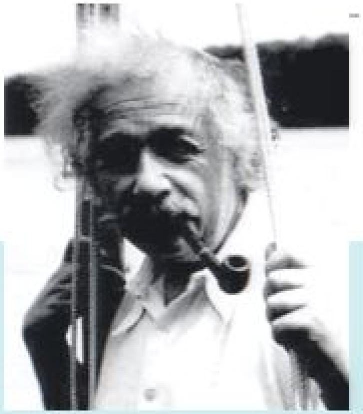

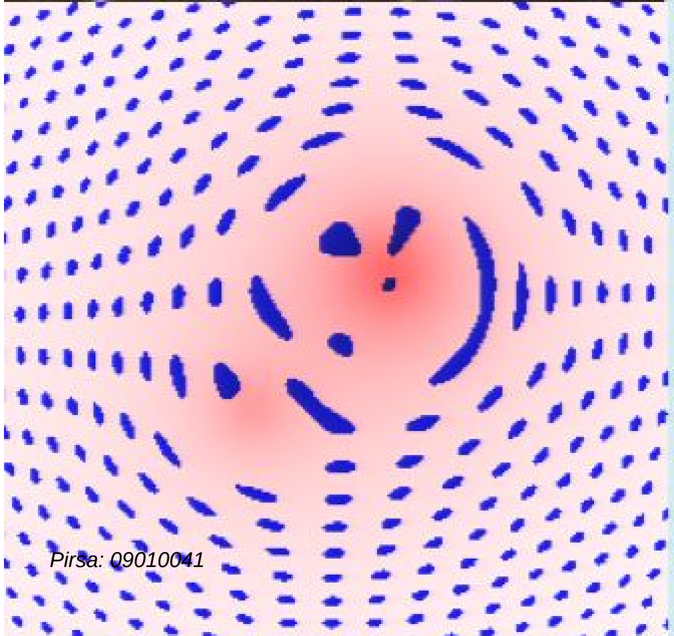

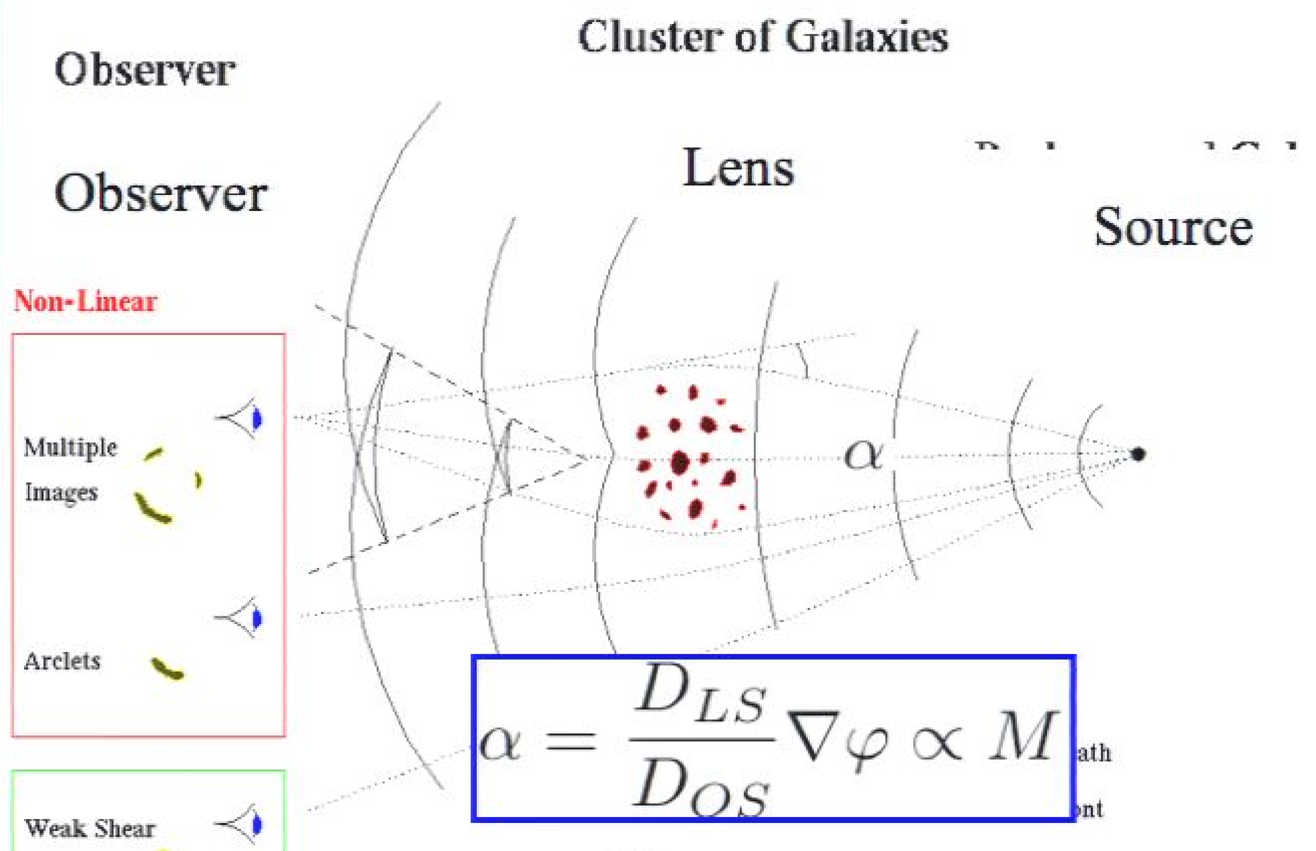

$$\boxed{\alpha = \frac{D_{LS}}{D_{OS}} \nabla \varphi \propto M}$$

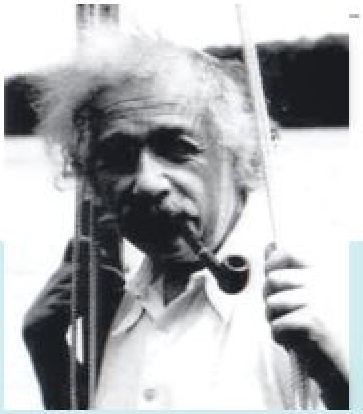

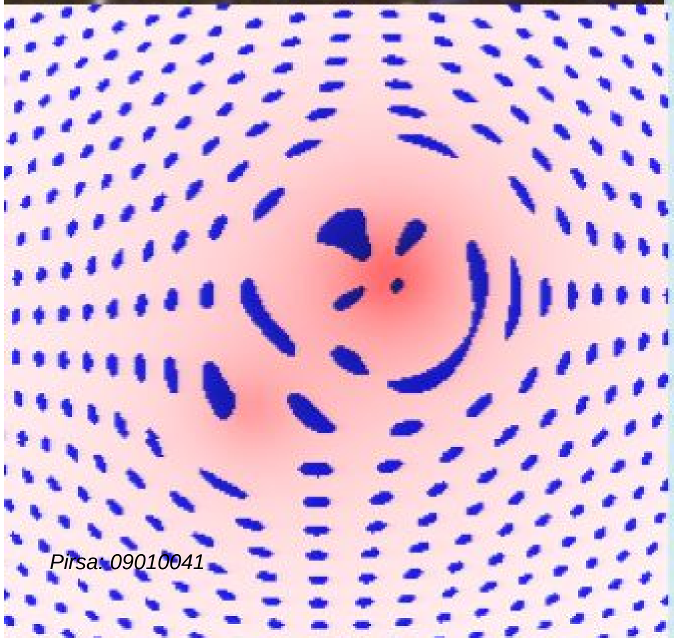

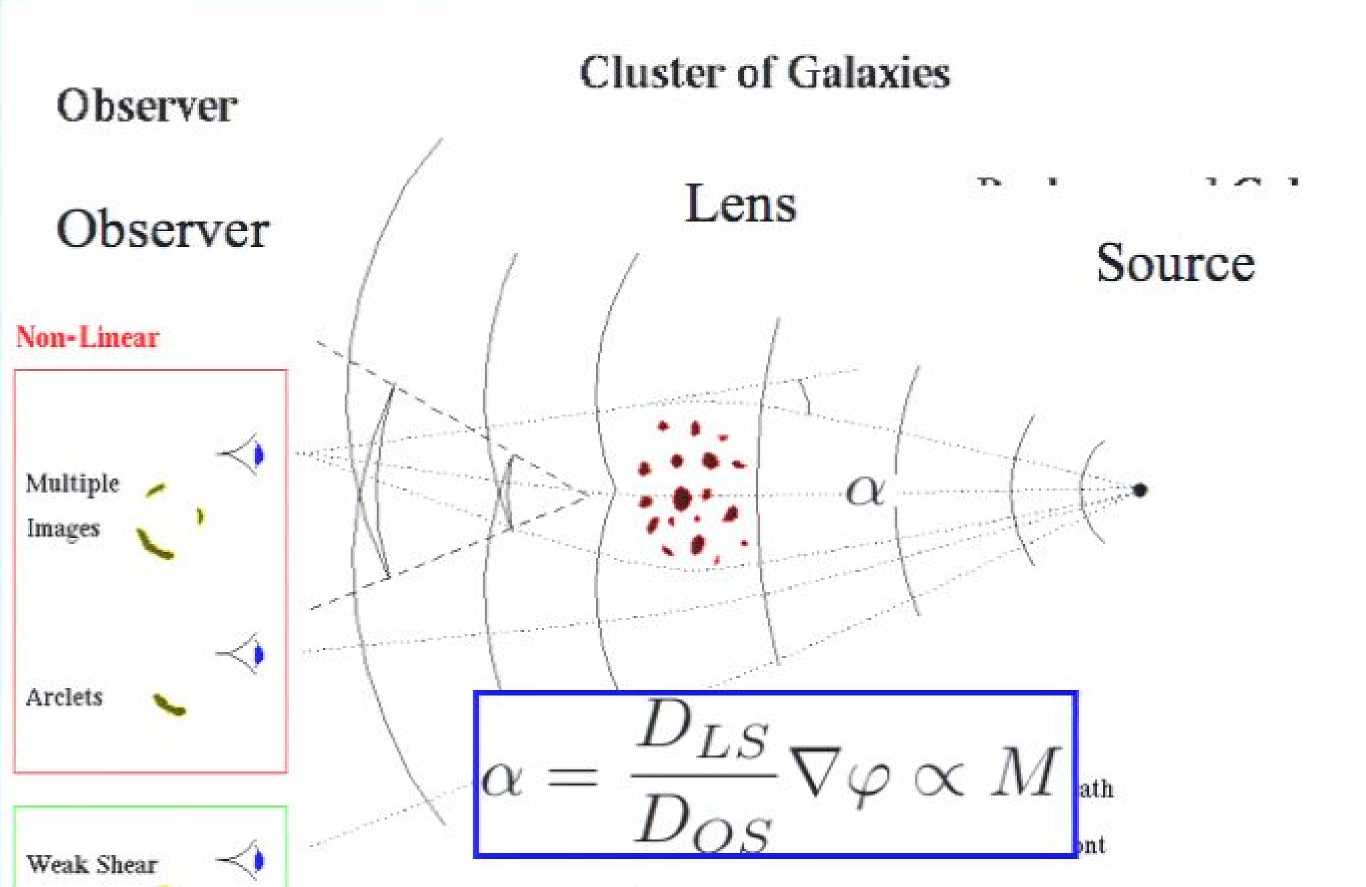

$$\alpha = \frac{D_{LS}}{D_{OS}} \nabla\varphi \propto M$$

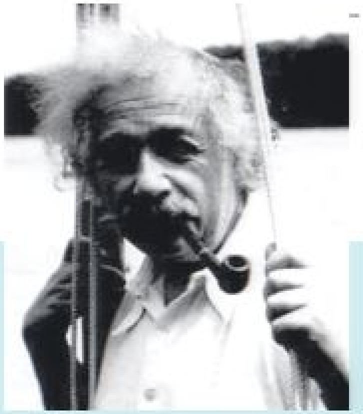

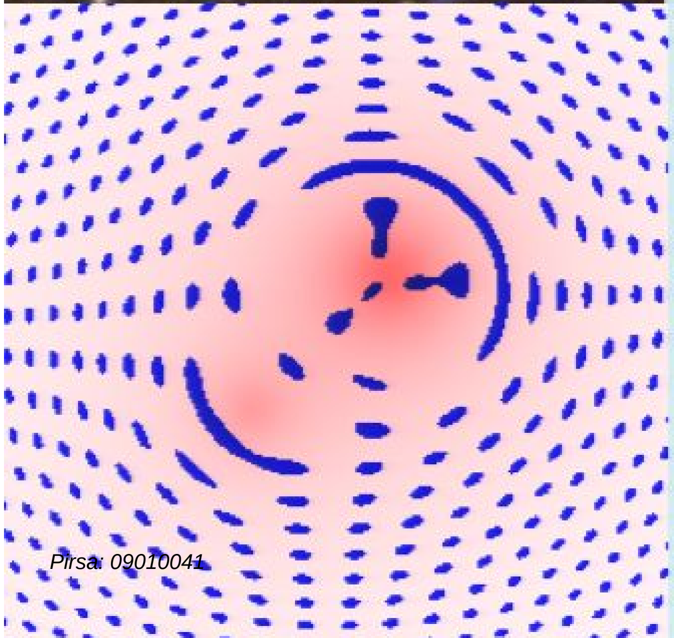

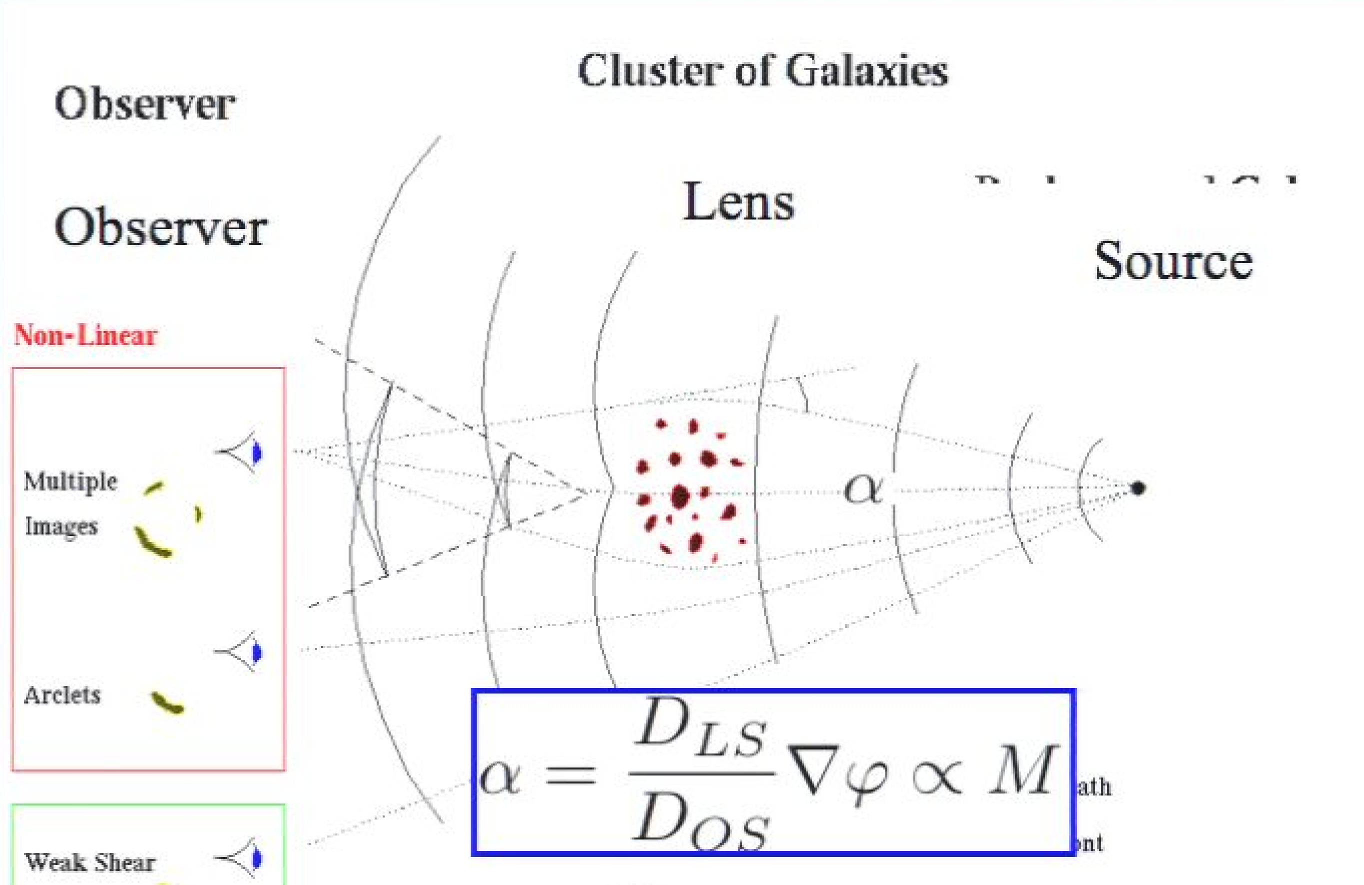

$$\alpha = \frac{D_{LS}}{D_{OS}} \nabla \varphi \propto M$$

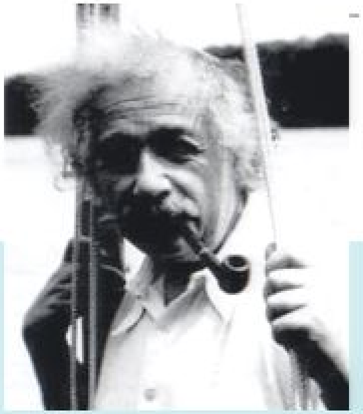

CFHT 1990

Z_cluster=0.375

Z_arc=0.725 (Soucail et al 1988)

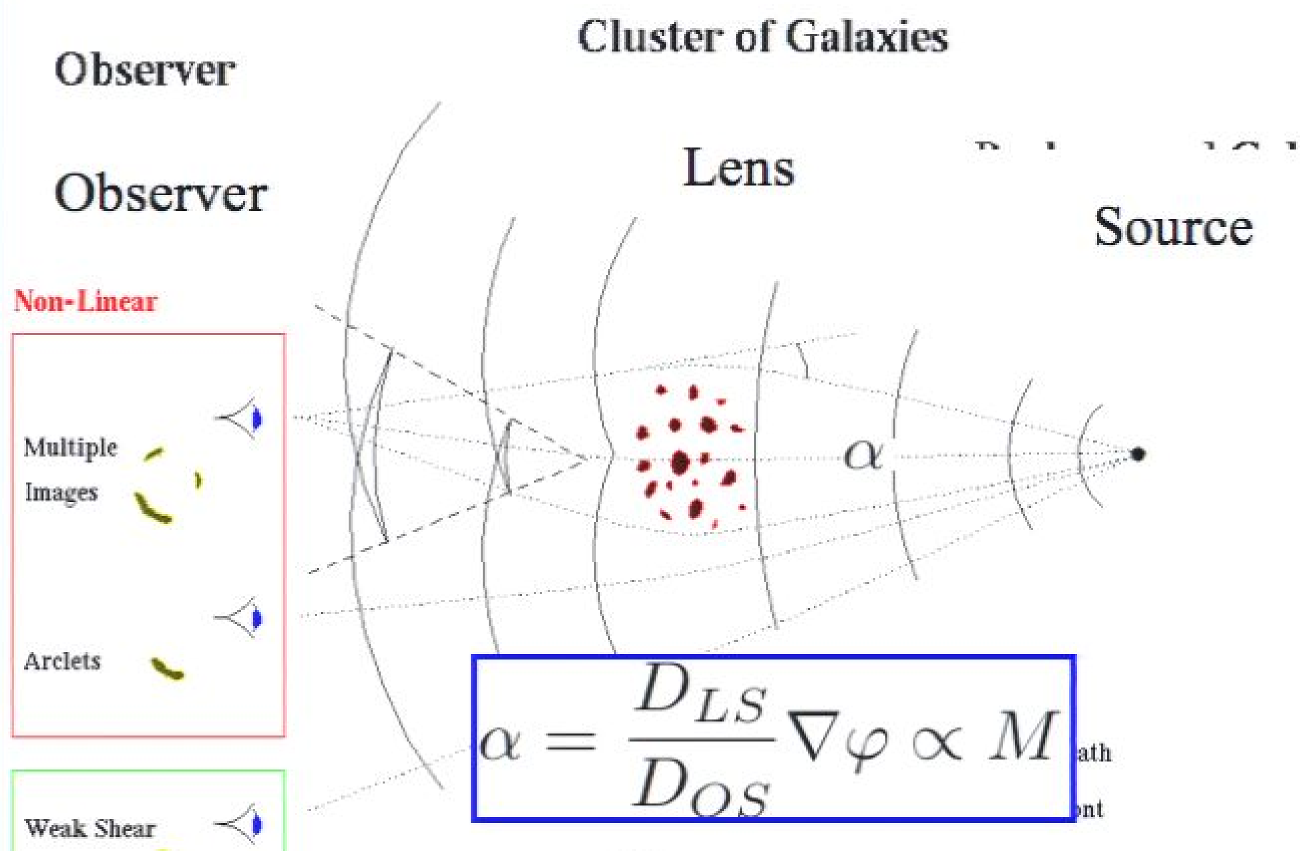

$$\alpha = \frac{D_{LS}}{D_{OS}} \nabla \varphi \propto M$$

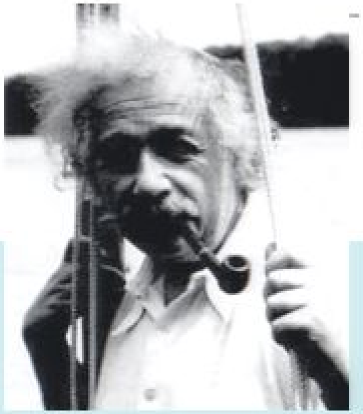

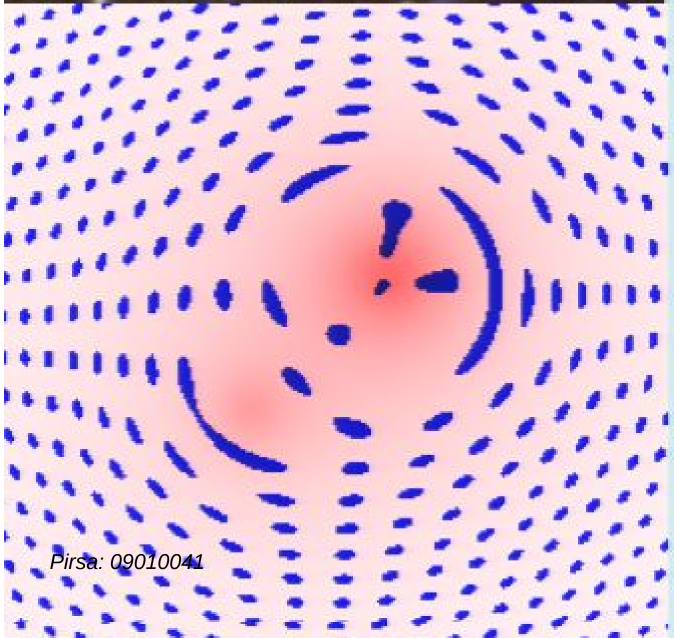

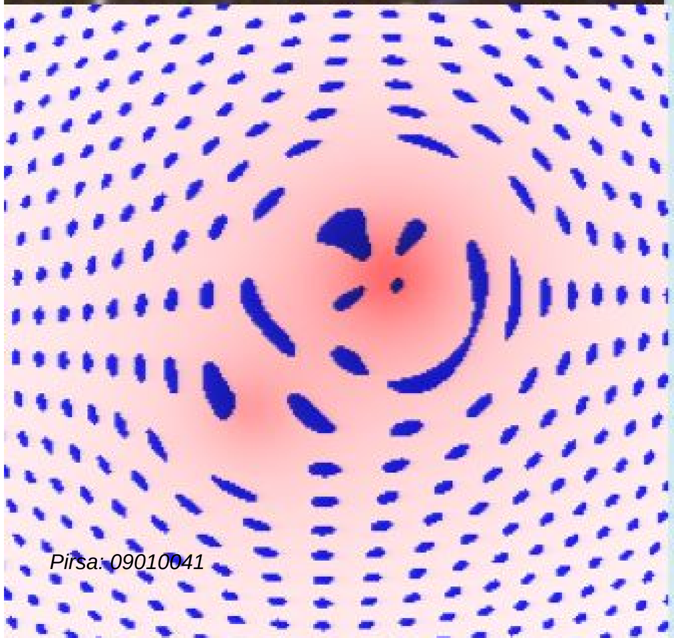

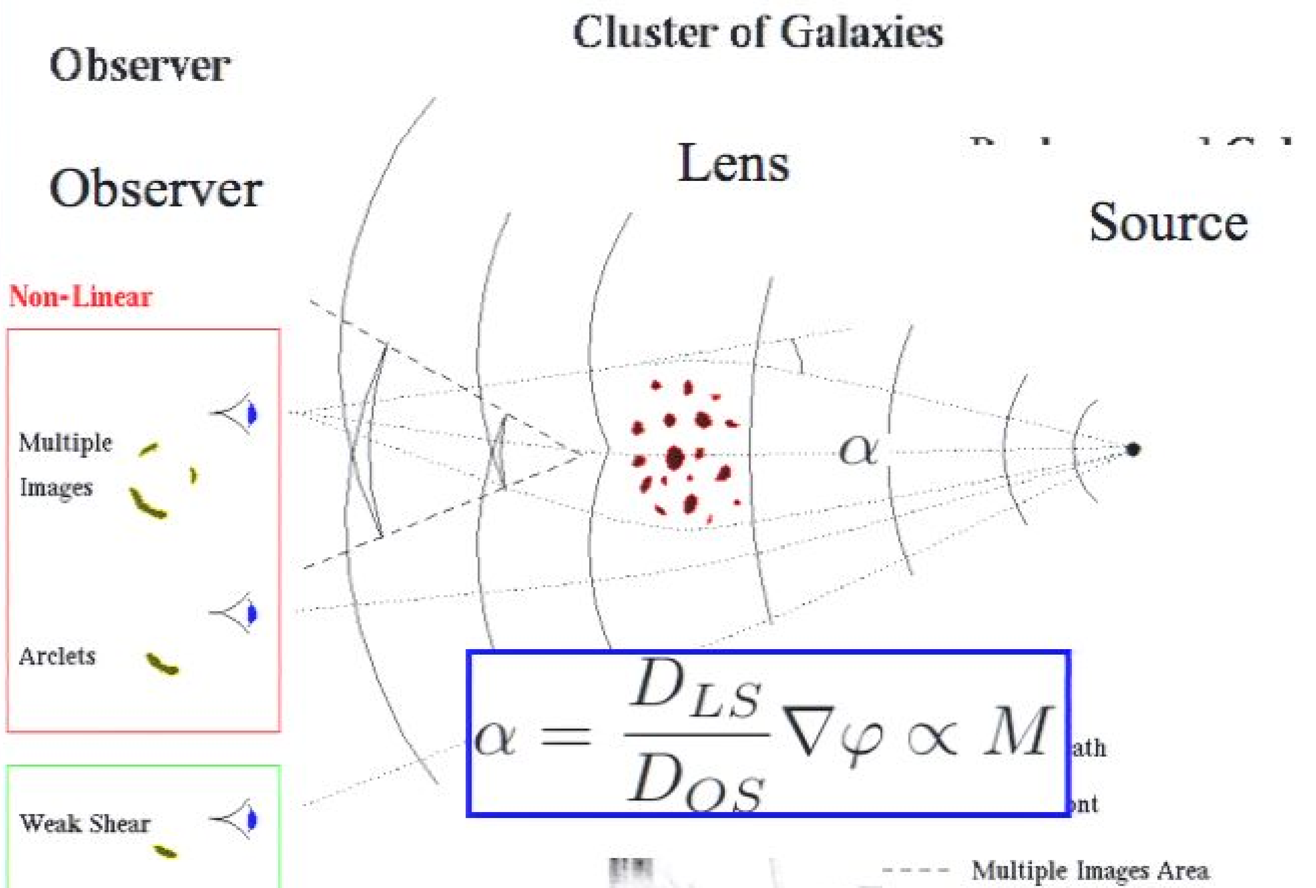

$$\alpha = \frac{D_{LS}}{D_{OS}} \nabla \varphi \propto M$$

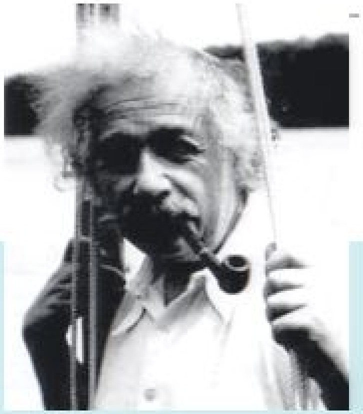

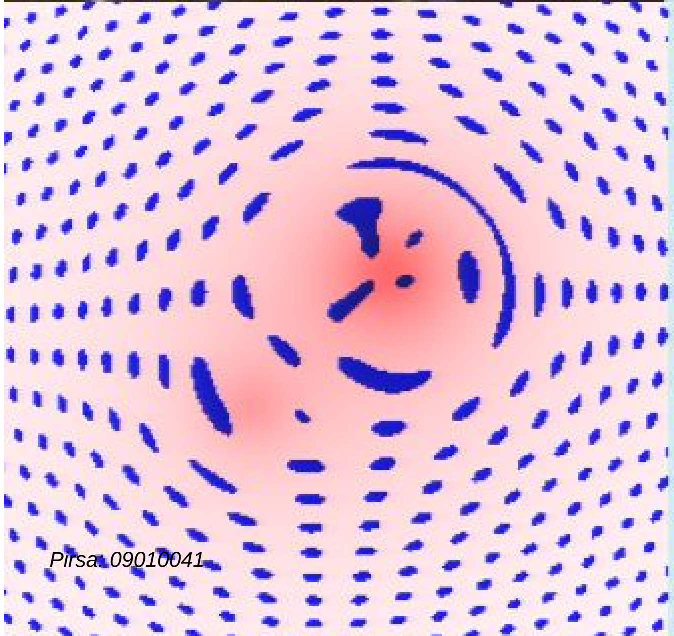

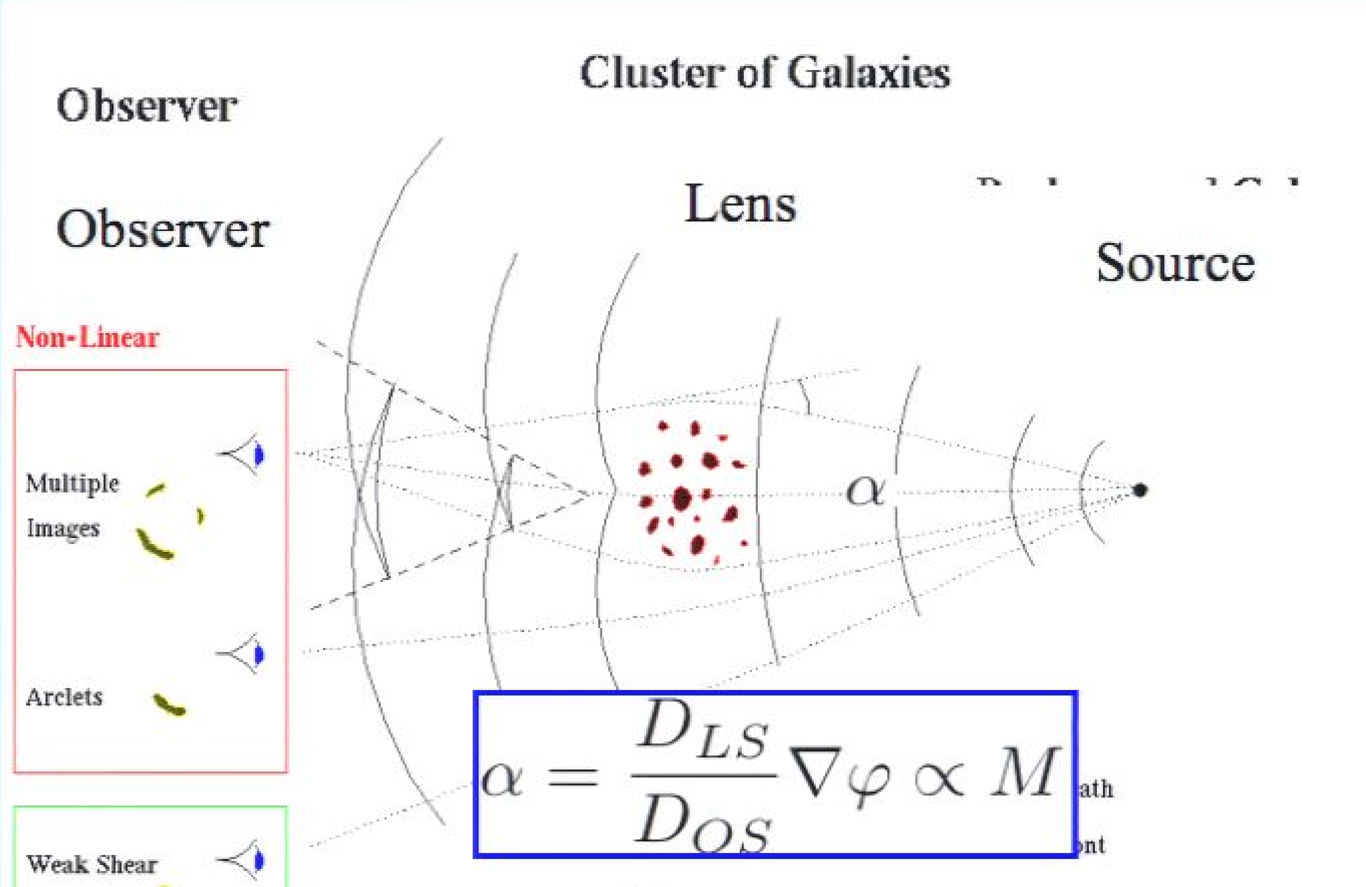

$$\alpha = \frac{D_{LS}}{D_{OS}} \nabla \varphi \propto M$$

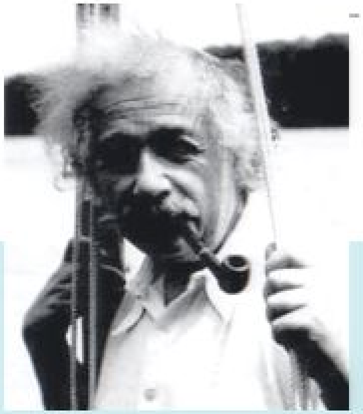

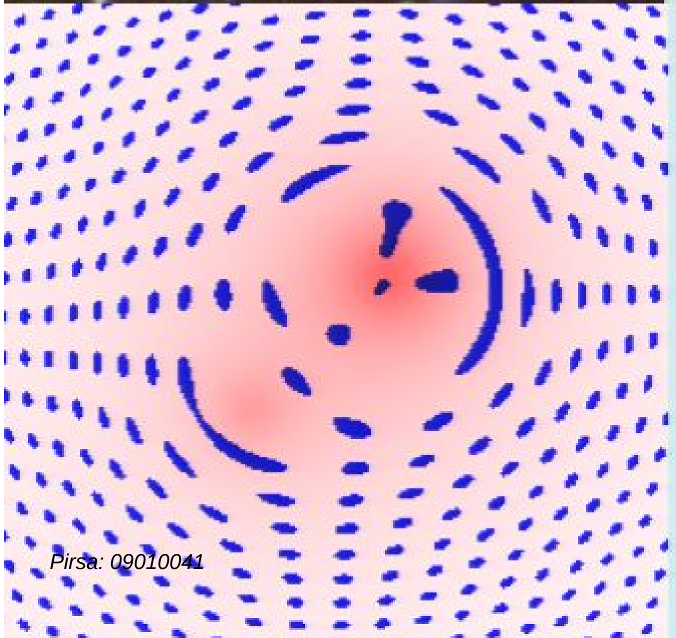

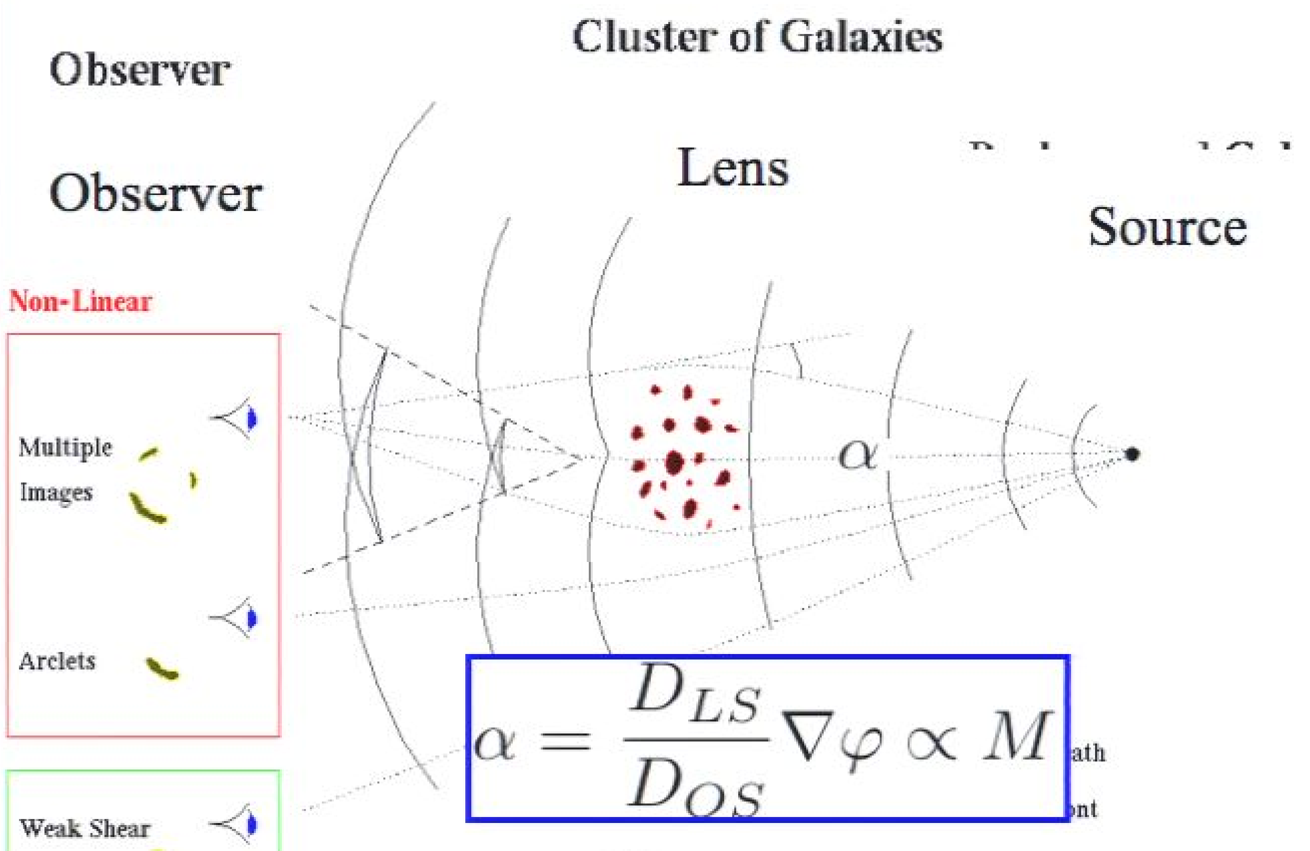

$$\boxed{\alpha = \frac{D_{LS}}{D_{OS}} \nabla \varphi \propto M}$$

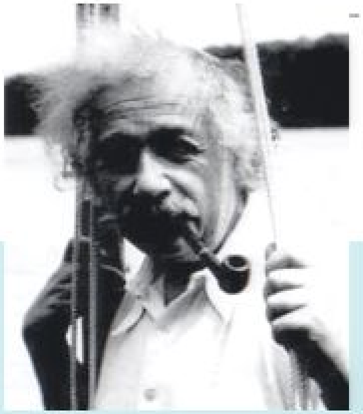

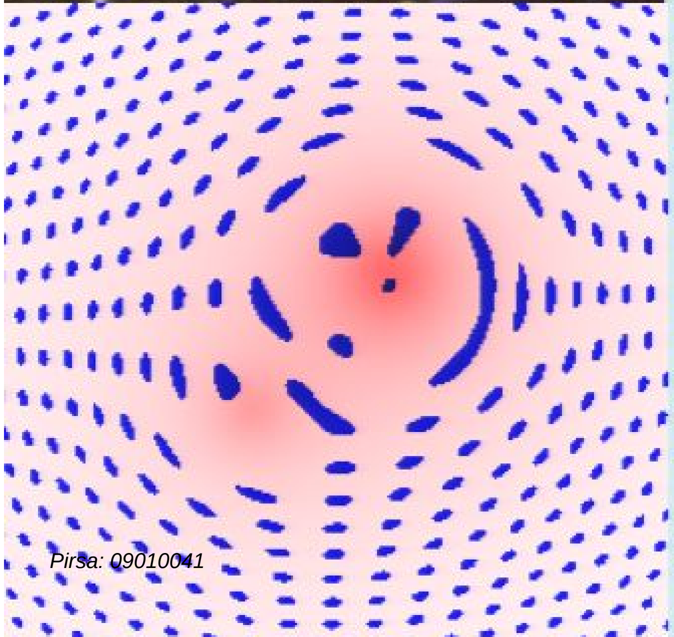

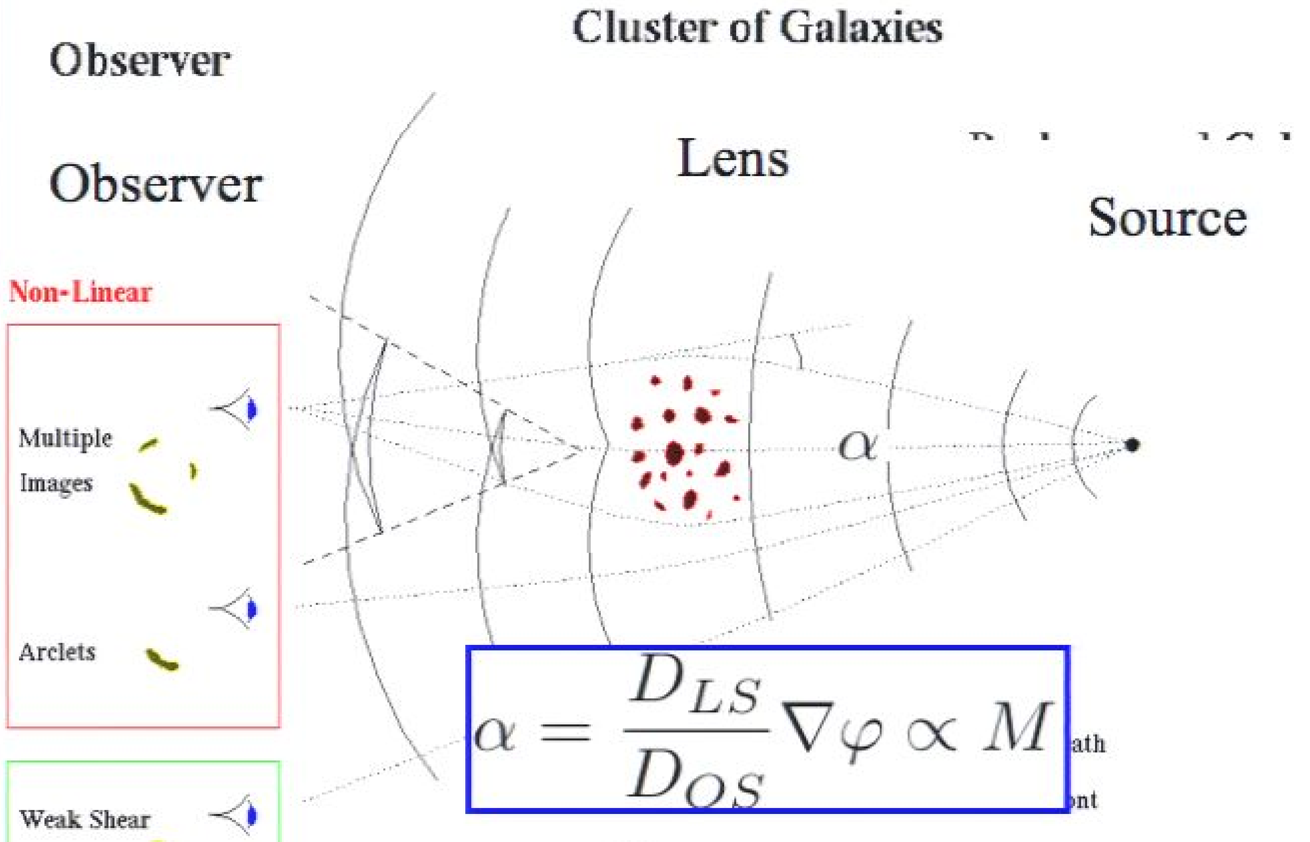

$$\alpha = \frac{D_{LS}}{D_{OS}} \nabla\varphi \propto M$$

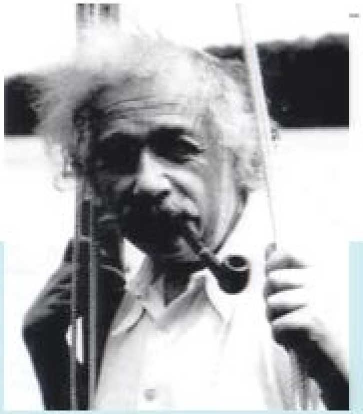

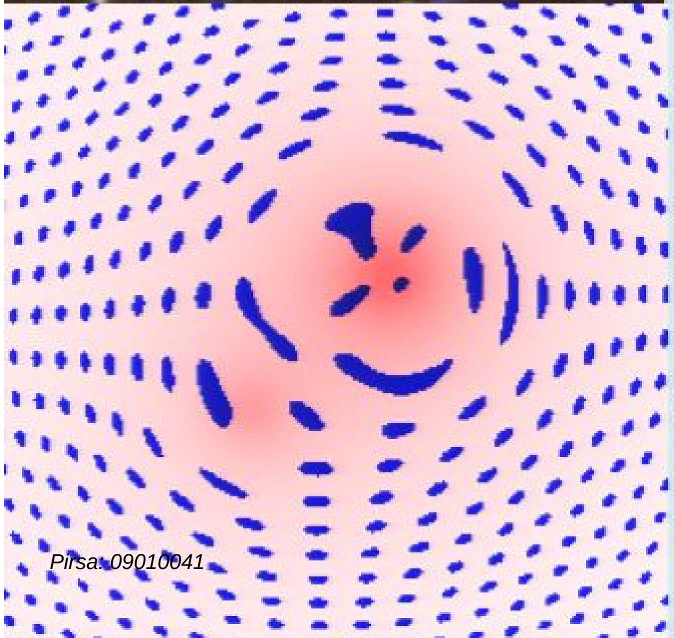

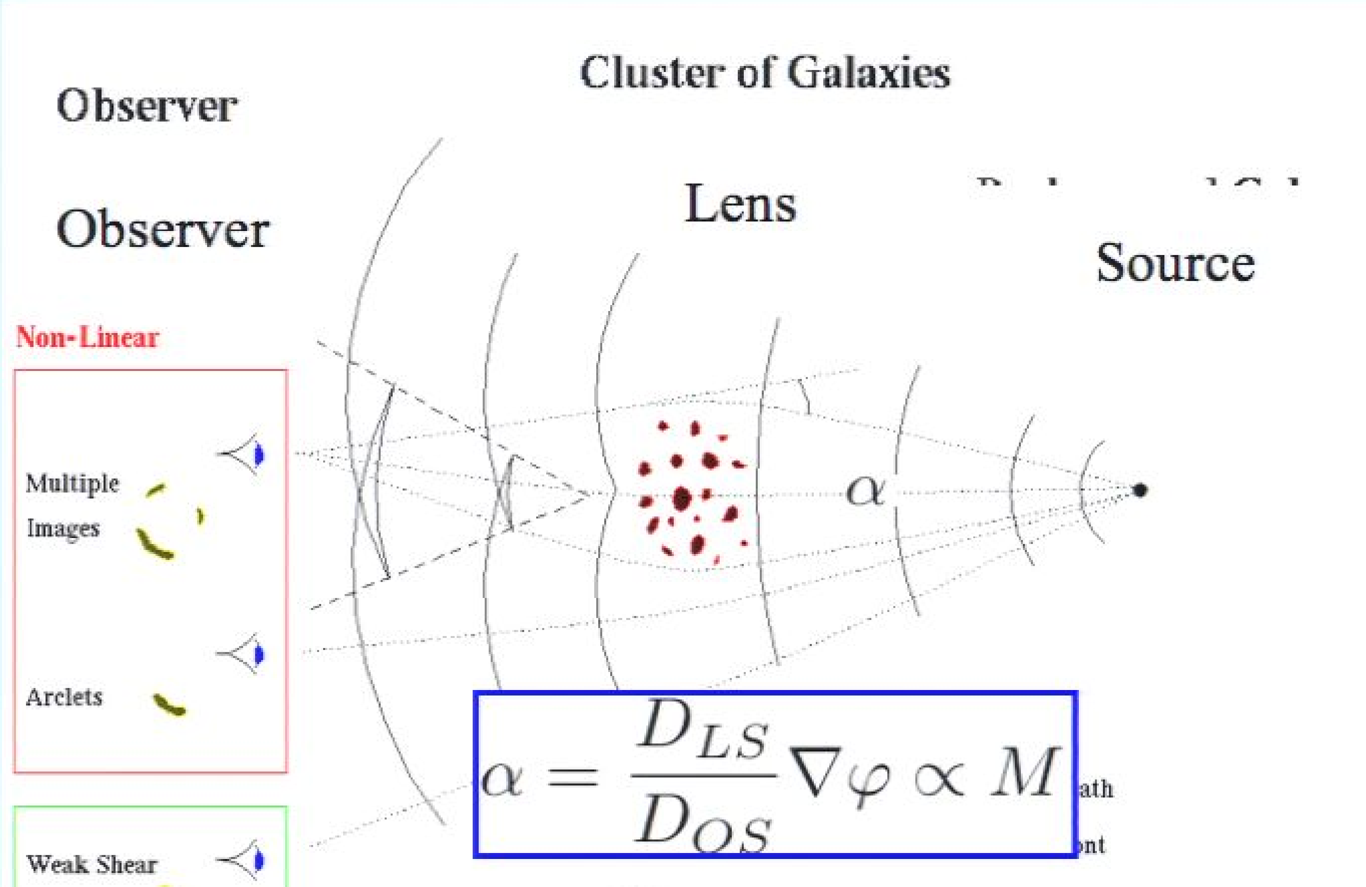

$$\alpha = \frac{D_{LS}}{D_{OS}} \nabla \varphi \propto M$$

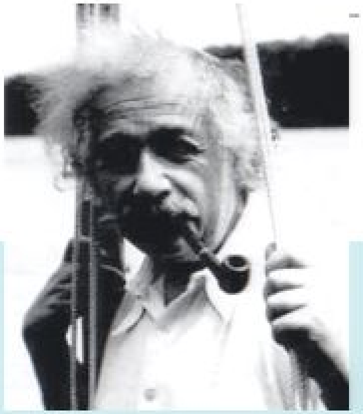

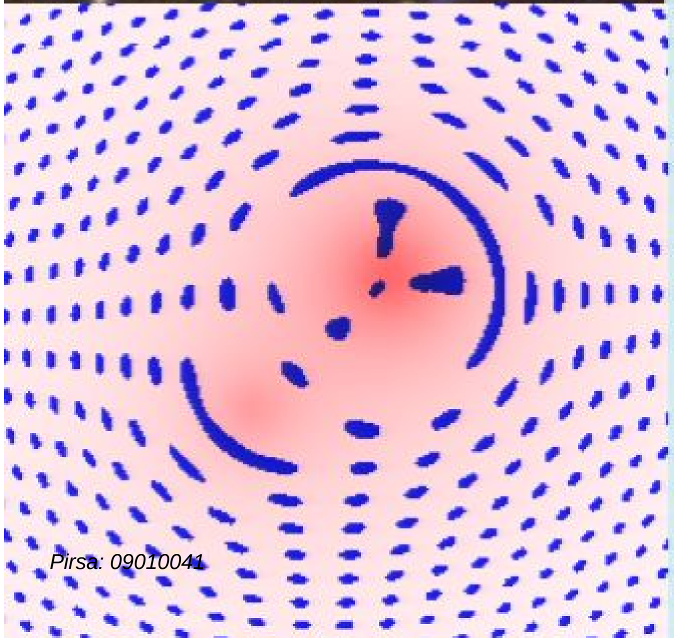

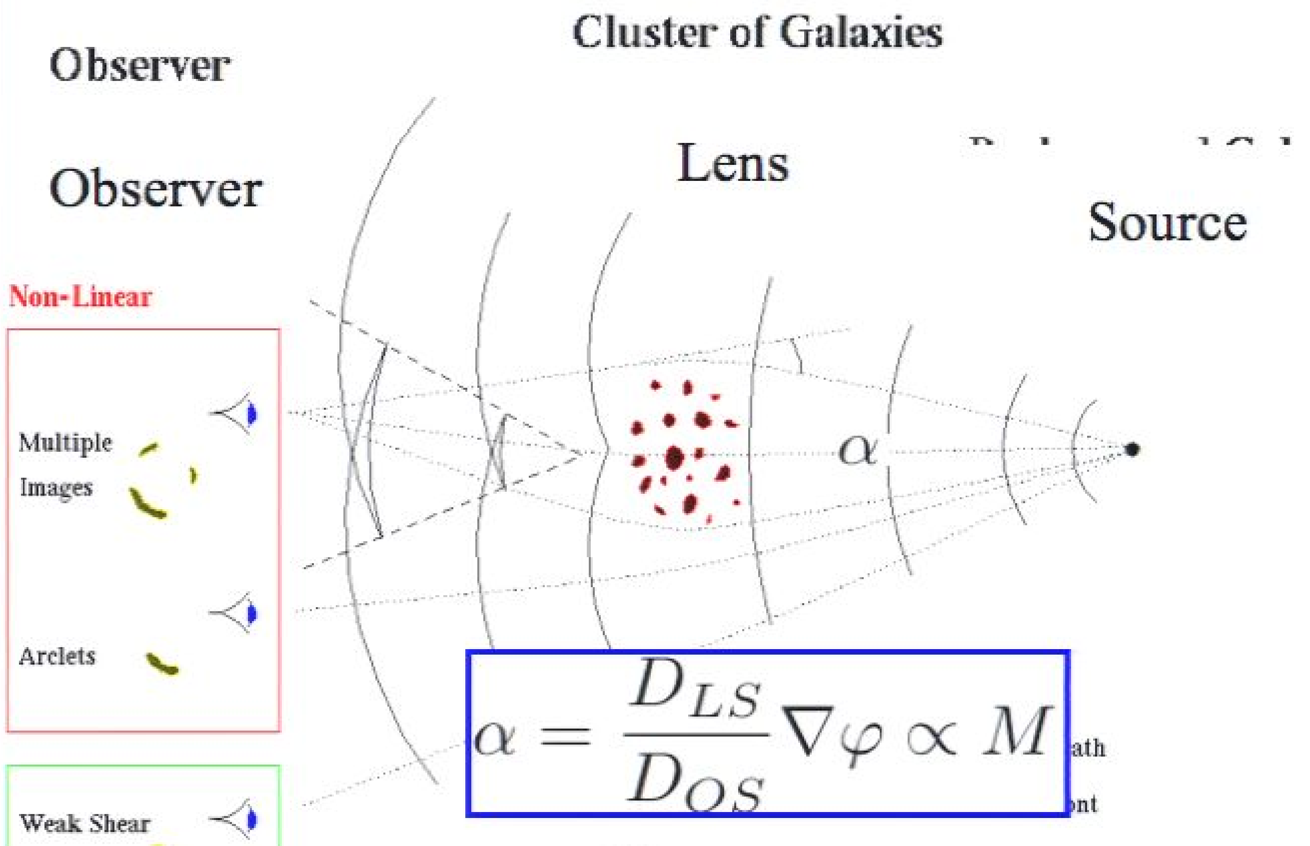

$$\boxed{\alpha = \frac{D_{LS}}{D_{OS}} \nabla \varphi \propto M}$$

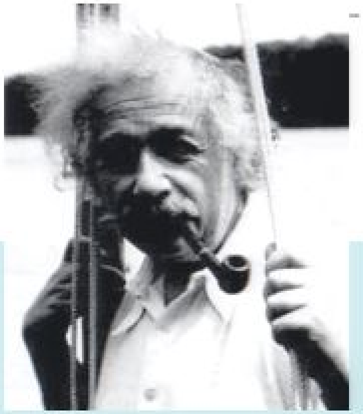

CFHT 1990

Z_cluster=0.375

Z_arc=0.725 (Soucail et al 1988)

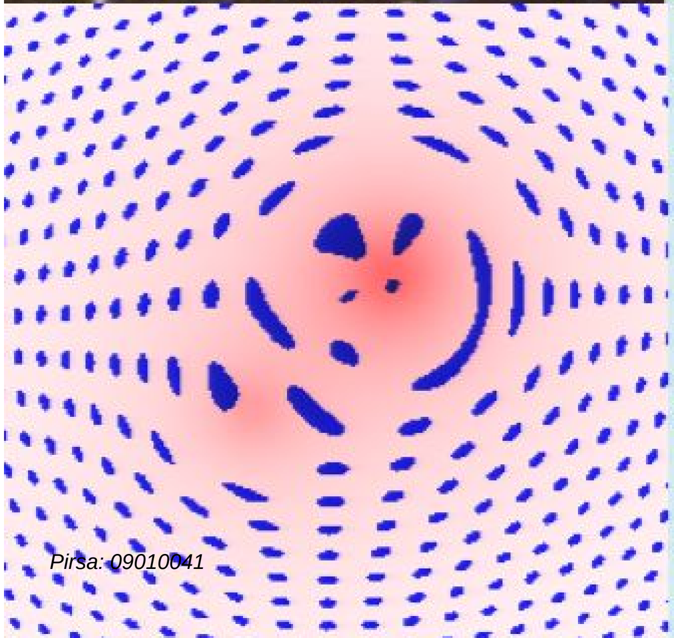

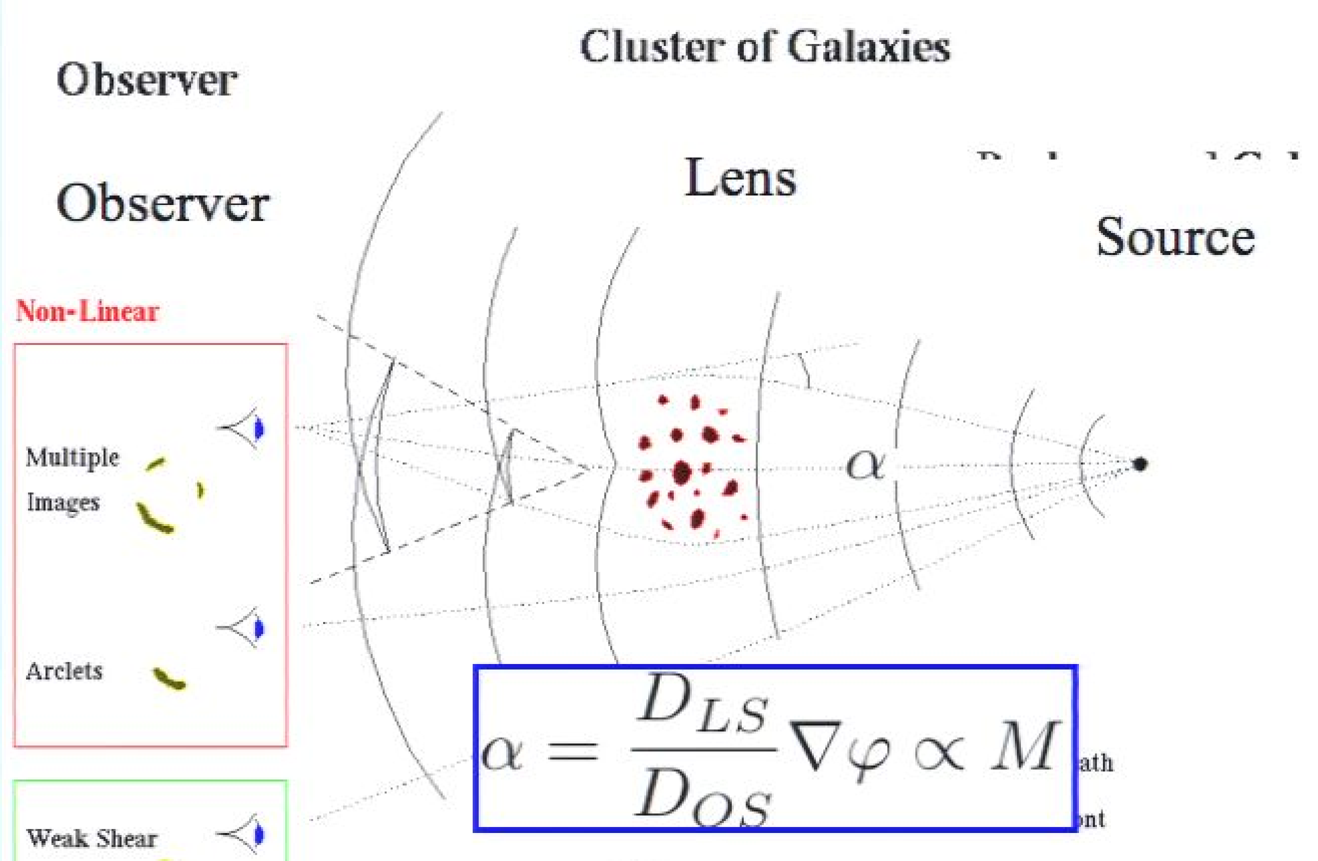

Cluster of Galaxies

Observer

Observer

Lens

Source

Non-Linear

Multiple Images

Arclets

Weak Shear

α

ath

nt

$$\alpha = \frac{D_{LS}}{D_{OS}} \nabla \varphi \propto M$$

Multiple Images Area

Linear

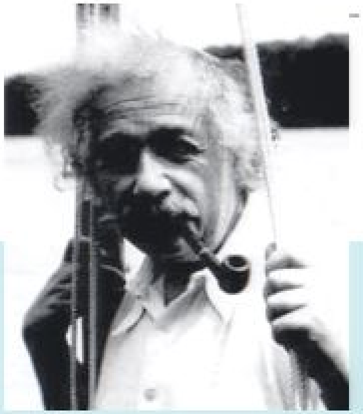

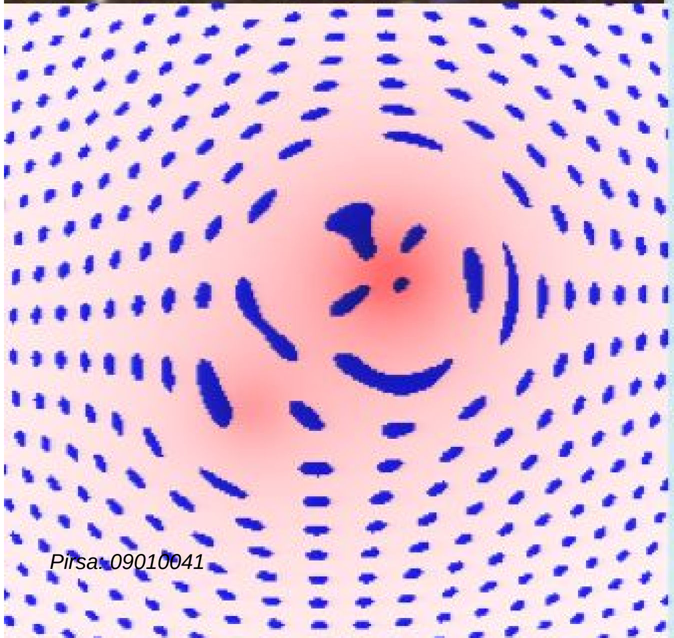

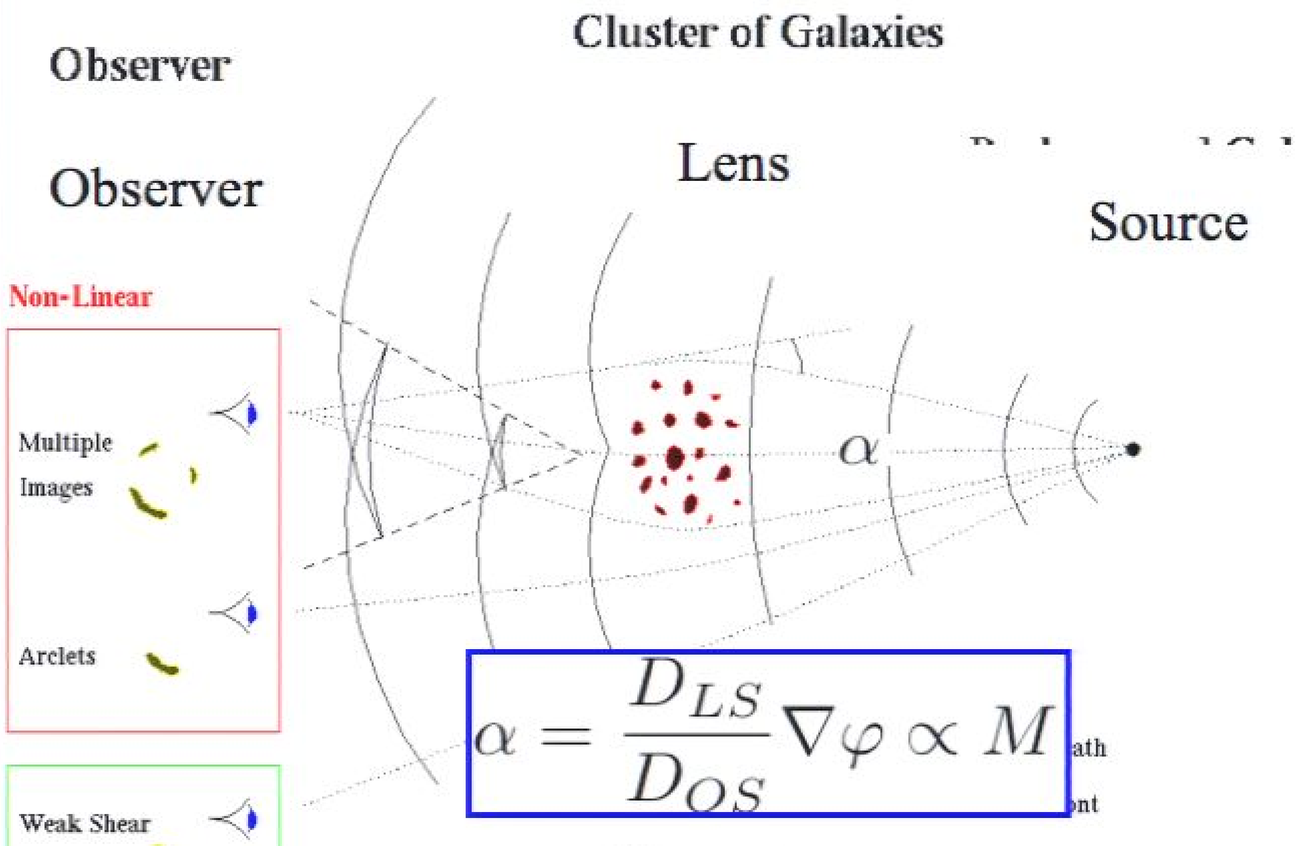

$$\alpha = \frac{D_{LS}}{D_{OS}} \nabla \varphi \propto M$$

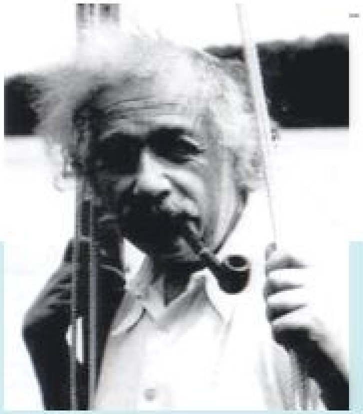

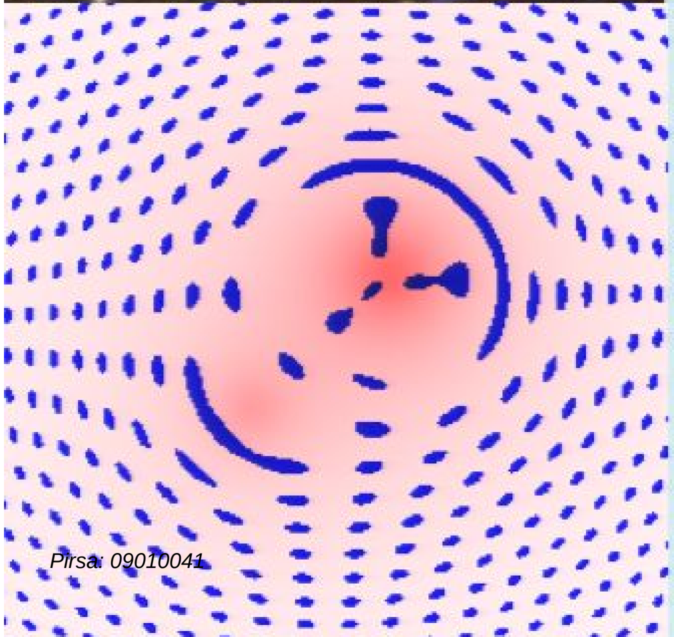

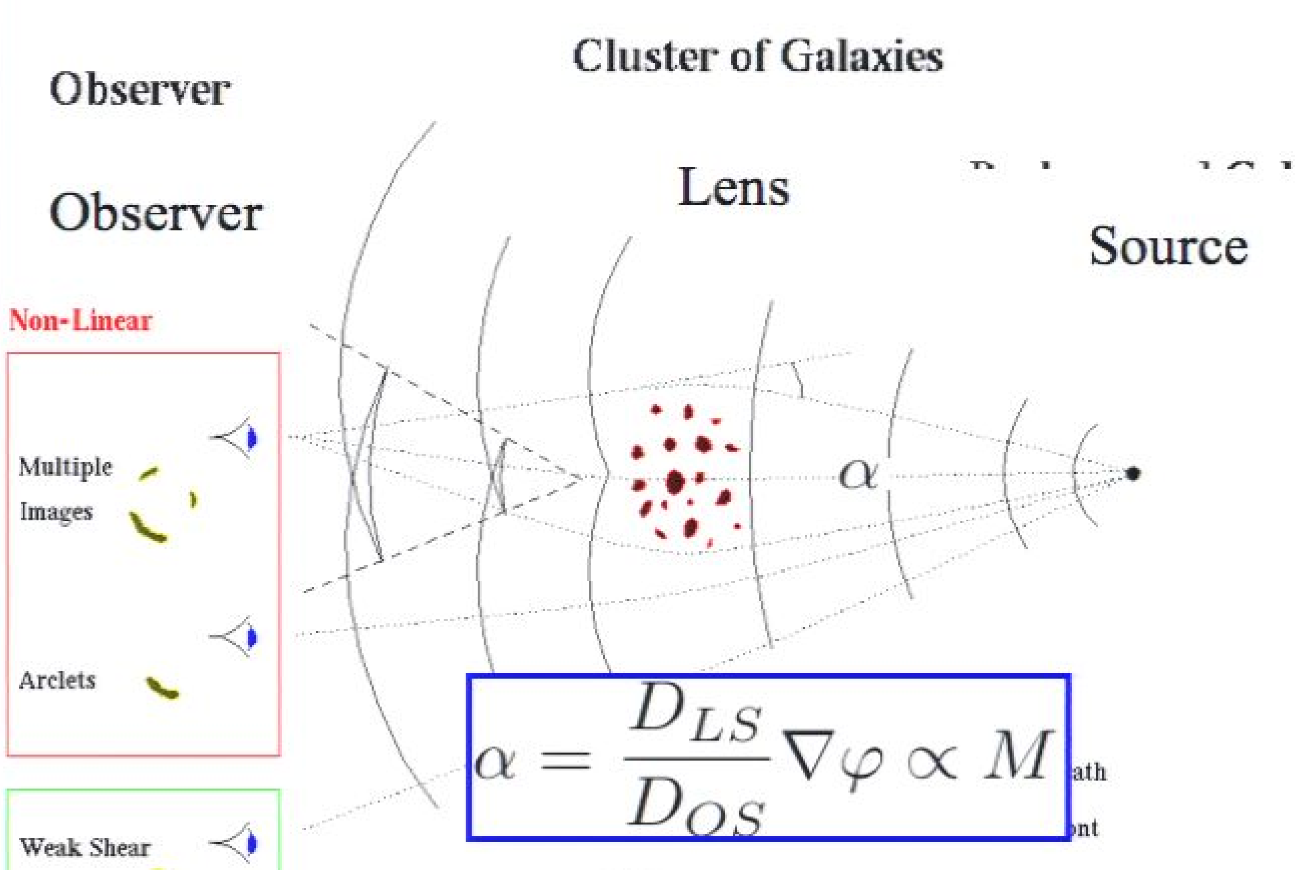

$$\alpha = \frac{D_{LS}}{D_{OS}}\nabla\varphi \propto M$$

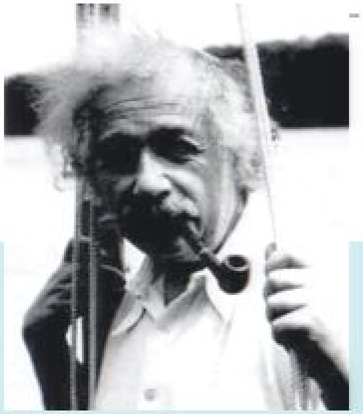

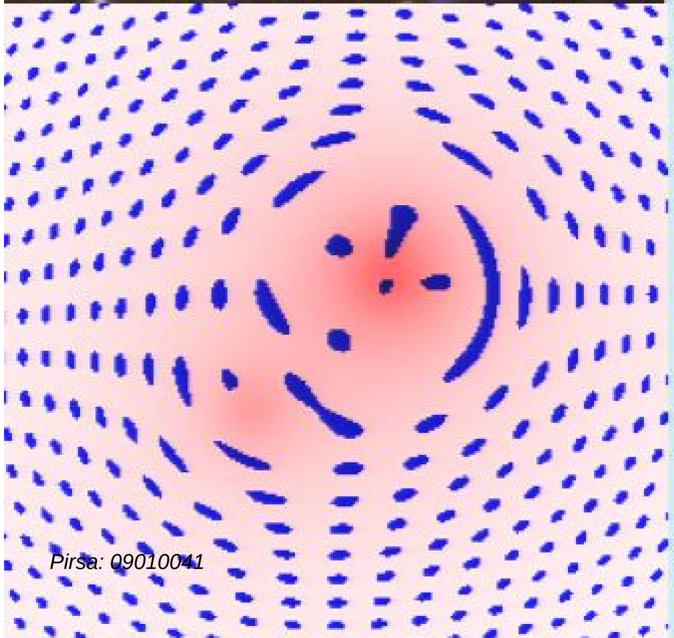

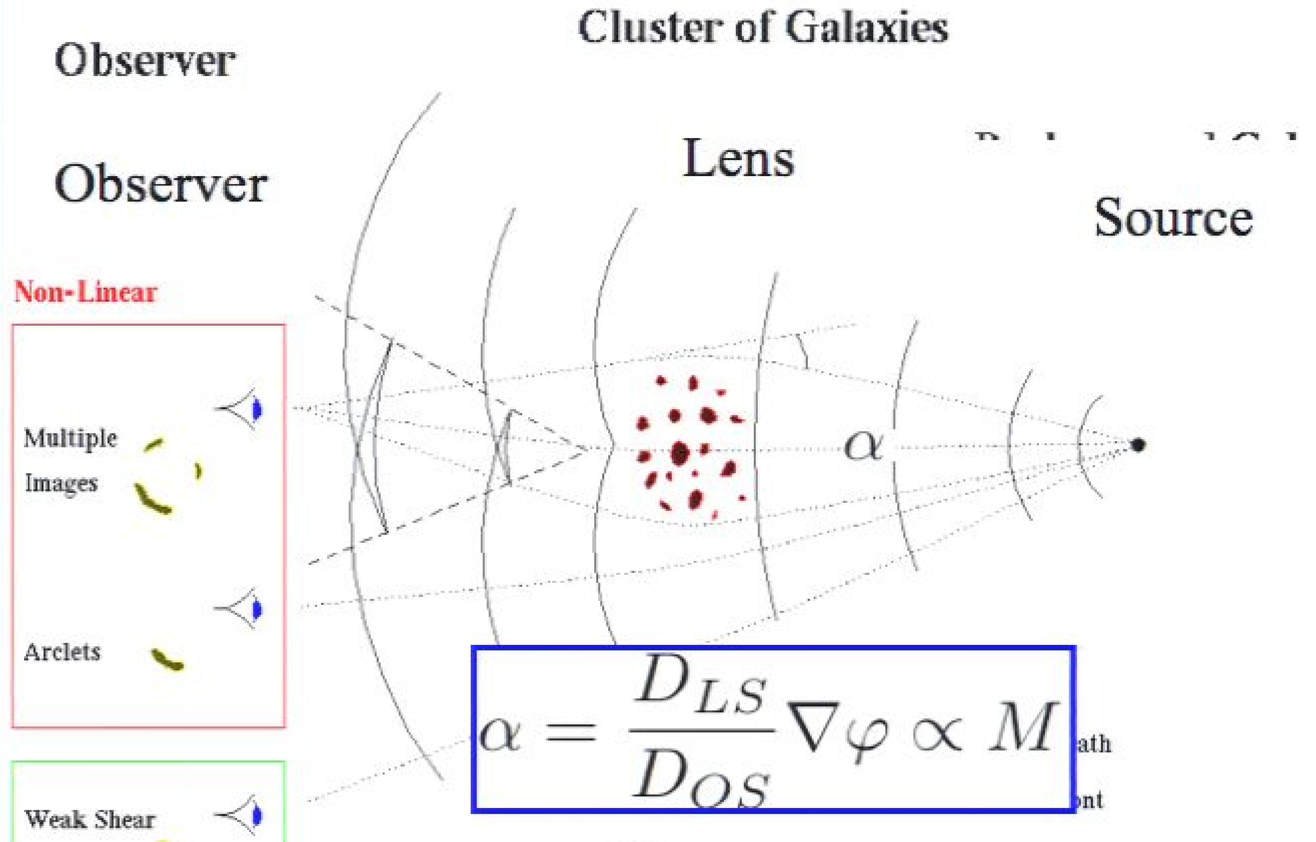

$$\boxed{\alpha = \frac{D_{LS}}{D_{OS}} \nabla \varphi \propto M}$$

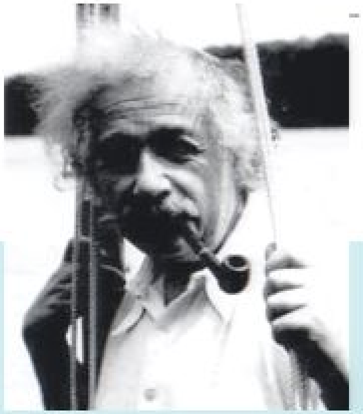

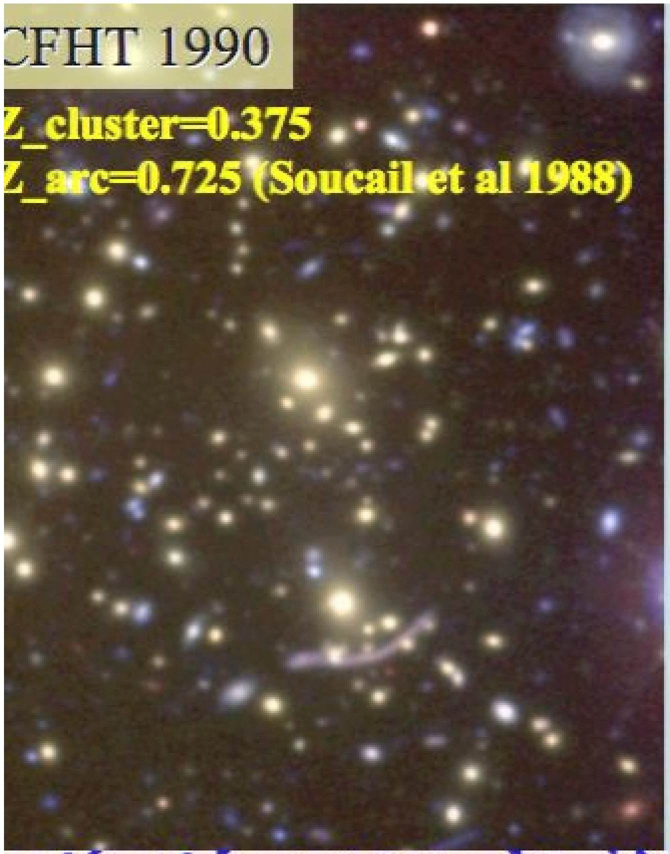

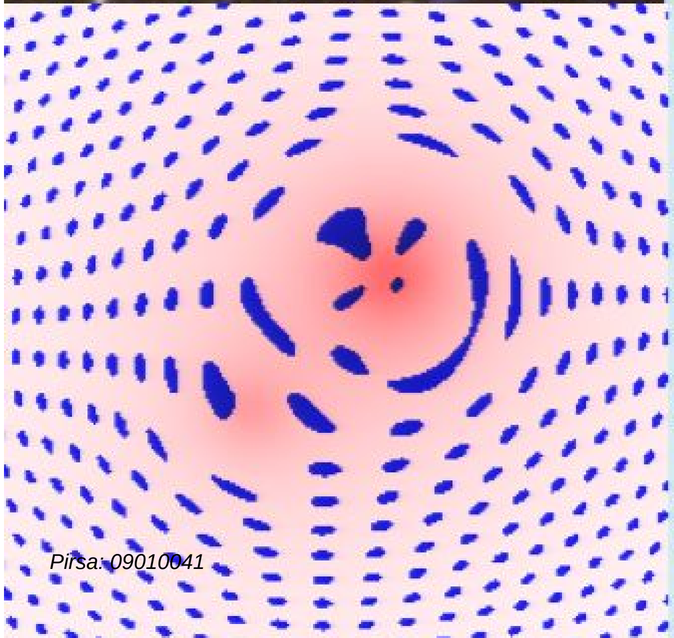

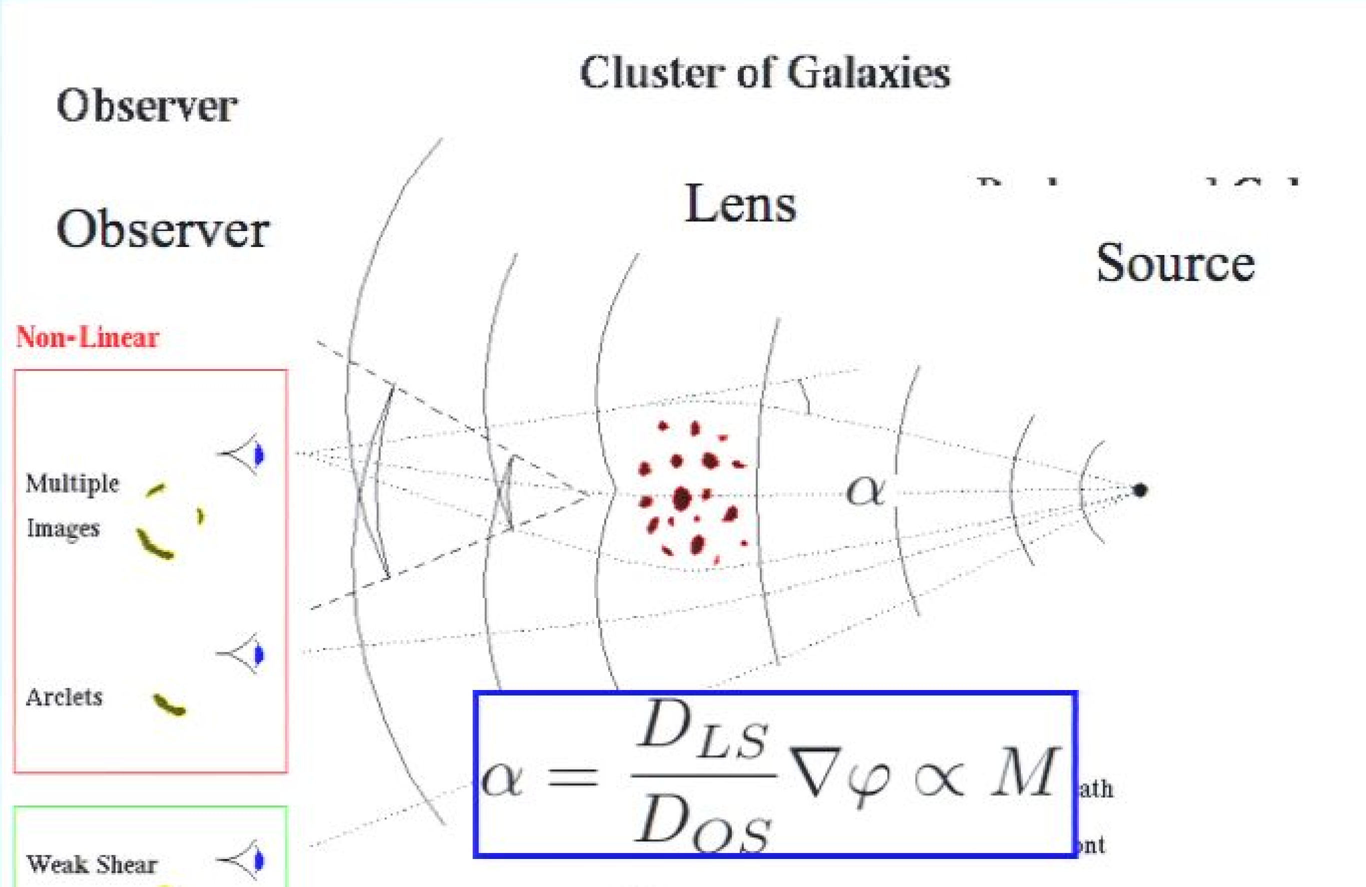

$$\boxed{\alpha = \frac{D_{LS}}{D_{OS}} \nabla\varphi \propto M}$$

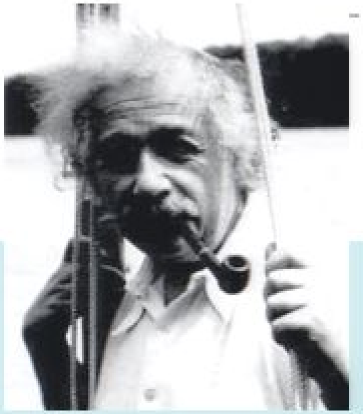

CFHT 1990

Z_cluster=0.375

Z_arc=0.725 (Soucail et al 1988)

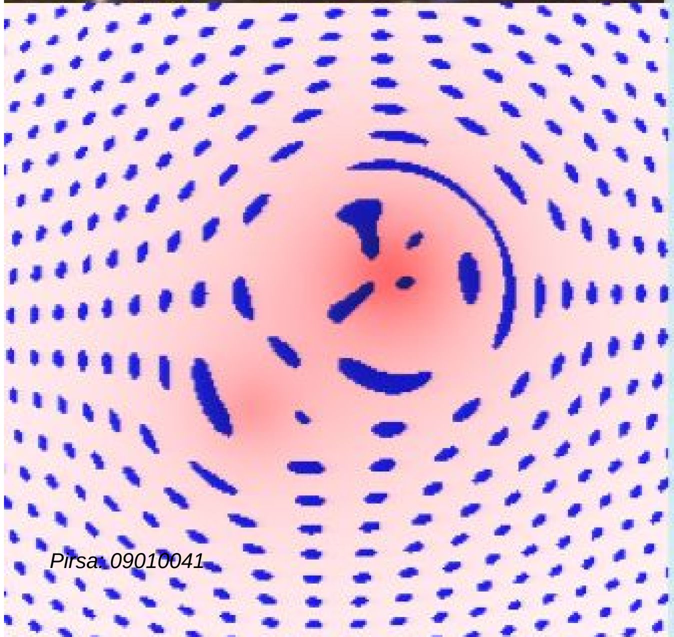

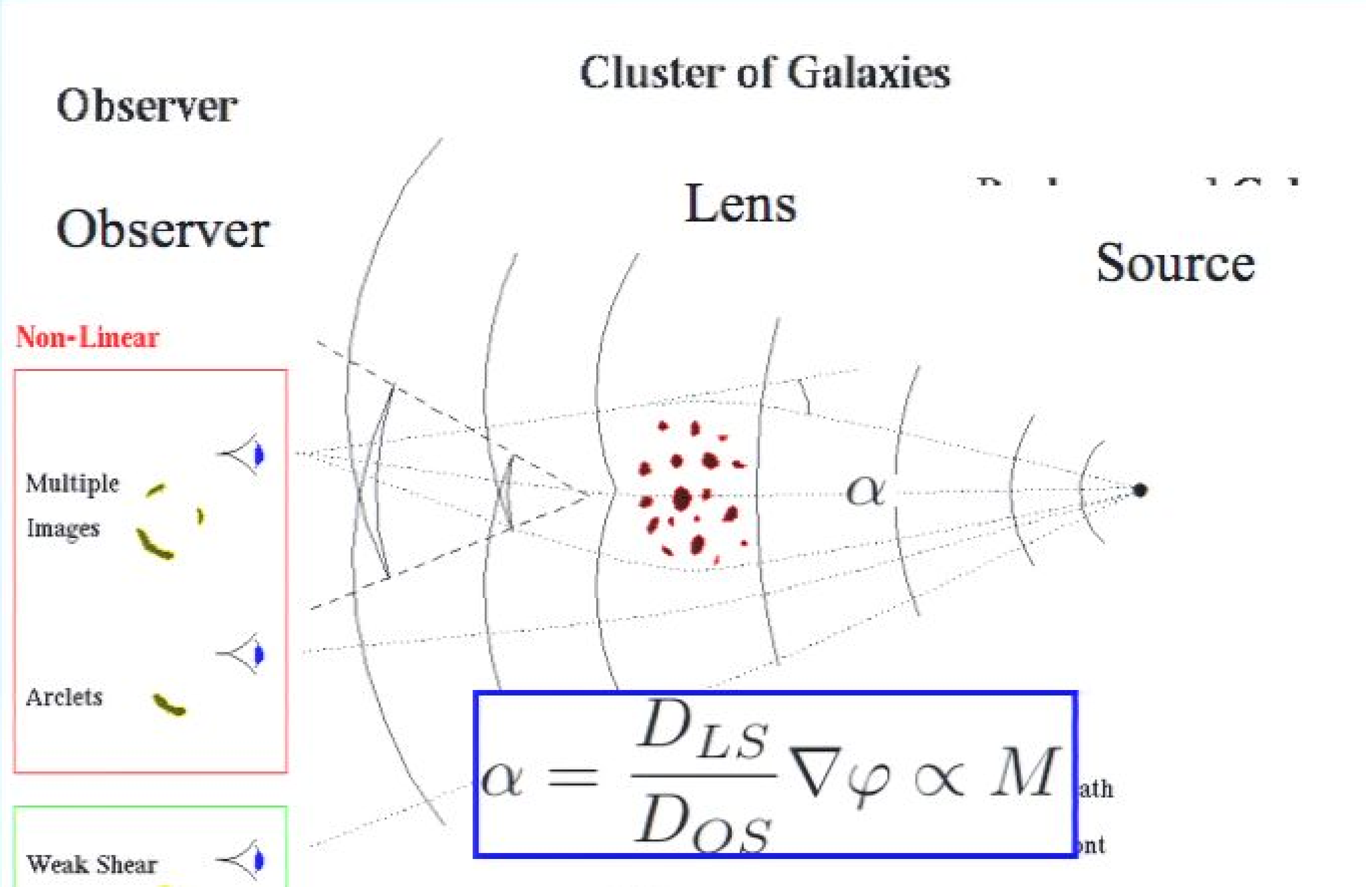

$$\alpha = \frac{D_{LS}}{D_{OS}} \nabla \varphi \propto M$$

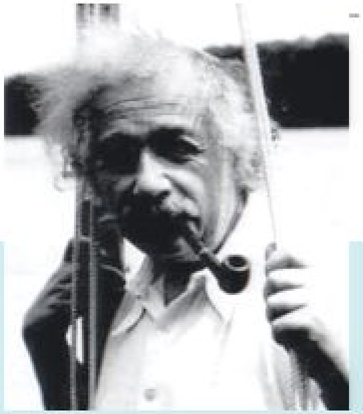

High Resolution from space

- Post COSTAR, Hubble has provided a unique view of multiply imaged galaxies: better dentification, fainter images, morphologies

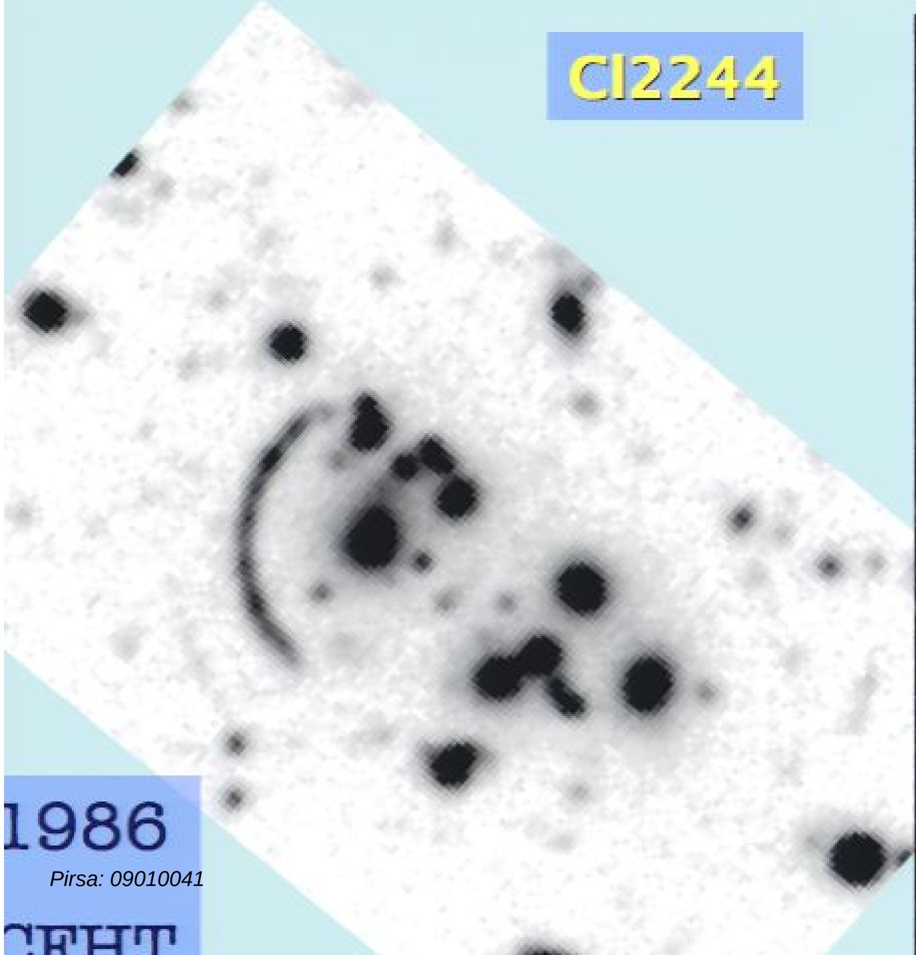

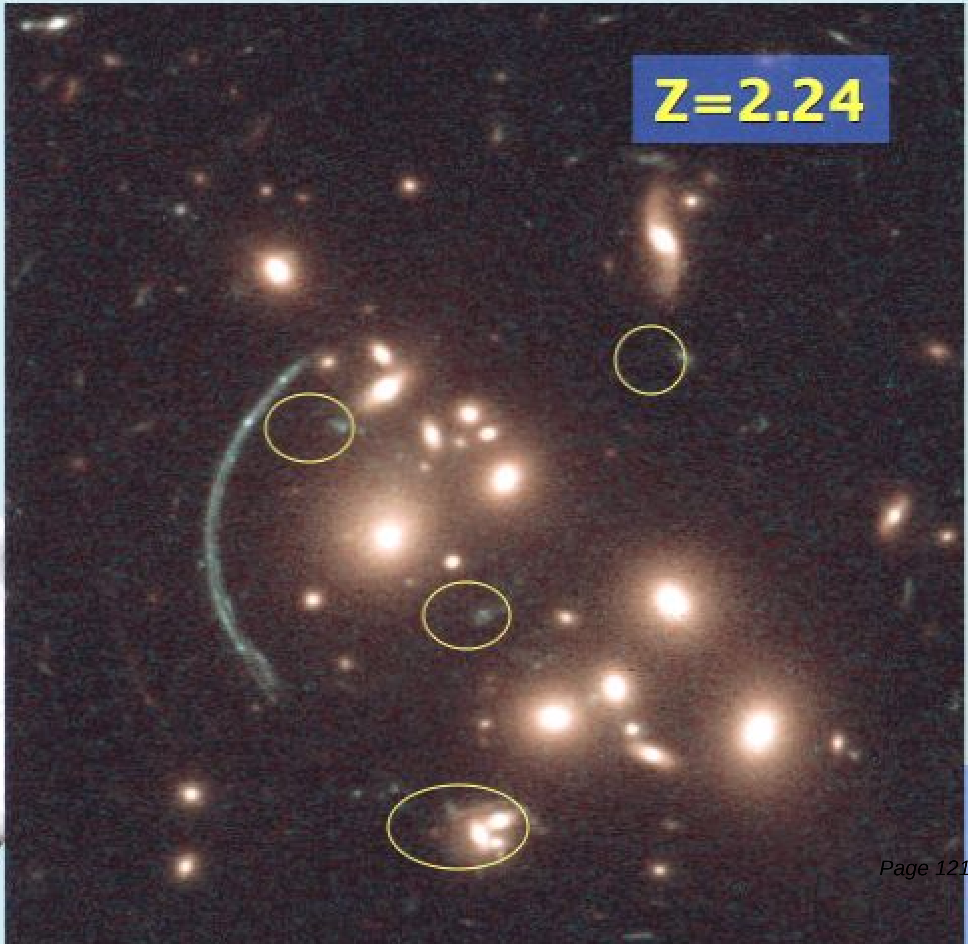

20 years ago - the first arc redshift

- 1987 the first giant luminous arc discovered
- 1988 the first spectrum confirming the gravitational lensing explanation (Soucail+ 88)
- Clusters are massive and *dense* enough to produce strong lensing - repository of DM
- Every massive cluster is essentially a lens

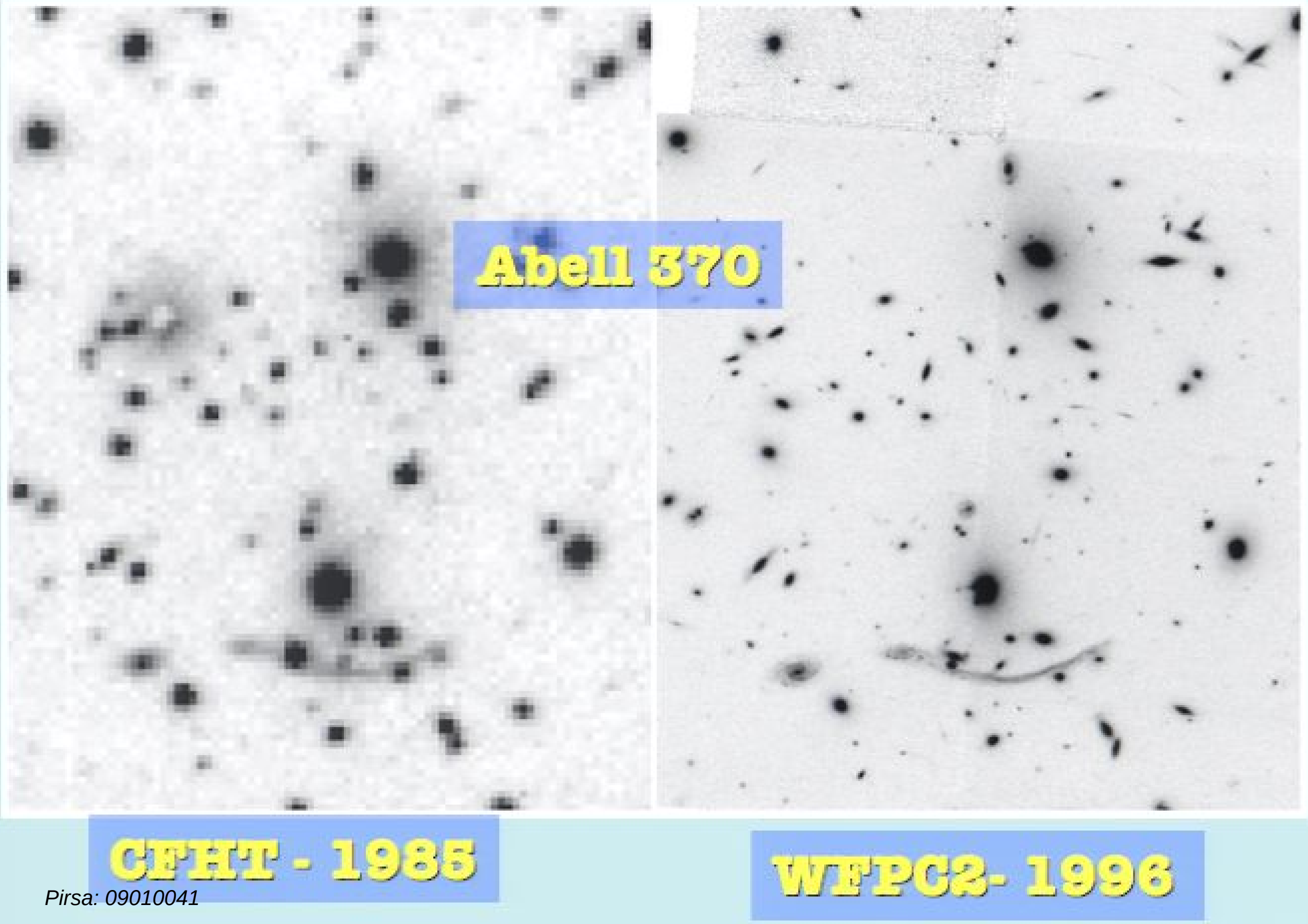

- Probing the mass distribution
- Link between the galaxies, X-ray gas, DM
- Lens Magnification
- Sensitivity to the geometry of the Universe

Quantifying light deflection

- Define the “projected gravitational potential” Ψ through

$$\psi(\vec{\theta}) = \frac{D_{\rm ds}}{D_{\rm d} D_{\rm s}} \frac{2}{c^2} \int \Phi(D_{\rm d}\vec{\theta}, z)\, dz \,.$$

⇒ “thin lens”

- Then the deflection is given by

$$\vec{\alpha}(\vec{\theta}) = \vec{\nabla}\psi = \frac{1}{\pi} \int \kappa(\vec{\theta}') \frac{\vec{\theta} - \vec{\theta}'}{|\vec{\theta} - \vec{\theta}'|^2} d^2\theta'$$

where κ is a scaled surface mass density in the lens plane

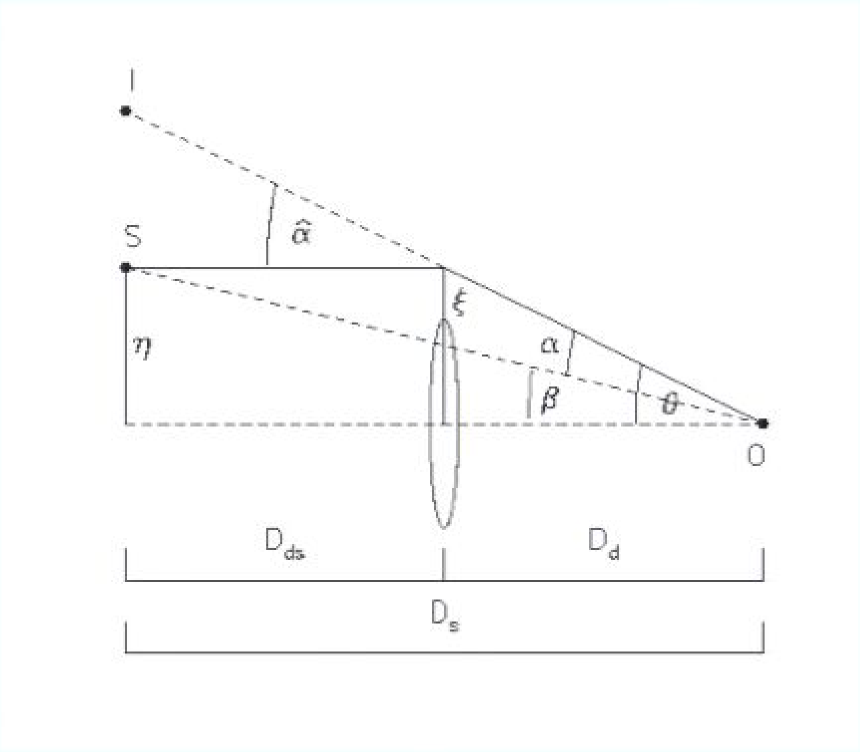

S=source
D=deflector
O=observer
I=image

Image deflection is related to the surface mass density in the lens plane

Lens Mapping

$$\mathcal{A}^{-1} = \begin{pmatrix} 1-\kappa-\gamma_1 & -\gamma_2 \\ -\gamma_2 & 1-\kappa+\gamma_1 \end{pmatrix}$$

Amplification matrix

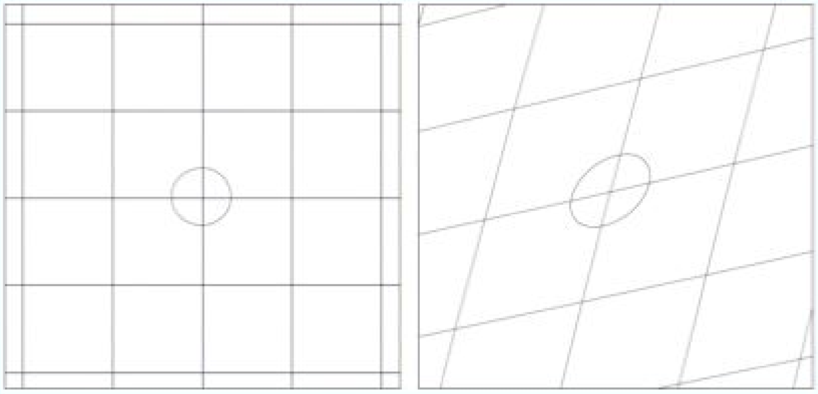

convergence $\boxed{\kappa = \Delta\varphi/2 = \Sigma/2\Sigma_{crit}}$

shear $\boxed{\gamma_1 = (\partial_{yy}\varphi - \partial_{xx}\varphi)/2 \qquad \gamma_2 = \partial_{xy}\varphi}$

$$\Sigma_{\rm cr} = \frac{c^2}{4\pi G}\frac{D_{\rm s}}{D_{\rm d}D_{\rm ds}}$$
$$= 0.35\,{\rm g\,cm}^{-2}\left(\frac{D}{1\,{\rm Gpc}}\right)^{-1}$$

Reduced shear: measured quantity

$$\boxed{g = \frac{\gamma}{1-\kappa}}$$

Strong lensing

multiple image geometries for an elliptical lens

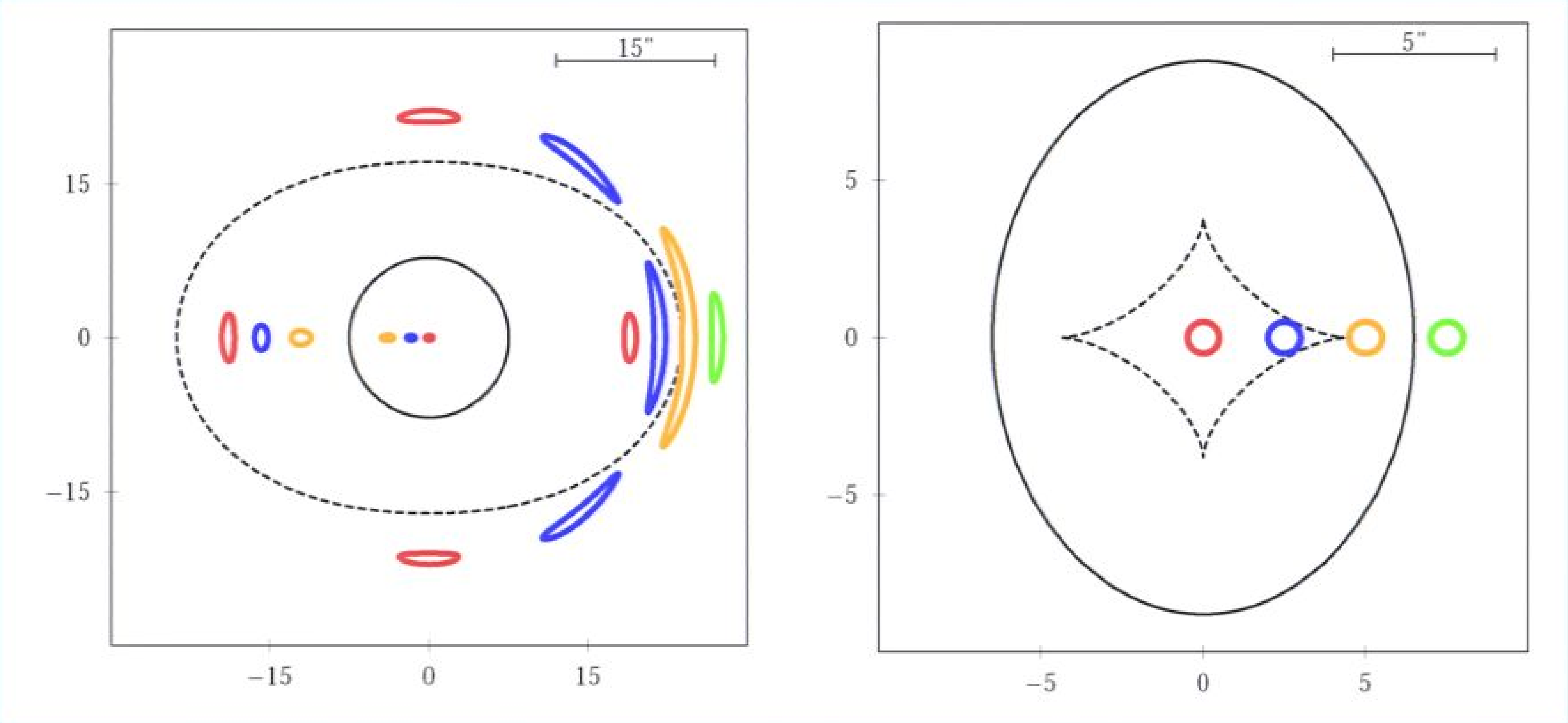

Image plane

critical curves

Source plane

caustics

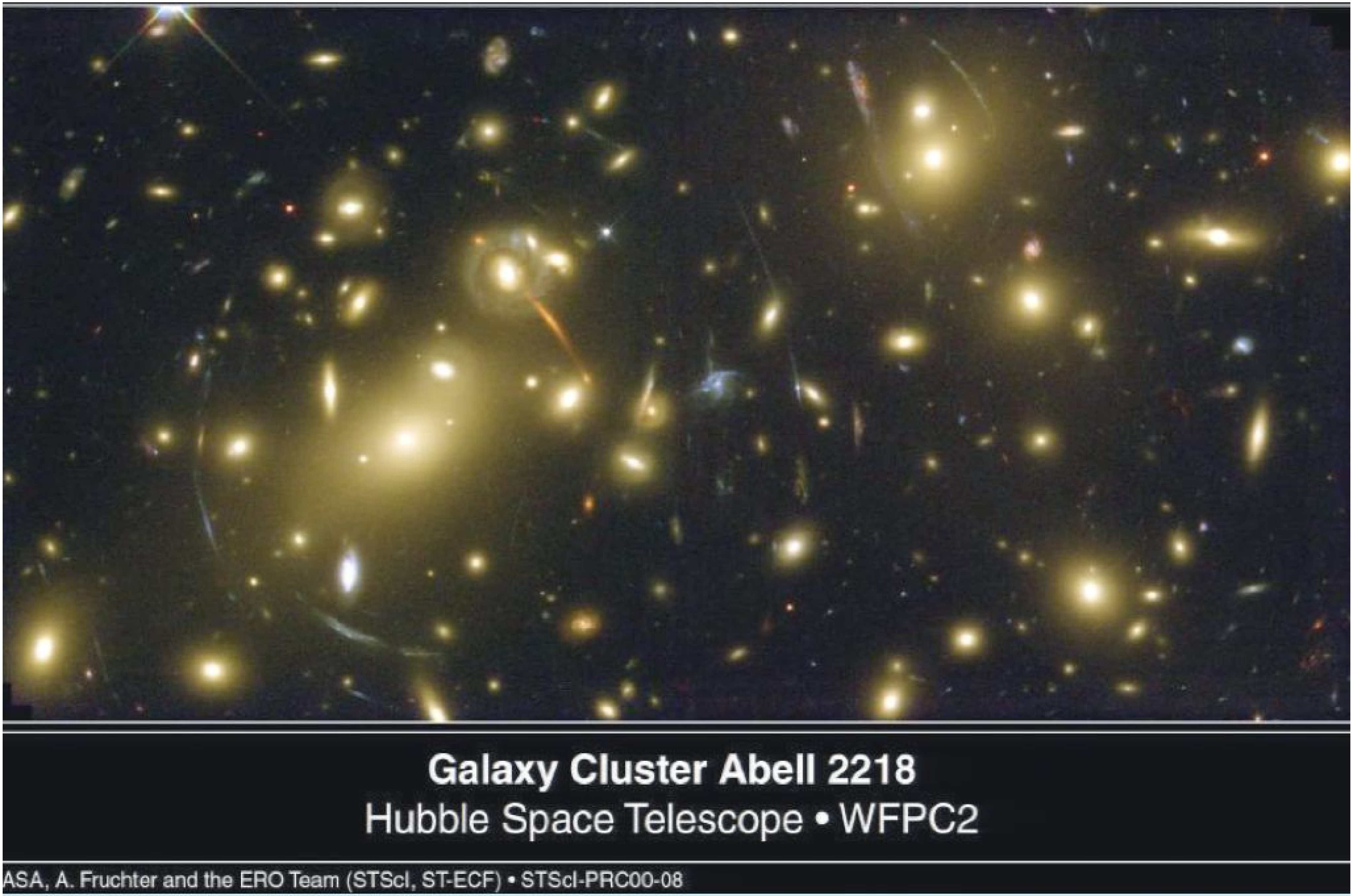

Galaxy Cluster Abell 2218

Hubble Space Telescope • WFPC2

ASA, A. Fruchter and the ERO Team (STScI, ST-ECF) • STScI-PRC00-08

~1% of mass in galaxies, ~10% of mass is hot gas, rest is DM

Measuring Weak Shear

- In the ***weak regime***,the shape of galaxies are linearly modified by the gravitational shear:

$$\varepsilon_I = \varepsilon_S + \gamma$$

- The average galaxy shape is an unbiased estimator of the gravitational shear:

$$\boxed{\gamma(x,y) <=> \Sigma(x,y)}$$

- Error on shear is a function of intrinsic shape, measurement error and number of galaxies

$$< \varepsilon_I >=< \underset{=0}{\cancel{\varepsilon_S} >} + < \gamma >$$

Galaxy Properties

$$\sigma^2(\varepsilon_I) = \sigma^2(\gamma) \propto \frac{\boxed{\sigma^2(\varepsilon_S)} + \boxed{\delta^2 \varepsilon_I}}{\boxed{N}}$$

PSF
correction
& method

Survey
size &
depth

Weak Lensing

$$M_{ij} \propto R_\theta \begin{pmatrix} a^2 & 0 \\ 0 & b^2 \end{pmatrix} R_{-\theta}$$

$$M^S = A^{-1} \, M^I \, {}^t A^{-1}$$

$$\boxed{\varepsilon_S = \frac{\varepsilon_I - g}{1 - g\varepsilon_I} \sim \varepsilon_I - \gamma}$$

Lensing equation for image moments

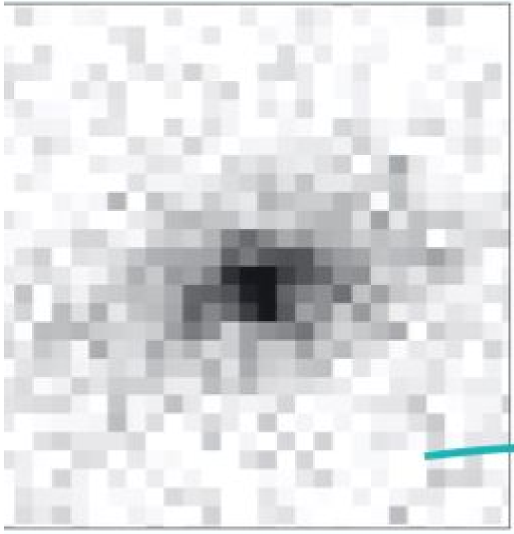

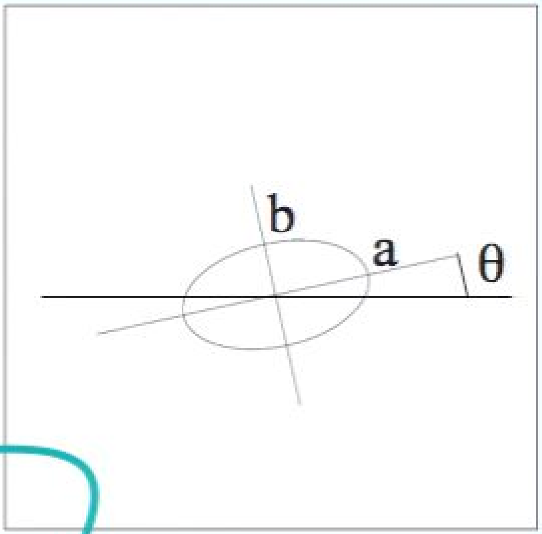

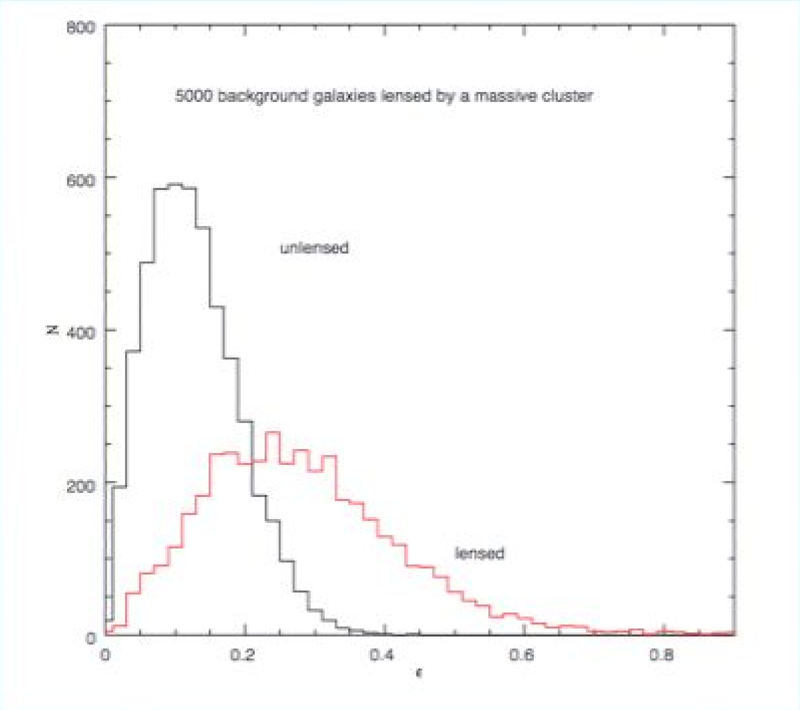

$$\varepsilon = \frac{a-b}{a+b}$$

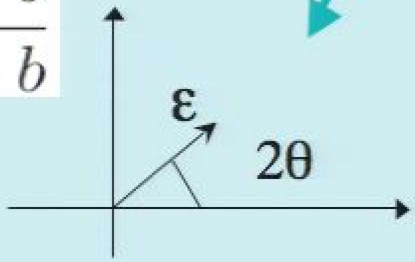

Ellipticity vector

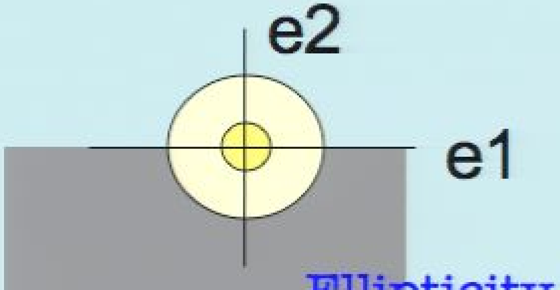

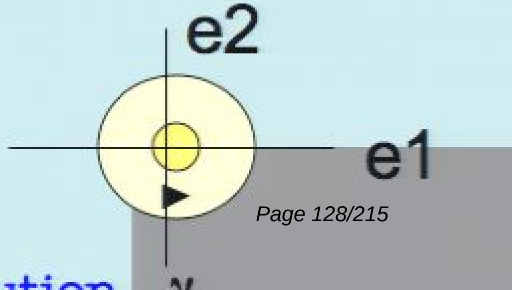

Ellipticity distribution

Photometric Redshift

Fitting SED templates with photometry from: 7 broad optical bands, 6 ntermediate bands + K-band + IRAC 3.6&4.5 mm, IR reduces catastrophic errors,intermediate bands reduce scatter for bright objects (Ilbert + 2008)

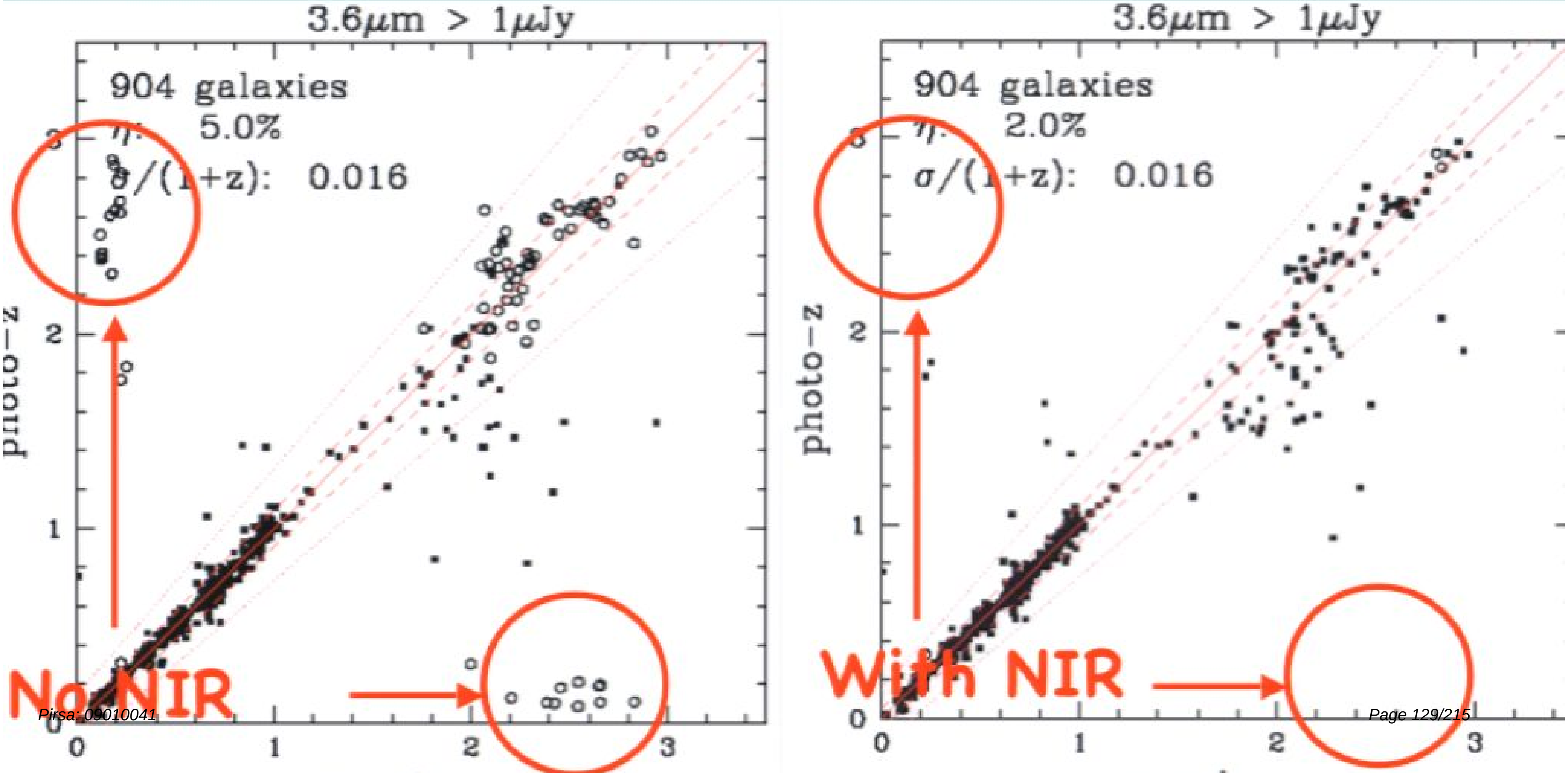

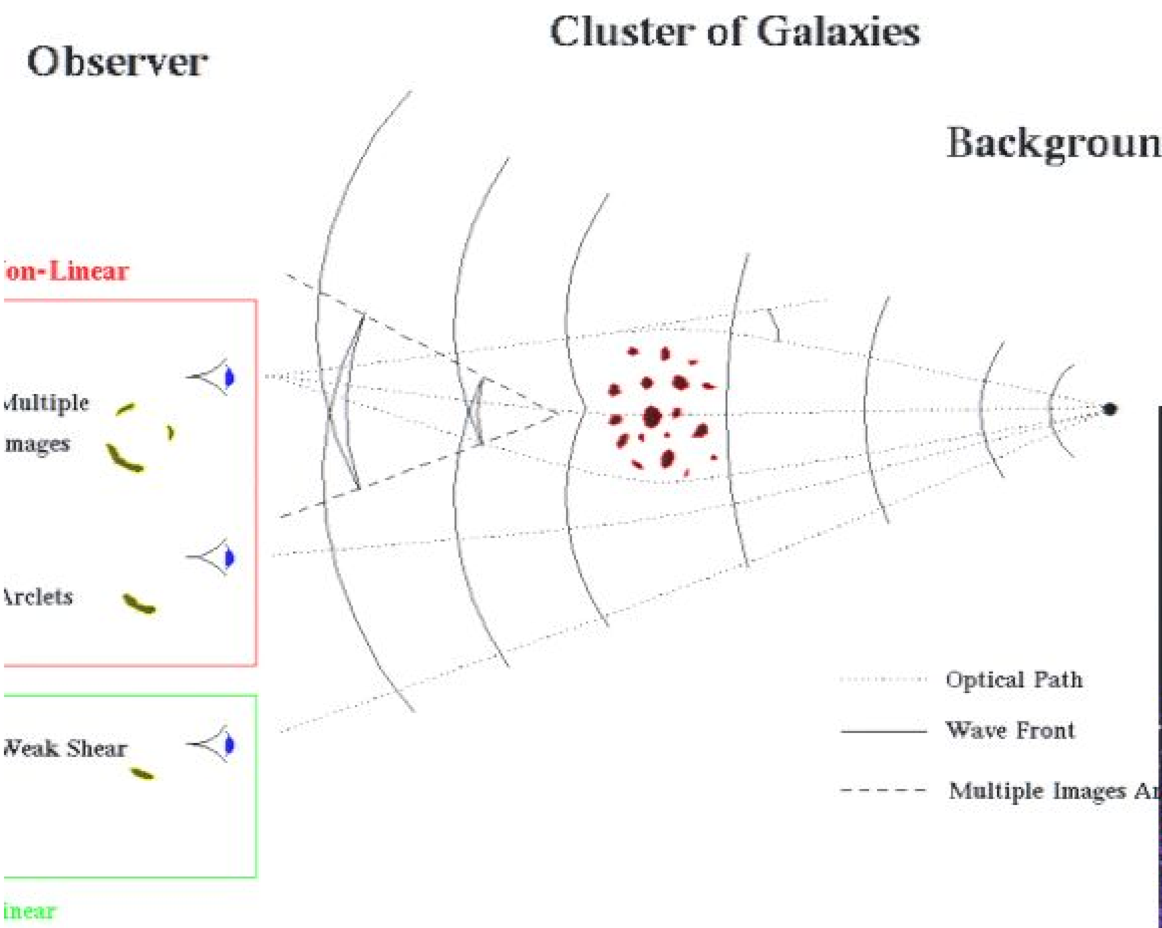
Observer
Cluster of Galaxies
Background Ga
on-Linear
Multiple
mages
Arclets
Weak Shear
inear
Optical Path
Wave Front
Multiple Images Ar

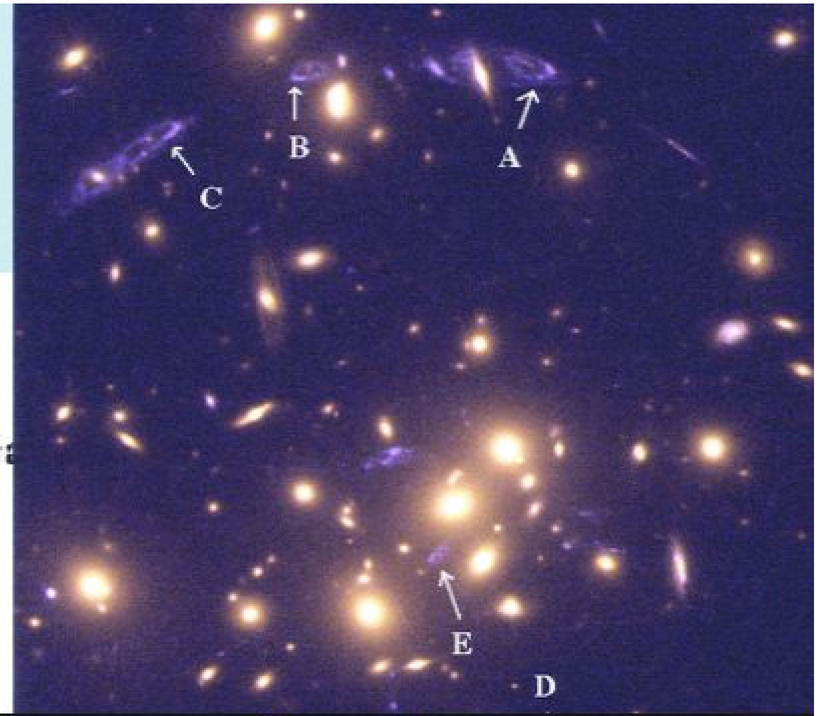
C
B
A
E
D

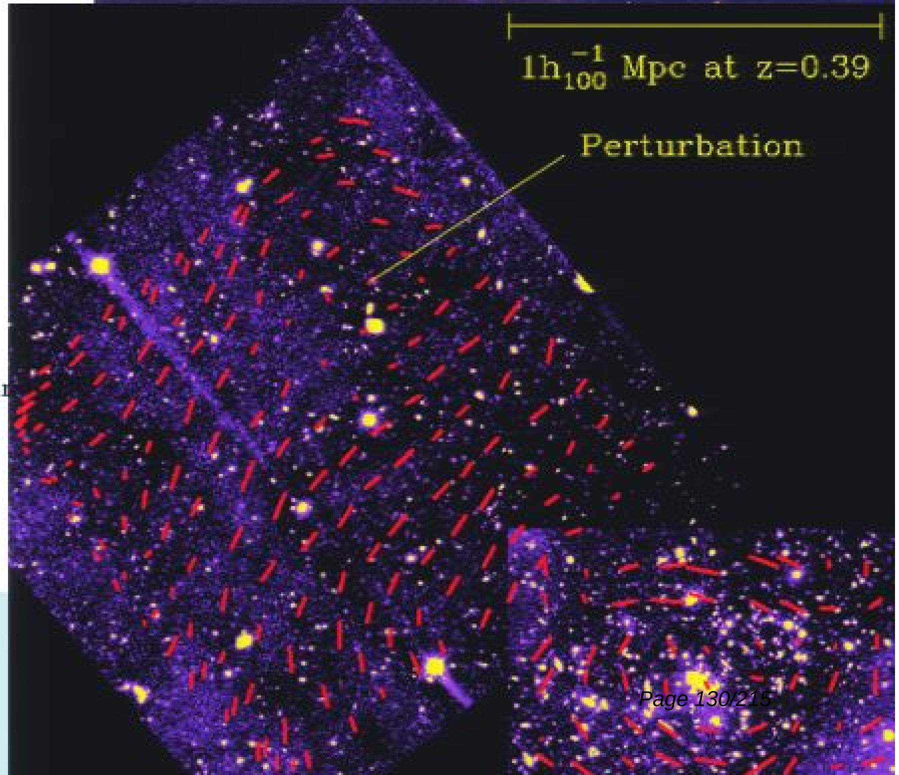
$1h_{100}^{-1}$ Mpc at z=0.39
Perturbation

Strong lensing

multiple images, highly distorted and magnified arcs, depletion of background number counts

- Projected surface mass density within the beam $\Sigma(r) > \Sigma_{crit}$
- Mass enclosed within the arc is tightly constrained

Weak lensing

coherent distortion in the shapes of background galaxies

- Shear field used to construct mass map

Kaiser & Squires 93

Isotropic effect of lensing: magnification

multiple images, highly distorted and magnified arcs, dilution/depletion of background galaxy number counts

Projected surface mass density within the beam

$$\Sigma(r) > \Sigma_{crit}$$

Mass enclosed within the arc is tightly constrained

$$\Sigma_{crit} = \left[\frac{D_d D_{ds}}{D_s} / 1Gpc \right]^{-1} \times 0.35$$

$$\Sigma(\theta_{arc}) \approx \Sigma(\theta_E)$$

$$M(\theta_{arc}) = \Sigma_{crit} \times \pi \times \left(D_d \theta_{arc} \right)^2$$

Mapping DM in clusters

DM potential = ‘smooth’ component + clumps

Associate clumps with bright early-type spectroscopically confirmed cluster members and use positions, magnitudes and redshifts of multiple images (strong lensing features), and the shapes of background galaxies (weak lensing) to partition the total mass

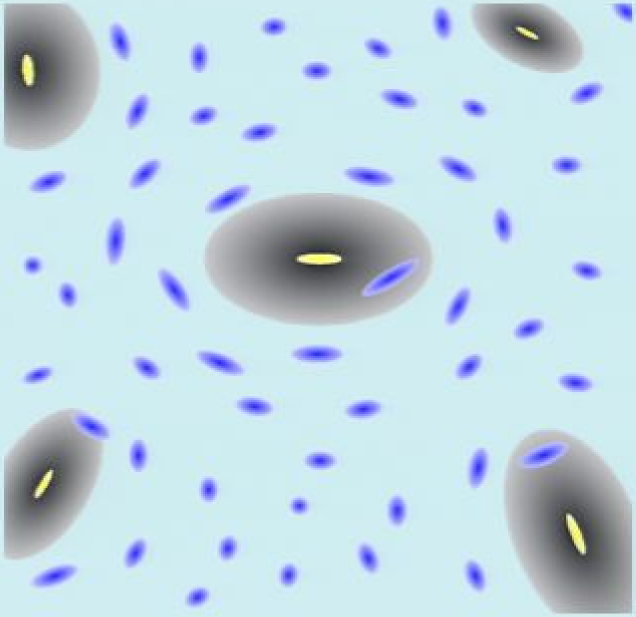

Mass modeling

- Identify all arcs, identify multiple images (using adaptive ray-tracing code LensInvert PN 03 - Bayesian MCMC)
- Model cluster mass as a smooth 'isothermal' ellipse (parametric model), parameters: velocity dispersion, ellipticity, tidal radius
- Add perturbations to model effect of cluster sub-halos

Galaxy halo properties

- Aperture radii, mass, velocity dispersion, total M/L ratios
- Mass function, radial distribution of DM
- Implications of the spatial distribution for the nature of dark matter

Tyson+ 90; PN+ 98; 02

Sub-halo properties

- cut radii
- mass, velocity dispersion
- M/L ratios
- mass function
- radial distribution

$$r_{core} = r^*_{core}\left(\frac{L}{L^*}\right)^{\frac{1}{2}} \quad r_{cut} = r^*_{cut}\left(\frac{L}{L^*}\right)^{\alpha} \quad \sigma = \sigma^*\left(\frac{L}{L^*}\right)^{\frac{1}{4}}$$

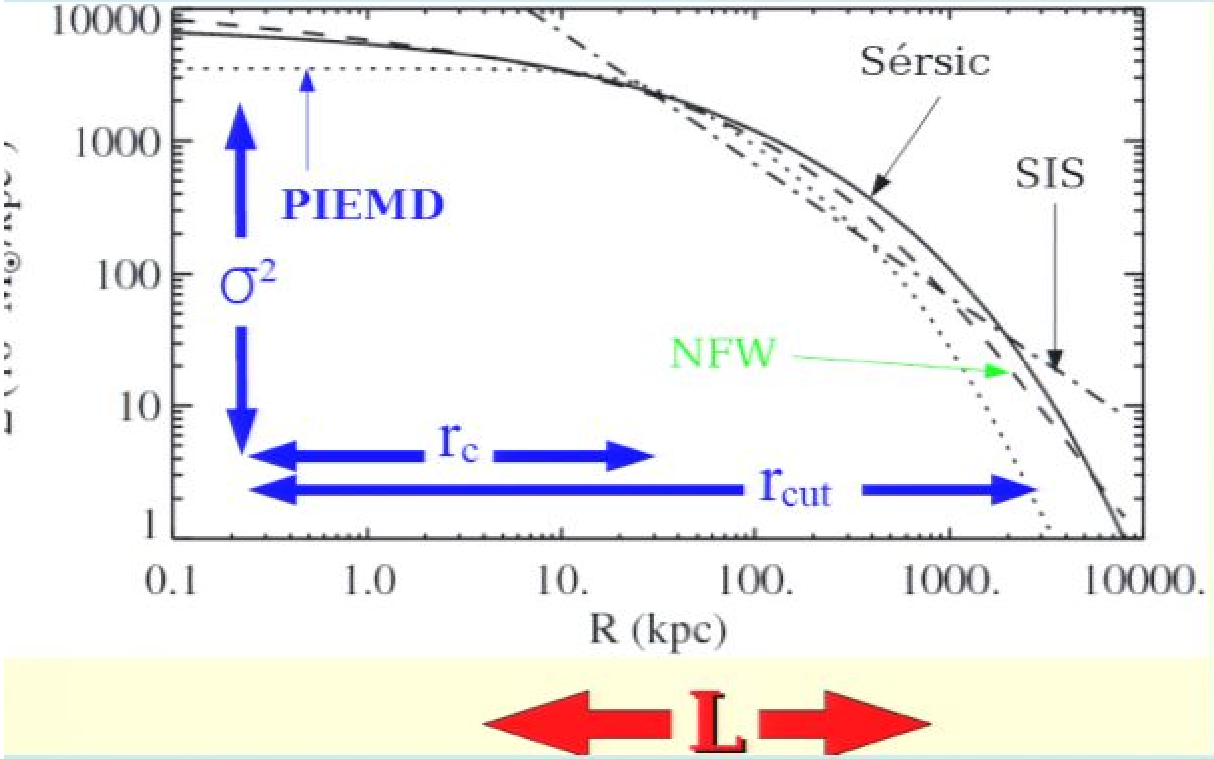

$$M \propto \sigma^2 r_{cut}$$

This mass mapping method has been tested using simulated clusters, with strong and weak lensing constraints

Mass modeling: Bayesian inference

Definition of chi^2 for a system:

$$\chi_i^2 = \sum_{j=1}^{n_i} \left(\frac{\theta_{ij}^{obs} - \theta_{ij}^{pred}}{\sigma_{ij}} \right)^2$$

$$P(d|s, M) = \frac{1}{\sqrt{2\pi\sigma}} \exp\left(\frac{-\chi^2}{2}\right)$$

Introduction of priors: velocity dispersions of galaxies, L of galaxies and total mass inferred from X-ray

$$P(s|d, M) = \frac{P(d|s, M)\, P(s|M)}{P(d|M)}$$

Calculate Evidence to calibrate models, derive posterior proba
the parameters, shows degeneracies clearly

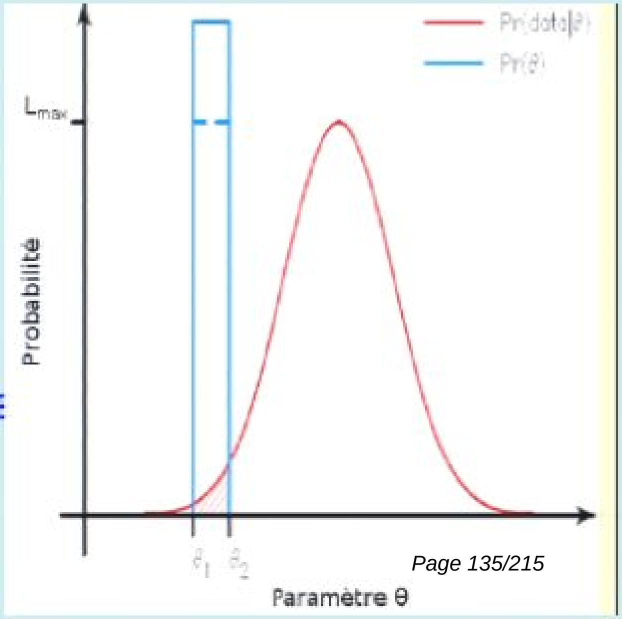

Sub-halo properties

- cut radii
- mass, velocity dispersion
- M/L ratios
- mass function
- radial distribution

$$r_{core} = r^*_{core} \left(\frac{L}{L^*}\right)^{\frac{1}{2}} \quad r_{cut} = r^*_{cut} \left(\frac{L}{L^*}\right)^{\alpha} \quad \sigma = \sigma^* \left(\frac{L}{L^*}\right)^{\frac{1}{4}}$$

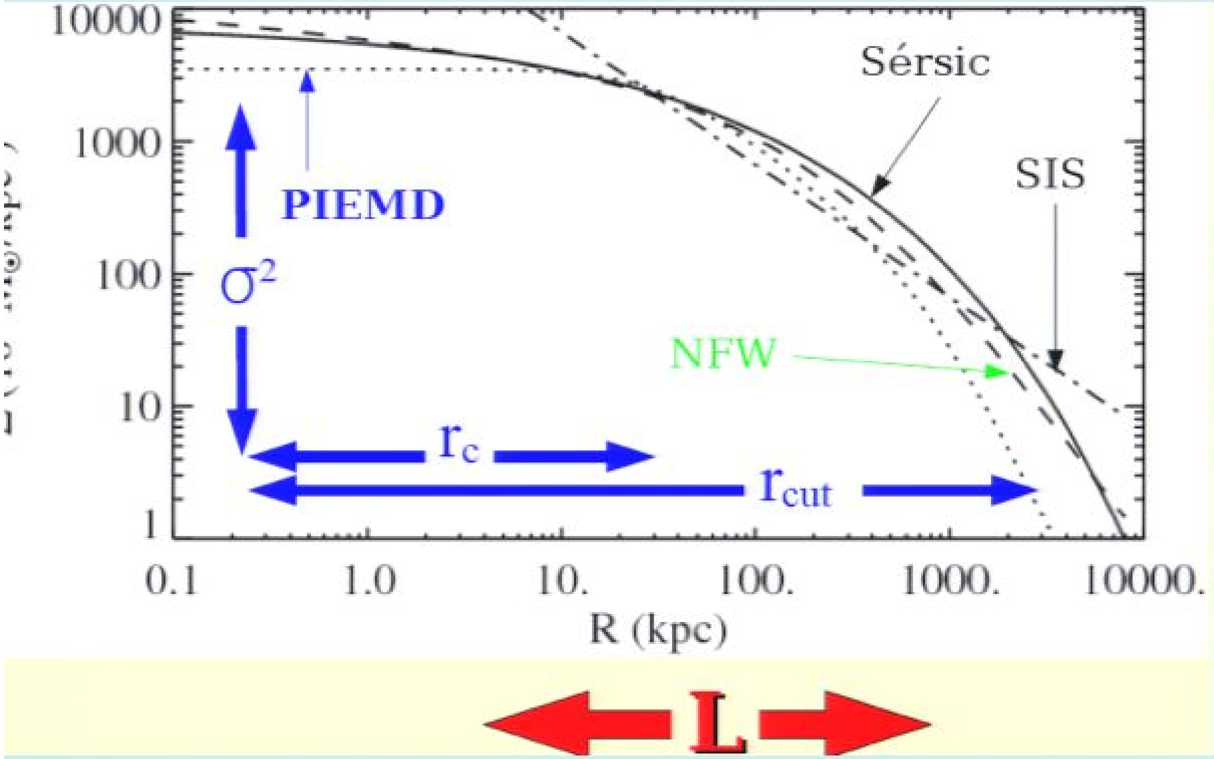

$$M \propto \sigma^2 r_{cut}$$

This mass mapping method has been tested using simulated clusters, with strong and weak lensing constraints

Mass modeling: Bayesian inference

Definition of chi² for a system:

$$\chi_i^2 = \sum_{j=1}^{n_i} \left(\frac{\theta_{ij}^{obs} - \theta_{ij}^{pred}}{\sigma_{ij}} \right)^2$$

$$P(d|s,M) = \frac{1}{\sqrt{2\pi}\sigma} \exp\left(\frac{-\chi^2}{2}\right)$$

Introduction of priors: velocity dispersions of galaxies, L of galaxies and total mass inferred from X-ray

$$P(s|d,M) = \frac{P(d|s,M)\,P(s|M)}{P(d|M)}$$

Calculate Evidence to calibrate models, derive posterior proba the parameters, shows degeneracies clearly

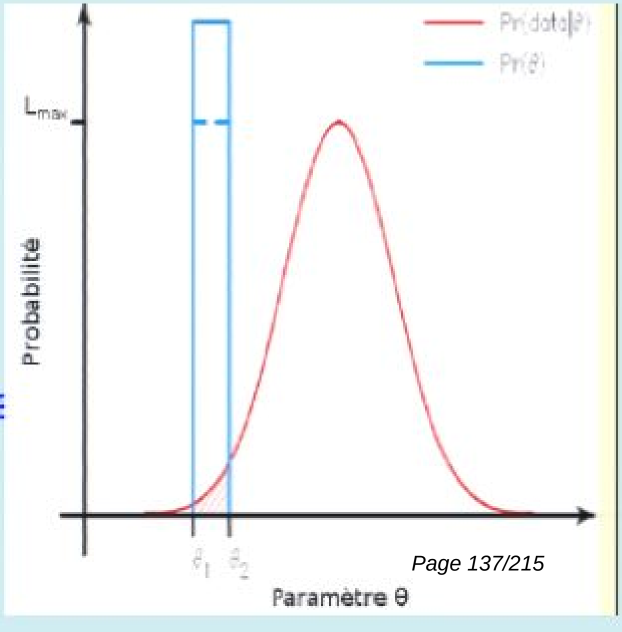

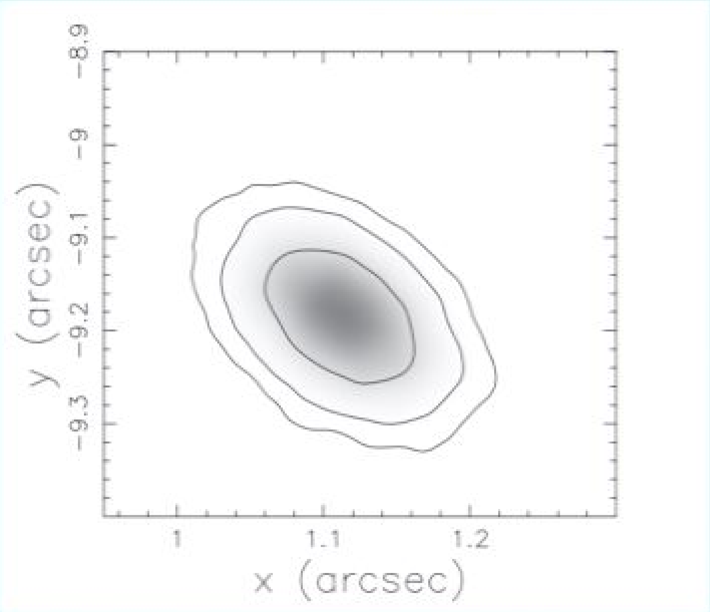

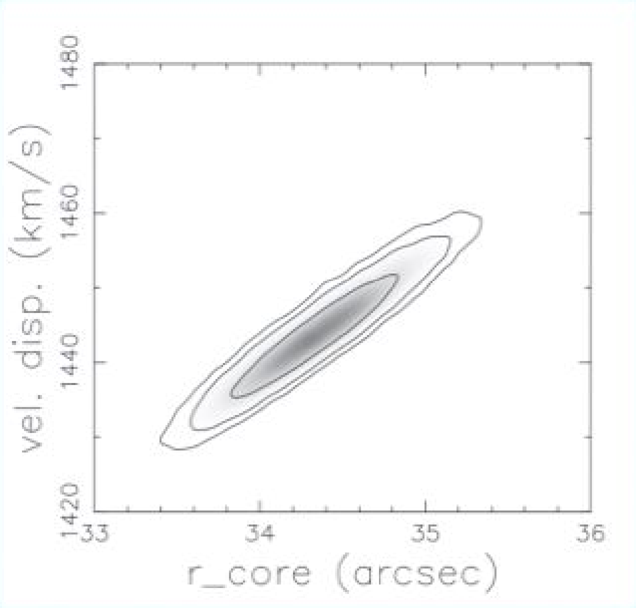

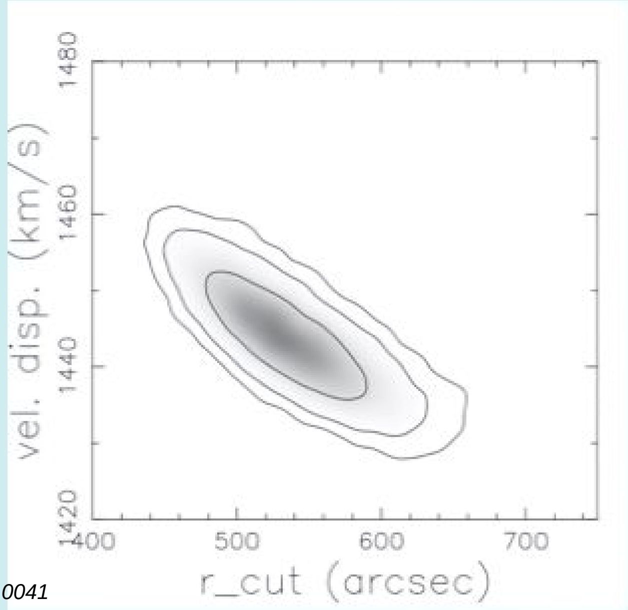

Marginalized posterior PDFs

Is maximum for the set of params
That provides the best fit and is consistent
With the prior PDF; evidence is the probability
of getting the data given assumed model M

Jullo+ 07

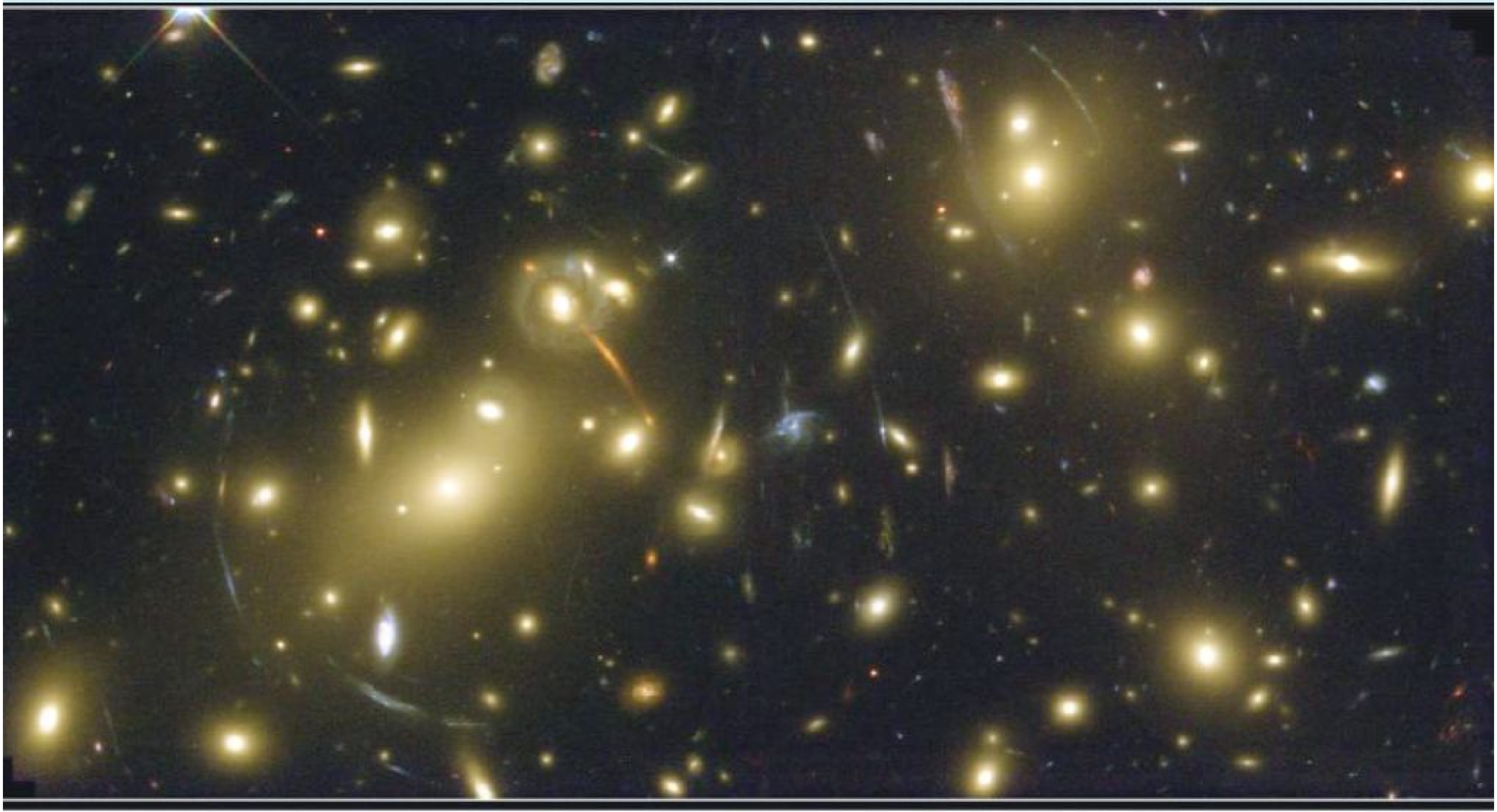

Galaxy Cluster Abell 2218

Hubble Space Telescope • WFPC2

ASA, A. Fruchter and the ERO Team (STScI, ST-ECF) • STScI-PRC00-08


R = 6.0 Mpc
z = 4.917
a = 0.170
diemand 2003

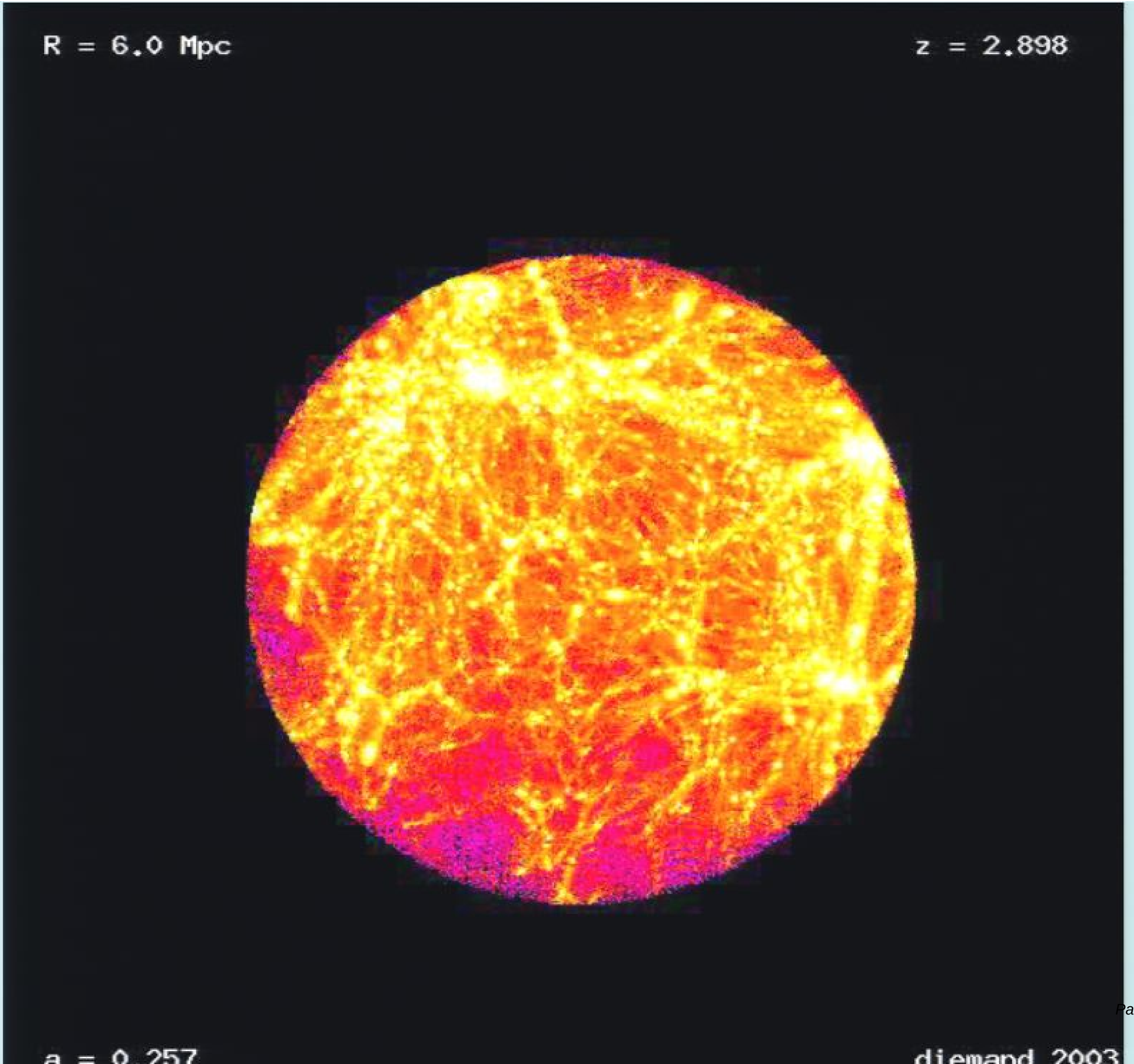
R = 6.0 Mpc
z = 2.898
a = 0.257
diemand 2003

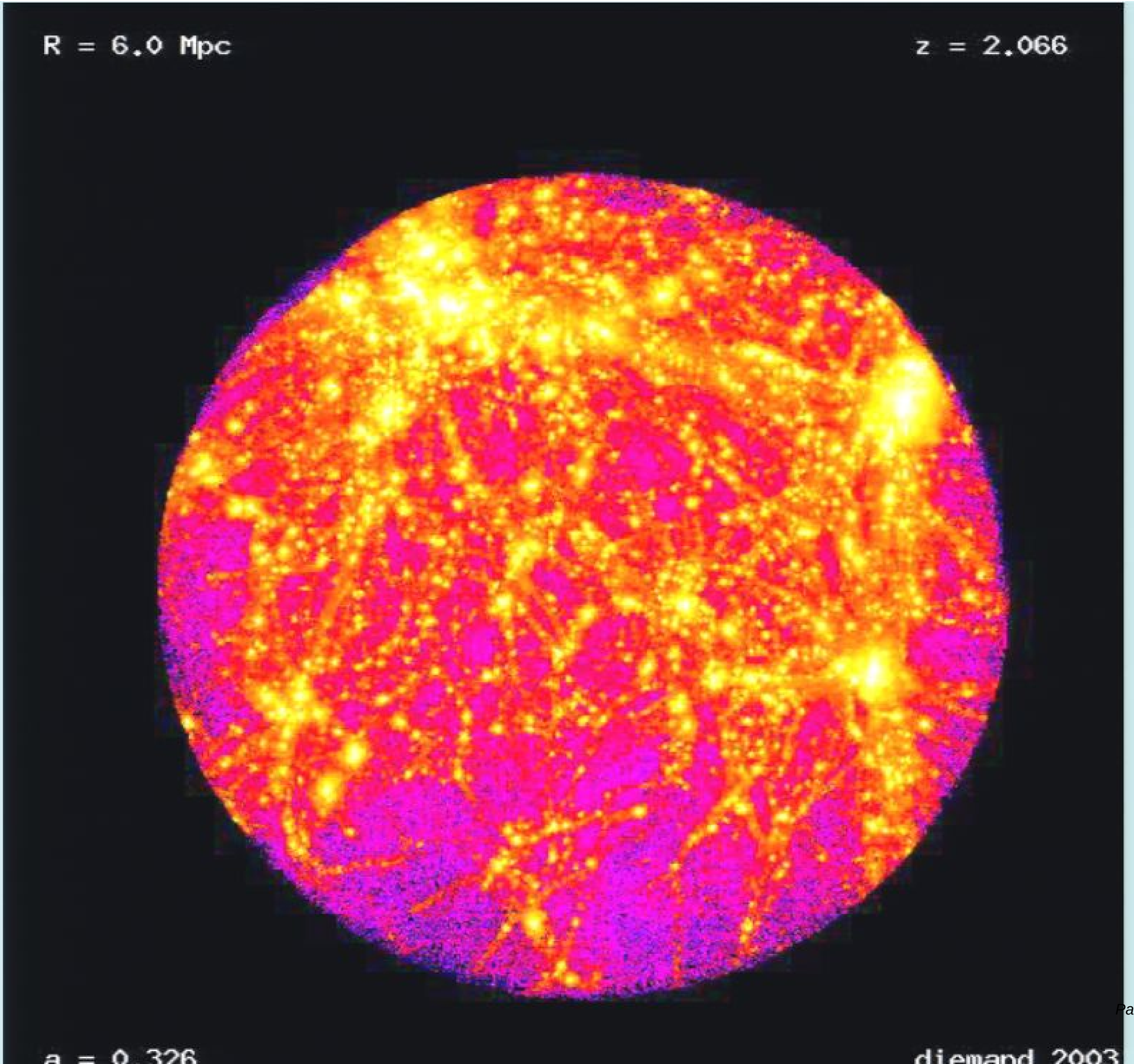
R = 6.0 Mpc
z = 2.066
a = 0.326
diemand 2003

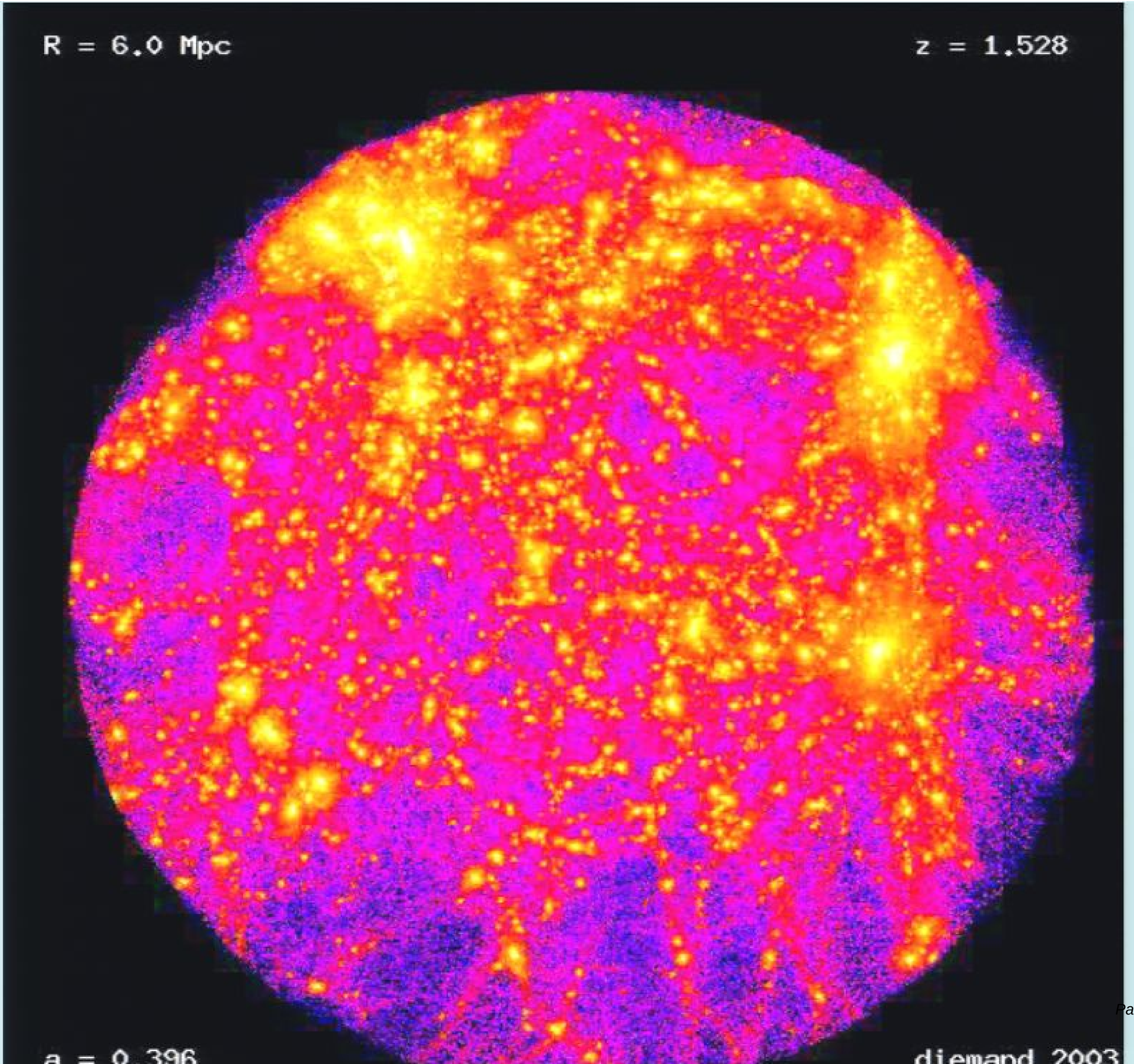
R = 6.0 Mpc
z = 1.528
a = 0.396
diemand 2003

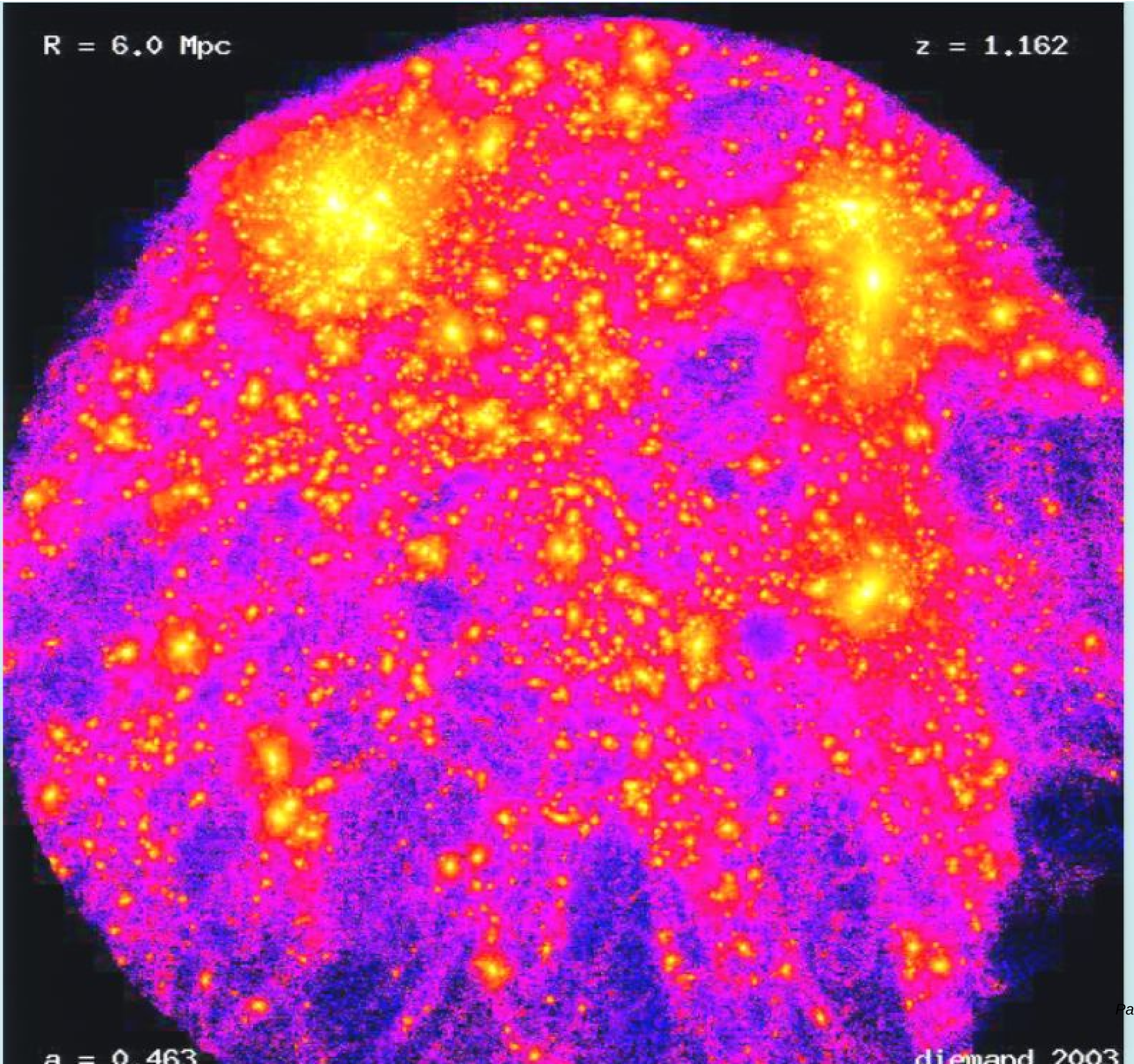
R = 6.0 Mpc
z = 1.162
a = 0.463
diemand 2003

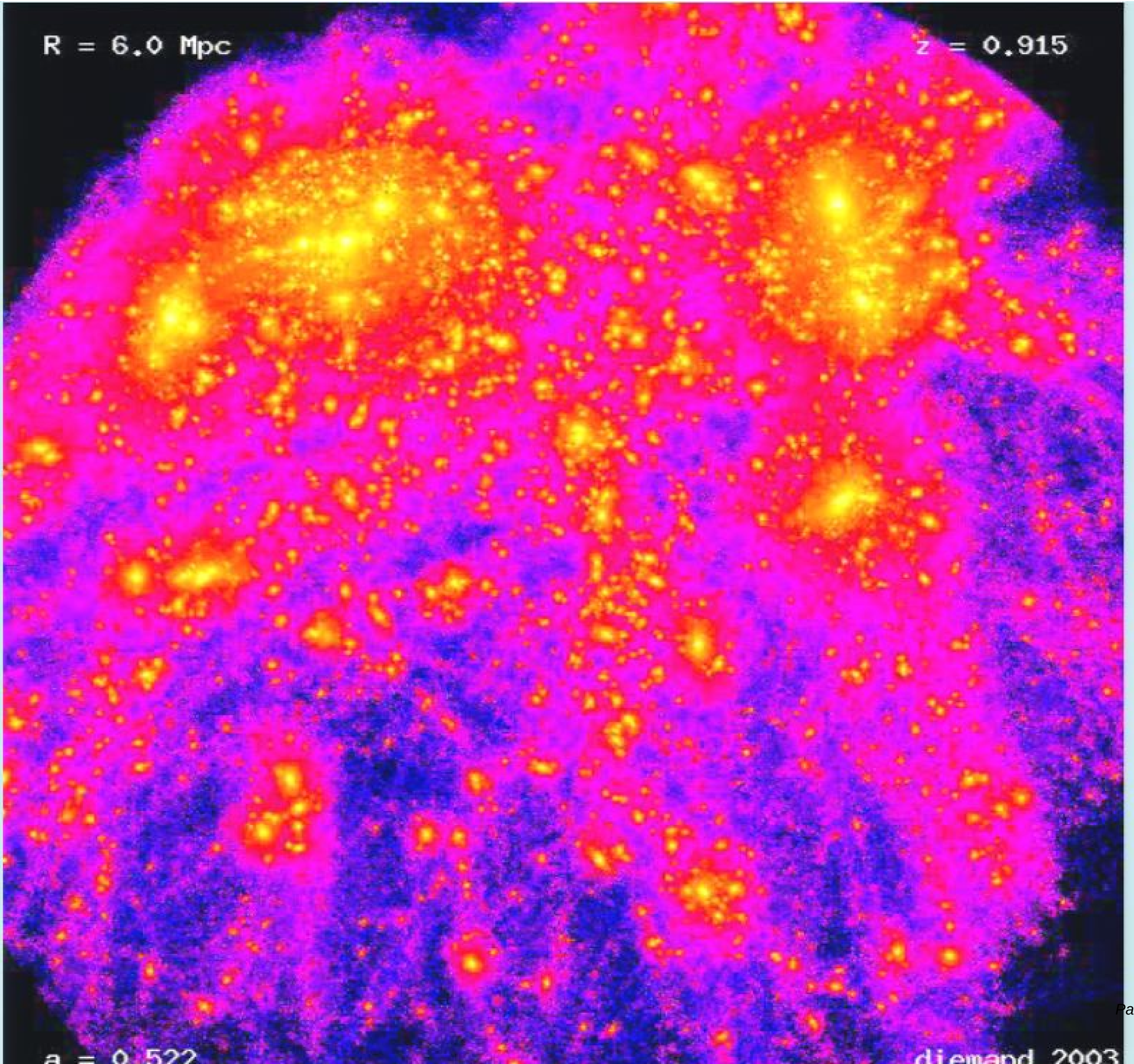
R = 6.0 Mpc
z = 0.915
a = 0.522
diemand 2003

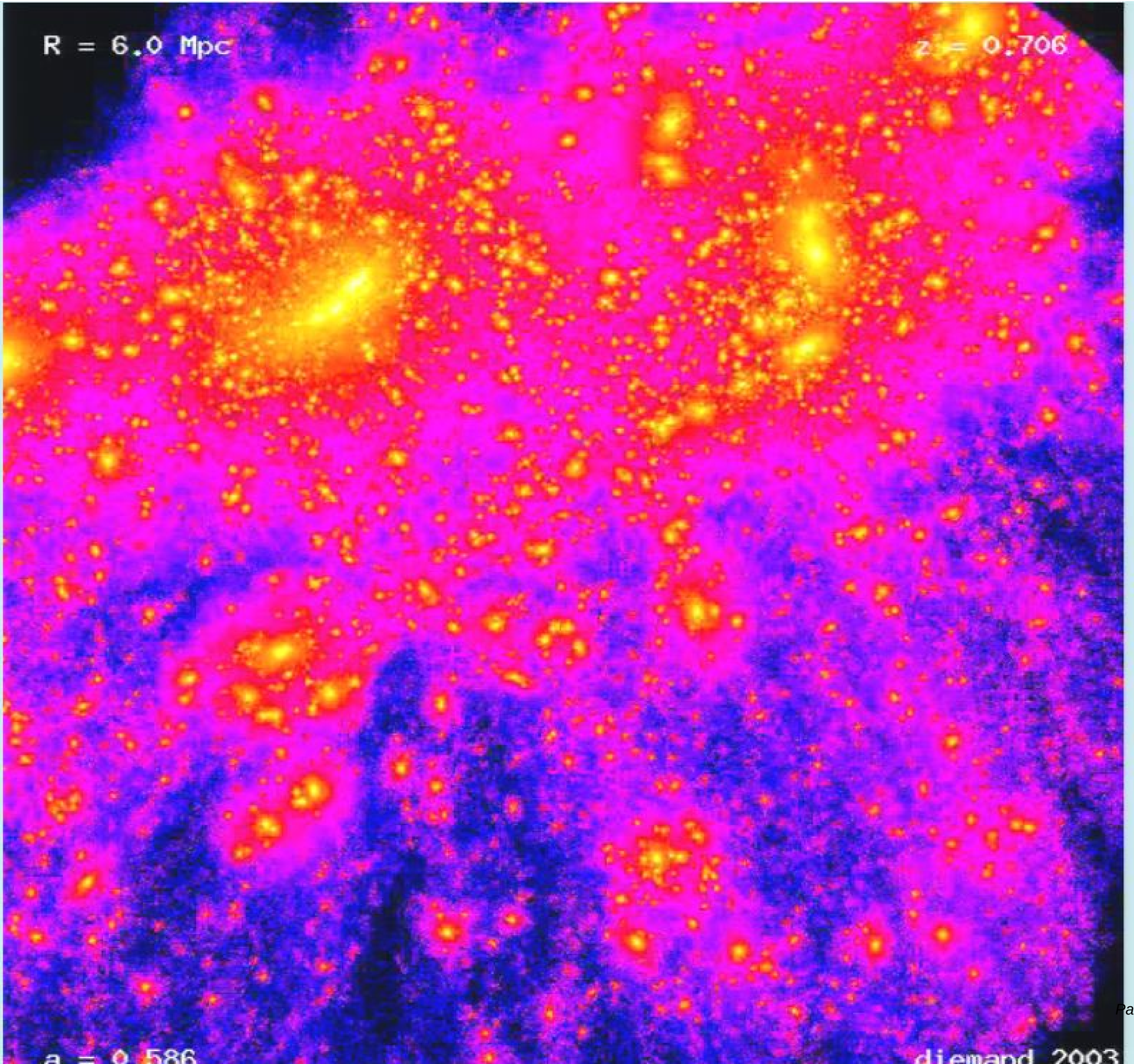
R = 6.0 Mpc
z = 0.706
a = 0.586
diemand 2003

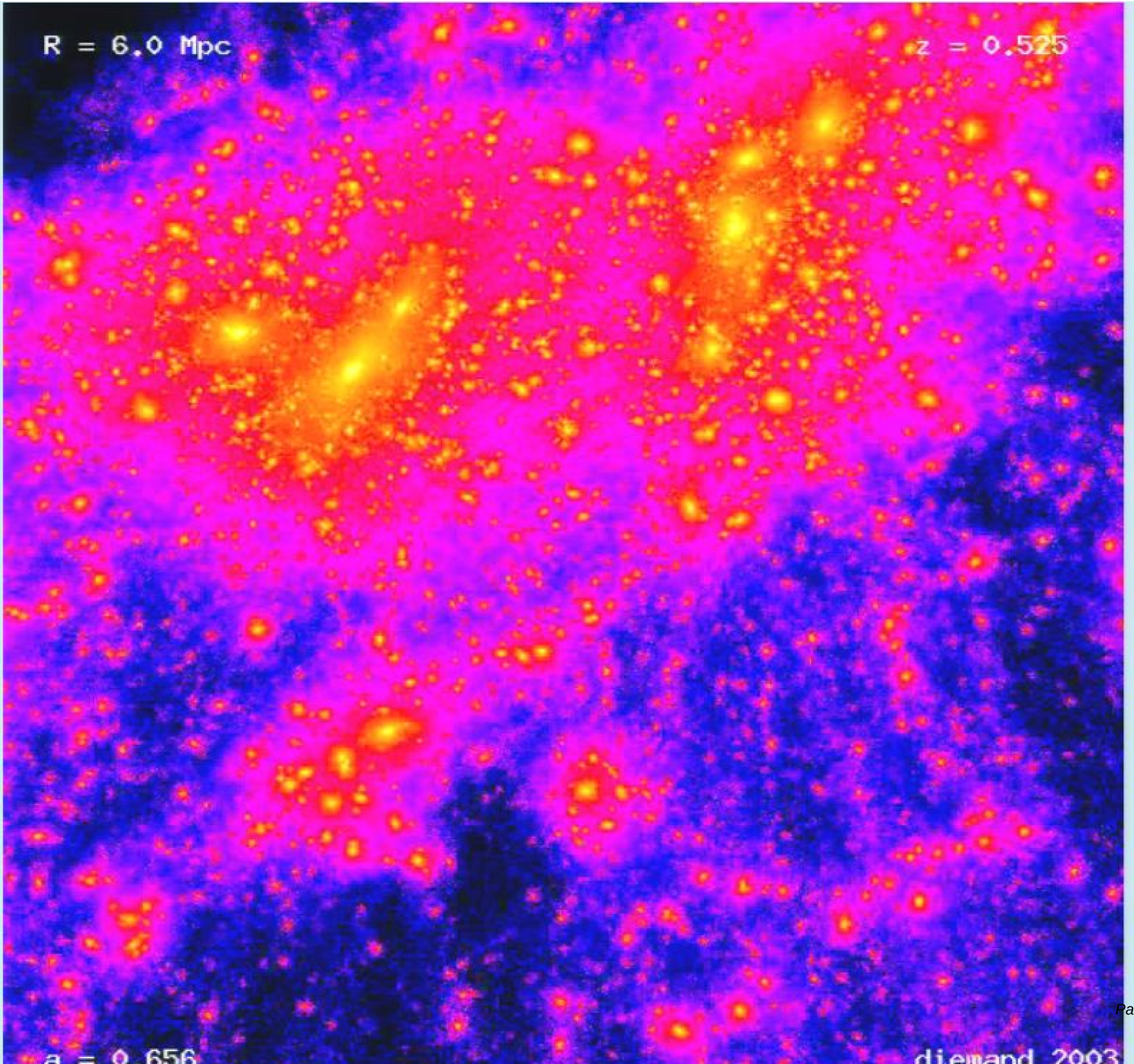

R = 6.0 Mpc
z = 0.525
a = 0.656
diemand 2003

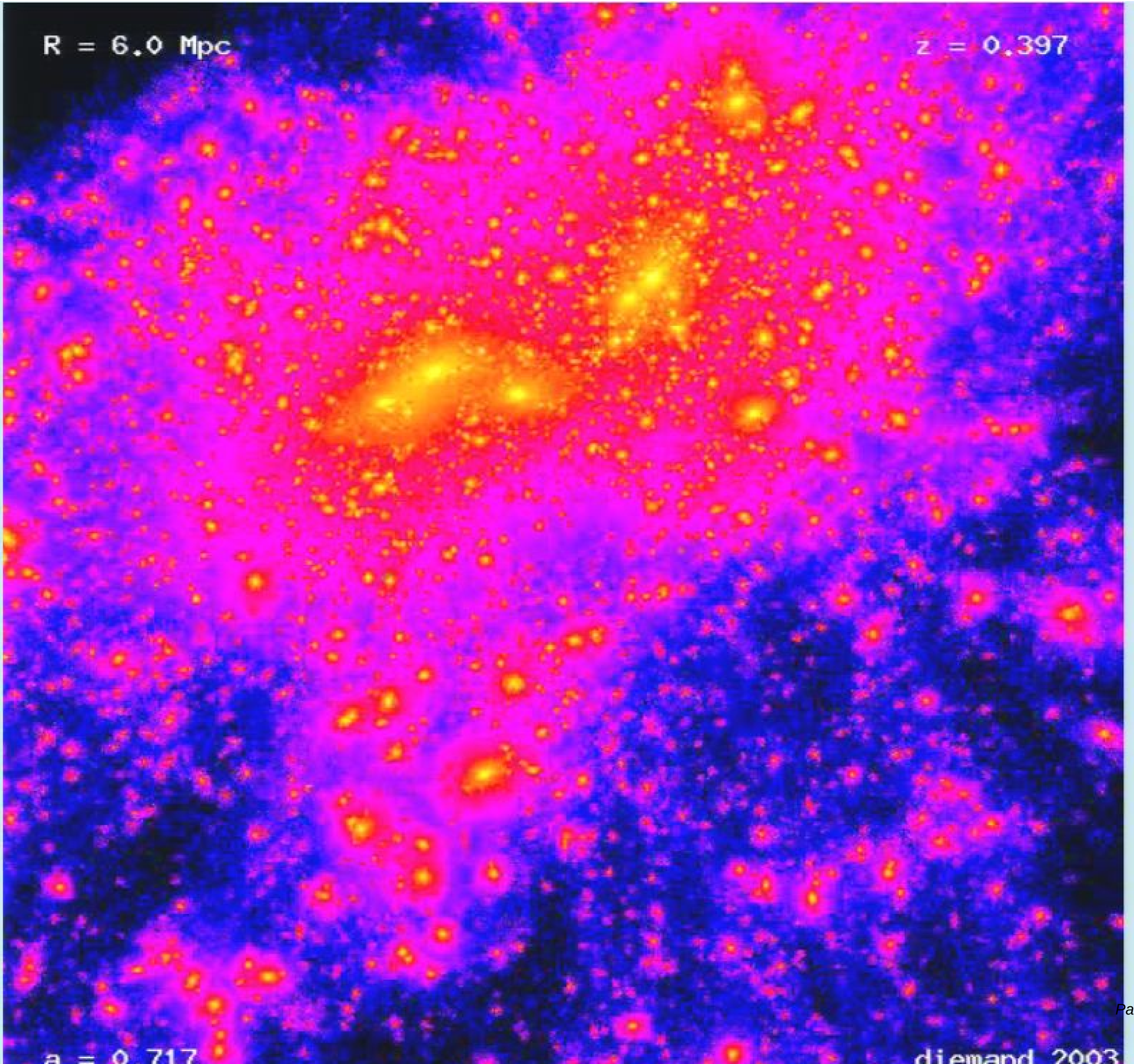
R = 6.0 Mpc
z = 0.397
a = 0.717
diemand 2003

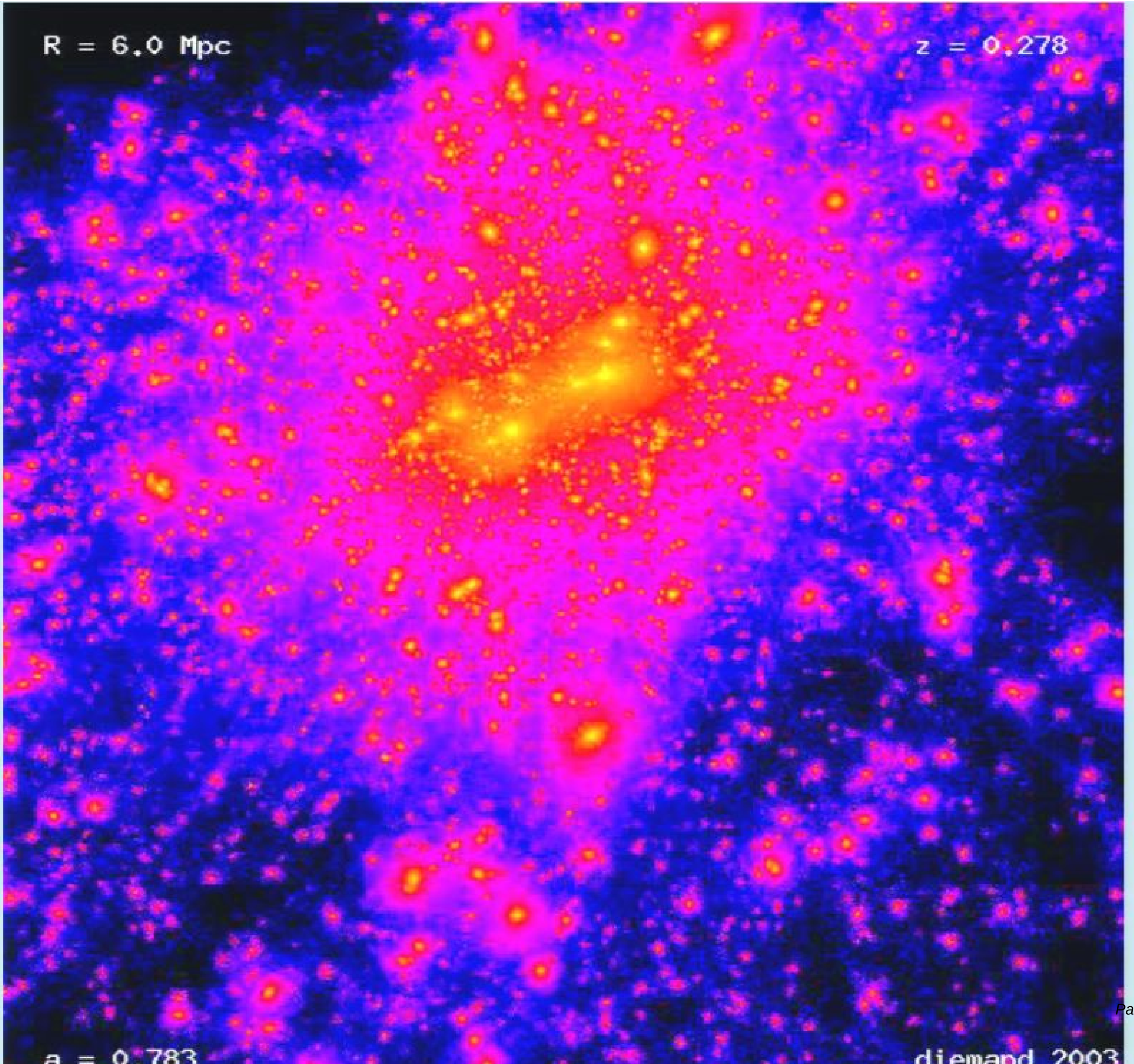
R = 6.0 Mpc
z = 0.278
a = 0.783
diemand 2003

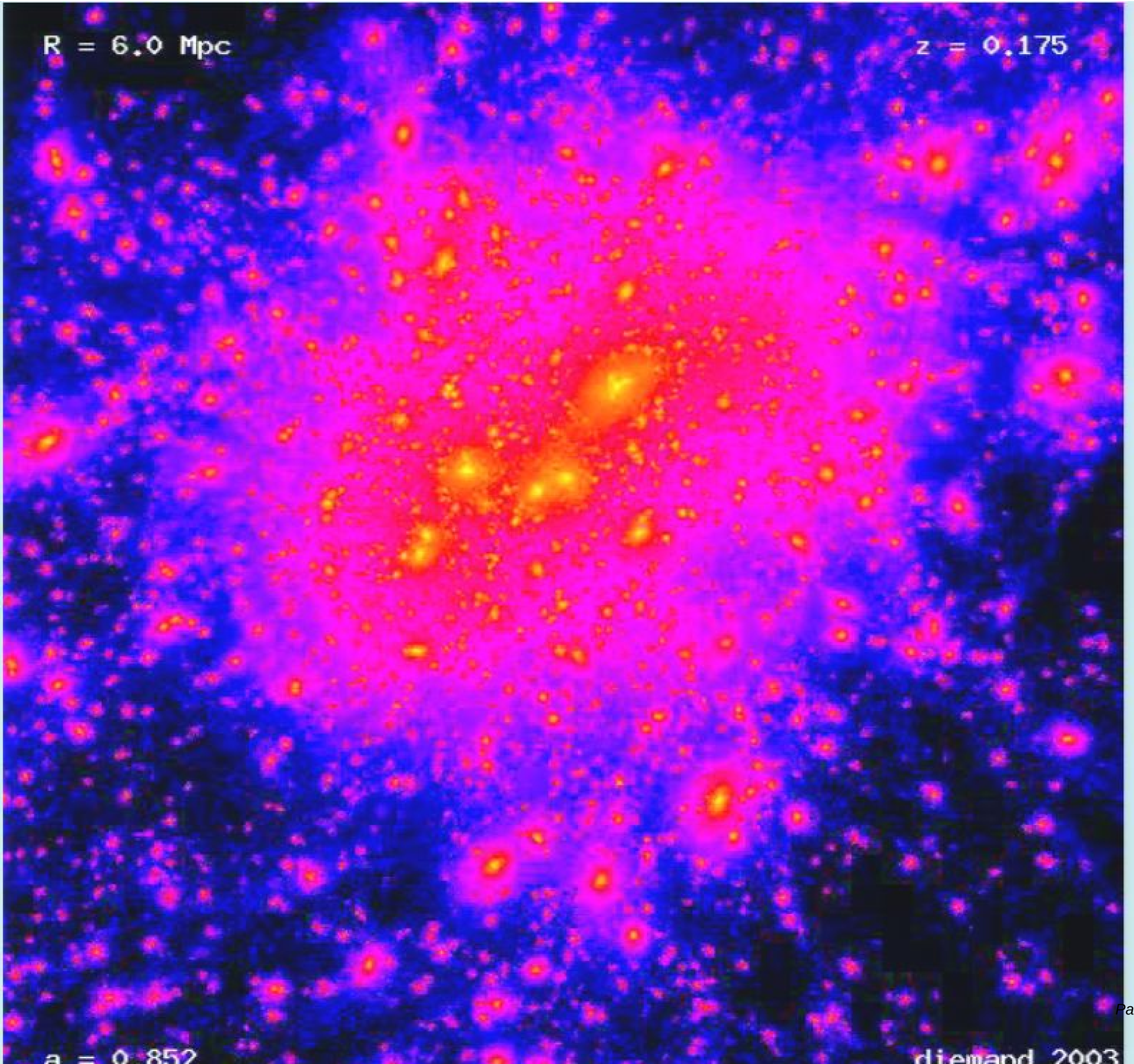
R = 6.0 Mpc
z = 0.175
a = 0.852
diemand 2003

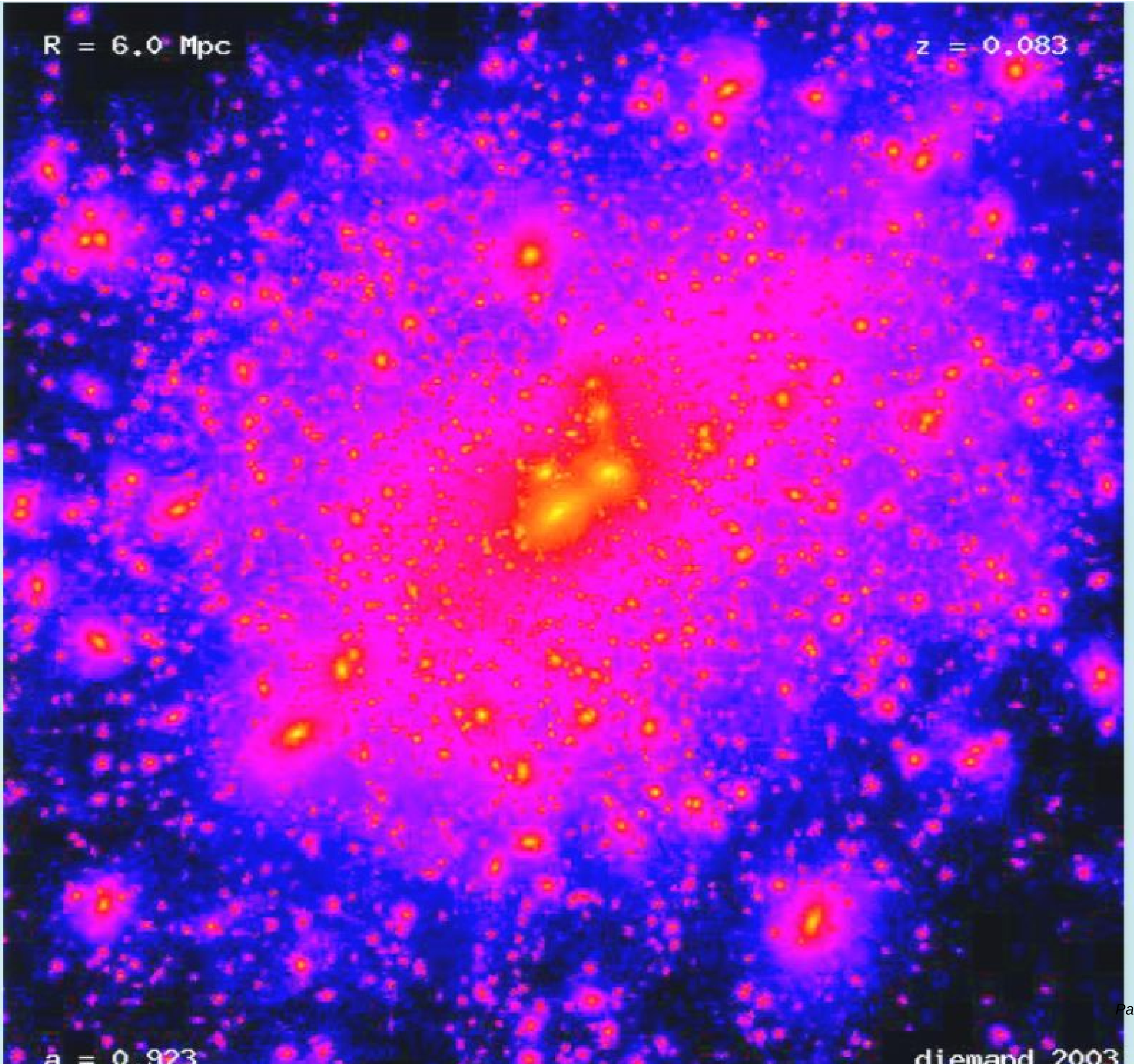
R = 6.0 Mpc
z = 0.083
a = 0.923
diemand 2003

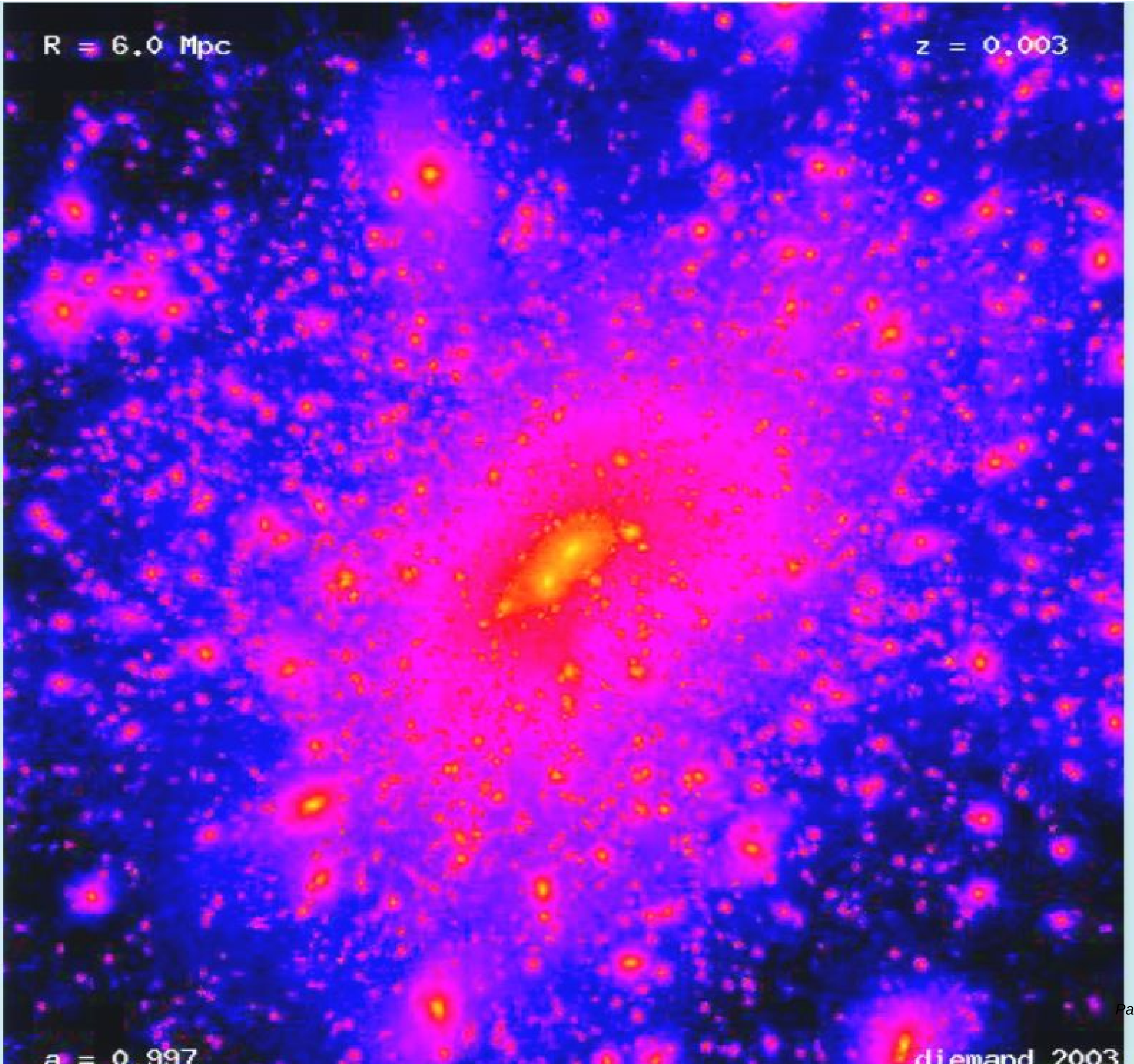
R = 6.0 Mpc
z = 0.003
a = 0.997
diemand 2003

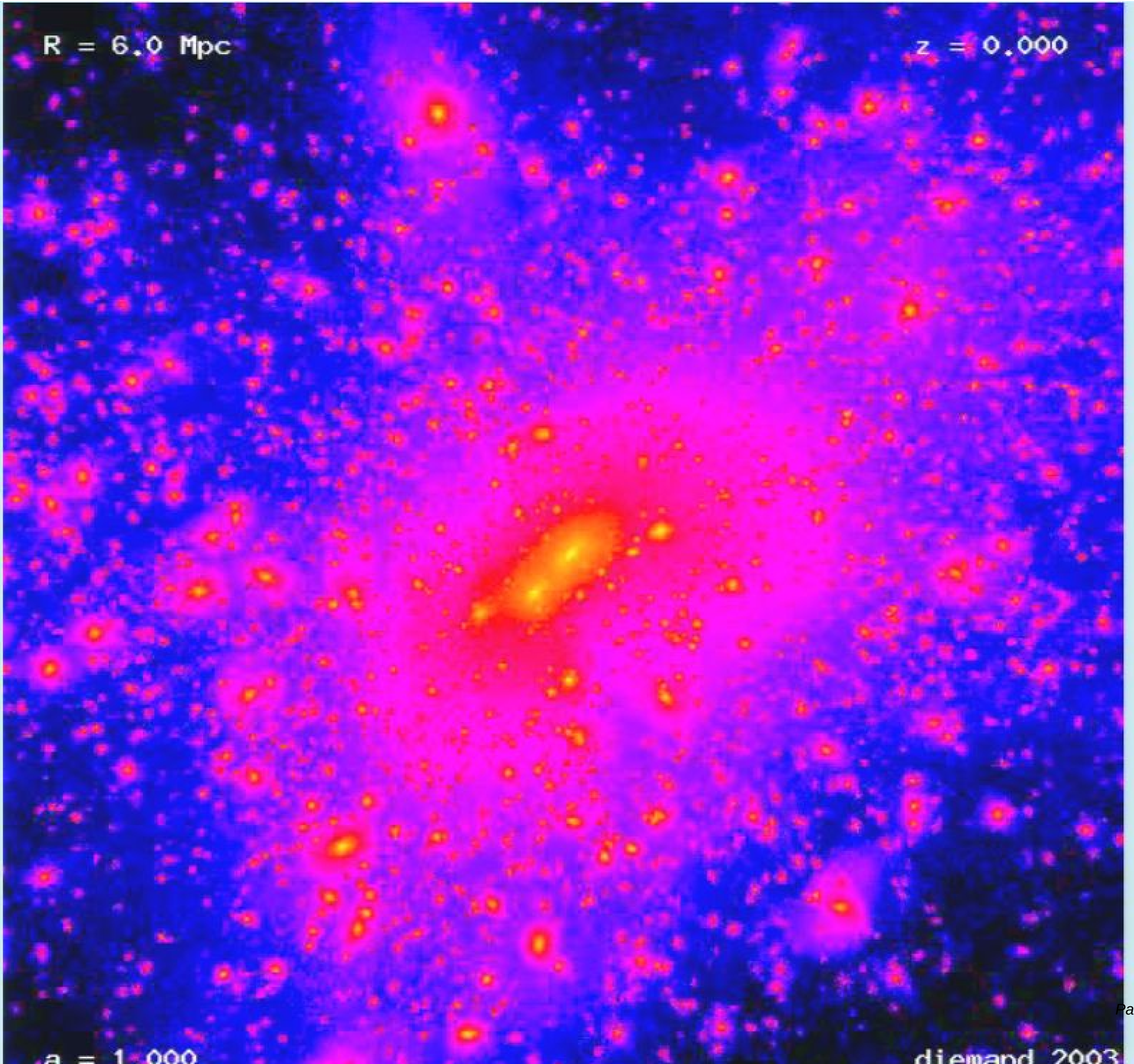
R = 6.0 Mpc
z = 0.000
a = 1.000
diemand 2003

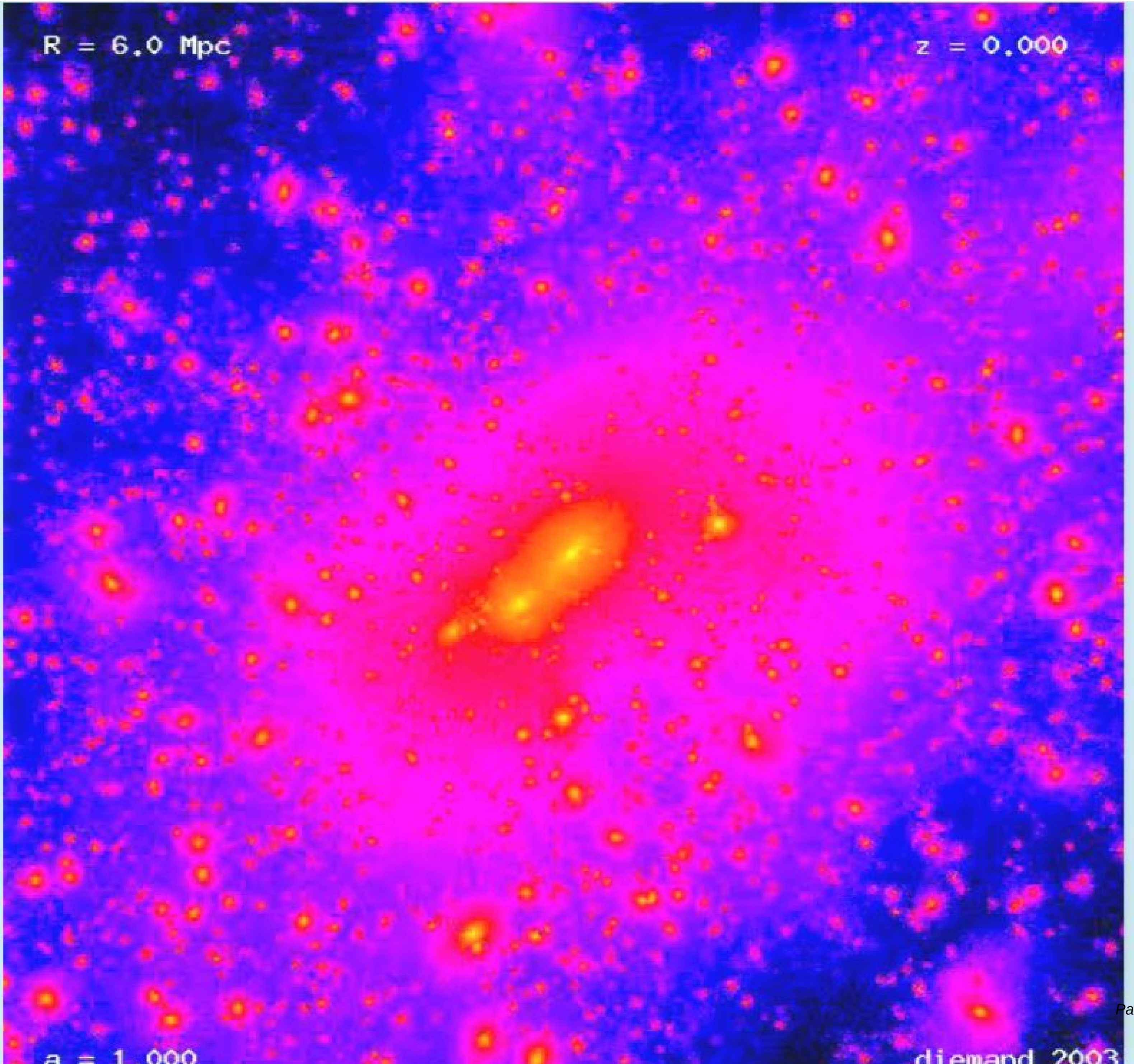
R = 6.0 Mpc
z = 0.000
a = 1.000
diemand 2003

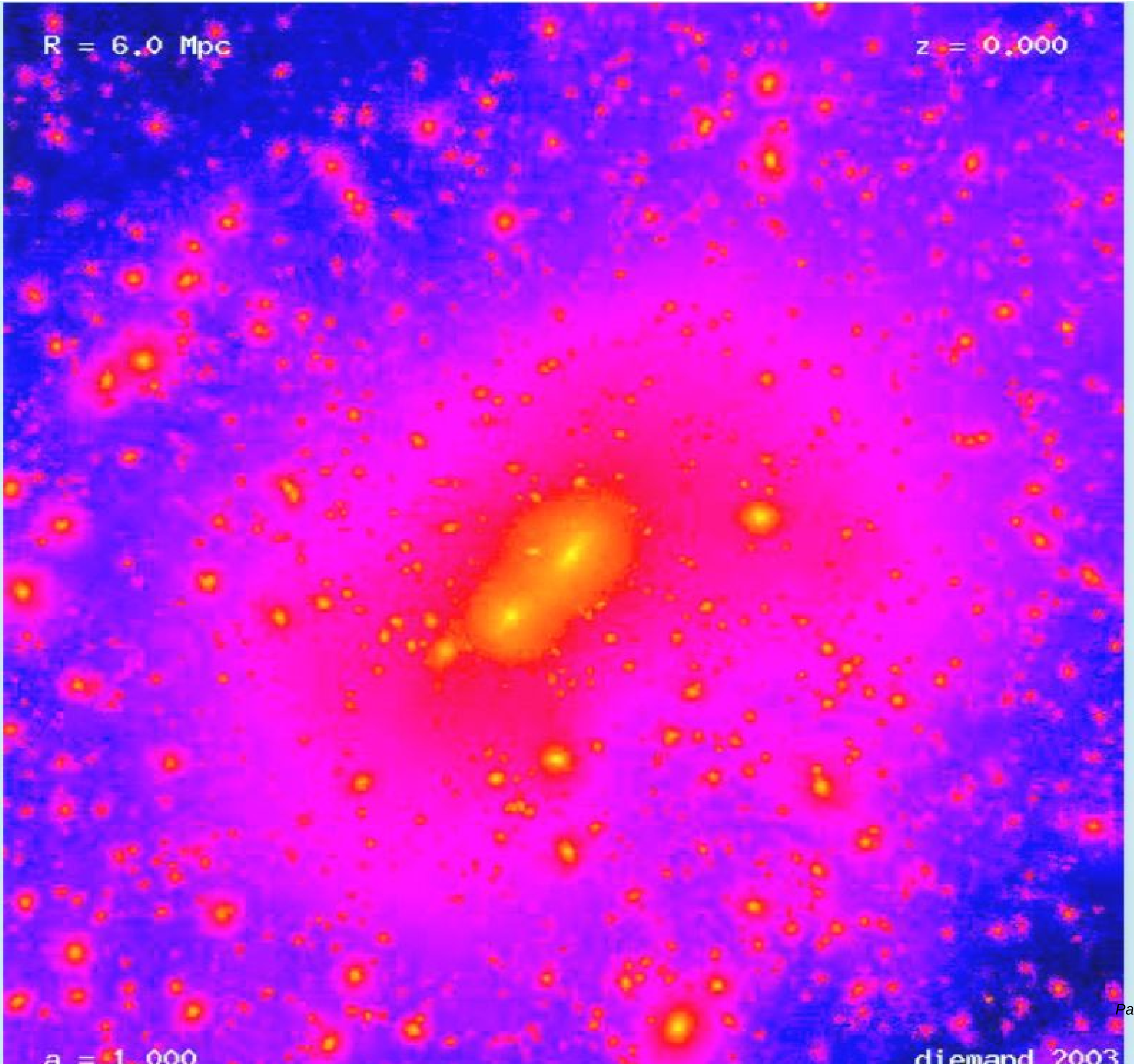
R = 6.0 Mpc
z = 0.000
a = 1.000
diemand 2003

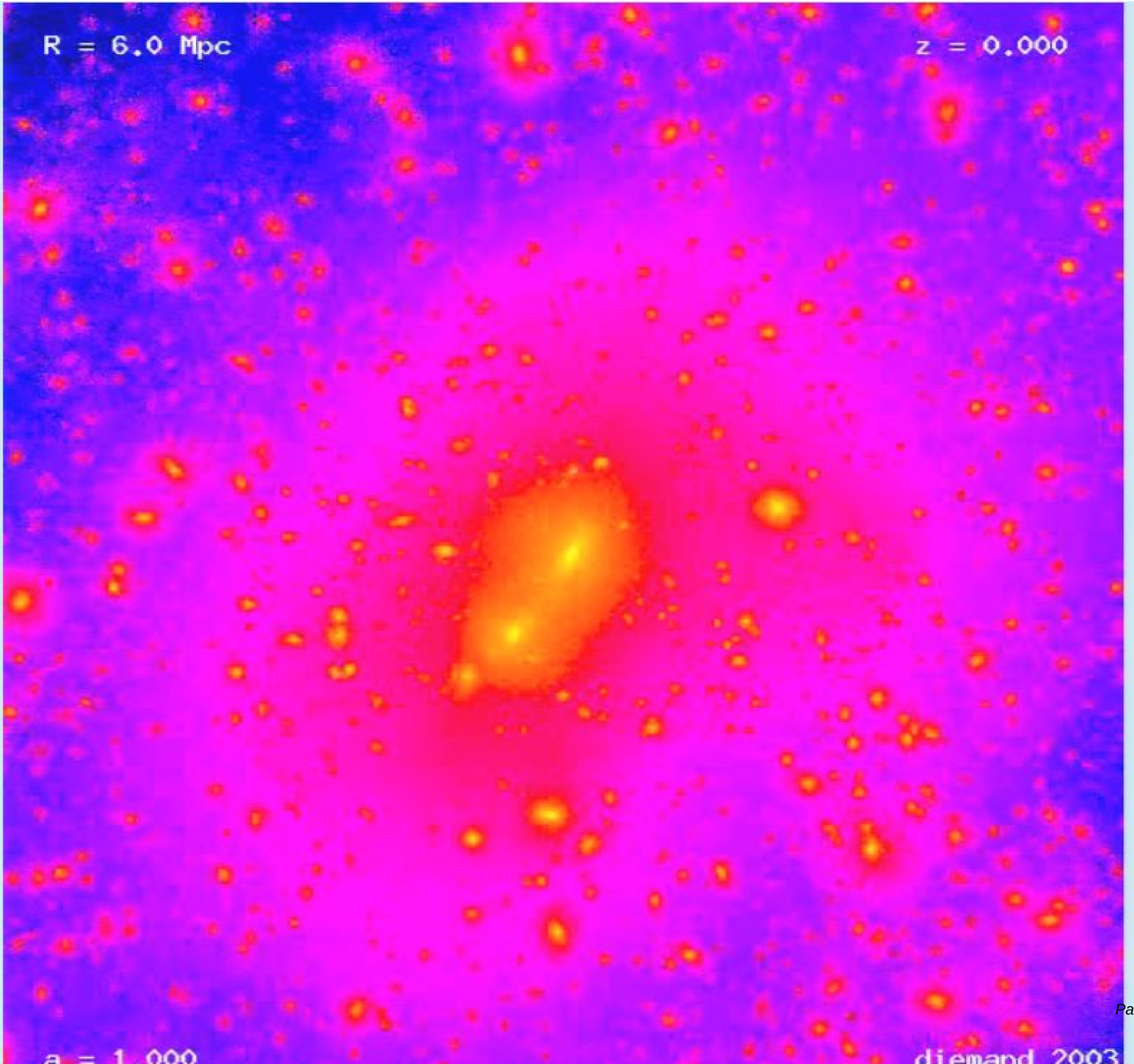
R = 6.0 Mpc
z = 0.000
a = 1.000
diemand 2003

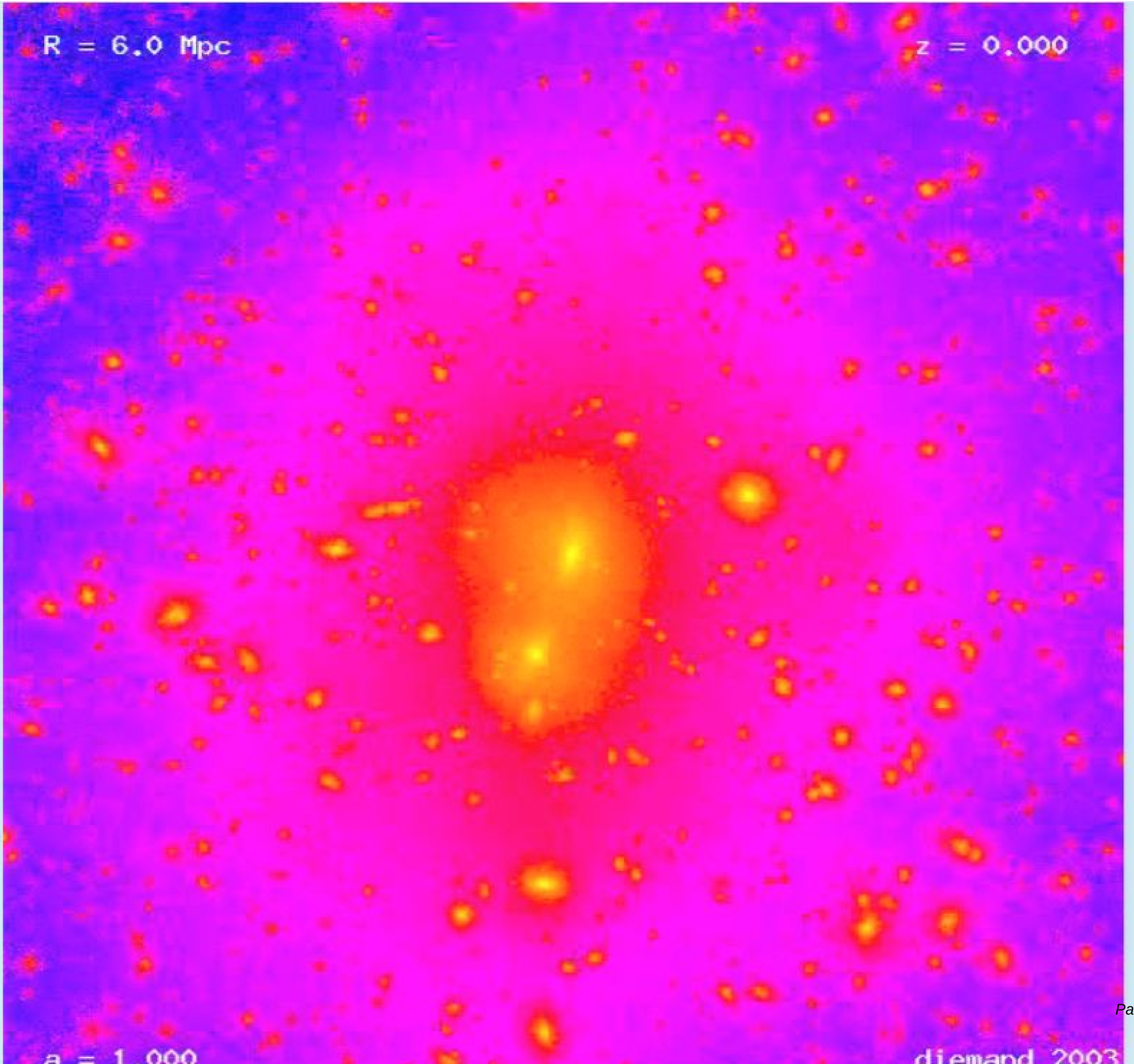
R = 6.0 Mpc
z = 0.000
a = 1.000
diemand 2003

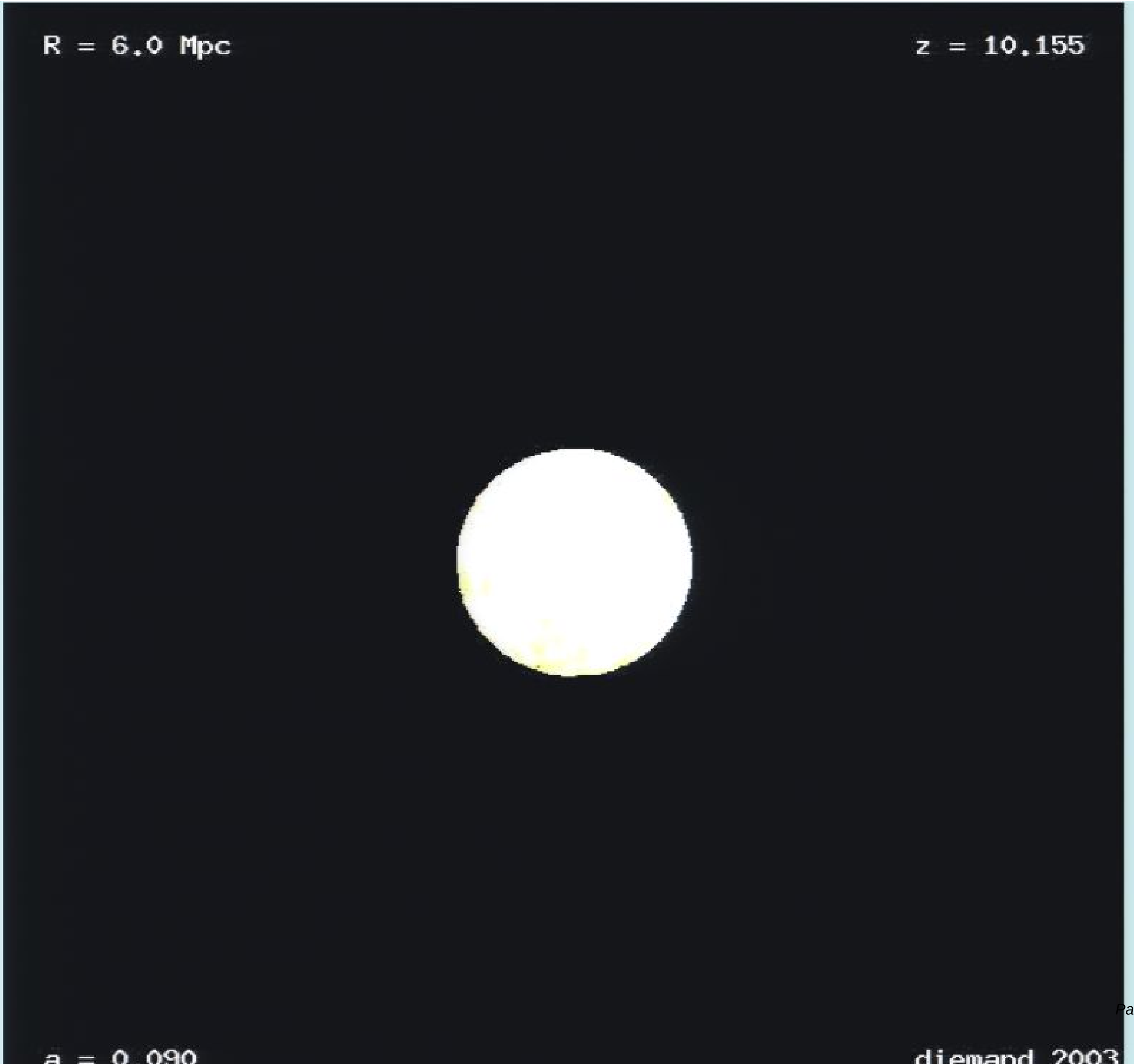
R = 6.0 Mpc
z = 10.155
a = 0.090
diemand 2003


R = 6.0 Mpc
z = 4.420
a = 0.186
diemand 2003

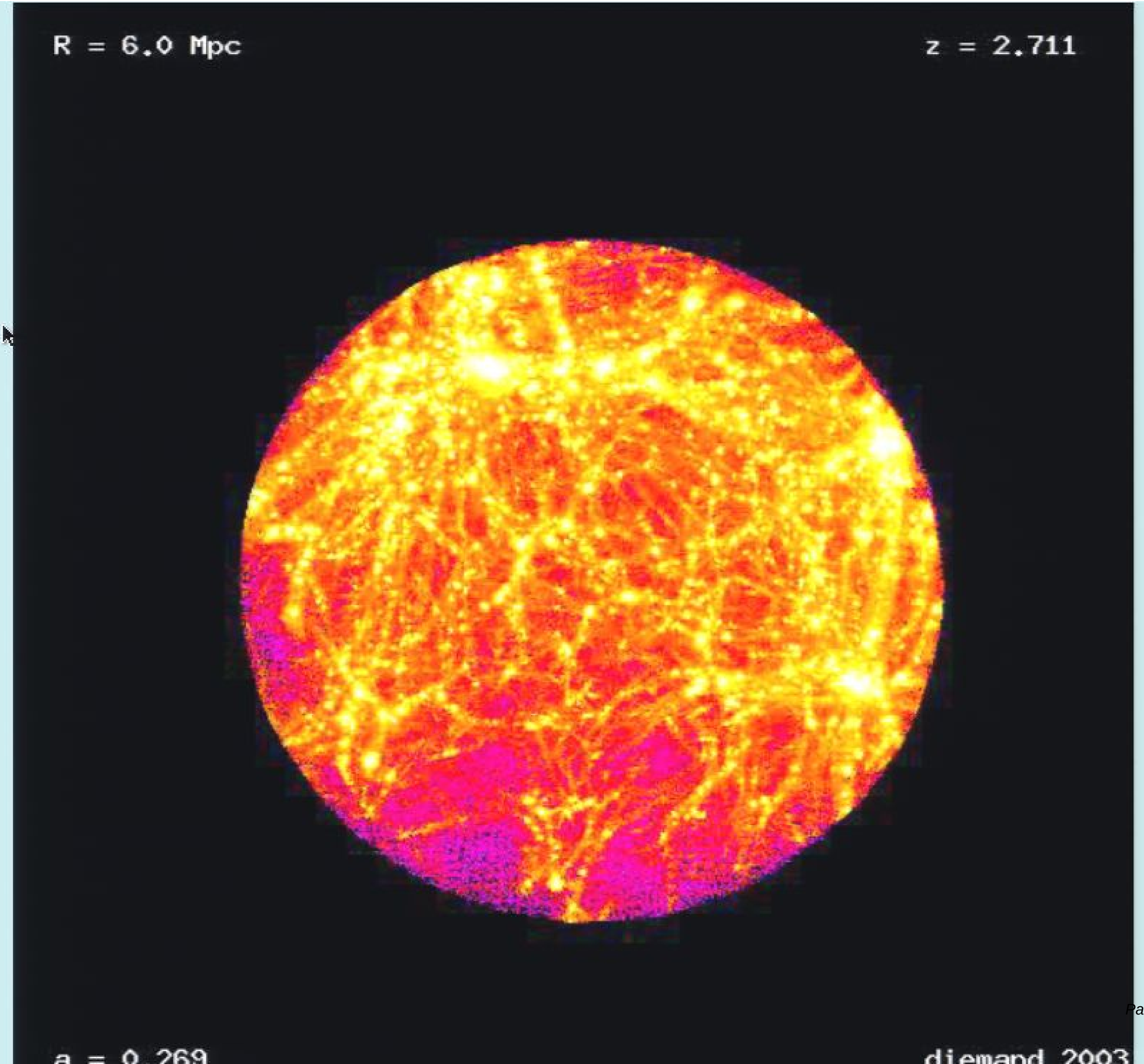
R = 6.0 Mpc
z = 2.711
a = 0.269
diemand 2003

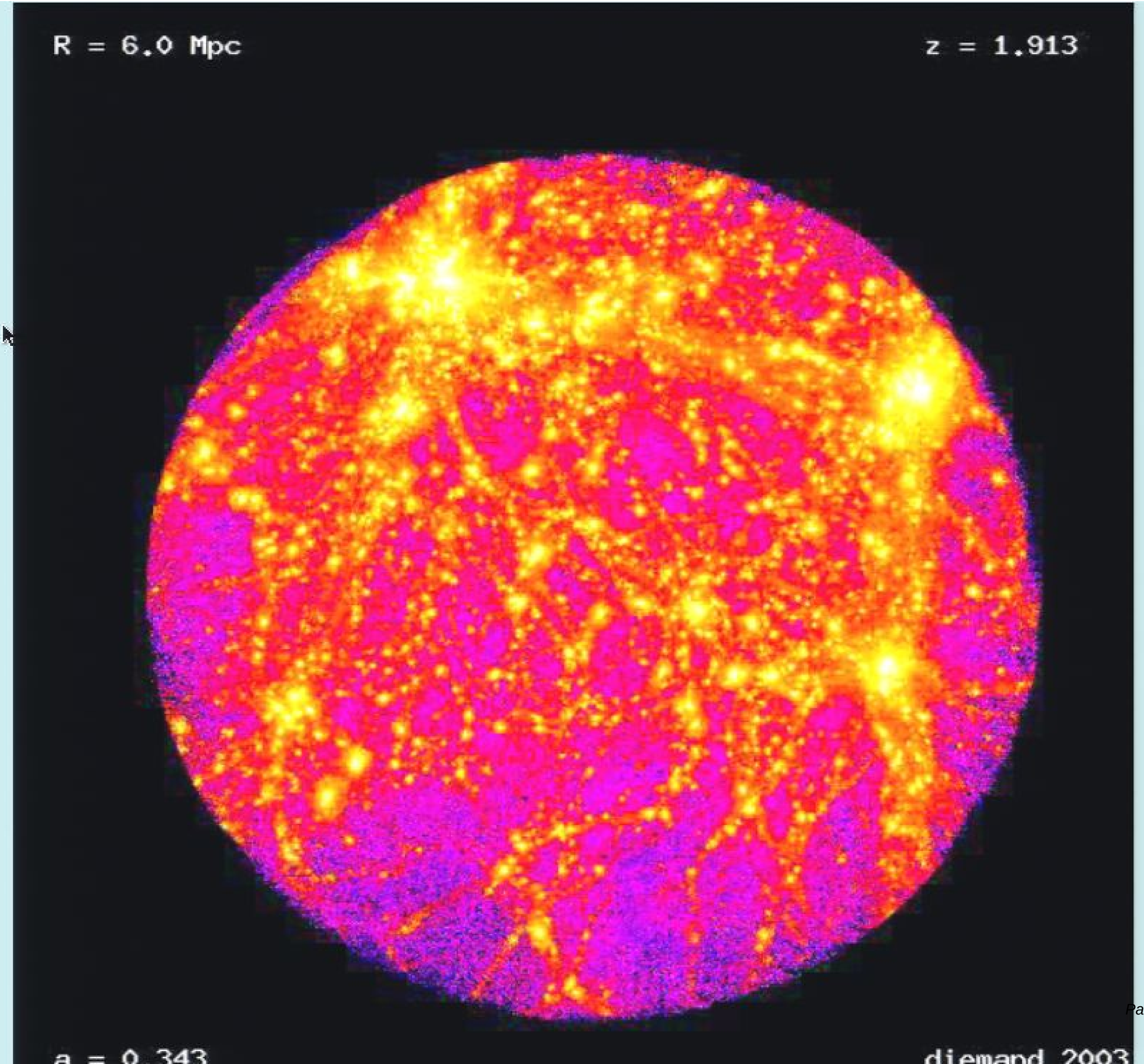
R = 6.0 Mpc
z = 1.913
a = 0.343
diemand 2003

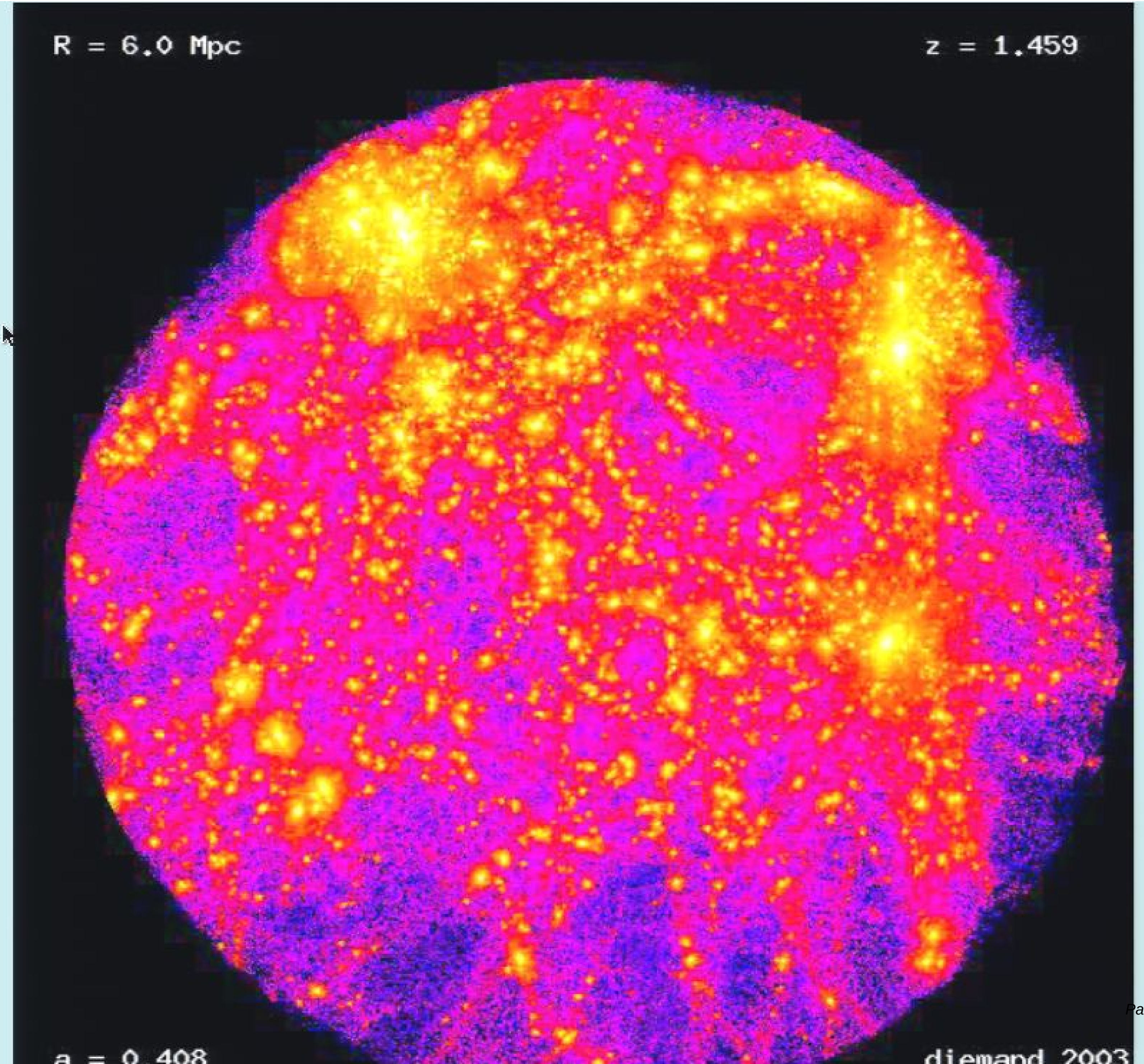
R = 6.0 Mpc
z = 1.459
a = 0.408
diemand 2003

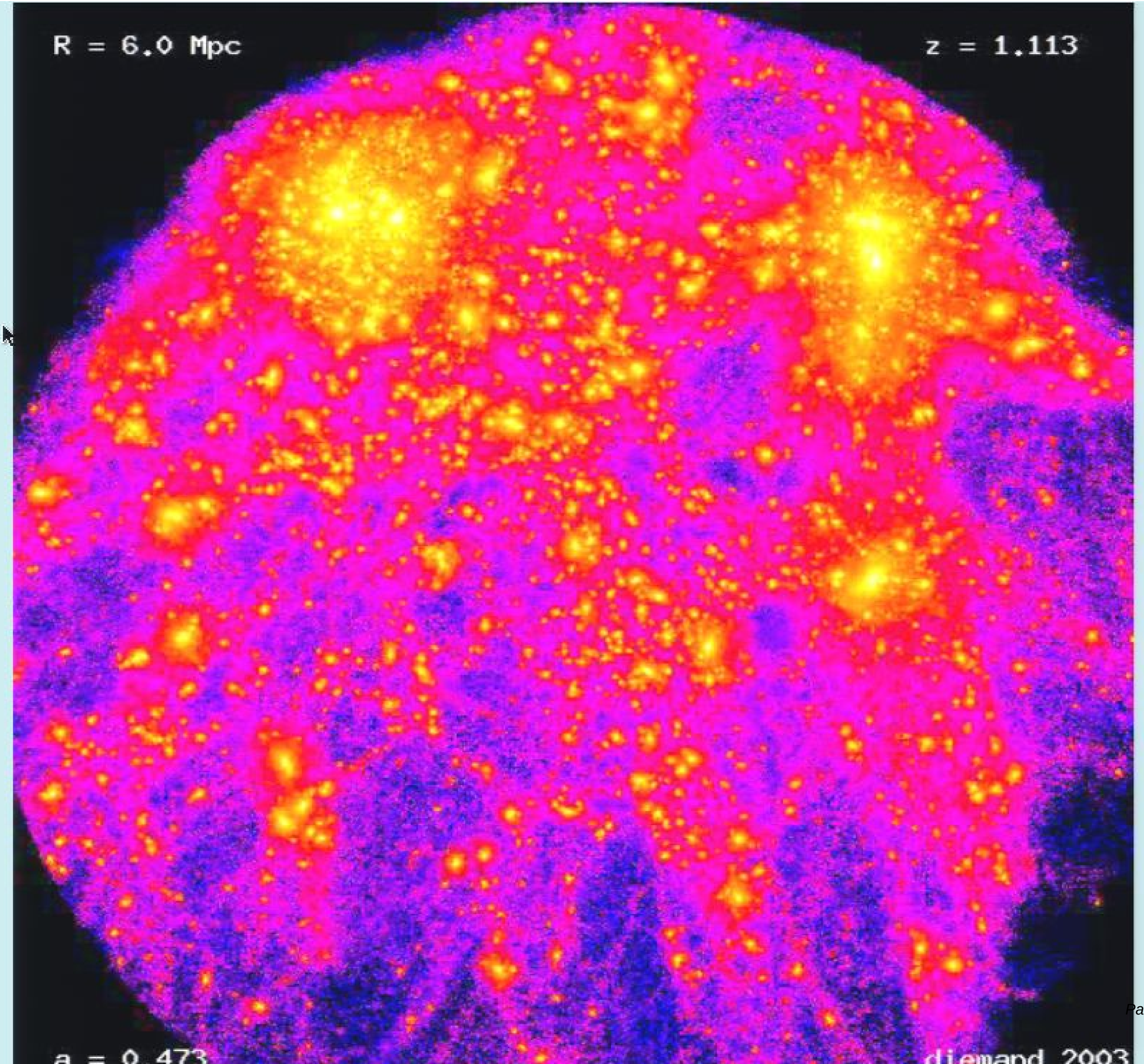
R = 6.0 Mpc
z = 1.113
a = 0.473
diemand 2003

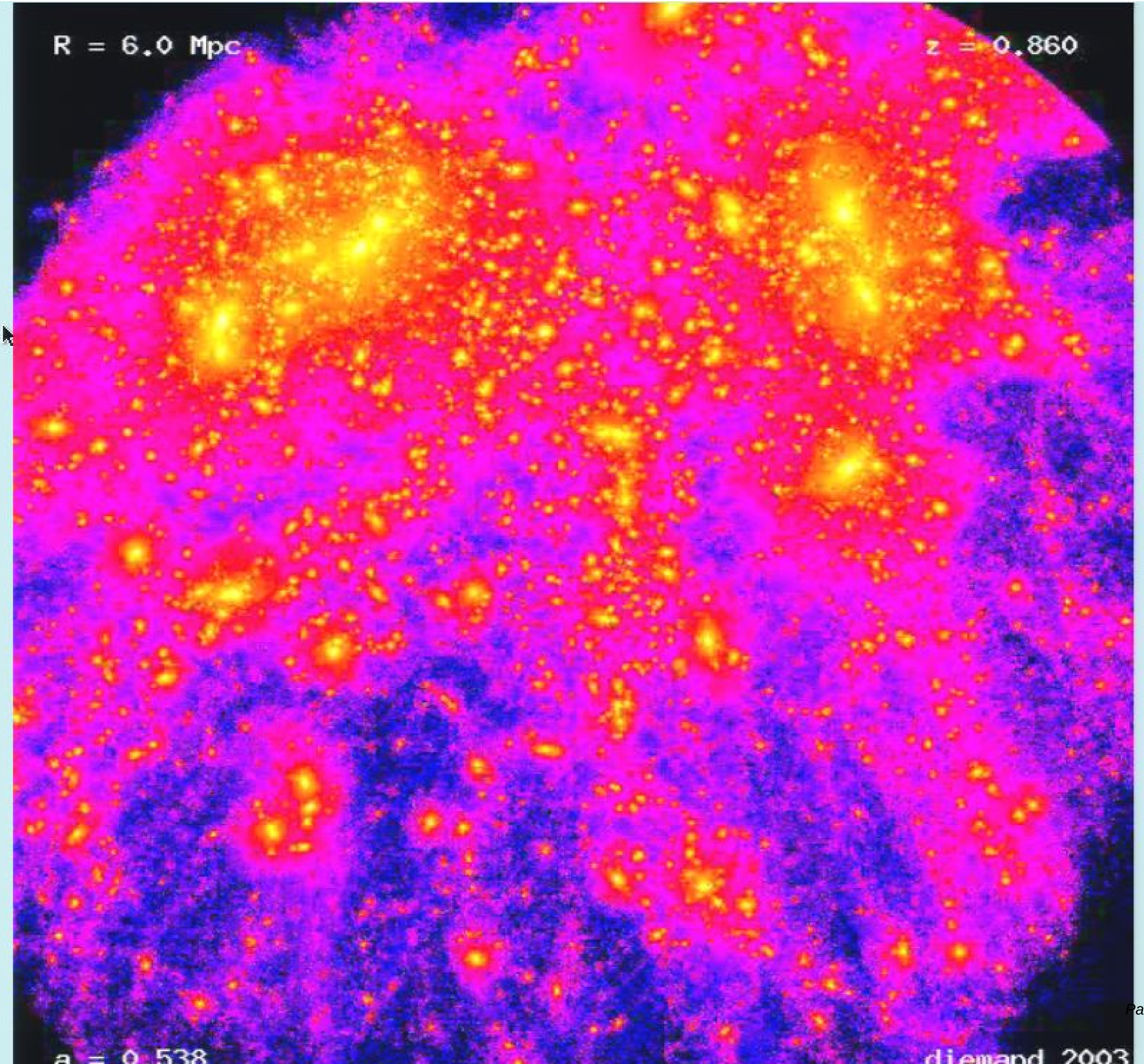
R = 6.0 Mpc
z = 0.860
a = 0.538
diemand 2003

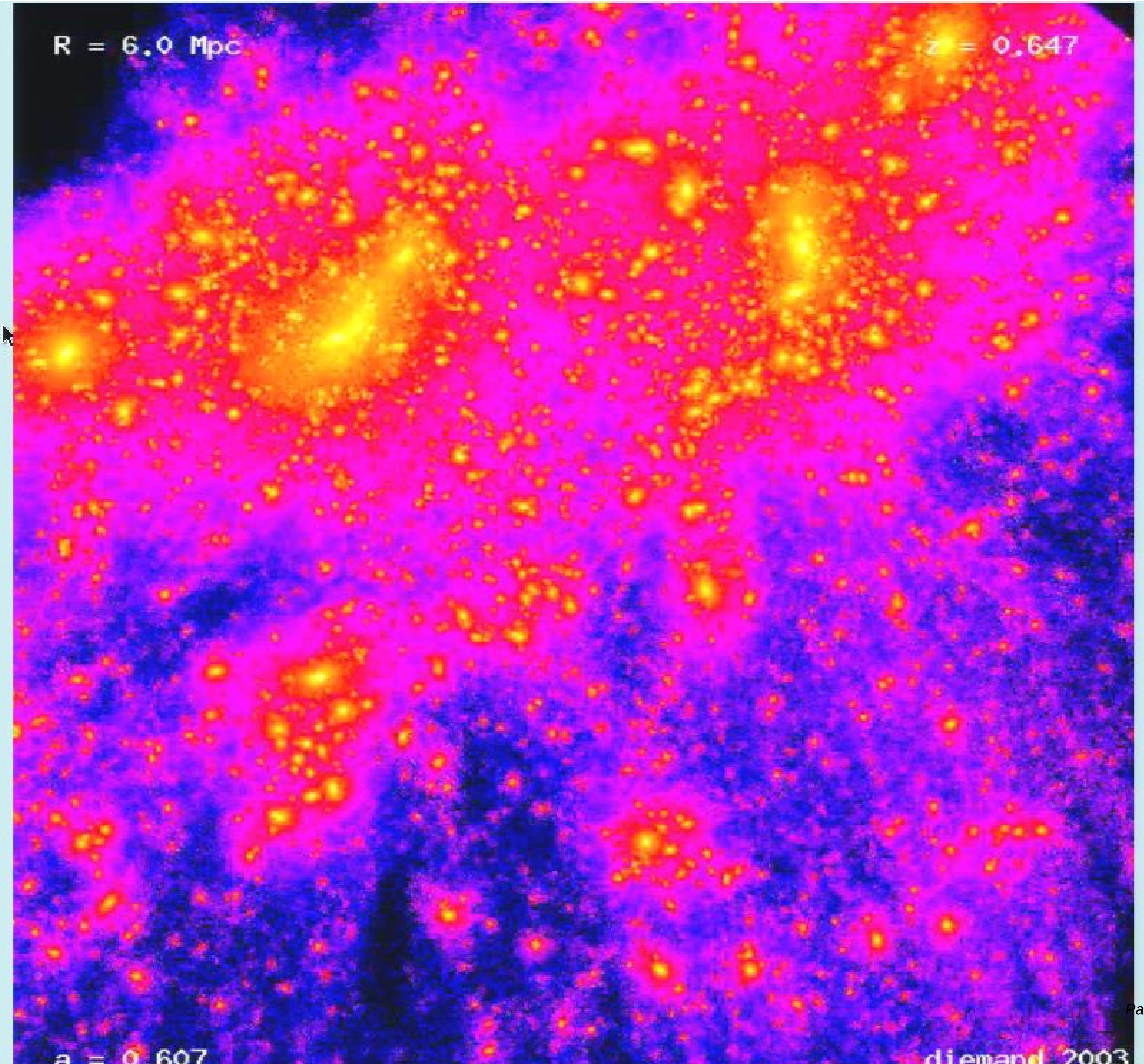
R = 6.0 Mpc
z = 0.647
a = 0.607
diemand 2003

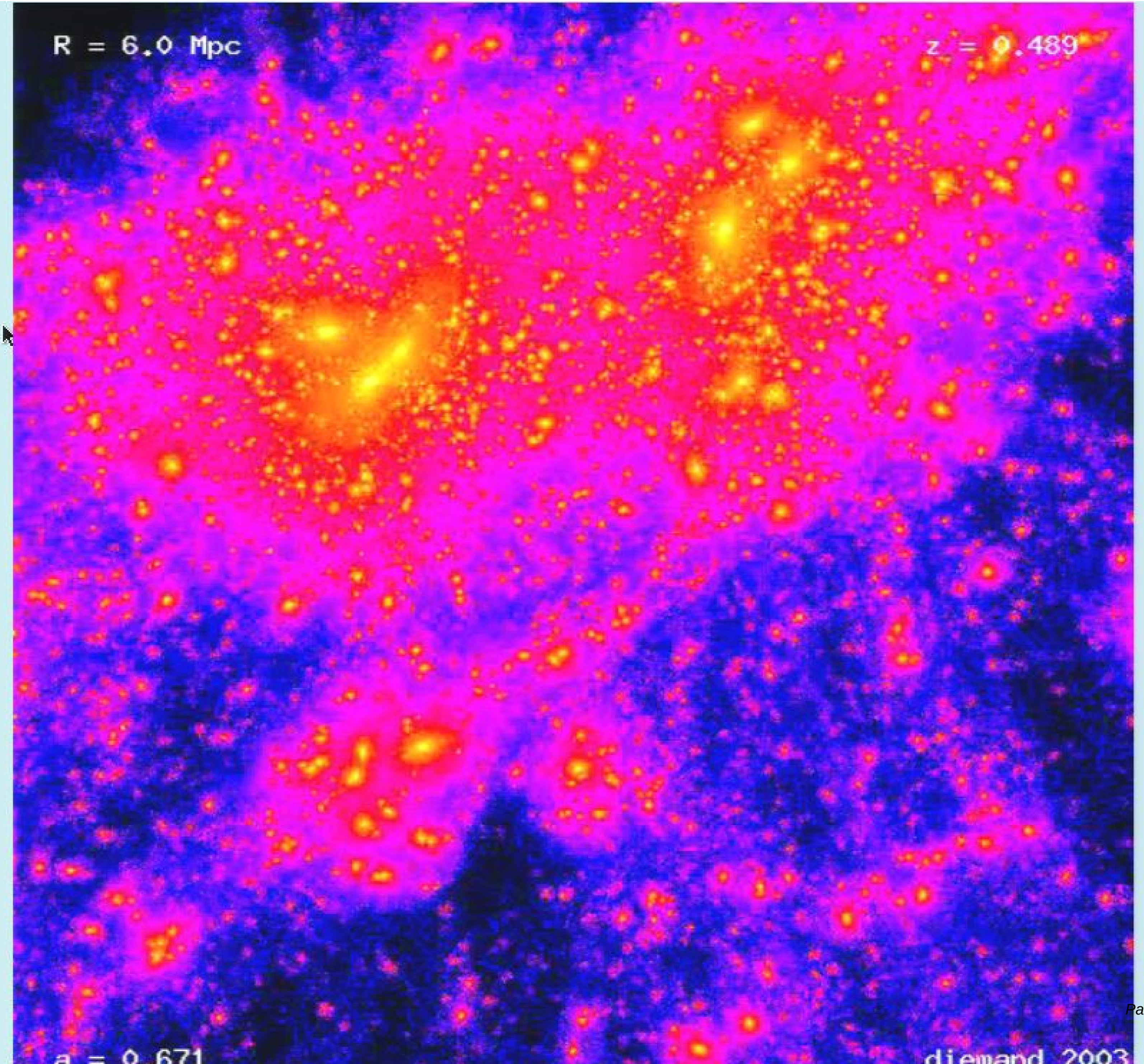
R = 6.0 Mpc
z = 0.489
a = 0.671
diemand 2003

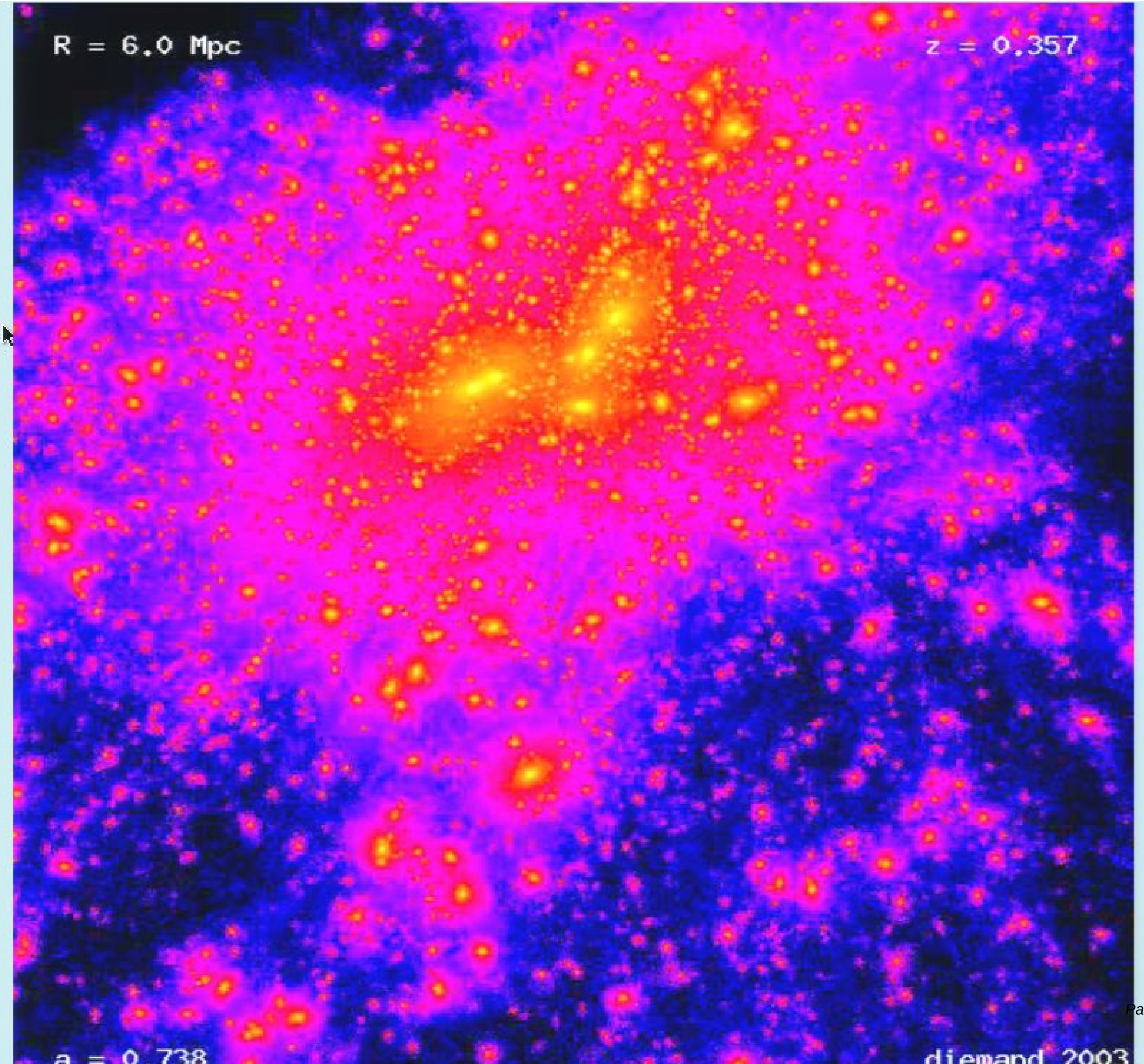
R = 6.0 Mpc
z = 0.357
a = 0.738
diemand 2003

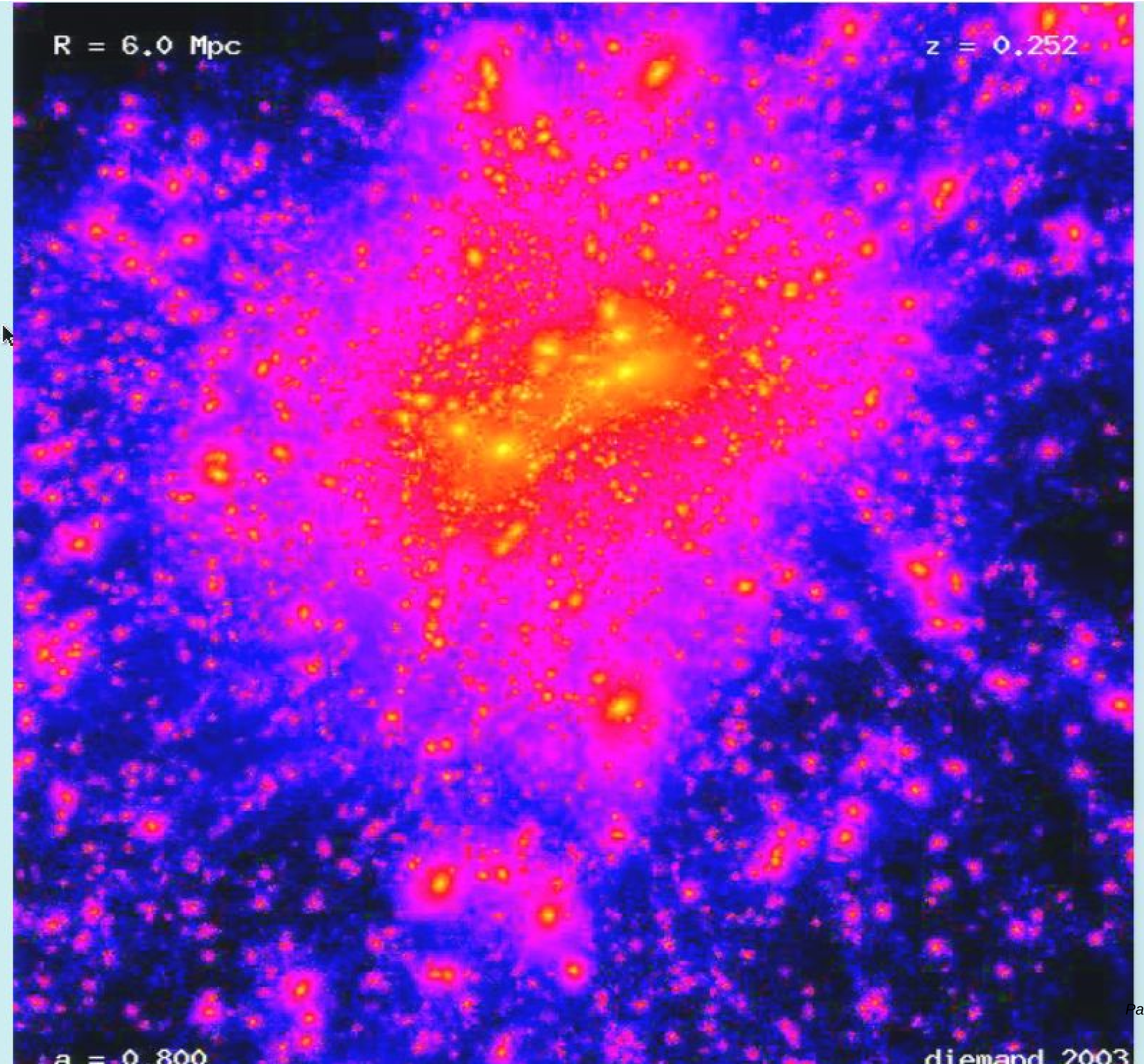
R = 6.0 Mpc
z = 0.252
a = 0.800
diemand 2003

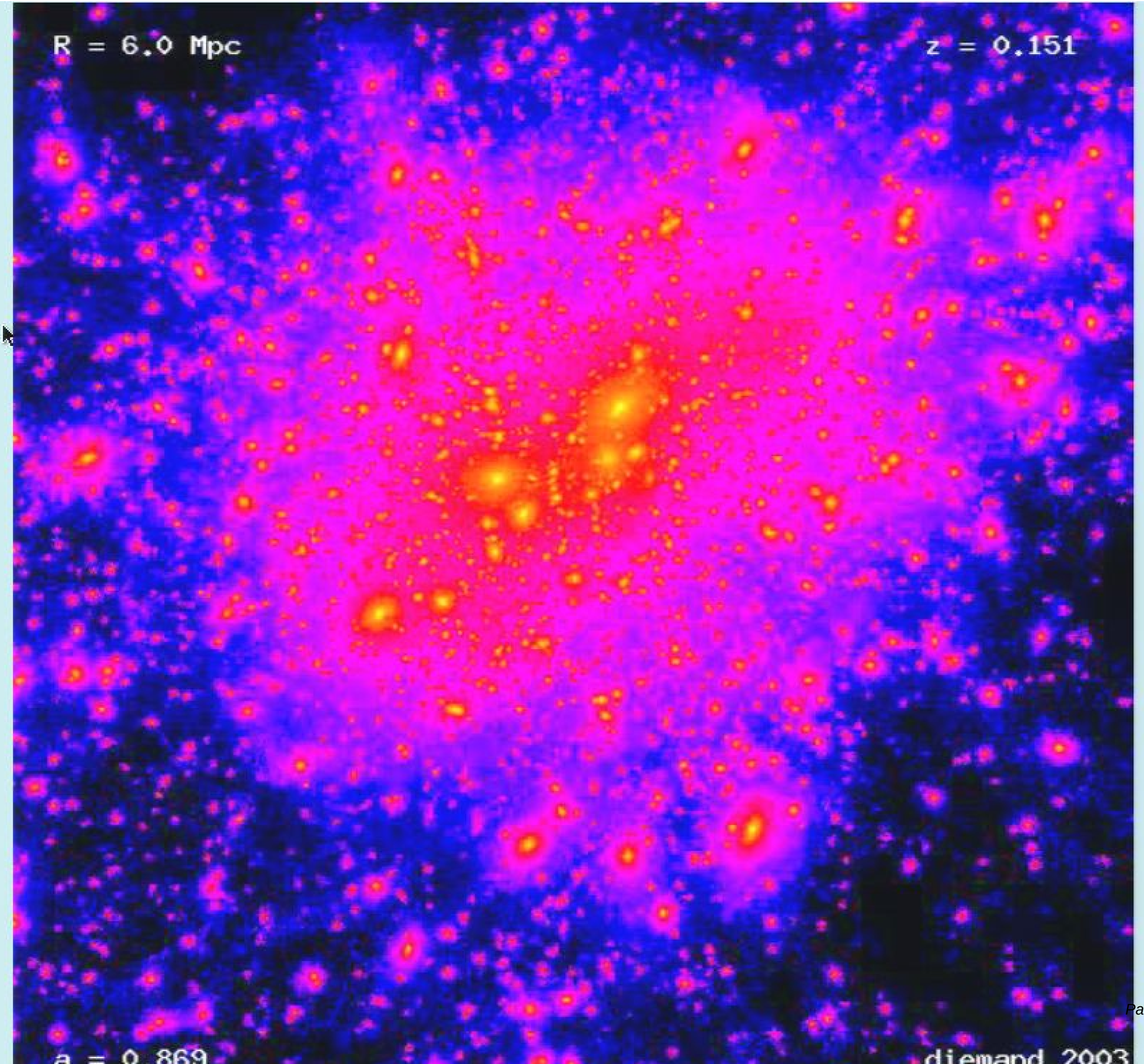
R = 6.0 Mpc
z = 0.151
a = 0.869
diemand 2003

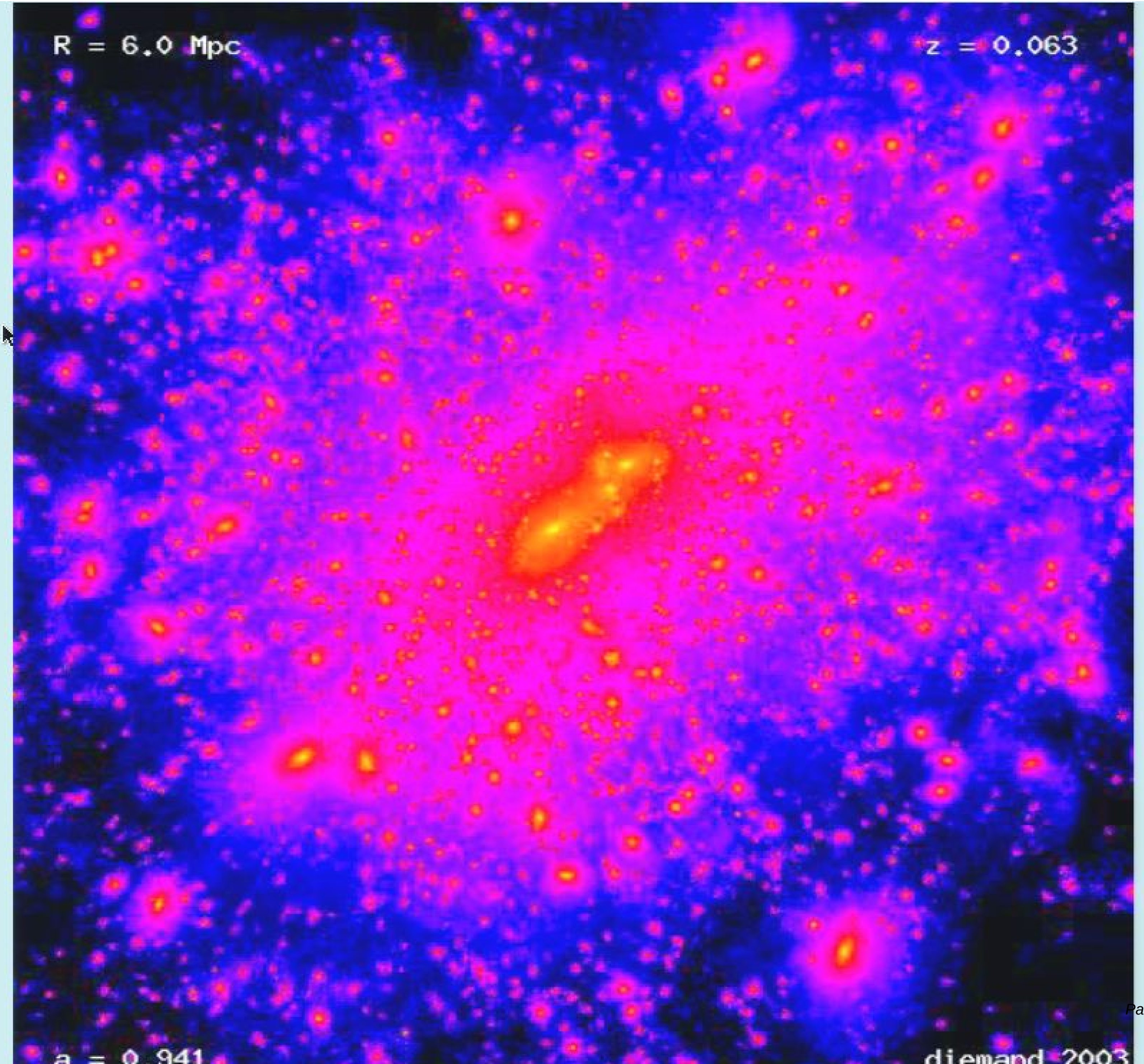
R = 6.0 Mpc
z = 0.063
a = 0.941
diemand 2003

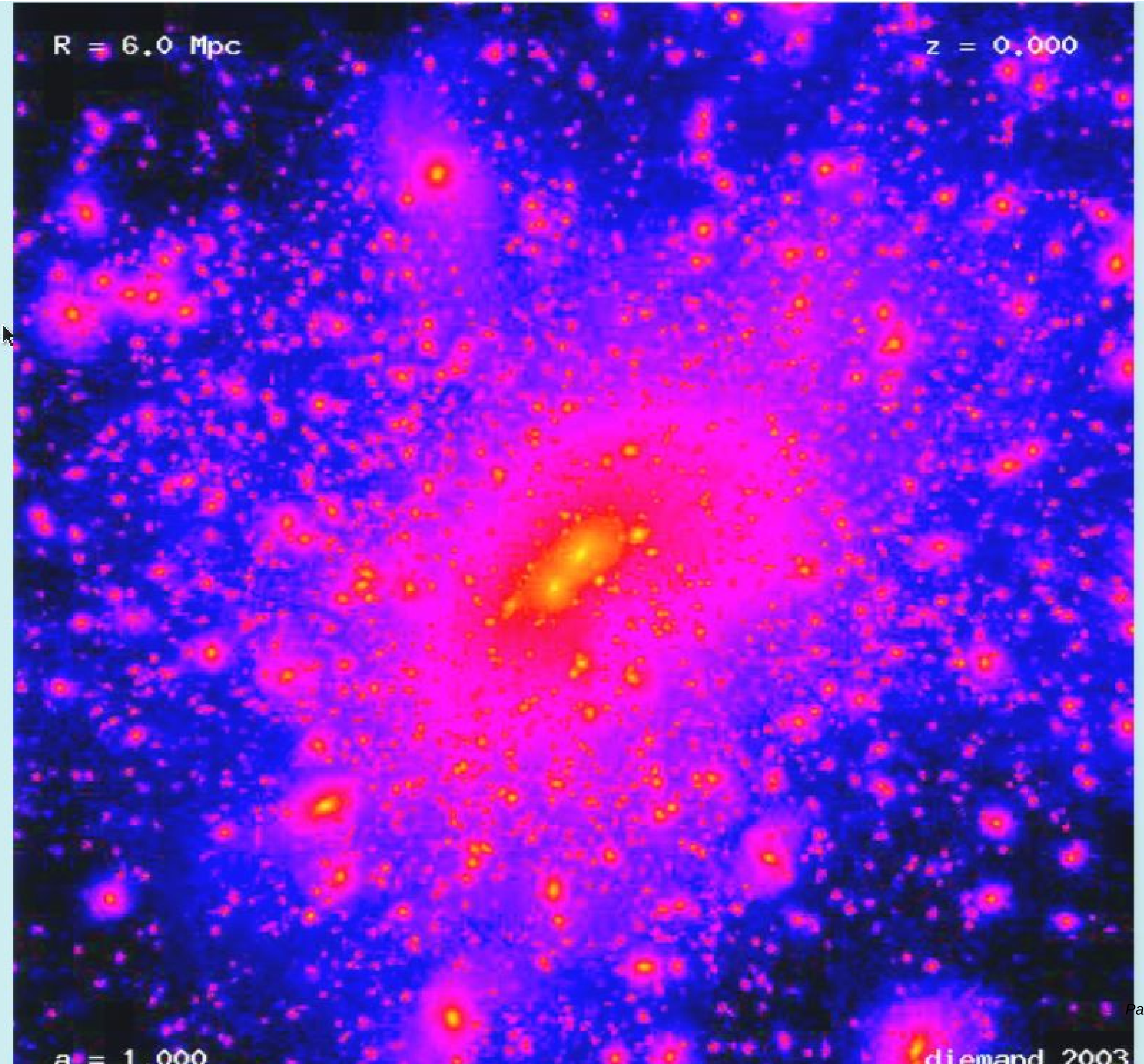
R = 6.0 Mpc
z = 0.000
a = 1.000
diemand 2003

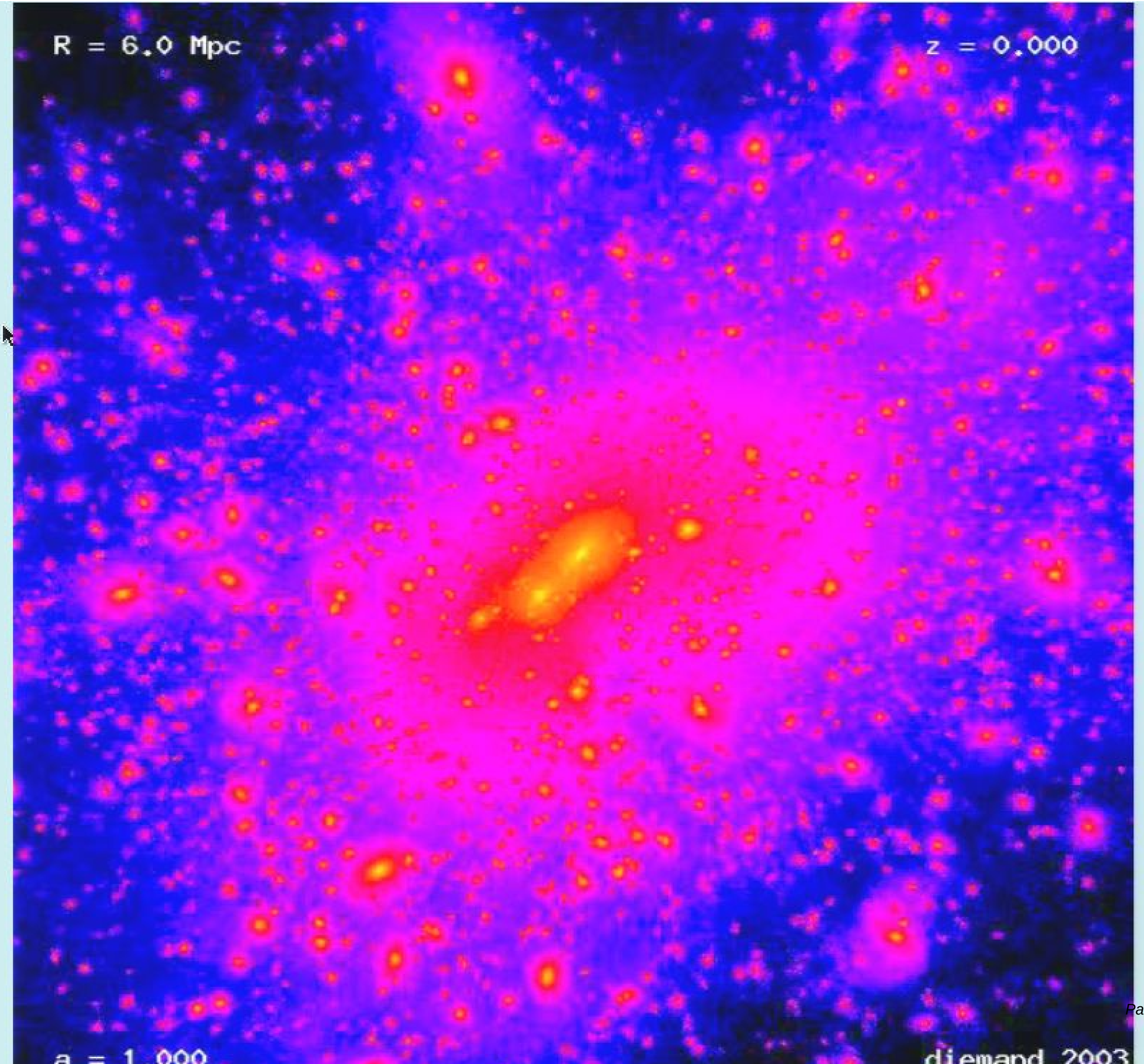
R = 6.0 Mpc
z = 0.000
a = 1.000
diemand 2003

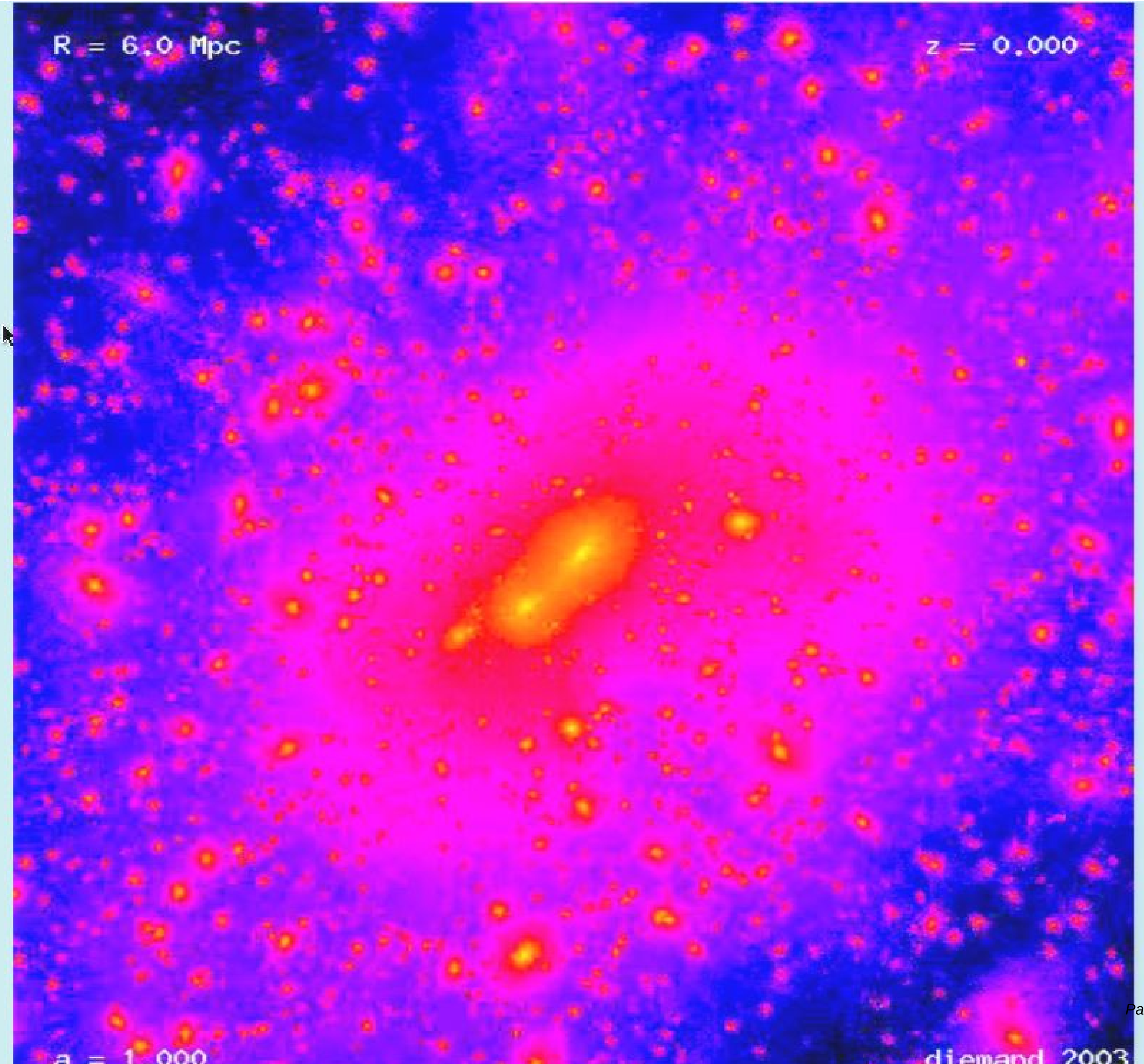
R = 6.0 Mpc
z = 0.000
a = 1.000
diemand 2003

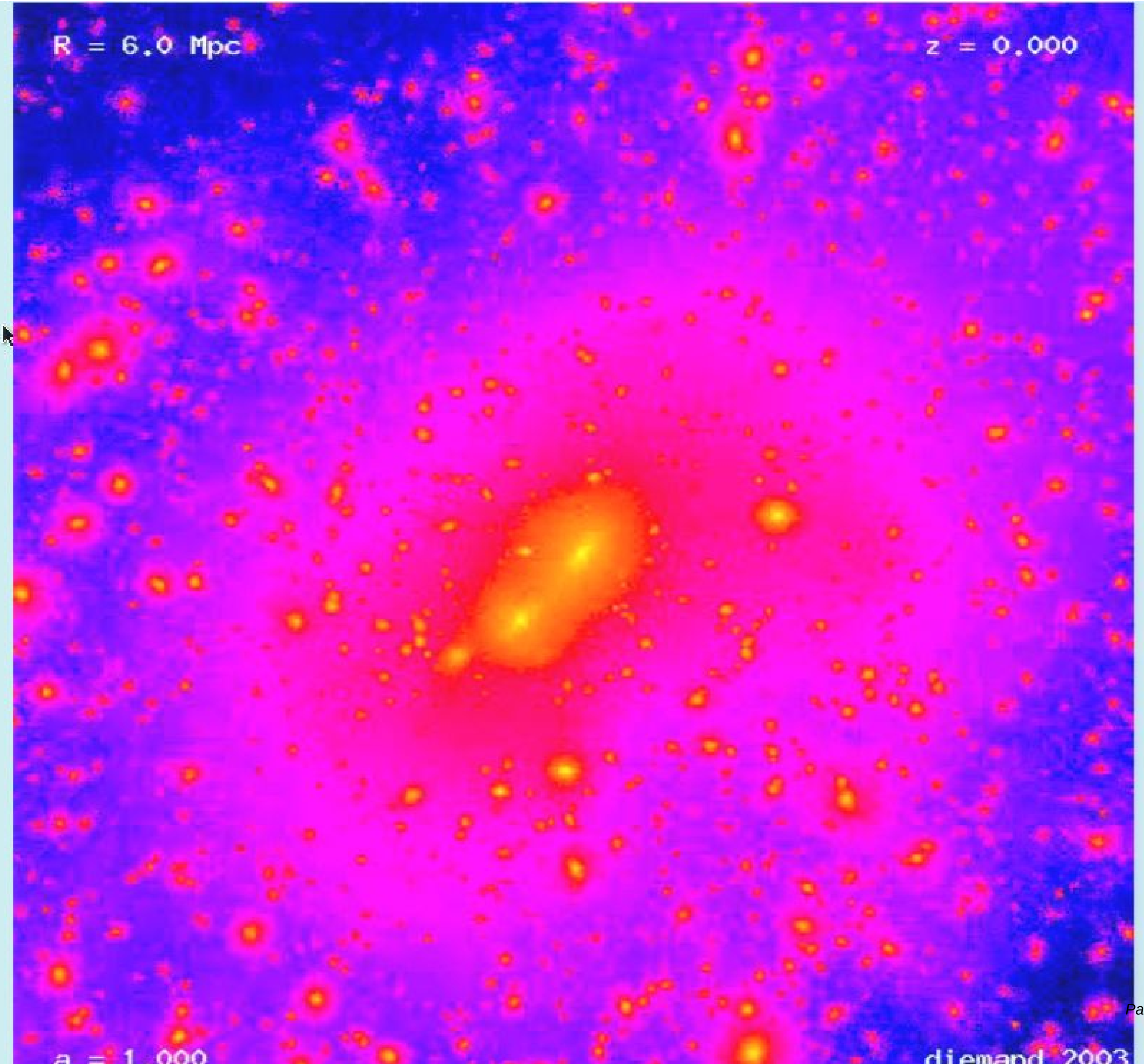
R = 6.0 Mpc
z = 0.000
a = 1.000
diemand 2003

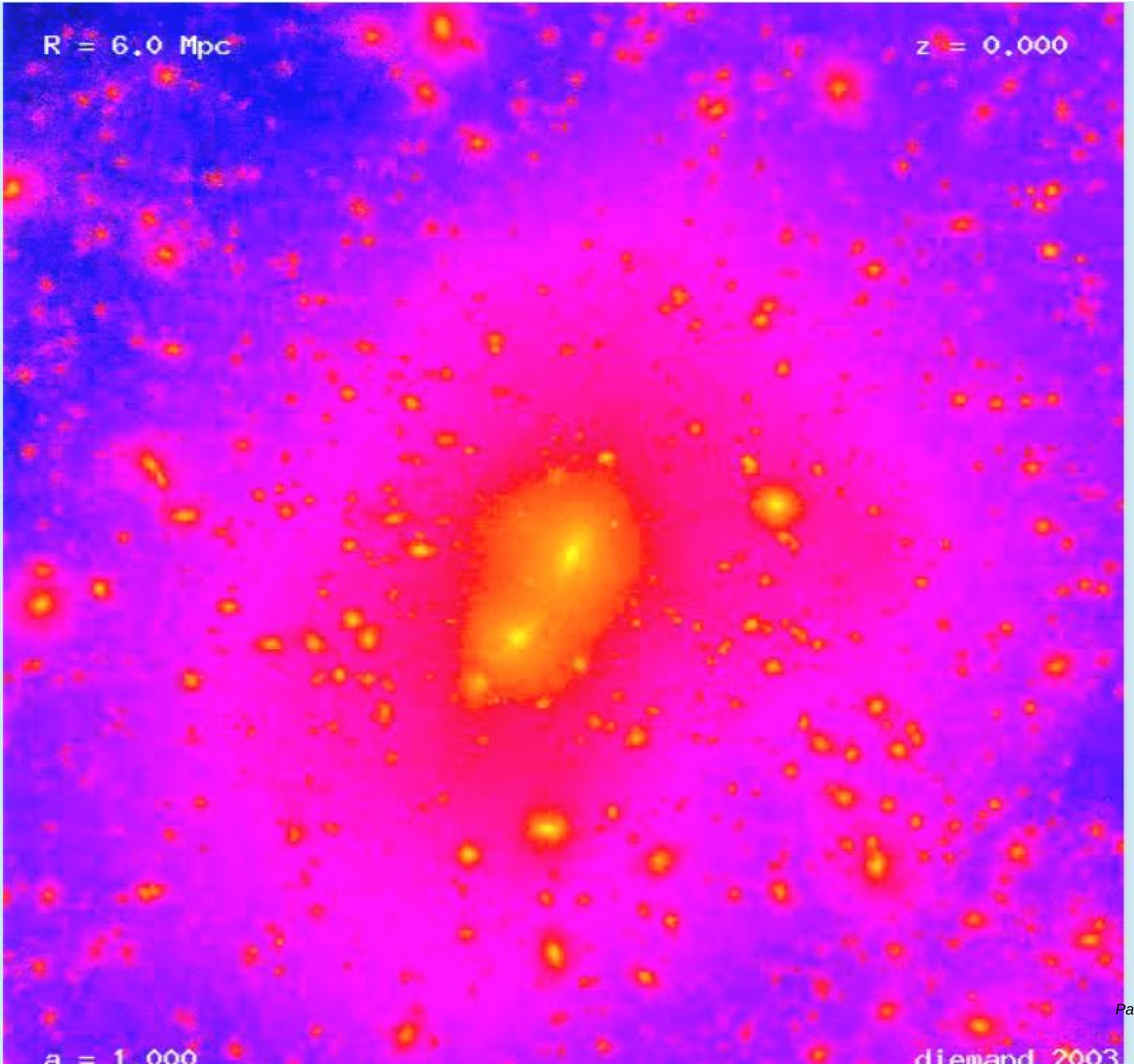
R = 6.0 Mpc
z = 0.000
a = 1.000
diemand 2003

Constraints on subhalo properties

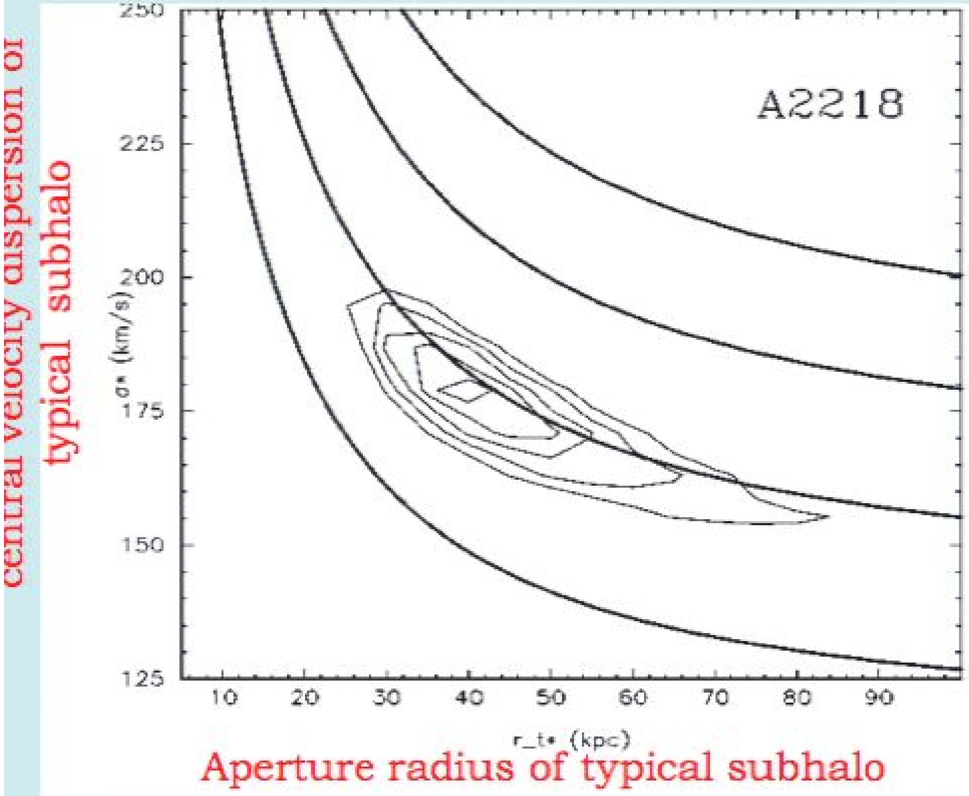

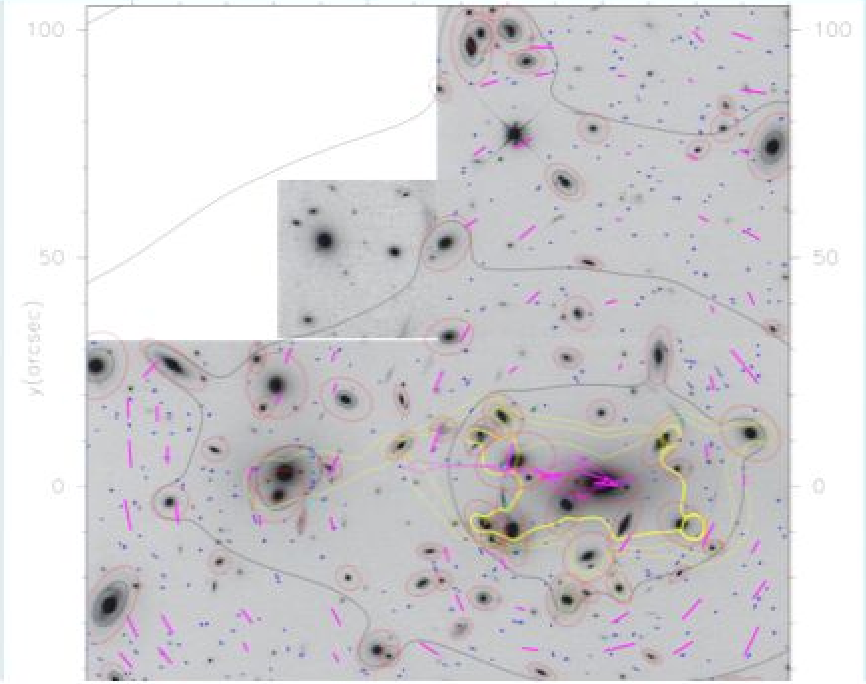

M_ap - mass within aperture

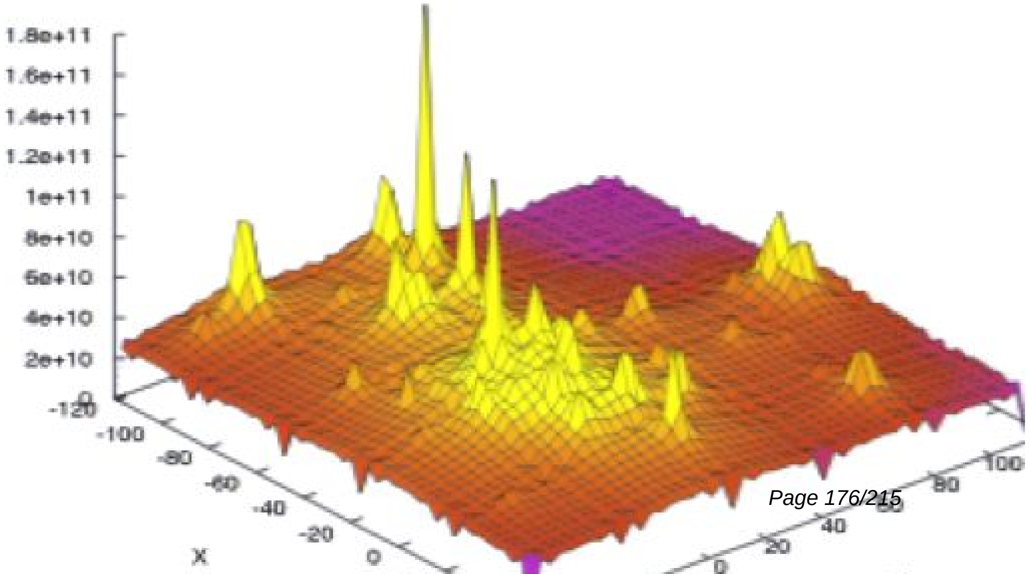

The detailed dark matter distribution in A2218

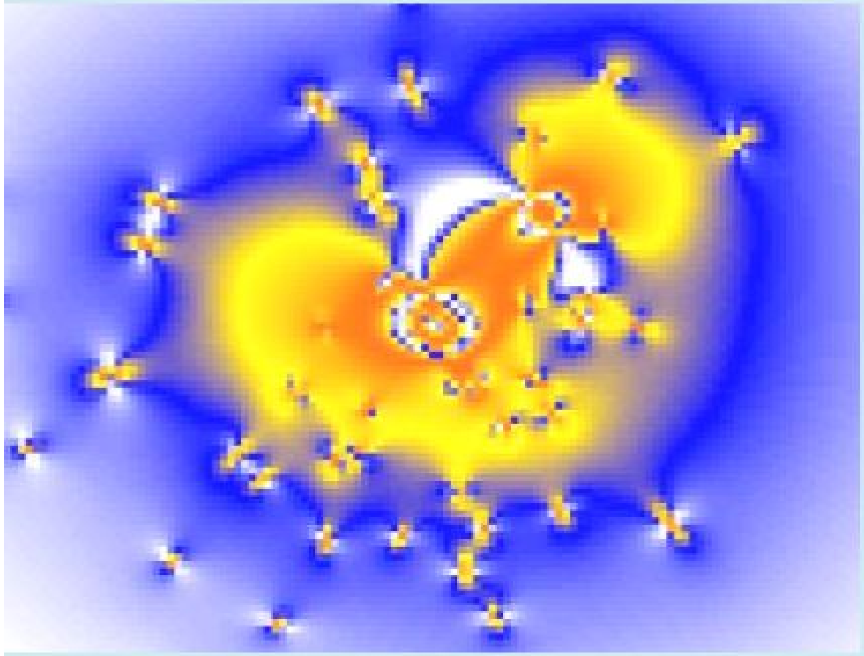

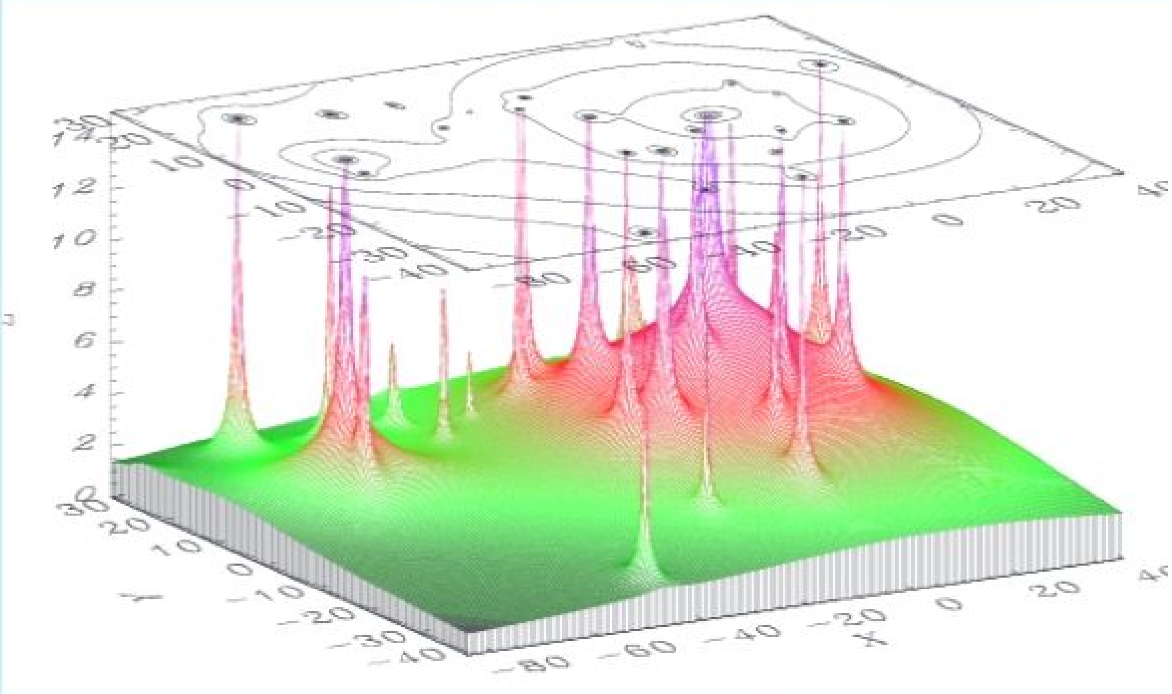

Sub-halo mass functions

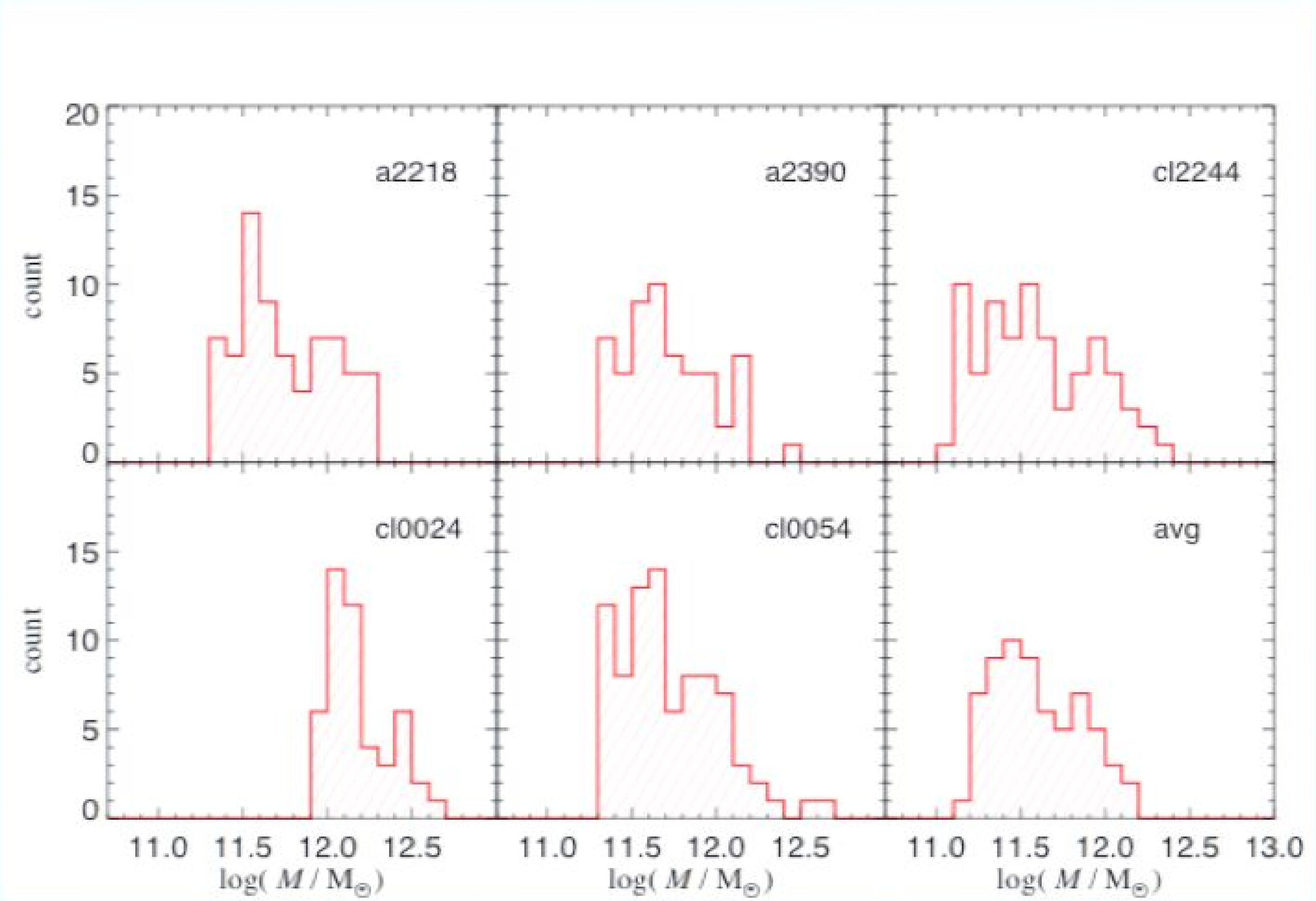

PN, Kneib, Smail & Ellis 06

Comparison with LCDM clusters in the Millenium Run

The subhalo mass function

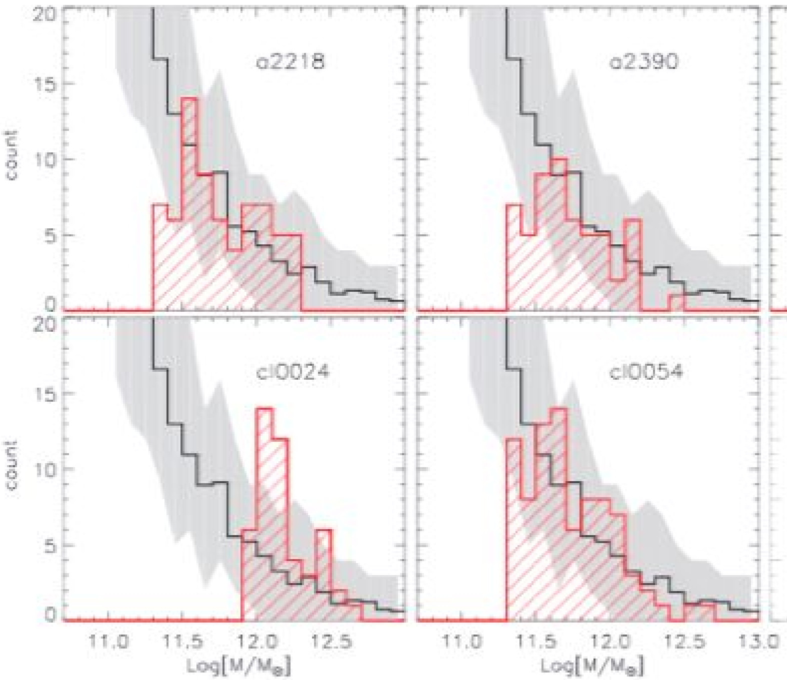

Springel+ 05
PN, De Lucia & Springel 07

Cl0024+16 extending analysis to 5 Mpc

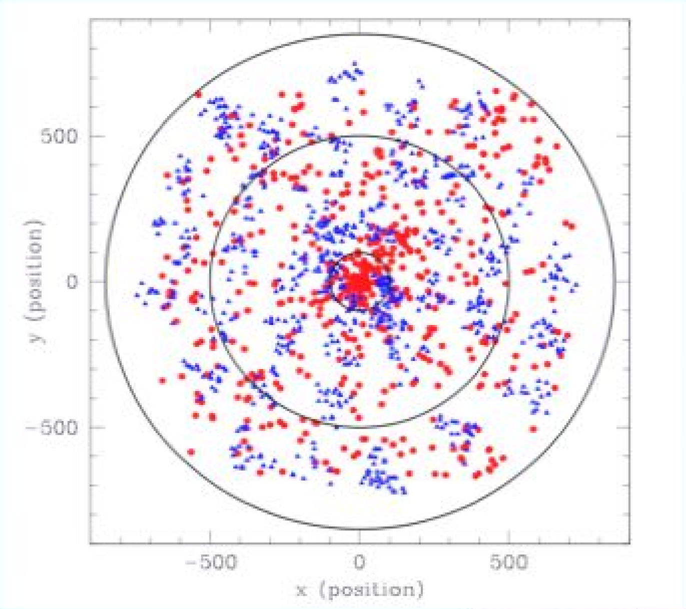

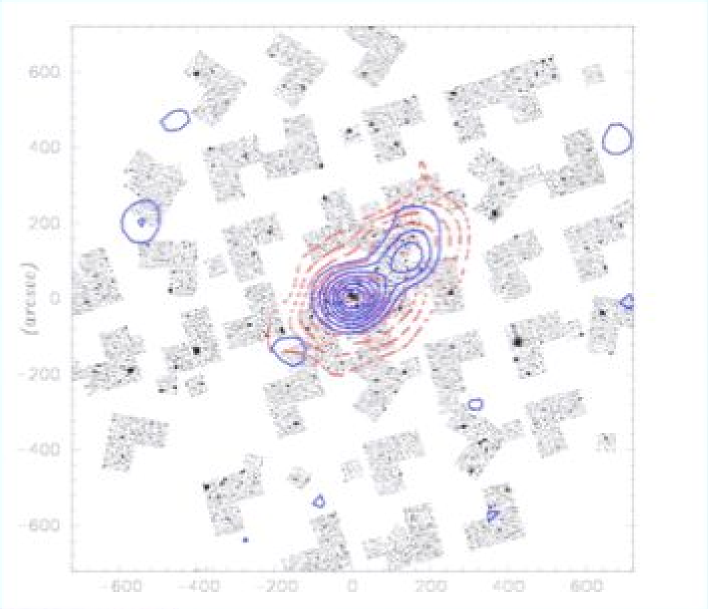

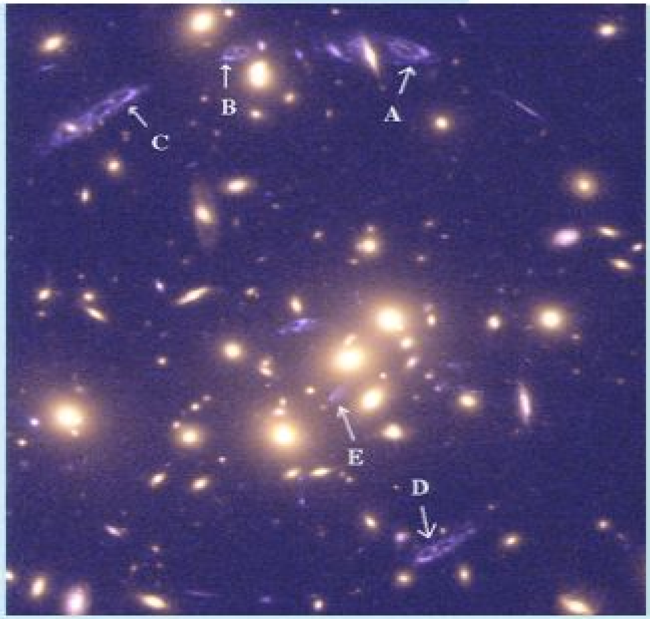

PN+ 08

Comparison with LCDM clusters in the Millenium Run

The subhalo mass function

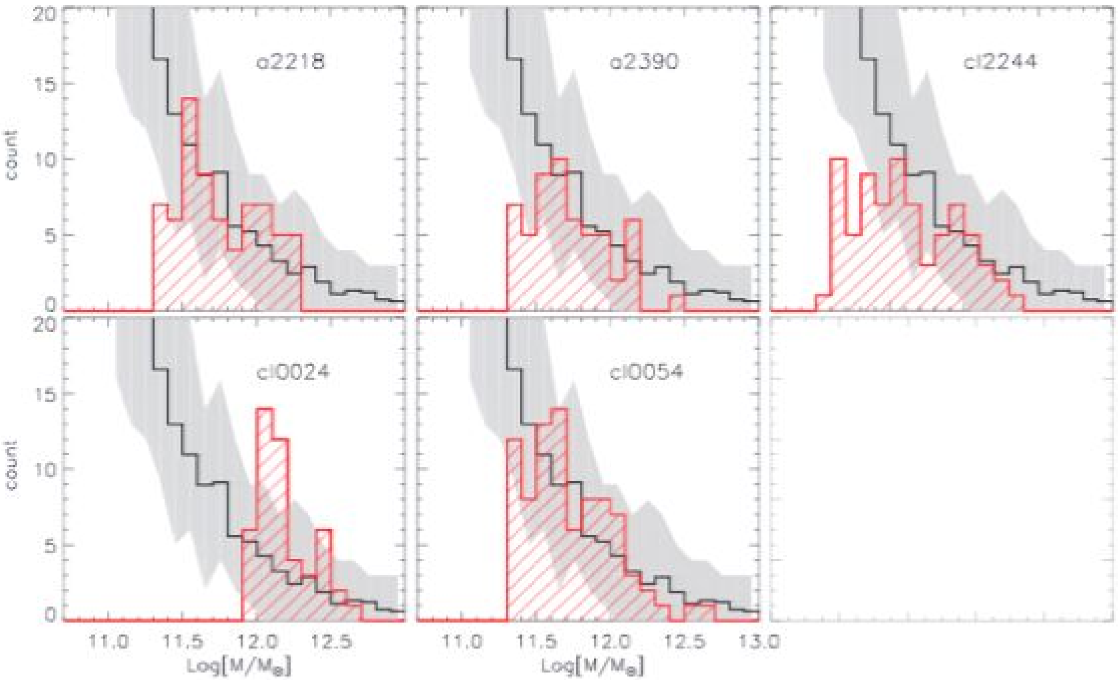

Springel+ 05

PN, De Lucia & Springel 07

Cl0024+16 extending analysis to 5 Mpc

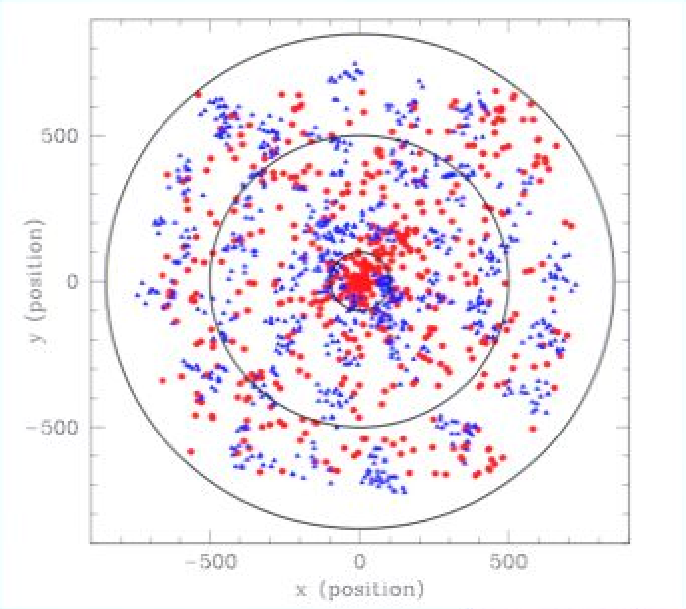

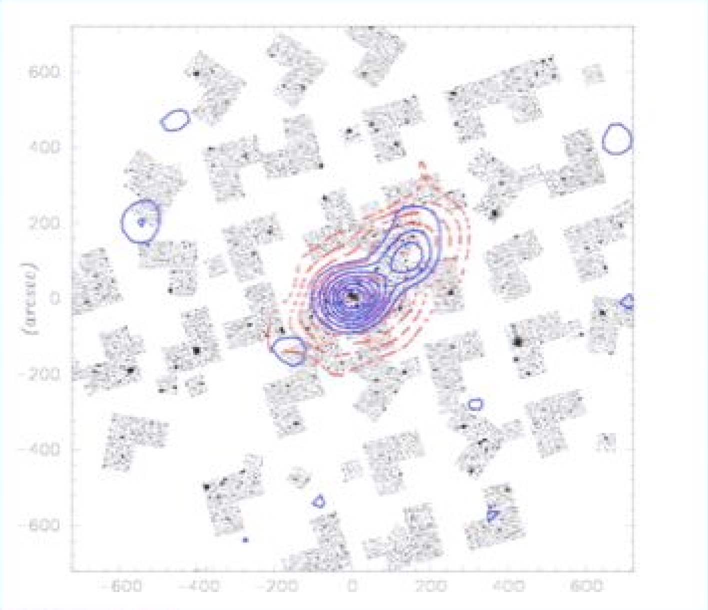

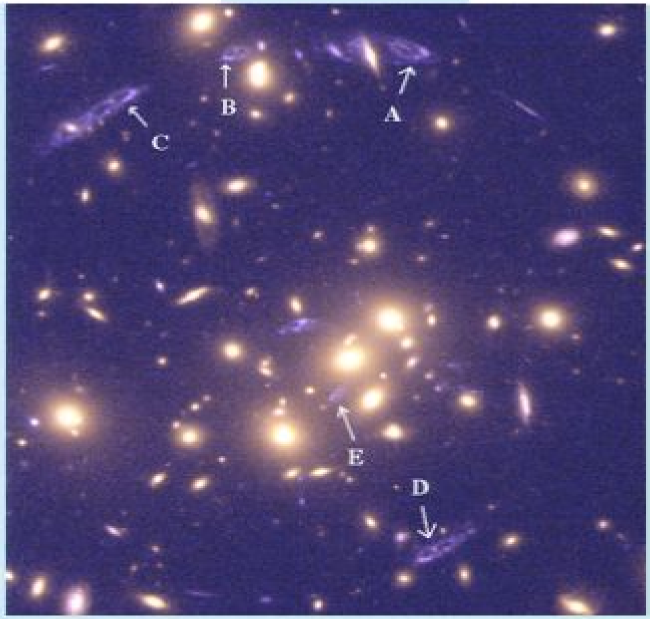

PN+ 08

Cl0024+1654 HST wide field sparse mosaic

- 76 orbits, 38 pointings
- Probe regions out to ~5Mpc

Aim: understand physics of clusters by comparing with other mass estimates: X-ray, dynamics, caustics in redshift space

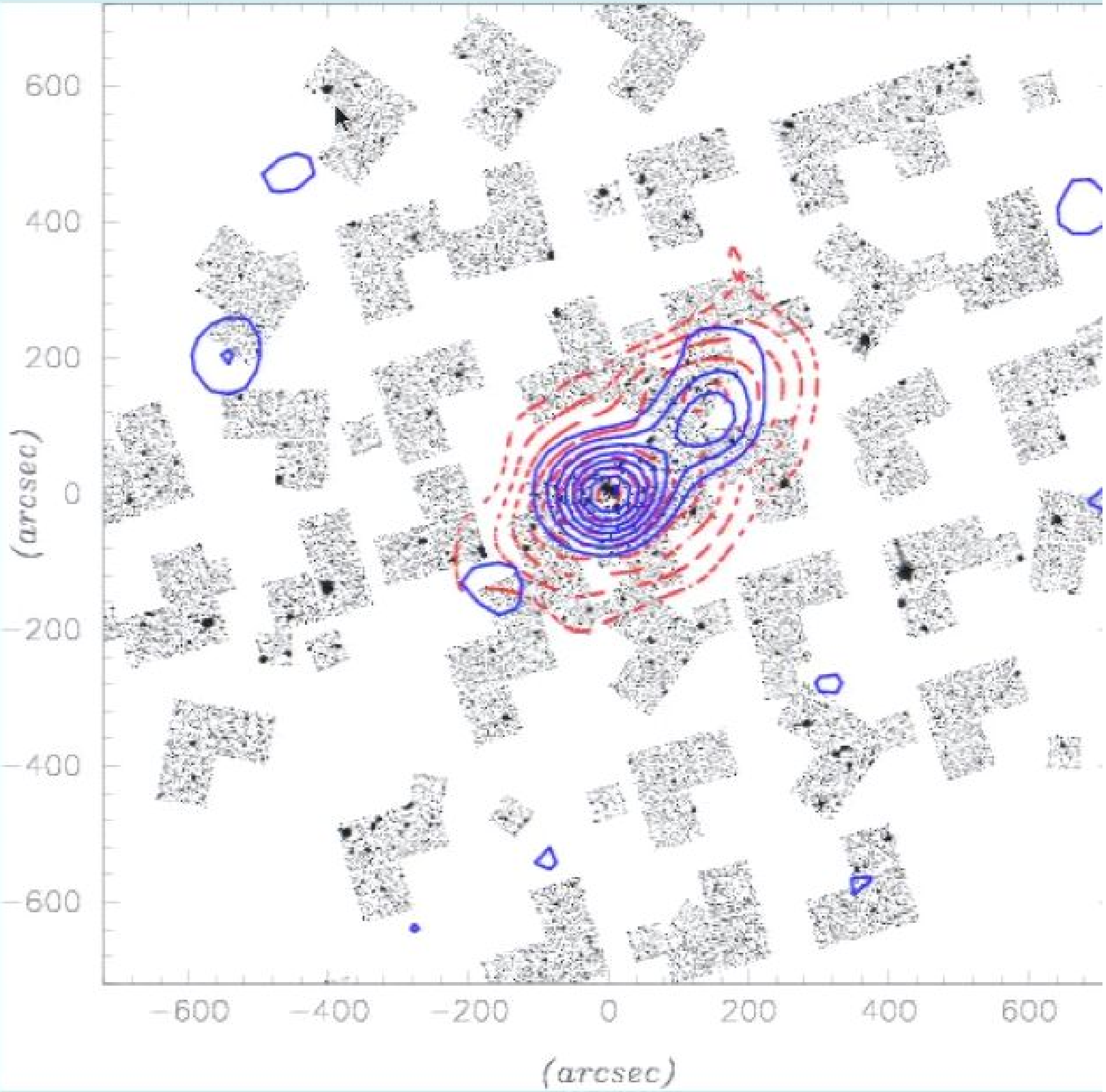

Treu+ 03, Kneib+ 03, Diaferio, Geller & Rines 05; RN+ 08

Cl0024+1654 HST wide field sparse mosaic

- 76 orbits, 38 pointings
- Probe regions out to ~5Mpc

Aim: understand physics of clusters by comparing with other mass estimates: X-ray, dynamics, caustics in redshift space

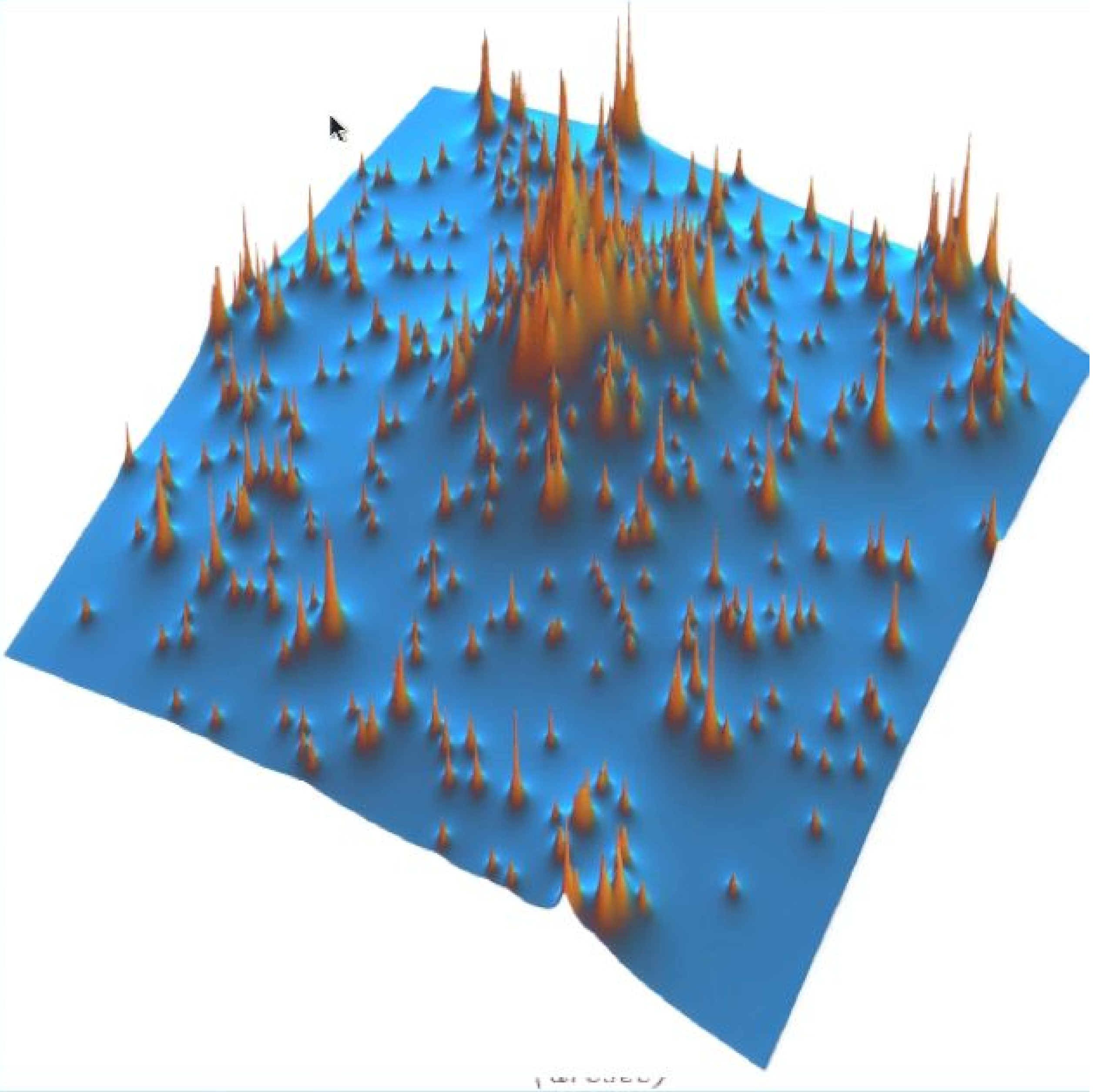

Treu+03, Kneib+03, Diaferio, Geller & Rines 05; RN+08

Mass of DM subhalo hosting L* galaxy

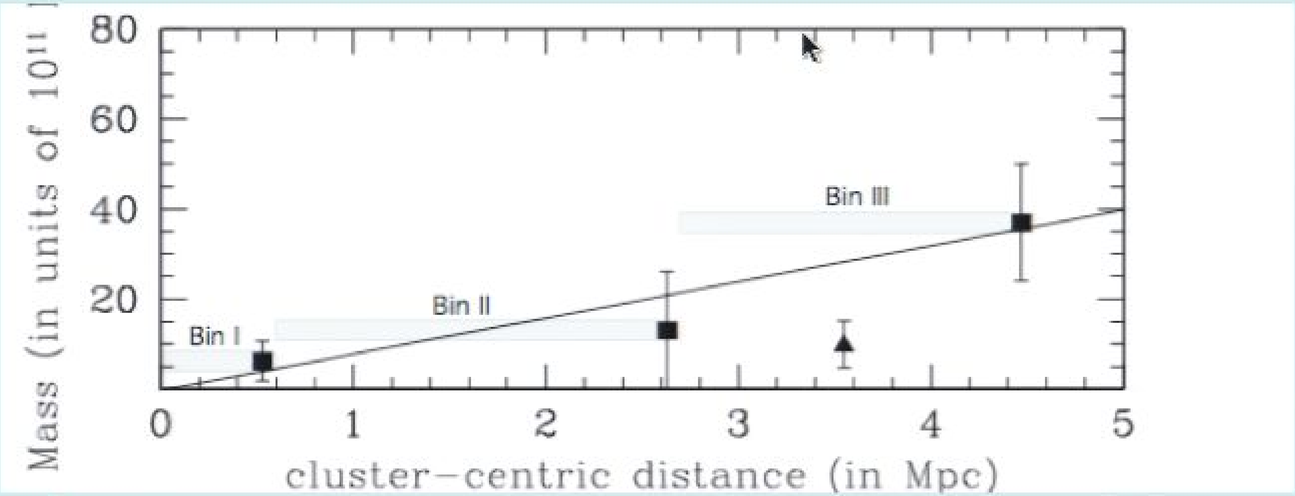

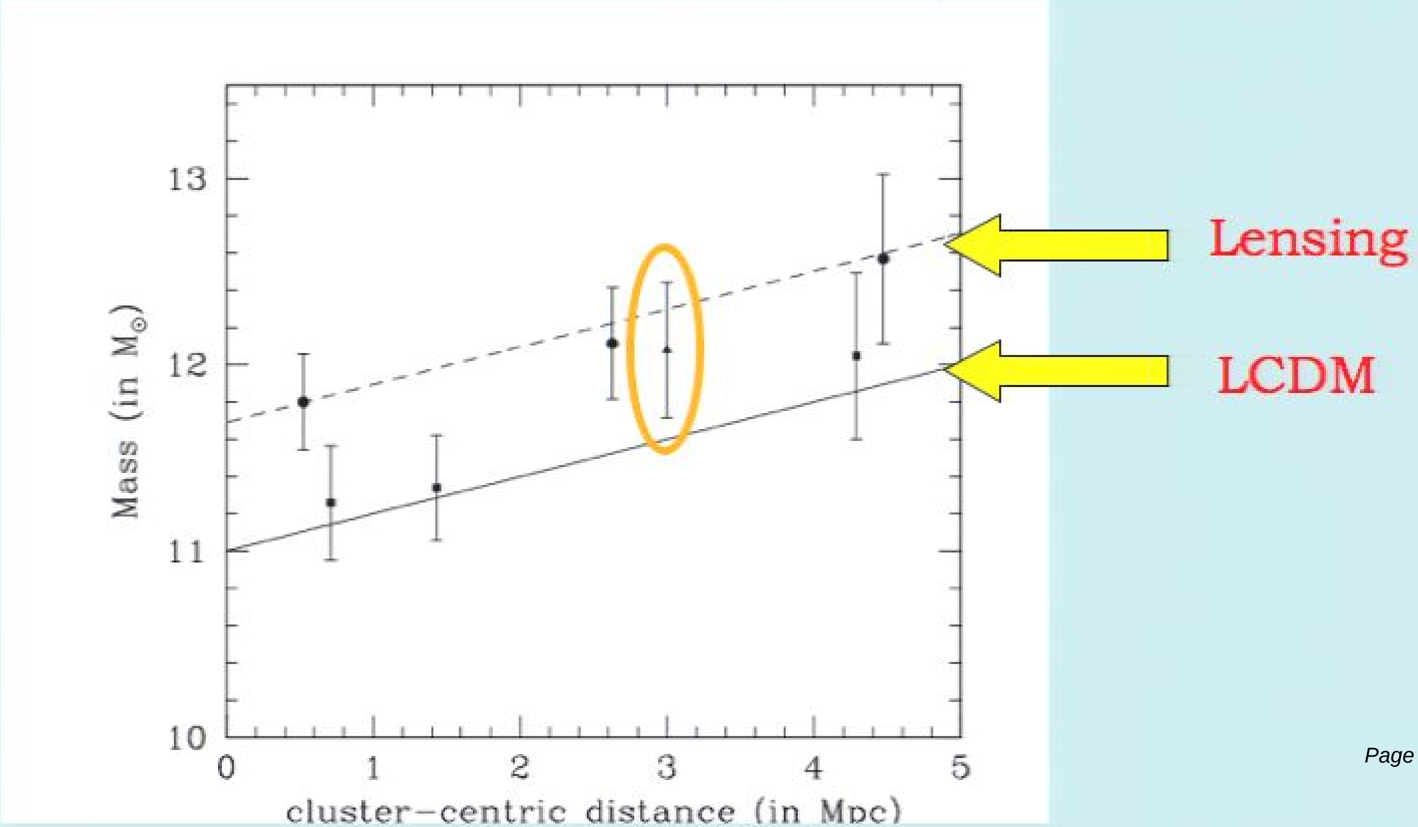

Lensing

LCDM

Subhalo mass functions as a function of radius

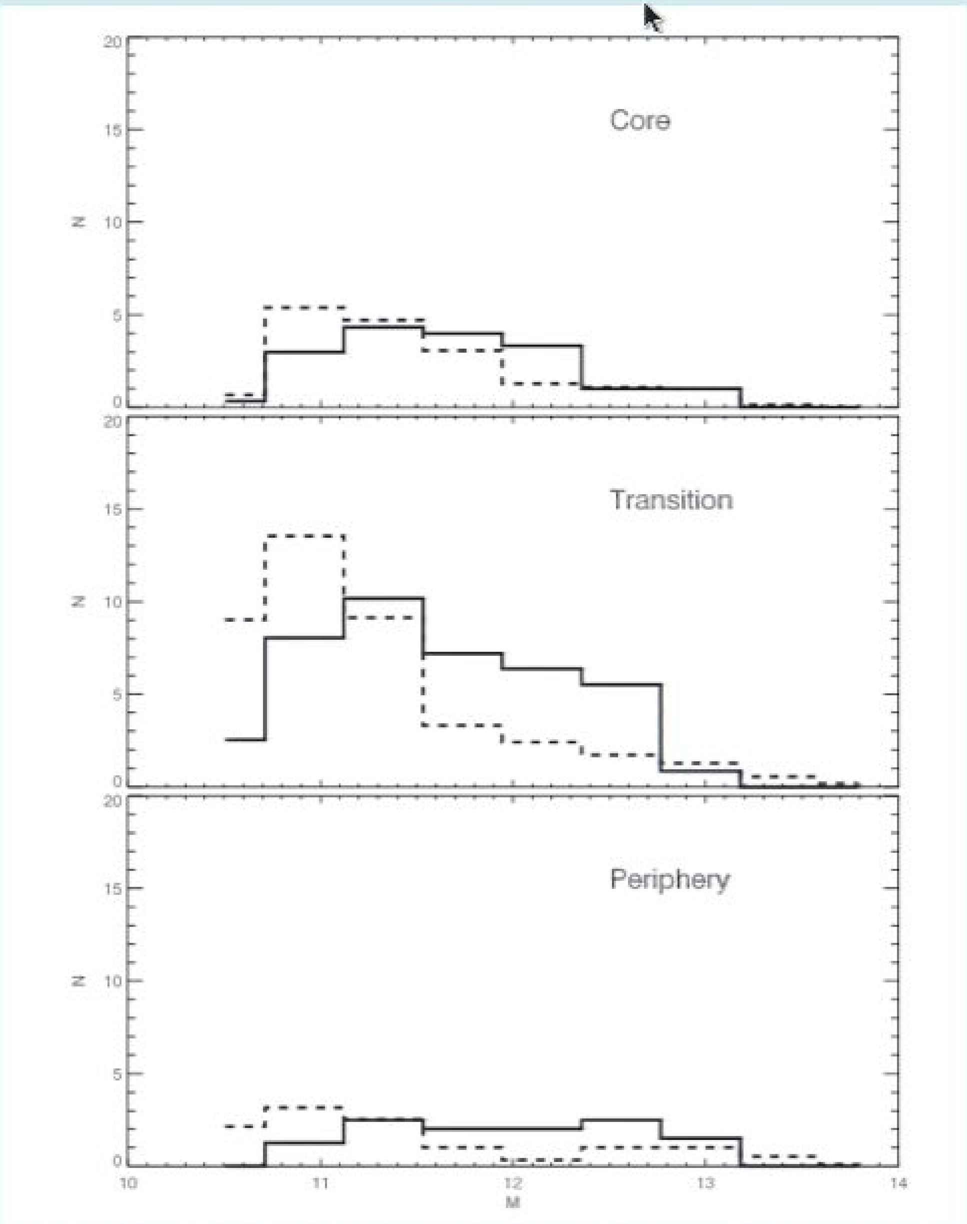

association of subhalos with bright galaxies in

Combined strong and weak lensing

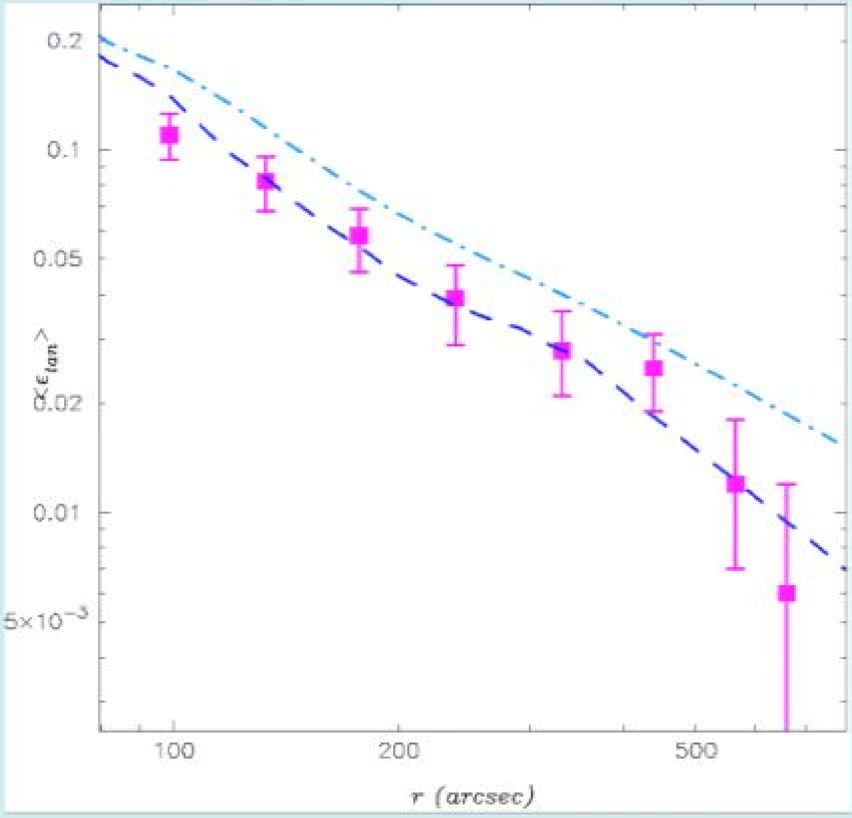

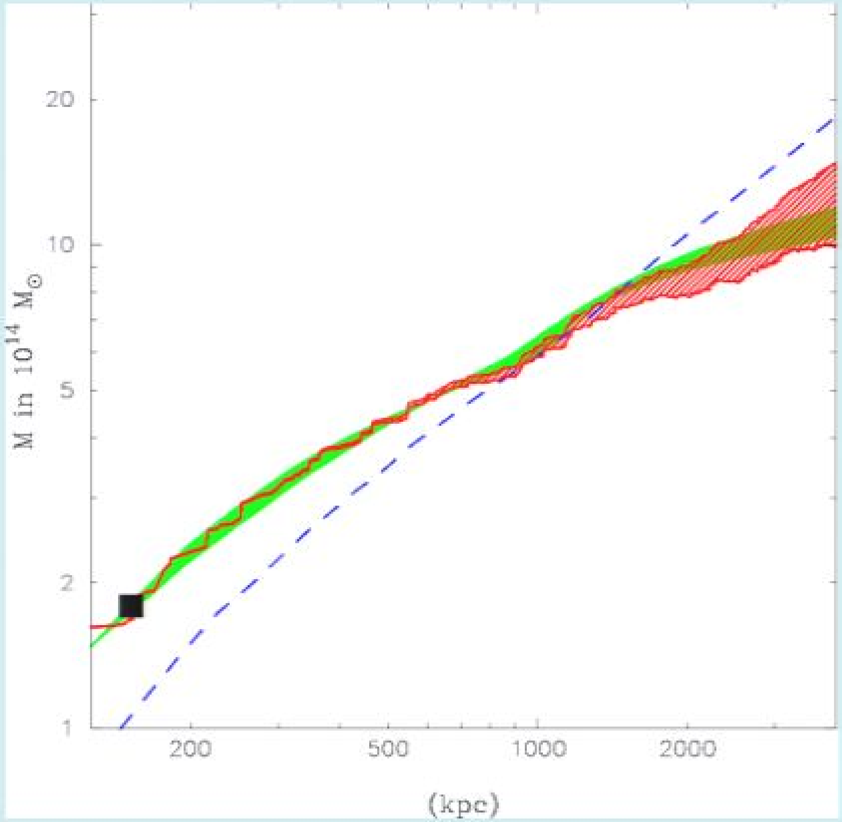

Constraints on density profiles

- Best-fit provided by NFW profile (steeper than r^{-2} at large r)
- No evidence for cores

Kneib, PN+ 03, Smith+ 05, Richard+ 05

Fitting density profiles to measured shear profiles

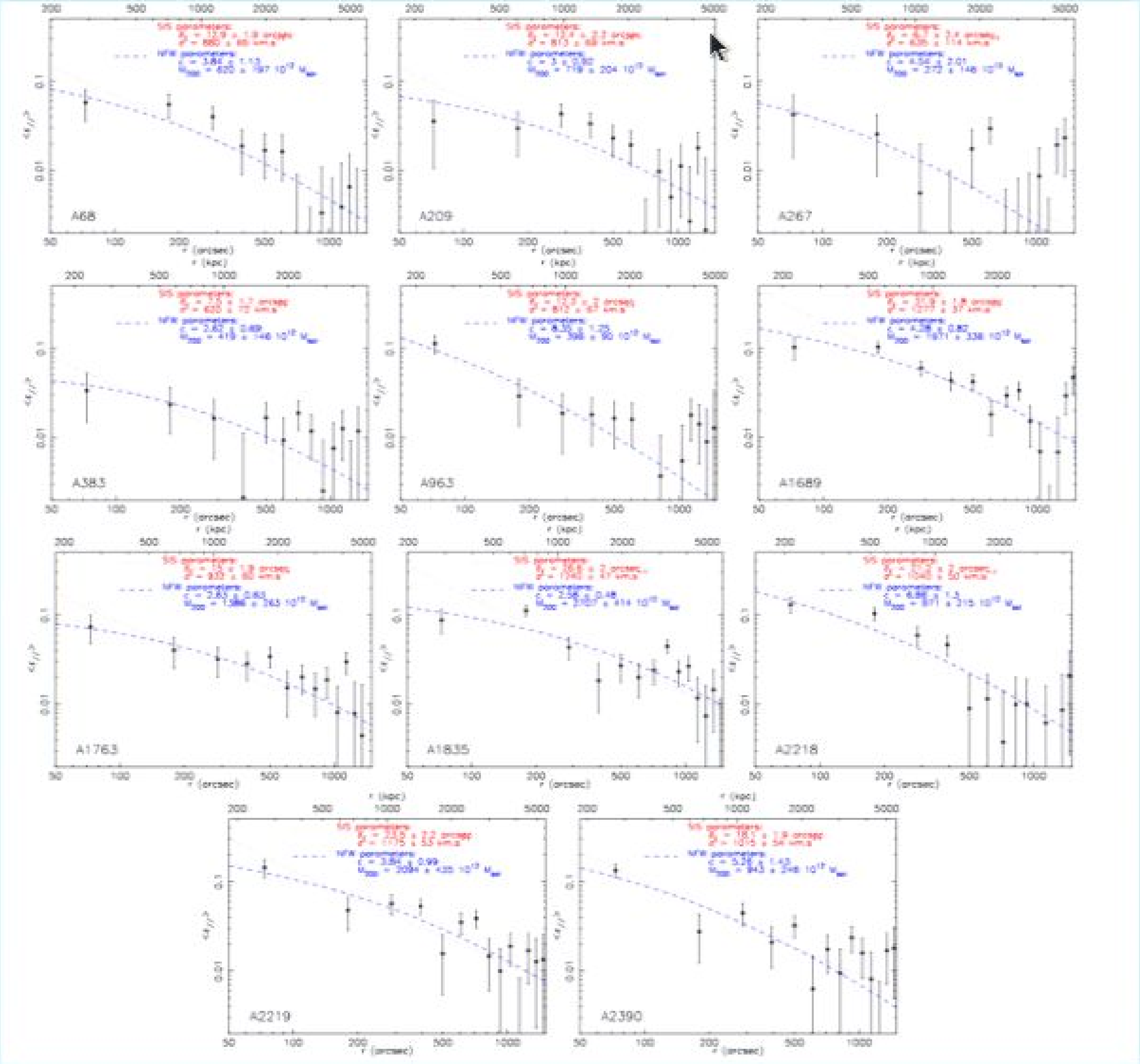

By and large best-fit provided by NFW profile (steeper than r^{-2}) at large r

Bardeau+ 07

Inner slope of the density profile

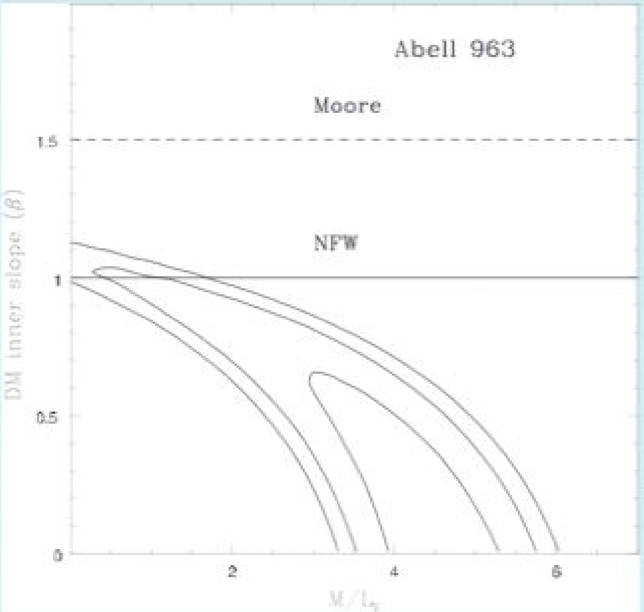

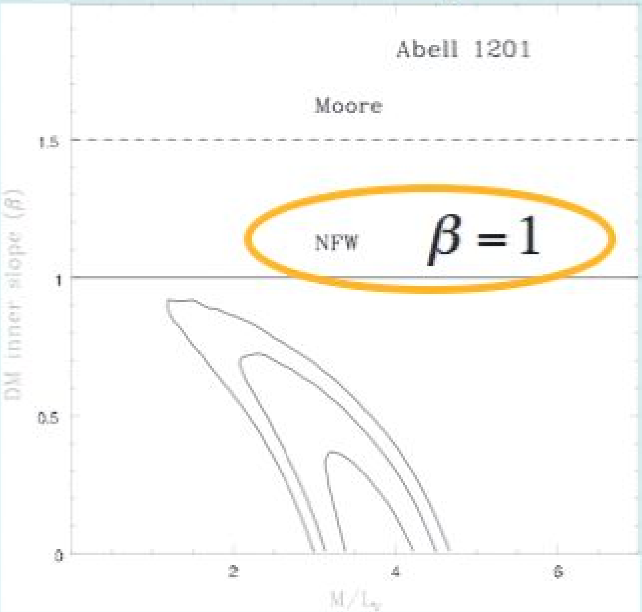

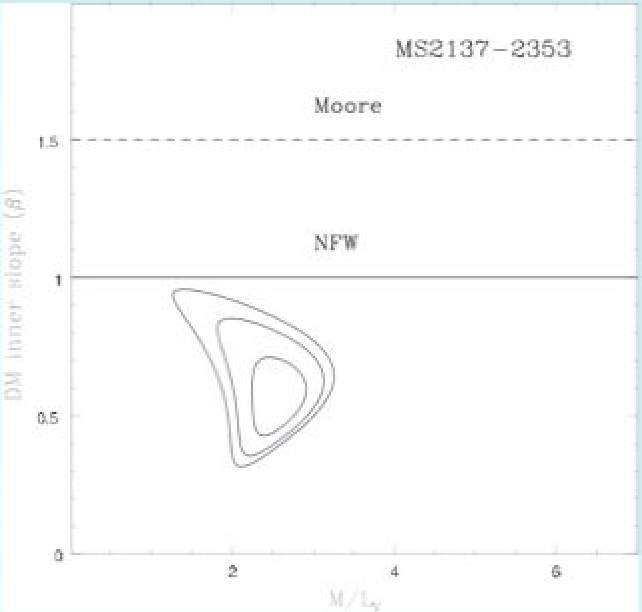

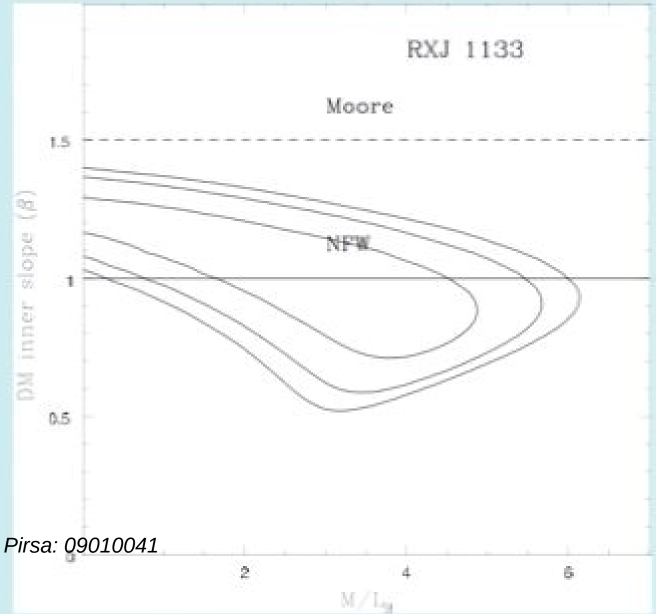

Clusters with radial and tangential arcs combining lensing with BCG vel. disp.

$$\boxed{\rho_{DM} \propto r^{-\beta}}$$

Radial Arcs: $\langle\beta\rangle = 0.52^{+0.05}_{-0.05}$

Tangential Arcs: $\beta < 0.57$

Sand+ 04; Limousin+ 07

Global correlations M_{lens}- L_X,T

- For ongoing surveys these scaling relations need to be calibrated with hydrodynamic simulations
- Sample of lensing clusters at z ~0.2
- At present M_{200}/r_{200} ~ vel disp (model); L_X ~ $M_{200}^{0.83}$

Smith+ 06; Bardeau+ 08

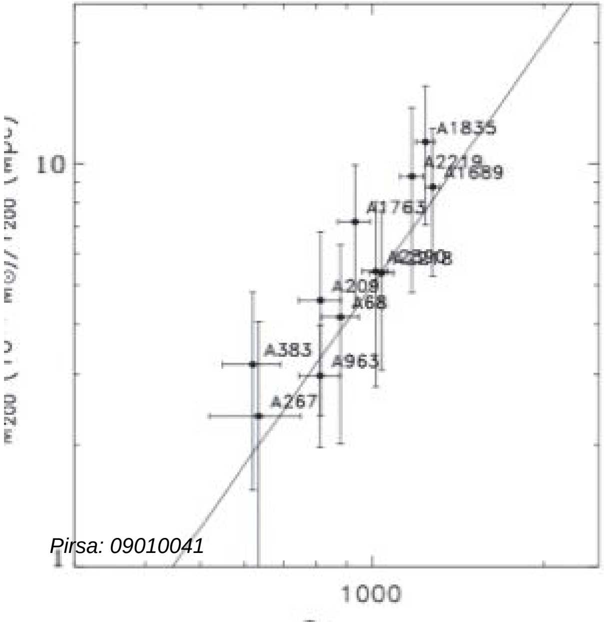

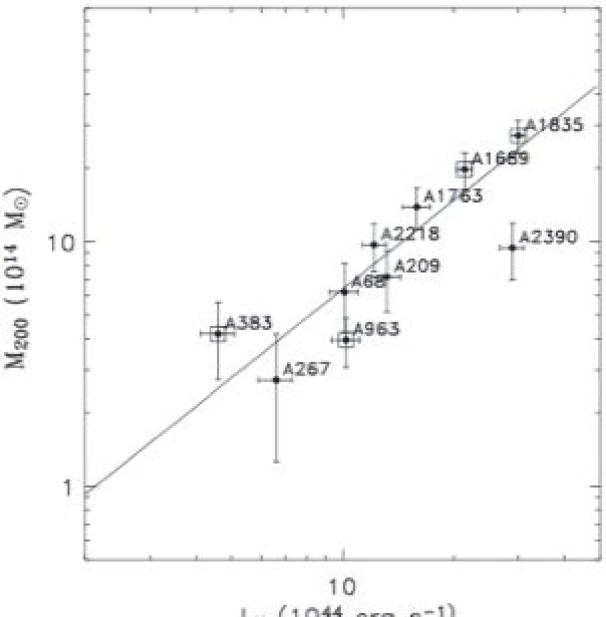

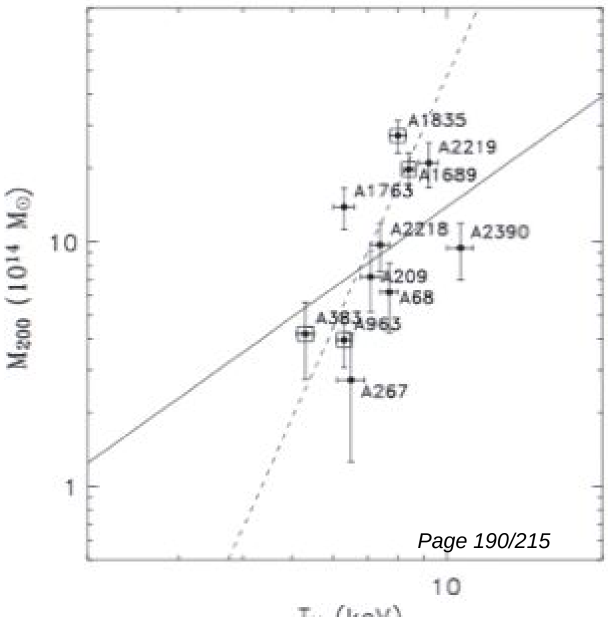

The c-M relation

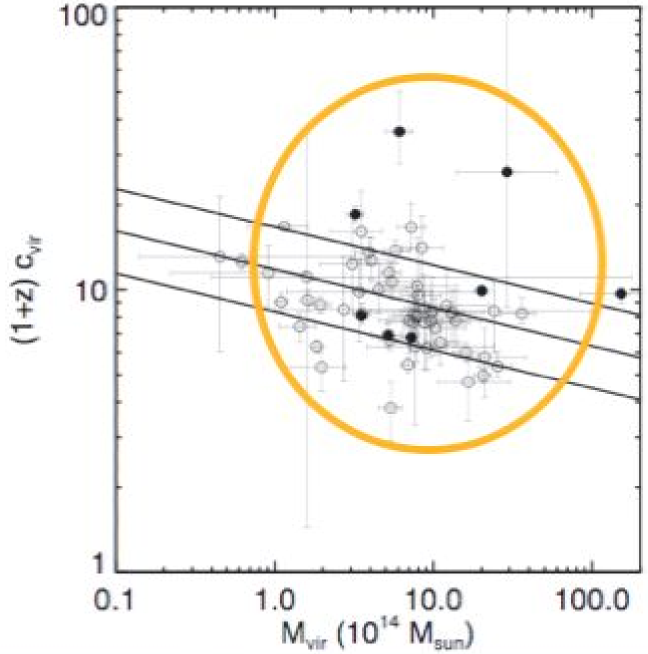

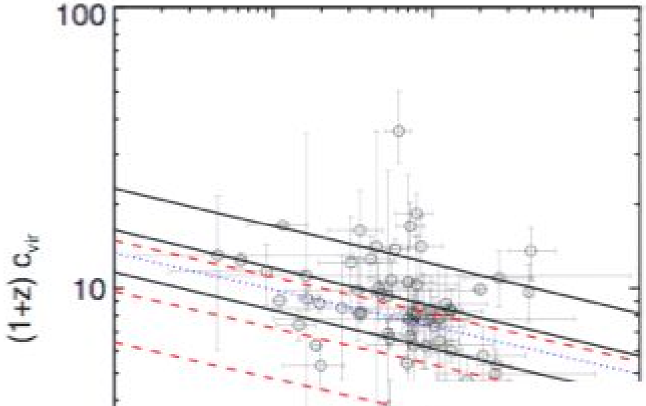

Comerford & Natarajan

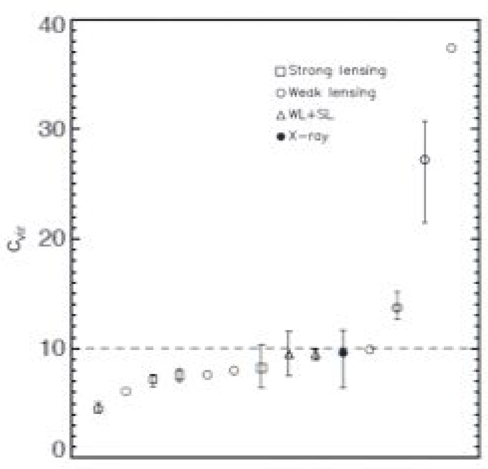

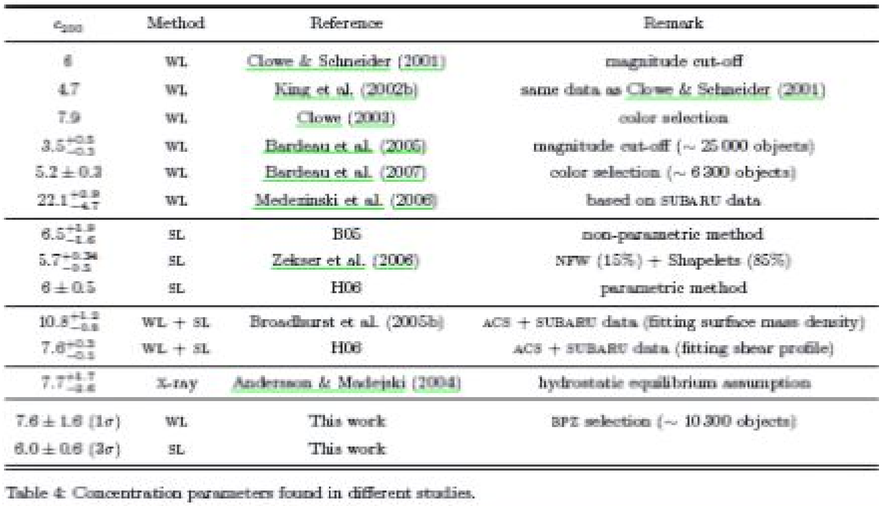

c_{200}	Method	Reference	Remark
6	WL	Clowe & Schneider (2001)	magnitude cut-off
4.7	WL	King et al. (2002b)	same data as Clowe & Schneider (2001)
7.9	WL	Clowe (2003)	color selection
$3.5^{+0.5}_{-0.3}$	WL	Bardeau et al. (2005)	magnitude cut-off ($\sim$ 25 000 objects)
5.2 ± 0.3	WL	Bardeau et al. (2007)	color selection ($\sim$ 6 300 objects)
$22.1^{+2.9}_{-4.7}$	WL	Medezinski et al. (2006)	based on SUBARU data
$6.5^{+1.9}_{-1.6}$	SL	B05	non-parametric method
$5.7^{+0.34}_{-0.5}$	SL	Zekser et al. (2006)	NFW (15%) + Shapelets (85%)
6 ± 0.5	SL	H06	parametric method
$10.8^{+1.2}_{-0.8}$	WL + SL	Broadhurst et al. (2005b)	ACS + SUBARU data (fitting surface mass density)
$7.6^{+0.3}_{-0.5}$	WL + SL	H06	ACS + SUBARU data (fitting shear profile)
$7.7^{+4.7}_{-2.6}$	X-ray	Andersson & Madejski (2004)	hydrostatic equilibrium assumption
7.6 ± 1.6 (1σ)	WL	This work	BPZ selection ($\sim$ 10 300 objects)
6.0 ± 0.6 (3σ)	SL	This work	

Table 4: Concentration parameters found in different studies.

C_{vir} scales as $M_{vir}^{-0.14}$

Lensing clusters systematically above the best-fit c-M power-law
Slope in good agreement with Hennawi+ (blue) and Bullock+(red)
Lensing concentrations higher than X-ray determinations

Comerford & PN 07

Where is the Matter in A2218?

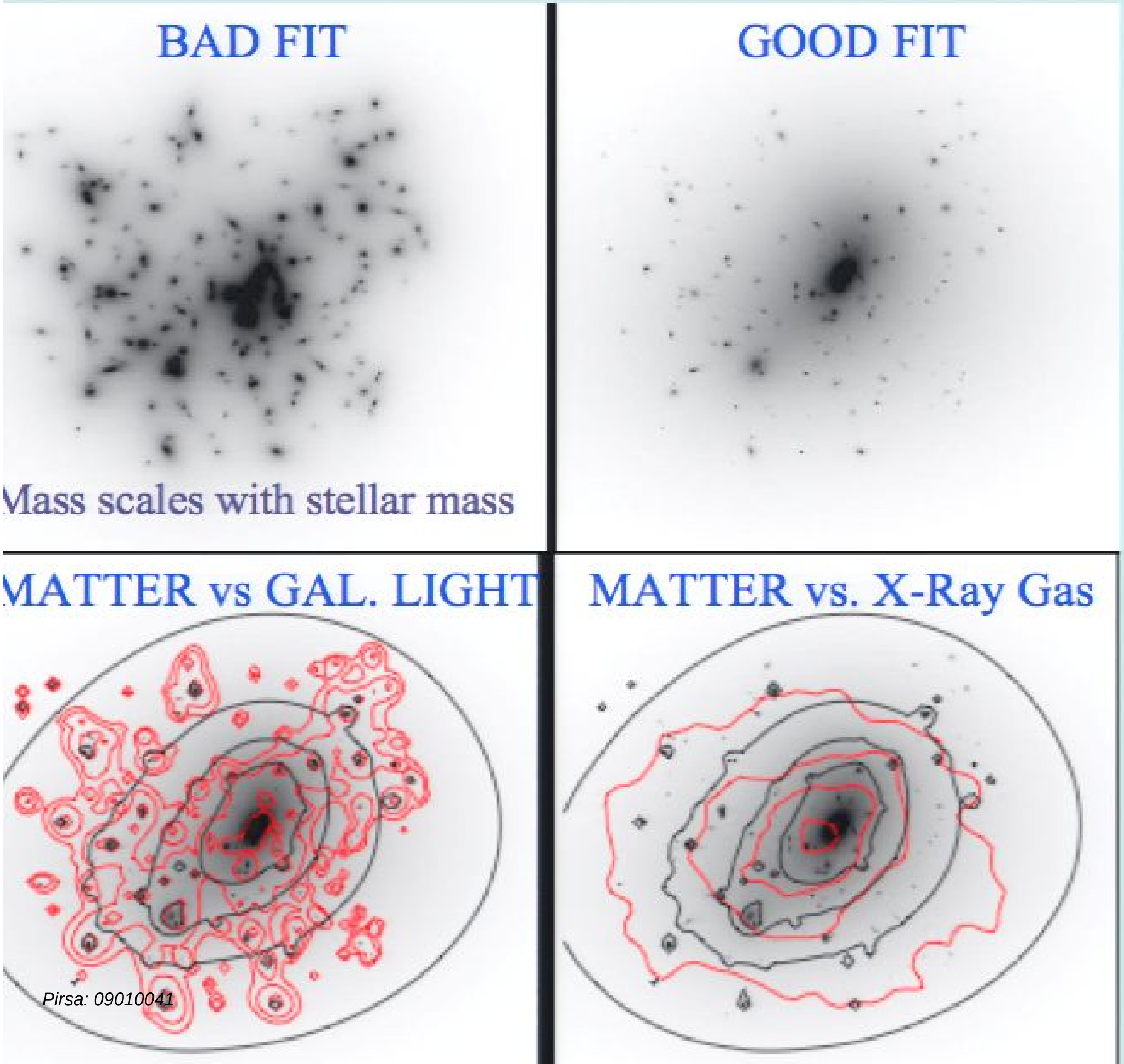

Strong Lensing constraints in Abell 2218:

- Mass distribution proportional only to the stellar mass produces a BAD FIT to the lensing data
- Require large scale smooth mass (DM) distribution
- Important difference between DM , Galaxy distribution and X-ray gas (different physics)
- But scaling relations ought to exist

Eliasdottir+ 08

Halo Mass Function

Cluster mass function evolves strongly with redshift
=> cosmological probe (growth factor)

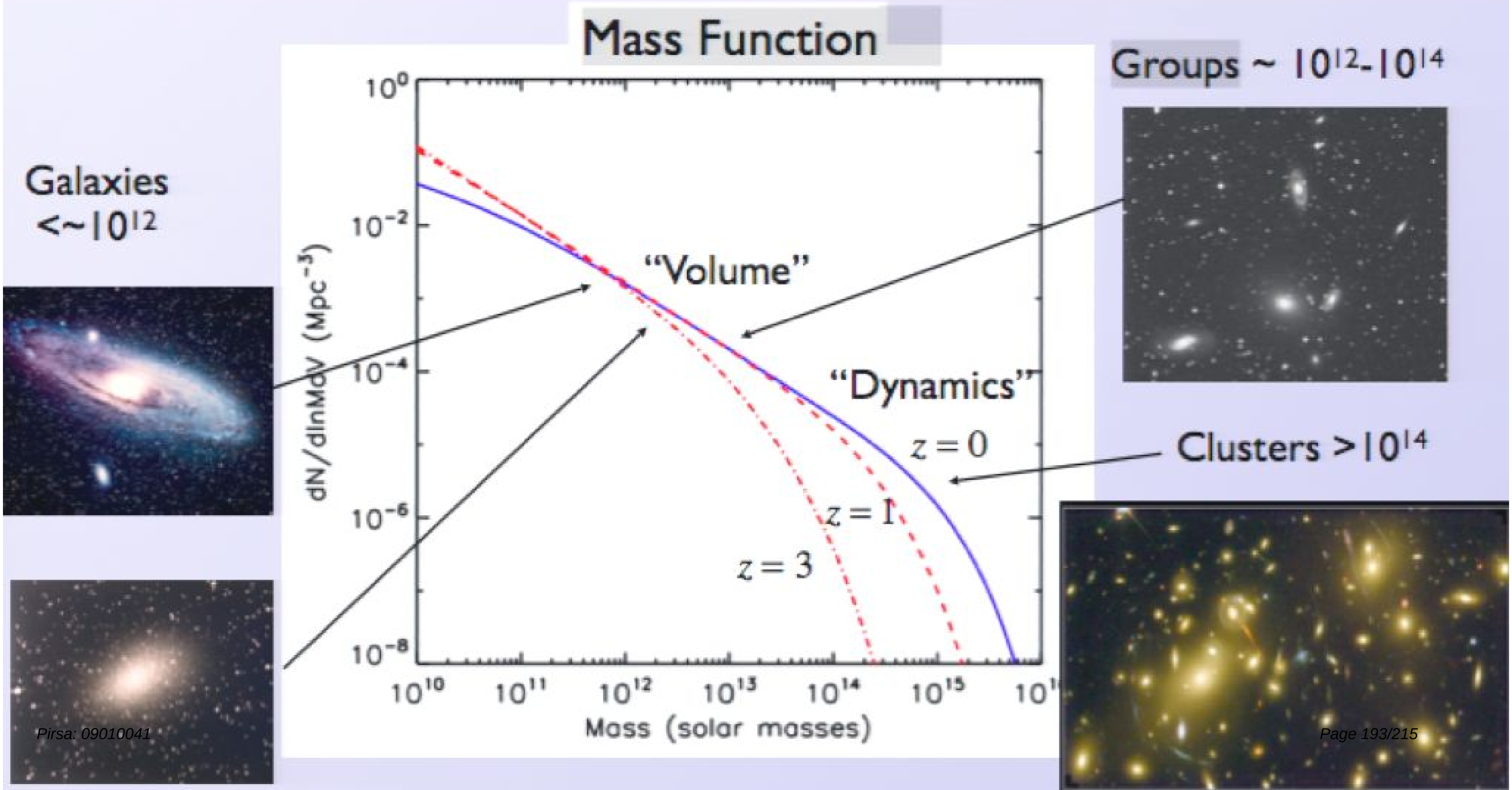

Mass Function

Galaxies
<~10^{12}

Groups ~ 10^{12}-10^{14}

Clusters >10^{14}

Counting clusters and cosmology

Measure the abundance evolution of cluster number counts = make a cluster catalog with (ID, z, M ...) with

$$\boxed{M > M_{det}}$$

Mass function:

$$\frac{dN}{dz\,d\log M} = \underbrace{\boxed{\frac{dV}{dz}}}_{\text{Geometry}} \underbrace{\boxed{\frac{dn}{d\log M}(M,z)}}_{\text{Dark Matter growth}}$$

JDEM predictions Bartlett + 09

WMAP-5 flat fiducial model

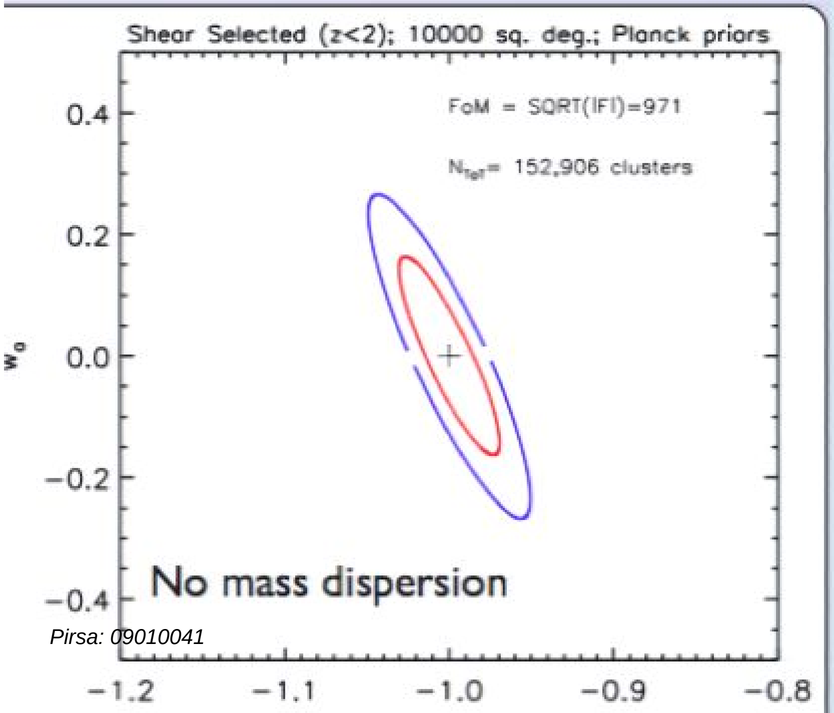

- ➡Dark matter sector understood
- ➡Mass function well-modeled by N-body simulations (e.g., Jenkins et al. (2001) - Millennium Simulation)
- ➡ lensing is the cleanest selection

Similar to X-ray work by Vikhlinin+ 08;

Ω_m-σ_8 from weak lensing-based cluster mass function

- Cosmology with X-ray cluster sample
  - –In principle:
    - Count clusters f(M,z)
  - –In reality:
    - Measure f(Mproxy,z)
    - scaling relation: Mproxy vs M
  - –Complications:
    - Mass dominated by non-baryonic DM
    - X-ray observables probe baryons
- Reliable calibration of mass-observable scaling relations is fundamental

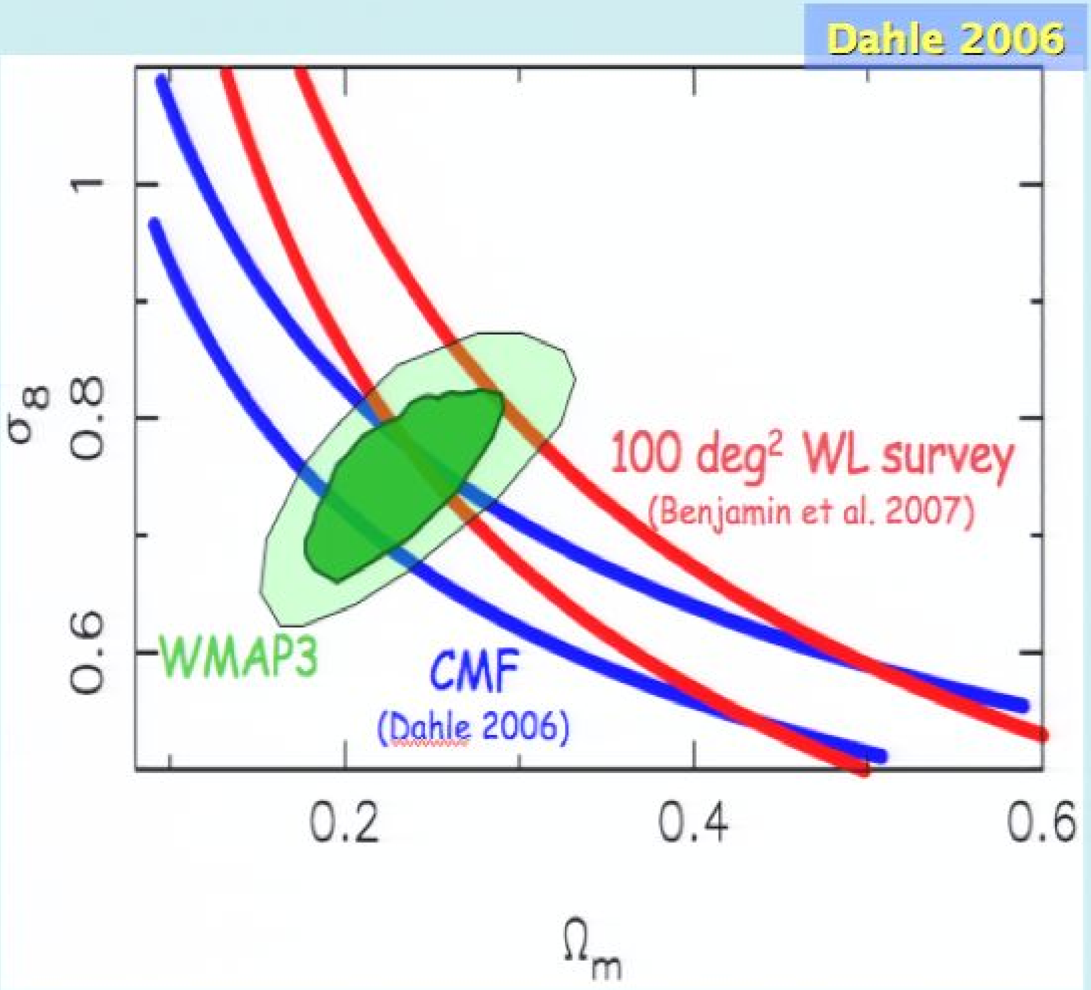

An optimist's tally of lensing tests of LCDM

Substructure: mass function of DM halos, spatial distribution of DM halos agree well

Density profiles of DM halos: profile outer slopes consistent with NFW (~ r_{vir}), inner slopes unclear but appear to be consistent with no cores, some dispersion

Tidal stripping: galaxy orbits and dynamics - reasonable agreement complicated by baryons; collisionless DM favored over fluid models

Lensing cross-sections and arc statistics: good agreement at low z, hints of excess at z > 0.6 super-lenses, structure along the line of sight

Concentration-Mass relation: in agreement within errors of the relation seen in LCDM simulations

Cluster arcs and dark energy

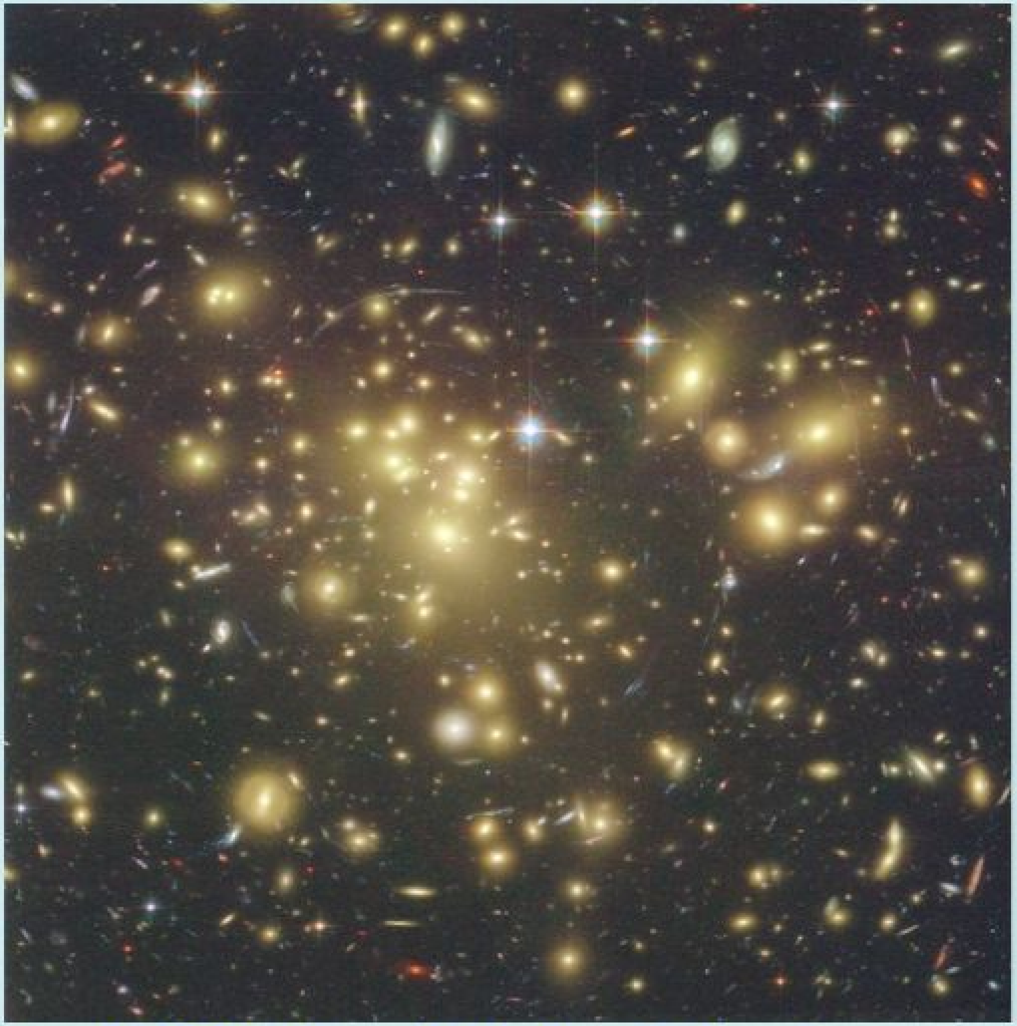

A1689, 32 multiply imaged systems,
19 with measured redshifts

Abell 1689

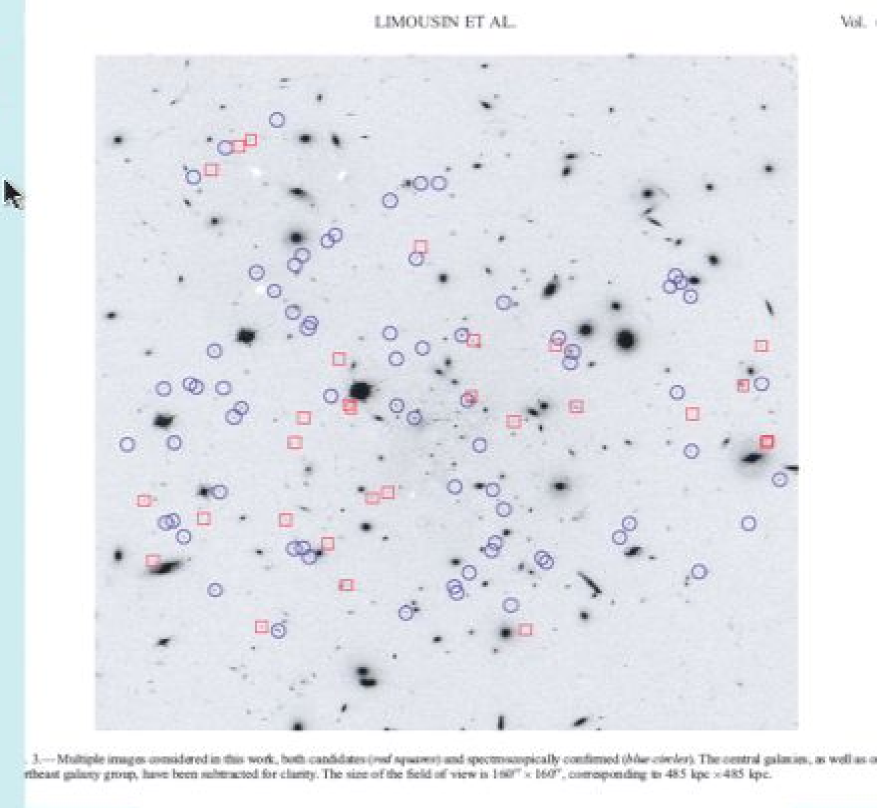

LIMOUSIN ET AL. Vol.

. 3.— Multiple images considered in this work, both candidates (*red squares*) and spectroscopically confirmed (*blue circles*). The central galaxies, as well as o rtheast galaxy group, have been subtracted for clarity. The size of the field of view is 160″ × 160″, corresponding to 485 kpc × 485 kpc.

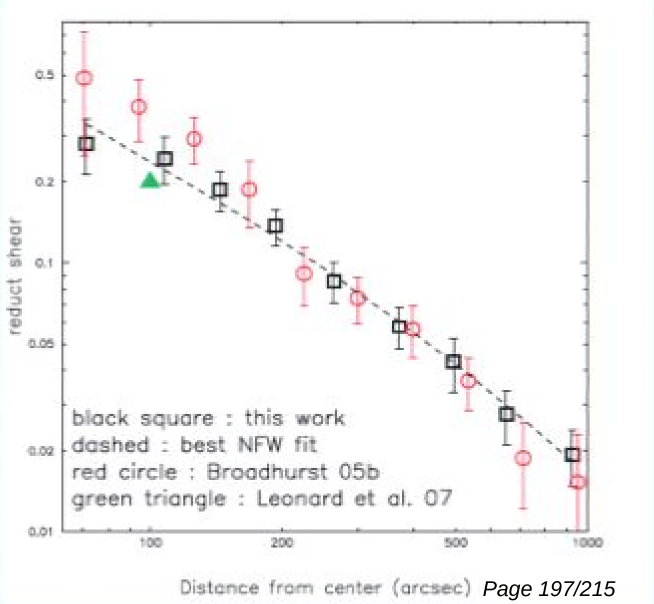

Einstein radii at multiple source redshifts

Ratio of the position of multiple images, depends on mass distribution and cosmological parameters

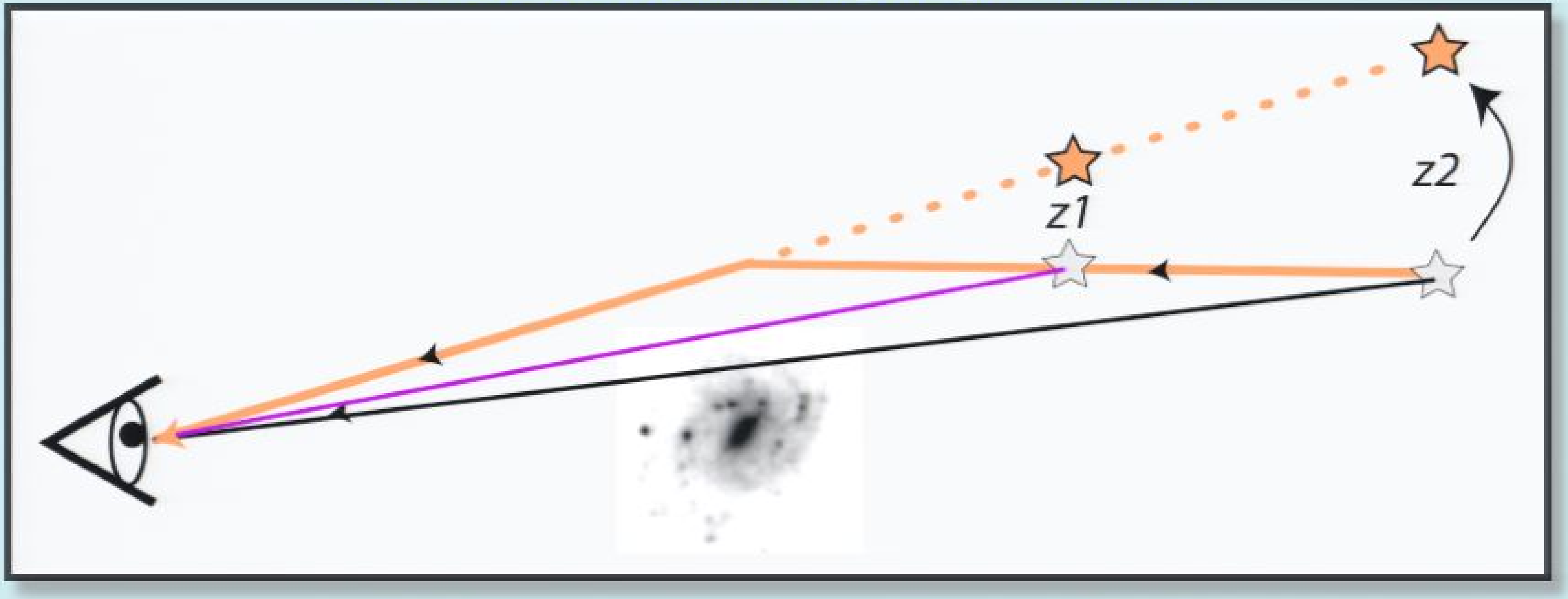

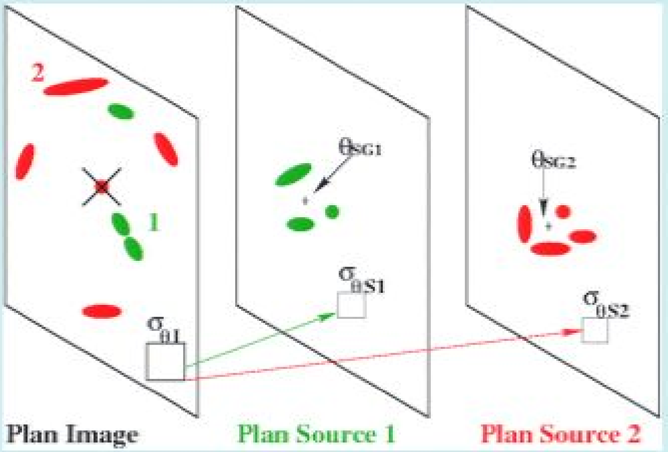

Allows constraining dark energy out to z_{source}

Multiple image families and sensitivity to dark energy

$$\boldsymbol{\theta} = \boldsymbol{\beta} + \boldsymbol{\alpha}(\boldsymbol{\theta}, \xi; M)$$

$$\xi = \frac{D(0, z_l)D(z_l, z_s)}{D(0, z_s)} \equiv \frac{D_{ol}\, D_{ls}}{D_{os}}$$

For multiple images of the same source

$$\boldsymbol{\beta}_f = \boldsymbol{\theta}_{f,i} - \boldsymbol{\nabla}\varphi_M(\boldsymbol{\theta}_{f,i}, \xi).$$

notation denotes the position of the ith image of family f

Taking the ratio of 2 distinct families of multiple images

$$\left\{\frac{D_{\rm ls1}}{D_{\rm os1}}\frac{D_{\rm os2}}{D_{\rm ls2}}\right\}\frac{\sum_{i=1}^{m}\boldsymbol{\nabla}\phi_M(\boldsymbol{\theta}_{1,i})}{\sum_{j=1}^{n}\boldsymbol{\nabla}\phi_M(\boldsymbol{\theta}_{2,j})} = \frac{-m\boldsymbol{\beta}_1 + \sum_{i=1}^{m}\boldsymbol{\theta}_{1,i}}{-n\boldsymbol{\beta}_2 + \sum_{j=1}^{n}\boldsymbol{\theta}_{2,j}}.$$

$$\Xi(z_1, z_{\rm s1}, z_{\rm s2}; \Omega_{\rm M}, \Omega_{\rm X}, w_{\rm X}) = \frac{D(z_1, z_{\rm s1})}{D(0, z_{\rm s1})}\frac{D(0, z_{\rm s2})}{D(z_1, z_{\rm s2})}$$

Feasibility study for smooth model clusters

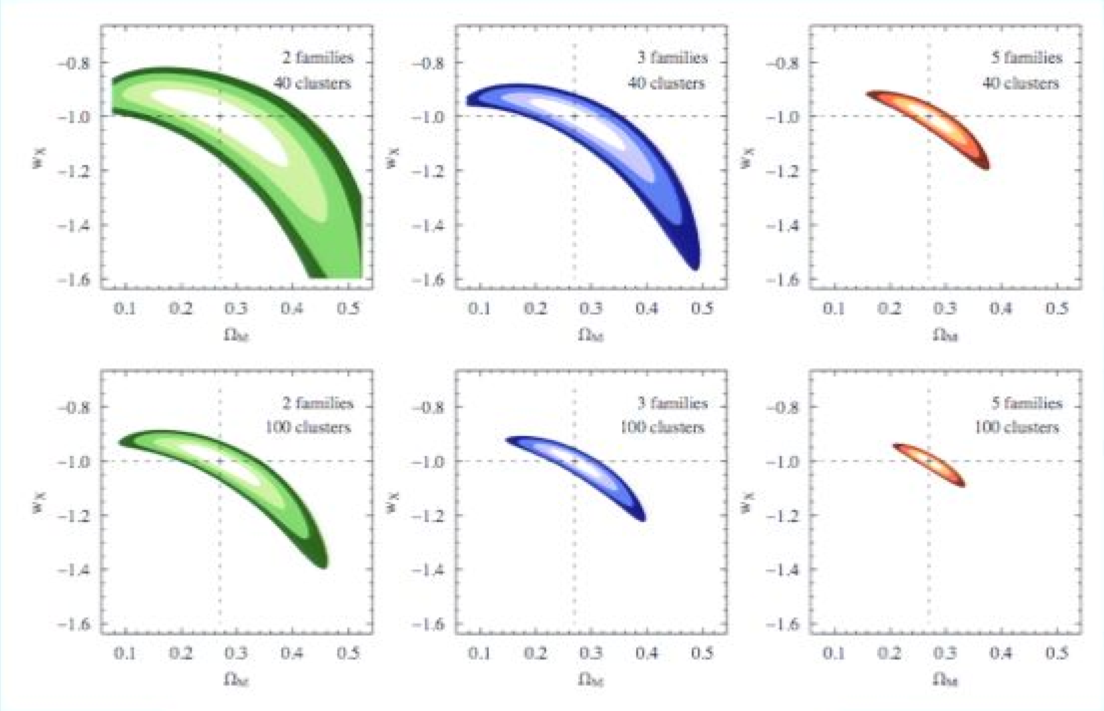

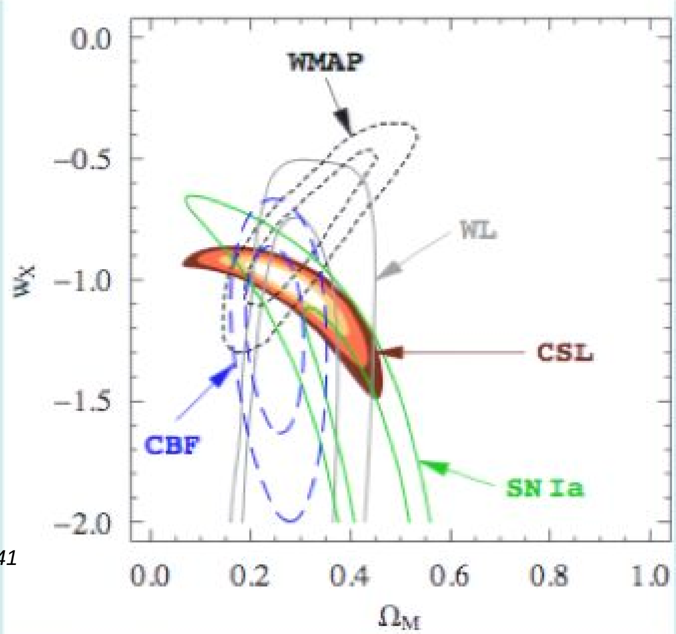

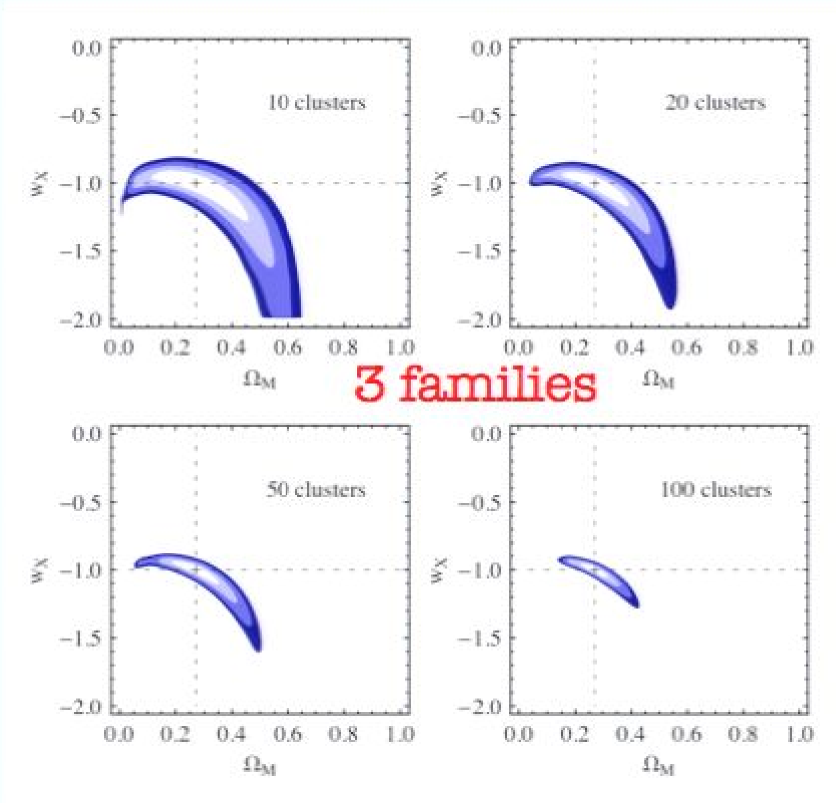

3 families

Gilmore & PN 08

Current limitations in the mass modeling

- Positional accuracy ~0.7- 0.5 arcsec (Abell 1689)
- Unknown redshifts for all sources (photo-z's ???)
- Width of intrinsic ellipticity distribution
- Finite number of background sources
- Structure along the line of sight behind the lens plane (environments of lenses Momcheva et al. '06, Oguri, Keeton& Dalal '05)

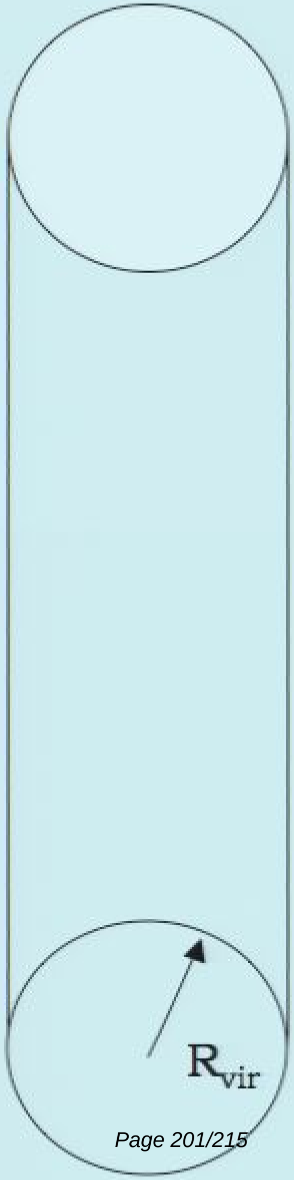

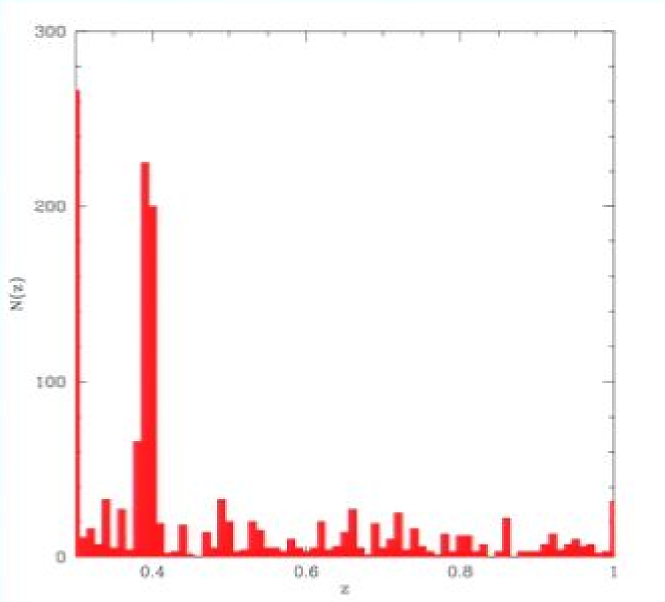

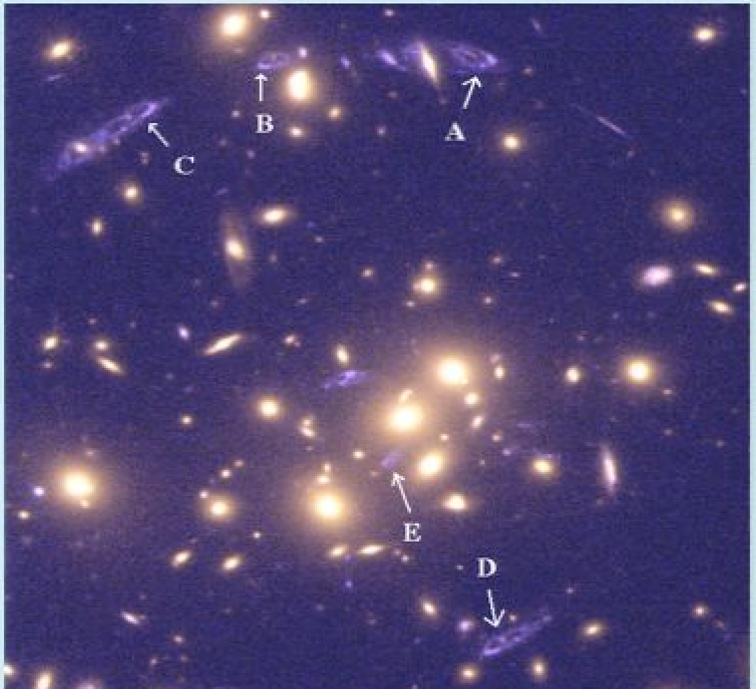

Multi-Scale Grid Based Modeling

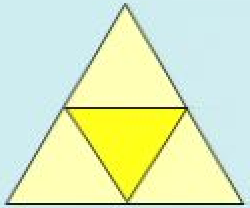

More flexible ”multi-scale” model:

- hexagonal/triangle padding- to match the natural shape of clusters
- Multi-scale: split triangles according to a mass densit threshold
- Circular mass clump at each grid point:
  - Truncated isothermal profile with a core
  - size of the mass clump depends on the grid: r_core =grid-size
  - Truncation also depends on the grid: r_cut/r_core = 3
  - one free parameter for each clump
- Add galaxy-scale mass clumps
- MCMC optimized
- Easy extension to WL regime

ACS field of A1689

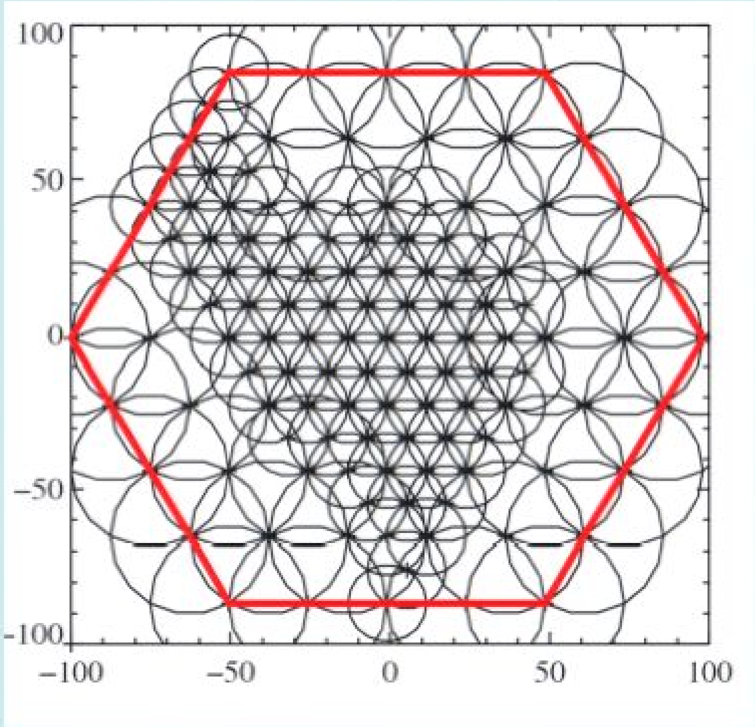

Work in progress!

Multiple image families and sensitivity to dark energy

$$\boldsymbol{\theta} = \boldsymbol{\beta} + \boldsymbol{\alpha}(\boldsymbol{\theta}, \xi; M)$$

$$\xi = \frac{D(0, z_l)D(z_l, z_s)}{D(0, z_s)} \equiv \frac{D_{ol}\, D_{ls}}{D_{os}}$$

For multiple images of the same source

$$\boldsymbol{\beta}_f = \boldsymbol{\theta}_{f,i} - \boldsymbol{\nabla}\varphi_M(\boldsymbol{\theta}_{f,i}, \xi)$$

notation denotes the position of the i$^{\mathrm{th}}$ image of family f

Taking the ratio of 2 distinct families of multiple images

$$\boxed{\left\{\frac{D_{\mathrm{ls}1}}{D_{\mathrm{os}1}}\frac{D_{\mathrm{os}2}}{D_{\mathrm{ls}2}}\right\}} \frac{\sum_{i=1}^{m} \boldsymbol{\nabla}\phi_M(\boldsymbol{\theta}_{1,i})}{\sum_{j=1}^{n} \boldsymbol{\nabla}\phi_M(\boldsymbol{\theta}_{2,j})} = \frac{-m\boldsymbol{\beta}_1 + \sum_{i=1}^{m} \boldsymbol{\theta}_{1,i}}{-n\boldsymbol{\beta}_2 + \sum_{j=1}^{n} \boldsymbol{\theta}_{2,j}}.$$

$$\Xi(z_1, z_{\mathrm{s}1}, z_{\mathrm{s}2}; \Omega_{\mathrm{M}}, \Omega_{\mathrm{X}}, w_{\mathrm{X}}) = \frac{D(z_1, z_{\mathrm{s}1})}{D(0, z_{\mathrm{s}1})}\frac{D(0, z_{\mathrm{s}2})}{D(z_1, z_{\mathrm{s}2})}$$

Einstein radii at multiple source redshifts

Ratio of the position of multiple images,depends on mass distribution and cosmological parameters

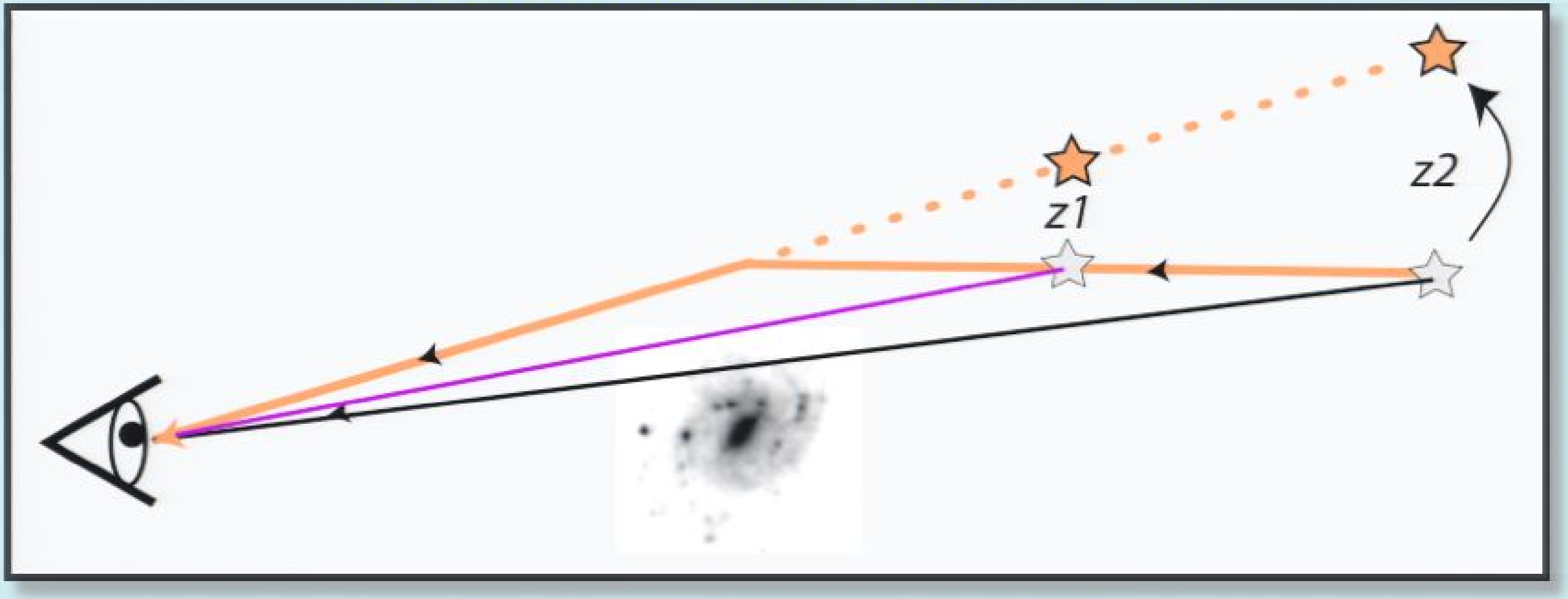

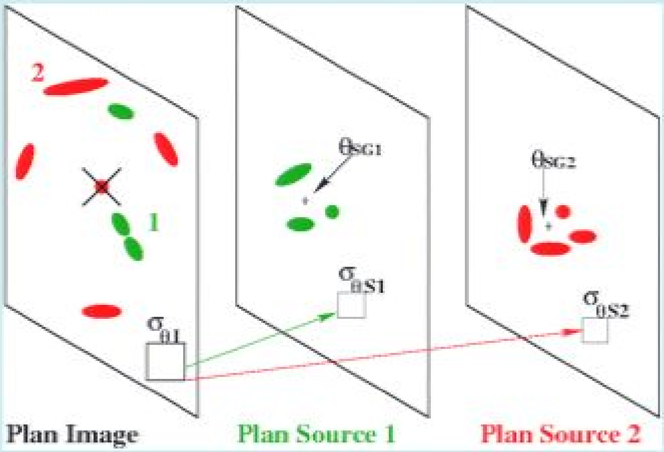

Allows constraining dark energy out to z_{source}

Multiple image families and sensitivity to dark energy

$$\boldsymbol{\theta} = \boldsymbol{\beta} + \boldsymbol{\alpha}(\boldsymbol{\theta}, \xi; M)$$

$$\xi = \frac{D(0, z_l) D(z_l, z_s)}{D(0, z_s)} \equiv \frac{D_{ol} D_{ls}}{D_{os}}$$

For multiple images of the same source

$$\boldsymbol{\beta}_f = \boldsymbol{\theta}_{f,i} - \boldsymbol{\nabla} \varphi_M(\boldsymbol{\theta}_{f,i}, \xi)$$

notation denotes the position of the i^{th} image of family f

Taking the ratio of 2 distinct families of multiple images

$$\boxed{\left\{ \frac{D_{ls1}}{D_{os1}} \frac{D_{os2}}{D_{ls2}} \right\}} \frac{\sum_{i=1}^{m} \boldsymbol{\nabla} \phi_M(\boldsymbol{\theta}_{1,i})}{\sum_{j=1}^{n} \boldsymbol{\nabla} \phi_M(\boldsymbol{\theta}_{2,j})} = \frac{-m\boldsymbol{\beta}_1 + \sum_{i=1}^{m} \boldsymbol{\theta}_{1,i}}{-n\boldsymbol{\beta}_2 + \sum_{j=1}^{n} \boldsymbol{\theta}_{2,j}}.$$

$$\Xi(z_1, z_{s1}, z_{s2}; \Omega_{\mathrm{M}}, \Omega_{\mathrm{X}}, w_{\mathrm{X}}) = \frac{D(z_1, z_{s1})}{D(0, z_{s1})} \frac{D(0, z_{s2})}{D(z_1, z_{s2})}$$

Feasibility study for smooth model clusters

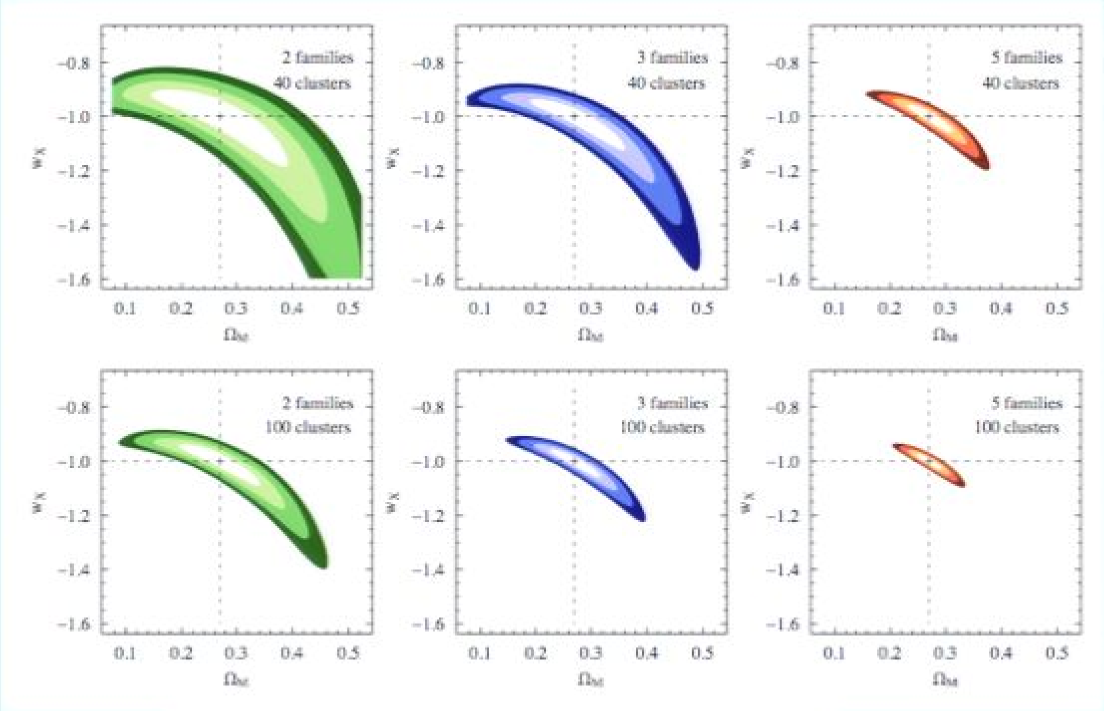

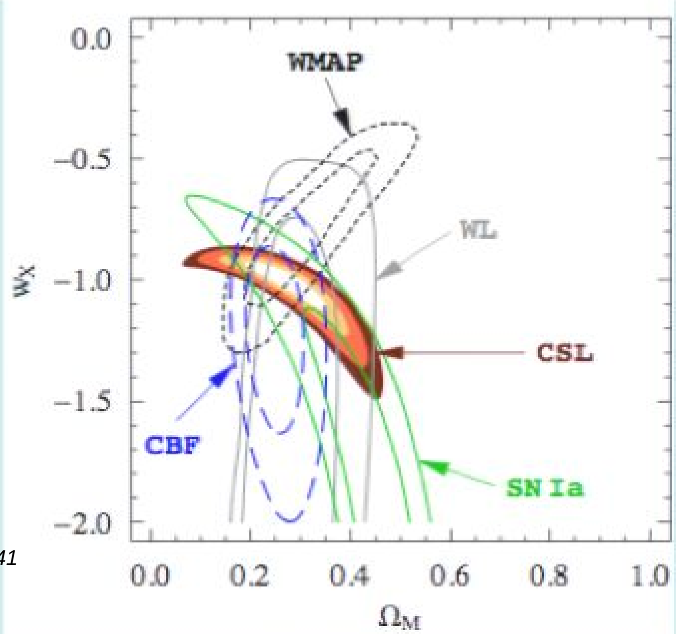

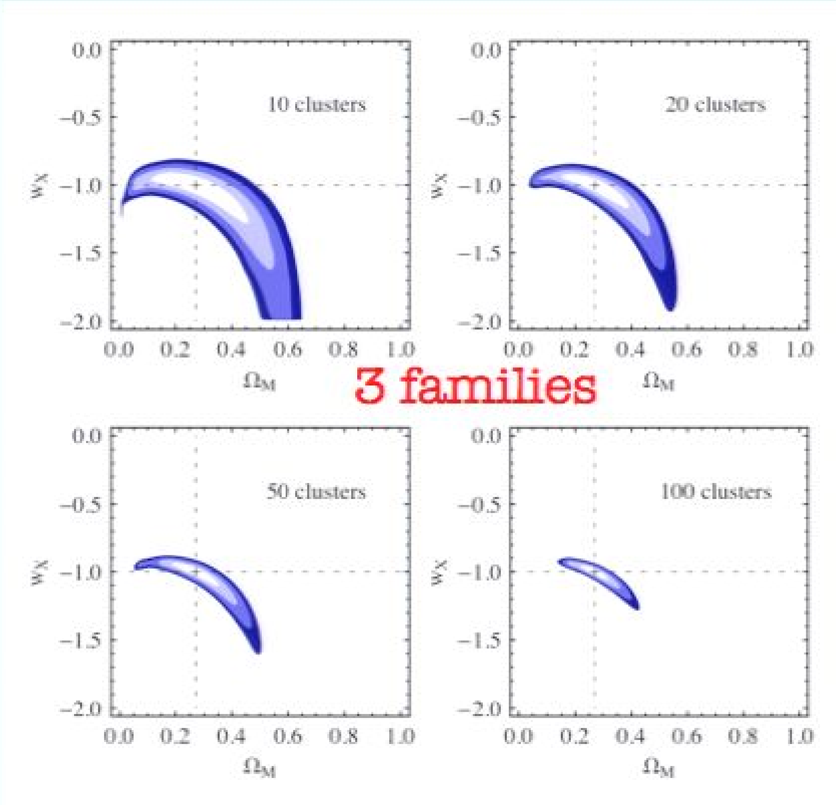

3 families

Gilmore & PN 08

Multi-Scale Grid Based Modeling

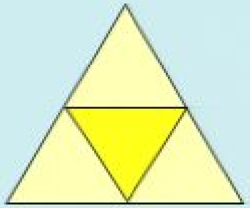

More flexible "multi-scale" model:

- hexagonal/triangle padding- to match the natural shape of clusters
- Multi-scale: split triangles according to a mass densit threshold
- Circular mass clump at each grid point:
  - Truncated isothermal profile with a core
  - size of the mass clump depends on the grid: r_core =grid-size
  - Truncation also depends on the grid: r_cut/r_core = 3
  - one free parameter for each clump
- Add galaxy-scale mass clumps
- MCMC optimized
- Easy extension to WL regime

ACS field of A1689

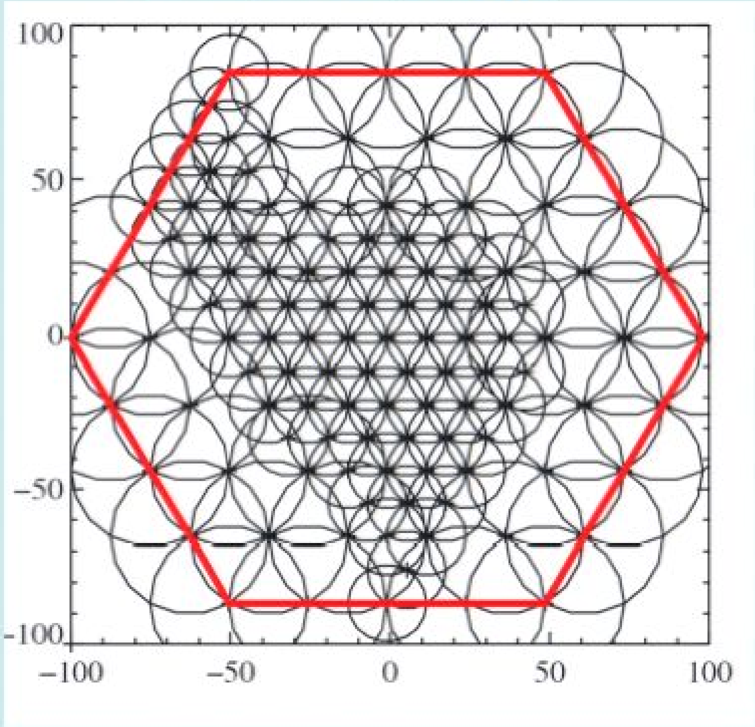

Work in progress!

Preliminary results for A1689

Mass model with 3 PIEMD potentials; 58 cluster galaxies Bayesian optimization: 32 constraints, 21 free parameters; RMS = 0.6 arcsec; 12 multiple images with spec z, flat Universe prior, LOS structure not included

$0.1 \leq \Omega_M \leq 0.58; -1.57 \leq w_X \leq -0.85$

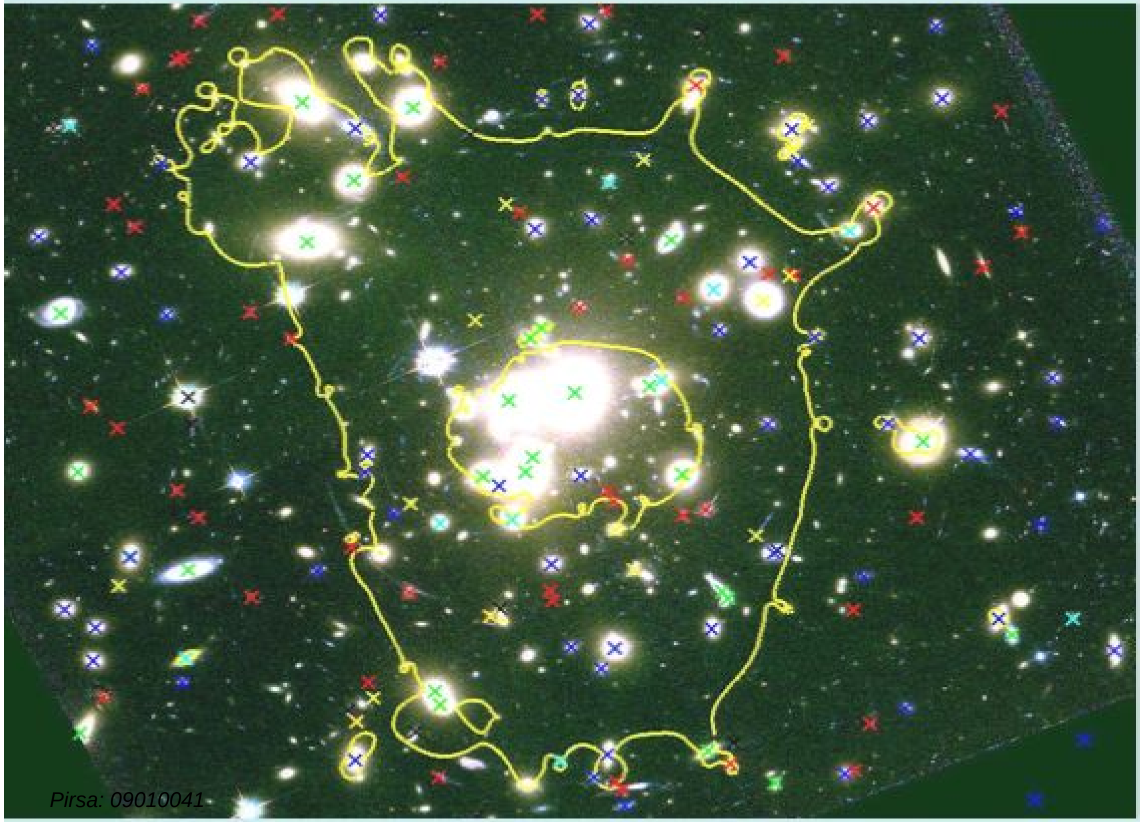

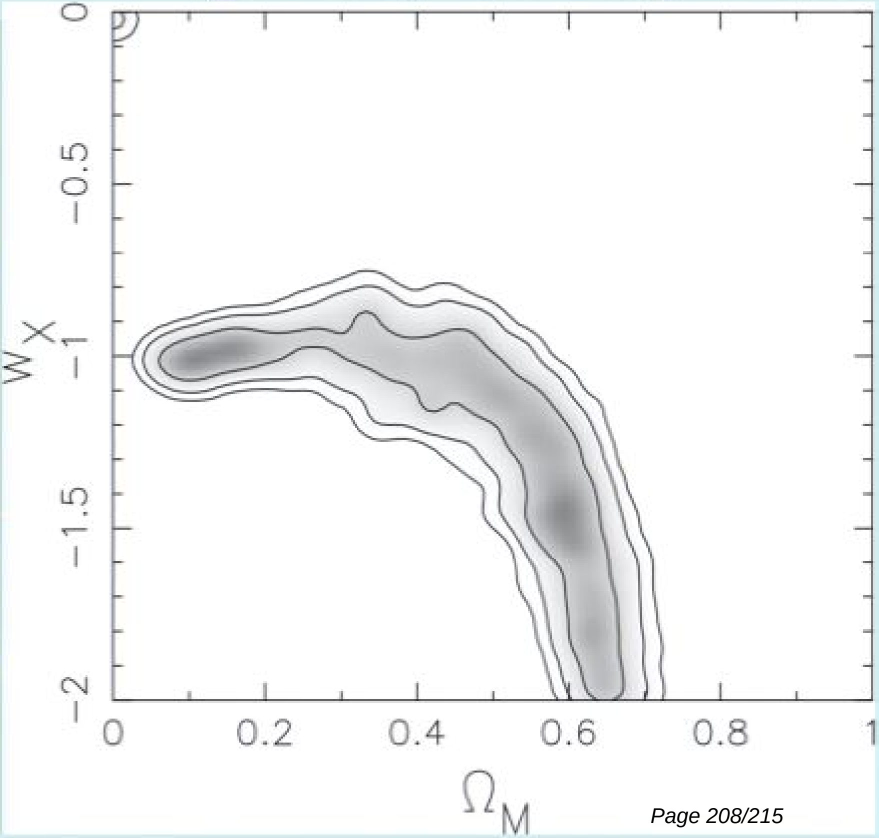

D'Aloisio & PN; Jullo & Kneib 09

Current limitations in the mass modeling

- Positional accuracy ~0.7- 0.5 arcsec (Abell 1689)
- Unknown redshifts for all sources (photo-z's ???)
- Width of intrinsic ellipticity distribution
- Finite number of background sources
- Structure along the line of sight behind the lens plane (environments of lenses Momcheva et al. '06, Oguri, Keeton& Dalal '05)

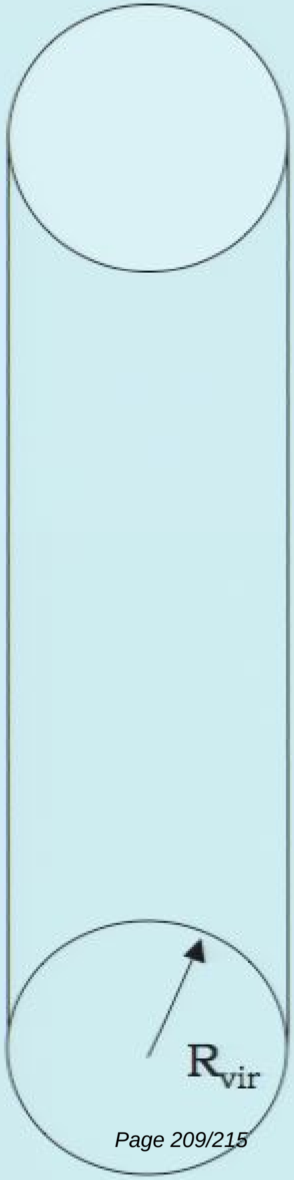

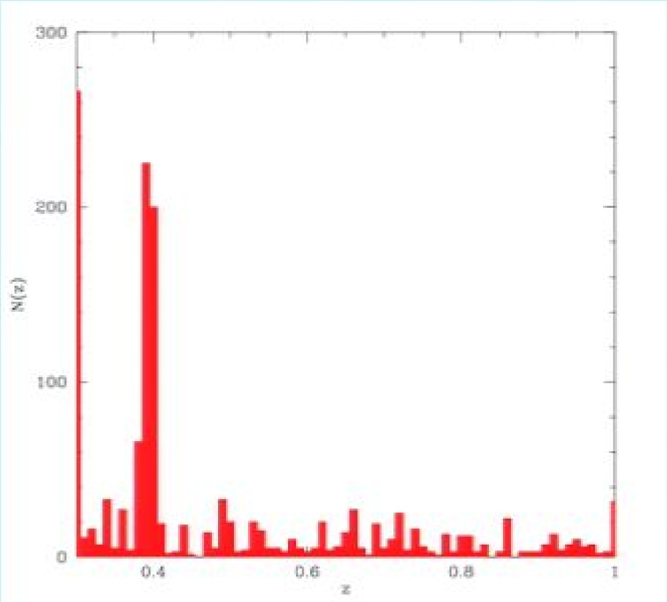

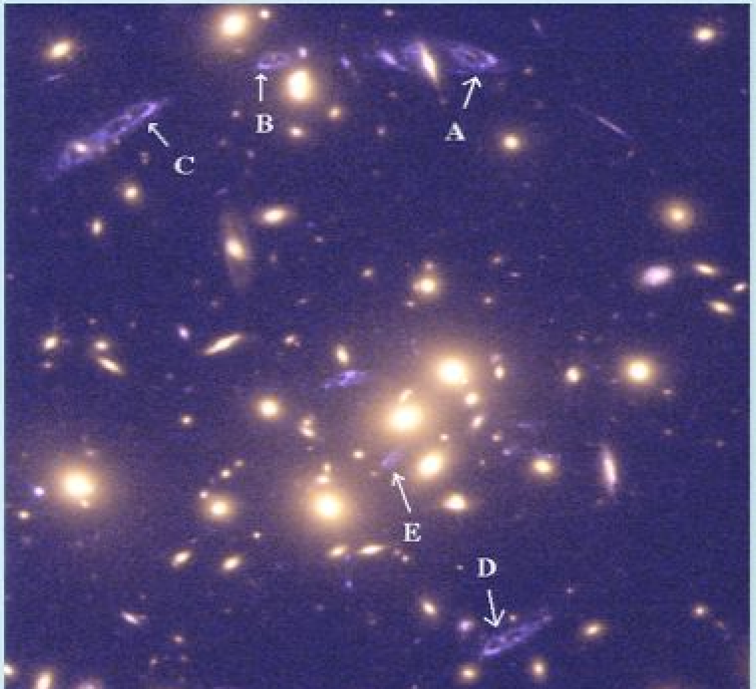

Effect of structure along the line of sight

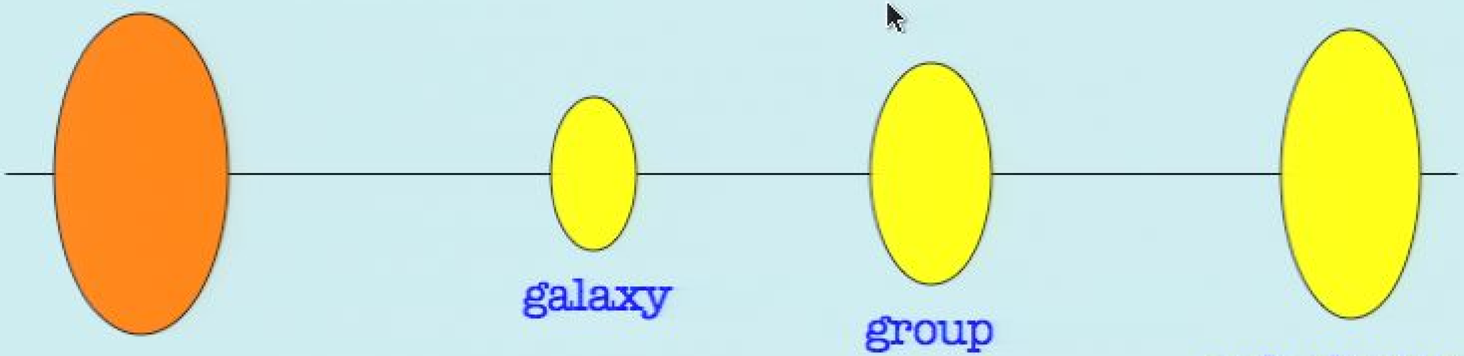

galaxy

group

sub-cluster

Foreground cluster lens

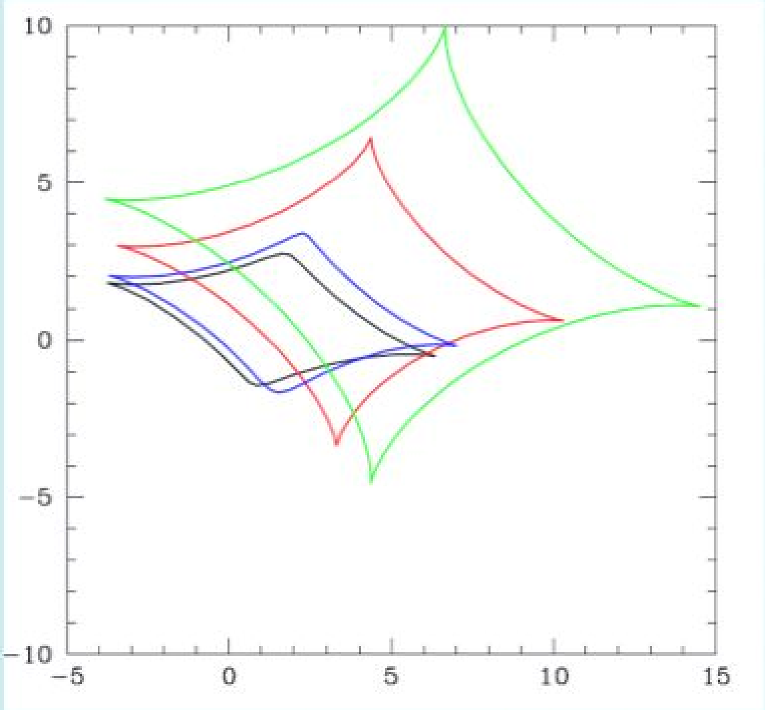

Area under caustic likely to produce multiple images

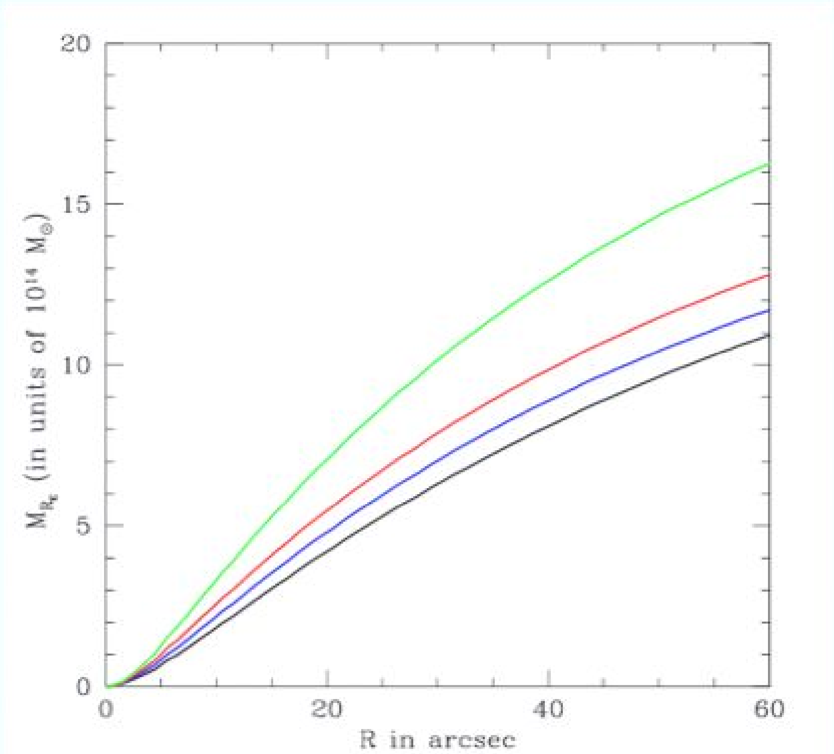

Contribution of structure behind the lens plane

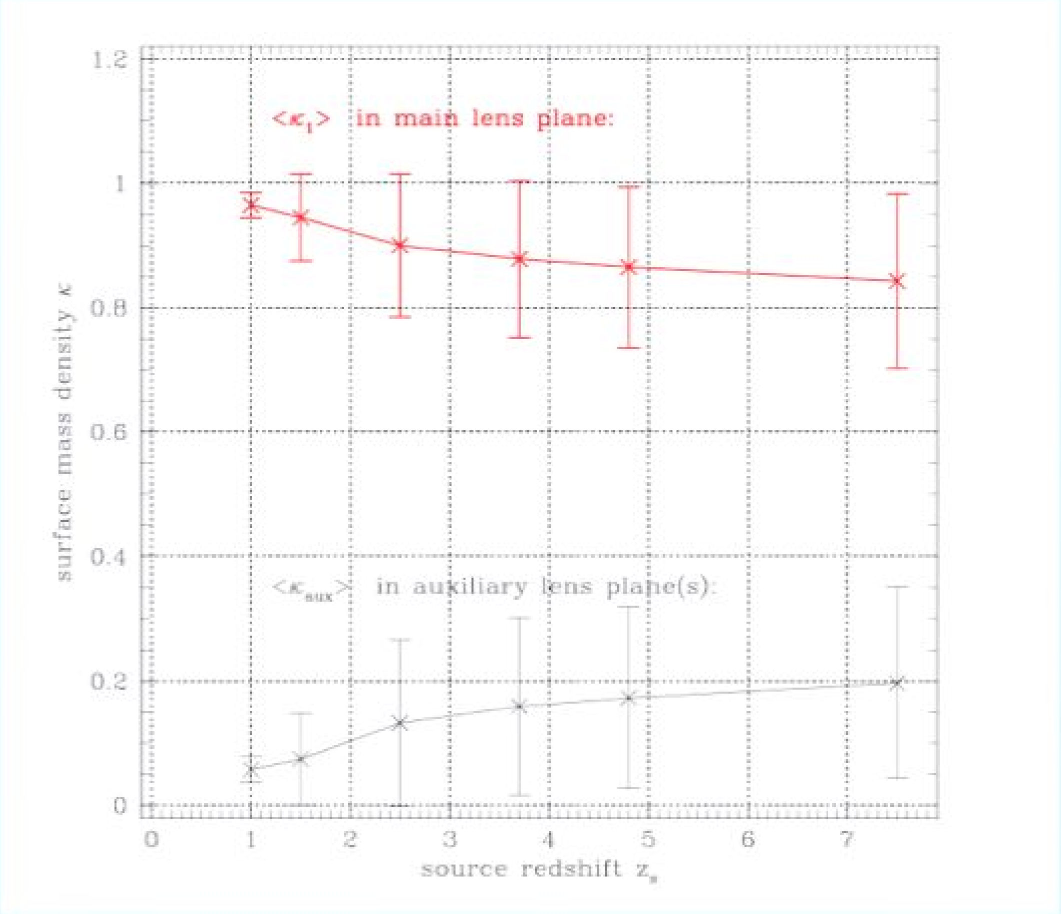

perturbations in the
positions of multiple images

RN: in prep

Future Cosmological ground-based Surveys

- 2009:VST-KIDS: 1000 deg^2
- 2009: DES: 5000 deg^2
- 2009+: Pan STARRS: ~20000 deg^2
- 2018: LSST: ~20000 deg^2

- But WL limited by ground based PSF to n_eff ~ 20-30 gal/$sqarcmin^2$ (limits the mass sensitivity of detecting clusters)
- Only going to space can we do better, with higher accuracy ellipticity measurements

Future Cosmological Space Missions

- 2013: JWST: 6.5m telescope - optimized for distant Universe, but can likely do some SN and Cluster cosmology
- 2015- JDEM: 1.5m telescope, 150Mpix (WL,BAO,SN)
- 2017- EUCLID: 1.2m telescope, 600 Mpix (WL,BAO)
- *Possibility of ESA joining NASA/DOE, should aim for the best possible given resource constraints* : a proper telescope/mission competitive to ground-based projects, which will enable the fundamental questions to be answered with a variety of probes.

Future prospects

- Clusters very useful and important laboratories for studying dark matter and dark energy
- Current lensing observations of clusters consistent with LCDM
- Future test for LCDM - tri-axiality distribution of clusters from combining X-ray, lensing and SZ data
- Strong lensing in clusters a very promising technique to constrain dark energy models
- More work needed in understanding the systematics before applying to real clusters
- Future surveys will establish clusters as very efficient cosmological probes

hi-z lensed galaxies behind clusters

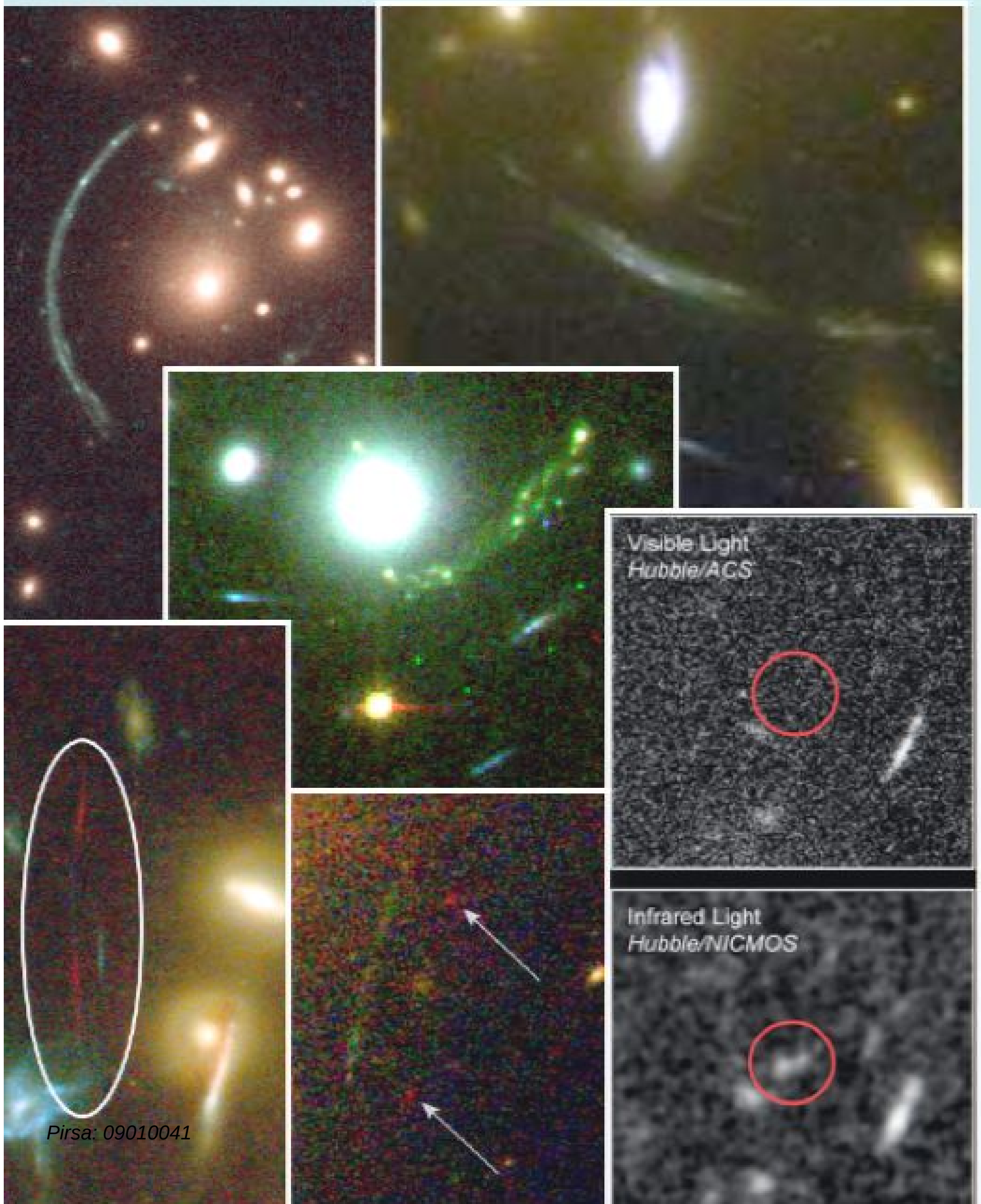

- **1987**: Cl2244 one of the first gravitational arcs, later recognized as a z=2.2 galaxy
- Ebbels et al **1996**: a z=2.5 LBG in a2218
- cB58 z=2.7 recognized as a strongly lensed source (Seitz et al **1998**)
- Franx et al **1997**: a LAE at z=4.9
- Ellis et al **2001**: LAE at z=5.6
- Kneib et al **2004**, Egami et al **2005**: LBG at z~6.8